

Distribution Agreement

In presenting this thesis or dissertation as a partial fulfillment of the requirements for an advanced degree from Emory University, I hereby grant to Emory University and its agents the non-exclusive license to archive, make accessible, and display my thesis or dissertation in whole or in part in all forms of media, now or hereafter known, including display on the world wide web. I understand that I may select some access restrictions as part of the online submission of this thesis or dissertation. I retain all ownership rights to the copyright of the thesis or dissertation. I also retain the right to use in future works (such as articles or books) all or part of this thesis or dissertation.

Signature:

Cara A. Mosley

Date

Design, Synthesis, and Biological Evaluation of
Subunit-Selective N-Methyl-D-Aspartate Receptor Antagonists

By

Cara Amelia Mosley
Doctor of Philosophy

Chemistry

Dennis C. Liotta
Advisor

Frank E. McDonald
Committee Member

Fredric M. Menger
Committee Member

Accepted:

Lisa A. Tedesco, Ph.D.
Dean of the James T. Laney School of Graduate Studies

Date

Design, Synthesis, and Biological Evaluation of
Novel N-Methyl-D-Aspartate Receptor Antagonists

By

Cara A. Mosley
B.S. Georgia Institute of Technology, 2004

Advisor: Dennis C. Liotta, Ph.D.

An abstract of
A dissertation submitted to the Faculty of the Graduate School of Emory University
in partial fulfillment of the requirements for the degree of Doctor of Philosophy in
Chemistry

2009

Abstract

Design, Synthesis, and Biological Evaluation of Subunit-Selective N-Methyl-D-Aspartate Receptor Antagonists

Part 1: Design, Synthesis, and Biological Evaluation of Novel NR1/NR2B-Selective NMDA Receptor Antagonists Towards the Treatment of Neurodegenerative Diseases

Part 2: Design, Synthesis, and Biological Evaluation of First-in-Class NR2C/2D-Selective NMDA Receptor Antagonists

By Cara A. Mosley

Part 1:

N-Methyl-D-Aspartate (NMDA)-selective ionotropic glutamate receptors are ligand-gated ion channels that mediate a Ca^{2+} -permeable component of excitatory synaptic transmission in the central nervous system. The receptors are tetrameric complexes comprised of glycine-binding NR1 subunits and glutamate-binding NR2 subunits, of which there are four different subtypes (NR2A, NR2B, NR2C and NR2D) that each endow the receptor with unique functional properties. Over-activation of NMDA receptors has been associated with a number of neurodegenerative diseases in both animal and human models including stroke, traumatic brain injury, epilepsy, schizophrenia, and neuropathic pain. As a potential treatment for these disorders, a number of NMDA receptor antagonists have been developed.

In Chapter 1, the synthesis and structure activity relationship analysis of novel enantiomeric propanolamines are presented. Compounds have been evaluated for potency against the NR1/NR2B subunit of the N-Methyl-D-Aspartate (NMDA) receptor. In addition, the pH sensitivity (fold shift) of the analogues is discussed. Fold shift, i.e. the

increased potency of a given compound at more acidic pH values, is hypothesized to be beneficial under ischemic conditions associated with stroke. In addition, the compounds described have been specifically designed to exhibit decreased off-target activity at the human-ether-a-go-go related gene (hERG) ion channel, which is often associated with cardiotoxicity *in vivo*.

A novel mechanism of action for literature-precedent NMDA receptor antagonists is also presented. Ion pore channel blockers, previously believed to be non-specific for all sub-types of NMDA receptors, are shown to exhibit both subunit selectivity and fold shifts. The pH sensitivity of the compounds is not reflective of the protonation state of the inhibitor under differential pH conditions. Rather, it is hypothesized that the pK_a of the NMDA receptor's proton sensor region is responsible for the observed fold shift *in vitro*.

In Chapter 2, a novel series of amide-based NR1/NR2B-selective NMDA receptor antagonists is described. Originating in a screening hit characterized by a thiosemicarbazide linker region, development of structure activity relationships led to a novel series of antagonists characterized by an amide scaffold. Similar to the enantiomeric propanolamines, design of analogues is targeted towards inducing pH sensitivity and eliminating off-target effects. Some of the studied compounds are potent, selective, non-competitive, and voltage-independent antagonists of NR2B-containing NMDA receptors. Like the founding member of this class of antagonists (ifenprodil), several interesting compounds of the series bind to the amino terminal domain of the NR2B subunit to inhibit function. Analogue potency is modulated by

linker length, flexibility, and hydrogen bonding opportunities. However, unlike previously described classes of NR2B-selective NMDA antagonists that exhibit off-target activity at a variety of monoamine receptors, the compounds described herein show much diminished effects against the hERG channel and α_1 adrenergic receptors. These data together suggest that masking charged atoms on the linker region of NR2B-selective antagonists can decrease undesirable side effects while still maintaining on-target potency. Selections of the compounds discussed have acceptable half-lives *in vivo* and are predicted to permeate the blood-brain barrier. The lead compound was neuroprotective *in vitro*, but did not exhibit neuroprotective properties in an *in vivo* model of neuropathic pain.

Part 2:

As a result of the development of NR1/NR2B-selective NMDA receptor antagonists as both drugs and research tools, greater than 1000 publications describe studies involving the NR1/NR2B subunit and its role in both physiologic and disease states. However, no useful and selective inhibitors of the NR1/NR2A-, NR2C, or NR2D receptors have been described to date. Based on the anatomical localization of the receptor, antagonists specific to the NR2C and NR2D subunit could potentially be beneficial in treating the over-active NMDA receptors which contribute to Parkinson's disease.

Herein, we describe the synthesis and biological activity of a new class of subunit-selective antagonists of NMDA receptors which contain the (*E*)-3-phenyl-2-

styrylquinazolin-4(3H)-one backbone. The inhibition of NMDA receptor function induced by these quinazolin-4-one derivatives is non-competitive and voltage-independent, suggesting that this family of compounds does not exert action on the agonist binding site of the receptor or block the channel pore. The compounds described here closely resemble the previously reported selective non-competitive antagonist **CP-465,022** ((S)-3-(2-chlorophenyl)-2-[2-(6-diethylaminomethyl-pyridin-2-yl)-vinyl]-6-fluoro-3H-quinazolin-4-one), known to target the closely related α -amino-3-hydroxy-5-methyl-4-isoxazolepropionic acid (AMPA)-selective glutamate receptor. However, modification of ring substituents resulted in analogues with greater than 100-fold selectivity for NMDA receptors over AMPA and kainate receptors. Furthermore, within this series of compounds, certain analogues were identified with 50-fold selectivity for NR2C/D-containing receptors over NR2A/B containing receptors. These compounds represent a new class of subunit-selective NMDA receptor antagonists.

Design, Synthesis, and Biological Evaluation of
Subunit-Selective N-Methyl-D-Aspartate Receptor Antagonists

By

Cara A. Mosley
B.S. Georgia Institute of Technology, 2004

Advisor: Dennis C. Liotta, Ph.D.

A dissertation submitted to the Faculty of the Graduate School of Emory University
in partial fulfillment of the requirements for the degree of Doctor of Philosophy in
Chemistry

2009

TABLE OF CONTENTS

List of Illustrations

Figures
Tables
Schemes
Graphs
Charts

List of Abbreviations

Part 1: Design, Synthesis, and Biological Evaluation of Novel NR1/NR2B-Selective NMDA Receptor Antagonists Towards Treatment of Neurodegenerative Diseases

CHAPTER 1	1
<hr/>	
1.1 STATEMENT OF PURPOSE	1
1.2 INTRODUCTION AND BACKGROUND	4
1.3 SYNTHESIS OF ENANTIOMERIC PROPANOLAMINE ANALOGUES	31
1.4 pKa DETERMINATION OF NMDA RECEPTOR CHANNEL BLOCKERS	34
1.5 RESULTS AND DISCUSSION	38
1.6 CHEMISTRY EXPERIMENTAL DETAIL	45
1.7 BIOLOGY EXPERIMENTAL DETAIL	57
CHAPTER 2	68
<hr/>	
2.1 STATEMENT OF PURPOSE	68
2.2 INTRODUCTION AND BACKGROUND	70
2.3 SYNTHESIS OF HYDRAZIDE-BASED ANALOGUES	77
2.4 BIOLOGICAL EVALUATION OF HYDRAZIDE-BASED ANALOGUES	85
2.5 CONCLUSIONS REGARDING HYDRAZIDE-BASED ANALOGUES	93
2.6 RATIONALE FOR PROPOSED AMIDE-BASED ANALOGUES	95
2.7 SYNTHESIS OF AMIDE-BASED ANALOGUES	101
2.8 RESULTS AND DISCUSSION	115
2.9 CONCLUSIONS	159

2.10 CHEMISTRY EXPERIMENTAL DETAIL	162
2.11 BIOLOGY EXPERIMENTAL DETAIL	247

Part 2: Design, Synthesis, and Biological Evaluation of First-in-Class NR2C/2D-Selective NMDA Receptor Antagonists

CHAPTER 3 **261**

3.1 STATEMENT OF PURPOSE	262
3.2 INTRODUCTION AND BACKGROUND	264
3.3 SYNTHESIS OF 987 ANALOGUES	270
3.4 RESULTS AND DISCUSSION	276
3.5 CONCLUSIONS	294
3.6 INTRODUCTION AND RATIONALE FOR NAPHTHYLPHENYL CARBAMOTHIOATE ANALOGUES (1063 SERIES)	296
3.7 SYNTHESIS OF 1063 ANALOGUES	299
3.8 RESULTS AND DISCUSSION	302
3.9 CONCLUSIONS REGARDING BOTH 987 AND 1063 SERIES INHIBITORS	309
3.10 CHEMISTRY EXPERIMENTAL DETAIL	310
3.11 BIOLOGY EXPERIMENTAL DETAIL	393

List of Illustrations

List of Figures	Page
Figure 1.1 NR2B Selective NMDA receptor antagonists with modest pH sensitivity	2
Figure 1.2 Exemplary Enantiomeric Propranolamine	4
Figure 1.3 Tetrameric composition of NMDA receptor	5
Figure 1.4 Domains of one subunit (NR1 or NR2) of the NMDA receptor	6
Figure 1.5 Cartoon of NMDA receptor semiautonomous domains and the ligands they bind	6
Figure 1.6 Anatomical localization of NR subunit mRNA in rat determined by in situ hybridization	7
Figure 1.7 Deactivation time courses for NR2A-, NR2B-, NR2C-, and NR2D-containing NMDA receptors	8
Figure 1.8 Pharmacological binding sites and ligands on NMDA receptors (modified)	12
Figure 1.9 Ion pore channel blockers	13
Figure 1.10 Structure of glycine site NMDA antagonist ACEA-1021	14
Figure 1.11 Structure of glutamate binding site NMDA antagonist CGS-19755	14
Figure 1.12 Ifenprodil-like pharmacophore of NR2B-selective NMDA receptor antagonists	16
Figure 1.13 Benzylpiperidine and phenylpiperidine NR2B-selective NMDA antagonists	17
Figure 1.14 Concentration-response curve of Ifenprodil-induced inhibition at 3 pH values	18
Figure 1.15 Screening hit for start of NR2B inhibitor program	19
Figure 1.16 Drugs withdrawn or restricted due to hERG binding	22
Figure 1.17 Phases of ventricular action potential (modified)	23
Figure 1.18 A normal QT interval from an ECG (yellow) compared to a prolonged QT signal (green)	23
Figure 1.19 hERG channel structure with important ligand-binding residues highlighted (modified)	24
Figure 1.20 Lead enantiomeric propranolamine 93-31 : properties and proposed analogues	29
Figure 1.21 Rationale for hybrid analogue 93-155	30
Figure 1.22 Proposed analogues with B ring modifications	31
Figure 1.23 Structures of Drugs in Table 1.4	36
Figure 1.24 Proposed analogue 33	40
Figure 2.1 Thiosemicarbazide 211 , screening hit	70
Figure 2.2 Comparison of screening hit 211 and enantiomeric propranolamine 93-4 .	71
Figure 2.3 96-1 , the sulfonamide analogue of 211	75
Figure 2.4 Proposed semicarbazide analogues	75
Figure 2.5 Proposed N-acetylpropanehydrazide analogues	76
Figure 2.6 Determining the effect of alkylation on semicarbazide analogues	76
Figure 2.7 Proposed <i>n</i> -butyl analogues	77
Figure 2.8 Proposed hydrazide analogues	77
Figure 2.9 Proposed phthalimide analogue	77
Figure 2.10 Retrosynthesis of hydrazide compounds	78
Figure 2.11 Isolated dialkylation product 13	83

Figure 2.12 SAR of hydrazide-based analogues	94
Figure 2.13 Comparison of lead enantiomeric propanolamine and semicarbazide compounds, as well as proposed hybrid amide analogues	96
Figure 2.14 General structure of proposed cyclic amide compounds	98
Figure 2.15 Proposed alkylated amide compounds 22 and 23 compared with 93-31 and 96-7	99
Figure 2.16 Proposed changes to A and B ring substitutions	100
Figure 2.17 Proposed amine analogues	101
Figure 2.18 Retrosynthetic analysis of amide analogues	102
Figure 2.19 <i>In vitro</i> analysis of compound 96-22	146
Figure 2.20 Homology Modeling of 96-22 in the ATD allosteric binding site	148
Figure 2.21 Results of rotorod locomotor assay with 96-22	149
Figure 2.22 Results of lactate dehydrogenase assay with 96 series compounds	151
Figure 2.23 MCAO results: summary of reduction of infarct volume following treatment with 96-22	152
Figure 2.24 The positive control, gabapentin (100 mg/kg i.p) significantly reduced mechanical allodynia	155
Figure 2.25 Administration of 96-22 (10, 30, and 100 mg/kg i.p.) did not reduce mechanical allodynia	155
Figure 3.1 Screening hits identified in Traynelis laboratory NR2C/NR2D inhibitor screening effort	263
Figure 3.2 Summary of weakly-subunit selective antagonists	265
Figure 3.3 Basal ganglionic circuitry of Parkinson's Disease	267
Figure 3.4 Comparison of purchased 987 analogues at NR1/NR2D-containing NMDA receptors	268
Figure 3.5 Proposed B ring 987 analogues	269
Figure 3.6 Effect of C ring substitution on potency and selectivity	269
Figure 3.7 Proposed C ring 987 analogues	270
Figure 3.8 Pfizer's styryl quinazolinone AMPA antagonist CP-465,022	277
Figure 3.9 Correlation between van der Waals radii and both potency and selectivity of 987 series	287
Figure 3.10 <i>In vitro</i> analysis of 987 class	292
Figure 3.11 Mutagenesis studies of 987 class compounds	293
Figure 3.12 Proposed binding site of 987 series compounds	294
Figure 3.13 Concentration-effect curves for more selective 987 series compounds	295
Figure 3.14 Hit compound 1063 found during NR2C/2D screening effort	297
Figure 3.15 Selectivity comparison of 987, 1105, and 1063 class NR2C/2D inhibitors	297
Figure 3.16 Proposed sulfur to oxygen oxidation of 1063	298
Figure 3.17 Proposed analogues of 1063 series	299
Figure 3.18 Activity of 1063-2 at various NR1-splice variant-containing NR1/NR2D receptors	305
Figure 3.19 Mutagenesis studies of binding interactions of 1063-2 with NR2D	306
Figure 3.20 Binding regions of 987 series, 1063 series, and 1105 series of NR2D inhibitors	307
Figure 3.21 The concentration of 1063-2 increases in the brain and plasma of rats over time	308

List of Tables

Table 1.1 Examples of NMDA antagonists utilized in clinical trials	11
Table 1.2 Effect of N-alkylation on fold shift of enantiomeric propanolamines	21
Table 1.3 Examples of medicinal chemistry methods to decrease hERG binding	27
Table 1.4 Activities and fold shifts of known channel blockers at NMDA receptor subtypes	35
Table 1.5 pK _a and protonation characteristics of known channel blockers	37
Table 1.6 <i>In vitro</i> analysis of 93-155 at NMDA and hERG receptors	38
Table 1.7 <i>In vitro</i> analysis of analogues with B ring modifications	40
Table 2.1 <i>In vitro</i> analysis of hydrazide-based compound towards rat glutamate receptor subtypes	86
Table 2.2 Hydrazide-based compound <i>in vitro</i> analysis at human NR1/NR2B NMDA receptors and off-target receptors	87
Table 2.3 Summary of amide compounds synthesized	109
Table 2.4 Summary of amine compounds synthesized	113
Table 2.5 <i>In vitro</i> analysis of amide-based compound towards rat glutamate receptor subtypes	116
Table 2.6 Linear amides: <i>in vitro</i> analysis at human NR1/NR2B NMDA receptors	119
Table 2.7 Cyclic amides: <i>in vitro</i> analysis of on-target NR1/NR2B NMDA potency	121
Table 2.8 A and B ring amide modifications: <i>in vitro</i> analysis of on-target NR1/NR2B NMDA potency	122
Table 2.9 Effect of B ring modifications in the enantiomeric propanolamine series: <i>in vitro</i> analysis of on-target NR1/NR2B NMDA potency	124
Table 2.10 Alkylated amides: <i>in vitro</i> analysis of on-target NR1/NR2B NMDA potency	125
Table 2.11 Effect of A ring substitution in enantiomeric propanolamine piperazines: <i>in vitro</i> analysis of on-target NR1/NR2B NMDA potency	127
Table 2.12 <i>In vitro</i> analysis of amide-based compound towards rat glutamate receptor subtypes	129
Table 2.13 Amines: <i>in vitro</i> analysis of on-target NR1/NR2B NMDA potency	130
Table 2.14 <i>In vitro</i> analysis of off-target hERG and α_1 potency	136
Table 2.15 Summary of <i>in vitro</i> properties of best analogues	139
Table 2.16 Pharmacokinetic data obtained for 96-22 , 96-37 , and 96-17	141
Table 2.17 MDR1-MDCK permeability of 96 series compounds	156
Table 3.1 Sample of attempted Suzuki conditions	272
Table 3.2 Optimization of subunit selectivity through evaluation of A and B ring substituents	278
Table 3.3 Optimization of subunit selectivity through evaluation of A ring substituents	279
Table 3.4 Optimization of subunit selectivity through evaluation of C ring substituents	280
Table 3.5 Substitutions for Ring B carboxylic acid and Ring A nitro groups	281
Table 3.6 Optimization of A and B ring substituents with best C ring substituents	282
Table 3.7 Optimization of linker and A ring substituents	283
Table 3.8 Optimization of B ring substituents of pyridinyl A ring analogues	284
Table 3.9 Summary of 1063 series <i>in vitro</i> activity at NMDA receptors	303
Table 3.10 <i>In vivo</i> pharmacokinetics parameters of NR2D inhibitors (mice)	308

List of Schemes

Scheme 1.1 Synthesis of <i>para</i> -phenoxy aniline intermediate 25	32
Scheme 1.2 Synthesis of 93-160	32
Scheme 1.3 Synthesis of 93-155	33
Scheme 1.4 Synthesis of 93-150	34
Scheme 2.1 Synthesis of 2 , fragment B	79
Scheme 2.2 Synthesis of 10 , fragment B	79
Scheme 2.3 Synthesis of hydrazide-based analogues: 96-1 , 96-4 , 96-5 , 96-10 , and 96-12	81
Scheme 2.4 Synthesis of phenolic hydrazide-based analogues 96-2 and 96-3	82
Scheme 2.5 Synthesis of alkylated hydrazide-based analogues: 96-6 and 96-7	83
Scheme 2.6 Synthesis of alkylated and phenolic N-acetylpropanehydrazide analogue 96-8	84
Scheme 2.7 Synthesis of N-ethylpropanehydrazide analogues 96-9 and 96-11	85
Scheme 2.8 Synthesis of carboxylic acids 35 , 36 , and 37	102
Scheme 2.9 Synthesis of <i>para</i> -arylurea 39	103
Scheme 2.10 Synthesis of ethanediamine and propanediamine fragments 45-50	104
Scheme 2.11 Synthesis of ethoxyamine 53	104
Scheme 2.12 Synthesis of thioethaneamine 55	105
Scheme 2.13 Synthesis of propaneamine 58	105
Scheme 2.14 Synthesis of cinnamyl amine 62	106
Scheme 2.15 Synthesis of chiral alkylated ethanediamine fragments 71 and 72	107
Scheme 2.16 Synthesis of n-butylamine 75	107
Scheme 2.17 Synthesis of piperazone 78 via Mitsunobu cyclodehydration	108
Scheme 2.18 Synthesis of piperazone 78 via N-amidation	109
Scheme 2.19 General synthesis of amide compounds in Table 2.3	109
Scheme 2.20 Synthesis of phenol 96-27	112
Scheme 2.21 General synthesis of amines in Table 2.4	113
Scheme 2.22 Synthesis of imidazolinones 96-23 and 96-45	114
Scheme 2.23 Synthesis of 96-46 via reductive amination of 96-22	115
Scheme 2.24 Synthesis of piperazone 96-67	115
Scheme 3.1 Synthesis of (<i>E</i>)-3-phenyl-2-styryl-quinazolin-4(3H)-ones	271
Scheme 3.2 Synthesis of C ring R ₈ -thiophene analogue 987-58	274
Scheme 3.3 Synthesis anthranilic acids from 5-iodoisatin	274
Scheme 3.4 Synthesis of quinazolinone 18	275
Scheme 3.5 Synthesis of saturated linker analogue 987-40	276
Scheme 3.6 Synthesis of thiocarbamate and carbamate 1063 analogues	300
Scheme 3.7 Failed synthesis of ester 1063 analogue via saponification	300
Scheme 3.8 Synthesis of ester 1063 analogues	301
Scheme 3.9 Synthesis of urea analogue 1063-12	302

List of Charts

Chart 2.1 Hydrazide-based analogue inhibition at rat glutamate receptor subtypes	87
Chart 2.2 Amide-based analogue inhibition at glutamate receptor subtypes	117
Chart 2.3 Amine-based analogue inhibition at glutamate receptor subtypes	130

List of Graphs

Graph 2.1 96-22 dosed at 3 mg/kg IV	142
Graph 2.2 96-37 dosed at 3 mg/kg IV	142
Graph 2.3 96-17 dosed at 3 mg/kg IV	143

List of Abbreviations

α_1:	α -adrenergic receptors (α_1 subtype)
Ac₂O:	Acetic anhydride
AcOH:	Acetic acid
ADME:	Absorption, Distribution, Metabolism, Excretion
aLQTS:	acquired Long QT Syndrome
AMPA:	α -amino-3-hydroxy-5-methyl-4-isoxazolepropionic acid
ATD:	Amino Terminal Domain
Boc:	tert-Butyloxycarbonyl
Bn:	Benzyl
CDI:	Carbonyldiimidazole
DBAD:	Di- <i>tert</i> -butyl azodicarboxylate
DCC:	N,N'-Dicyclohexylcarbodiimide
1,2-DCE:	1,2-Dichloroethane
DCM:	Dichloromethane (methylene chloride, CH ₂ Cl ₂)
DIAD:	Diisopropyl azodicarboxylate
DIPEA:	N,N-diisopropylethylamine
DMAP:	4-(Dimethylamino)pyridine
1,2-DME:	1,2-Dimethoxyethane
DMF:	N,N,-dimethylformamide
DMS:	Dimethyl sulfide
DMSO:	Dimethyl Sulfoxide
DRG:	Dorsal Root Ganglion
EDC:	1-Ethyl-3-(3-dimethylaminopropyl)carbodiimide hydrochloride
EtOAc:	Ethyl Acetate
FDA:	Food and Drug Administration
GABA:	γ -aminobutyric acid
GPe:	Global Pallidus (external)
GPi:	Global Pallidus (internal)
hERG:	human Ether-a-go-go Related Gene
HMPA:	Hexamethylphosphoramide
HPLC:	High Performance Liquid Chromatography
IC₅₀:	half-maximal Inhibitory Concentration
IPCF:	isopropyl chloroformate
K_i:	Inhibitory Constant
LDA:	Lithium diisopropylamide
LDH:	Lactate Dehydrogenase
MCAO:	Middle Cerebral Arterial Occlusion
Ms:	Mesyl, Mesylate (OCH ₃)
MsCl:	Methanesulfonyl chloride
PCP:	Phencyclidine

PK:	Pharmacokinetics
Pyr:	Pyridine
LBD:	Ligand Binding Domain
NMDA:	N-Methyl-D-Aspartate
NMM:	N-methylmorpholine
NMR:	Nuclear Magnetic Resonance
PD:	Parkinson's Disease
rt:	room temperature
SAR:	Structure Activity Relationship
SNc:	Substantia nigra pars compacta
STN:	Subthamic Nucleus
T_{1/2}:	Half-life
TdP:	Torsades de Pointes
TFA:	Trifluoroacetic acid
THF:	Tetrahydrofuran
TBAF:	Tetrabutylammonium fluoride
TBDMS:	tert-Butyldimethylsilane
TBDPS:	<i>tert</i> -Butyldiphenylsilane
TBDPSCI:	<i>tert</i> -Butyl(chloro)diphenylsilane
TBI:	Traumatic Brain Injury
TLC:	Thin Layer Chromatography
TMSNCO:	Trimethylsilyl isocyanate
UHP:	Urea hydrogen peroxide

Part 1:

Design, Synthesis, and Biological
Evaluation of Novel NR1/NR2B-
Selective NMDA Receptor
Antagonists Towards the
Treatment of Neurodegenerative
Diseases

Chapter 1.

Part I: Design, Synthesis, and Biological Evaluation of Enantiomeric Propranolamine NR1/NR2B NMDA Receptor Antagonists

Part 2: Evaluation of the pK_a Properties of Voltage-dependent Channel Blocker NMDA Receptor Antagonists

1.1 Statement of Purpose

Our research group is interested in the development of pH-sensitive NR2B-selective N-Methyl-D-Aspartate (NMDA) receptor antagonists for use in the prophylaxis and treatment of ischemic disorders. NMDA receptor over-activation has been implicated in neuronal death resulting from hypoxia,¹⁻⁴ brain and spinal cord injury,⁵ Parkinson's disease,⁶⁻⁸ neuropathic pain.⁹⁻¹² It has also been suggested that the receptor contributes to chronic neurodegenerative diseases such as Alzheimer's disease¹³⁻¹⁶ and Huntington's disease.¹⁷⁻¹⁹ Acidification of the brain pH is known to occur via a number of mechanisms involved in the aforementioned disease states, particularly hypoxic ischemia, and affects a variety of biochemical processes including glutamate receptor function.²⁰⁻²²

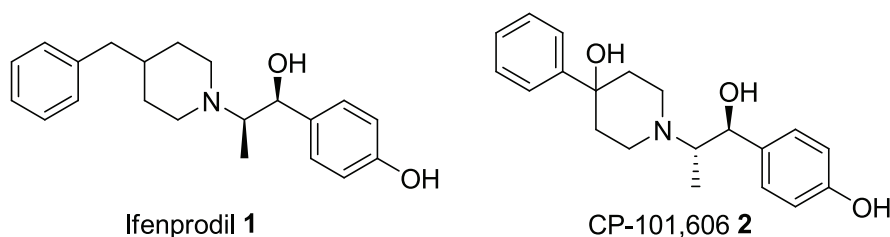


Figure 1.1 NR2B Selective NMDA receptor antagonists with modest pH sensitivity

NMDA receptors are tonically inhibited by protons at physiologic pH (7.4),²³ and the small molecule NMDA receptor antagonists ifenprodil (**1**, Figure 1.1) and CP-101,606, (traxoprodil, **2**, Figure 1.1) both specific for NR2B-subtypes of NMDA receptors, were found to modestly enhance receptor inhibition under acidic conditions.²⁴ However, these compounds exhibited severe side effects in animal and human models, postulated to be a result of non-specific drug binding. Thus, compounds which inhibit NR2B-containing NMDA receptors preferentially under ischemic conditions associated with hypoxia, but have attenuated side effects compared to past failed clinical agents offer a potential method of improved neuroprotective treatment.

The search for NR2B-selective pH-sensitive NMDA receptor antagonists originated with work previously done in our research group regarding enantiomeric propanolamines (exemplified by **3**, Figure 1.2).²⁵ Compounds in this class were highly potent against NR2B-containing receptors compared to other NMDA receptor subtypes (NR2A-, NR2C-, and NR2D-containing receptors) and glutamate receptor family members (AMPA and kainate receptors). The propanolamines also exhibited increased activity at acidic pH compared with more alkaline physiologic pH (a quality referred to as “fold shift”). Unfortunately, these compounds generally exhibited poor drug-like characteristics, specifically poor selectivity versus a closely related receptor (hERG). Therefore, propanolamines with decreased off-target activity were desired. This was achieved using the following strategy:

1. Structure activity relationships were utilized to design analogues with NR2B NMDA potency, significant fold shift, and decreased off-target effects

2. Novel propranolamine analogues were synthesized.
3. The analogues were tested for *in vitro* NMDA receptor activity in NR1/NR2B-containing NMDA receptors at pH 6.9 and pH 7.6. All *in vitro* biological evaluation of NMDA receptors was carried in the laboratory of Dr. Stephen Traynelis in the Emory School of Medicine, Department of Pharmacology.

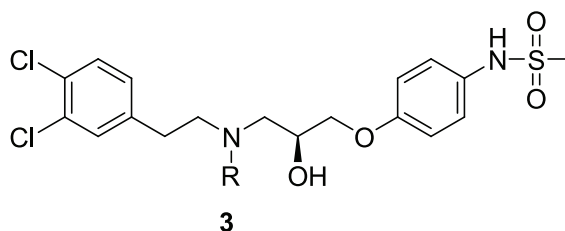


Figure 1.2 Exemplary Enantiomeric Propranolamine

1.2 Introduction and Background

1.2.1. NMDA Receptor structure, function, and localization

Glutamate is the major excitatory neurotransmitter in the central nervous system (CNS), and is involved in post-synaptic effects in a number of ionotropic and metabotropic receptors.²⁶⁻²⁸ Three classes of ionotropic receptors are stimulated by glutamate, and are named based on the synthetic agonists that activate them: AMPA (α -amino-3-hydroxy-5-methyl-4-isoxazolo-propionic acid) receptors, kainate receptors, and NMDA (N-methyl-D-aspartate) receptors. The NMDA receptor in particular has garnered much attention due to the pivotal role the receptor plays in synaptic plasticity²⁹⁻³⁰ and neuronal development,³¹⁻³⁴ as well as higher brain functions such as learning, memory, and motor function.

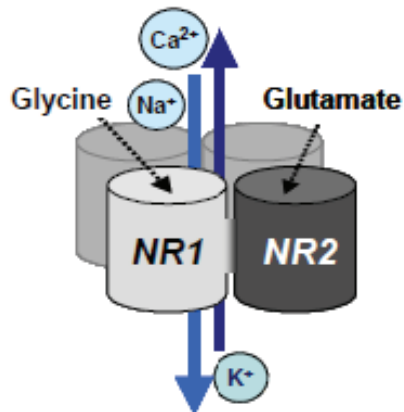


Figure 1.3 Tetrameric composition of NMDA receptor. Subunits in the background are also NR1 and NR2, although the specific architecture is unknown.

NMDA receptors are ligand-gated cation channels that reside in cellular membranes. The receptors (Figure 1.3) are heterooligomeric assemblies of one NR1 subunit and one or more NR2A, NR2B, NR2C, or NR2D subunit. Multiple receptor isoforms are possible due to the presence of splice variants of NR1 (a-h) and differential expression of NR2 genes (A-D). Functional receptor stoichiometry requires a tetramer composed of two NR1 subunits and two NR2 subunits (named by convention “NR1/NR2X-containing NMDA receptors,” where X=A, B, C, or D) arranged such that a pore is formed between subunits which allows cation permeability. Each NR1 or NR2 subunit contains two extracellular domains, an amino terminal domain (ATD) and a ligand binding domain (LBD), as well as a transmembrane domain and an intracellular C-terminal domain (Figure 1.4).

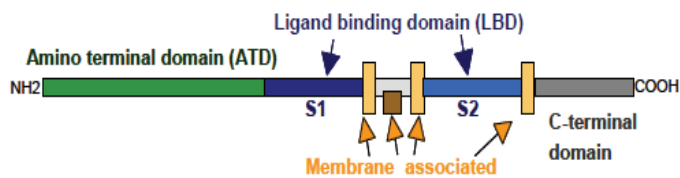


Figure 1.4 Domains of one subunit (NR1 or NR2) of the NMDA receptor

The ligand binding domain on NR1 subunits binds the coagonist glycine while the ligand binding domain on NR2 subunits binds glutamate (Figure 1.5). Both glycine and glutamate co-binding are required for receptor activation, which involves a proteinaceous conformational shift to induce de-blocking of magnesium ions that reside in the channel pore at membrane resting potential. Depolarization, which releases magnesium from the channel pore, allows the passage of calcium and other ions into the cell, propagating neuron to neuron synaptic transmission. The importance of NMDA receptor function relies on the two signals generated by activation of the receptors: 1.) electrical depolarizing current for neuronal excitation and 2.) biochemical intracellular ionic influx, which can trigger intracellular signaling pathways.

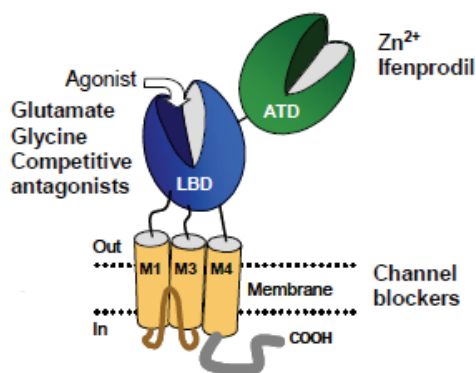


Figure 1.5 Cartoon of NMDA receptor semiautonomous domains and the ligands they bind.

Only one subunit (NR1 or NR2) is shown

Receptor localization and pharmacology varies based on receptor subtype. While NR1 subunits are ubiquitously expressed throughout the central nervous system, NR2 subunits exhibit differential anatomical localization.³⁵ NR2A mRNA is enriched in the striatum, NR2B mRNA is found primarily in the frontal cortex, NR2C mRNA is localized in the cerebellum, and the basal ganglion structures contain highest levels of NR2D mRNA. The distribution of NR2A-D containing receptors in the rat brain is illustrated in Figure 1.6.

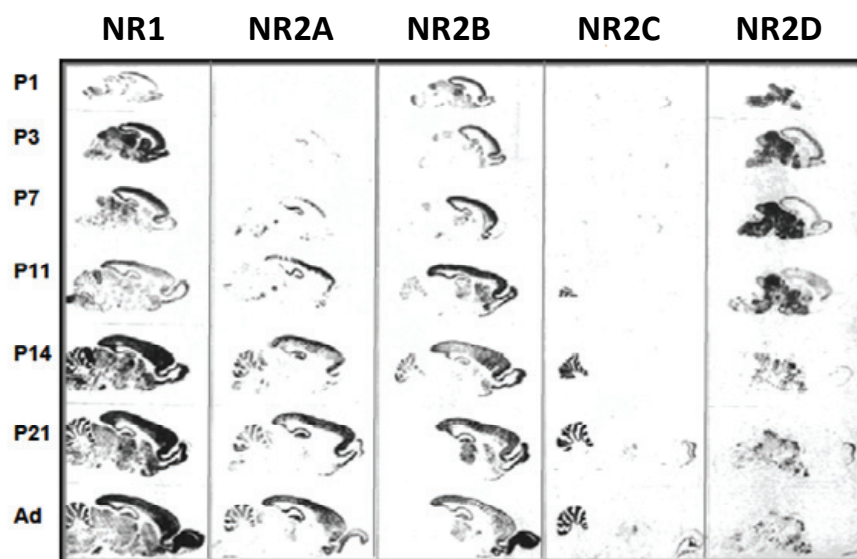


Figure 1.6 Anatomical localization of NR subunit mRNA in rat determined by in situ hybridization³⁵

Not only are NR2 subtypes differentially expressed in the central nervous system, receptor pharmacology and electrophysiology is also variable.³⁶⁻³⁷ The amplitude of receptor firing and the time-course of receptor activation vary

significantly based on NR2 subunit (Figure 1.7). For example, NR2A-containing receptors open with a large amplitude and shorter deactivation time compared to NR2B-, NR2C, or NR2D-containing receptors. While NR2A-containing receptors require merely 0.05 milliseconds deactivation time, NR2D-containing receptors require 1.7 seconds before subsequent firing. Other qualities that vary between receptor subtypes include agonist (glutamate and glycine) IC_{50} values, open probability, conductance, calcium ion permeability, and magnesium ion sensitivity. As a result of the differential expression and pharmacology of the NMDA receptors based on NR2 subunit, specific receptor subtype and localization determines the physiologic processes in which the receptor is involved.

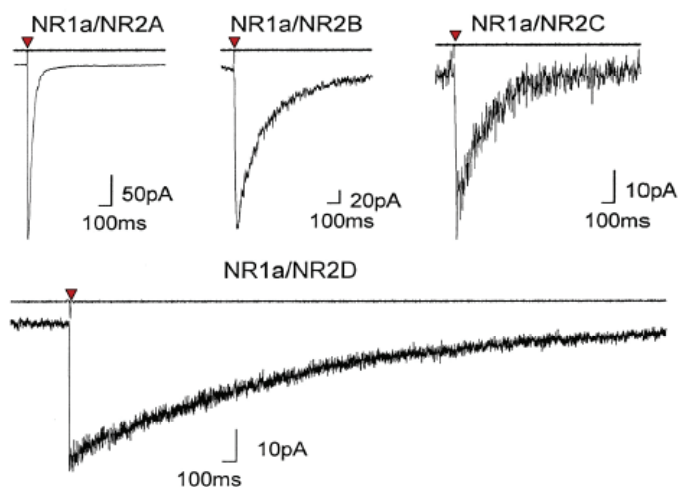


Figure 1.7 Deactivation time courses for NR2A-, NR2B-, NR2C-, and NR2D-containing NMDA receptors.³⁶

1.2.2. NMDA receptor over-activation and excitotoxicity

Under physiologic conditions, glutamate stimulates NMDA receptor activation allowing and influx of calcium ions intracellularly. Ca^{2+} influx stimulates both

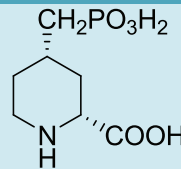
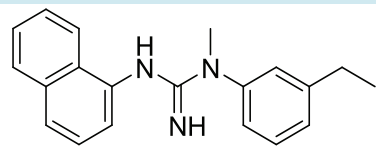
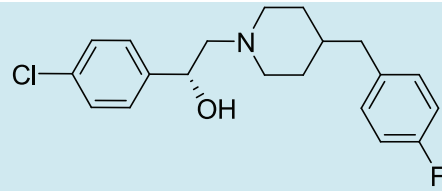
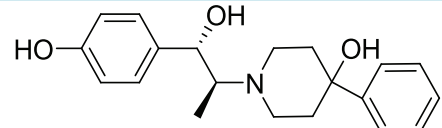
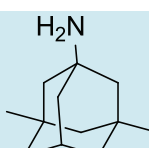
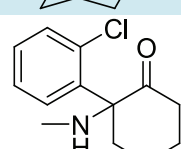
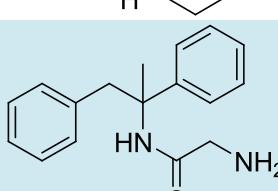
electrochemical signaling along an axon and intracellular signaling cascades. Under hypoxic or ischemic conditions, in which oxygen supply to the brain has been decreased or severed completely, neuronal death in the area of infarct causes intracellular contents, including glutamate, to flood the extracellular space.³⁸ Excess glutamate release results in sustained over-activation of glutamate receptors, including NMDA receptors. Over-stimulation triggers calcium ions to flood the intracellular space, bringing about excitotoxic signaling, necrosis, and apoptosis, ultimately resulting in further release of glutamate from the effected cells. This glutamate and calcium feedback mechanism perpetuates and amplifies the ischemic insult in neurons, and can cause significant and irreversible damage to brain tissues of affected areas. Therefore, inhibitors of NMDA receptors, which would potentially slow or stop glutamate-mediated damage, have long been thought to be potential treatments for conditions resulting from hypoxia including stroke and traumatic brain injury (TBI). Glutamate also contributes to the “slow excitotoxicity” of cellular mechanisms, and is at least partly responsible for chronic neurodegenerative diseases including Alzheimer’s disease, dementia, Parkinson’s disease, Huntington’s disease, and amyotrophic lateral sclerosis.³⁹ Notably, under-activation of the receptors is thought to be involved in schizophrenic patients. NR1/NR2B-containing NMDA receptors outside the central nervous systems have been implicated in chronic neuropathic pain.⁴⁰

1.2.3 Therapeutic uses of NMDA receptor antagonists

As a consequence of aberrant NMDA receptor behavior in a variety of disease states in animal models, NMDA receptor antagonists have been tested in a number of clinical trials toward treatment of all of the aforementioned diseases (a number are highlighted in Table 1.1).⁴¹ Over 9,000 individuals have partaken in stroke and TBI trials, but unfortunately no effective therapeutics have been introduced to date. This can be attributed to a number of reasons, including difficulty of carrying out such trials, the heterogeneity of the stroke population, variability in the duration between time of infarct and drug administration compared with animal models, and severe dose-limiting side effects at therapeutic concentrations. Side effects of channel blocker and glutamate and glycine binding site antagonists are similar to the psychotomimetic effects seen with phenylcyclidine (PCP, and non-selective channel blocker NMDA antagonist) such as delusion, agitation, hallucination, and confusion,⁴²⁻⁴³ thought to be a result of the negative effects of global NMDA inhibition. Efforts to specifically target one subtype of the receptor, namely NR1A/NR2B-containing NMDA receptors, have led to compounds with decreased psychosis-like side effects.⁴⁴ Unfortunately, these too have proved ineffective in the clinic either due to neutral results when compared with placebo arms,⁴⁵ cardiotoxicity related to off-target receptors (opioid, hERG, α_1 -adrenergic, and sigma receptors, among other), or induction of drug dependence.⁴⁶ The only Food and Drug Administration (FDA)-approved NMDA receptor antagonists are both low-affinity channel blockers. Memantine (Namenda ©, Forest Pharmaceuticals) in particular has low receptor affinity allowing rapid binding to the open channel

magnesium binding site.⁴⁷ The drug then quickly dissociates, and it is this long “off-time” that is thought to prevent impairment of normal synaptic transmission and reduce side effects traditionally observed with channel blockers.⁴⁸⁻⁴⁹

Table 1.1 Examples of NMDA antagonists utilized in clinical trials

Drug	Structure	Mechanism of Action	Clinical Trial Indication
Selfotel		Competitive antagonist, Glutamate binding site	Stroke and TBI
Aptiganel		High affinity ion channel blocker	Stroke and TBI
Eliprodil		NR1A/NR2B allosteric site antagonist	Stroke and TBI
CP-101,606		NR1A/NR2B allosteric site antagonist	TBI
Memantine[†]		Low-affinity ion channel blocker	Dementia and Huntington's Disease
Ketamine[‡]		Low affinity ion channel blocker	Analgesia
Remacemide		Uncompetitive NMDA antagonist	Epilepsy, Stroke, and Huntington's Disease

[†]Approved for treatment of mild to moderate Alzheimer's disease (Namenda ©, Forest Pharmaceuticals).

[‡]Approved as an anesthetic (Ketanest S ©, Pfizer Inc.).

1.2.4. Classes of NMDA receptor antagonists

The NMDA receptor has a number of pharmacological sites that are responsive to small molecule modulation (Figure 1.8), all of which have been exploited in the development of antagonists to attenuate NMDA hyperfunction.⁵⁰ The majority of compounds may be categorized into four classes of inhibitors: ion pore channel blockers, glycine site antagonists, glutamate site antagonists, and subunit-selective antagonists. The first three of these will be discussed here. For a discussion of subunit-selective antagonists, see section 1.2.5.

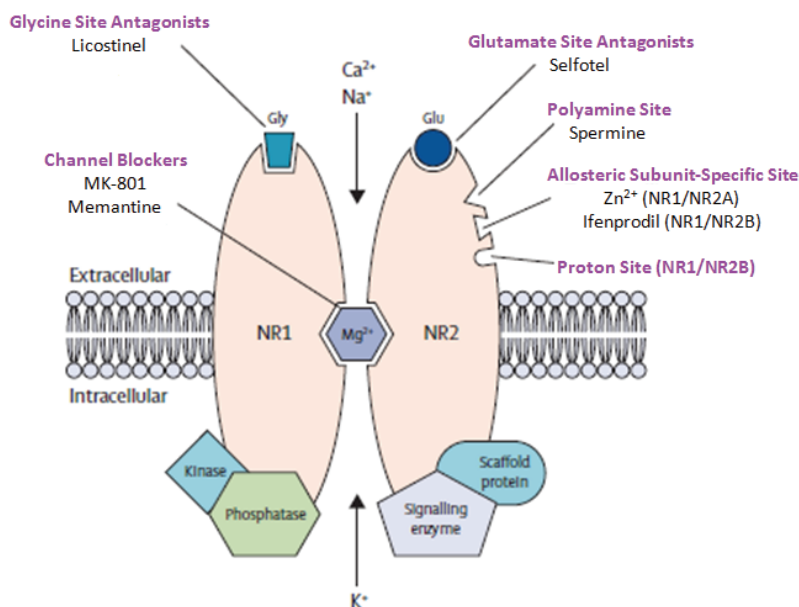


Figure 1.8 Pharmacological binding sites and ligands on NMDA receptors (modified).⁵¹

The first class of antagonists to be developed was ion pore channel blockers. These compounds bind within the ion conduction path, and are characterized by varying affinities towards the open or closed state of the receptor. Because blocking of

the channel pore causes global NMDA antagonism, channel blockers are often associated with severe side effects. Channel blockers are generally organic cations (Figure 1.9). The clinically approved NMDA receptor antagonist, Memantine (**5**, Namenda ©, Forest Pharmaceuticals), is a member of this class.⁵²⁻⁵³ It is characterized by weak and fleeting binding to the open state of the receptor after extrusion of magnesium from the channel pore (use-dependent and voltage dependent).⁴⁷ In contrast, MK-801 (**4**, Figure 1.9) exhibits higher potency and duration of pore binding to the closed receptor, and is associated with severe side-effects.⁵⁴

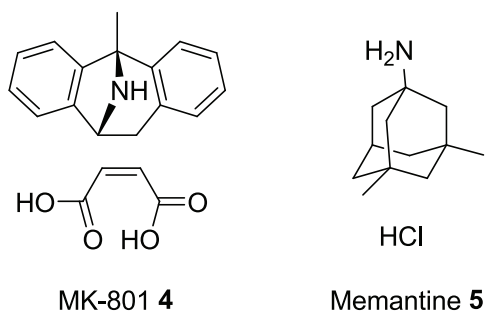
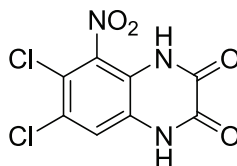


Figure 1.9 Ion pore channel blockers

Competitive antagonists for the glycine binding site on the NR1 subunit have also been described.⁵⁵ The most prominent class of compounds, quinoxaline-2,3-diones, can be exemplified by one of the most potent analogs in the series, ACEA-1021 (**6**, Licostinel, Figure 1.10).⁵⁶⁻⁵⁷ While Licostinel and related analogs are highly potent against NMDA receptors ($IC_{50} = 5.9$ nM), they also exhibited moderate activity against related glutamate receptors such as AMPA ($IC_{50} \sim 2$ μ M). Permeation across the blood brain barrier is also an obstacle due to the charged nature the analogues. Clinical trials

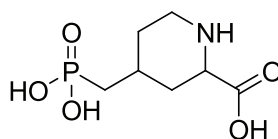
of Licostinel indicated the drug was safe, but crystals were found in the urine of patients, indicative of poor aqueous solubility and metabolism.⁵⁸



ACEA-1021, Licostinel, **6**

Figure 1.10 Structure of glycine site NMDA antagonist ACEA-1021.

Competitive NR2 subunit glutamate binding site antagonists are most commonly phosphono-amino acid compounds (exemplified by CGS-19755, Selfotel, **7**, Figure 1.11).⁵⁹⁻⁶⁰ Like glycine site antagonists, the glutamate site antagonists are often charged molecules, and thus have difficulty penetrating the blood brain barrier.⁶¹ In addition, untoward side effects are observed in both animal and human models due to the global inhibition of NMDA and other glutamate receptors.



CGS-19755, Selfotel, **7**

Figure 1.11 Structure of glutamate binding site NMDA antagonist CGS-19755

1.2.5. NR2B-selective NMDA receptor antagonists

NR1/NR2B-containing NMDA receptors (NR2B NMDA receptors) have been the focus of intense pharmacological study.²⁷ Evidence suggests that NR2B subtype-selective blockade of NMDA receptors can be beneficial in cerebral ischemia, epilepsy,

Parkinson's disease, depression, and Alzheimer's disease.⁶²⁻⁶⁴ In addition, mice over-expressing NR2B-containing receptors show an increased sensitivity to pain, and NR2B-selective antagonists are antinociceptive in certain models of pain.^{11,65} While NR1 is ubiquitously expressed in the central nervous system, NR2B-containing receptors are primarily found in the forebrain, dorsal root ganglion, striatum, and spinal cord.^{12,35,66} Most notably, NR2B subunits are absent in the cerebellum. Because of their differential distribution, the hypothesis follows that antagonists selective for NR2B-containing NMDA receptors may not give rise to psychotomimetic symptoms associated with global NMDA inhibition which results from treatment with channel blockers and glutamate binding site antagonists.

A multitude of NR2B-selective NMDA receptor antagonists have been described in the literature.⁶⁷ This class of compounds generally binds the amino terminal domain of the NR2B at an allosteric polyamine site (Figures 1.5 and 1.8), and thus inhibition cannot be overcome with high concentrations of glutamate or glycine.

Structurally, the most common and well-developed analogues resemble the first-in-class NR2B-selective NMDA antagonist ifenprodil (**1**, Figure 1.1).⁶⁸ The general ifenprodil-like pharmacophore can be described as a non-polar aryl A ring connected via a basic amine linker, 9-11 Å in length, to an aryl B ring, which traditionally contains a hydrogen bond donor substituent (**8**, Figure 1.12).⁶⁹⁻⁷¹

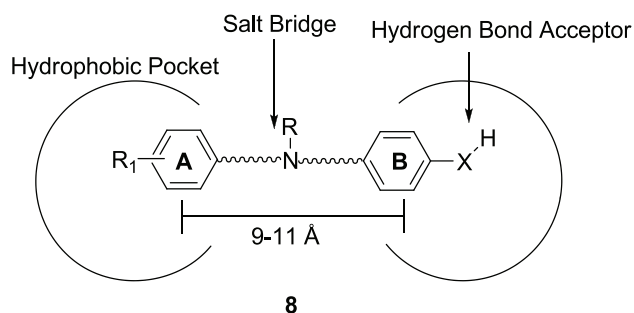


Figure 1.12 Ifenprodil-like pharmacophore of NR2B-selective NMDA receptor antagonists

A number of ifenprodil analogues with improved pharmacokinetic and pharmacodynamic properties have been described and subjected to human clinical trials, the most promising analogue being traxoprodil (**2**, CP-101,606, Pfizer).⁷² Traxoprodil was well-tolerated in safety studies and showed effectiveness in patients suffering from mild to moderate traumatic brain injury.⁴⁴ However, a recent study indicated rats and rhesus monkeys self-administered traxoprodil preferentially to phencyclidine (PCP), suggesting NR2B inhibition may play a role in substance abuse.⁴⁶ Further development of traxoprodil was subsequently ceased.

Early ifenprodil-like antagonists often contained 4-benzylpiperidine or 4-phenylpiperidine A rings and phenolic-containing B rings (Figure 1.13). However, these compounds were plagued by undesirable metabolic properties and off-target activity at the hERG and α_1 receptors.⁷³ One solution has been to replace the phenolic functionality with alternative hydrogen bond donors. Analogues containing acyclic N-methyl sulfonamides and ureas,⁷⁴ as well as heterocyclic phenolic isosteres such as benzimidazoles,⁷⁴ benzimidazolones, benzoxalones, benzothiazoles, and benzoxazinones⁷⁵ have been described as effective NR2B-selective antagonists.

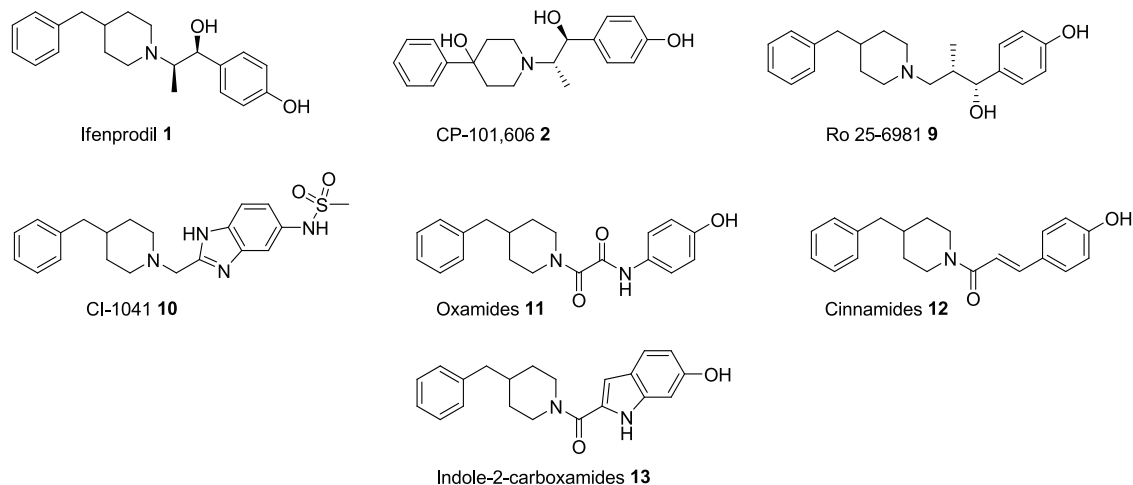


Figure 1.13 Benzylpiperidine and phenylpiperidine NR2B-selective NMDA antagonists

An alternative approach has been to mask the charge of the basic nitrogen centrally located within the linker region. This has been accomplished by probing series' of N-acyl-4-benzyl-piperidines (Figure 1.13), particularly oxamides (**11**)⁷⁵ cinnamides (**12**).⁷⁶ These amide-based compounds are postulated to have a more drug-like metabolic profile and some exhibit neuroprotective activity in animals.

1.2.6. Brain acidification

At physiologic pH, 50% of NMDA receptors in the forebrain (i.e. NR2B-containing NMDA receptors) are inhibited by protons ($IC_{50} = 7.3$).^{23,77-79} The pH of the interstitial brain undergoes a number of moderate pH changes throughout synaptic transmission.²¹ However, during the course of seizure or ischemia, the pH of affected areas can decrease from 0.1 to 1.0 pH units.⁸⁰⁻⁸¹ Under such acid conditions, the innate neuroprotection of NR2B-containing NMDA receptors to limit the toxic effects of

excessive extracellular glutamate release is overcome. Acidification may also occur in other pathological processes including neuropathic pain,⁸²⁻⁸³ Parkinson's disease,²⁰⁻²¹ epilepsy, and traumatic brain injury.

In 1998, Drs. Stephen Traynelis and Raymond Dingledine of Emory University School of Medicine discovered that the NR2B-selective NMDA receptor antagonists ifenprodil and traxoprodil inhibit receptors via a novel mechanism involving the receptor's proton sensor region.²⁴ Ifenprodil was found to be more potent at pH 6.5 relative to pH 7.5 (Figure 1.14), and was found to be 18 times more effective as a neuroprotectant in rat cerebral cortex cultures at pH 6.5. The hypothesis followed that administration of the phenethanolamines enhanced endogenous proton inhibition by increasing receptor sensitivity. In other words, the pK_a of the proton sensor was shifted to a more alkaline pH in the presence of a small molecule inhibitor, causing a larger number of receptors to be inhibited at physiologic pH and unaffected by media acidification.

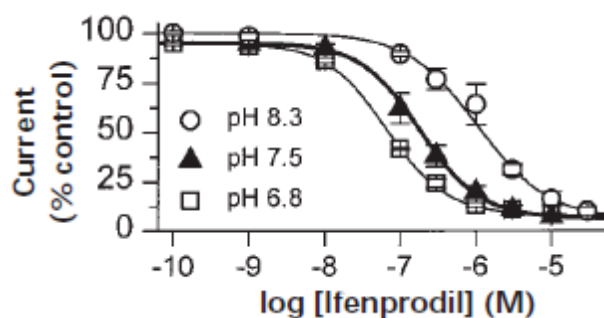


Figure 1.14 Concentration-response curve of Ifenprodil-induced inhibition at 3 pH values²⁴

1.2.7. Structure activity relationships of enantiomeric propanolamine analogues

The lack of clinical successes with NR2B-selective NMDA receptor antagonists, particularly the ifenprodil analogue eliprodil,⁸⁴ was attributed largely to dose-limiting toxicity as a result of activity against N-, P-, and Q-type calcium channels.⁸⁵ It was hypothesized that novel phenylethanamines with increased activity at acidic pH values could be administered at lower doses, and thus would have decreased off-target effects. The ideal compound would have no activity at physiologic pH but be very potent under ischemic conditions. Such a compound could potentially be used as prophylactic neuroprotectant therapy in patients who are at risk or have a history or ischemic events.

Inspired by the differential activity of ifenprodil at acidic and basic pH values, the Liotta group explored the structure-activity relationships (SAR) surrounding a second series of propanolamines based on screening hit **13** (AM-92016, Figure 1.15), a known potassium channel blocker.⁸⁶ These compounds fit the generalized ifenprodil-like pharmacophore, as they possess a hydrophobic A ring connected to a hydrogen bond donor-containing B ring via an amine linker.

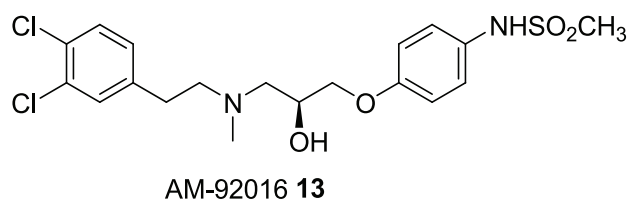


Figure 1.15 Screening hit for start of NR2B inhibitor program

The activity of the analogues was measured in both rat and human NR2B-containing NMDA receptors at two pH values. The pH boost, or fold shift, is defined as the ratio of IC₅₀ values at pH 7.6 and pH 6.9:

$$\text{Fold Shift} = (\text{IC}_{50} \text{ value at pH 7.6}) / (\text{IC}_{50} \text{ value at pH 6.9})$$

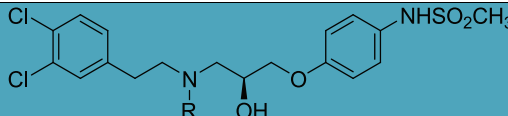
The more potent a compound is at acidic pH compared to the alkaline pH, the larger the fold shift. Consequently, the larger the magnitude of the fold shift, the greater likelihood of having decreased side effects resulting from physiologic NMDA receptor blockage.

The optimal linker length between the A ring and B ring was found to be 7 atoms, about 9-11 Å. The most potent analogues contained an A ring decorated with 3,4-dichloro-substitution. However 3-chloro-4-fluoro-, and 4-chloro- substitution also gave similar activity. A *para*-methanesulfonamide was found to be the most potent B ring substitution.

Although changes on the A Ring, B ring, and linker region were found to affect an analogue's fold shift, the most profound changes in the series were controlled by functionalization of the centrally located amine. As illustrated in Table 1.2, fold shift increases concurrently with chain length according to the trend N-methyl < N-ethyl < N-propyl < N-butyl > N-pentyl, indicative of the limited space in the binding pocket. Chirality was also an important determinant of fold shift. It was found that the *S* enantiomer (shown in Table 1.2) was always more potent against rat receptors while compounds with the *R* configuration were more effective against human receptors. This is illustrated by the lead compound in the series, (*S*)- **93-31**, which has a fold shift of 17

in rat NR2B-containing NMDA receptors but a fold shift of 6 in human receptors. Conversely, the *R*-enantiomer of **93-31**, **93-88**, has a fold shift of 6 in rat NR2B-containing NMDA receptors but 22 in human receptors.

Table 1.2 Effect of N-alkylation on fold shift of enantiomeric propanolamines



R	Compound ID	IC ₅₀ pH 6.9 (nM) [†]	IC ₅₀ pH 7.6 (nM) [†]	Fold Shift
Hydrogen	93-4	18	37	2
Methyl	93-1	39	259	7
Ethyl	93-5	11	89	8
Propyl	93-6	50	496	10
Butyl	93-31	27	454	17
Pentyl	93-87	141	653	5

[†] Measured in rat NR2B-containing NMDA receptors (NR1/NR2B)

The lead compound in the series, *n*-butyl analogue **93-31**, was found to be neuroprotective in an *in vivo* model of transient focal ischemia and attenuated mechanical allodynia in the spinal nerve ligation model of neuropathic pain. As hypothesized, the side effects of the drug were minimal and **93-31** did not affect locomotor function.⁸⁷

1.2.8. The human Ether-*a*-go-go Related Gene (hERG) ion channel

Drug interactions with the hERG channel, which cause potentially fatal acquired long QT syndrome (aLQTS) and ventricular tachycardia (torsade de pointes, TdP), has been the most common cause of black box labeling restrictions or withdrawal of marketed drugs in the last decade (10 examples, Figure 1.16).⁸⁸ As a result of post-

marketing reports of sudden death and TdP, the Food and Drug Administration mandates no new drugs can be marketed without evaluation of safety as it relates to hERG binding.⁸⁹ Accordingly, determining hERG binding and cardiac safety in pre-clinical models has become the primary goal of pharmaceutical development before entering clinical trials.

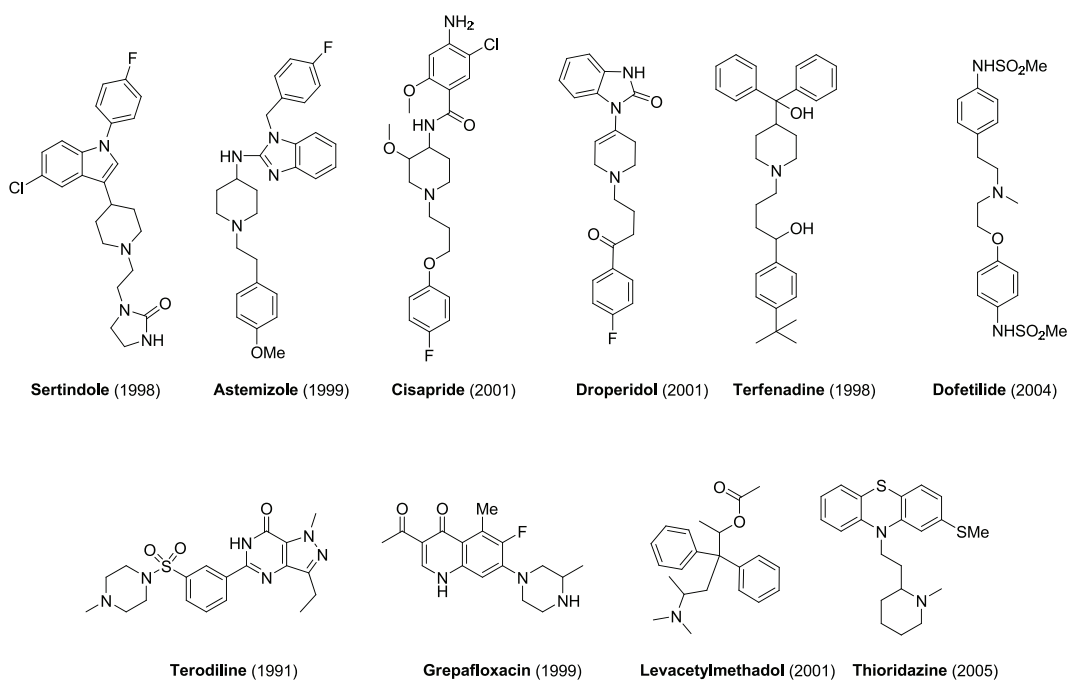


Figure 1.16 Drugs withdrawn or restricted due to hERG binding

The QT wave of an electrocardiogram represents the duration of ventricular action potential in myocardial cells.⁹⁰ Under normal conditions, the action potential consists of rapid depolarization (increase of influx/intracellular current of Na⁺ ions), a plateau phase (dynamic equilibrium of Ca²⁺ ions into and K⁺ ions out of the cell), and a repolarization phase (K⁺ ion efflux) (Figure 1.17).

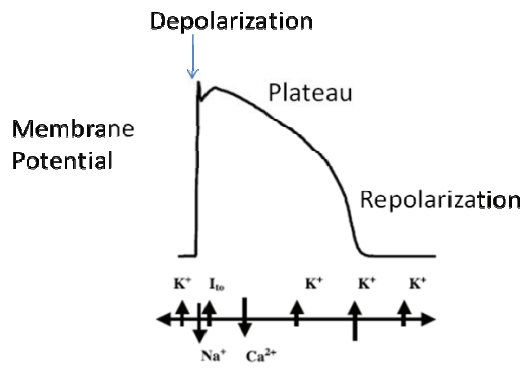


Figure 1.17 Phases of ventricular action potential (Modified)⁹⁰

In normal individuals, the QT interval lasts between 200 to 300 milliseconds (Figure 1.18). However, a person with genetic long QT syndrome or drug-induced aLQTS may have a QT interval of up to 400 milliseconds. Prolonged QT intervals of 440 milliseconds or greater have been associated with ventricular tachycardia, TdP, and increased mortality.⁹¹ The most important component of the repolarization phase is the rapid delayed rectifier K^+ current mediated by the hERG channel.⁹²⁻⁹³

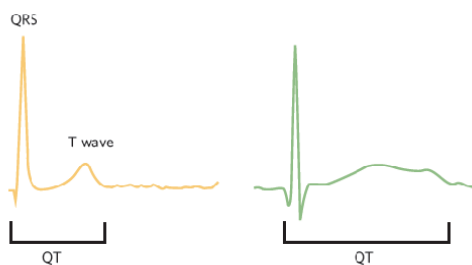


Figure 1.18 A normal QT interval from an ECG (yellow) compared to a prolonged QT signal (green)⁹¹

Structurally, the hERG channel is a tetrameric transmembrane protein, with each subunit composed of six helices. Individual subunits contain a potential-sensing

domain and a pore-forming domain.⁹⁴ The transmembrane pore resembles a narrowing cylinder and is constructed with a traditional K^+ signature sequence, Ser-Val-Gly-Phe-Gly, which forms a K^+ selectivity filter (Figure 1.19). The carbonyl oxygen atoms of these residues serve as coordination sites and direct dehydrated K^+ atoms to proceed single-file through the ion conduction pathway.⁹⁵

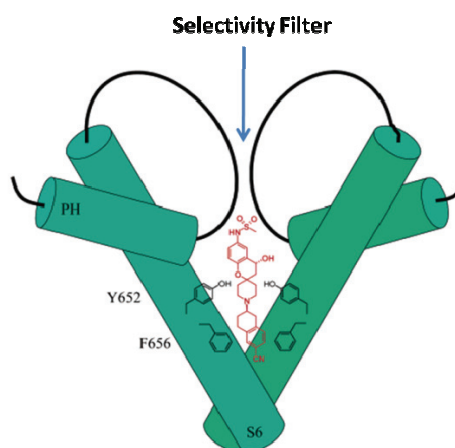


Figure 1.19 hERG channel structure with important ligand-binding residues highlighted (modified)⁷³

hERG blockage is thought to be the pharmacologic cause of clinical QT prolongation and TdP.⁹⁶ The channel is known to be quite promiscuous, and binds a number of drug classes: antiarrhythmics, psychiatric, antimicrobials, and antihistamines. Two residues that lie in the pore, Phe656 and Tyr652, were found to be critical for hERG-ligand binding, and it is hypothesized that Tyr652 participates in cation- π interactions with amine-containing ligands while Phe656 participates in hydrophobic interactions. Upon binding, the pore is occluded from ion permeation.⁹⁷⁻⁹⁸

The pharmacophore of hERG ligand resembles that of the NR2B NMDA antagonists (Figures 1.12 and 1.16). Similar to the ifenprodil-like compounds previously

developed, a number of hERG blockers also contain two aromatic rings flanking an amine which is ionized at physiologic pH. The hERG-active compounds sertindole, astemizole, cisapride, droperidol, and terfenadine all contain piperidines asymmetrically located between the aryl termini, similar to NR2B NMDA antagonists ifenprodil, CP-101,606, and the other antagonists listed in figure 1.12. Dofetilide in particular bears a striking resemblance to the enantiomeric propanolamines previously developed in the Liotta group. This hERG blocker contains a centrally located N-methyl amine flanked by two aryl methyl sulfonamides (the 93 series compounds have only one methyl sulfonamide) and a phenoxy oxygen located at one terminus of the linker region.

A number of strategies are traditionally used by medicinal chemists to decrease or eliminate drug-hERG binding, and can be categorized into four main divisions (Table 1.3): discrete structural modifications, formation of zwitterions, control of logP, and attenuation of pK_a .⁷³

Discrete structural modifications have been used to optimize compounds without a centrally located amine that could potentially participate in π -cation interactions. In one example, the hERG binding of a series of NR2B NMDA antagonists developed by Pfizer (Table 1.3)⁷⁴ was mitigated by acetylation of benzimidazole **14** to afford compound **15**, and resulted in a 22-fold decrease in hERG binding.

The most well-known example of utilizing zwitterions formation to reduce hERG affinity is terfenadine (**16**, marketed as Seldane © in the United States, Aventis Pharmaceuticals, Table 1.3). Although approved in 1982, Seldane was withdrawn from

the market in 1997 after post-market analysis indicated the drug prolonged the QT interval and was associated with TdP adverse events.⁹⁹⁻¹⁰⁰ Interestingly, it was found that the carboxylic acid metabolite **17** (fexofenidine) was responsible for the parent compound's antihistamine activity. Compound **17** had decreased hERG binding, and did not affect the QT interval *in vivo*. The lowered hERG binding was attributed to the increased polarity of the compound which limited the ability of **17** to bind within the ion channel. Subsequently, **17** was marketed as Allegra © (Sanofi-Aventis Pharmaceuticals) and brought to market in 1996.

The partition coefficient (logP) is a measure of the differential solubility of a compound in two immiscible solvents, generally expressed as the ratio:

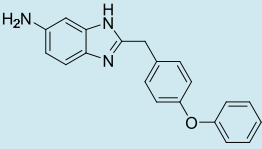
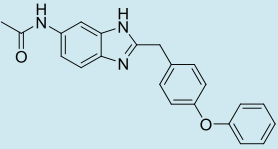
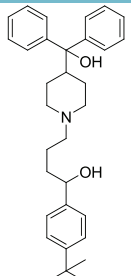
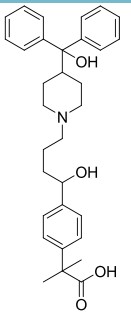
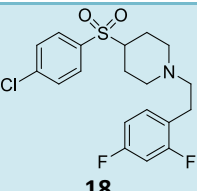
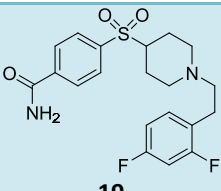
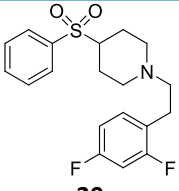
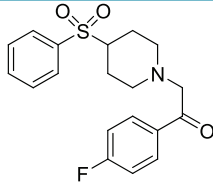
$$\log P_{(octanol/water)} = \log ([drug]_{octanol}) / ([drug]_{water})$$

LogP is a measure of drug-like hydrophobicity of a compound, and generally utilized for optimizing Absorption Distribution Metabolism Excretion (ADME) parameters. Because the hERG channel is known to be relatively hydrophobic, the logP property can also be tuned to decrease hERG affinity. Increasing hydrophilicity by incorporating additional hydrogen-bonding moieties, such as replacement of the chlorine substituent of **18** (logP = 3.78) with the amide of **19** (logP = 7.33), decreased hERG binding by nearly 50-fold (Table 1.3).¹⁰¹

Finally, alteration in pK_a has been used to attenuate hERG binding. Decreasing the basicity of the centrally located nitrogen with pendant groups is hypothesized to minimize the cation- π interaction of protonated amines with the aromatic residues which line the ion channel pore.⁹⁷ An example of this is a comparison of compounds **20**

and **21**, where **21** has a ketone at the β -position to the amine.¹⁰¹ Compound **21** has a calculated pK_a of 5.25 compared to the pK_a of 7.52 of parent compound **20**, and exhibits significantly decreased hERG activity.

Table 1.3 Examples of medicinal chemistry methods to decrease hERG binding

Method	hERG Active	IC ₅₀ (nM)	hERG IC ₅₀ (nM)	hERG Optimized	IC ₅₀ (nM)	hERG IC ₅₀ (nM)
Discrete Structural Modification	 14	180	120	 15	93	2,600
Zwitterion Formation	 Terfenadine (Seldane®) 16	1	56	 Fexofenadine (Allegra®) 17	15	2,300
Modulation of logP	 18	1.4	150	 19	0.52	7,100
Modulation of pK_a	 20	0.33	1,000	 21	2.4	6,800

1.2.9. Rationale for inhibitor design

The structural similarities between the Liotta group's enantiomeric propanolamines and traditional hERG blockers, coupled with the knowledge that screening hit AM 92016 (**13**) was an antiarrhythmic agent, suggested this family of compounds had a substantial likelihood of being a ligand for the hERG channel and may cause QT prolongation. Biological testing proved this to be true, and unfortunately the lead compound, **93-31**, exhibited similar affinity for both the off-target hERG channel ($K_i = 56$ nM) and on-target NR2B-containing NMDA receptors ($IC_{50} = 27$ nM in rat receptors). Although *in vitro* hERG binding does not necessarily correlate to causing QT prolongation *in vivo*, the low therapeutic index of this compound was the inspiration for further medicinal chemistry efforts to decrease hERG binding but maintain good NR2B NMDA selectivity and fold shift.

Notwithstanding activity at the hERG channel, compound **93-31** is a potential drug candidate. It embodies an example of an enantiomerically pure propanolamine with differentially increased activity under acidic pH conditions that showed excellent neuroprotective properties *in vivo*.⁸⁷ We hypothesized large fold shift, coupled with excellent selectivity for NR2B-containing NMDA receptors located in the forebrain, would represent a new class of NMDA antagonists with a novel dual mode of action. Compounds like **93-31**, with dual selectivity (pH sensitivity and NR1/NR2B-subtype selective), would exhibit decreased side effects compared with simple NR2B-selective antagonists, as the dually-selective compounds would be inactive at NR2B-containing receptors at physiologic conditions. This novel class of inhibitors would preferentially

act at the target NR1/NR2B receptors under acidic conditions associated with hypoxic ischemic events. By this reasoning, we expect compounds of this type to be not only neuroprotective, but potential prophylactic agents. Therefore, we sought a potential NR2B NMDA antagonist drug candidate via decreasing the hERG activity of lead compound **93-31** and optimizing drug-like characteristics.

It was envisaged that the information regarding optimization of the lead enantiomeric propranolamine **93-31** could be obtained via synthesis of analogues with specific functional group manipulations (Figure 1.20). The analogues described below were designed to probe the effect of steric, electronic, and lipophilic changes on both on target NR1/NR2B NMDA receptor antagonism and off-target hERG blockage.

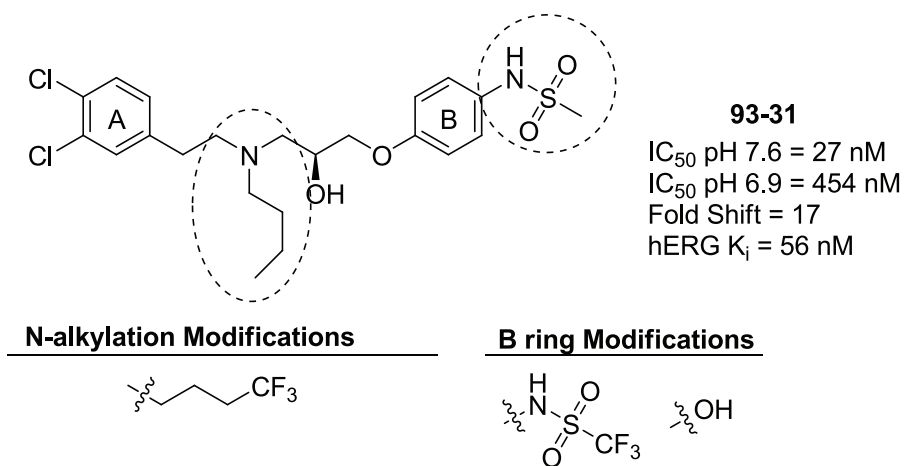


Figure 1.20 Lead enantiomeric propranolamine **93-31**: properties and proposed analogues

The 4,4,4-trifluorobutyl analogue **93-155** was proposed as a result of the observation illustrated in Figure 1.21. While **93-31** exhibited 97% hERG binding at a concentration of 3 μ M, the pentafluorobenzyl analogue **93-51** was bound only 40% of

hERG receptors (at 3 μM), although it showed both a significant decrease in on-target NR2B-containing NMDA receptor potency and fold shift. It was hypothesized that the hybrid **93-155** structure may embody the positive characteristics of both **93-31** and **93-51**, namely the desired potency and fold shift of **93-31** coupled with the decreased hERG activity of **93-51**. Incorporation of the trifluorobutyl substituent would inductively decrease the pK_a of the ammonium proton, and as such this modification would be categorized as a pK_a modulation approach to decreasing hERG activity.

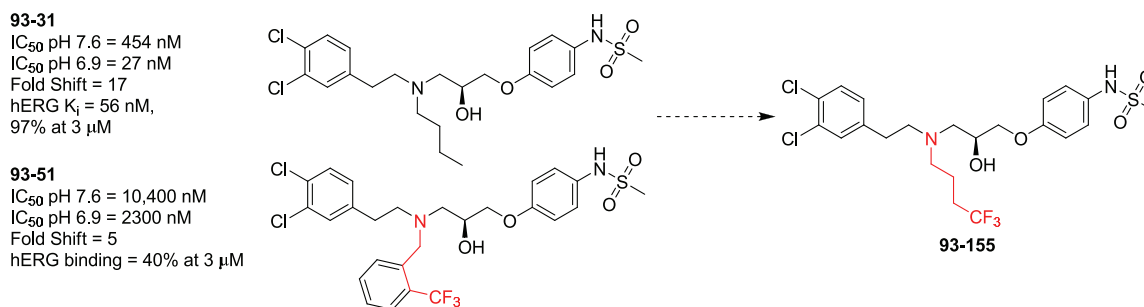


Figure 1.21 Rationale for hybrid analogue **93-155**

Two analogues with modified B ring substitution were proposed to probe the enantiomeric propanolamine B ring pharmacophore and to potentially decrease hERG binding compared to **93-31** (Figure 1.22). Compound **93-160** replaces the traditional methanesulfonamide B ring with a trifluoromethanesulfonamide. This alteration will significantly decrease the pK_a of the sulfonamide N-H, and may affect hydrogen bond donor interactions. However, because fluorine is an isostere of carbon, this modification should not drastically effect how the analogue binds within the active site.

The corresponding phenolic analogue to **93-31** is **93-150**. This compound was hypothesized to have similar activity to **93-31** due to the observation that numerous other NR2B NMDA antagonists are phenols (Figure 1.12), as the phenol satisfies the NR2B NMDA pharmacophore which requires a hydrogen bond donor substituent on the B ring. In addition, the phenol may decrease the ability of **93-150** to bind within the lumen of the hERG channel.

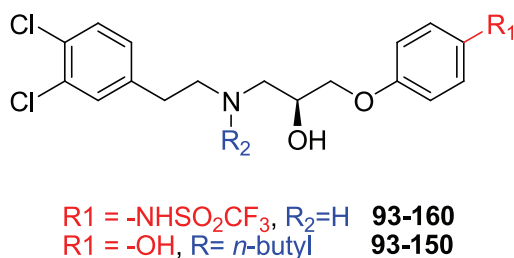
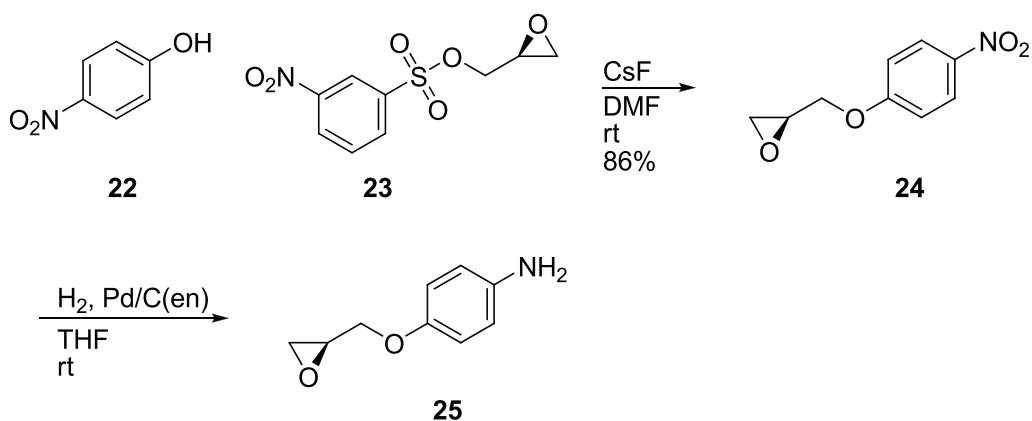


Figure 1.22 Proposed analogues with B ring modifications

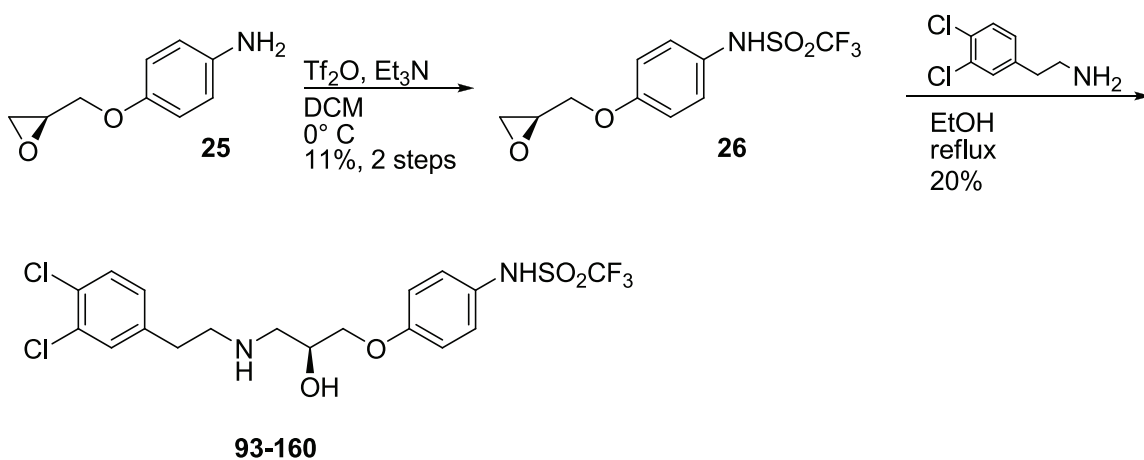
1.3 Synthesis of Enantiomeric Propanolamine Analogues

The synthesis of both sulfonamide-containing analogues **93-155** and **93-160** began by alkylation of *para*-nitrophenol (**22**) with (*S*)-(+)-glycidyl nosylate (**23**) under basic conditions, affording phenoxy epoxide **24** (Scheme 1.1).¹⁰² The nitro group was then reduced to the aniline using Pd/C catalyst poisoned with ethylene diamine¹⁰³ to give compound **25**.¹⁰⁴ The poisoned catalyst was required to reduce side product formation resulting from epoxide opening.

Scheme 1.1 Synthesis of *para*-phenoxy aniline intermediate 25

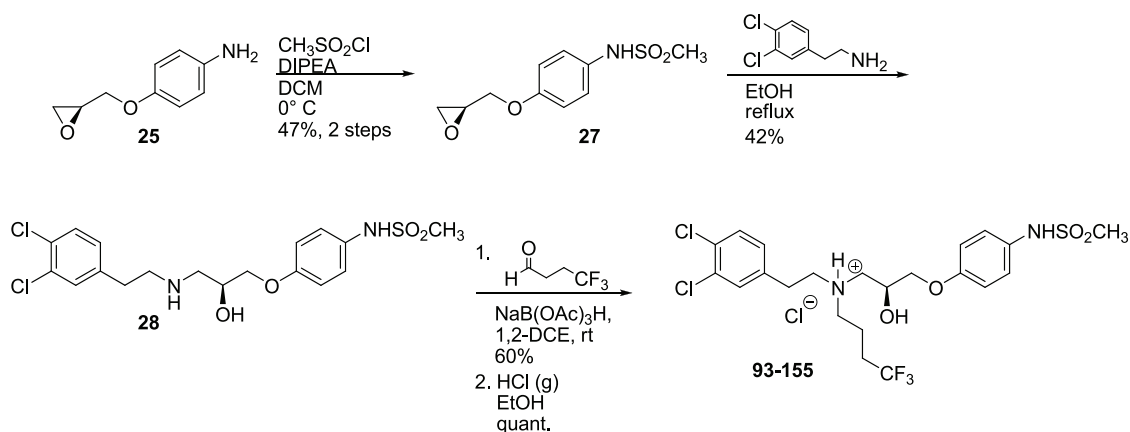
Aniline **25** was found to be unstable on silica gel, and thus was immediately converted after work-up and concentration to the desired sulfonamide. In the case of **93-160** (Scheme 1.2), **25** was treated with trifluoromethanesulfonic anhydride and base to yield trifluoromethylsulfonamide **26**. Treatment of epoxide **26** with 3,4-dichlorophenethylamine effected ring opening at the epoxide C-3 position.

Scheme 1.2 Synthesis of 93-160



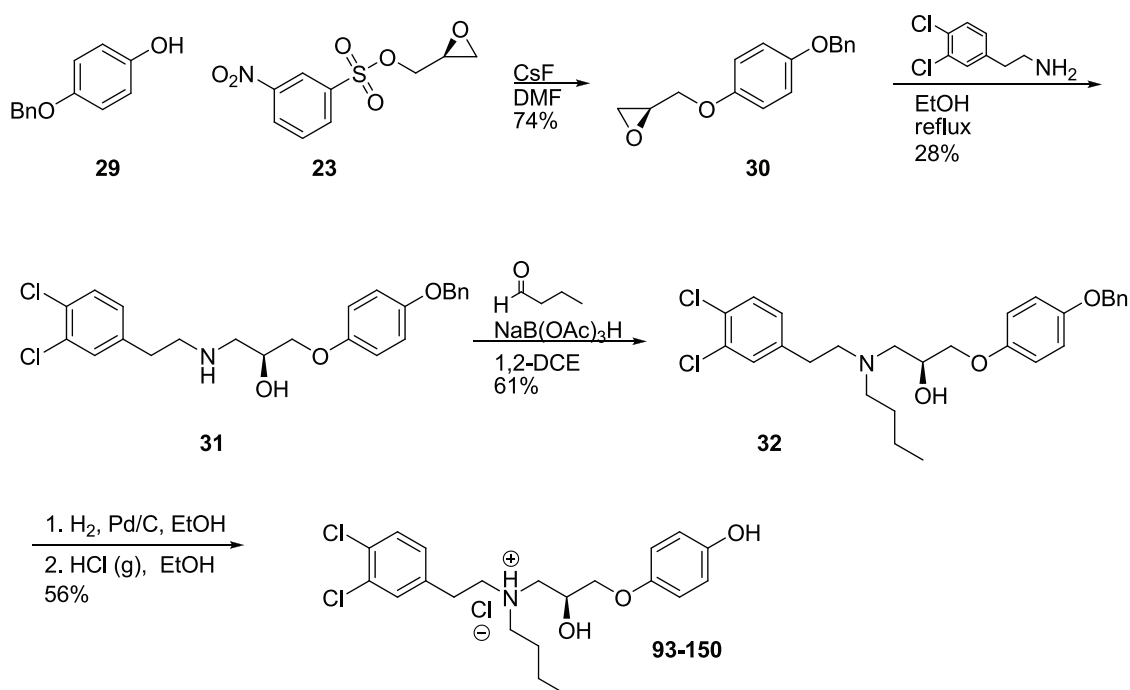
Synthesis of **93-155** (Scheme 1.3) proceeds from common intermediate **25** by formation of the methanesulfonamide using methanesulfonyl chloride and base to afford **27**. Oxirane opening with 3,4-dichlorophenethylamine to gave **28**. N-alkylation was carried out by reductive amination on the central amine using butyraldehyde and sodium triacetoxyborohydride to yield **93-155** after treatment of the free base with HCl.

Scheme 1.3 Synthesis of 93-155



Phenolic compound **93-150** was prepared in a similar manner to **93-155** and **93-160** (Scheme 1.4). Displacement of (*S*)-(+)-glycidyl nosylate (**23**) with *para*-benzyloxyphenol (**29**) gave the glycidyl aryl ether **30**. Oxirane **30** was then opened at the C-3 position with 3,4-dichlorophenethylamine to afford amine **31**. Reductive amination using butyraldehyde yielded the *n*-butyl compound **32**. Finally, deprotection of the benzyl group under hydrogenolysis with palladium on carbon catalyst produced the desired compound **93-150**.

Scheme 1.4 Synthesis of 93-150

1.4 pK_a determination of NMDA receptor channel blockers1.4.1. Rationale for pK_a experiments

The physical location of the NMDA receptor proton sensor, responsible for endogenous proton inhibition and increased receptor sensitivity, is unknown. However, point mutations deep within the channel pore were found to significantly influence the pH sensitivity of the receptor.¹⁰⁵⁻¹⁰⁶ This suggests the proton sensor could be located near, or have long distance contacts with, the ion channel pore. The Traynelis group hypothesized that if the proton sensor was located near the pore, channel blockers may also exhibit pH-dependent fold shifts similar to those of the previously described NR2B-selective antagonists.

Biological testing of a variety of channel blockers across NR1/NR2A-, NR1/NR2B, NR1/NR2C-, and NR1/NR2D-containing NMDA receptors, indicated structural and functional differences existed within the pores of all subtypes (Table 1.4).¹⁰⁷ These structurally diverse compounds have various proposed binding site interactions within the channel pore in addition to different kinetics of channel blockage.¹⁰⁸⁻¹¹¹ Therefore the observed result comprising differential activity at various NR2-containing receptors, measured by the Traynelis lab, was not unexpected (Table 1.4).

The hypothesis followed that the channel blockers may also exhibit differential fold shifts. In fact, the open-state trapping blockers MK-801, ketamine, and norketamine all exhibited fold shifts of greater than five (Table 1.4). In particular, the enantiomers of MK-801 showed differential activity at NR1/NR2A-containing receptors. (+)-MK-801 (**4**, Figure 1.9) had an IC₅₀ of 15 nM, while (-)-MK-801 had an IC₅₀ of 354 nM, both measured at pH 7.6. In addition, both enantiomers exhibited differential fold shifts when activity at pH 7.6 and 6.9 were compared.¹⁰⁷

Table 1.4 Activities and fold shifts[†] of known channel blockers[‡] at NMDA receptor subtypes

Antagonist	NR1/NR2A			NR1/NR2B			NR1/NR2C			NR1/NR2D		
	IC ₅₀ (μM)		FS ^a	IC ₅₀ (μM)		FS	IC ₅₀ (μM)		FS	IC ₅₀ (μM)		FS
	pH 7.6	pH 6.9		pH 7.6	pH 6.9		pH 7.6	pH 6.9		pH 7.6	pH 6.9	
(+)-MK-801	0.03	0.01	2.5	0.01	0.01	1.0	0.02	0.01	1.8	0.03	0.03	1.2
(-)-MK-801	0.35	0.05	6.4	0.03	0.02	1.4	0.04	0.03	1.2	0.17	0.06	2.8
(+/-)-Ketamine	3.31	0.54	6.2	0.93	0.24	3.8	1.65	0.66	2.5	2.42	1.23	2
(+)-Ketamine	16.1	2.35	6.9	1.55	0.40	3.8	1.11	0.70	1.6	1.5	0.78	1.9
(+/-)-Norketamine	50.9	6.99	7.3	8.74	1.90	4.6	5.6	1.2	4.7	7.5	2.6	2.9
Dextrometorphan	11.3	5.12	2.2	3.74	1.28	2.9	1.07	0.47	2.3	5.4	2.4	2.2

Antagonist	NR1/NR2A			NR1/NR2B			NR1/NR2C			NR1/NR2D		
	IC ₅₀ (μM)			IC ₅₀ (μM)			IC ₅₀ (μM)			IC ₅₀ (μM)		
	pH 7.6	pH 6.9	FS ^a	pH 7.6	pH 6.9	FS	pH 7.6	pH 6.9	FS	pH6 7.6	pH 6.9	FS
Levomethorphan	12.7	5,61	2.3	2.24	0.07	3.3	1.06	0.31 9	3.3	2.6	1.12	2.2
Phencyclidine	0.82	0.17	4.9	0.16	0.06	2.6	0.16	0.08	2.1	0.22	0.19	1.2
CNS1102/ Aptiganel	0.13	0.04	3.7	0.07	0.03	2.5	0.09	0.04	2.4	0.14	0.13	1.1
Memantine	4.36	2.25	1.9	1.2	0.86	1.4	0.61	0.50	1.2	0.82	0.58	1.4
Remacimide	80.9	44.2	1.8	35	60.3	0.5	91.9	43.1	2.1	62.9	76.3	0.8

† Fold Shift = (IC₅₀ pH 7.6)/(IC₅₀ 6.0)

‡ Structures of MK-801, Figure 1.9. Structures of Ketamine, Phencyclidine, Aptiganel, Memantine, and Remacimide can be found in Table 1.1

^a FS = Fold Shift

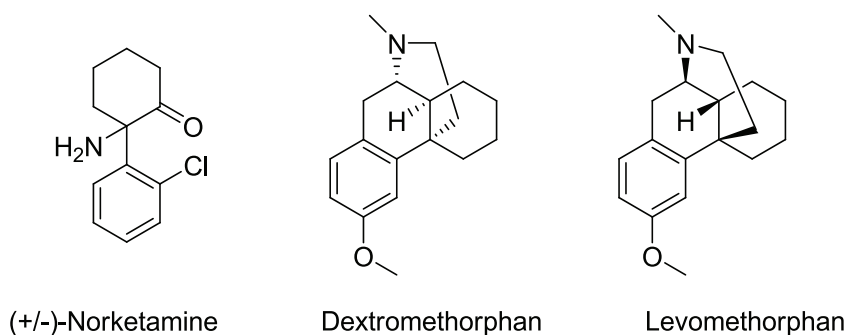


Figure 1.23 Structures of Drugs in Table 1.4. For the remainder of drug structures, see Figure 1.9 and Table 1.1.

The channel blocker ketamine is known to have enhanced potency under acidic conditions.¹¹² This finding has been correlated to pK_a of ketamine, measured experimentally to be 7.5, hence ketamine is susceptible to significant ionization changes between pH 6.9 and 7.6. The increased fraction of compound which exists in the protonated form versus the unprotonated form under acidic conditions is thought to account for the fold shift of ca. 6 seen in NR1/NR2A-containing receptors.

1.4.2. Determination of pKa values of selected channel blockers

To determine if the differential activity of other channel blockers under acidification conditions could also be attributed to pK_a, various known channel blockers were obtained, and their pK_as were measured both experimentally and by computational calculation. The results, compared with other known channel blocker protonation statistics, are shown in Table 1.5.¹⁰⁷

Table 1.5 pK_a and protonation characteristics of known channel blockers[†]

Antagonist	pK _a		Protonated Species (%)	
	Experimental	Predicted	pH 7.6	pH 6.9
(+)-MK-801	8.37	8.0	85.5	96.7
(-)-MK-801	8.37	8.0	85.5	96.7
(+/-)-Ketamine¹¹²	7.5	6.5	44.3	80.0
(+)-Ketamine¹¹²	7.5	6.5	44.3	80.0
(+/-)-Norketamine	6.8	6.4	14.6	44.3
Dextromethorphan¹¹³	9.2	9.1	97.6	99.5
Levomethorphan¹¹³	9.2	9.1	97.6	99.5
Phencyclidine¹¹⁴	8.5	8.2	88.8	97.6
CNS1102/Aptiganel	10.3	9.1	96.9	99.4
Memantine¹¹⁵	10.3	10.8	99.8	100
Remacimide	8.14	7.8	61.3	88.0

[†] Orange color indicates results determined in this work.

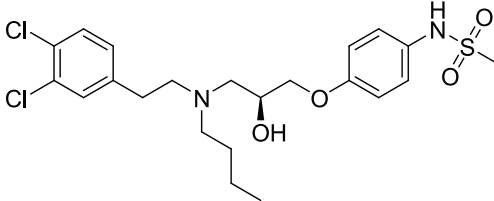
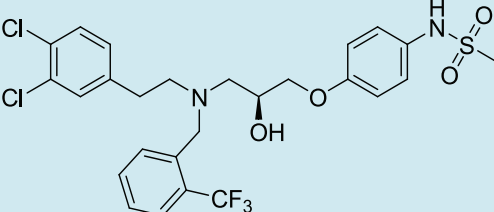
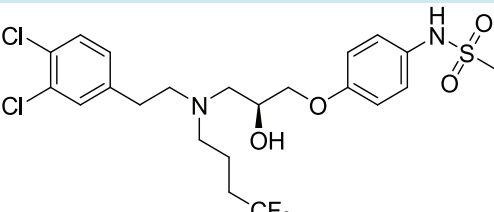
1.5 Results and Discussion

1.5.1. Structure activity relationships (SAR) of novel enantiomeric propanolamines.

Analogue potency at pH 6.9 and 7.6 was determined in the Traynelis laboratory using two electrode voltage clamp recordings in *Xenopus laevis* oocytes expressing recombinant rat NMDA receptors. hERG binding assays were outsourced to MDS Pharma.

The activity of the 4,4,4-trifluorobutyl analogue **93-155** is shown in comparison to **93-31** and **93-51** in Table 1.6.

Table 1.6 *In vitro* analysis of 93-155 at NMDA and hERG receptors

Compound	Structure	IC ₅₀ NMDA (nM) [†]		Fold Shift	hERG Binding [‡]
		pH 7.6	pH 6.9		
93-31		454	27	17	97%
93-51		10,400	2,300	5	40%
93-155		6,070	3,700	2	ND

[†] Determined in rat oocytes, NR1/NR2B-containing NMDA receptors

[‡] Percent binding at 3 μM

ND = not determined

The hypothesis that the hybrid structure (**93-155**) between **93-31** and **93-51** may exhibit potency similar to that of **93-31** proved incorrect. The IC_{50} value of **93-155** (6,070 nM) was intermediate to both **93-31** (454 nM) and **93-51** (10,400 nM) at pH 7.6. Unfortunately, **93-155** also exhibited decreased potency at pH 6.9 (3,700 nM) compared to **93-51**, giving a fold shift of only two. Due to the fact that **93-155** did not satisfy two of the three hypothesized properties, namely increased potency at pH 6.9 and a fold shift similar to **93-31**, the hERG value was not determined.

The decreased activity of **93-155** may be attributed to conformational flexibility. While **93-31** has a number of C-C bonds with the ability to rotate in the *n*-butyl chain, **93-51** has increased rigidity as a result of the benzyl system. Therefore, increased IC_{50} at pH 6.9 and fold shift may be inherent with a flexible hydrophobic chain. One can also envisage a decreased pK_a of the centrally located amine as a result of the additional trifluoromethane substituent, although this effect would be minimal when traversing such a long distance. Another notable difference between **93-155** and **93-51** is chain geometry. In particular, it may be possible that a *cis*-double bond within the N-alkylated chain, such as in compound **33** (Figure 1.24), would be a more appropriate isostere of the **93-51** trifluorobenzyl substituent, and represents an optimized hybrid compound. However, analogue **33** was not prepared in the course of this work.

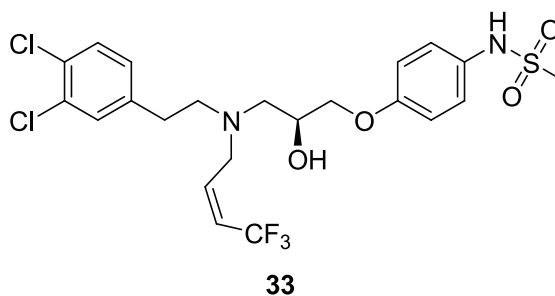


Figure 1.24 Proposed analogue 33

The activity and SAR of B ring modifications within the enantiomeric propranolamine series is illustrated in Table 1.7.

Table 1.7 *In vitro* analysis of analogues with B ring modifications

Compound	Structure	IC ₅₀ NMDA [†]		Fold Shift	hERG Binding [‡]
		pH 7.6	pH 6.9		
93-4		37	18	2	83%
93-31		454	27	17	97%
93-160		1,270	800	0.62	ND
93-138		384	149	3	33%
93-150		3,550	360	10	60%

[†] Determined in rat oocytes, NR1/NR2B-containing NMDA receptors

‡ Percent binding at 3 μ M
ND = not determined

The replacement of the methanesulfonamide of **93-4** with the trifluoromethanesulfonamide of **93-160** yielded surprising results. Compound **93-160** exhibited decreased potency at both pH values when compared to **93-4**. **93-160** also exhibited a reverse fold-shift of 0.62, meaning the compound is more potent at physiologic pH than under the acidic conditions associated with hypoxia. The molecular determinants of the reverse fold shift are unclear. Seemingly the trifluoromethyl group is an isostere to the methyl group. Thus size should not account for the differences in potency or fold shift observed. It remains to suggest the inductive effects of the trifluoromethyl group, which cause a reduction of the sulfonamide N-H pK_a . QuikProp¹¹⁶ calculations suggest the pK_a of the sulfonamide N-H of **93-160** is 5.1, compared to a pK_a of 9.8 for the methylsulfonamide N-H of **93-31**. Therefore at physiologic pH, there is a much larger percentage of deprotonated (zwitterionic) species of **93-160** compared to **93-31**. This differential protonation state may reduce the ability of **93-160** to form the appropriate hydrogen bonds between the compound and the allosteric NR2B site. Regardless, the properties of **93-160** were antithetical to the desired properties for an optimized analogue. This resulted in a lack of interest in the hERG-binding activity, and thus this property was not determined.

The replacement of the methanesulfonamide of **93-31** with a phenol (**93-150**) yielded a good example of an optimized enantiomeric propanolamine. As in the case of **93-4** and **93-31**, functionalization of the central amine nitrogen of the parent amine **93-**

138 caused a concomitant slight potency decrease at pH 6.9 (**93-138** IC_{50} = 149 nM, **93-150** IC_{50} = 360 nM) and a much more significant decrease in potency at pH 7.6 (**93-138** IC_{50} = 384 nM, **93-150** IC_{50} = 3,550 nM). As a result of the large drop in physiologic potency, fold shift increased from **93-138** (fold shift = 3) to **93-150** (fold shift = 10). The SAR of both pairs of compounds, **93-138** and **93-150**, and **93-4** and **93-31**, clearly indicate that the length of the N-substituent influences fold shift.

Compound **93-150** also exhibited a > 30% decrease in off-target hERG binding (60% binding at 3 μ M) compared to **93-31** (97% binding at 3 μ M). Therefore it appears that replacement of the methylsulfonamide with a phenol decreases interactions with the hERG channel. However, **93-150** had increased hERG activity compared to free amine compound **93-138** (33% binding at 3 μ M). This is most likely a result of both increased lipophilicity and change in the pK_a of the amine nitrogen with the additional *n*-butyl substituent.

As a consequence of these studies, one can make a number of conclusions regarding analogue potency and fold shift at NR1/NR2B-containing NMDA receptors and off-target hERG receptors:

1. Functionalization of the central amine decreases potency at pH 6.9 only slightly, but results in a large potency drop at pH 7.6, giving rise to a large fold shift. This relationship holds true regardless of B ring substituent.
2. Decreasing the basicity of the central amine nitrogen results in decreased potency and fold shift.

3. Decreasing the pK_a of the sulfonamide N-H results in decreased potency and fold shift.
4. Replacement of the B ring sulfonamide with a phenol yields compounds with similar potencies and fold shifts, but a decreased off-target hERG profile.

Since the discovery of the aforementioned SAR, NeurOp Inc. has further explored a number of hydrogen bonding substituents which are tolerated on the B ring which give exceptional fold shifts and off-target profiles.¹¹⁷

1.5.2. The role of pK_a in determining channel blocker fold shift

Table 1.5 summarizes the pK_a values determined for known channel blockers which have been either previously published in the literature or determined during the course of this work.¹⁰⁷ The pK_a values of chiral, achiral, and racemic compounds were examined. In addition, the percent of ionized drug was calculated at both pH 7.6 and 6.9.

It has been reported that the increased potency of ketamine has been attributed to the larger percentage of protonated drug at acidic pH values relative to physiologic pH.¹¹² With a pK_a of 7.5, ketamine undergoes a large shift in the quantity of ionized species between the pH values of 6.9 and 7.6. At pH 7.6, only 44% of ketamine is protonated, compared with 80% at pH 6.9. The pK_a of norketamine was determined in this study to be 6.8, somewhat lower than that of ketamine. Given the structural similarities of ketamine and norketamine however, similar ionization properties are

expected. A significant increase in protonated norketamine results during acidification (44% at pH 6.9 versus 15% at pH 7.6) as well. Thus, the increased percentage of protonated species at pH 6.9 may account for the fold shift of 7.3 observed in NR1/NR2A-containing NMDA receptors *in vitro* when treated with norketamine.

Unlike ketamine, an increase in the percent of protonated species cannot account for the fold shift of 6.4 seen for (-)-MK-801 on NR1/NR2A-containing NMDA receptors. The pK_a of both MK-801 enantiomers was determined to be 8.37. This is greater than the pK_a of ketamine, making MK-801 less sensitive to pH changes from 6.7 to 7.9. With nearly 97% of the drug is protonated at pH 6.9 compared with 86% at pH 7.6, this small difference in ionization could not significantly contribute to pH sensitivity. One can conclude that the fold shift associated with one enantiomer of MK-801 selectively can be attributed to the structural determinants of binding within the pore and/or the receptor's gating mechanism and not ionization state of the drug.

Taken together, these results suggest that contrary to previous hypotheses, subunit-selective NMDA antagonist channel blockers could be developed as neuroprotectants. Gating kinetics, structural determinants, or both, of the channel pore appear to vary considerably between NR2A-D-containing receptors. This gives rise to distinctly different potencies when treated with a number of antagonists. The pore is shown to have significant sensitivity, as demonstrated by increased affinity towards one enantiomer over another in some cases, typical of protein-ligand interactions. In addition to exhibiting a range of affinities for NR2A-D-containing receptors *in vitro*, a selection of channel blockers also exhibit pH dependence. Thus, similar to the NR2B-

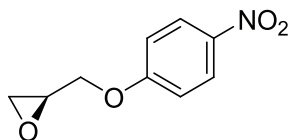
selective NMDA antagonists discussed in Section 1.3.1, subunit-selective pH-dependent channel blockers may represent a novel dual mechanism of NMDA receptor inhibition. This dual mechanism has the potential to specifically target receptors located in particular brain loci in addition to exhibiting increased potency under hypoxic ischemia conditions relative to physiologic pH. Compounds of this class would potentially exhibit decreased side effects compared to NMDA antagonists previously developed.

1.6. Chemistry Experimental Detail

All reagents were obtained from commercially suppliers and used without further purification. Reaction progress was monitored by thin layer chromatography (TLC) on precoated glass plates (silica gel 60 F₂₅₄, 0.25 mm thickness) purchased from EM Science. Flash chromatography was carried out on silica gel 60 (230-400 mesh). ¹H and ¹³C NMR spectra were recorded on an INOVA-400 (400 MHz), INOVA-600 (600 MHz), or Mercury 300 Vx (300 MHz). The spectra obtained were referenced to the residual solvent peak. Chemical shifts are reported in parts per million and coupling constants in Hertz (Hz). Mass spectra were performed by the Emory University Mass Spectrometry center on either a VG 70-S Nier Johnson or JEOL instrument. Elemental analyses were performed by Atlantic Microlab, Inc (Norcross, GA). C, H, N agreed with proposed structures within ± 0.4 of theoretical values unless otherwise indicated.

1.6.1. Experimental details of compounds synthesized in Chapter 1

(S)-2-((4-nitrophenoxy)methyl)oxirane (**24**).



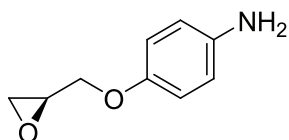
Cesium Fluoride (3.28 g, 21.6 mmol, 3 equiv) was added to a solution of 4-nitrophenol (1.0 g, 7.19 mmol, 1.0 equiv) in anhydrous DMF (3.0 mL). After stirring for 1 h, (S)-glycidyl 3-nitrobenzenesulfonate (1.86 g, 7.19 mmol, 1.0 equiv) was added. The resulting suspension stirred at room temperature for 24 h. The mixture was poured over ice. After melting, the solution was extracted with ethyl acetate (3 x 20 mL). The combined organic layers were dried over MgSO₄ and concentrated *in vacuo* to give a white solid. The crude product was purified by column chromatography on silica gel (50% EtOAc/Hexanes) to give a white solid (1.23 g, 86%). Characterization agrees with previously reported spectra.¹⁰² 99.6% ee based on chiral HPLC with Chiralcel OD column (46 mm i.d. x 250 mm, eluent hexane-EtOH-Et₂NH 90:10:0.1 v/v; flow rate, 1.0 mL/min; UV monitoring at 254 nm). ¹H NMR (400 MHz, CDCl₃) δ 8.21 (d, *J* = 7.1 Hz, 2H), 7.00 (d, *J* = 7.1 Hz, 2H), 4.38 (dd, *J*₁ = 11.3 Hz, *J*₂ = 1.7 Hz, 1H), 4.02 (dd, *J*₁ = 11.3 Hz, *J*₂ = 2.9 Hz, 1H), 3.41-3.38 (mult, 1H), 2.95 (t, *J* = 5.7 Hz, 1H), 2.78 (dd, *J*₁ = 5.7 Hz, *J*₂ = 1.3 Hz, 1H). ¹³C NMR (100 MHz, CDCl₃) δ 163.6, 142.1, 126.2, 114.9, 69.7, 50.0, 44.7.

Palladium on Carbon catalyst poisoned with ethylenediamine [Pd/C(en)].

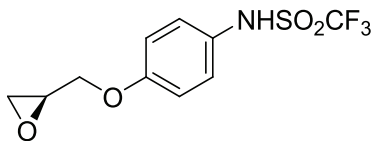
An oven-dried and evacuated 1 L 3-neck round bottom flask fitted with an oven-dried and evacuated 500 mL addition funnel was backfilled with Argon (g) and charged with

Palladium on activated carbon (5% w/w 0.200 g). With gentle stirring, ethylenediamine (0.42 g, 0.1 M) in methanol (70 mL) was added via addition funnel dropwise (CAUTION: FIRE HAZARD!) The mixture was stirred at room temperature for 32 hours. The catalyst was collected by filtration and washed with methanol and ether. The black solid was dried for 24 hours under high vacuum before using.

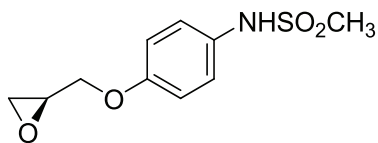
(S)-4-(oxiran-2-ylmethoxy)aniline (25).



Epoxide **24** (500 mg, 3.0 mmol) was dissolved in anhydrous THF (5.0 mL). To this solution, poisoned palladium-carbon catalyst [**Pd/C(en)**] was added (50 mg, 10 wt%). A hydrogen balloon was added and the heterogeneous mixture stirred at room temperature for 12 h. The catalyst was removed by filtration, and the filtrate was concentrated *in vacuo* to give pink oil. This crude oil was immediately dissolved in anhydrous DCM for the next step. ^1H NMR (400 MHz, CDCl_3) δ 6.77 (d, $J = 8.9$ Hz, 2H), 6.64 (d, $J = 8.9$ Hz, 2H), 4.13 (dd, $J_1 = 11.1$ Hz, $J_2 = 1.7$ Hz, 1H), 3.90 (dd, $J_1 = 11.1$ Hz, $J_2 = 2.9$ Hz, 1H), 3.32 (mult, 1H), 2.88 (t, $J = 4.8$ Hz, 1H), 2.74 (dd, $J_1 = 4.8$ Hz, $J_2 = 1.4$ Hz, 1H).

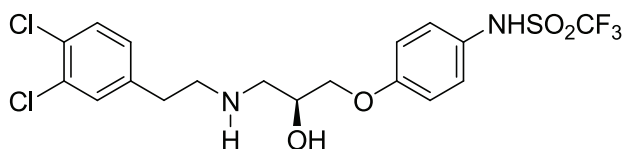
(S)-1,1,1-trifluoro-N-(4-(oxiran-2-ylmethoxy)phenyl)methanesulfonamide (26).

The crude solution of **25** (2.0 g, 12 mmol) in DCM (20.0 mL) was cooled to 0 °C. To this solution, triethylamine was added (1.84 mL, 13.2 mmol, 1.1 equiv), followed by trifluoromethanesulfonic anhydride (2.22 mL, 13.2 mmol, 1.1 equiv). The solution was stirred at 0 °C for 1 hour. After warming to room temperature the mixture was stirred for 12 h. Distilled water (50 mL) was added and the pH was adjusted to 4-5 with aqueous HCl (10% v/v in water). The resulting solution was extracted with DCM (3x 20 mL). The combined organic layers were dried over MgSO₄ and concentrated *in vacuo* to give a brown oil. The crude product was purified by column chromatography on silica gel (5% EtOAc/DCM) to give a yellow oil (0.400 g, 11% over 2 steps). ¹H NMR (400 MHz, CDCl₃) δ 7.22 (d, *J* = 9.0 Hz, 2H), 6.91 (d, *J* = 9.0 Hz, 2H), 4.26 (dd, *J*₁ = 11.1 Hz, *J*₂ = 1.4 Hz, 1H), 3.92 (dd, *J*₁ = 11.1 Hz, *J*₂ = 3.0 Hz, 1H), 3.38 (mult, 1H), 2.95 (t, *J* = 4.4 Hz, 1H), 2.80 (dd, *J*₁ = 4.8 Hz, *J*₂ = 1.3 Hz, 1H). ¹³C NMR (100 MHz, CDCl₃) δ 158.3, 154.6, 127.2, 126.6, 115.7, 69.2, 50.4, 44.9. ¹⁹F NMR (400 MHz, CDCl₃) δ -75.58.

(S)-N-(4-(oxiran-2-ylmethoxy)phenyl)methanesulfonamide (27).

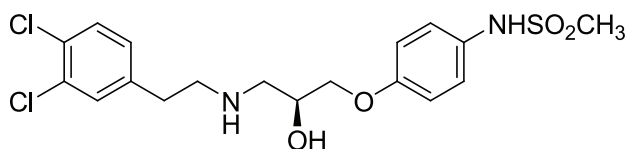
The crude solution of **25** (0.610 g, 3.79 mmol) in DCM (5.0 mL) was cooled to 0 °C. To this solution, N,N-diisopropylethylamine was added (0.58 mL, 4.17 mmol, 1.1 equiv), followed by methanesulfonyl chloride (0.33 mL, 4.17 mmol, 1.1 equiv). The solution stirred at 0 °C for 1 h. After warming to room temperature, 20 mL of distilled water was added and stirred for 20 minutes. The resulting solution was extracted with DCM, and the organics layers were dried over MgSO₄ and concentrated *in vacuo* to give a pink solid. The crude product was purified by column chromatography on silica gel (10% EtOAc/DCM) to give a white solid (0.380 g, 47% over 2 steps). ¹H NMR (400MHz, CDCl₃) δ 7.19 (dd, *J*₁ = 6.9 Hz, *J*₂ = 2.0 Hz, 2H), 6.91 (dd, *J*₁ = 6.9 Hz, *J*₂ = 2.0 Hz, 2H), 4.24 (dd, *J*₁ = 11.2 Hz, *J*₂ = 2.8 Hz, 1H), 3.92 (dd, *J*₁ = 11.2 Hz, *J*₂ = 5.6 Hz, 1H), 3.34-3.36 (mult, 1H), 2.95 (s, 3H), 2.92 (t, *J* = 4.4 Hz, 1H), 2.77 (dd, *J*₁ = 5.6 Hz, *J*₂ = 2.4 Hz, 1H). ¹³C NMR (100 MHz, CDCl₃) δ 39.2, 44.8, 50.5, 69.3, 115.9, 124.8, 129.8, 157.8. LRMS calcd for C₁₀H₁₃NO₄S, 243.05653 [M]⁺; found, 243.06 [M]⁺.

(S)-N-(4-(3-(3,4-dichlorophenethylamino)-2-hydroxypropoxy)phenyl)-1,1,1-trifluoromethanesulfonamide (93-160).



Compound **26** (0.150 g, 0.5 mmol) was dissolved in ethanol (6.0 mL). To this solution, 3,4-dichlorophenethylamine (0.7 mL, 0.5 mmol, 1.0 equiv) was added. The mixture was refluxed for 6 h, before concentrating *in vacuo* to give a yellow oil. The crude material was purified by column chromatography on silica gel (10% EtOH/DCM) to give a white solid (0.051 g, 20%). ^1H NMR (400 MHz, CDCl_3) δ 7.57 (t, $J = 8.9$ Hz, 3H) 7.24 (d, $J = 8.3$ Hz, 2H), 6.81 (d, $J = 8.9$ Hz, 2H), 6.63 (d, $J = 9.2$ Hz, 2H), 4.25-3.94 (mult, 1H), 3.81 (t, $J = 5.1$ Hz, 2H), 3.10-3.02 (mult, 3H), 2.87-2.82 (mult, 3H). ^{19}F NMR (400 MHz, CDCl_3) δ -70.95. HRMS calcd for $\text{C}_{18}\text{H}_{19}\text{Cl}_2\text{F}_3\text{N}_2\text{O}_4\text{S}$, 487.04741 $[\text{M}+\text{H}]^+$; found, 487.04642 $[\text{M}+\text{H}]^+$.
 Anal. ($\text{C}_{18}\text{H}_{19}\text{Cl}_2\text{F}_3\text{N}_2\text{O}_4\text{S}$) C, H, N.

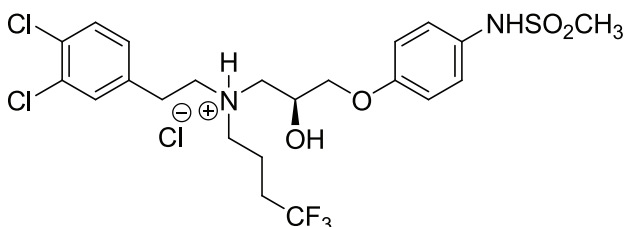
(S)-N-(4-(3-(3,4-dichlorophenethylamino)-2-hydroxypropoxy)phenyl)methanesulfonamide (28).



To a solution of **5** (0.315 g, 1.19 mmol) in ethanol (6.0 mL) was added 3,4-dichlorophenethylamine (0.18 mL, 1.19 mmol, 1.0 equiv) dropwise to give a white heterogeneous suspension. The mixture was refluxed for 6 h. The resulting solution was cooled and then concentrated *in vacuo* to give a yellow oil. The crude product was

purified by column chromatography on silica gel (10% MeOH/DCM) to give a white solid (0.217 g, 42%). ^1H NMR (400 MHz, CDCl_3) δ 7.35 (d, J = 8.4 Hz, 1H), 7.30 (d, J = 2.0 Hz, 1H), 7.18 (dd, J_1 = 6.8 Hz, J_2 = 2.4 Hz, 2H), 7.04 (dd, J_1 = 6.8 Hz, J_2 = 2.4 Hz, 1H), 6.88 (dd, J_1 = 6.8 Hz, J_2 = 2.0 Hz, 2H), 4.05-4.00 (mult, 1H), 3.96 (s, 1H), 3.94 (d, J = 2.4 Hz, 1H), 2.95 (s, 3H), 2.93-2.75 (mult, 6H). ^{13}C NMR (100 MHz, CDCl_3) δ 157.4, 140.3, 130.9, 130.6, 130.5, 123.0, 128.4, 125.0, 115.7, 70.9, 68.3, 51.7, 50.7, 39.2, 35.3. HRMS calcd for $\text{C}_{18}\text{H}_{22}\text{Cl}_2\text{N}_2\text{O}_4\text{S}$, 432.06773 $[\text{M}]^+$; found, 432.0735 $[\text{M}]^+$.

(S)-N-(4-(3-((3,4-dichlorophenethyl)(4,4,4-trifluorobutyl)amino)-2-hydroxypropoxy)phenyl)-methanesulfonamide·HCl (93-155).

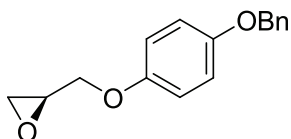


4,4,4-trifluorobutyraldehyde (0.400 g, 0.92 mmol, 1.0 equiv) was added to a solution of **28** (0.116 g, 0.92 mmol, 1.0 equiv) in 1,2-dichloroethane (5.0 mL). The mixture was stirred for 10 minutes before adding sodium triacetoxyborohydride (0.587 g, 2.77 mmol, 3.0 equiv). The grey suspension was stirred for 12 h. After completion, NaHCO_3 (sat'd sol'n, 50 mL) was added and the layers were separated. The organics were dried over MgSO_4 and concentrated *in vacuo* to give a yellow oil. The crude material was purified by column chromatography on silica gel (5% MeOH/DCM) to give a clear oil (0.301 g, 60%). ^1H NMR (400 MHz, CDCl_3) δ 7.34 (d, J = 8.3 Hz, 1H), 7.27 (d, J = 2.0 Hz, 1H), 7.19 (d, J = 8.9 Hz, 2H), 7.01 (d, J = 8.3 Hz, 1H), 6.89 (d, J = 8.9 Hz, 2H), 3.98-3.93

(mult, 1H), 3.92 (d, $J = 4.5$ Hz, 2H), 2.95 (s, 3H), 2.88-2.65 (mult, 5H), 2.06-2.01 (mult, 2H), 1.78-1.63 (mult, 1H). ^{13}C NMR (100 MHz, CDCl_3) δ 149.6, 139.1, 133.3, 130.8, 130.7, 129.6, 128.3, 125.0, 115.7, 70.4, 66.7, 55.7, 53.2, 39.2, 33.0, 31.5, 15.5. HRMS calcd for $\text{C}_{22}\text{H}_{27}\text{Cl}_2\text{F}_3\text{N}_2\text{O}_4\text{S}$, 543.11001 $[\text{M}+\text{H}]^+$; found: 543.10930 $[\text{M}+\text{H}]^+$.

The free amine (0.167 g, 0.31 mmol) was dissolved in ethanol and HCl gas was bubbled through the solution to form **93-155** as the HCl salt upon evaporation of the solvent (0.178 g, quant.) Anal. ($\text{C}_{22}\text{H}_{27}\text{Cl}_2\text{F}_3\text{N}_2\text{O}_4\text{S}\cdot\text{1HCl}$) C, H, N.

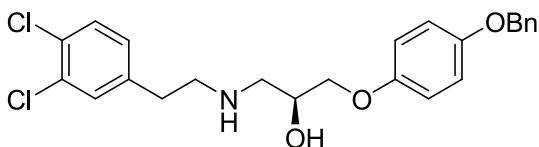
(S)-2-((4-(benzyloxy)phenoxy)methyl)oxirane (30).



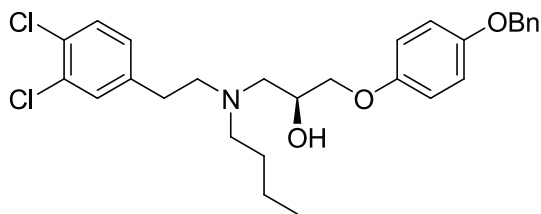
Cesium Fluoride (5.23 g, 34.5 mmol, 3.0 equiv) was added to a solution of 4-benzyloxyphenol (2.3 g, 11.5 mmol) in DMF (12.0 mL). After stirring for 1 h, (*S*)-glycidyl 3-nitrobenzenesulfonate (2.98 g, 11.5 mmol, 1.0 equiv) was added. The reaction was stirred for 24 h at room temperature. The reaction mixture was poured into 300 mL of ice water, and stirred until ice melted. The organics were extracted with EtOAc. The combined organic layers were concentrated *in vacuo* to give a peach solid. The crude product was purified by column chromatography on silica gel to give a white solid (5.09 g, 74%). 99.3 % ee based on chiral HPLC with Chiralcel OD column (46 mm i.d. x 250 mm, eluent hexane-EtOH-Et₂NH 90:10:0.1 v/v; flow rate, 1.0 mL/min; UV monitoring at 254 nm). ^1H NMR (400 MHz, CDCl_3) δ 7.44-7.32 (mult, 5H), 6.93-6.85 (mult, 4H), 5.02 (s,

2H), 4.17 (dd, $J_1 = 10.8$ Hz, $J_2 = 3.2$ Hz, 1H), 3.91 (dd, $J_1 = 11.7$ Hz, $J_2 = 6.0$ Hz, 1H), 3.37-3.32 (mult, 1H), 2.90 (t, $J = 4.8$ Hz, 1H), 2.75 (dd, $J_1 = 4.8$ Hz, $J_2 = 2.4$ Hz, 1H).

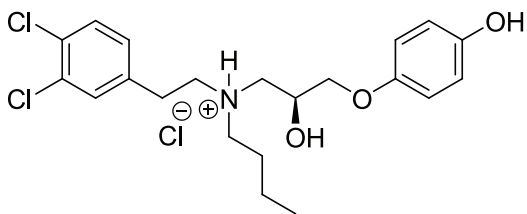
(S)-1-(4-(benzyloxy)phenoxy)-3-(3,4-dichlorophenethylamino)propan-2-ol (31).



To a solution of **30** (5.09 g, 19.9 mmol) in ethanol (60.0 mL) was added 3,4-dichlorophenethylamine (2.95 mL, 19.9 mmol, 1.0 equiv) dropwise. The mixture was refluxed for 7 h, resulting in a colorless solution. The solution was cooled and concentrated *in vacuo* to give a yellow oil. The crude material was purified by column chromatography on silica gel (10% MeOH/DCM) to give a white solid (2.49 g, 28%). ^1H NMR (400 MHz, CDCl_3) δ 7.43-7.30 (mult, 7H), 7.04 (dd, $J_1 = 8.6$ Hz, $J_2 = 2.0$ Hz, 1H), 6.82 (dd, $J_1 = 8.6$ Hz, $J_2 = 2.4$ Hz, 2H), 5.02 (s, 2H), 4.12-3.99 (mult, 1H), 3.92 (s, 1H), 3.91 (d, $J = 1.6$ Hz, 1H), 2.93-2.75 (mult, 6H). ^{13}C NMR (100 MHz, CDCl_3) δ 166.1, 153.4, 153.1, 140.3, 137.4, 130.8, 130.6, 128.8, 128.4, 128.1, 127.7, 116.0, 115.6, 71.2, 70.8, 68.5, 51.8, 50.8, 35.8. HRMS calcd for $\text{C}_{24}\text{H}_{25}\text{Cl}_2\text{NO}_3$, 446.12909 $[\text{M}+\text{H}]^+$; found, 446.1341 $[\text{M}+\text{H}]^+$.

(S)-1-(4-(benzyloxy)phenoxy)-3-(butyl(3,4-dichlorophenethyl)amino)propan-2-ol (32).

Butyraldehyde (4.7 mL, 5.6 mmol, 1.0 equiv) was added to a solution of **31** (2.49 g, 5.6 mmol) in 1,2-dichloroethane (25.0 mL). The mixture was stirred for 10 minutes before adding sodium triacetoxyborohydride (3.5 g, 17 mmol, 3.0 equiv). The grey suspension was stirred for 12 hours. NaHCO₃ (sat'd, 50 mL) was added and the layers were separated. The organics were dried over MgSO₄ and concentrated *in vacuo* to give a yellow oil. The crude material was purified by column chromatography on silica gel (33% Hexanes/EtOAc) to give a white solid (1.71 g, 61%). ¹H NMR (400 MHz, CDCl₃) δ 7.44-7.31 (mult, 6H), 7.27 (d, *J* = 2.0 Hz, 1H), 7.01 (dd, *J*₁ = 8.4 Hz, *J*₂ = 2.4 Hz, 1H), 6.90 (dd, *J*₁ = 6.6 Hz, *J*₂ = 2.0 Hz, 2H), 6.84 (dd, *J*₁ = 6.6 Hz, *J*₂ = 2.8 Hz, 2H), 5.02 (s, 2H), 3.99-3.86 (mult, 3H), 2.83-2.53 (mult, 8H), 1.48-1.41 (mult, 2H), 1.32-1.21 (mult, 2H), 0.92 (t, *J* = 7.2 Hz, 3H). ¹³C NMR (100 MHz, CDCl₃) δ 153.4, 153.3, 140.5, 137.4, 132.5, 130.8, 130.6, 128.8, 128.4, 128.1, 127.7, 116.0, 115.7, 71.0, 70.9, 66.5, 57.4, 55.8, 54.2, 33.0, 29.3, 20.7, 14.2. HRMS calcd for C₂₈H₃₃Cl₂NO₃, 502.19169 [M+H]⁺; found, 502.1945 [M+H]⁺.

(S)-4-(3-(butyl(3,4-dichlorophenethyl)amino)-2-hydroxypropoxy)phenol (93-150).

To a solution of **32** (1.0 g, 2.0 mmol) in ethanol (10.0 mL) was added 5% Pd/C catalyst (0.300 g, 30 wt%). The heterogeneous solution was subjected to hydrogenolysis at 40 psi for 5 h. The resulting mixture was filtered through a pad of Celite, and the filtrate was concentrated *in vacuo* to give a clear oil. The crude material was purified by column chromatography on silica gel (2% MeOH/DCM) to give a white solid (0.456 g, 56%). ^1H NMR (400 MHz, CDCl_3) δ 7.32 (d, $J = 8.4$ Hz, 1H), 7.25 (d, $J = 2.4$ Hz, 1H), 6.99 (dd, $J_1 = 8.0$ Hz, $J_2 = 2.0$ Hz, 1H), 6.73-6.71 (mult, 4H), 3.98-3.89 (mult, 1H), 3.88 (s, 1H), 3.88 (d, $J = 4.8$ Hz, 1H), 2.82-2.49 (m, 8H), 1.42 (dd, $J_1 = 8.4$ Hz, $J_2 = 2.4$ Hz, 2H), 1.28 (dd, $J_1 = 8.0$ Hz, $J_2 = 2.0$ Hz, 2H), 0.90 (t, $J = 7.2$ Hz, 3H). ^{13}C NMR (100 MHz, CDCl_3) δ 152.8, 150.2, 140.5, 132.5, 130.8, 130.5, 130.3, 128.4, 116.3, 115.8, 70.9, 66.6, 57.1, 55.7, 54.1, 32.9, 29.3, 20.7, 14.2. HRMS calcd for $\text{C}_{21}\text{H}_{27}\text{Cl}_2\text{NO}_3$, 412.14474 $[\text{M}+\text{H}]^+$; found, 412.14530 $[\text{M}+\text{H}]^+$.

The amine was dissolved in ethanol and HCl gas was bubbled through the solution to give **93-150** as the HCl salt upon evaporation of the solvent. Anal ($\text{C}_{21}\text{H}_{27}\text{Cl}_2\text{NO}_3 \cdot 1\text{HCl}$) C, H, N.

1.6.2. Combustion analysis (Atlantic Microlab, Inc)

Compound ID	Molecular Formula	Theoretical	Experimental
93-160	C ₁₈ H ₁₉ Cl ₂ F ₃ N ₂ O ₄ S	C: 44.36, H: 3.93, N: 5.75	C: 44.55, H: 3.91, N:5.77
93-155	C ₂₂ H ₂₇ Cl ₂ F ₃ N ₂ O ₄ S·1HCl	C: 45.57, H: 4.87, N: 4.83	C: 45.70, H: 4.90, N: 4.78
93-150	C ₂₁ H ₂₇ Cl ₂ NO ₃ ·1HCl	C: 56.20, H: 6.29, N: 3.12	C: 56.12, H: 6.22, N: 3.09

All values are within $\pm 0.4\%$

1.6.3. Determination of pK_a values

A PCA200 pK_a Titrator (Sirius Analytical Instruments, East Sussex, UK) was used to determine pK_a values. Refinement Pro Software (Sirius Analytical Instruments, East Sussex, UK) was used to analyzed data from the titrations.

A representative example procedure is as follows: MK-801 (2-5 mg) was dissolved at 1.3 mM in 80% MeOH/water (v/v) with 0.15 M KCl. Three serial titrations were performed from pH 2 to 12. The pK_a was determined by the Yasuda-Shedlovsky extrapolation as described by the manufacturer.

1.6.4. Calculation of percent protonated species

The Henderson-Hasselbach equation was used to determine the percentage of protonated drug species at a given pH. The pKa values determined in the course of this study or the values reported in the literature were utilized in the calculations. The pHs of interest were 6.9 and 7.6, thus the fraction of protonated drug ([HA]) was calculated at each pH.

The Henderson-Hasselbach equation is as follows:

$pH = pK_a + \log([A^-]/[HA])$ refers to the ionization: $HA + H_2O \leftrightarrow H_3O^+ + A^-$

An example calculation for determining the fraction of protonated MK-801 ($pK_a = 8.37$)

at pH 6.9 is as follows:

$$pH = pK_a + \log([A^-]/[HA])$$

$$6.9 = 8.37 + \log([A^-]/[HA])$$

$$-1.47 = \log([A^-]/[HA])$$

$$0.0338844 = [A^-]/[HA]$$

$$[A^-] = 0.338844 * [HA]$$

The fraction of ionized drug corresponds to:

$$[HA] = [HA]/([HA] + [A^-])$$

$$[HA] = [HA]/([HA] + 0.338844 * [HA])$$

$$[HA] = 1/1.0338844$$

$$[HA] = 0.967 = 96.7\%$$

Therefore, 96.7% of MK-801 is protonated at pH 6.9.

1.7. Biology Experimental Detail

1.7.1. In vitro NMDA antagonism assay (Dr. Stephen Traynelis Laboratory, Emory University School of Medicine)

Expression of glutamate receptors in *Xenopus laevis* oocytes.

All protocols involving the use of animals were approved by the Emory University IACUC. crRNA was synthesized from linearized template cDNA for rat glutamate receptor subunits according to manufacturer specifications (Ambion).

Quality of synthesized cRNA was assessed by gel electrophoresis, and quantity was estimated by spectroscopy and gel electrophoresis. Stage V and VI oocytes were surgically removed from the ovaries of large, well-fed and healthy *Xenopus laevis* anesthetized with 3-amino-benzoic acid ethyl ester (1-3 gm/l) as previously described.¹⁰⁵ Clusters of isolated oocytes were incubated with 292 U/ml Worthington (Freehold, NJ) type IV collagenase or 1.3 mg/ml collagenase (Life Technologies, Gaithersburg, MD; 17018-029) for 2 hr in Ca²⁺-free solution comprised of (in mM) 89 NaCl, 1 KCl, 2.4 NaHCO₃, 0.82 MgSO₄, 10 HEPES, with slow agitation to remove the follicular cell layer. Oocytes were then washed extensively in the same solution and maintained in Barth's solution comprised of (in mM) 88 NaCl, 1 KCl, 2.4 NaHCO₃, 10 HEPES, 0.82 MgSO₄, 0.33 Ca(NO₃)₂, and 0.91 CaCl₂ and supplemented with 100 µg/ml gentamycin, 10 µg/ml streptomycin, and 10 µg/ml penicillin. Oocytes were manually defolliculated and injected within 24 hrs of isolation with 3-5 ng of NR1-1a (hereafter NR1) subunit and 7-10 ng of NR2 subunit in a 50 nl volume, or 5-10 ng in 50 nl of AMPA or kainate receptor cRNAs, and incubated in Barth's solution at 15°C for 1-7 d. Glass injection pipettes had tip sizes ranging from 10-20 microns, and were backfilled with mineral oil.

Two electrode voltage clamp recording from *Xenopus laevis* oocytes

Two electrode voltage-clamp recordings were made 2-7 days post-injection as previously described.¹⁰⁵ Oocytes were placed in a dual-track plexiglass recording chamber with a single perfusion line that splits in a Y-configuration to perfuse two

oocytes. Dual recordings were made at room temperature (23°C) using two Warner OC725B or OC725C two-electrode voltage clamp amplifiers, arranged as recommended by the manufacturer. Glass microelectrodes (1-10 Megaohms) were filled with 300 mM KCl (voltage electrode) or 3 M KCl (current electrode). The bath clamps communicated across silver chloride wires placed into each side of the recording chamber, both of which were assumed to be at a reference potential of 0 mV. Oocytes were perfused with a solution comprised of (in mM) 90 NaCl, 1 KCl, 10 HEPES, and 0.5 BaCl₂; pH was adjusted to 7.4 or 7.6 by addition of 1 M NaOH. Oocytes expressing NR1/NR2A were pre-incubated before recording in recording solution supplemented with 50 μM BAPTA-AM at room temperature. Oocytes were recorded under voltage clamp at -40 mV. Final concentrations for control application of glutamate (50-100 μM) plus glycine (30 μM) to oocytes expressing NMDA receptors were achieved by dilution from 100 and 30-100 mM stock solutions, respectively. In addition, 10 μM final EDTA was obtained by adding a 1:1000 dilution of 10 mM EDTA, in order to chelate contaminant divalent ions such as extracellular Zn²⁺. Homomeric GluR1 AMPA receptors were activated by 100 μM glutamate. Homomeric GluR6 kainate receptors were incubated in concanavalin A (10 μM) for 5 minutes, and activated by 100 μM glutamate. Concentration-response curves for experimental compounds acting on NMDA receptors were obtained by applying in successive fashion a maximally effective concentration of glutamate/glycine, followed by glutamate/glycine plus variable concentrations of experimental compounds. Concentration-response curves consisting of 5 to 8 concentrations were obtained in this manner. The baseline leak current at -40 mV was measured before and

after recording, and the full recording linearly corrected for any change in leak current. Oocytes with glutamate-evoked responses smaller than 50 nA were not included in the analysis. The level of inhibition produced by experimental compounds was expressed as a percent of the initial glutamate response, and averaged together across oocytes from a single frog. Each experiment consisted of recordings from 3 to 10 oocytes obtained from a single frog. Results from ≥ 3 experiments using oocytes from 3 different frogs were pooled, and the percent responses at antagonist concentrations for each oocyte were fitted by the equation,

$$\text{Percent Response} = (100 - \text{minimum}) / (1 + ([\text{conc}] / IC_{50})^{nH}) + \text{minimum}$$

where *minimum* is the residual percent response in saturating concentration of the experimental compounds, IC_{50} is the concentration of antagonist that causes half of the achievable inhibition, and nH is a slope factor describing steepness of the inhibition curve. *Minimum* was constrained to be greater than or equal to 0.

1.7.2. *In vitro* binding studies for secondary effects (MDS Pharma, Inc.)

Compounds were evaluated for binding to the human ether-a-go-go potassium channel (hERG) expressed in HEK293 cells by displacement of ^3H -astemizole according to the methods by Finlayson et al.¹¹⁸ Compounds were incubated at 10 μM , in duplicate, and the amount of ^3H -astemizole determined by liquid scintillation spectroscopy. In some cases, a seven concentration (each concentration in duplicate) displacement curve was generated to determine IC_{50} .

K_i values for human hERG channels determined by displacement of 1.5 nM ^3H astemizole from HEK-293 cell membranes transfected with human recombinant hERG channels (MDS Pharma). Data from multipoint displacement curves were fit by a non-linear, least squares regression analysis and the K_i calculated using the Cheng and Prusoff equation.

References

- (1) Park, C. K.; Nehls, D. G.; Graham, D. I.; Teasdale, G. M.; McCulloch, J. *Ann. Neurol.* **1988**, *24*, 543.
- (2) Dirnagl, U.; Iadecola, C.; Moskowitz, M. A. *Trends Neurosci.* **1999**, *22*, 391.
- (3) Whetsell, W. O., Jr. *J. Neuropathol. Exp. Neurol.* **1996**, *55*, 1.
- (4) Lipton, S. A. *Curr. Opin. Neurol. Neurosurg.* **1993**, *6*, 588.
- (5) Wang, C. X.; Shuaib, A. *Curr Drug Targets CNS Neurol Disord* **2005**, *4*, 143.
- (6) Loftis, J. M.; Janowsky, A. *Pharmacol. Ther.* **2003**, *97*, 55.
- (7) Dunah, A. W.; Wang, Y.; Yasuda, R. P.; Kameyama, K.; Haganir, R. L.; Wolfe, B. B.; Standaert, D. G. *Mol. Pharmacol.* **2000**, *57*, 342.
- (8) Hallett, P. J.; Standaert, D. G. *Pharmacol. Ther.* **2004**, *102*, 155.
- (9) Dickenson, A. H.; Chapman, V.; Green, G. M. *Gen. Pharmacol.* **1997**, *28*, 633.
- (10) Dickenson, A. H.; Sullivan, A. F. *Neuropharmacology* **1987**, *26*, 1235.
- (11) Boyce, S.; Wyatt, A.; Webb, J. K.; O'Donnell, R.; Mason, G.; Rigby, M.; Sirinathsinghji, D.; Hill, R. G.; Rupniak, N. M. *Neuropharmacology* **1999**, *38*, 611.
- (12) Standaert, D. G.; Testa, C. M.; Young, A. B.; Penney, J. B., Jr. *J. Comp. Neurol.* **1994**, *343*, 1.
- (13) Henneberry, R. C. *Neurobiol. Aging* **1989**, *10*, 611.
- (14) Snyder, E. M.; Nong, Y.; Almeida, C. G.; Paul, S.; Moran, T.; Choi, E. Y.; Nairn, A. C.; Salter, M. W.; Lombroso, P. J.; Gouras, G. K.; Greengard, P. *Nat. Neurosci.* **2005**, *8*, 1051.
- (15) Beal, M. F. *Ann. Neurol.* **1992**, *31*, 119.

- (16) Olney, J. W.; Wozniak, D. F.; Farber, N. B. *Arch. Neurol.* **1997**, *54*, 1234.
- (17) Li, L.; Fan, M.; Icton, C. D.; Chen, N.; Leavitt, B. R.; Hayden, M. R.; Murphy, T. H.; Raymond, L. A. *Neurobiol. Aging* **2003**, *24*, 1113.
- (18) Estrada Sanchez, A. M.; Mejia-Toiber, J.; Massieu, L. *Arch. Med. Res.* **2008**, *39*, 265.
- (19) Fan, M. M.; Raymond, L. A. *Prog. Neurobiol.* **2007**, *81*, 272.
- (20) Chesler, M. *Prog. Neurobiol.* **1990**, *34*, 401.
- (21) Chesler, M.; Kaila, K. *Trends Neurosci.* **1992**, *15*, 396.
- (22) Amato, A.; Ballerini, L.; Attwell, D. *J. Neurophysiol.* **1994**, *72*, 1686.
- (23) Traynelis, S. F.; Cullcandy, S. G. *Nature* **1990**, *345*, 347.
- (24) Mott, D. D.; Doherty, J. J.; Zhang, S.; Washburn, M. S.; Fendley, M. J.; Lyuboslavsky, P.; Traynelis, S. F.; Dingledine, R. *Nat. Neurosci.* **1998**, *1*, 659.
- (25) Tahirovic, Y. A.; Geballe, M.; Gruszecka-Kowalik, E.; Myers, S. J.; Lyuboslavsky, P.; Le, P.; French, A.; Irier, H.; Choi, W. B.; Easterling, K.; Yuan, H.; Wilson, L. J.; Kotloski, R.; McNamara, J. O.; Dingledine, R.; Liotta, D. C.; Traynelis, S. F.; Snyder, J. P. *J. Med. Chem.* **2008**, *51*, 5506.
- (26) Dingledine, R.; Borges, K.; Bowie, D.; Traynelis, S. F. *Pharmacol. Rev.* **1999**, *51*, 7.
- (27) Loftis, J. M.; Janowsky, A. *Pharmacol. Ther.* **2003**, *97*, 55.
- (28) Mayer, M. L.; Armstrong, N. *Annu. Rev. Physiol.* **2004**, *66*, 161.
- (29) Lisman, J. *Philos T Roy Soc B* **2003**, *358*, 829.
- (30) Miyamoto, E. *J Pharmacol Sci* **2006**, *100*, 433.
- (31) Rudhard, Y.; Kneussel, M.; Nassar, M. A.; Rast, G. F.; Annala, A. J.; Chen, P. E.; Tigaret, C. M.; Dean, I.; Roes, J.; Gibb, A. J.; Hunt, S. P.; Schoepfer, R. *J. Neurosci.* **2003**, *23*, 2323.
- (32) Colonnese, M. T.; Zhao, J. P.; Constantine-Paton, M. *J. Neurosci.* **2005**, *25*, 1291.
- (33) Colonnese, M. T.; Constantine-Paton, M. *J. Comp. Neurol.* **2006**, *494*, 738.
- (34) Waters, K. A.; Machaalani, R. *Resp Physiol Neurobi* **2005**, *149*, 123.
- (35) Akazawa, C.; Shigemoto, R.; Bessho, Y.; Nakanishi, S.; Mizuno, N. *J. Comp. Neurol.* **1994**, *347*, 150.
- (36) Vicini, S.; Wang, J. F.; Li, J. H.; Zhu, W. J.; Wang, Y. H.; Luo, J. H.; Wolfe, B. B.; Grayson, D. R. *J. Neurophysiol.* **1998**, *79*, 555.
- (37) Popescu, G. *Cell. Mol. Life Sci.* **2005**, *62*, 2100.

- (38) Rothman, S. M.; Olney, J. W. *Ann. Neurol.* **1986**, *19*, 105.
- (39) Lipton, S. A.; Rosenberg, P. A. *N. Engl. J. Med.* **1994**, *330*, 613.
- (40) Petrenko, A. B.; Yamakura, T.; Baba, A.; Shimoji, K. *Anesth. Analg.* **2003**, *97*, 1108.
- (41) Muir, K. W. *Curr. Opin. Pharmacol.* **2006**, *6*, 53.
- (42) Albers, G. W.; Atkinson, R. P.; Kelley, R. E.; Rosenbaum, D. M. *Stroke* **1995**, *26*, 254.
- (43) Muir, K. W.; Lees, K. R. *Stroke* **1995**, *26*, 503.
- (44) Merchant, R. E.; Bullock, M. R.; Carmack, C. A.; Shah, A. K.; Wilner, K. D.; Ko, G.; Williams, S. A. *Ann. N.Y. Acad. Sci.* **1999**, *890*, 42.
- (45) Saltarelli, M. D.; Weaver, J. J.; Hsu, C.; Bednar, M. M. *Stroke* **2004**, *35*, 241.
- (46) Nicholson, K. L.; Mansbach, R. S.; Menniti, F. S.; Balster, R. L. *Behav. Pharmacol.* **2007**, *18*, 731.
- (47) Johnson, J. W.; Kotermanski, S. E. *Curr. Opin. Pharmacol.* **2006**, *6*, 61.
- (48) Parsons, C. G.; Danysz, W.; Quack, G. *Neuropharmacology* **1999**, *38*, 735.
- (49) Lipton, S. A. *Nat Rev Neurosci* **2007**, *8*.
- (50) Gerber, A. M.; Vallano, M. L. *Mini-Rev. Med. Chem.* **2006**, *6*, 805.
- (51) Kalia, L. V.; Kalia, S. K.; Salter, M. W. *Lancet Neurology* **2008**, *7*, 742.
- (52) Lipton, S. A. *J Alzheimers Dis* **2004**, *6*, S61.
- (53) Robinson, D. M.; Keating, G. M. *Drugs* **2006**, *66*, 1515.
- (54) Wong, E. H.; Kemp, J. A.; Priestley, T.; Knight, A. R.; Woodruff, G. N.; Iversen, L. L. *Proc. Natl. Acad. Sci. U. S. A.* **1986**, *83*, 7104.
- (55) Cai, S. X. *Curr. Top. Med. Chem.* **2006**, *6*, 651.
- (56) Cai, S. X.; Kher, S. M.; Zhou, Z. L.; Ilyin, V.; Espitia, S. A.; Tran, M.; Hawkinson, J. E.; Woodward, R. M.; Weber, E.; Keana, J. F. W. *J. Med. Chem.* **1997**, *40*, 730.
- (57) Woodward, R. M.; Huettner, J. E.; Guastella, J.; Keana, J. F.; Weber, E. *Mol. Pharmacol.* **1995**, *47*, 568.
- (58) Petty, M. A.; Weintraub, P. M.; Maynard, K. I. *Cns Drug Rev* **2004**, *10*, 337.
- (59) Jarvis, M. F.; Murphy, D. E.; Williams, M.; Gerhardt, S. C.; Boast, C. A. *Synapse* **1988**, *2*, 577.

- (60) Lehmann, J.; Hutchison, A. J.; McPherson, S. E.; Mondadori, C.; Schmutz, M.; Sinton, C. M.; Tsai, C.; Murphy, D. E.; Steel, D. J.; Williams, M.; et al. *J. Pharmacol. Exp. Ther.* **1988**, *246*, 65.
- (61) Dawson, D. A.; Wadsworth, G.; Palmer, A. M. *Brain Res.* **2001**, *892*, 344.
- (62) Gogas, K. R. *Curr Opin Pharmacol* **2006**, *6*, 68.
- (63) Chazot, P. L. *Curr. Med. Chem.* **2004**, *11*, 389.
- (64) Waxman, E. A.; Lynch, D. R. *Neuroscientist* **2005**, *11*, 37.
- (65) Wei, F.; Wang, G. D.; Kerchner, G. A.; Kim, S. J.; Xu, H. M.; Chen, Z. F.; Zhuo, M. *Nat. Neurosci.* **2001**, *4*, 164.
- (66) Monyer, H.; Burnashev, N.; Laurie, D. J.; Sakmann, B.; Seeburg, P. H. *Neuron* **1994**, *12*, 529.
- (67) Layton, M. E.; Kelly, M. J.; Rodzinak, K. J. *Curr. Top. Med. Chem.* **2006**, *6*, 697.
- (68) Williams, K. *Mol. Pharmacol.* **1993**, *44*, 851.
- (69) Chenard, B. L.; Menniti, F. S. *Curr. Pharm. Des.* **1999**, *5*, 381.
- (70) Nikam, S. S.; Meltzer, L. T. *Curr. Pharm. Des.* **2002**, *8*, 845.
- (71) Borza, I.; Domany, G. *Curr Top Med Chem* **2006**, *6*, 687.
- (72) Chenard, B. L.; Bordner, J.; Butler, T. W.; Chambers, L. K.; Collins, M. A.; Decosta, D. L.; Ducat, M. F.; Dumont, M. L.; Fox, C. B.; Mena, E. E.; Menniti, F. S.; Nielsen, J.; Pagnozzi, M. J.; Richter, K. E. G.; Ronau, R. T.; Shalaby, I. A.; Stemple, J. Z.; White, W. F. *J. Med. Chem.* **1995**, *38*, 3138.
- (73) Jamieson, C.; Moir, E. M.; Rankovic, Z.; Wishart, G. *J. Med. Chem.* **2006**, *49*, 5029.
- (74) McCauley, J. A.; Theberge, C. R.; Romano, J. J.; Billings, S. B.; Anderson, K. D.; Claremon, D. A.; Freidinger, R. M.; Bednar, R. A.; Mosser, S. D.; Gaul, S. L.; Connolly, T. M.; Condra, C. L.; Xia, M.; Cunningham, M. E.; Bednar, B.; Stump, G. L.; Lynch, J. J.; Macaulay, A.; Wafford, K. A.; Koblan, K. S.; Liverton, N. J. *J. Med. Chem.* **2004**, *47*, 2089.
- (75) Barta-Szalai, G.; Borza, I.; Bozo, E.; Kiss, C.; Agai, B.; Proszenyak, A.; Keseru, G. M.; Gere, A.; Kolok, S.; Galgoczy, K.; Horvath, C.; Farkas, S.; Domany, G. *Bioorg. Med. Chem. Lett.* **2004**, *14*, 3953.
- (76) Borza, I.; Kolok, S.; Gere, A.; Agai-Csongor, E.; Agai, B.; Tarkanyi, G.; Horvath, C.; Barta-Szalai, G.; Bozo, E.; Kiss, C.; Bielik, A.; Nagy, J.; Farkas, S.; Domany, G. *Bioorg. Med. Chem. Lett.* **2003**, *13*, 3859.
- (77) Giffard, R. G.; Monyer, H.; Christine, C. W.; Choi, D. W. *Brain Res.* **1990**, *506*, 339.

- (78) Tang, C. M.; Dichter, M.; Morad, M. *Proc. Natl. Acad. Sci. U. S. A.* **1990**, *87*, 6445.
- (79) Traynelis, S. F.; Cullcandy, S. G. *J Physiol-London* **1991**, *433*, 727.
- (80) Siesjo, B. K. *Prog. Brain Res.* **1985**, *63*, 121.
- (81) Silver, I. A.; Erecinska, M. J. *Cereb. Blood Flow Metab.* **1992**, *12*, 759.
- (82) Jendelova, P.; Sykova, E. *Glia* **1991**, *4*, 56.
- (83) Sykova, E.; Svoboda, J. *Brain Res.* **1990**, *512*, 181.
- (84) Lees, K. R. *Neurology* **1997**, *49*, S66.
- (85) Bath, C. P.; Farrell, L. N.; Gilmore, J.; Ward, M. A.; Hicks, C. A.; O'Neill, M. J.; Bleakman, D. *Eur. J. Pharmacol.* **1996**, *299*, 103.
- (86) Traynelis, S. F.; Liotta, D. C.; Snyder, J. P.; Altas, Y.; Mott, D. D.; Doherty, J. J.; Dingledine, R. (Emory University, USA). pH-Dependent NMDA Receptor Antagonists. WO 2002072542, September 19, 2002.
- (87) Dingledine, R. J.; Traynelis, S. F.; Liotta, D. C. (Emory University, USA). Methods of Identifying Improved NMDA Receptor Antagonists. WO 2009061935, May 14, 2009.
- (88) Roden, D. M. *N. Engl. J. Med.* **2004**, *350*, 2620.
- (89) Guth, B. D. *Toxicol. Sci.* **2007**, *97*, 4.
- (90) Finlayson, K.; Witchel, H. J.; McCulloch, J.; Sharkey, J. *Eur. J. Pharmacol.* **2004**, *500*, 129.
- (91) Sanguinetti, M. C.; Tristani-Firouzi, M. *Nature* **2006**, *440*, 463.
- (92) Sanguinetti, M. C.; Jiang, C. G.; Curran, M. E.; Keating, M. T. *Cell* **1995**, *81*, 299.
- (93) Trudeau, M. C.; Warmke, J. W.; Ganetzky, B.; Robertson, G. A. *Science* **1995**, *269*, 92.
- (94) Cabral, J. H. M.; Lee, A.; Cohen, S. L.; Chait, B. T.; Li, M.; Mackinnon, R. *Cell* **1998**, *95*, 649.
- (95) Zhou, Y. F.; Morais-Cabral, J. H.; Kaufman, A.; MacKinnon, R. *Nature* **2001**, *414*, 43.
- (96) Abbott, G. W.; Sesti, F.; Splawski, I.; Buck, M. E.; Lehmann, W. H.; Timothy, K. W.; Keating, M. T.; Goldstein, S. A. N. *Cell* **1999**, *97*, 175.
- (97) Mitcheson, J. S.; Chen, J.; Lin, M.; Culberson, C.; Sanguinetti, M. C. *Proc. Natl. Acad. Sci. U. S. A.* **2000**, *97*, 12329.
- (98) Fernandez, D.; Ghanta, A.; Kauffman, G. W.; Sanguinetti, M. C. *J. Biol. Chem.* **2004**, *279*, 10120.

- (99) Rampe, D.; Wible, B.; Brown, A. M.; Dage, R. C. *Mol. Pharmacol.* **1993**, *44*, 1240.
- (100) Woosley, R. L. *Annu. Rev. Pharmacool. Toxicol.* **1996**, *36*, 233.
- (101) Fletcher, S. R.; Burkamp, F.; Blurton, P.; Cheng, S. K. F.; Clarkson, R.; O'Connor, D.; Spinks, D.; Tudge, M.; van Niel, M. B.; Patel, S.; Chapman, K.; Marwood, R.; Shephard, S.; Bentley, G.; Cook, G. P.; Bristow, L. J.; Castro, J. L.; Hutson, P. H.; MacLeod, A. M. *J. Med. Chem.* **2002**, *45*, 492.
- (102) Kitaori, K.; Furukawa, Y.; Yoshimoto, H.; Otera, J. *Tetrahedron* **1999**, *55*, 14381.
- (103) Sajiki, H.; Hattori, K.; Hirota, K. *J. Org. Chem.* **1998**, *63*, 7990.
- (104) Sajiki, H.; Hattori, K.; Hirota, K. *Chem-Eur J* **2000**, *6*, 2200.
- (105) Traynelis, S. F.; Burgess, M. F.; Zheng, F.; Lyuboslavsky, P.; Powers, J. L. *J. Neurosci.* **1998**, *18*, 6163.
- (106) Kashiwagi, K.; Pahk, A. J.; Masuko, T.; Igarashi, K.; Williams, K. *Mol. Pharmacol.* **1997**, *52*, 701.
- (107) Dravid, S. M.; Erreger, K.; Yuan, H. J.; Nicholson, K.; Le, P.; Lyuboslavsky, P.; Almonte, A.; Murray, E.; Mosely, C.; Barber, J.; French, A.; Balster, R.; Murray, T. F.; Traynelis, S. F. *J. Physiol-London* **2007**, *581*, 107.
- (108) Sobolevsky, A. I.; Koshelev, S. G.; Khodorov, B. I. *J. Neurosci.* **1999**, *19*, 10611.
- (109) Sobolevskii, A. I.; Khodorov, B. I. *Neurosci. Behav. Physiol.* **2002**, *32*, 157.
- (110) Blanpied, T. A.; Clarke, R. J.; Johnson, J. W. *J. Neurosci.* **2005**, *25*, 3312.
- (111) Yuan, H. J.; Erreger, K.; Dravid, S. M.; Traynelis, S. F. *J. Biol. Chem.* **2005**, *280*, 29708.
- (112) Macdonald, J. F.; Bartlett, M. C.; Mody, I.; Pahapill, P.; Reynolds, J. N.; Salter, M. W.; Schneiderman, J. H.; Pennefather, P. S. *J. Physiol-London* **1991**, *432*, 483.
- (113) Moffat, A. C.; Osselton, M. D.; Widdop, B.; 3rd ed. Vol. 2; Pharmaceutical Press: London, 2004.
- (114) Mozayani, A. *Forensic Sci. Rev.* **2003**, *15*, 62.
- (115) Freudenthaler, S.; Meineke, I.; Schreeb, K. H.; Boakye, E.; Gundert-Remy, U.; Gleiter, C. H. *Br. J. Clin. Pharmacol.* **1998**, *46*, 541.
- (116) Jorgensen, W. L. *Science* **2004**, *303*, 1813.
- (117) Liotta, D. C.; Snyder, J. P.; Traynelis, S. F.; Wilson, L. J.; Mosley, C. A.; Dingledine, R. J.; Myers, S.; Tahirovic, Y. A. (Emory University, USA and NeurOp, Inc., USA). NMDA Receptor Antagonists for Neuroprotection. WO 2009006437, January 8, 2009.

(118) Finlayson, K.; Turnbull, L.; January, C. T.; Sharkey, J.; Kelly, J. S. *Eur. J. Pharmacol.* **2001**, *430*, 147.

Chapter 2. Design, Synthesis, and Biological Evaluation of NR1/NR2B-Selective NMDA Receptor Antagonists

2.1 Statement of Purpose

The Traynelis lab found a number of additional compounds further to the aforementioned propanolamine series (discussed in Chapter 1) during their search for NR2B-selective NMDA antagonists. A second class, exemplified by compound **211** (Figure 2.1), is characterized by a thiosemicarbazide backbone. We hypothesized that this class may represent a generalized scaffold which could be optimized based on structural similarity to the previously developed propanolamines. We envisaged compounds of this type may have intrinsically decreased hERG activity due to the lack of a centrally located amine which could be protonated at physiological pH, and thus would not associate with the lumen of the K⁺ channel.

Design of **211** analogues would encompass a four-pronged approach towards safe and effective NR2B-selective pH dependent NMDA receptor antagonist (heretofore referred to as 96 series compounds). Exemplary compounds would potentially exhibit four important properties:

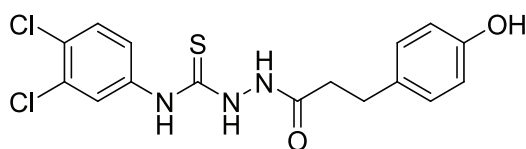
1. Selectivity for NR1/NR2B-containing NMDA receptors over other glutamate family subtype receptors.
2. Potency against NR1/NR2B-containing NMDA receptors.
3. A large therapeutic index for NMDA versus off-target binding.

4. Increased activity at acidic pH values relative to physiologic pH (i.e. exhibit fold shift).

In addition, drug-like characteristics in terms of absorption, distribution, metabolism, and excretion (ADME) parameters, as well as and *in vivo* biological activity as neuroprotectants is required. These project goals were achieved using the following strategy:

1. A series of novel antagonists based on **211** were synthesized.
2. The novel analogs were tested for *in vitro* NMDA receptor activity in NR2A-, NR2B-, NR2C-, and NR2D-containing NMDA receptors at pH 6.9 and pH 7.6. In addition, kainate and AMPA receptor activity was measured. All *in vitro* biological evaluation of NMDA receptors were carried out in the laboratory of Dr. Stephen Traynelis in the Emory School of Medicine Department of Pharmacology.
3. Off-target *in vitro* monoamine receptor activity of all compounds less than 500 nM was determined.
4. Pharmacokinetics studies on most active analogues were conducted *in vivo* (rat).
5. Locomotor effects were analyzed using the Rotarod assay *in vivo* (mice).
6. An *in vitro* analysis of neuroprotection was performed using the lactate dehydrogenase (LDH) assay.
7. An *in vivo* (mice) ischemic stroke model, the middle cerebral arterial occlusion model (MCAO), with the most active analogue was conducted.

8. An *in vivo* neuropathic pain study (mice) with the most active analogue was performed.
9. *In vitro* brain penetration studies for selected analogues were determined.
10. Molecular modeling and mutagenesis studies were utilized to determine where the most active compounds bind the receptor.

**211****Figure 2.1 Thiosemicarbazide 211, screening hit**

2.2 Introduction and Background

2.2.1. Biological Screening Hit and Medicinal Chemistry Program Rationale

The Traynelis group came to be interested in **211** (Figure 2.1) during the course of a biological screen for NR1/NR2B-containing NMDA receptor antagonists. Compound **211** was thought to be an inhibitor of the ifenprodil binding site on the amino terminal domain, similar to the compounds described in Chapter 1. Structural similarities rapidly became apparent when comparing **211** to enantiomeric propranolamine **93-4** (Figure 2.2).

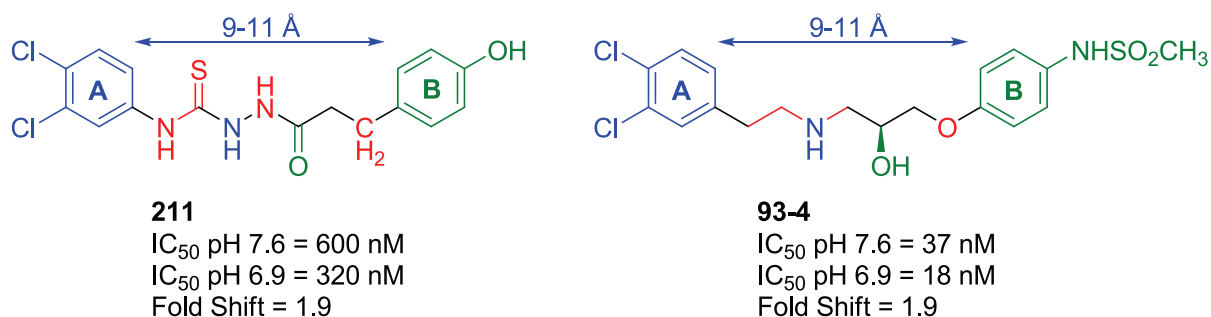


Figure 2.2 Comparison of screening hit **211** and enantiomeric propanolamine **93-4**.

Definite similarities are indicated in blue, indefinite similarities in green, and differences in red.

Exact similarities between **211** and **93-4** (highlighted in blue, Figure 2.2) include a 3,4-dichlorophenyl A ring, a seven atom linker bridging the A and B phenyl rings comprising a distance of 9-11 Å, and an amine located at position 3 of the linker. Diffuse similarities (highlighted in green, Figure 2.2) include an oxygen substituent at position C5 of the linker. However, the oxidation state between the two compounds differs, with **211** containing a carbonyl compared to the alcohol of **93-4**. Both compounds also contain a hydrogen bond donor substituent at the *para* position of the B ring. Compound **211** has a hydroxyl whereas **93-4** bears a methanesulfonamide. There are particularly significant differences in the compounds (highlighted in red, Figure 2.2). The first is the lack of a phenoxy oxygen at position 7 of the linker in **211**. The second is the heteroatom-laden thiosemicarbazide linker functionality present in **211** compared with the simple β -amino alcohol of **93-4**.

Compound **211** exhibited activity *in vitro* against NR2B-containing NMDA receptors with an IC_{50} of 320 nM at pH 6.9 and an IC_{50} of 600 nM at 7.6, giving a fold shift of 1.9. Although the potency at both pH values is significantly less than **93-4**, the

fold shifts between the two are essentially identical. Inspired by success in the enantiomeric propanolamine series at incorporating fold shift using medicinal chemistry methods, compound **211** offered a potential starting point for such an effort on a novel (albeit structurally similar) scaffold. Furthermore, we hypothesized **211** would be a poor substrate for hERG binding due to the lack of a centrally located amine, which would be protonated at physiologic pH. In theory **211** cannot make cation- π interactions with Tyr652 of the K⁺ channel, and represents an inherently safer drug compared with **93-4** or other basic amine-based NMDA receptor antagonists.

Although the two scaffolds are similar, the Liotta group sought to distinguish the subtleties of the thiosemicarbazide scaffold compared to the enantiomeric propanolamine series. This included an investigation into A and B ring modifications as well as changes within the linker region. The structure activity relationships of on-target NR1/NR2B NMDA receptor potency, fold shift, and off-target (hERG and α_1 -adrenergic receptors) binding were explored to determine if, and to what extent, lessons gleaned from enantiomeric propanolamine series optimization could be transferrable to a secondary scaffold. Issues to be addressed throughout the course of the medicinal chemistry effort around thiosemicarbazide **211** included:

1. Is the 3,4-dichloro A ring substitution optimal in both series?
2. Is a basic nitrogen required in the linker region for fold shift?
3. Does alkylation of the centrally located nitrogen increase fold shift?

4. How does affecting the basicity of the nitrogen influence hERG and α_1 -adrenergic binding? Can these effects be differentiated from on-target potency and fold shift?
5. Is the optimal linker length 7 atoms in both series?
6. How does linker geometry affect NMDA potency, off-target binding, and fold shift?
7. What is the optimal B ring substitution?

2.2.2. The α_1 -adrenergic receptor

The enantiomeric propanolamines, in addition to having nanomolar potency at the hERG channel, also had high affinity for the α_1 -adrenergic receptor.¹ The adrenergic receptors are G-protein coupled receptors which mediate the effects of endogenous catecholamines, particularly the neurotransmitter norepinephrine (noradrenaline) and the hormone epinephrine (adrenaline).² The two predominant classes of adrenergic receptors, α and β , are further divided into nine adrenergic receptor subtypes. In particular, α_1 receptors have received much attention due to their participation in a number of physiological processes including control of smooth muscle contraction and blood pressure regulation via peripheral vasoconstriction. Local vasoconstriction in the nasal cavity can relieve congestion, and α_1 agonists such as phenylephrine are used for this purpose. In the eye, α_1 agonists induce long-term dilation of the pupil, and are often utilized in eye exams. More recently, α_1 receptors were found to regulate smooth

muscle movement in the prostate, and α_1 agonists are marketed to treat urinary incontinence and the benign prostate hyperplasia (BPH).³

The general structures of α_1 agonists fall into two classes: phenethylamines and imidazolines.⁴ The phenethylamines are structural analogs of norepinephrine and epinephrine, and the pharmacophore generally accepted is a basic amine 3-4 atoms away from a phenyl ring. The enantiomeric propanolamines contain the phenethylamine functionality, and therefore their binding to α_1 was not unexpected. However, we sought to eliminate α_1 -binding (agonism or antagonism) of the new class of compounds in order to avoid any untoward side effects.

2.2.3. Rationale for proposed hydrazide-based analogues

As discussed in Chapter 1, multiple known NR2B-selective NMDA receptor antagonists contain a phenolic B ring. Therefore the first difference explored between **211** and the enantiomeric propanolamines was B ring substitution, namely compound **96-1** with a *para*-arylmethanesulfonamide in lieu of the phenol present in **211** (Figure 2.3). Although both phenols and sulfonamides are hydrogen bond donors with similar pK_as, the phenol proved to have decreased off-target binding in the case of the enantiomeric propolamine series.

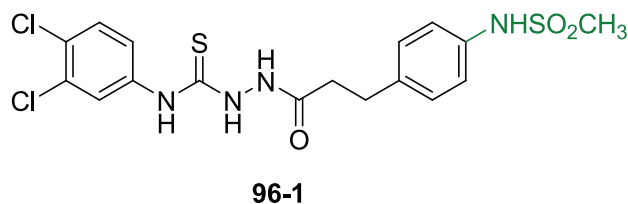


Figure 2.3 96-1, the sulfonamide analogue of 211

The thiosemicarbazide functionality linker region was probed through a number of strategies. First, biological systems rapidly metabolize sulfur to oxygen *in vitro* and *in vivo*. Therefore it was possible that the active compound with NR2B NMDA receptor antagonist activity was the oxygen-containing semicarbazide **96-2** (Figure 2.4). We also explored the relative effect of *para*-arylmethansulfonamide versus phenolic B ring substitution, as in **96-5**.

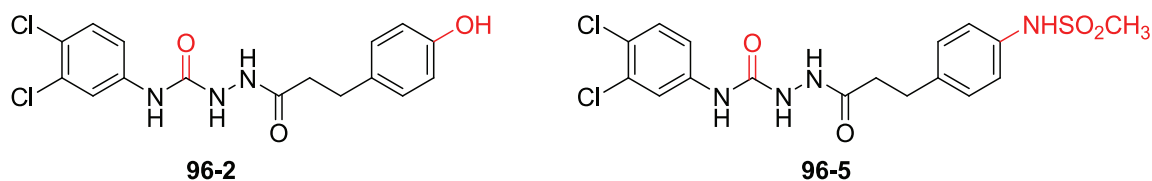


Figure 2.4 Proposed semicarbazide analogues

Decreasing the substantial rigidity and removing one hydrogen bond donor of the thiosemicarbazide functionality was explored in a series of N-acetylpropanehydrazides including **93-3** and **93-4**, in addition to the 6-atom linker analogue **96-10** (Figure 2.5).

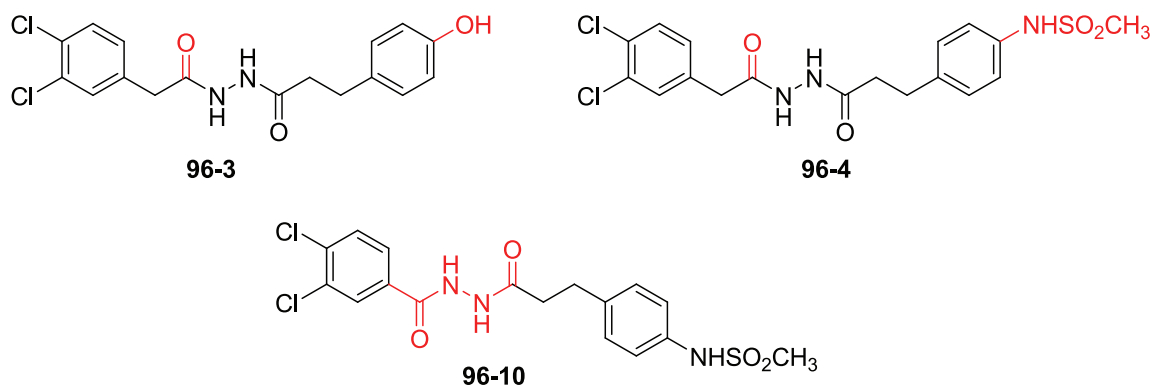


Figure 2.5 Proposed N-acetylpropanehydrazide analogues

Alkylation of the nitrogen at position 3 of the linker was probed to determine if this position mapped to the amine of the enantiomeric propanolamine series (Figure 2.6). We hypothesized that *n*-butyl analogues **96-6**, **96-7**, and **96-8** may exhibit increased fold shift when compared to the parent compounds **96-4**, **96-5**, and **96-3**, respectively (Figure 2.7).

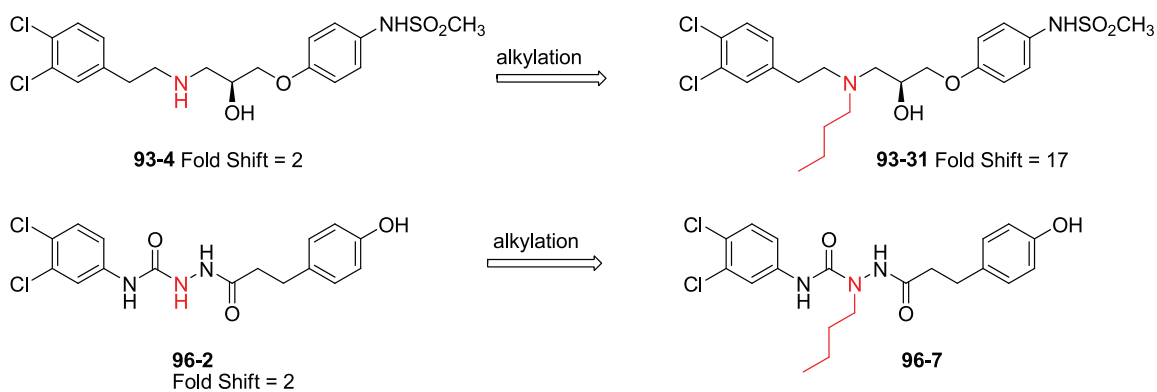
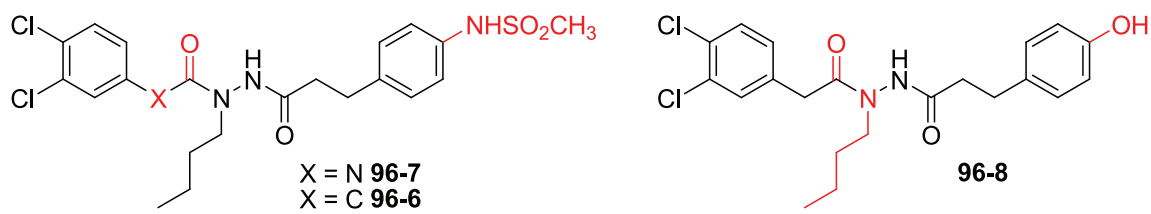


Figure 2.6 Determining the effect of alkylation on semicarbazide analogues

Figure 2.7 Proposed *n*-butyl analogues

A series of N-ethylpropanehydrazide analogues was proposed in order to further probe the effects of increased flexibility within the linker region (Figure 2.8).

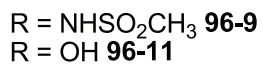
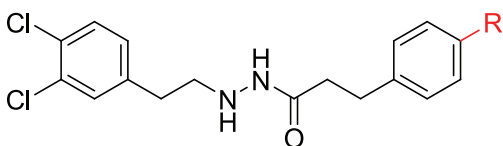


Figure 2.8. Proposed hydrazide analogues

Finally, the hydrazide linker was rigidified through the cyclic phthalimide compound **96-12** (Figure 2.9).

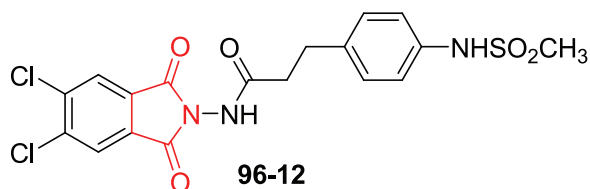


Figure 2.9 Proposed phthalimide analogue

2.3 Synthesis of hydrazide-based analogues

Retrosynthetically, it was envisaged that compounds of type **96-1** through **96-12** would come from scission of the carbon-nitrogen bond between hydrazide fragment B

and an electrophilic dichloro-aryl fragment A species (Figure 2.10).⁵ Fragment B could be defined as **1** or **2** based on whether B ring substitution was a *para*-methanesulfonamide moiety (**2**) or *para*-phenol (**1**).

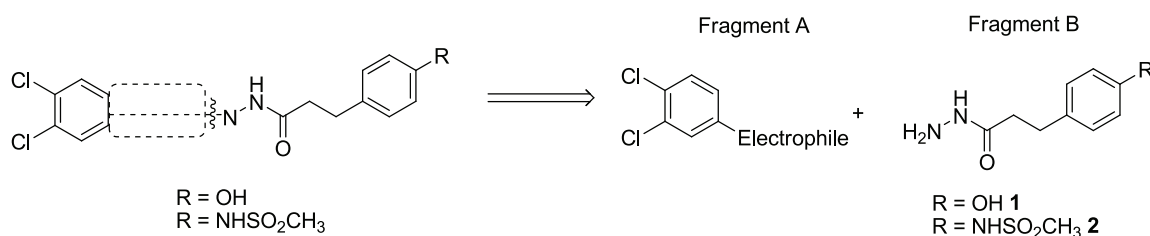
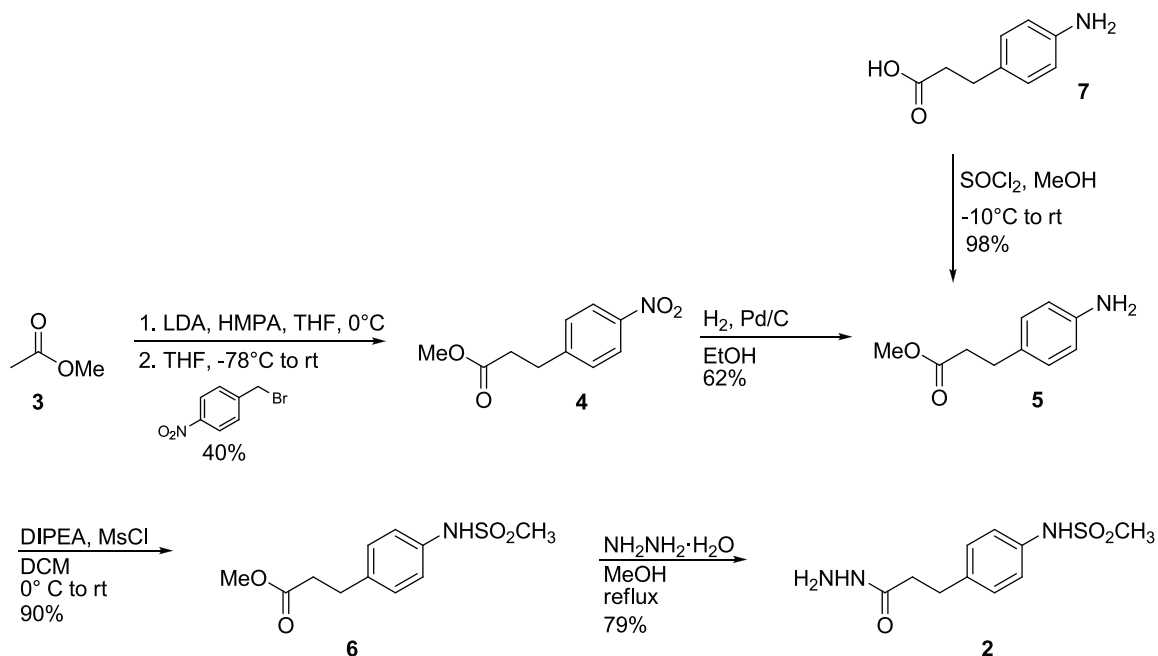


Figure 2.10 Retrosynthesis of hydrazide compounds

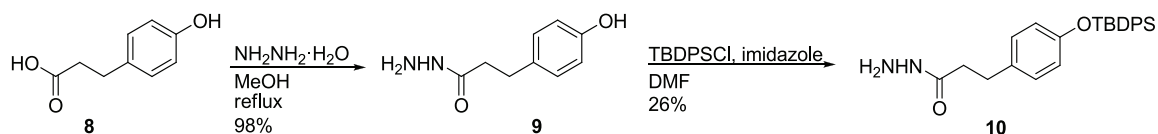
The *para*-arylmethanesulfonamide fragment **2** was synthesized as illustrated in Scheme 2.1. The initial route utilized to synthesize **2** began with alkylation of methyl acetate (**3**) with *para*-nitrobenzyl bromide to give methyl ester **4**. The nitro group was then reduced via hydrogenolysis to aniline **5**, which was subsequently treated with methanesulfonyl chloride and base to yield *para*-arylmethanesulfonamide **6**. Finally, the methyl ester functionality was converted to a hydrazide using hydrazine monohydrate in refluxing methanol to afford **2**. A more succinct synthesis in which carboxylic acid **7** was converted to methyl ester **5** before completing the synthesis as described above, was found. This alternative synthesis was preferred due to the higher yield obtained in the methyl ester formation (98%) as opposed to the alkylation strategy (40% in the first step).

Scheme 2.1 Synthesis of 2, fragment B



The phenol fragment B, compound **1**, was reacted with electrophilic fragment A compounds as the TBDPS-protected phenol (**10**, Scheme 2.2). Synthesis began with 3-(4-hydroxyphenyl)propanoic acid (**8**). Hydrazinolysis of **8** gave **9**.⁶ Subsequent TBDPS protection of the phenol afforded **10**.

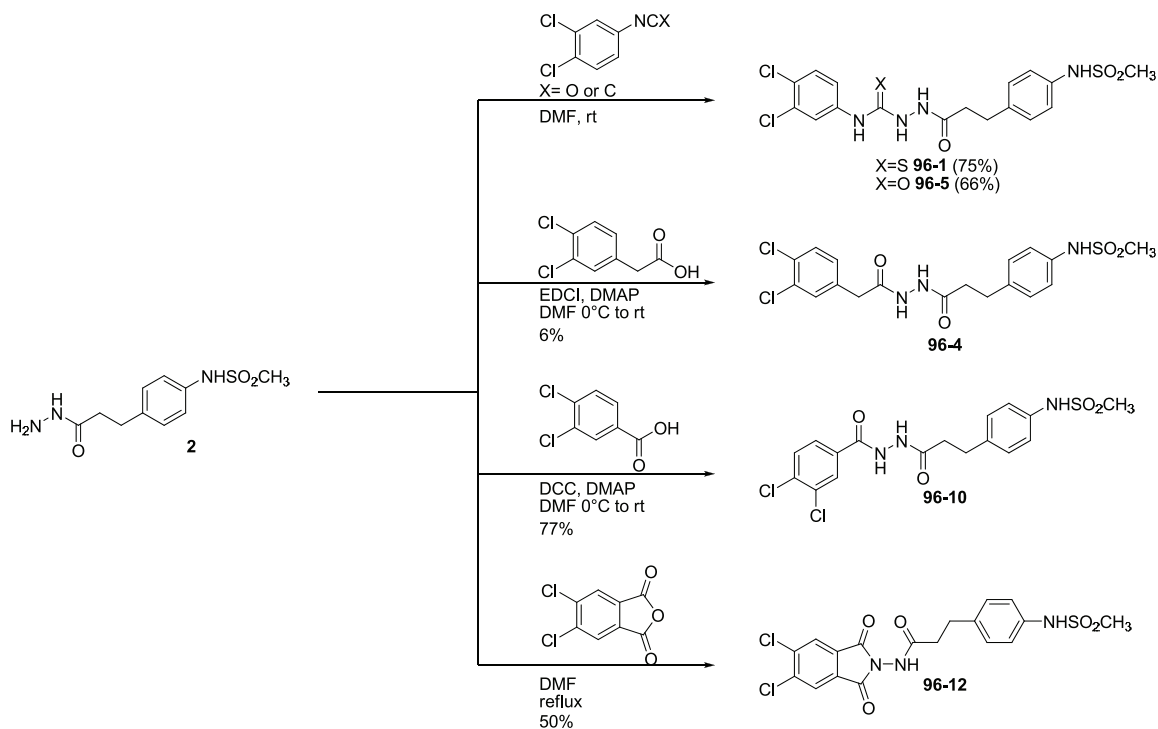
Scheme 2.2 Synthesis of 10, fragment B



With the two fragment B building blocks in hand; semicarbazide, thiosemicarbazide, N-acetylpropanehydrazide, and N-ethylpropanehydrazide analogues were synthesized by allowing **2** or **10** to react with the appropriate electrophilic fragment A.

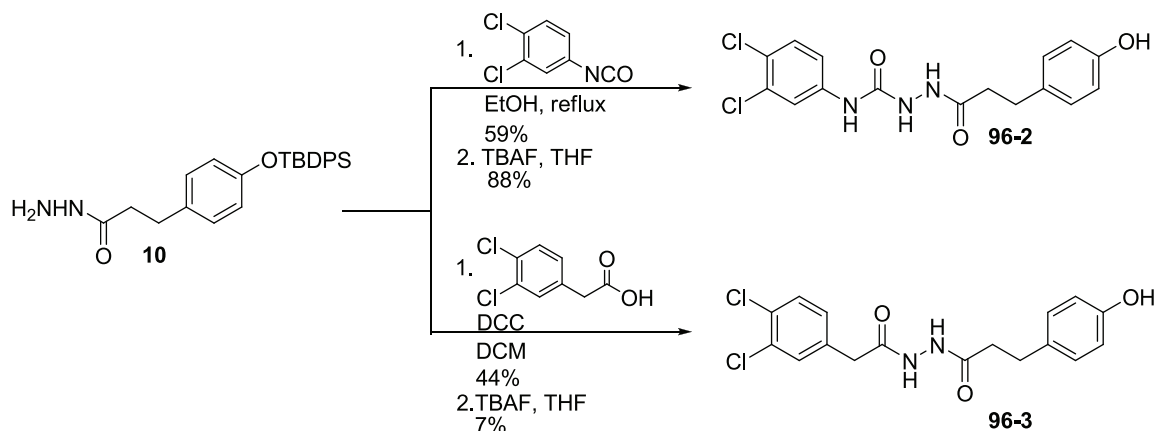
A selection of analogues generated from the *para*-arylmethanesulfonamide hydrazide fragment **2** is illustrated in Scheme 2.3. Compound **2** was reacted with 3,4-dichlorophenyl isothiocyanate or 3,4-dichlorophenyl isocyanate to give thiosemicarbazide **96-1** or semicarbazide **96-5** respectively. Subjecting **2** and 3,4-dichlorophenylacetic acid to carbodiimide-mediated coupling conditions with 1-Ethyl-3-(3-dimethylaminopropyl)carbodiimide hydrochloride (EDC) afforded N-acetylpropanehydrazide analogue **96-4**. Both chromatographic separation and recrystallization were required to obtain pure **96-4**, contributing to the low yield. Compound **2** was also used to synthesize analogues with 6-atom linker regions. Carbodiimide-mediated coupling between **2** and 3,4-dichlorophenylbenzoic acid yielded **96-10**. The fused phthalimide-hydrazide analogue **96-12** was made by refluxing hydrazide **2** with 3,4-dichlorophenylmaleic anhydride.

Scheme 2.3 Synthesis of hydrazide-based analogues: 96-1, 96-4, 96-5, 96-10, and 96-12



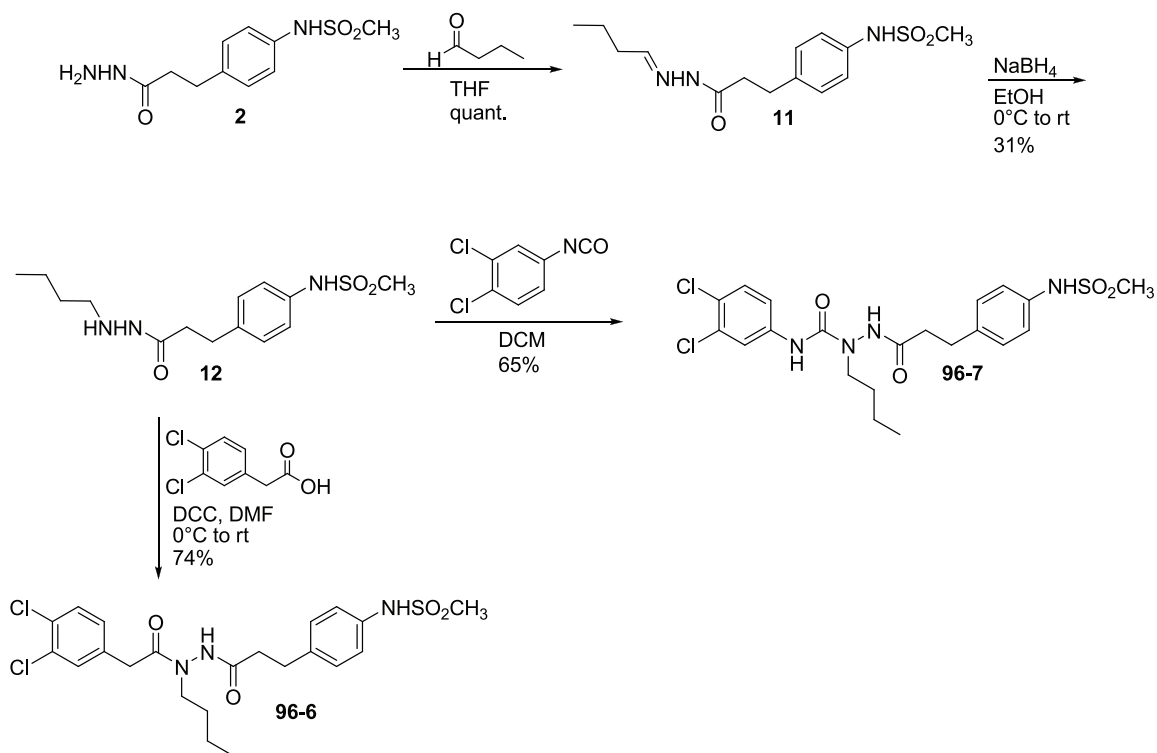
Synthesis of **96-2** and **96-3**, both containing phenolic substitution, was conducted as illustrated in Scheme 2.4. Protected phenol **10** was reacted with 3,4-dichlorophenylisocyanate affording the semicarbazide functionality. The TBDPS group was then removed by fluoride-mediated deprotection with TBAF to give **96-2**. Subjection of **10** to carbodiimide-mediated coupling conditions with 3,4-dichlorophenyl acetic acid successfully installed the N-acetylpropanehydrazide functionality. Finally, TBAF deprotection of the TBDPS group afforded phenol analogue **96-3**.

Scheme 2.4 Synthesis of phenolic hydrazide-based analogues 96-2 and 96-3

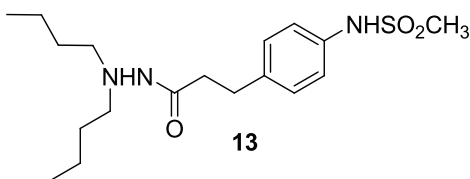


The effects of alkylation at the 3-position of the linker region were probed with semicarbazide and acetylpropanehydrazide analogues **96-6**, **96-7**, and **96-8** (Figure 2.7). Compounds **96-6** and **96-7**, both containing the *para*-arylmethanesulfonamide B ring, were synthesized according to Scheme 2.5. Fragment B compound **2** was converted to the Schiff base **11** with butyraldehyde. Precise stoichiometric quantities of the aldehyde were required to prevent over-alkylation of the terminal hydrazide nitrogen during the following reductive step. After isolation of **11**, reduction with sodium borohydride cleanly afforded N-butylpropanehydrazide **12**.

Scheme 2.5 Synthesis of alkylated hydrazone-based analogues: 96-6 and 96-7

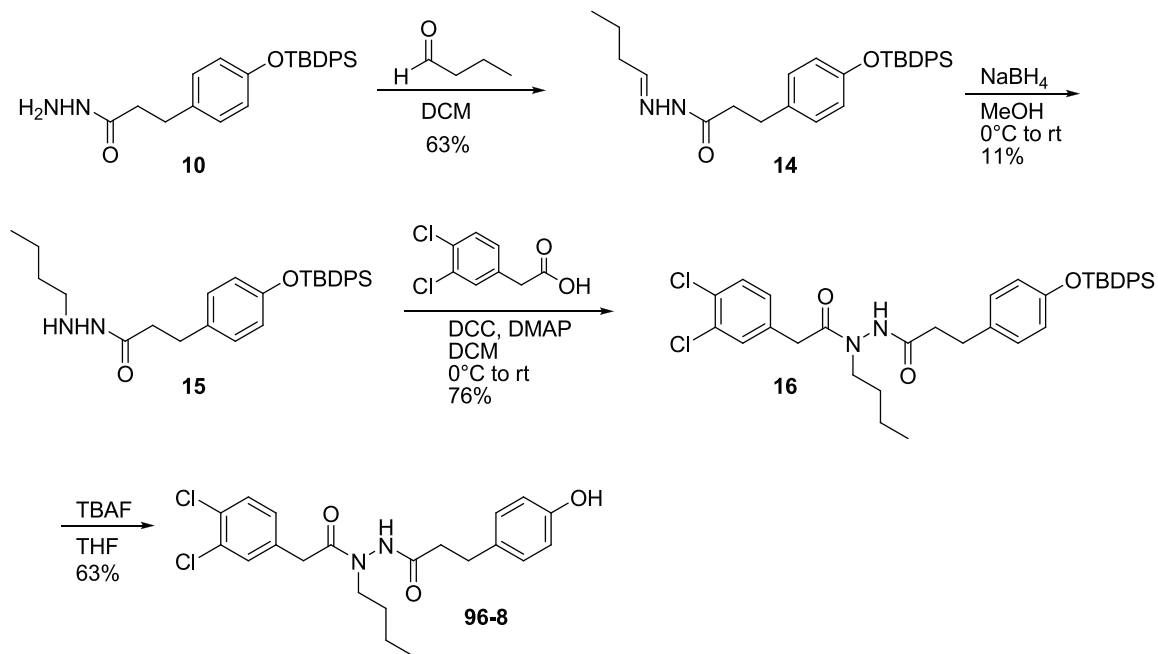


Chromatography was required to prevent the excess butyraldehyde used in Schiff base formation from inducing a subsequent alkylation during the reduction to give **13** (Figure 2.11). Initial attempts to perform the reductive amination in one pot failed due to near-quantitative conversion to **13**. The sensitivity of this reaction arises from the increased reactivity of mono-alkylated compound **12** towards further reaction with butyraldehyde due to the electron donating nature of the *n*-butyl group.⁷

Figure 2.11 Isolated dialkylation product **13**

The phenolic analogue **96-8** was prepared in a similar fashion to **96-6** (Scheme 2.6). Treatment of hydrazide **10** with butyraldehyde, followed by chromatographic isolation, gave Schiff base **14**. Reduction of **14** with sodium borohydride yielded alkylated hydrazide **15**, albeit in low yield. Carbodiimide-mediated coupling with 3,4-dichlorophenylacetic acid afforded **16**. Finally, the B ring TBDPS group was deprotected with TBAF to give **96-8**.

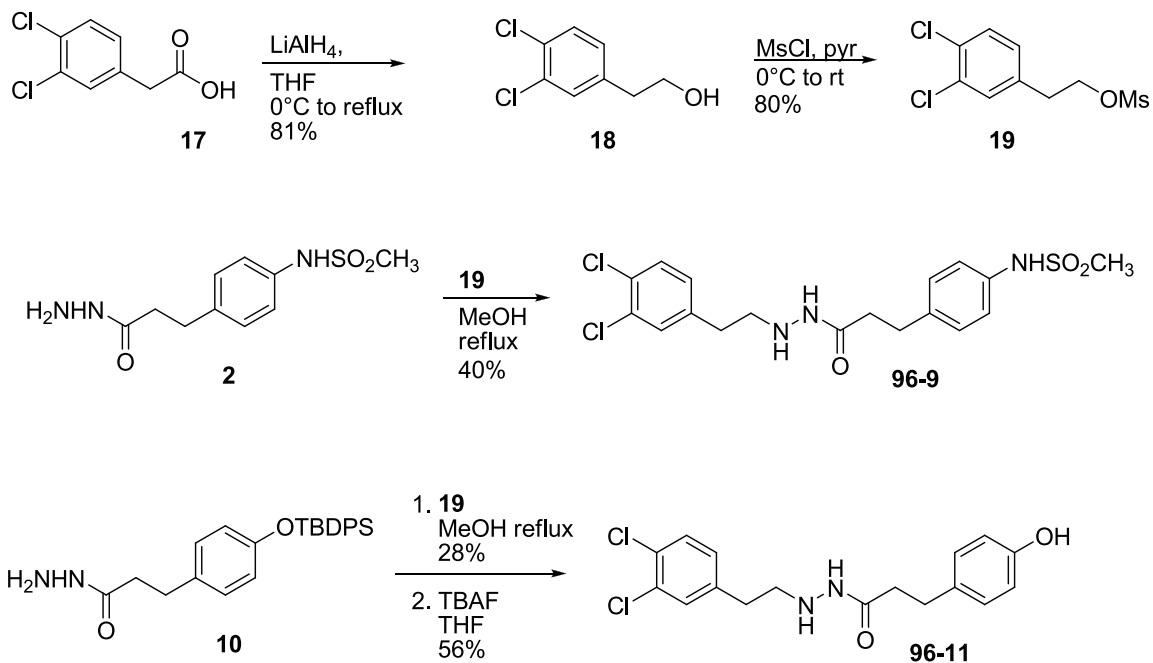
Scheme 2.6 Synthesis of alkylated and phenolic N-acetylpropanehydrazide analogue **96-8**



N-ethylpropanehydrazide analogues **96-9** and **96-11** were prepared by coupling hydrazide fragment **2** or **10** with mesylate **19** (Scheme 2.7). Lithium aluminum hydride reduction of 3,4-dichlorophenylacetic acid (**17**) gave alcohol **18**. Treatment of **18** with methanesulfonyl chloride yielded **19**. Refluxing mesylate **19** and the appropriate

hydrazide A fragment gave N-ethylhydrazides **96-9** and **20**. Analogue **96-11** was obtained through TBAF-mediated deprotection of **20**.

Scheme 2.7 Synthesis of N-ethylpropanehydrazide analogues 96-9 and 96-11



2.4 Biological evaluation of hydrazide-based compounds

2.4.1. Selectivity of hydrazide-based compounds for glutamate receptor subtypes

The potency and selectivity of all compounds were evaluated using two electrode voltage clamp analysis on recombinant NMDA receptor function.⁵ First, the effects of 3 μM of each compound was screened against current responses produced by maximally effective concentrations of NMDA receptor co-agonists glutamate (50 μM) and glycine (30 μM) at rat NR1/NR1A-, NR1/NR2B-, NR1/NR2C-, and NR1/NR2D-containing NMDA receptors. In addition to NMDA receptors, representative members of

related glutamate receptor families, specifically AMPA (GluR1) and kainate (GluR6), were evaluated (Table 2.1). Compounds that exhibited less than 50% response possessed marked inhibition. The data indicates that compounds had little or no effect on response in NR1/NR1A-, NR1/NR2C-, NR1/NR2D-, GluR1 or GluR6. However, all but three compounds (**96-2**, **96-3**, and **96-8**), exhibited reduced responses (less than 50%) against the NR1/NR2B-subtype of NMDA receptor.

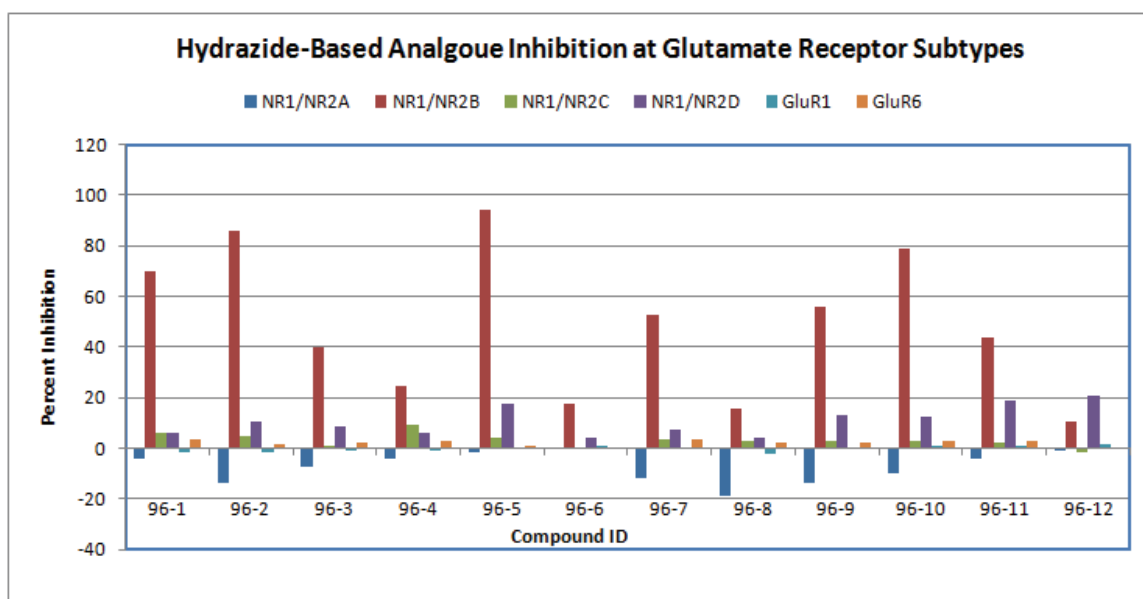
Table 2.1 *In vitro* analysis of hydrazide-based compound towards rat glutamate receptor subtypes

Compound ID	Percent Response (%)					
	NMDA Receptor Subtype				Other glutamate receptors	
	NR1/NR2A	NR1/NR2B	NR1/NR2C	NR1/NR2D	GluR1	GluR6
96-1	104	30*	94	94	101	96
96-2	114	14*	95	90	101	98
96-3	107	60*	99	92	101	98
96-4	104	75*	91	94	101	97
96-5	101	6*	96	82	100	99
96-6	100	82*	100	96	100	100
96-7	112	47*	96	93	100	96
96-8	119	85*	97	96	102	98
96-9	114	44*	97	87	100	98
96-10	110	21*	97	87	100	97
96-11	104	56*	98	81	99	97
96-12	101	90*	102	79	98	100

Data shown are the current response in *Xenopus* oocytes expressing the indicated recombinant rat receptors recorded under two electrode voltage clamp ($V_{\text{HOLD}} = 40$ mV) in response to maximally effective concentration of glutamate (50 μM) and glycine (30 μM) in the presence of 3 μM of the indicated compound, expressed as a percent of controlled response in the absence of test compound. Measurements are the mean of 4 to 10 oocytes for each compound at each receptor subtype. For compounds showing a greater than 10% change from control, * indicates $p < 0.05$ (paired t-test)

This data can also be viewed as percent inhibition (Chart 2.1), the opposite of percent response. For hydrazide-based analogues **96-1** through **96-12**, it is clear that these compounds have minimal effects at all receptor subtypes other than NR1/NR2B, suggesting compounds of this class have high selectivity for the NR1/NR2B-containing NMDA receptors.

Chart 2.1 Hydrazide-based analogue inhibition at rat glutamate receptor subtypes



Graphical representation of the data presented in Table 2.1. Percent inhibition = 100 – Percent Response.

The concentration-effect curves for hydrazide compounds against recombinant human NR1/NR2B-containing NMDA receptors were then determined. The IC_{50} for synthesized compounds can be found in Table 2.2.

Table 2.2 Hydrazide-based compound *in vitro* analysis at human NR1/NR2B NMDA receptors and off-target receptors

ID	Structure	NR2B IC_{50}^{\dagger} (nM) pH 7.6	NR2B IC_{50}^{\dagger} (nM) pH 6.9	Fold Shift	hERG ^a	α_1 -adrenergic ^b
211		600 [†]	320 [†]	1.9		
96-1		270	180	1.6	13	<1

ID	Structure	NR2B IC ₅₀ [†] (nM) pH 7.6	NR2B IC ₅₀ [†] (nM) pH 6.9	Fold Shift	hERG ^a	α ₁ -adrenergic ^b
96-2		119	70	1.7		
96-3		7,140	3,330	2.1		
96-4		5,750	3,820	1.5		
96-5		28	15	1.9	3	5
96-6		92,600	119,800	0.8		
96-7		7,540	2,140	3.5		
96-8		117,300	104,800	1.1		
96-9		4,810	1,340	3.6		
96-10		521	240	2.2		
96-11		26,200	6,060	4.3		
96-12		41,800	6,640	6.3		

[†] The IC₅₀ value was determined from two electrode voltage clamp recordings of human NR1/NR2B receptor function, fitted as described in the experimental section. For all experiments, data are the fitted IC₅₀ value for the mean composite averaged from between 16 and 29 oocytes from 3 or more different frogs.

[‡] The IC₅₀ was determined as described above in rat NR1/NR2B receptors.

^a Binding to the human ether a-go-go potassium channel (hERG) expressed in HEK293 cells by displacement with 1.5 nM ³[H]-astemizole. Each result represents an average of displacement experiments done in duplicate at 10 μM of the test compound.

^b Percent displacement of 0.25 nM ³[H] prazosin from Wistar rat brain membranes. Each result represents the average of displacement binding experiments done at 3 μM. All binding assays were performed by MDS Pharma, Bothell, WA.

2.4.2. Structure activity relationships of hydrazide-based analogues (pH 7.6 data only)

The initial screening hit **211** (rat IC₅₀ = 600 nM) contained a *para*-phenol B ring (Table 2.2). Our previous studies focused on compounds with *para*-arylmethanesulfonamide B rings. The hybrid *para*-arylmethanesulfonamide thiosemicarbazide compound, **96-1**, exhibited increased potency relative to **211**, with an IC₅₀ value of 270 nM. This result is consistent with our previous work in the enantiomeric propranolamine series in which phenol **93-150** was less potent than the sulfonamide-containing analogue **93-4** (Chapter 1).

Replacement of the sulfur, embedded in the thiosemicarbazide functionality, with oxygen, yielded various semicarbazide analogues (Table 2.2). This alteration resulted in significantly enhanced potency, as observed for **96-2** and **96-5** relative to the parent thiosemicarbazide analogues, regardless of B ring substitution. Potency of the semicarbazide *para*-arylmethanesulfonamide compound **96-5** (IC₅₀ = 28 nM) was increased nearly ten times relative to the thiosemicarbazide counterpart **96-1**. The relative effect of the semicarbazide phenol compound **93-2** was less dramatic but followed the same trend, with an IC₅₀ value of 119 nM. The increased potency of the oxygen-containing compounds suggests that the oxygen present in the semicarbazide moiety makes additional beneficial hydrogen bonding contacts with the ifenprodil

binding pocket. Furthermore, the more potent oxygen-containing analogues eliminate the liability of potential sulfur oxidation during metabolism, critical if the compounds were to be utilized *in vivo*.

Replacement of the A ring aniline nitrogen with carbon at the 1 position of the linker yielded analogues characterized by N-acetylpropanehydrazide and N-ethylpropanehydrazide linker regions. Elimination of the terminal N-H hydrogen bond donor resulted in a dramatic decrease in potency, regardless of B ring substitution or linker composition. Phenolic N-acetylpropanehydrazide analogue **96-3** had 60-fold reduced potency ($IC_{50} = 7,140$ nM) compared with semicarbazide analogue **96-2**. Similarly, the *para*-arylmethanesulfonamide N-acetylpropanehydrazide **96-4** ($IC_{50} = 5,750$) was 200-fold less potent than semicarbazide **96-5**. Additional removal of the carbonyl at the two position of the linker region, as in N-ethylpropanehydrazides **96-9** and **96-11**, also influenced potency. However, the effect was dependent on B ring functionality. Replacement of the 2-carbonyl with a methylene group resulted in the significant reduction of potency observed for phenol **96-11** ($IC_{50} = 26,200$ nM) compared to semicarbazide **96-2** (> 200-fold reduction) and N-acetylpropanehydrazide **96-3** (ca. 3-fold reduction). In contrast, while *para*-arylmethanesulfonamide N-ethylpropanehydrazide **96-9** ($IC_{50} = 4,810$ nM) was 170-fold less potent than semicarbazide **96-5**, **96-9** was slightly more potent than the corresponding N-acetylpropanehydrazide counterpart **96-4**. Although the effect of carbonyl deletion at position 2 of the linker is questionable, the data clearly indicates the importance of an aniline nitrogen at position 1 for potency.

The effect of alkylation of the terminal hydrazide nitrogen in the semicarbazide functionality (position 3 of the linker) was explored via a series of *n*-butyl compounds. In our primary suppositions, alkylated compounds were proposed in an attempt to enhance pH sensitivity (i.e. fold shift). Herein the activity of these compounds at physiologic pH is discussed; the effect of alkylation on fold shift will be presented in the following section. Results at pH 7.6 indicated that regardless of linker composition or B ring substitution, alkylation severely compromised NR1/NR2B potency. The alkylated semicarbazide **96-7** ($IC_{50} = 7,540$ nM) and alkylated N-acetylpropanehydrazide **96-6** ($IC_{50} = 92,600$ nM) both exhibited decreased potencies compared with parent non-alkylated compounds **96-5** (ca. 269-fold reduction) and **96-4** (ca. 16-fold reduction). A similar result was observed within the phenol series where alkylated N-acetylpropanehydrazide **96-8** ($IC_{50} = 117,300$ nM) had a 16-fold reduction of potency compared with the non-alkylated counterpart **96-3**.

Finally, two analogues were synthesized which possessed a 6-atom linker. N-benzoylpropanehydrazide analogue **96-10** ($IC_{50} = 521$ nM) was the only modestly potent bishydrazide analogue, even without an aniline N-H hydrogen bond donor. Phthalimide analogue **96-12** showed poor activity ($IC_{50} = 41,800$ nM).

2.4.3. Structure activity relationships of hydrazide-based analogues on fold shift.

The effect of hydrazide-based antagonists on NR1/NR2B-containing NMDA receptors at both physiologic pH (7.6) and a more acidic pH characteristic of ischemic conditions (pH 6.9) were evaluated.

As indicated in Table 2.2, no linker changes resulted in significant alteration of the fold shift associated with lead compound **211** (fold shift = 1.9). Although all semicarbazide (no alkylation), thiosemicarbazide (no alkylation), and N-acetylpropanehydrazide compounds were modestly more potent at pH 6.9, generally fold shift did not exceed two. However, both phenolic and *para*-arylmethanesulfonamide N-ethylpropanehydrazide analogues **96-9** (fold shift = 3.6) and **96-11** (fold shift = 4.3) exhibited modest increases in fold shift. The increased flexibility of the N-ethylpropanehydrazide compared with the rigid planarity of semicarbazide, thiosemicarbazide, and N-acetylpropanehydrazide compounds was hypothesized to be responsible for the apparent increase in pH sensitivity.

Finally, the hypothesis that the profound effect of alkylation at position 3 of the linker region on fold shift observed with the enantiomeric propanolamines would be transferrable to **211**-type compounds proved to be false. In the case of the enantiomeric propanolamines, addition of a butyl group at position 3 enhanced fold shift from 2 to 17. A similar effect was not observed in the case of the hydrazide-based compounds. Alkylated carbazides, both the *para*-arylmethanesulfonamide **96-6** (fold shift = 0.8) and phenol **96-8** (fold shift = 1.1), exhibited negligible fold shift. In contrast to the enantiomeric propanolamines, where relative pH 7.6 activity is decreased while activity at 6.9 is enhanced upon alkylation, potency of hydrazide-based analogue activity at both pH 7.6 and 6.9 are markedly decreased with alkylation. Only *n*-butyl semicarbazide **96-7** exhibited a modest fold shift (3.5).

2.4.4. Structure activity relationships of hydrazide-based analogues on off-target receptors.

The hypothesis that the thiosemicarbazide functionality would be characterized by inherently low hERG binding proved correct. Neither thiosemicarbazide **96-1** (hERG binding 13% at 3 μ M) nor semicarbazide **96-5** (3% hERG binding at 3 μ M) exhibited appreciable hERG or α_1 activity. Both **96-1** and **96-5** represent compounds that have increased rigidity and hydrophilicity (both of which effect logP) compared with the enantiomeric propanolamines. In addition, the hydrazide functionalities lack a nitrogen which would be protonated at physiologic pH. This limited the ability of this class of compounds to interact with the lumen of the K⁺ channel and participating in π -cation interactions. The absence of a basic nitrogen was also responsible for the lack of α_1 agonism, as the hydrazide functionality did not satisfy the generally accepted α_1 pharmacophore.

2.5 Conclusions regarding hydrazide-based analogues

Several important observations can be gleaned from the structure activity relationship analysis of the hydrazide-based analogues, summarized in Figure 2.12 and the list below. As indicated, **96-5** was the most promising hydrazide-based analogue. This semicarbazide showed on-target NR1/NR2B potency of 28 nM and negligible hERG binding (3% at 3 μ M). Both of these results represent significant improvements over screening hit **211**. The structural modifications leading to the increase in beneficial properties included replacement of the thiosemicarbazide functionality of **211** with the

semicarbazide of **96-5**, as well as incorporation of a *para*-arylmethanesulfonamide B ring as opposed to the *para*-phenol of **211**. However, neither **96-5** nor other hydrazide-analogues exhibit appreciable fold shifts. Together, this information was used to further design potentially improved pH-sensitive NR2B-selective NMDA receptor antagonists.

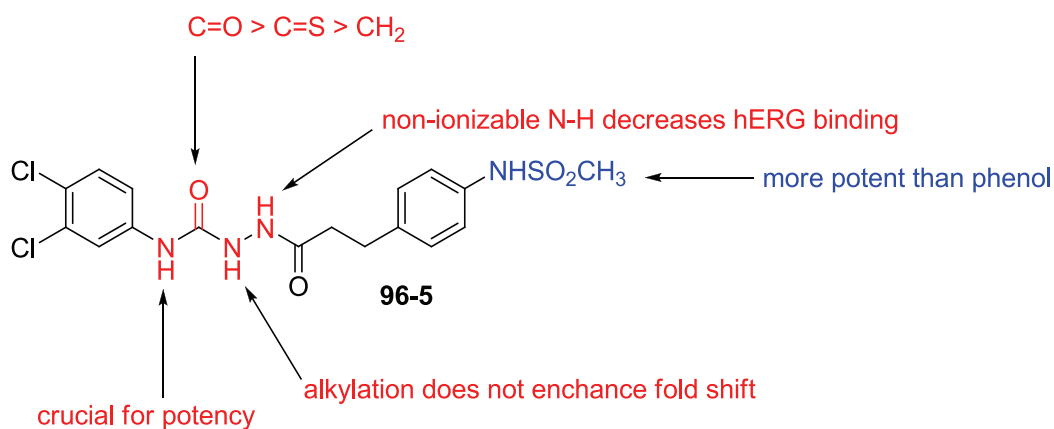


Figure 2.12 SAR of hydrazide-based analogues

- 1.) The thiosemicarbazide and semicarbazide scaffold has high selectivity and affinity for NR1/NR2B-containing NMDA receptors.
 - a. Removal of the A ring aniline nitrogen most profoundly affected (decreased) potency.
 - b. Removal of the carbonyl at position two of the linker decreased potency.
 - c. Semicarbazides were more potent than thiosemicarbazides.
- 2.) Compounds containing *para*-arylmethanesulfonamide B rings had increased potency relative to their phenol counterparts.

- 3.) Alkylation at position 3 of the linker region did not induce positive changes in fold shift.
- 4.) Increased flexibility of the linker region may increase likelihood of a compound exhibiting fold shift greater than ca. 2.
- 5.) Compounds of the thiosemicarbazide and semicarbazide class had decreased hERG binding.
 - a. The lack of a centrally located amine nitrogen which could be protonated at physiologic pH, and thus associate with the hERG channel, was hypothesized to account for this observation.

2.6 Rationale for proposed amide-based analogues

Only five hydrazide-based compounds exhibited nanomolar potency, most notably **96-5**. Although hERG binding was minimized, we hypothesized that further development of this class of compounds as neuroprotectants would be met with limited success. The hydrazide and semicarbazide compounds were structurally rigid with limited bond rotation and flexibility, which may be important for inducing potency and fold shift. In addition, we presumed the likelihood of hydrazide-based compounds exiting general circulation and crossing the blood-brain barrier was minimal. Because of the hydrophilic nature of the molecules, which possess multiple hydrogen bond donor and acceptors, passive diffusion across the tight junctions of the brain cardiovascular system would be most likely impossible. Nor could the compounds be transported into brain tissue via amino acid transporters.

As a result of these observations, we sought to incorporate the structure-activity relationships gleaned from the hydrazide-based series to a series of more flexible amide-based compounds. Amides are known to be significantly more flexible than hydrazides or semicarbazides, and reduced linker rigidity coupled with increased hydrophilicity was envisaged to yield compounds with a more diverse SAR profile in terms of both potency and fold shift. In addition, the increased hydrophobicity would translate into compounds potentially likely to cross the blood-brain barrier. By attenuating the basic nitrogen centrally located within the linker region, the amides were also hypothesized to have decreased hERG binding.

Compounds of the general structure **20** (Figure 2.13) were proposed as initial targets for further synthetic efforts.

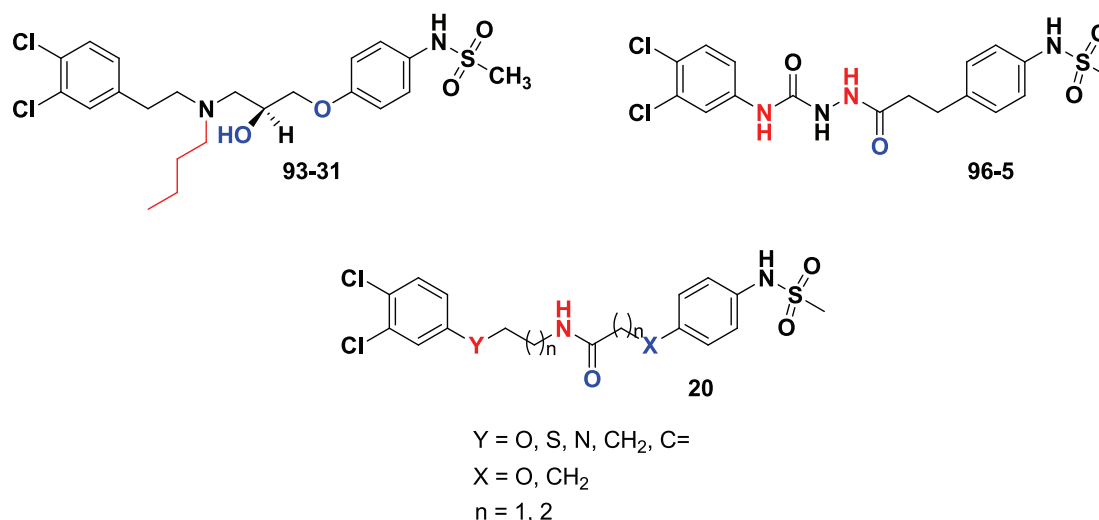


Figure 2.13 Comparison of lead enantiomeric propanolamine and semicarbazide compounds, as well as proposed hybrid amide analogues

We probed the effects of combining the enhancing properties of both the enantiomeric propanolamine and hydrazide series'. The 3,4-dichlorophenyl A ring and *para*-arylmethanesulfonamide B ring were maintained for initial comparison with both previously developed series. The aniline nitrogen, crucial for activity of **96-5**, was an intriguing position to be studied in the amide target structures. By altering this position to include a number of atomic and saturation level changes, a number of conformations, bond lengths, and hydrogen bonding donor/acceptor possibilities would be explored. The ethylene linker between the A ring aniline nitrogen and the centrally located amide would add increased flexibility and decreased hydrophilicity. Although both the enantiomeric propanolamines and the hydrazides contained oxygen atoms incorporated at position 5, the oxidation state varied between the two. We chose to utilize the carbonyl as part of the centrally located amide functionality. The amide could first serve as a synthetic handle, and could be reduced or further functionalized to generate additional novel compounds. The importance of the B ring phenoxy oxygen present in the enantiomeric propanolamine series, but lacking in the hydrazide-based compound series, would also be probed through both methylene and oxygen substitution at this position. Finally, the linker length was examined by extending linker regions on both flanks of the centrally located amide.

A number of NR2B-selective NMDA receptor antagonists are known to contain a piperidine motif beside the hydrophobic A ring (see introduction, Chapter 1). We hypothesized that incorporation of the ethanediamine linker into various heterocyclic structures; including piperazines, acyl piperazines, diacyl piperazines, and

imidazolinones, would yield novel antagonists with different characteristic heterocyclic functionalities proximal to the A ring (**21**, Figure 2.14). These compounds would vary in conformation, hydrogen bond donor/acceptor opportunities, and basicity. Notably, the acyl piperazines were proposed to have decreased hERG binding relative to piperazine-containing compounds due to the attenuated amine basicity. The effect of varying the heterocyclic core of the NR2B pharmacophore was unknown in terms of potency and fold shift.

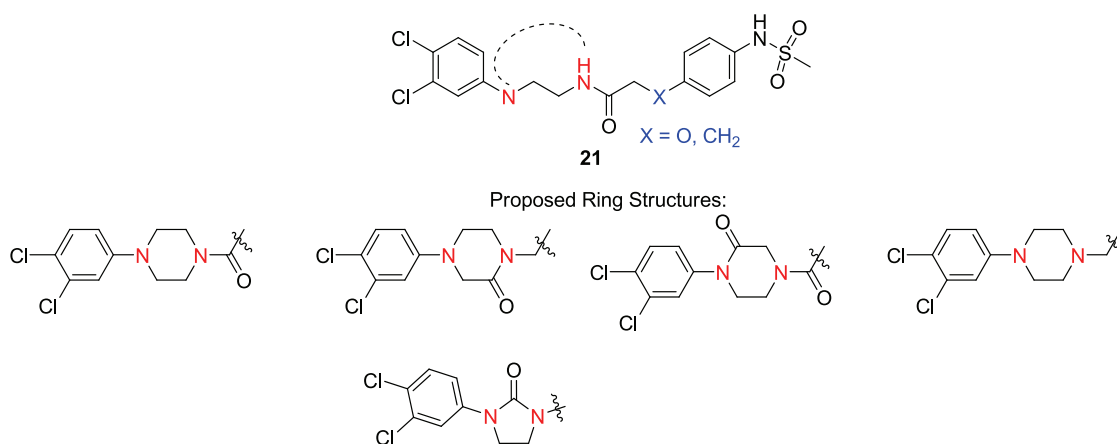


Figure 2.14 General structure of proposed cyclic amide compounds

Alkylation of the amine in the enantiomeric propanolamine series gave rise to a significant increase in fold shift over parent free base compounds. In contrast, alkylation of hydrazide-based compounds led to a significant decrease in potency at both pH 7.6 and 6.9, giving non-potent compounds with negligible fold shifts. However, the position of alkylation in the proposed amide series would not map directly to either previously developed series (**22**, Figure 2.15). The 3- position of the enantiomeric propanolamine and **96-7** type compounds were alkylated, whereas the 4- position of amide **22** would be

modified. Herein, we probed the effect of alkylation of the amides differentially at positions 1, 3, and 4 of the linker region to determine how positional substitution would influence fold shift. Alkylation on carbon at the 3-position of **22** was carried out in an enantiomeric fashion, as the enantiomers potentially interact with the chiral binding pocket differentially. Alkylation at the 3-position on nitrogen, on compounds such as **23**, required moving the amide one unit to the left. This alkylation more closely resembles that observed for the enantiomeric propanolamines as opposed to the chiral 3-position alkylation of **22**.

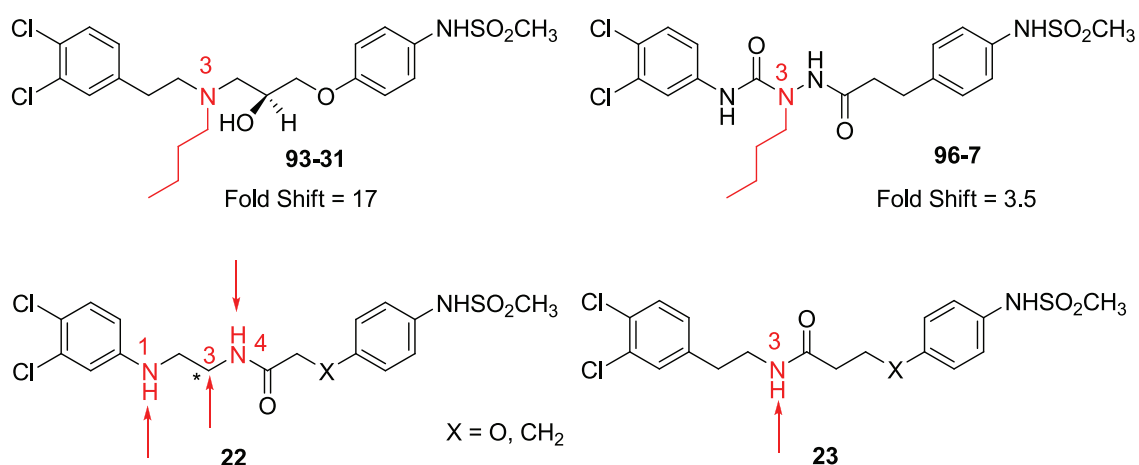


Figure 2.15 Proposed alkylated amide compounds **22** and **23** compared with **93-31** and **96-7**.

Note: red arrows indicate sites of alkylation

The previously identified optimal A and B ring substitutions were 3,4-dichlorophenyl and *para*-arylmethanesulfonamido, respectively. We sought to perform some simple changes to both rings to potentially effect potency and hERG binding (**21**, Figure 2.16).

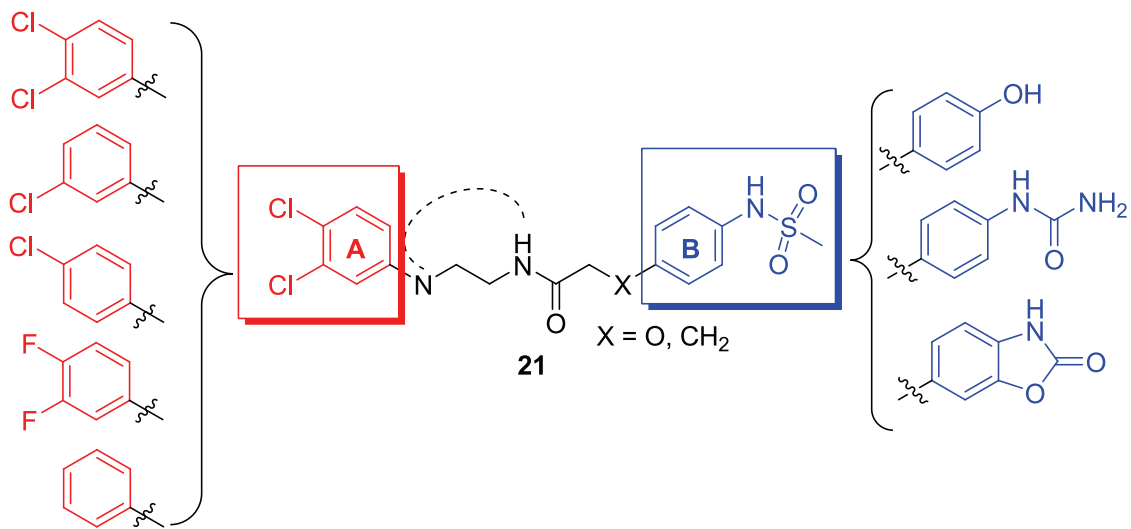


Figure 2.16 Proposed changes to A and B ring substitutions

Various A ring regio- and chemo-substitutions in the enantiomeric propanolamine series were found to affect potency.^{1,8} As such, we incorporated various fluorine, chlorine, and hydrogen substitutions to address whether the same trends would be apparent. These changes were made on both straight chain amides linker analogues and acyl piperazine containing compounds.

B ring composition was also altered to probe the effect such a change would have on hERG binding. As discussed in Chapter 1 and the hydrazide-based compound sections, B ring substitution can have a significant influence on off-target activity. We sought to retain a pK_a of ca 9-10 for on-target NMDA binding.⁹ Hence, we targeted compounds with phenol, urea, and benzoxazolidinone B ring functionalities.

To exploit the synthetic ease of reducing amides, the amines of the corresponding amides were also targets (**24**, **25**, and **26**, Figure 2.17). We sought to

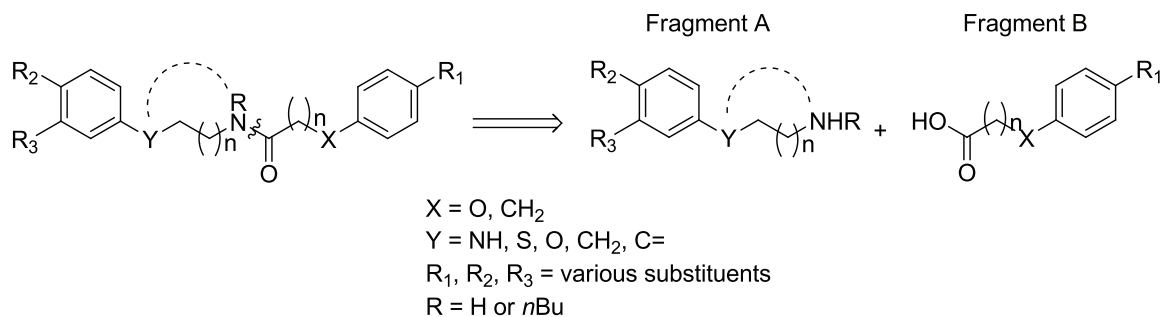
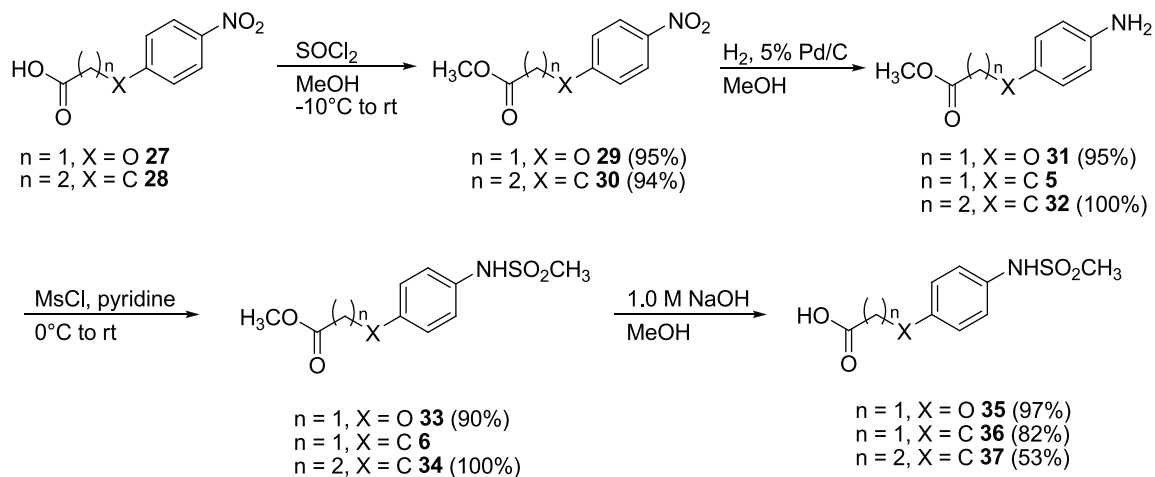


Figure 2.18 Retrosynthetic analysis of amide analogues

Carboxylic acid fragments not commercially available were prepared as illustrated in Schemes 2.8 and 2.9.

Scheme 2.8 Synthesis of carboxylic acids **35**, **36**, and **37**

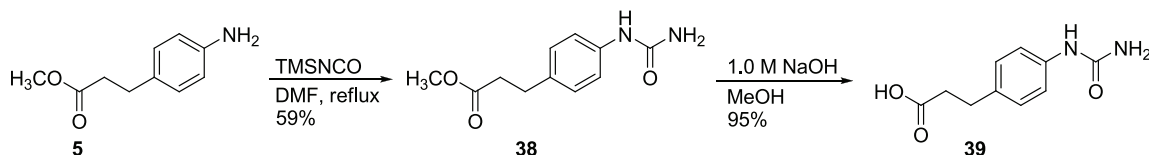


Synthesis of *para*-arylmethanesulfonamides **35** and **37** began with 2-(4-nitrophenoxy)acetic acid (**27**) and 4-(4-nitrophenyl)butanoic acid (**28**), respectively (Scheme 2.8). The methyl esters (**29** and **30**) were formed with treatment of the carboxylic acids with thionyl chloride and methanol.¹¹ Reduction of the aryl nitro group using hydrogenolysis yielded anilines **31** and **32**. Aniline **5** was prepared as shown

previously in Scheme 2.1. Formation of the methanesulfonamide by mesylation under basic conditions afforded *para*-arylmethanesulfonamides **33**, **6**, and **34**. Finally, saponification of the methyl ester functionality gave carboxylic acids **35**, **36**, and **37**.

Intermediate **5** was also utilized in the synthesis of *para*-arylurea B ring fragment **39** (Scheme 2.9). Treatment of aniline **5** with trimethylsilyl isocyanate gave urea **38**.¹² Saponification of the methyl ester afforded carboxylic acid **39**.

Scheme 2.9 Synthesis of *para*-arylurea **39**

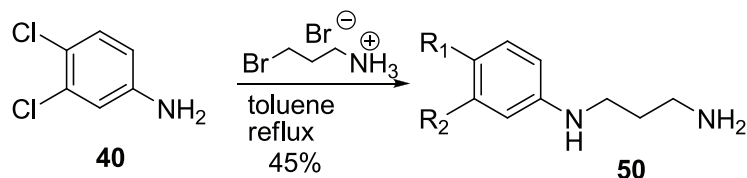
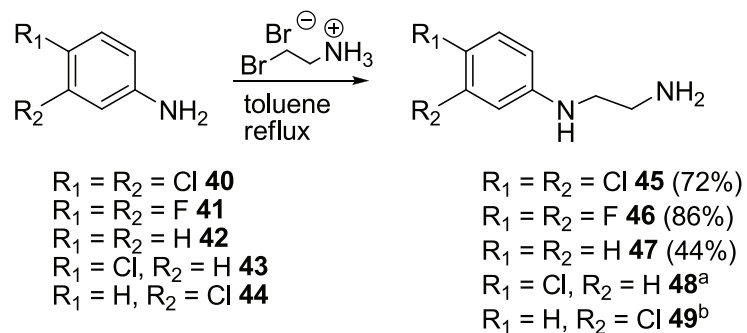


All other carboxylic acids used for amide bond formation were commercially available or prepared by other lab members.

Synthesis of fragment A amines to generate compounds of type **20** were prepared as shown in Schemes 2.10-14.

The phenyl-1,2-ethanediamine and corresponding propanediamine fragment A amines (**45-49**, **50**) were synthesized by refluxing an appropriate aniline (**40-44**) with the corresponding bromoalkylamine hydrobromide (Scheme 2.10).¹³

Scheme 2.10 Synthesis of ethanediamine and propanediamine fragments 45-50

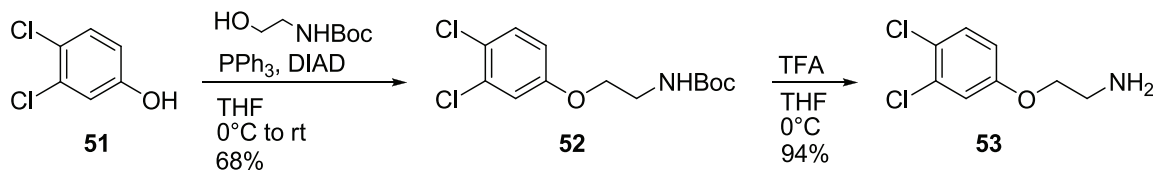


^a prepared by Rose Santangelo

^b prepared by Dr. Yesim Tahirovic

The phenoxy-containing fragment A amine (**53**) was prepared via Mitsunobu reaction between 3,4-dichlorophenol (**51**) and N-Boc-ethanolamine to give intermediate **52** (Scheme 2.11). Deprotection of the Boc group with trifluoroacetic acid yielded phenoxyethanamine **53**.¹⁴

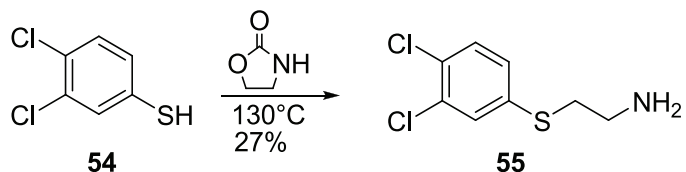
Scheme 2.11 Synthesis of ethoxyamine 53



Refluxing 3,4-dichlorothiophenol (**54**) with oxazolidinone under neat conditions yielded the sulfur-containing 3,4-dichlorophenylthioethanamine (**55**, Scheme 2.12).¹⁵

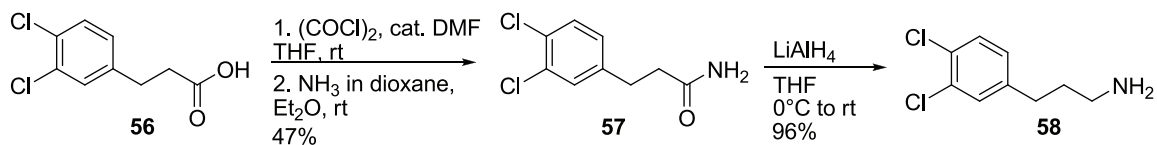
This transformation occurred through initial ring opening of the oxazolidinone followed by decarboxylation to afford **55**.

Scheme 2.12 Synthesis of thioethaneamine 55



The sp^3 -hybridized carbon-containing fragment A amine was synthesized as illustrated in Scheme 2.13.¹⁶ The acid chloride of **56** was formed with oxalyl chloride, followed by amination with ammonia to give propionamide **57**. Reduction of the amide with lithium aluminum hydride yielded amine **58**.

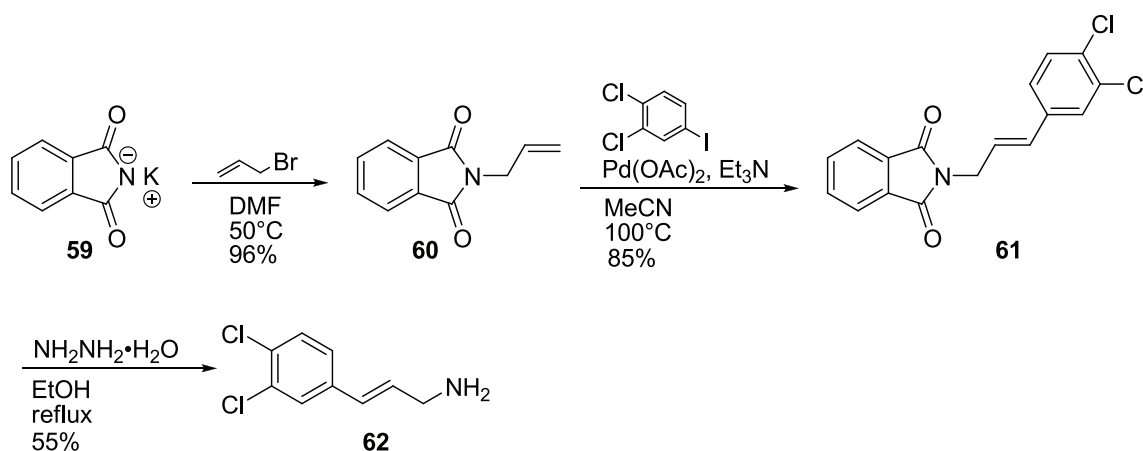
Scheme 2.13 Synthesis of propaneamine 58



The carbon-containing fragment A amine with sp^2 -hybridization was also synthesized (Scheme 2.14).¹⁷ Heck reaction between allyl phthalamide¹⁸ and 3,4-dichloriodobenzene yielded the *trans*-cinnamylamine **61**. In accordance with the observation of Malek et al., reaction occurred completely regioselectively at the γ -position of **60**.¹⁹ The use of phenyl iodine (strong σ -donor) substrate and PPh_3 as a ligand favors a neutral mechanism of migratory insertion due to dissociation of a PPh_3

ligand.²⁰ Sterics then control the formation of linear (β -attack) product **61**. The use of bidentate ligands and aryl triflates (weakly associated anionic ligand) however, would have led to a cationic mechanism of migratory insertion. Under such conditions, insertion occurs with high selectivity for the carbon with lower charge density (α -attack), despite steric preferences. This would lead to a branched product, which was not observed in the course of this work. The phthalimide protecting group was removed via hydrazinolysis to give free amine **62**.

Scheme 2.14 Synthesis of cinnamyl amine **62**

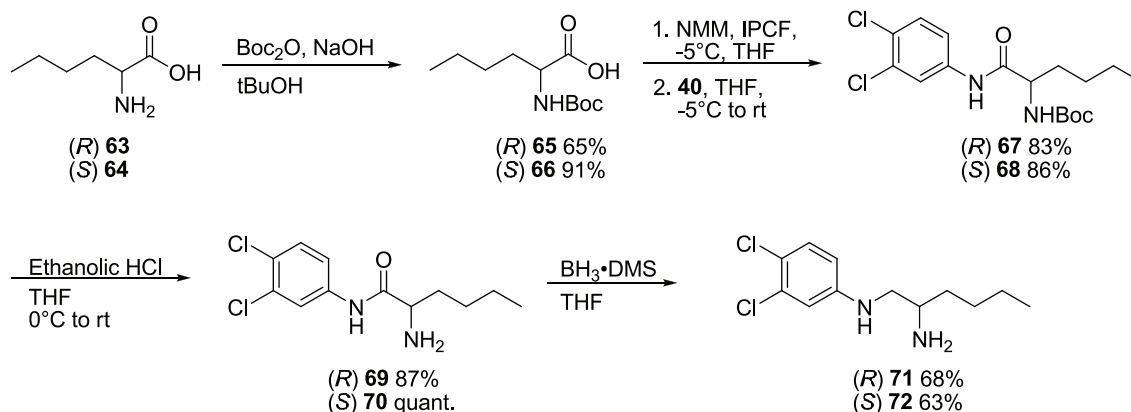


Synthesis of fragment A *n*-butylamines utilized in coupling reactions with carboxylic acid to give compounds of type **22** and **23** are shown in Schemes 2.15 and 2.16.

The chiral *n*-butyl ethanediamines **71** and **72** were synthesized from chiral amino acid derivatives (Scheme 2.15).²¹ Reaction of Boc-protected D- or L- norleucine (**65** and **66**) with isopropyl chloroformate (IPCF) and N-methylmorpholine (NMM) gave an intermediate mixed anhydride. Treatment of the mixed anhydride with 3,4-

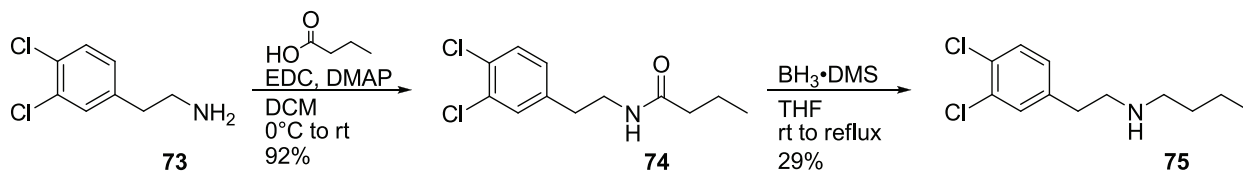
dichloroaniline (**40**) afforded carboxamides **67** and **68**. Deprotection of the Boc protecting group with ethanolic hydrochloric acid yielded α -amino amides **69** and **70**. Finally, reduction of the amide functionality of **69** and **70** yielded diamines **71** and **72**, respectively.

Scheme 2.15 Synthesis of chiral alkylated ethanediamine fragments 71 and 72



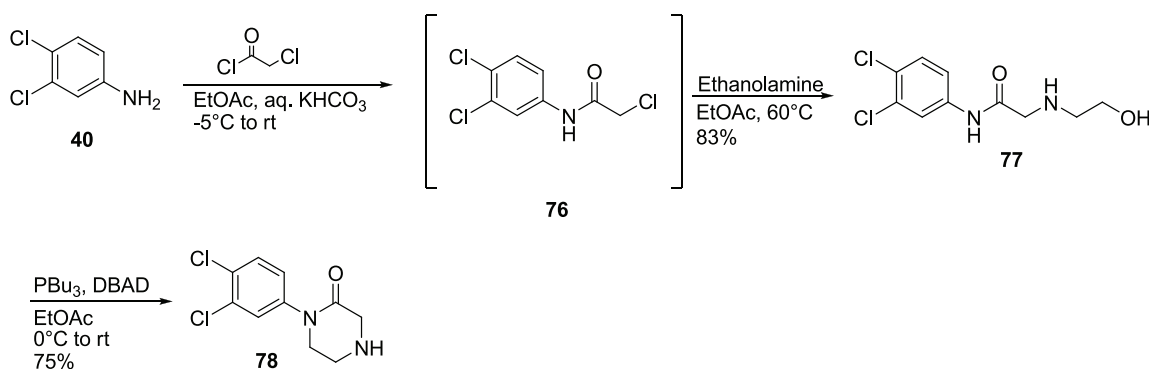
N-(3,4-dichlorophenethyl)butan-1-amine (**75**) was obtained as shown in Scheme 2.16. Carbodiimide-mediated coupling between 3,4-dichlorophenethylamine (**73**) and butyric acid gave amide **74**. Reduction with borane dimethyl sulfide afforded *n*-butylamine **75**.

Scheme 2.16. Synthesis of *n*-butylamine 75



N-Arylpiperazone **78** (Scheme 2.17) was required in the synthesis of **21**-type amide analogues. Amidoalcohol **77** was generated from acylation of 3,4-dichloroaniline under Scotten-Baumann conditions to give intermediate α -chloroamide **76**.²² Removal of the aqueous layer followed by addition of ethanolamine yielded amidoalcohol **77** upon heating to 60°C. Mitsunobu cyclodehydration of **77** proceeded with nucleophilic attack on the amide nitrogen to provide piperidone **78**. Weissman et al. suggest the increased acidity of the amide N-H compared to the amine accounts for selective 6-membered ring formation as opposed to aziridination, which would result if cyclization occurred at the amine. Use of tributylphosphine (PBU₃) and di-*tert*-butyl azodicarboxylate (DBAD) was crucial for the cyclodehydration to proceed with good yield. The more common Mitsunobu reagents triphenylphosphine (PPh₃) and diisopropyl azodicarboxylate (DIAD) gave a significantly decreased yield.

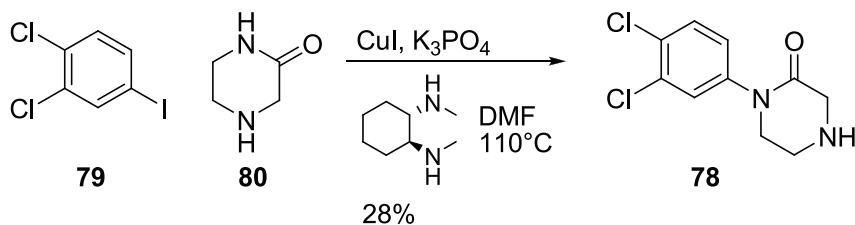
Scheme 2.17 Synthesis of piperazone 78 via Mitsunobu cyclodehydration



Buchwald's N-amidation of aryl halides²³ was explored as a one pot alternative route to N-arylpiperazone **78** (Scheme 2.18). Subjection of 3,4-dichloriodobenzene and

2-oxopiperidone to copper-catalyzed N-amidation reaction conditions yielded **78**, albeit in low yield.

Scheme 2.18 Synthesis of piperazine **78** via N-amidation



With a number of amine fragment A compounds and carboxylic acid fragment B compounds in hand, a diversity of amides were synthesized as potential antagonists. Reactions were carried out in DMF with EDC as the carbodiimide coupling reagent (Scheme 2.19). Reactions generally proceeded in moderate to good yield. The results are summarized in Table 2.3.

Scheme 2.19 General synthesis of amide compounds in Table 2.3

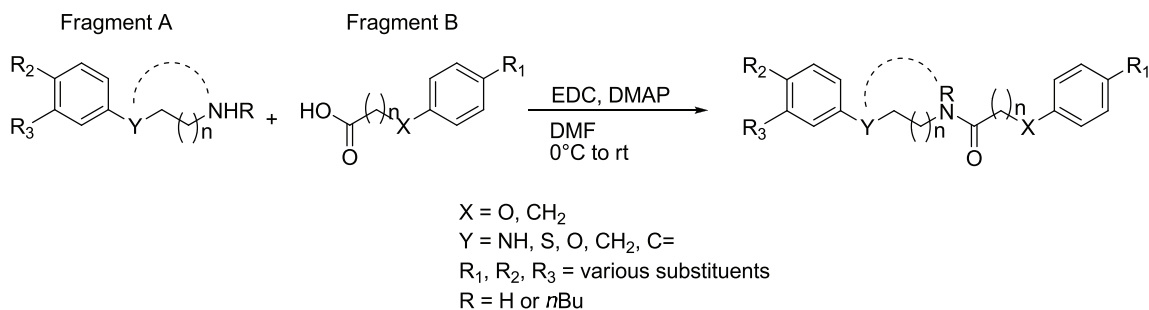
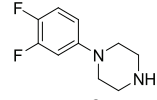
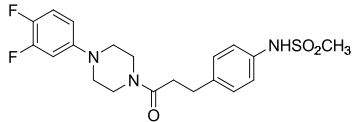
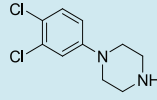
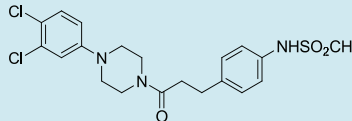
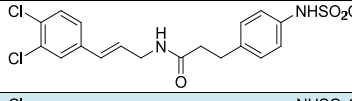
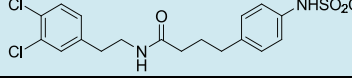
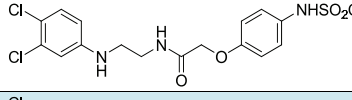
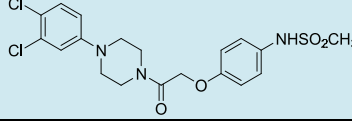
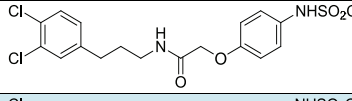
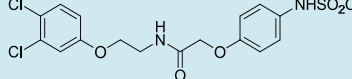
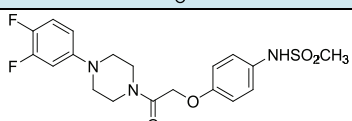
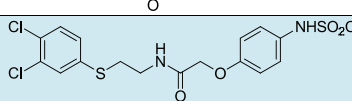
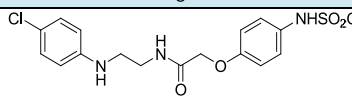
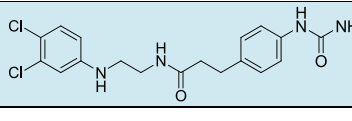
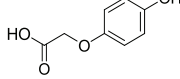
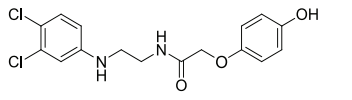
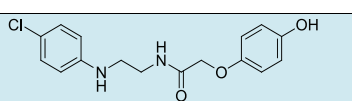
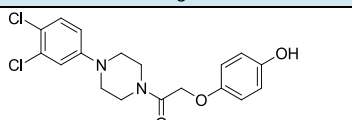


Table 2.3 Summary of amide compounds synthesized

Compound ID	Fragment A Amine	Fragment B Carboxylic Acid	Compound Structure	Yield (%)
96-13	45	36		74

Compound ID	Fragment A Amine	Fragment B Carboxylic Acid	Compound Structure	Yield (%)
96-14	 81^a	36		40
96-15	 82^a	36		28
96-17	62	36		80
96-19	73	37		68
96-22	45	35		55
96-30	82	35		85
96-32	58	35		43
96-34	53	35		41
96-35	81	35		41
96-37	55	35		69
96-38	48	35		60
96-39	45	39		25
96-40	45	 83		53
96-42	48	83		49
96-43	82	83		62

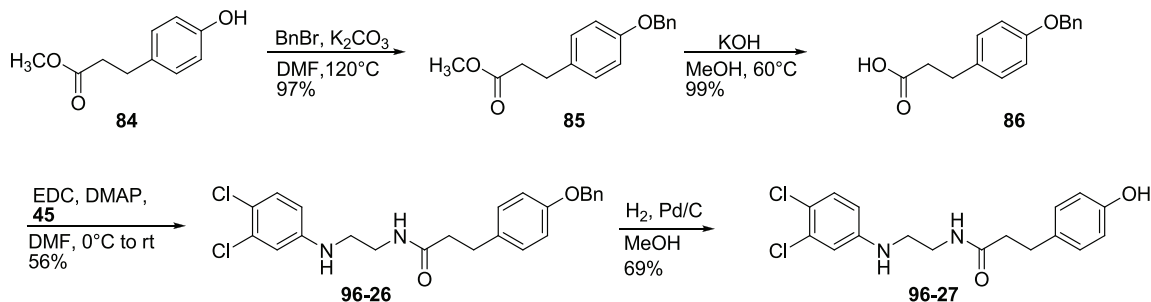
Compound ID	Fragment A Amine	Fragment B Carboxylic Acid	Compound Structure	Yield (%)
96-47	71	35		72
96-50	62	35		71
96-51	72	35		79
96-53	46	35		46
96-56	47	35		33
96-58	50	35		64
96-59	50	36		40
96-62	75	37		63
96-63	49	35		69
96-64	49	36		68
96-68	78	36		69

^acommercially available

The **96-13** analogue with a phenolic B ring was synthesized as illustrated in Scheme 2.20. Protection of phenol **84** with benzyl bromide gave compound **85**.²⁴ Saponification yielded carboxylic acid **86**, which underwent carbodiimide-mediated coupling with amine **45** to afford amide **96-26**. Deprotection of the benzyl group was carried out under hydrogenolysis conditions to give **96-27**. It is probable that protection

of the phenol before amide bond formation was not required, as indicated with **96-40**, **96-42** and **96-43** (see Table 2.3), all of which underwent smooth EDC coupling in the presence of an unprotected phenol.

Scheme 2.20 Synthesis of phenol 96-27



A number of amide analogues in Table 2.3 were reduced to their corresponding amines (Table 2.4). Reduction was accomplished with either lithium aluminum hydride (LAH) or borane dimethyl sulfide (BMS) (Scheme 2.21). In some cases, extended reaction time during the course of lithium aluminum hydride reduction resulted in A ring dehalogenation. Consequently, borane dimethyl sulfide-mediated reduction gave appreciably higher yields, most likely because BMS is a milder reducing reagent, which did not cause dehalogenation. In addition, work up of BMS reactions did not include elimination of problematic aluminum salts typical of LAH reductions. A selection of free amines were converted to HCl salts to confer increased water solubility and aid in handling (i.e. generation of powders as opposed to oils).

Scheme 2.21 General synthesis of amines in Table 2.4

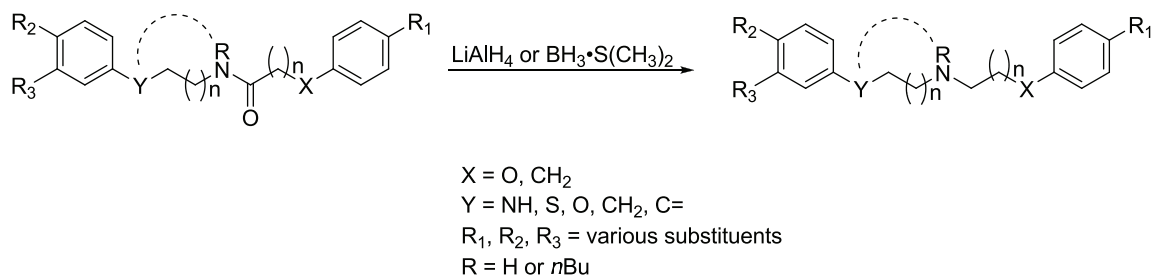
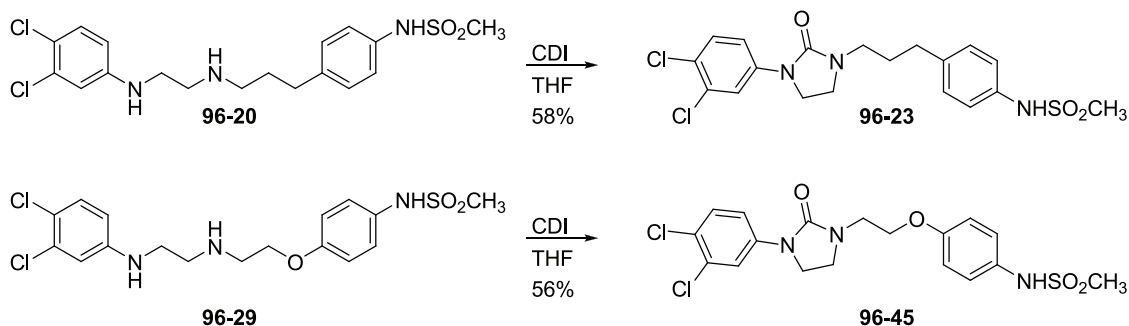


Table 2.4 Summary of amine compounds synthesized

Compound ID	Structure	Parent Amide	Yield (%)
96-20		96-13	74
96-21		96-15	21
96-24		96-19	23
96-25		96-22	34
96-31		96-30	79
96-33		96-32	42
96-36		96-34	34
96-41		96-38	78
96-48		96-47	63
96-52		96-51	82
96-55		96-37	78
96-62		96-60	41

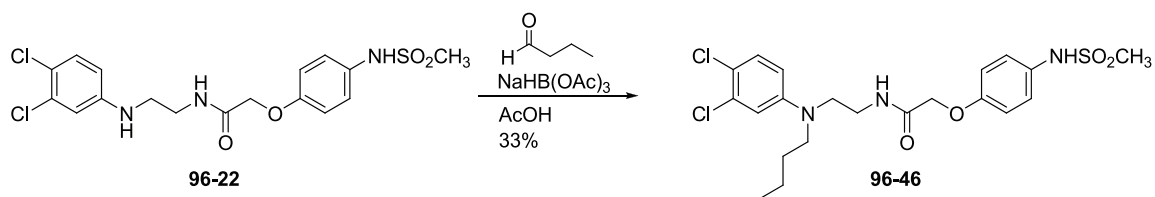
The ethanediamine linker of amine-containing compounds was incorporated into a cyclic urea moiety as illustrated in Scheme 2.22. Upon treatment with carbonyldiimidazole (CDI), cyclization to the imidazolinone occurred in reasonable yields to give **96-23** and **96-45**.

Scheme 2.22 Synthesis of imidazolinones **96-23** and **96-45**



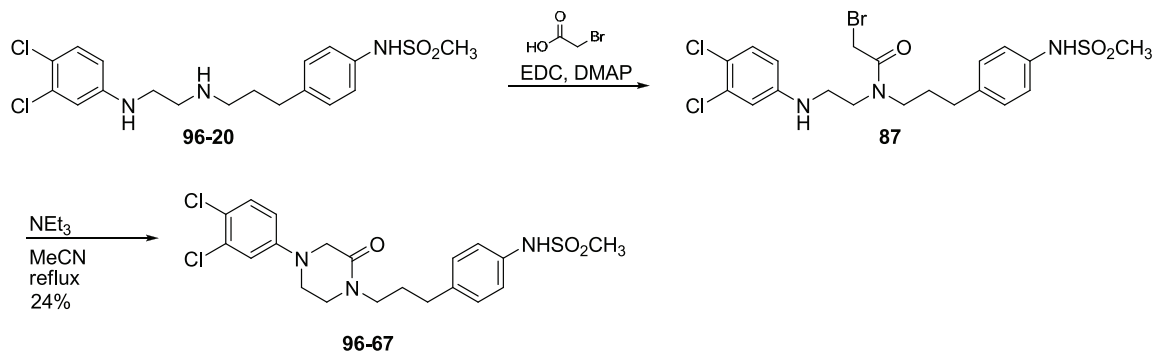
Alkylated analogue **96-46**, with a pendant *n*-butyl chain on the A ring aniline nitrogen, was synthesized by reductive amination of **96-22** with butyraldehyde (Scheme 2.23).²⁵ Due to the electron-withdrawing character of the 3,4-dichloroaniline, the reaction was carried out under acidic conditions with sodium triacetoxyborohydride. Maryanoff et al. proposed these conditions to be optimum for performing reductive aminations of weakly basic anilines. Although they report 60% to 90% yields with anilines, herein we observed significantly lowered conversion with the majority of the reaction mixture composed of butanol and unreacted **96-22**.

Scheme 2.23 Synthesis of 96-46 via reductive amination of 96-22



Piperazine analogue **96-67** was prepared via a method similar to that described by Naito, et al (Scheme 2.24).²⁶ EDC-mediated amide bond formation between N-phenylethanediamine linker analogue **96-20** and α -bromoacetic acid yielded intermediate α -bromoamide **87**. The crude material was immediately subjected to cyclization conditions with triethylamine to construct piperazine **96-67**.

Scheme 2.24 Synthesis of piperazine 96-67



2.8 Results and Discussion

2.8.1 Selectivity and structure activity relationships of 96 series compounds

Amide analogue selectivity

The potency and selectivity of amide-based compounds were evaluated using two electrode voltage clamp analysis on recombinant NMDA receptor function.⁵ First,

the effects of 3 μM of each compound was screened against current responses produced by maximally effective concentrations of NMDA receptor co-agonists glutamate (50 μM) and glycine (30 μM) at rat NR1/NR1A-, NR1/NR2B-, NR1/NR2C-, and NR1/NR2D-containing NMDA receptors. In addition to NMDA receptors, representative members of related glutamate receptor families, specifically AMPA (GluR1) and kainate (GluR6), were evaluated (Table 2.5). Compounds that exhibited less than 50% response possessed marked inhibition. The data indicate that compounds had little or no effect on response in NR1/NR1A-, NR1/NR2C-, NR1/NR2D-, GluR1 or GluR6. All but two compounds (**96-14** and **96-19**), exhibited reduced responses (less than 50%) against the NR1/NR2B-subtype of NMDA receptor. This data can also be viewed as percent inhibition (Chart 2.2), the opposite of percent response.

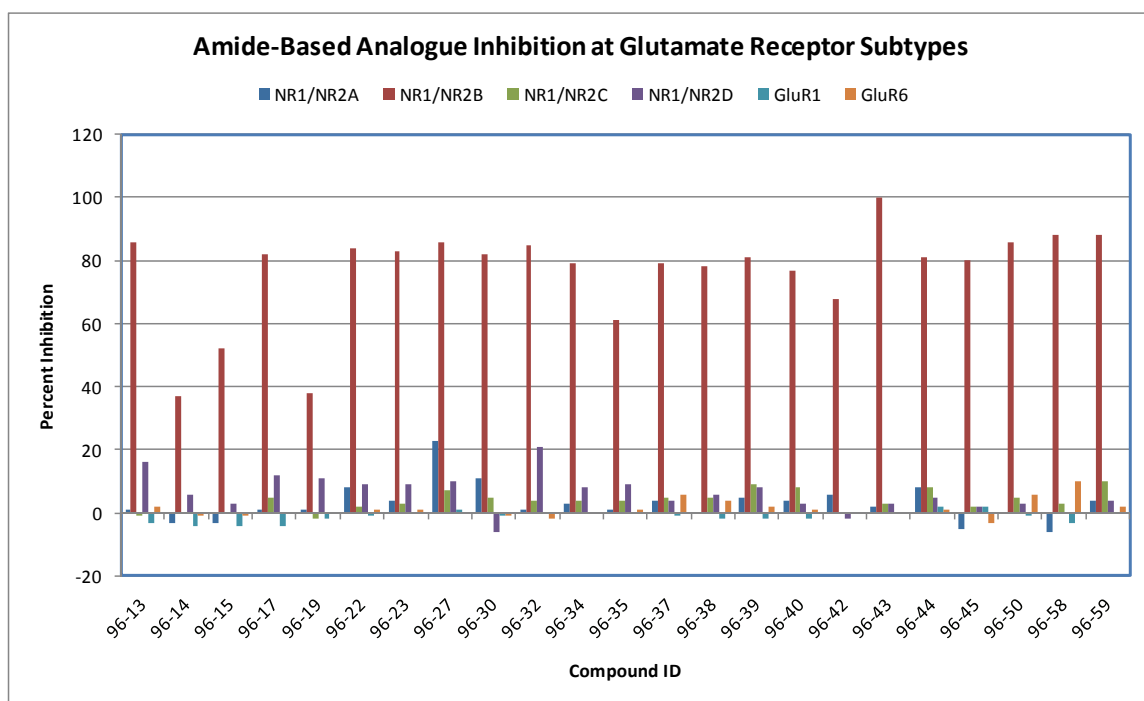
Table 2.5 *In vitro* analysis of amide-based compound towards rat glutamate receptor subtypes

Compound	Percent Response (%)					
	NMDA Receptor Subtype				Other glutamate receptors	
	NR1/NR2A	NR1/NR2B	NR1/NR2C	NR1/NR2D	GluR1	GluR6
96-13	99	14*	101	84*	103	98
96-14	103	63*	100	94	104	101
96-15	103	48*	100	97	104	101
96-17	99	18*	95	88*	104	100
96-19	99	62*	102	89*	102	100
96-22	92	16*	98	91	101	99
96-23	96	17*	97	91	100	99
96-27	77	14*	93	90	99	100
96-30	89	18*	95	106	101	101
96-32	99	15*	96	79*	100	102
96-34	97	21*	96	92	100	100
96-35	99	39*	96	91	100	99
96-37	96	21*	95	96	101	94
96-38	100	22*	95	94	102	96
96-39	95	19*	91	92	102	98
96-40	96	23*	92	97	102	99
96-42	94	32*	100	102	100	100
96-43	98	42*	97	97	100	100
96-44	92	19*	92	95	98	99

Compound	Percent Response (%)					
	NMDA Receptor Subtype				Other glutamate receptors	
	NR1/NR2A	NR1/NR2B	NR1/NR2C	NR1/NR2D	GluR1	GluR6
96-45	105	20*	98	98	98	103
96-50	100	14*	95	97	101	94
96-58	106	12*	97	100	103	90
96-59	96	12*	90	96	100	98

Data shown are the current response in *Xenopus* oocytes expressing the indicated recombinant rat receptors recorded under two electrode voltage clamp ($V_{\text{HOLD}} = 40$ Mv) in response to maximally effective concentration of glutamate (50 μM) and glycine (30 μM) in the presence of 3 μM of the indicated compound, expressed as a percent of controlled response in the absence of test compound. Measurements are the mean of 4 to 10 oocytes for each compound at each receptor subtype. For compounds showing a greater than 10% change from control, * indicates $p < 0.05$ (paired t-test)

Chart 2.2 Amide-based analogue inhibition at glutamate receptor subtypes



Graphical representation of the data presented in Table 2.5. Percent inhibition = 100 – Percent Response.

Structure activity relationships of amide analogues (pH 7.6)

The concentration-effect curve for all compounds against human recombinant NR1/NR2B-containing NMDA receptors was determined for all compounds at pH 7.6 and

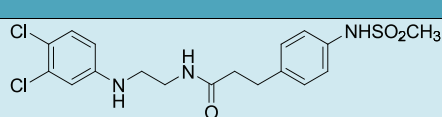
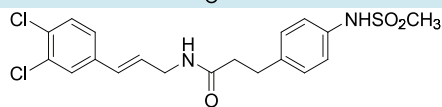
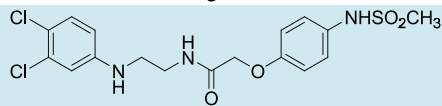
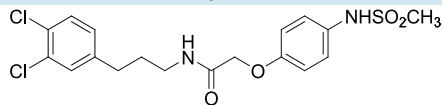
6.9. Herein we discuss the structure activity relationship (SAR) at physiologic pH (pH 7.6).

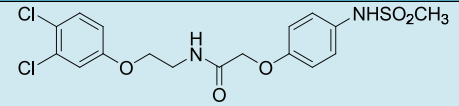
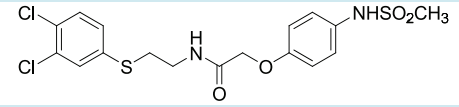
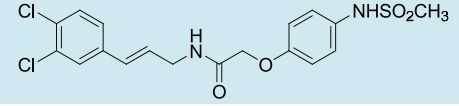
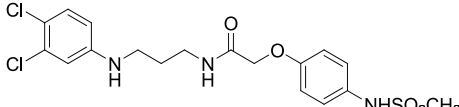
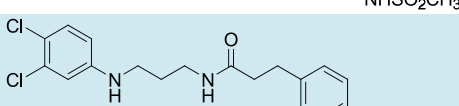
Within the linear amide series (Table 2.6), ethanediamine amide **96-13** showed excellent potency ($IC_{50} = 65$ nM). Incorporation of a phenoxy oxygen proximal to the B ring, as in **96-22**, yielded a compound with similar potency ($IC_{50} = 54$ nM). The eight-atom linker analogues of **96-13** and **96-22**, **96-59** ($IC_{50} = 750$ nM) and **96-58** ($IC_{50} = 193$ nM) respectively, were both found to be less active than their seven-atom counterparts. This result suggests the seven-atom linker is optimal in the linear amide series, similar the result found in the enantiomeric propanolamine series. The phenoxy oxygen, present in the enantiomeric propanolamine series but not the hydrazide series, clearly improved on-target potency for both the 7- and 8- membered ethanediamine linker analogues.

Due to the added potency of compounds containing the B ring linker phenoxy oxygen, this structural component was retained in a number of amides which were screened to determine the effect of the altering the aniline nitrogen proximal to the A ring on activity. In contrast to the effect observed in the semicarbazide series, where replacing the aniline nitrogen with carbon led to a 200-fold decrease in activity, propaneamide **96-32** ($IC_{50} = 64$ nM) had similar potency observed for **96-22**. Substitution of the aniline nitrogen with an oxygen (**96-34**, $IC_{50} = 380$ nM) or sulfur (**96-37**, $IC_{50} = 362$ nM) however, did lead to significant decreases in potency. The cinnamyl amides **96-17** ($IC_{50} = 50$ nM) and **96-50** ($IC_{50} = 72$ nM) both exhibited activity similar to the ethanediamine amides **96-13** and **96-22** as well as propaneamide **96-32**. In the case of

cinnamyl amides **96-17** and **96-50**, incorporation of the phenoxy oxygen led to a slight decrease in potency. The sp^2 -carbon- and sp^3 -carbon-containing analogues showed similar potency, suggesting conformation at this position is not crucial to on-target binding. In addition, the similar activity observed between cinnamyl amides **96-17** and **96-50**, propaneamides **96-32**, and aniline nitrogen containing analogues **96-13** and **96-22** suggests the presence of a hydrogen bond donor or hydrogen bond neutral species is optimal in this position. This hypothesis is supported by the fact that hydrogen bond acceptor analogues with oxygen (**96-32**) or sulfur (**95-37**) in this position exhibited decreased potency. We postulated the presence of a hydrogen bond acceptor(s) in the allosteric binding site pocket which can interact with the aniline nitrogen of **96-13** and **96-22** in a positive fashion, but have less productive interactions with the oxygen-containing **96-32** and sulfur-containing **96-37** analogues. This hydrogen bond acceptor was later found to be D101 by homology modeling.

Table 2.6 Linear amides: *in vitro* analysis at human NR1/NR2B NMDA receptors

Compound ID	Structure	NR1/NR2B IC ₅₀ (nM) [†]		Fold Shift
		pH 7.6	pH 6.9	
96-13		65	30	2.1
96-17		50	20	
96-22		54	15	
96-32		64	25	

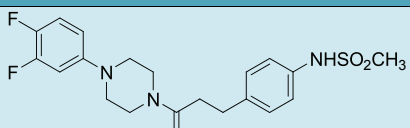
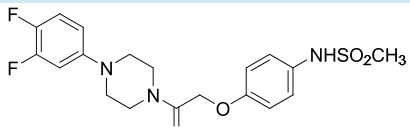
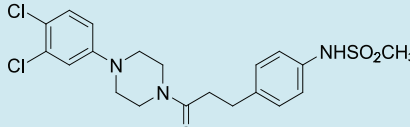
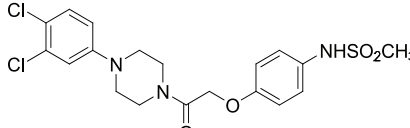
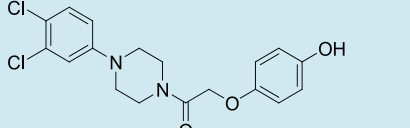
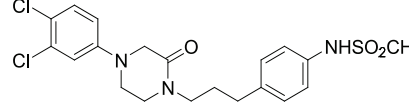
Compound ID	Structure	NR1/NR2B IC ₅₀ (nM) [†]		Fold Shift
		pH 7.6	pH 6.9	
96-34		380	120	3.1
96-37		362	45	8.0
96-50		72	70	1.0
96-58		193	90	2.1
96-59		750	260	2.9

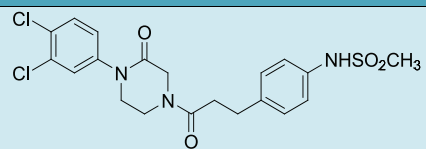
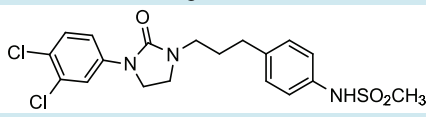
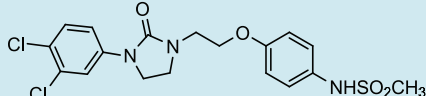
[†] The IC₅₀ value was determined from two electrode voltage clamp recordings of human NR1/NR2B receptor function, fitted as described in the experimental section. For all experiments, data are the fitted IC₅₀ value for the mean composite averaged from between 16 and 29 oocytes from 3 or more different frogs.

The effect of rigidifying the ethanediamine linker by incorporation of a number of heterocyclic structures was also probed (Table 2.7). The 3,4-dichlorophenyl acyl piperazines **96-15** (IC₅₀ = 3,600 nM) and **96-30** (IC₅₀ = 166 nM) both showed decreased activity compared to their linear counterparts. However, phenoxy-oxygen-containing **96-30** only showed a modest decrease in potency, while **96-15** exhibited a 55-fold reduction in potency. Within the acyl piperazine series, 3,4-difluoro- A ring substitution significantly decreased potency relative to the 3,4-dichloro-substituted counterparts. The effect of the phenoxy oxygen is consistent with the trend observed for 3,4-dichloro-substituted acyl piperazines, wherein phenoxy oxygen incorporation (i.e. **96-35**, IC₅₀ = 2,540 nM) resulted in increased activity (i.e. **96-14**, IC₅₀ = 12,200 nM). Migration of the

amide carbonyl from within the chain to the piperazine resulted in an increase of activity observed for **96-67** ($IC_{50} = 980$ nM), an intermediate potency between acyl piperazine **96-15** and imidazolinone **96-45**. Imidazolinone activity was less affected by the presence of the phenoxy oxygen than the acyl piperazines. Both **96-23** ($IC_{50} = 637$ nM) and **96-45** ($IC_{50} = 45$ nM) were less active than the parent amides. The acyl piperazines and imidazolinones give further evidence of the confounding influence of phenoxy oxygen incorporation on activity, the effect of which was highly dependent on the particular scaffold.

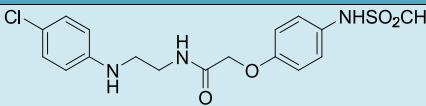
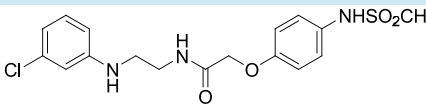
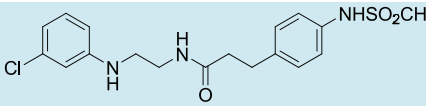
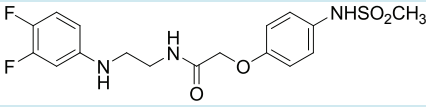
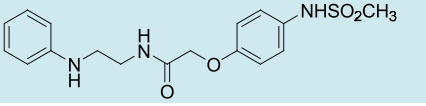
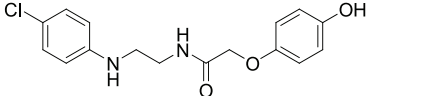
Table 2.7 Cyclic amides: *in vitro* analysis of on-target NR1/NR2B NMDA potency

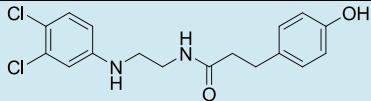
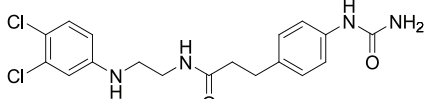
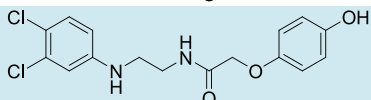
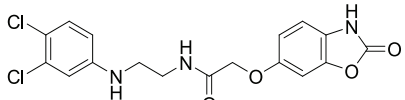
Compound ID	Structure	NR1/NR2B IC_{50} (nM)		Fold Shift
		pH 7.6	pH 6.9	
96-14		12,200	2,830	4.3
96-35		2,540	1,360	1.9
96-15		3,600	650	5.5
96-30		166	32	5.1
96-43		1,330	820	1.6
96-67		980	650	1.5

Compound ID	Structure	NR1/NR2B IC ₅₀ (nM)		Fold Shift
		pH 7.6	pH 6.9	
96-68		4,400	930	4.7
96-23		637	150	4.3
96-45		730	290	2.5

A and B ring decoration was also probed in an attempt to elucidate the subtleties of altering the periphery of the amide compounds on NR2B potency (Table 2.8).

Table 2.8 A and B ring amide modifications: *in vitro* analysis of on-target NR1/NR2B NMDA potency

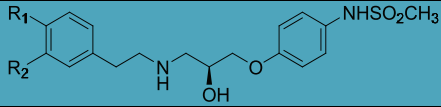
Compound ID	Structure	NR1/NR2B IC ₅₀ (nM)		Fold Shift
		pH 7.6	pH 6.9	
96-38		977	510	1.9
96-63		1,110	290	3.8
96-64		1,360	1,260	1.1
96-53		1,270	4,040	0.3
96-56		5,700	5,300	1.1
96-42		1,480	930	1.6

Compound ID	Structure	NR1/NR2B IC ₅₀ (nM)		Fold Shift
		pH 7.6	pH 6.9	
96-27		470	170	2.7
96-39		553	330	1.7
96-40		515	280	1.9
96-44 [†]		150	79	1.9

[†]Prepared by Sarah Burroughs

Differential substitution at the 3- and 4- positions of the A ring were compared to the 3,4-dichloro A ring analogue **96-22**. Both positions proved crucial to activity as 4-chloro **96-38** (IC₅₀ = 977 nM) and 3-chloro **96-39** (IC₅₀ = 1,110 nM) exhibited micromolar activity, representing a ca. 19-fold reduction in activity compared to **96-22**. 3,4-difluoro substitution (**96-53**, IC₅₀ = 1,270 nM) or no substitution (**96-56**, IC₅₀ = 5,700 nM) further decreased activity. We therefore presumed 3,4-dichloro-substitution was optimal for 96 series A ring potency. This result mimics the pattern observed in the enantiomeric propanolamine series (Table 2.9), although the effect is more significant in the amide series. In the case of the enantiomeric propanolamines, 4-chloro- substitution was also found to contribute most towards potency.¹ 3-Chloro- and 3,4-difluoro-substitution both resulted in dramatic decreases in activity.

Table 2.9 Effect of B ring modifications in the enantiomeric propranolamine series: *in vitro* analysis of on-target NR1/NR2B NMDA potency

			
Compound	R ₁	R ₂	NR1/NR2B IC ₅₀ (nM)
93-4	Cl	Cl	50
93-48	H	Cl	628
93-49	Cl	H	101
93-56	F	F	357

Alterations in B ring functionality, although incorporated to potentially effect hERG binding, also influenced NR2B activity (Table 2.8). B ring analogues with *para*-phenol (**96-40**, IC₅₀ = 515 nM), *para*-arylhurea (**96-39**, IC₅₀ = 553 nM), and *para*-benzimidazolone (**96-44**, IC₅₀ = 150 nM) moieties showed decreased potency compared to *para*-arylmethanesulfonamide **96-22**. The effect of B ring substitution was not as dramatic as A ring substitution, however. This result is most likely due to the fact that all B ring substitution compounds tested retained hydrogen bond donors in the *para*-position, known to be important to interaction with the NR2B allosteric binding pocket. The pharmacophore determinants of the A ring are significantly less understood, although hydrophobic moieties are always preferred.

Alkylation at various positions within the linker chain was proposed to effect fold shift. However, their incorporation had a significant influence on physiologic NR2B NMDA potency as well (Table 2.10).

Table 2.10 Alkylated amides: *in vitro* analysis of on-target NR1/NR2B NMDA potency

Compound ID	Structure	NR1/NR2B IC ₅₀ (nM)		Fold Shift
		pH 7.6	pH 6.9	
96-46		27,500	21,000	1.3
96-47		No block/ peculiar fit	No block/ peculiar fit	No block/ peculiar fit
96-51		18,800	2,480	7.6
96-62		>100,000	28,000	>1

When an *n*-butyl chain was incorporated at the 1- position of **96-22**, as in **96-46** (IC₅₀ = 27,500 nM) a dramatic loss in activity resulted. Similarly, the addition of a pendant *n*-butyl group at the 3- position on nitrogen, as in **96-62** (IC₅₀ > 100,000 nM), resulted in a complete loss of potency. The enantiomers **96-47** and **96-51** contained alkylation at the 3- position on carbon. Not surprisingly, the chiral environment of the binding pocket interacted with these compounds in different fashions. While **96-51** (IC₅₀ = 18,800 nM) exhibited a significant decrease in potency compared to non-alkylated analogue **96-22**, antipode **96-47** did not cause substantive blockage of the receptor, and its IC₅₀ could not be determined. Clearly alkylated amides are not appreciably tolerated by the binding pocket, either due to steric bulk or conformational arrangement. This observation mimics the results seen in with alkylated hydrazide-based compounds, but is opposite of the trend observed with the enantiomeric propanolamines. Both the

tertiary alkyl amides and alkyl hydrazide-based compounds are significantly less flexible than the enantiomeric propanolamines, and these compounds may be unable to assume the appropriate binding pose for productive ligand-protein interactions, which would account for the decreased activity observed.

Structure activity relationships of amides (fold shift)

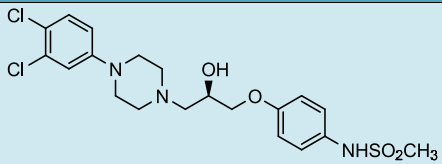
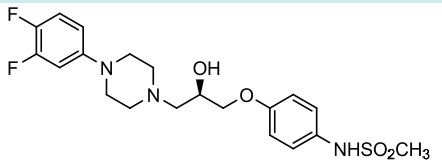
In our initial hypothesis, we sought to develop amide-based compounds that also exhibited fold shifts. Within the linear amide series (Table 2.6), analogues generally exhibited fold shifts from ca. 1 to ca. 4. Linker length did not appreciably affect fold shift. Eight-atom analogues **96-58** (fold shift = 2.1) and **96-59** (fold shift = 2.9) showed similar pH dependence to seven-atom analogues **96-22** (fold shift 4.3) and **96-13** (fold shift 2.1). Here again we see the bizarre effect of the B ring phenoxy oxygen on fold shift. Seven atom ethanediamine amides had a greater fold shift in the presence of the phenoxy oxygen, while eight atom ethanediamine amides and cinnamyl amides (**96-17** fold shift = 2.5; **96-50** fold shift = 1.0) exhibited a smaller fold shift.

The greatest effector of fold shift amongst the linear amides was the 1-position proximal to the A ring. The substitutions effected fold shift as follows: S > NH > CH₂ > O > CH. This trend only roughly follows bond length between the 1 and 2 position of the linker. The C-S bond of **96-37** has the highest fold shift (8) and the longest bond length. The C-N bond of **96-22** is of intermediate length and has a modest fold shift (4.3). The C=C bond of **96-50** has both the shortest bond length and the smallest fold shift. However, if length was the only factor controlling fold shift, one would expect the eight

atom linker analogues to exhibit higher fold shift than **96-37**. This was not the case, thus bond length cannot fully explain the fold shift phenomenon.

The cyclic amide analogues (Table 2.7) generally exhibited greater fold shift than linear amides. Among 3,4-dichlorophenylacyl piperazines (**96-35** and **96-15**, fold shift = ca. 5) and 3,4-dichlorophenylimidazolinones (**96-23** fold shift = 4.3, **96-45** fold shift = 2.5), the absence of a phenoxy oxygen was beneficial for fold shift. The 3,4-difluorophenylacyl piperazines exhibit the opposite effect, with **96-14** (fold shift = 4.3) having a slightly larger fold shift than **96-35** (fold shift = 1.9). Notably, we did not observe an increase in fold shift when changing from 3,4-dichlorophenyl to 3,4-difluorophenyl, as observed quite dramatically in the enantiomeric propranolamine series. As illustrated in Table 2.11, aryl fluorine substitution in the piperazine series robustly induced increased potency at both pH values, and conferred a significant fold shift relative to the dichloro-containing counterpart.

Table 2.11 Effect of A ring substitution in enantiomeric propranolamine piperazines: *in vitro* analysis of on-target NR1/NR2B NMDA potency

Compound ID	Structure	NR1/NR2B IC ₅₀ (nM)		Fold Shift
		pH 7.6	pH 6.9	
93-94		1,020	296	3.0
96-108		557	31	18

A and B ring modifications also played a role in affecting fold shift (Table 2.8). The 3-chloro substituted analogue **96-39** (fold shift = 3.8) was found to more closely resemble the fold shift observed with 3,4-dichloro analogue **96-22** than the 4-chloro substituted analogue **96-38** (fold shift = 1.9). This suggests an opposing relationship between the 3- and 4-position to both on-target potency and fold shift. The absence of any halogens on the A ring eliminated all fold shift, as in **96-56**, which exhibited a fold shift of 1.1. Similar to the aforementioned acyl piperazine series, 3,4-difluoro substitution had a deleterious effect on fold shift. In particular, **96-53**, the 3,4-difluoro analogue of **96-22**, exhibited a reverse fold shift (0.3).

Replacement of the *para*-arylmethanesulfonamide with another hydrogen bond donor decreased fold shift (Table 2.8). While the phenol **96-27** exhibited a moderate fold shift of 2.7, urea **96-39** (fold shift = 1.7) and benzimidazolone **96-44** (fold shift = 1.9) both had fold shift values less than two.

Amides possessing alkylation modifications were also examined for fold shift. Incorporation of the *n*-butyl chain at the 1-position of **96-22** decreased fold shift to 1.3. However, chiral alkylation at the 3-position of **96-22**, as in **96-51**, did yield a compound with a significant fold shift of 7.6. The antipode of **96-47** did not exhibit this same activity, suggesting the preference of the chiral binding pocket for the stereochemistry present in **96-51**.

2.8.2 Selectivity and structure activity relationships of amine analogues

Amine analogue selectivity

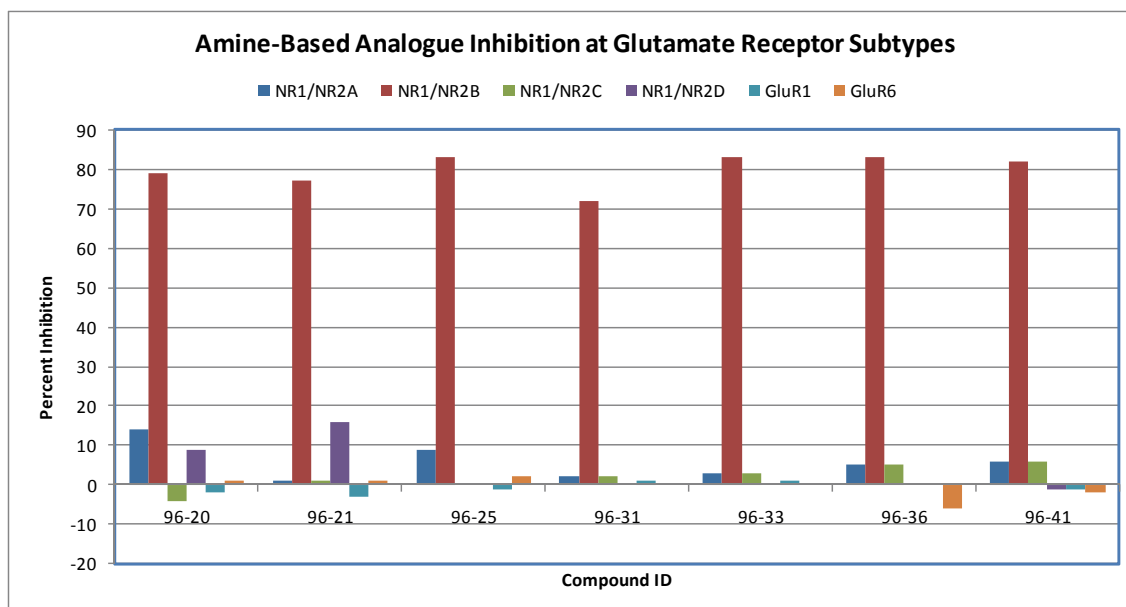
The potency and selectivity of amine-based compounds were evaluated using two electrode voltage clamp analysis on recombinant NMDA receptor function. First, the effects of 3 μM of each compound was screened against current responses produced by maximally effective concentrations of NMDA receptor co-agonists glutamate (50 μM) and glycine (30 μM) at rat NR1/NR1A-, NR1/NR2B-, NR1/NR2C-, and NR1/NR2D-containing NMDA receptors. In addition to NMDA receptors, representative members of related glutamate receptor families, specifically AMPA (GluR1) and kainate (GluR6), were evaluated (Table 2.12). Compounds that exhibited less than 50% response possessed marked inhibition. The data indicate that compounds had little or no effect on response in NR1/NR1A-, NR1/NR2C-, NR1/NR2D-, GluR1 or GluR6. This data can also be viewed as percent inhibition (Chart 2.3), the opposite of percent response.

Table 2.12 *In vitro* analysis of amide-based compound towards rat glutamate receptor subtypes

Compound ID	Percent Response (%)					
	NMDA Receptor Subtype				Other glutamate receptors	
	NR1/NR2A	NR1/NR2B	NR1/NR2C	NR1/NR2D	GluR1	GluR6
96-20	86	21*	104	91	102	99
96-21	99	23*	99	84	103	99
96-25	91	17*	100	100	101	98
96-31	98	28*	98	--	99	100
96-33	97	17*	97	--	99	100
96-36	95	17*	95	--	100	106
96-41	94	18*	94	101	101	102

Data shown are the current response in *Xenopus* oocytes expressing the indicated recombinant rat receptors recorded under two electrode voltage clamp ($V_{\text{HOLD}} = 40 \text{ Mv}$) in response to maximally effective concentration of glutamate (50 μM) and glycine (30 μM) in the presence of 3 μM of the indicated compound, expressed as a percent of controlled response in the absence of test compound. Measurements are the mean of 4 to 10 oocytes for each compound at each receptor subtype. For compounds showing a greater than 10% change from control, * indicates $p < 0.05$ (paired t-test)

Chart 3.3

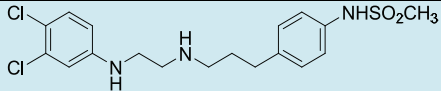
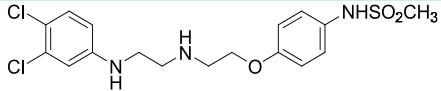


Graphical representation of the data presented in Table 2.12. Percent inhibition = 100 – Percent Response.

Structure activity relationships of amine analogues (pH 7.6)

Although we anticipated amines of parent amides to exhibit significant off-target hERG binding, we sought to determine how a centrally located basic amine would affect physiologic potency and fold shift (Table 2.13).

Table 2.13 Amines: *in vitro* analysis of on-target NR1/NR2B NMDA potency[†]

Compound ID	Structure	NR1/NR2B IC ₅₀ (nM)		Fold Shift
		pH 7.6	pH 6.9	
96-20 (96-13)		18 (65)	2 (30)	9.0 (2.1)
96-25 (96-22)		39 (54)	11 (15)	3.5 (4.3)

Compound ID	Structure	NR1/NR2B IC ₅₀ (nM)		Fold Shift
		pH 7.6	pH 6.9	
96-33 (96-32)		104 (64)	27 (26)	3.9 (2.5)
96-36 (96-34)		98 (120)	23 (38)	4.3 (3.1)
96-55 (96-37)		290 (362)	640 (45)	0.5 (8.0)
96-41 (96-38)		77 (977)	50 (510)	1.6 (1.9)
96-21 (96-15)		3,360 (3,600)	210 (650)	12.0 (5.5)
96-31 (96-30)		1,940 (166)	572 (32)	3.4 (5.1)
96-48 (96-47)		5,890 (no block)	2,300 (no block)	2.6 (-)
96-52 (96-51)		12,600 (18,800)	1,910 (2,480)	6.6 (7.6)
96-60 (96-62)		2,800 (>100)	450 (28)	6.2 (>1)

* Activity of parent amide is shown below in parenthesis.

Regarding activity at physiologic pH: in general, amines exhibited increased, or only slightly decreased, potency relative to amide counterparts.

Amine analogues of **96-13** and **96-22**, namely **96-20** (IC₅₀ = 18 nM) and **96-25** (IC₅₀ = 39 nM) respectively, both exhibited modestly increased potency relative to parent amides. Amine **96-20** was the most potent compound synthesized. Other 1-N, 4-N, 7-O linker analogues, regardless of decoration surrounding the rest of the analogue, also exhibited increased potency relative to amide counterparts. 4-chlorophenylethanediamine **96-41** exhibited a ca. 13-fold improvement in potency

relative to parent amide **96-38**. Similarly, the 3-position carbon-alkylated enantiomers **96-48** ($IC_{50} = 5,890$ nM) and **96-52** ($IC_{50} = 12,600$ nM), also containing 1-N, 4-N, 7-O linker backbones, exhibited significant increases in activity compared to parent amides.

Reduction of the carbon- and oxygen-containing amides yielded amines with slightly reduced, but still extremely potent, activity (**96-33**, $IC_{50} = 104$ nM; **96-34**, $IC_{50} = 98$ nM). In contrast, the sulfur-containing amine **96-55** ($IC_{50} = 290$ nM) exhibited slightly increased potency relative to amide **96-37**.

An exception to this trend was observed with piperazine analogues **96-21** ($IC_{50} = 3,360$ nM) and **96-31** ($IC_{50} = 1,940$). The phenoxy oxygen-containing **96-31** exhibited a 12-fold reduction in potency relative to the parent amide **96-30**. Indicative of the perplexing influence of the phenoxy oxygen, the piperazine **96-21** showed similar activity to the parent amide **96-15**.

Structure activity relationships of amines (fold shift)

As hypothesized, amines generally exhibited an increase in fold shift relative to their parent amides (Table 2.13). While linear ethanediamine amide **96-13** exhibited a fold shift of 2.1, the corresponding amine **96-20** had an impressive fold shift of 9.9. The carbon-containing analogue **96-33** (fold shift = 3.9) and oxygen-containing analogue **96-36** (fold shift = 4.3) also displayed heightened fold shifts relative to parent amides, although less than observed for **96-20**. Decreased potency at pH 7.6 accounted for the increased fold shifts in **96-33** and **96-36**, whereas heightened potency at both pH values occurred in the case of **96-20**, resulting in the large boost in fold shift observed. The 1-

N, 4-O, 7-O backbone analogues exhibited relatively similar fold shifts regardless of amide or amine functionality. A ring 3,4-dichloro and 4-chloro substituted amines **96-25** (fold shift = 3.5) and **96-41** (fold shift = 1.6) both had fold shifts within one unit of the amide parent. Interestingly, both exhibited increased potency by concomitant levels relative to the amides at both pH values, resulting in the unchanged fold shift observed. The *n*-butyl 1-N, 4-O, 7-O amine system of **96-52** also exhibited fold shift (6.6), albeit somewhat lower than the parent **96-51**. Not surprisingly, the *n*-butylamine **96-60**, with *n*-butyl position similar to that of the enantiomeric propanolamine series (3-position), showed a significant improvement in fold shift (6.2). Finally, piperazine **96-21** (fold shift = 12.0) had a large increase in potency at pH 6.9 relative to amide **96-15**, giving the largest measured fold shift of any amide-based analogue thus far.

2.8.3 Off-target effects of 96 series analogues

The development of previous classes of NR2B-selective NMDA receptor antagonists, including enantiomeric propanolamines, has been hindered by interactions with off target receptors including hERG and α_1 adrenergic receptors. Accordingly, we evaluated the effect of the **211**-type hydrazide based compounds and amide based compounds discussed above at these targets (Table 2.14).

The thiosemicarbazide **96-1** and thiosemicarbazide **96-5** both exhibited minimal hERG and α_1 -adrenergic activity. This confirmed our original hypothesis that a centrally located nitrogen, that can be ionized at physiological pH, is an important structural

feature for off-target activity. Accordingly, elimination of the charge within the linker is a plausible mechanism of eliminating untoward effects.

The influence of attenuating amine basicity on hERG and α_1 -adrenergic binding was also readily observed in the amide series as well. Ethanediamine analog **96-20**, which exhibited an excellent on-target NR2B IC_{50} of 18 nM and a fold shift of ca. 10, exhibited hERG binding of 14 nM, as well as significant α_1 activity (52% at 3 μ M). The greater affinity of **96-20** for the hERG channel compared with NR2B NMDA receptors prevents the compound from possessing a large enough NR2B versus hERG therapeutic index to be a selective and useful antagonist. However, masking the charge of the centrally located nitrogen of **96-20** dramatically reduced hERG by greater than 300-fold, with amide **96-13** exhibiting a K_i of 4,620 nM. A similar effect is observed within all linear amine-amide pairs including **96-22** and **96-25**, **96-32** and **96-33**, and **96-38** and **96-41**. Amine **96-25** exhibited 97% hERG binding, while amide **96-22** had activity reduced to 43% and a measured K_i of 12,000 nM. Also important is the 40-fold decrease in hERG binding observed with the incorporation of the phenoxy oxygen proximal to the B ring, illustrated by comparing the hERG activity of **96-13** (hERG K_i = 4,620 nM) and **96-22** (hERG K_i = 12,000 nM). Neither amide **96-13** nor **96-22** exhibited significant α_1 -adrenergic binding.

Within the linear amide series, hERG activity was also influenced by functionality proximal to the A ring. Sulfur-containing analogue **96-37** showed significant hERG binding (75% displacement at 10 μ M). The corresponding oxygen-containing analogue **96-34** reduced hERG binding (42% displacement at 10 μ M), but exhibited minimal

change in displacement of α_1 ligands. This result reinforces the value of incorporating additional oxygen atoms within the linker region, which clearly confer decreased hERG and α_1 -adrenergic activity. While the sp^3 -carbon linkage-containing amide **96-32** exhibited negligible hERG activity and α_1 -adrenergic activity, the sp^2 -carbon analogue showed minimal binding to the hERG channel ($K_i \sim 3,000$ nM) without actions at the α_1 -adrenergic receptor.

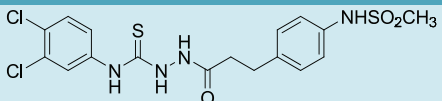
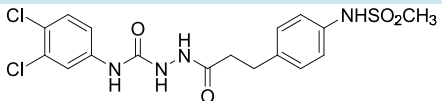
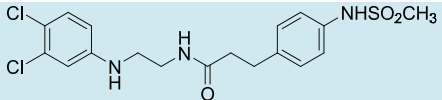
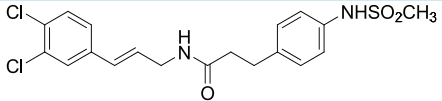
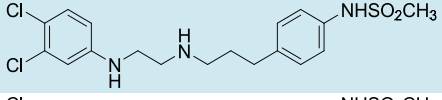
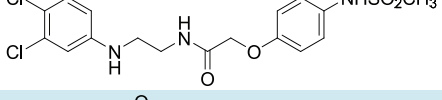
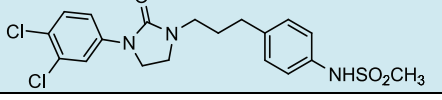
Rigidifying the linker region also had a profound influence on off-target effects. While amide **96-22** exhibited minimal hERG binding, the additional two atom bridge composing acyl piperazine **96-30** showed increased affinity for hERG binding (93% displacement at 10 μ M) and the highest α_1 -adrenergic activity of all compounds tested. The corresponding piperazine amine showed hERG and α_1 affinities similar to that of parent amide **96-30**. 3,4-difluorophenylacylpiperazine analogue **96-35** retained reduced, but still significant, hERG binding (41% at 10 μ M). The phenolic B ring and 3,4-dichloro-A ring acyl piperazine analogue exhibited intermediate hERG activity (48% at 10 μ M). These results suggest the piperazine scaffold has innate increased affinity for the hERG lumen. Consequently, decreasing hERG in this scaffold could prove difficult. It is apparent that both A ring and B ring substitution effect hERG binding of acyl piperazines dramatically.

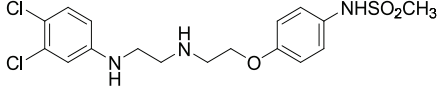
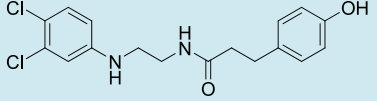
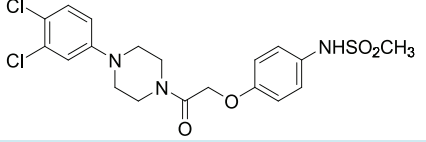
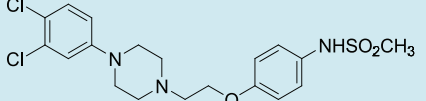
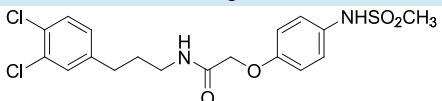
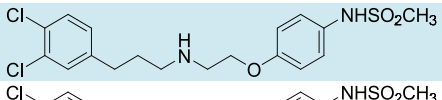
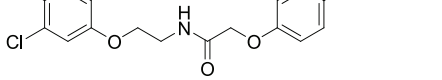
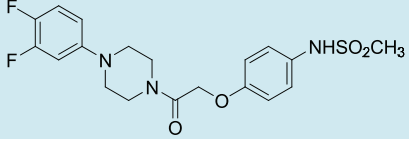
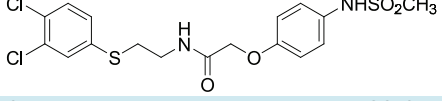
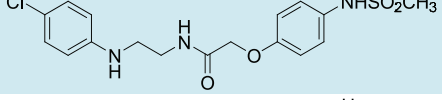
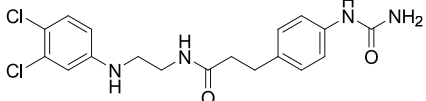
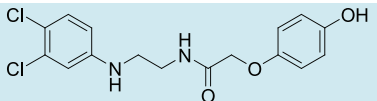
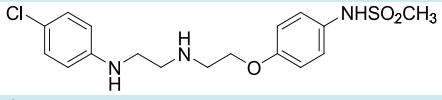
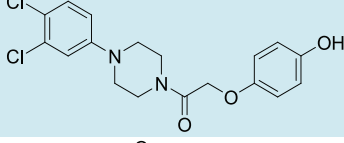
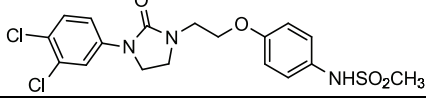
Imidazolinones **96-23** and **96-45** exhibited hERG receptor activity at levels intermediate between linear amides and acyl piperazines, but had negligible α_1 -adrenergic activity. The primary determinant controlling hERG activity in cyclic versus linear chain analogues is hydrophobicity. Removing the ethanediamine N-H bonds in the

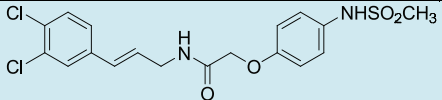
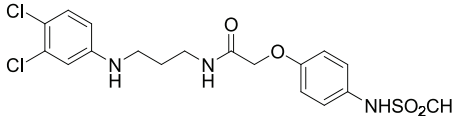
case of both the acyl piperazines and imidazolinones resulted in a significant increase in hydrophobicity. Such properties are favorable for interactions with the hERG channel, and resulted in significant off-target binding.

Finally, various B ring hydrogen bond donor moieties were examined to determine their effect on hERG binding. As expected, replacing the *para*-arylmethanesulfonamide with a *para*-arylurea (**96-39**, 18% hERG binding at 10 μ M) or *para*-phenol (**96-40**, 19% hERG binding at 10 μ M) resulted in decreased hERG binding. Again, the decrease in hydrophobicity is thought to account for the decrease in off-target hERG affinity.

Table 2.14 *In vitro* analysis of off-target hERG and α_1 potency

Compound	Structure	hERG (% displacement at 10 μ M) ^a	hERG K _i (nM)	α_1 -adrenergic (% displacement at 3 μ M) ^b
96-1		13		<1
96-5		3		5
96-13		65	4,620	1
96-17		47		16
96-20		>98	14	52
96-22		43	12,000	<1
96-23		81		<1

96-25		97	49
96-27		11	22
96-30		93	90
96-31		94	87
96-32		<1	<1
96-33		97	66
96-34		42	11
96-35		41	11
96-37		75	5
96-38		29	12
96-39		18	<1
96-40		19	19
96-41		97	53
96-43		48	31
96-45		71	23

96-50		72	22
96-58		83	19

^a Binding to the human ether a-go-go potassium channel (hERG) expressed in HEK293 cells by displacement with 1.5 nM ³[H]-astemizole. Each result represents an average of displacement experiments done in duplicate at 10 μM of the test compound.

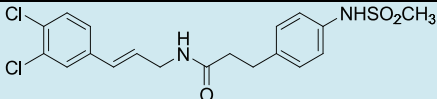
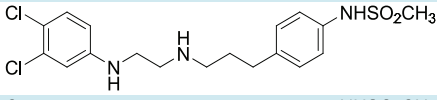
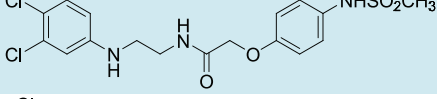
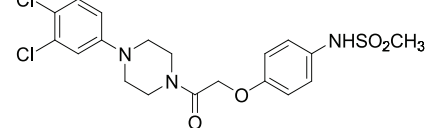
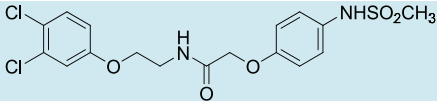
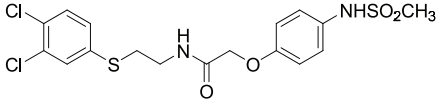
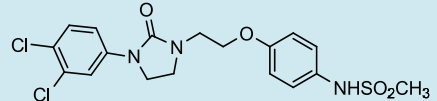
^b Percent displacement of 0.25 nM ³[H] prazosin from Wistar rat brain membranes. Each result represents the average of displacement binding experiments done at 3 μM. All binding assays were performed by MDS Pharma, Bothell, WA.

2.8.4 Compound selection process for further *in vitro* and *in vivo* testing of 96 series analogues

Our initial criterion for development of 96 series type class of NR2B-selective NMDA receptor antagonists was four-fold, including: selectivity for NR2B-subtype NMDA receptors, excellent on-target NR1/NR2B potency, decreased off-target profile, and differential activity at pH 7.6 versus 6.9.

All compounds synthesized were highly selective for the NR1/NR2B-subtype of receptor. In addition, a number of compounds exhibited two or more of the remaining criterion. Unfortunately, no analogues possessed potency, negligible off-target effects, and fold shift (we consider a fold shift of 5 to 10 to be significant). Table 2.15 summarizes the best compounds.

Table 2.15 Summary of *in vitro* properties of best analogues

Compound ID	Structure	NR2B IC ₅₀ pH 7.6 (nM)	NR2B IC ₅₀ pH 6.9 (nM)	Fold Shift	hERG [†]
96-17		50	20	2.5	47
96-20		18	2	9.0	K _i = 14
96-22		65	15	4.5	K _i = 12,000
96-30		166	32	5.1	93
96-34		380	120	3.1	42
96-37		362	45	8.0	75
96-45		730	290	2.5	71

[†] % displacement at 10 μM unless stated otherwise

During the course of our studies, we proved that amide-based compounds could exhibit fold shift and on-target potency. However, these compounds, exemplified by **96-30** and **96-37**, also bound significantly to the hERG receptor. Amine compound **96-20** also exhibited excellent on-target potency and fold shift, but possessed higher IC₅₀ for hERG than NMDA. Attempts to build-in fold shift within the 96 series were often met with increases in off-target binding. We propose that fold shift and hERG binding have similar molecular determinants, such as preference for a centrally located ionizable amine.

However, we did prove our initial hypothesis that suggested amides could exhibit both fold shift and decreased hERG binding. This finding lends credence to the argument that an ionizable nitrogen is not required for NR2B NMDA antagonism, and furthermore, attenuating the basicity of the charged nitrogen is a successful strategy to decrease off-target hERG binding.

We previously discontinued development of the enantiomeric propranolamine series due to hERG safety issues; therefore we chose safety as the defining characteristic for further testing of the 96 series compounds. We envisaged utilizing compounds **96-17**, **96-22**, and **96-37** for further studies. Compounds **96-17** and **96-22** exhibited modest fold shift (ca. 2-5), but excellent on-target potency and side effect profile. Sulfur-containing analogue **96-37** exhibited fold shift but higher than desired hERG binding. In addition, we hypothesized the compounds would have differential rates of metabolism. Enantiomeric propranolamines with fold shift (but poor hERG profile) were efficacious in a model of ischemic stroke, a condition where acidification is known to occur.¹ Compounds with fold shift are thought to be advantageous in such ischemic disease states. However, the role of fold shift is unknown in non-ischemic neurodegenerative diseases in which the NR2B-subtype of NMDA receptor is involved. Therefore, we proposed utilizing the best compound in a model of both ischemic stroke and neuropathic pain to evaluate the effects of a potent and safe NR2B-selective NMDA receptor antagonist in two disease states with differential reliance on acidification conditions.

2.8.5. In vitro and in vivo analysis of 96 series compounds

Pharmacokinetic Studies

The Rapid Rat pharmacokinetic study was performed by Ricerca Biosciences. The three compounds **96-17**, **96-22**, and **96-37** were formulated in 98% (2-hydroxypropyl)- β -cyclodextrin (5% in water)/2% dimethylacetamide. Each compound was dosed intravenously at 3 mg/kg to 3 male Sprague-Dawley rats. Blood was collected at four time-points (0.25, 2, 3, and 4 hours-post IV) and analyzed for test compound by HPLC/MS/MS methods. The first three time-point samples were obtained from the orbital plexus. The animals were sacrificed and the final time-point sample was taken from the aorta.

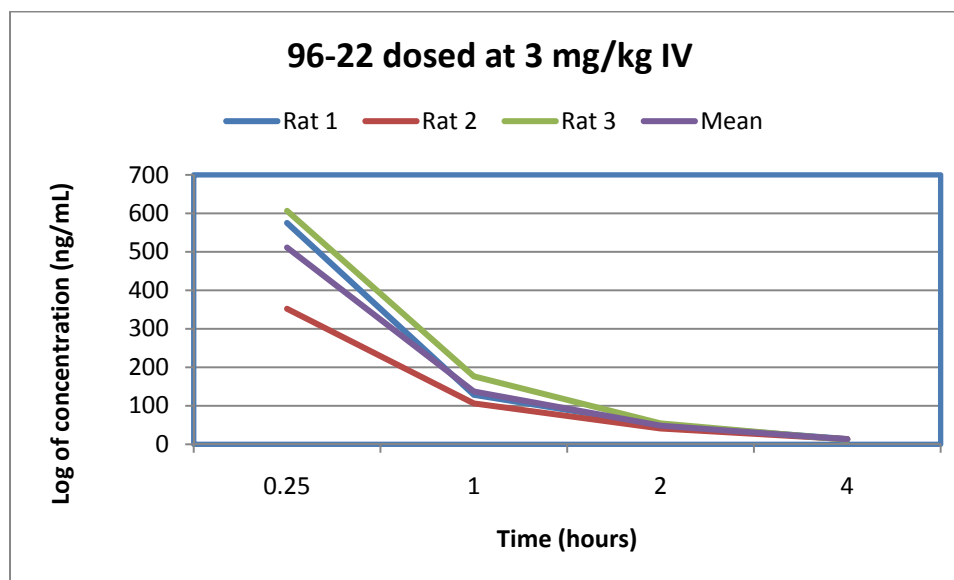
The results of the pharmacokinetic study are summarized in Table 2.16.

Table 2.16 Pharmacokinetic data obtained for 96-22, 96-37, and 96-17

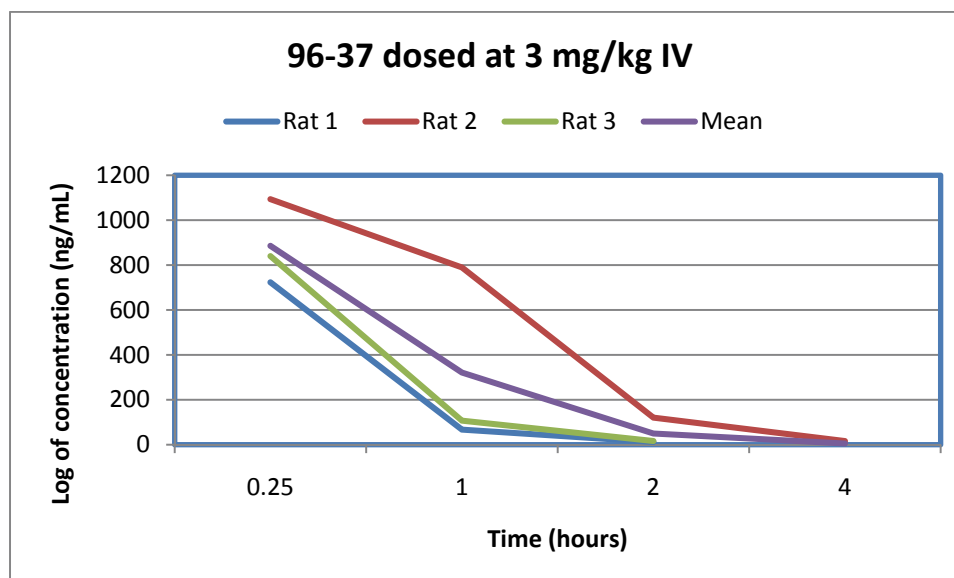
Compound	Rat	T _{1/2} (hours)	T _{max} (hours)	C _{max} (ng/mL)	AUC (hr*ng/mL)	CL (mL/hr/kg)
96-22	1	0.95	0.25	575.04	607.4	4790.53
	2	1.03	0.25	352.05	409.61	6982.90
	3	0.78	0.25	606.45	665.34	4421.04
Mean		0.92	0.25	511.18	560.78	5398.16
Standard Deviation		0.13	0	138.7	134.09	1384.81
96-37	1	0.3	0.25	723.27	638.41	4750.58
	2	0.59	0.25	1093.48	1586.79	1874.44
	3	0.31	0.25	840	747.15	4064.80
Mean		0.4	0.25	885.59	990.78	3563.27
Standard Deviation		0.16	0	189.27	519.01	1502.23
96-17	1	0.51	0.25	1426	1348.96	2214.41
	2	0.47	0.25	1514.68	1475.19	2030.02
	3	0.37	0.25	1514.09	1451.85	2104.10
Mean		0.45	0.25	1484.92	1425.33	2116.18
Standard Deviation		0.07	0	51.03	67.16	92.79

The half-lives for the three compounds can be illustrated in the Graphs 2.1-3 below.

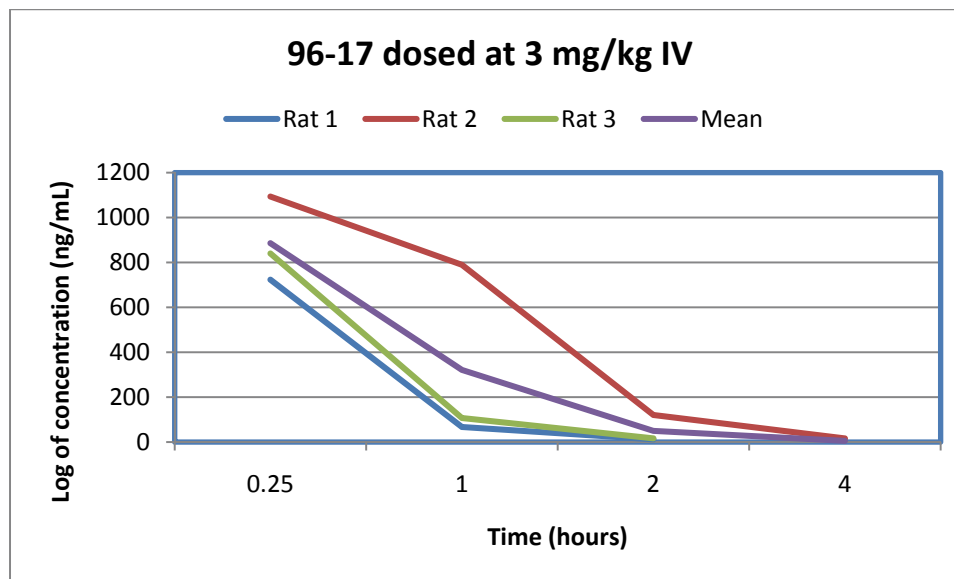
Graph 2.1



Graph 2.2



Graph 2.3



Compound **96-17** exhibited the largest area under the curve (AUC) of the three compounds evaluated, i.e. the largest amount of drug in the bloodstream after dosing. The AUC trend was as follows: **96-17** > **96-37** > **96-22**. However, ethanediamine amide **96-22** had the best plasma half-life of nearly an hour. The half-life trend was as follows: **96-22** ($t_{1/2} = 0.92$ hr) > **96-17** ($t_{1/2} = 0.45$ hr) > **96-37** ($t_{1/2} = 0.40$ hr). Area under the curve is arguably a deceiving parameter, as drugs can partition out of the bloodstream and into tissue, leading to a high internal tissue concentration but low plasma concentration. Therefore, because half-life is one of the most important and straightforward pharmacokinetic parameters, in addition to **96-22** exhibiting higher fold shift and better off-target profile compared to **96-17**, we chose **96-22** to initiate a series of further *in vitro* and *in vivo* experiments.

In vitro analysis of NMDA receptor antagonism

Compound **96-22** inhibits NR1/NR2B current responses with a half-maximally effective concentration of 36 nM (mouse subunits, n=11 oocytes from 2 frogs), 57 nM (rat, n=5-18 oocytes from 3 frogs), and 54 nM (human, n=6-24 oocytes from 4 frogs). For all inhibition curves, the Hill slope ranged between 0.81-0.94. The amino acid identity between murine and human NR1 and NR2B subunits is ~98% with most changes occurring in a region of the receptor not expected to be part of the binding pocket for NR2B-selective inhibitors. Compound **96-22** did not inhibit receptor function fully, but rather showed a maximal inhibition of 88% in rat NR1/NR2B, 78% in mouse NR1/NR2B, and 90% inhibition in human (Figure 2.19A-B). This result is consistent with that for other NR2B-selective antagonists, which act by a non-competitive mechanism to bring about incomplete inhibition.²⁷⁻³¹ Compound **96-22** (3 μ M) had minimal effects on recombinant heterodimeric NMDA receptors that contain other rat NR2 subunits (Figure 2.19A). Determination of the IC₅₀ value at rat NR1/NR2A (82 μ M, n=7), NR1/NR2C (58 μ M, n=6), NR1/NR2D (107 μ M, n=5) suggested that compound **96-22** was more than 1000-fold selective for rat NR1/NR2B over all other NR1/NR2 NMDA receptors. There were no detectable effects on recombinant kainate receptors (GluR6), recombinant AMPA (GluR1) receptors, or voltage-gated Na⁺ or K⁺ currents recorded from cultured cortical neurons (Figure 2.19A). Furthermore, consistent with other NR2B-selective ligands, inhibition of NR1/NR2B receptor responses by compound **96-22** was not surmountable by increasing the concentrations of glycine or glutamate 10-fold (Figure

2.19C), suggesting inhibition is non-competitive. The inhibition produced by **96-22** was voltage-independent (n=5; Figure 2.19D).

These data are consistent with compound **96-22** exerting a negative allosteric effect on NR2B receptor function through direct interaction with at least a portion of the ifenprodil binding site, which has been proposed to be contained within the amino terminal domain of the NR2B receptor.³²⁻³⁴ To test whether **96-22** and its analogues bind to the amino terminal domain, we evaluated a rat NR2B subunit in which residues within the amino terminal domain between S28 and H405 were deleted. We hypothesized that deletion of the amino terminal domain from the NR2B subunit, NR2B(Δ ATD), would render the receptors insensitive to inhibition by **96-22**. Functional properties of this deletion construct are similar to that of wild-type receptors (e.g., glutamate and glycine EC₅₀s are not altered, data not shown). As expected, **96-22** had virtually no effect on the current response of NR1/NR2B(Δ ATD) when activated by maximal concentrations of glutamate and glycine (Figure 2.19B). In addition, Asp101 (D101) within NR2B has been suggested to play an important role in ifenprodil binding. We find that mutation of this residue to alanine NR2B(D101A) increased the IC₅₀ to ~30 μ M (n=4 oocytes). This ca. 500-fold reduction in potency by NR2B(D101A) is consistent with **96-22** binding to the ifenprodil site on the NR2B subunit. Similar results were found for compounds semicarbazide **96-5**, amide **96-13**, and amine **96-20**, which were 51-, 102-, 177-fold less potent when evaluated at NR2B (D101A) (n=7, 13, 20 oocytes, respectively). A recently published homology model suggests the protonated piperidine of ifenprodil makes an electrostatic interaction with D101.³⁵ Presumably, the amide

compounds described here could make no such salt bridge. However, since D101A mutation reduces the potency (increases the IC_{50} value) for **96-15** and **96-22**, we hypothesize that the amide compounds make H-bond(s) to D101 and are situated similarly to ifenprodil within the ligand binding site of the NR2B ATD.³⁶

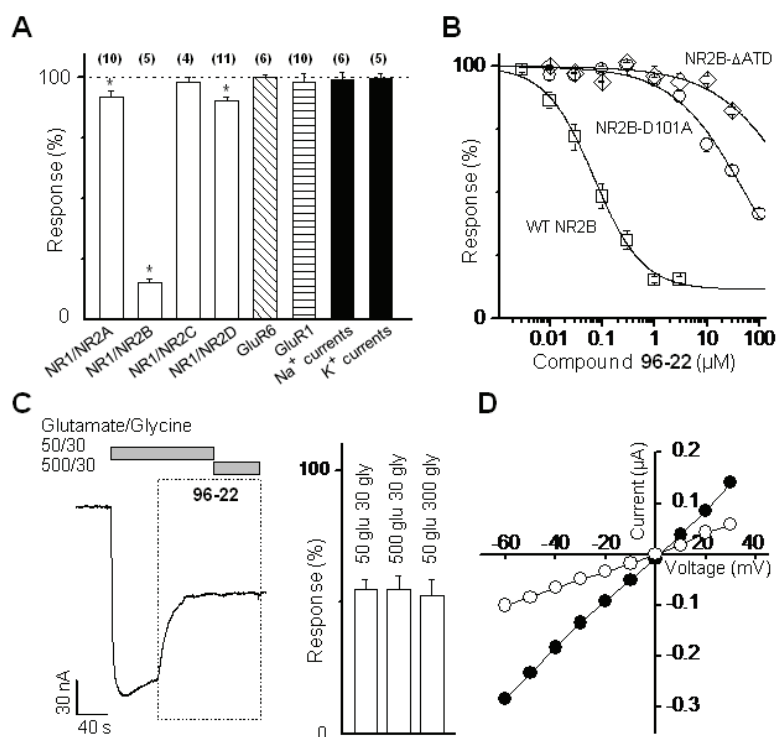


Figure 2.19 In vitro analysis of compound **96-22**

96-22 is an NR2B-selective, noncompetitive, voltage-independent NMDA receptor inhibitor. **(A)** Two electrode voltage clamp recordings from *Xenopus* oocytes were used to measure the mean \pm SEM response to glutamate and glycine coapplied with 3 μ M compound **96-22** on various glutamate receptors expressed as a percent of the maximal response evoked by saturating concentrations of agonists (50 μ M glutamate plus 30 μ M glycine) for the indicated NMDA receptors. Similar experiments were performed on recombinant GluR1 AMPA receptors (100 μ M glutamate), and recombinant GluR6 kainate receptors pre-treated with 10 μ M concanavalin-A (100 μ M glutamate). The effect of 3 μ M compound **96-22** was also evaluated on voltage-dependent sodium and potassium whole cell currents recorded from cultured cortical neurons and elicited by incremental 10 mV step depolarizations from -90 mV to +50 mV. The amplitudes of Na⁺ currents and K⁺ currents in the absence and presence of 3 μ M compound **96-22** were measured at -10 mV and +50 mV, respectively. The numbers in parenthesis are the number of oocytes or neurons tested under each condition. * $p < 0.05$, paired- t -test. **(B)** Concentration-effect curves for compound **96-22** were generated in oocytes expressing wild type and mutant NR1/NR2B receptors. The IC_{50} values of compound **52** were 0.057 μ M on rat wild type receptors

(n=18), 52 μM on mouse amino terminal domain D101A point mutants (n=4) and 563 μM on rat amino terminal domain deletion mutants (n=3). **(C)** Increasing the concentration of glutamate does not surmount the inhibition by 0.054 μM of compound **96-22** (n=4), suggesting compound **96-22** inhibits the receptor by a noncompetitive mechanism. The mean \pm SEM response as a percent control is summarized for experiments raising either glutamate or glycine concentration in the *right panel*. **(D)** Inhibition by compound **96-22** is independent of membrane potential. A representative recording from an oocyte expressing rat NR1/NR2B shows the current-voltage relationship for responses evoked by of 50 μM glutamate plus 30 μM glycine as closed circles and 0.054 μM compound **96-22** coapplied with 50 μM glutamate plus 30 μM glycine as open circles (representative of 8 experiments).

Homology modeling of **96-22** in the allosteric site of the NR2B amino terminal domain was performed (Figure 2.20) based on the binding site of ifenprodil (See Experimental for details) to elucidate the particulars of binding site ligand-protein contacts. The centrally located piperidine nitrogen of ifenprodil is thought to make a salt bridge with D101.³⁵ Because D101A mutation caused significant reduction of potency with **96-22**, **96-20**, and **96-5**, we biased docking results to force poses in which D101 was involved. As illustrated in Figure 2.20, D101 makes a salt bridge with the aniline nitrogen of **96-22**. By extension, we predict D101 to be involved in salt bridge contacts with all aniline-containing compounds (including **96-20** and **96-5**). The amide N-H forms a hydrogen bond with neighboring D104. In addition, the sulfonamide makes three hydrogen bonds with backbone residues P259, S281, and T282.

Taken together, the *in vitro* mutagenesis and computation modeling agree that contact with D101 is a crucial for NR2B potency. Within the amide series, compounds that potentially make this contact are consistently potent. Amide compounds can potentially form a maximum of one salt bridge (D101) and one hydrogen bonding contact (D104) within the linker region. The increased potency of amine compounds is

attributable to the ability of forming a maximum of two salt bridges, generally stronger than hydrogen bonds.

Figure 2.20 Homology Modeling of 96-22 in the allosteric binding site. Left panel: the amino terminal domain (grey) with 96-22 binding in the hinge region of the clamshell domain. Right panel: close-up view of hydrogen bonding interactions (highlighted in orange) 96-22 makes with the ifenprodil binding pocket.

Locomotor Activity and Rotorod Performance

NMDA receptor antagonists have been plagued by serious psychotic and ataxic side effects when utilized in animal models.³⁷⁻³⁹ The ability of NMDA receptor antagonists to influence locomotor function can readily be determined in mice. Figure 2.21 shows the motor coordination in a rotorod assay. Mice were placed on a rotating rod that was accelerated from 3 to 35 rpm over 5 minutes, and the latency time until

the mouse fell was recorded. Mice were tested 4 times each day for two consecutive days. On day three mice were injected intraperitoneally (ip) with 30 mg/kg **96-22** prior to the first trial. Dosing of **96-22** does not affect motor performance more than injection of vehicle. In contrast, the effects of NMDA receptor antagonist channel blocker MK-801 results in significant impairment and decreased latency to fall. This result suggests **96-22** did not alter the motor function of the mouse, and supports the argument that selective NR2B subtype NMDA antagonism results in decreased locomotor toxicity.

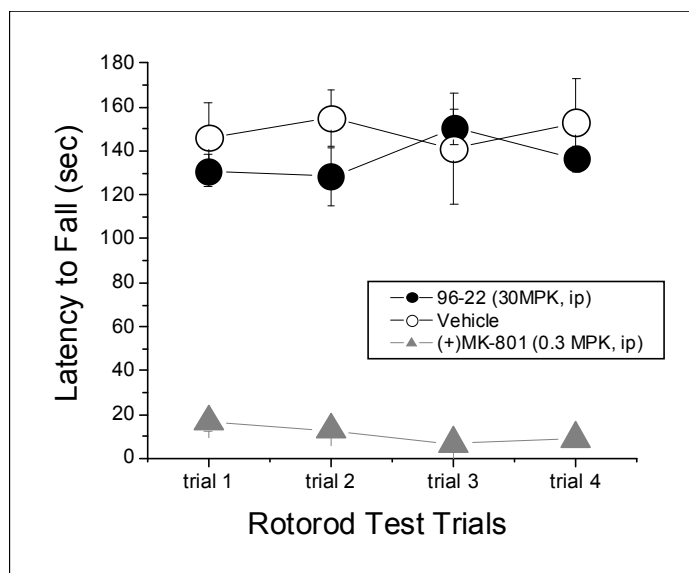


Figure 2.21 Results of rotorod locomotor assay with 96-22

Neuroprotection Assays

The neuroprotective ability of the 96-series compounds was measured by two methods, one *in vitro* and one *in vivo*. Two of the most common models of NMDA-mediated excitotoxicity were explored: (1) lactate dehydrogenase release in NMDA-

mediated neurotoxicity of cultured rat neurons and (2) the transient focal ischemia produced by occlusion of the middle cerebral artery (MCAO) in mice.

In vitro neuroprotection model: lactate dehydrogenase release from cortical neuron cultures

Excitatory amino acid-mediated neuronal injury is measured biochemically by lactate dehydrogenase (LDH) release into the media from cultured primary cortical neurons of rats.⁴⁰ Furthermore, the quantity of LDH released from neurons is indicative of compound's neuroprotective efficacy. Cortical neuronal cultures were treated with 100 mM NMDA and 100 mM glycine to activate NMDA (but not kainate or AMPA) receptors selectively. A number of 96 series compounds were evaluated, and the results are shown in Figure 2.22. A subset of the NMDA and glycine-treated cultures were exposed to varying concentrations of test compounds for 10 minutes. Cultures were washed with non-selective glutamate antagonist cocktail. The cultures were then returned to an incubator for 24 hours before spectrophotometrically determining LDH release.

Treatment of cortical neurons with 100 μ M NMDA and glycine caused nearly 30% LDH release, due to over stimulation of NMDA receptors resulting in neuronal death. In contrast, treatment with 96-series compounds **96-17**, **96-22**, and **96-37** (all at 10 μ M) resulted in LDH levels similar to that observed with treatment with vehicle. At a concentration of 10 μ M however, toxicity was observed with compound **96-30**. Overall,

these results prove that the compounds tested were neuroprotective in cortical cultures with overactivated NMDA receptors, even at concentrations much higher than the IC₅₀s.



Figure 2.22 Results of lactate dehydrogenase assay with 96 series compounds

In vivo neuroprotection model: Middle Cerebral Arterial Occlusion (MCAO)

We also evaluated compound **96-22** in an *in vivo* model of neuroprotection using the MCAO model of transient focal ischemia (Figure 2.23). Compound **96-22** was administered to C57Bl/6 mice (30 mg/kg) via intraperitoneal injection 30 minutes prior to surgery. Occlusion of the middle cerebral artery was performed for 30 minutes, after which blood flow was restored. Following reperfusion, a second dose of **96-22** (30

mg/kg) was administered. After 24 hours, the mice were sacrificed. The brains, once removed, were sliced into 2 mm sections and stained for viable cells with 2,3,5-triphenyltetrazolium chloride (TTC). The slices were then imaged by a threshold digital measure of > 30 % reduction in staining intensity.

The infarct volume of **96-22**-treated mice (average = 63 mm³) tended to be smaller than the vehicle only group (average = 78 mm³). However, this trend did not reach statistical significance. Like other NR2-selective NMDA receptor antagonists,⁴¹⁻⁴³ we hypothesize **96-22** was neuroprotective in this model. However, statistical significance was not achieved due to experimental problems related to generating reproducible infarcts. The MCAO surgery is a precise surgery, and technique in animal handling is crucial.

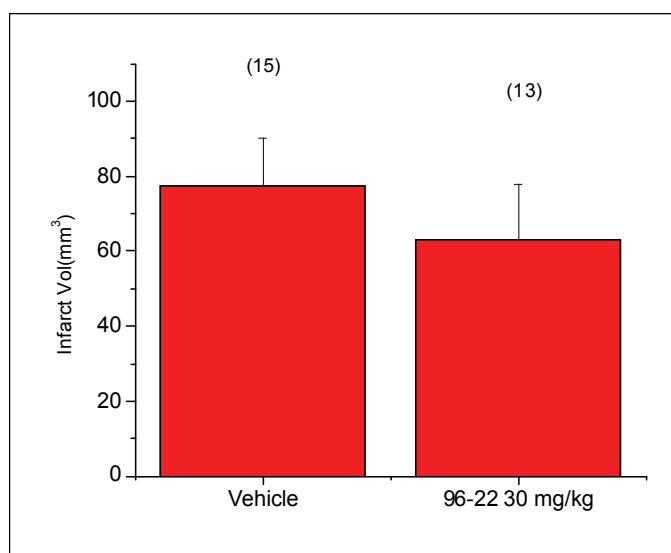


Figure 2.23 MCAO results: summary of reduction of infarct volume following treatment with 96-22

In vivo neuropathic pain model

Lead compound **96-22** appeared to show neuroprotection in one, or possibly two, models of ischemia. Both of these conditions are thought to involve brain acidification, a process in which the fold shift of **96-22** (ca. 4.5) was thought to be important. We also sought to determine the effect of using a strong NR2B NMDA antagonist with low hERG activity on a disease state which was not known to be characterized by acidification conditions, namely neuropathic pain.

Neuropathic pain is pain caused by or initiated from a primary lesion or dysfunction in the nervous system.⁴⁴ This includes situations where there is nerve injury due to trauma or disease. Additionally, neuropathic pain encompasses pain that results in the absence of a physical lesion of the nerve. The susceptibility of an individual to developing neuropathic pain is poorly understood. While the majority of people who suffer nerve injury do not develop neuropathic pain, a small fraction develops excruciatingly painful and long-lasting pain, which can often be debilitating.

The mechanism by which neuropathic pain operates is complex, but clearly relies, at least partly, on hyperfunction of NMDA receptors. Following nerve injury, the dorsal root ganglion (DRG) elicits spontaneous and persistent discharges, including heightened release of excitatory amino acids, including glutamate.⁴⁵⁻⁴⁶ Over-activation of glutamate receptors (including NMDA and AMPA) occurs, resulting in spinal sensitization.⁴⁷⁻⁴⁸ Clinically, spinal sensitization presents as hyperalgesia (painful response to a normally non-painful stimulus) and allodynia (increased sensitivity to pain).⁴⁹

A number of lines of evidence implicate the NMDA receptor in neuropathic pain. Accordingly, NMDA receptor antagonists have been shown to block spinal sensitization resulting from nerve injury, including NR2B-selective CP-101,606 (traxoprodil).⁵⁰⁻⁵¹ In particular, it has been hypothesized that NR2B subtype receptors contribute predominantly towards mediating pain and spinal sensitization relative to NR2A-, NR2C-, or NR2D-containing receptors.⁵²⁻⁵⁴ Therefore, we sought to evaluate our safe, potent, and NR2B-selective NMDA antagonist **96-22** in a model of neuropathic pain.

The Chung model⁵⁵ was chosen due to previous success with enantiomeric propanolamines in exhibiting efficacy (outsourced to Algos Therapeutics). Briefly, the spinal cord ligation model was used to induce chronic neuropathic pain. The rats were anesthetized and the L5 and L6 spinal nerves were ligated with a suture. The wound was closed and the animals were allowed to heal for 21 days, allowing the animals to develop neuropathic pain. Thirty minutes prior to testing (-30), a baseline von Frey test was measured. This involves inserting metal filaments of varying diameters at the rat's foot. While normally not considered painful, increases in injury-induced responsiveness was considered indicative of allodynia. At time 0, compound **96-22** was administered (3 test groups, 10 animals each, 10, 30, and 100 mg/kg doses). Further von Frey analyses were conducted at multiple time points post-dosing for 240 minutes. The results are summarized in Figures 2.24 and 2.25.

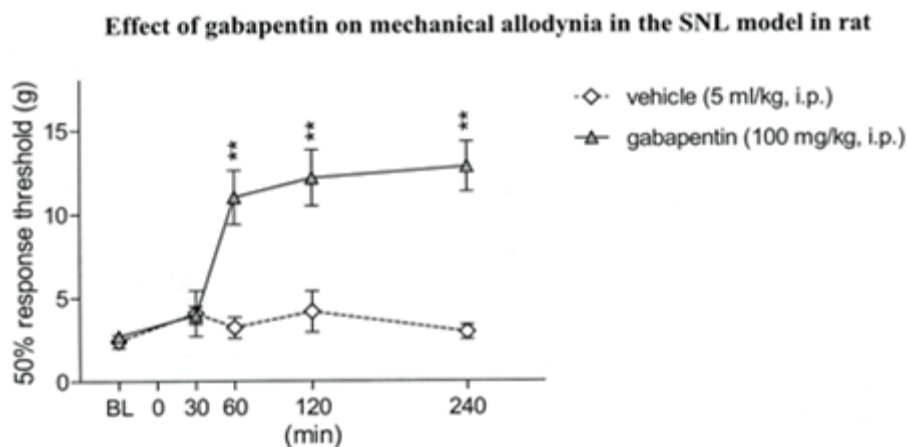


Figure 2.24 The positive control, gabapentin (100 mg/kg i.p.) significantly reduced mechanical allodynia. Shown are the mean von Frey thresholds for the experimental group indicated.

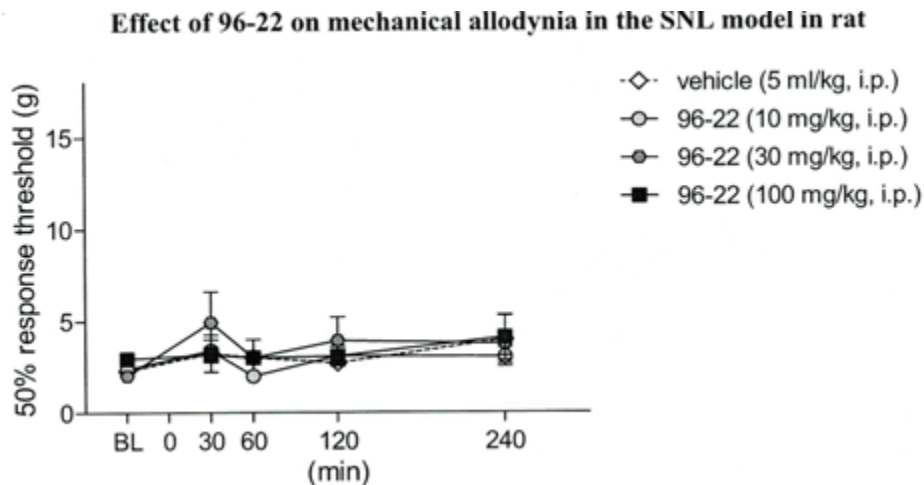


Figure 2.25 Administration of 96-22 (10, 30, and 100 mg/kg i.p.) did not reduce mechanical allodynia. Shown are the mean von Frey thresholds for the experimental groups indicated

Figure 2.24 illustrates the positive control gabapentin, which reduces mechanical allodynia relative to the vehicle after a period of one hour. In contrast, **96-22** had no efficacy attenuating allodynia at any time point for any of the dosing regimens tested (Figure 2.25).

The findings of the neuropathic pain study were somewhat surprising. The absence of an effect, even at the high dose of 100 mg/kg, led us to examine reasons for

the negative result. We subsequently submitted three compounds for blood-brain permeability analysis. We estimated brain penetration for linear amide **96-22**, acyl piperazine **96-30**, and imidazolinone **96-45** using the MDR1-MDCK *in vitro* assay (Table 2.17).

Table 2.17 MDR1-MDCK permeability of 96 series compounds

Compound ID	$P_{app}(A-B)^a$	$P_{app}(B-A)$	Efflux ratio ^b
96-22	1.80	63.2	35
96-30	4.76	42.4	8.9
96-45	12.9	40.2	3.1

^a P_{app} is the apparent permeability for the apical to basal (A-B) and the basal to apical (B-A) direction across MDR1-MDCK cell monolayers in Transwell wells. Papp units are $\times 10^{-6}$ cm/s.

^b Efflux ratio = $P_{app}(A-B)/P_{app}(B-A)$

It was determined that **96-22** was not expected to appreciably pass the blood-brain barrier ($P_{app}(A-B) = 1.80$) and was deemed a substrate for P-glycoprotein efflux (efflux ratio = 35). The p-glycoprotein pump (Pgp) is a well known proteinaceous mechanism responsible for efflux of non-native compounds, all of great structural diversity, from the cell. The low estimated brain permeability was most likely the cause of the negative result observed in the neuropathic pain study. Moreover, any **96-22** that did cross the blood-brain barrier would quickly be ejected from cells via the Pgp efflux pump. Acyl piperazine **96-30** showed increased estimated brain penetration, but was also deemed a Pgp efflux substrate. The compound with the highest brain potential was imidazolinone **96-45**, which also exhibited the lowest Pgp efflux. Thus, tying up the chain nitrogen atoms in **96-22** into a cyclic functionality such as acyl piperazine or imidazolinone led to increased blood brain barrier permeation. The decrease in

lipophilicity due to elimination of the two hydrogen bond donors of **96-22** likely accounts for the increased brain permeation potential. Furthermore, the more lipophilic compounds were less likely to be Pgp efflux substrates.

Our negative neuropathic pain results may have disproved a current hypothesis that suggests NMDA antagonists that act outside the central nervous system could be beneficial in treating pain.⁵⁶ The DRG is located in the peripheral nervous system, and operates at the hub of aberrant afferent discharges associated with pain. In addition, the NR2B-subtype NMDA receptors are differentially expressed on DRG neurons.⁵⁷ The NR2B-selective antagonist ifenprodil was found to be effective at inhibiting NMDA and glycine-induced current in rat neurons *in vitro*. Presumably, a NMDA receptor which acted at the peripheral nervous system would not cause cognitive, locomotor, or psychosis-like side effects because the compound would not be interacting with NMDA receptors within the brain or central nervous system. Compounds such as ifenprodil, or the 96 series developed herein, would possess the benefits of being both NR2B-NMDA subtype selective and tissue (DRG) selective, offering a safe and effective pain management strategy.

The finding that **96-22** did not substantially cross the blood brain barrier suggests the compound is concentrated in systemic circulation. Partitioned outside of the central nervous system, we hypothesized we would still see an effect in the neuropathic pain model due to the ability of **96-22** to act at the NR2B-containing receptors of the DRG, if the hypothesis described above was valid. Our failure to observe efficacy with a non-

brain penetrating NR2B-selective NMDA receptor antagonist in the Chung model provides evidence against this theory.

Naturally, alternative reasons for the inability of **96-22** to show efficacy in the *in vivo* neuropathic pain model can be rationalized. In DRG neurons over-activated with NMDA and glycine *in vitro*, the IC₅₀ of ifenprodil was substantially higher (2.64 μM) than NR2B-receptors found within the central nervous system (IC₅₀ = 500 nM), possibly due to differential post-translational modification of the NR2B receptors in the DRG.⁵⁶ Consequently, a higher dosing regimen **96-22** may have been needed to generate a substantial *in vivo* drug concentration. In addition, human liver microsomal metabolic data showed **96-22** is rapidly metabolized, with only 22% percent of drug detectable after 30 minutes (1% remaining after 60 minutes). Therefore, although ip or iv injection would bypass digestive metabolism, substantial P450 metabolism would occur when the compounds were delivered ip (both *in vivo* studies administered in this manner). Combined, the poor brain permeability and high metabolic rate suggest **96-22** was not present in the brain in appreciable amounts to affect NR2B-subtype receptors in the neuropathic pain model. In contrast, **96-22** did show a trend towards decreasing infarct volume, partially contributing to neuroprotection observed in the MCAO stroke model. It is assumed a breakdown of the blood brain barrier occurs during ischemia.⁵⁸ Such a breakdown would potentially allow **96-22** to pass into the brain and affect NR2B-subtype receptors, responsible for decreased infarct volume shown in the MCAO study.

2.9 Conclusions

The development of NMDA receptor antagonists, useful for the treatment of a number of neurodegenerative diseases, has been hindered (both in our lab and by others) by the presence of untoward side effects as a result of global NMDA receptor antagonism and undesired off-target activity. Our work in the enantiomeric propanolamine series resulted in lead compound **93-31**, which was selective, potent, and had a fold shift of 17. Unfortunately, **93-31** and the majority of enantiomeric propanolamines exhibited higher affinity for off-target hERG binding than NMDA receptor antagonism. The likelihood of hERG binding to induce QT prolongation *in vivo*, a known red flag safety issue for the Federal Drug Administration, was the impetus to develop a series of NR2B-selective NMDA receptor antagonists that did not exhibit hERG binding.

In the course of this study we sought NR2B-selective NMDA receptor antagonists that were potent, displayed pH sensitivity, and had a decreased off-target profile. Beginning with screening hit thiosemicarbazide structure **211**, a novel series of hydrazide-based compounds were synthesized and evaluated biologically for NR2B NMDA receptor antagonism. The aniline nitrogen proximal to the A was found to be crucial for NR2B potency. While semicarbazide **96-5** was selective, potent, and contained a safe hERG profile, **96-5** nor any other hydrazide-based compound exhibited fold shift. We hypothesized the absence of a centrally located amine which would be ionizable at physiologic pH was responsible for the negligible hERG binding.

We further pursued amide-based antagonists with increased flexibility which incorporated both the aniline nitrogen proximal to the A ring and a centrally located amide. We probed a series of 1-position substitutions among amide analogues, and found nitrogen-containing ethanediamine amide analog **96-22** to be optimal. The ethanediamine linker was incorporated into both acyl piperazine and imidazolinone moieties, and a number of these compounds also exhibited excellent potency. While members of the linear amide series were both potent and had negligible hERG binding, acyl piperazine and imidazolinones had much higher affinity for the K⁺ channel. The unexpected dramatic increase in off-target affinity as a result of a 2-carbon chain addition suggests the heightened hydrophobicity of the cyclic analogues increases the likelihood of hERG binding, and these scaffolds may have inherent hERG activity that will require additional medicinal chemistry efforts to eliminate. Fold shift among linear and cyclic amides varied tremendously from 8 to -0.5. The amide-based compounds which exhibited fold shift (i.e. **96-37**, fold shift = 8) prove that an ionizable nitrogen is not required for fold shift, a theory previously disseminated following work within the enantiomeric propanolamine series. However, the molecular determinants of a given amide analogue's fold shift were not clear, and we could not induce fold shift among amides via alkylation of the centrally located nitrogen, a proven strategy in the enantiomeric propanolamine series. In addition, the amide compounds that did exhibit significant fold shift also had greater affinity for the hERG channel than low-to-moderate fold shift-inducing analogues. Amine compounds resulting from reduction of the parent amides exhibited both increased fold shift and increased hERG binding. Taken together,

we hypothesize that the pharmacophores involved for fold shift and hERG binding are similar, particularly a centrally located nitrogen and hydrophobicity.

Further *in vitro* and *in vivo* testing was conducted to probe the drug-like characteristics of the amides. The pharmacokinetic half-lives of three compounds were determined, and **96-22** again proved superior, exhibiting a half-life of nearly an hour. **96-22** showed significant neuroprotection in an *in vitro* model of NMDA-induced over-activation in neuronal cultures. In addition, **96-22** showed a trend (although not statistically significant) towards limiting injury infarct volume and exhibiting neuroprotective properties in an *in vivo* mouse model of ischemic stroke. Together, these results suggest NR2B-selective amide compounds with decreased hERG activity and moderate fold shift are a potential treatment for ischemic disorders. In contrast, **96-22** proved ineffective in the rat Chung model of neuropathic pain. We hypothesize the inability of the compound to potentially cross the blood brain barrier was responsible for the lack of activity observed in the neuropathic pain model, and may have been a contributing factor towards the inability of **96-22** to show statistical significance in decreasing infarct volume in the MCAO model. In addition, we expect this work will be utilized as proof-of-principle evidence against treatment of neuropathic pain by inhibiting NR2B receptors in the peripheral nervous system DRG.

The amide-based compounds described herein encompass increased drug-like characteristics over the previous enantiomeric propanolamine series, including high potency with minimal hERG binding. These novel analogues have provided insight into ways in which off-target effects can be mitigated while retaining high potency and

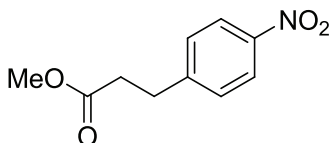
selectivity at NR2B containing receptors, and represent a starting point for further development of the potential uses of NR2B-selective NMDA receptor antagonists.

2.10 Chemistry Experimental Detail

All reagents were obtained from commercial suppliers and used without further purification. Reaction progress was monitored by thin layer chromatography (TLC) on pre-coated glass plates (silica gel 60 F254, 0.25 mm). Proton and carbon NMR spectra were recorded on an INOVA-400 (400 MHz), VNMRS 400 (400 MHz), INOVA-600 (600 MHz), or Mercury 300 Vx (300 MHz). The spectra obtained were referenced to the residual solvent peak. Mass spectra were performed by the Emory University Mass Spectroscopy Center on either a VG 70-S Nier Johnson or JEOL instrument. Elemental analyses were performed by Atlantic Microlab Inc. C, H, N agreed with proposed structures within $\pm 0.4\%$ of theoretical values unless indicated otherwise. When noted, flash chromatography was performed on a Teledyne ISCO Combiflash Companion with prepackaged Teledyne RediSep disposable normal phase silica columns. HPLC (Varian) was used to determine the purity of some compounds. HPLC was performed on a C₁₈ analytical column with UV detection using methanol and acetonitrile at 1 mL/minute according to the following ratios: (a) 50% acetonitrile/50% methanol over 10 minutes (b) 30% acetonitrile/70% methanol-70% acetonitrile/30% methanol gradient over 10 minutes (c) 20% acetonitrile/80% methanol-80% acetonitrile/20% methanol gradient over 10 minutes.

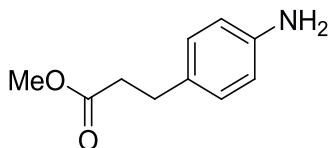
2.10.1 Experimental details of compounds synthesized in Chapter 2

Methyl 3-(4-nitrophenyl)propanoate (4).



Diisopropylamine (12.8 mL, 91 mmol, 1.21 equiv) was dissolved in anhydrous THF (100 mL) and cooled to -78°C . Butyllithium (1.6 M in THF, 62 mL, 1.32 mmol, 1.1 equiv) was added dropwise. The mixture was stirred for 1 hr at -78°C before addition of HMPA (6.0 mL). After stirring another hour at -78°C , methyl acetate (6.5 mL, 90 mmol, 1.20 equiv) was added dropwise and stirred for 1 additional hour. Finally, 4-nitrobenzyl bromide (16.0 g, 75 mmol) in THF (60.0 mL) was added dropwise giving a red solution. The mixture was warmed to room temperature and stirred for 12 h. The reaction was quenched with water and the mixture was extracted with DCM (3x). The combined organics were dried over MgSO_4 and concentrated *in vacuo* to give a brown residue. The crude material was purified using silica gel chromatography (1 EtOAc/1 Hexanes) to give a yellow solid (5.86 g, 37%). $^1\text{H NMR}$ (400 MHz, CDCl_3) δ 8.15 (d, $J = 8.2$ Hz, 2H), 7.37 (d, $J = 8.2$ Hz, 2H), 3.68 (s, 3H), 3.06 (t, $J = 7.3$ Hz, 2H), 2.68 (t, $J = 7.3$ Hz, 2H).

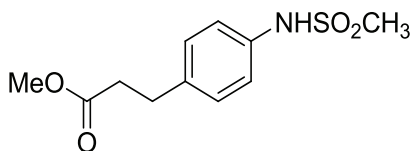
Methyl 3-(4-aminophenyl)propanoate (5).



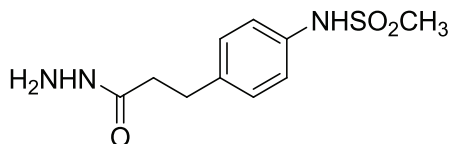
Compound **4** (5.86 g, 28 mmol) and was dissolved in ethanol (250 mL). To this solution, 5% Pd/C catalyst (0.293 g, 5 wt%) was added. The mixture was hydrogenolyzed at 40 psi

for 1 h. The catalyst was removed by filtration over a pad of celite and the resulting solution was concentrated *in vacuo* to give a yellow oil which was used without further purification (3.64 g, 73%). ^1H NMR (300 MHz, CDCl_3) δ 7.00 (d, $J = 8.3$ Hz, 2H), 6.64 (d, $J = 8.3$ Hz, 2H), 3.67 (s, 3H), 3.59 (bs, 2H), 2.85 (t, $J = 7.6$ Hz, 2H), 2.58 (t, $J = 7.6$ Hz, 2H).

Compound **5** can also be synthesized from **7**. Thionyl chloride (1.65 mL, 22.6 mmol, 3.3 equiv) was added dropwise to a solution of dry methanol (6.65 mL, 164 mmol, 24 equiv) at -10°C . After stirring for 10 minutes, the propionic acid **7** (1.13 g, 6.84 mmol) was added to give a yellow suspension. The solution was stirred for 1 h and slowly warmed to room temperature. The resulting solution was concentrated *in vacuo* to give a yellow solid. The solid was suspended in EtOAc, and solid NaHCO_3 was added until the salt dissolved fully. The layers were separated and the organics were washed with brine, dried over MgSO_4 , and concentrated *in vacuo* to give a yellow solid (1.06 g, 98%). ^1H NMR (300 MHz, CDCl_3) δ 7.00 (d, $J = 8.3$ Hz, 2H), 6.64 (d, $J = 8.3$ Hz, 2H), 3.67 (s, 3H), 3.59 (bs, 2H), 2.85 (t, $J = 7.6$ Hz, 2H), 2.58 (t, $J = 7.6$ Hz, 2H). ^{13}C NMR (150 MHz, CDCl_3) δ 173.8, 144.9, 130.7, 129.3, 115.5, 51.8, 36.4, 30.4. m/z (EI^+) calc'd for $\text{C}_{10}\text{H}_{11}\text{NO}_2$, 180.09 $[\text{M}+\text{H}]^+$; found, 180.30 $[\text{M}+\text{H}]^+$.

Methyl 3-(4-(methylsulfonamido)phenyl)propanoate (6).

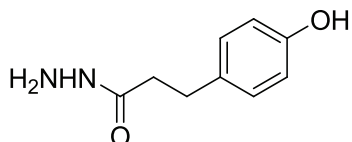
The ester **5** (7.38 g, 41.2 mmol) was dissolved in pyridine (17.0 mL, excess). After cooling to 0°C, methanesulfonyl chloride (4.55 mL, 57.7 mmol, 1.4 equiv) was added dropwise. The reaction was warmed to room temperature and stirred for 20 h. The reaction was quenched with water and the mixture was extracted with DCM (3x). The layers were separated and the organics were washed with brine and concentrated *in vacuo* to give a red solid. The crude material was purified using silica gel chromatography (1 EtOAc/1 Hexanes) to give a white solid (9.26 g, 87%). ¹H NMR (400 MHz, CDCl₃) δ 7.20 (d, *J* = 8.6 Hz, 2H), 7.15 (d, *J* = 8.6 Hz, 2H), 6.45 (bs, NH, 1H), 3.68 (s, 3H), 3.00 (s, 3H), 2.94 (t, *J* = 7.5 Hz, 2H), 2.63 (t, *J* = 7.5 Hz, 2H). ¹³C NMR (100 MHz, CDCl₃) δ 173.4, 137.6, 135.2, 129.4, 121.4, 51.7, 38.5, 35.5, 30.1. *m/z* (APCI) calc'd for C₁₁H₁₅NO₄S, 257.07; found, 257.56 [M]⁺.

3-(4-(Methylsulfonamido)phenyl)propanehydrazide(2).

Compound **5** (3.53 g, 14.0 mmol) was dissolved in MeOH (50.0 mL) and hydrazine monohydrate (5.20 mL, 106 mmol, 7.7 equiv) was added. The solution was refluxed for 12 h. The resulting solution was concentrated *in vacuo* to give a white solid. The crude material was purified using silica gel chromatography (10-20% MeOH/DCM gradient) to

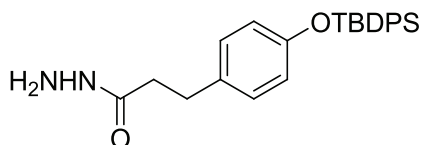
give a white solid (2.80 g, 79%). ^1H NMR (d_6 -DMSO) δ 9.59 (s, 1H), 8.95 (s, 1H), 7.15 (d, J = 8.6 Hz, 2H), 7.10 (d, J = 8.6 Hz, 2H), 4.16 (bs, 2H), 2.93 (s, 3H), 2.76 (t, J = 7.3 Hz, 2H), 2.28 (t, J = 7.3 Hz, 2H).

3-(4-Hydroxyphenyl)propanehydrazide (**9**).



3-(4-hydroxyphenyl)propanoic acid (**8**, 1.8 g, 10 mmol) was dissolved in hydrazine monohydrate (0.58 mL, 12 mmol, 1.2 equiv). The mixture was heated to 110°C and stirred for 30 min, upon which a white precipitate formed. After cooling to room temperature the white solid was collected by filtration and washed with benzene (1.76 g, 98%). The solid was pulverized before further use. ^1H NMR (300 MHz, d_6 -DMSO) δ 9.21 (bs, 1H), 8.98 (bs, 1H), 7.02 (d, J = 8.5 Hz, 2H), 6.69 (d, J = 8.5 Hz, 2H), 4.19 (bs, 2H), 2.74 (t, J = 7.3 Hz, 2H), 2.29 (t, J = 7.3 Hz, 2H). ^{13}C NMR (400 MHz, d_6 -DMSO) δ 171.6, 156.1, 131.9, 129.7, 115.7, 36.2, 30.9.

3-(4-(Tert-butyldiphenylsilyloxy)phenyl)propanehydrazide (**10**).

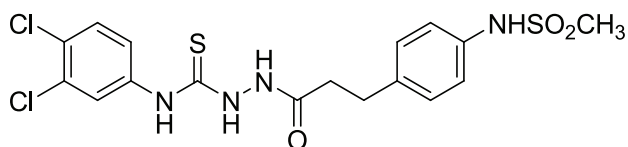


Compound **9** (5.0 g, 28 mmol) was dissolved in DMF (20.0 mL). Imidazole (5.0 g, 69 mmol, 2.5 equiv) was added, followed by dropwise addition of TBDPSCI (18.0 mL, 69 mmol, 2.5 equiv). The reaction was stirred at room temperature for 12 h. The mixture

was poured into 300 mL ice in a large beaker and left to melt, upon which DCM was added. The layers were separated and the organics were washed with NH_4Cl (aq.), dried over MgSO_4 , and concentrated *in vacuo* to give a pink residue. The crude material was purified using silica gel chromatography (2% MeOH/DCM) to give a white foam (3.06 g, 26%). ^1H NMR (300 MHz, CDCl_3) δ 7.73-7.68 (mult, 4H), 7.42-7.34 (mult, 6H), 6.89 (d, J = 8.5 Hz, 2H), 6.67 (d, J = 8.5 Hz, 2H), 6.43 (bs, 1H), 3.80 (bs, 2H), 2.83 (t, J = 7.3 Hz, 2H), 2.35 (t, J = 7.3 Hz, 2H), 1.09 (s, 9H).

4-(3,4-Dichlorophenyl)-1-(3-(4-

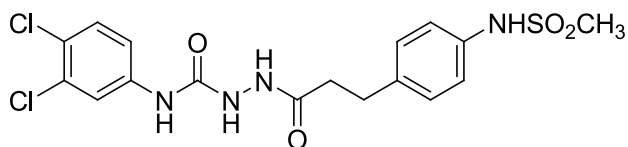
(methylsulfonamido)phenyl)propanoyl)thiosemicarbazide (96-1).



Hydrazide **2** (0.499 g, 1.94 mmol) was dissolved in DMF (15.0 mL). To this solution, 3,4-dichlorophenylisothiocyanate (0.278 mL, 1.94 mmol, 1.0 equiv) was added. The orange solution was stirred for 12 h at room temperature. The solution was concentrated *in vacuo* to give an orange residue. The crude material was purified using silica gel chromatography (3 EtOAc/1 Hexanes) to give a white foam (0.670 g, 75%). ^1H NMR (600 MHz, CD_3OD) δ 7.96 (s, 1H), 7.76 (s, 1H), 7.44 (d, J = 9.1 Hz, 1H), 7.35 (dd, J_1 = 9.1 Hz, J_2 = 1.9 Hz, 1H), 7.22 (d, J = 8.6 Hz, 2H), 7.16 (d, J = 8.6 Hz, 2H), 2.95 (t, J = 7.6 Hz, 2H), 2.91 (s, 3H), 2.61 (t, J = 7.6 Hz, 2H). ^{13}C NMR (150 MHz, CD_3OD) δ 183.7, 174.9, 164.9, 140.1, 138.7, 137.6, 132.8, 131.3, 131.1, 130.6, 130.5, 129.9, 122.3, 122.2, 39.2, 36.6, 31.4.

HRMS calc'd for $C_{17}H_{18}Cl_2N_4O_3S_2$, 459.01176 $[M-H]^+$; found, 459.01074 $[M-H]^+$. Anal. ($C_{17}H_{18}Cl_2N_4O_3S_2$) C, H, N.

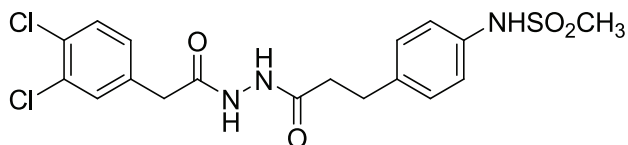
4-(3,4-Dichlorophenyl)-1-(3-(4-(methylsulfonamido)phenyl)propanoyl)semicarbazide (96-5).



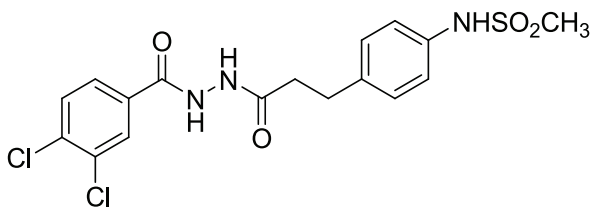
Hydrazide **2** (0.100 g, 0.39 mmol) was dissolved in DMF (3.0 mL). To this solution, 3,4-dichlorophenyisocyanate (0.073 g, 0.39 mmol, 1.0 equiv) was added and the mixture was stirred at room temperature for 12 h. The resulting solution was concentrated *in vacuo* to give a white solid. The crude material was purified using silica gel chromatography (10% -50% MeOH/DCM gradient) to give a white solid (0.114 g, 66%). 1H NMR (400 MHz, d_6 -DMSO) δ 9.69 (bs, 1H), 9.60 (bs, 1H), 9.12 (bs, 1H), 8.27 (bs, 1H), 7.85 (d, $J = 2.4$ Hz, 1H), 7.51 (d, $J = 8.8$ Hz), 7.41 (m, 1H), 7.20 (d, $J = 8.0$ Hz, 2H), 7.13 (d, $J = 8.8$ Hz, 2H), 2.94 (s, 3H), 2.80 (t, $J = 8.0$ Hz, 2H), 2.43 (t, $J = 7.2$ Hz, 2H). ^{13}C NMR (100 MHz, d_6 -DMSO) δ 172.2, 155.8, 140.7, 137.4, 136.9, 131.5, 131.1, 129.7, 123.8, 120.9, 120.6, 119.3, 35.5, 30.6. HRMS calc'd for $C_{17}H_{18}Cl_2N_4O_4S$, 444.0426 $[M]^+$; found 444.04663 $[M]^+$. Anal. ($C_{17}H_{18}Cl_2N_4O_4S$) C, H, N.

N'-(2-(3,4-dichlorophenyl)acetyl)-3-(4-(methylsulfonamido)phenyl)propanehydrazide

(96-4).

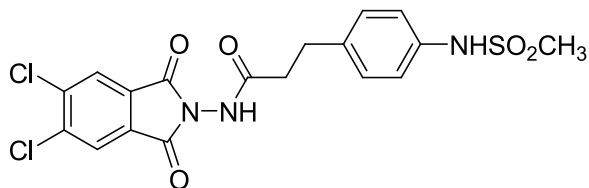


3,4-dichlorophenylacetic acid (0.800 g, 3.9 mmol), EDCI (0.750 g, 3.9 mmol, 1.0 equiv) and DMAP (0.470 g, 3.9 mmol, 1.0 equiv) were dissolved in DMF (10.0 mL) at 0°C and stirred for 45 minutes. Hydrazide **2** (1.0 g, 3.9 mmol, 1.0 equiv) was added and the mixture was warmed to room temperature and stirred for 12 h. The reaction was quenched with 1.0 N HCl and extracted with EtOAc (3x). The combined organics were dried over MgSO₄ and concentrated *in vacuo* to give an off white powder. The crude material was purified using silica gel chromatography (5% MeOH/DCM) to give a white solid which was further purified by recrystallization with EtOAc (0.103 g, 6.0%). ¹H NMR (400 MHz, *d*₆-DMSO) δ 10.89 (s, 1H), 9.88 (s, 1H), 9.60 (s, 1H), 7.59 (d, *J* = 8.6 Hz, 1H), 7.57 (d, *J* = 1.9 Hz, 1H), 7.28 (dd, *J*₁ = 8.6 Hz, *J*₂ = 1.9 Hz, 1H), 7.18 (d, *J* = 8.6 Hz, 2H), 7.10 (d, *J* = 8.6 Hz, 2H), 2.94 (s, 3H), 2.78 (t, *J* = 7.3 Hz, 2H), 2.40 (t, *J* = 7.3 Hz). ¹³C NMR (150 MHz, *d*₆-DMSO) δ 170.2, 168.1, 136.8, 136.3, 131.1, 130.8, 130.4, 129.6, 129.4, 129.3, 129.0, 120.2, 34.7, 30.0, 24.4. HRMS calc'd for C₁₈H₁₉Cl₂N₃O₄S, 444.04733 [M]⁺; found, 444.04802 [M]⁺. Anal. (C₁₈H₁₉Cl₂N₃O₄S) C, H, N.

3,4-Dichloro-N'-(3-(4-(methylsulfonamido)phenyl)propanoyl)benzohydrazide (96-10).

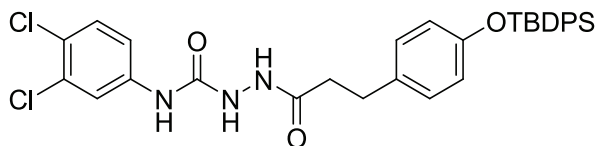
Hydrazide **2** (0.500 g, 1.9 mmol) was dissolved in DMF (10.0 mL). To this solution, 3,4-dichlorobenzoic acid (0.370 g, 1.9 mmol, 1.0 equiv) was added. Finally, DCC (1.0 M in DCM, 1.9 mL, 1.9 mmol, 1.0 equiv) was added. The mixture was stirred at room temperature for 12 hours. The white precipitate was removed by filtration, and the filtrate was concentrated *in vacuo* to give a brown residue. The crude material was purified using silica gel chromatography (10% MeOH/DCM) to give a white solid (0.648 g, 77%). ^1H NMR (600 MHz, CD_3OD) δ 8.03 (d, $J = 1.9$ Hz, 1H), 7.86 (dd, $J_1 = 8.1$ Hz, $J_2 = 1.9$ Hz, 1H), 7.66 (d, $J = 8.1$ Hz, 1H), 7.25 (d, $J = 8.6$ Hz, 2H), 7.19 (d, $J = 8.6$ Hz, 2H), 2.97 (t, $J = 7.6$ Hz, 2H), 2.92 (s, 3H), 2.61 (t, $J = 7.6$ Hz, 2H). ^{13}C NMR (150 MHz, CD_3OD) δ 174.4, 166.8, 138.8, 137.8, 137.5, 134.1, 134.1, 132.1, 131.0, 130.6, 128.6, 122.4, 39.1, 36.7, 31.8. HRMS calc'd for $\text{C}_{17}\text{H}_{17}\text{Cl}_2\text{N}_3\text{O}_4\text{S}$, 430.02474 $[\text{M}+\text{H}]^+$; found, 430.03129 $[\text{M}+\text{H}]^+$.
 Anal. ($\text{C}_{17}\text{H}_{17}\text{Cl}_2\text{N}_3\text{O}_4\text{S}$) C, H, N.

N-(5,6-dichloro-1,3-dioxisoindolin-2-yl)-3-(4-(methylsulfonamido)phenyl)propanamide (96-12).



Hydrazide **2** (0.250 g, 0.972 mmol) was dissolved in DMF (5.0 mL). To this solution, 5,6-dichloroisobenzofuran-1,3-dione (0.211 g, 0.972 mmol, 1.0 equiv) was added. The mixture was refluxed for 12 hr. The resulting solution was concentrated *in vacuo* to give a yellow residue. The crude material was purified using silica gel chromatography (10% MeOH/DCM) to give a yellow solid (0.220 g, 50%). ^1H NMR (400 MHz, CDCl_3) δ 8.11 (s, 1H), 8.07 (s, 1H), 7.89 (s, 1H), 7.23-7.24 (mult, 2H), 7.19-7.17 (mult, 2H), 3.35 (bs, 2H), 3.00-2.95 (mult, 2H), 2.91 (s, 3H), 2.70 (t, $J = 7.6$ Hz, 1H), 2.60 (t, $J = 7.6$ Hz, 1H). ^{13}C NMR (150 MHz, CDCl_3) δ 189.0, 174.2, 138.7, 137.9, 137.7, 137.4, 135.6, 133.2, 130.6, 122.3, 39.1, 36.7, 31.9. HRMS calc'd for $\text{C}_{18}\text{H}_{15}\text{Cl}_2\text{N}_3\text{O}_5\text{S}$, 456.01889 $[\text{M}+\text{H}]^+$; found, 456.01001 $[\text{M}+\text{H}]^+$. Anal. ($\text{C}_{18}\text{H}_{15}\text{Cl}_2\text{N}_3\text{O}_5\text{S} \cdot 0.25 \text{CH}_3\text{OH}$) C, H, N.

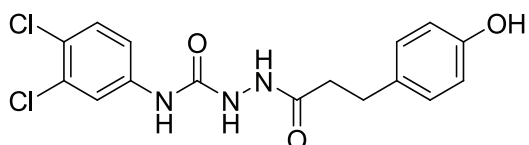
2-(3-(4-(Tert-butyldiphenylsilyloxy)phenyl)propanoyl)-N-(3,4-dichlorophenyl)hydrazinecarboxamide.



Hydrazide **10** (0.093 g, 0.22 mmol) was dissolved in ethanol (3.0 mL). To this solution, 3,4-dichlorophenylisocyanate was added dropwise (0.050 g, 0.27 mmol, 1.2 eq). The

mixture was refluxed for 1 hour. The resulting solution was concentrated *in vacuo* to give a colorless oil. The crude was purified by column chromatography on silica gel (3.5% MeOH/DCM) to give a colorless oil (0.080 g, 59%). ^1H NMR (400 MHz, CDCl_3) δ 8.29 (bs, 1H), 8.04 (bs, 1H), 7.84 (bs, 1H), 7.7-7.67 (mult, 4H), 7.42-7.30 (mult, 7H), 7.11 (d, $J = 8.3$ Hz, 1H), 6.84 (d, $J = 8.3$ Hz, 3H), 6.67 (d, $J = 8.6$ Hz, 2H), 2.80 (t, $J = 7.3$ Hz, 2H), 2.47 (t, $J = 7.3$ Hz, 2H), 1.08 (9H, s). ^{13}C NMR (600 MHz, CDCl_3) δ 174.7, 155.3, 154.5, 137.6, 135.7, 133.1, 132.3, 130.4, 130.2, 129.1, 128.0, 120.6, 120.0, 118.4, 35.9, 30.6, 26.7, 19.7, 15.5. HRMS calc'd for $\text{C}_{32}\text{H}_{33}\text{Cl}_2\text{N}_3\text{O}_3\text{Si}$, 606.17476 $[\text{M}+\text{H}]^+$; found, 606.17465 $[\text{M}+\text{H}]^+$.

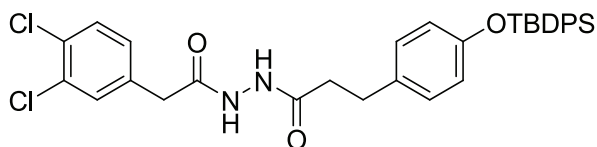
4-(3,4-Dichlorophenyl)-1-(3-(4-hydroxyphenyl)propanoyl)semicarbazide (96-2).



The semicarbazide above (0.080 g, 0.10 mmol) was dissolved in THF (1.0 mL). To this solution, TBAF (1.0 M in THF, 0.4 mL, 0.4 mmol, 3.0 equiv) was added dropwise. The mixture was stirred at room temperature for 2 h. A white precipitate formed, and the solution was concentrated *in vacuo* to give white solid. The crude was purified by column chromatography on silica gel to give a white solid (0.039 g, 88%). ^1H NMR (300 MHz, d_6 -DMSO) δ 9.14 (bs, 1H), 7.83 (mult, 1H), 7.46 (d, $J = 8.6$ Hz, 1H), 7.49-7.45 (mult, 1H), 6.98 (d, $J = 8.6$ Hz, 2H), 6.63 (d, $J = 7.9$ Hz, 2H), 2.78-2.60 (mult, 2H), 2.39-2.30 (mult, 2H). ^{13}C NMR (600 MHz, d_6 -DMSO) δ 171.6, 156.2, 154.0, 140.7, 131.8, 131.5,

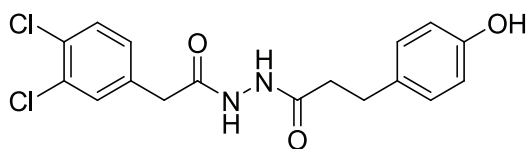
131.1, 129.7, 123.8, 115.7, 36.0, 30.5. HRMS calc'd for $C_{16}H_{15}Cl_2N_3O_3$, 368.2146 $[M]^+$; found, 368.0563 $[M]^+$. Anal. ($C_{16}H_{15}Cl_2N_3O_3$) C, H, N.

3-(4-(Tert-butyl-diphenylsilyloxy)phenyl)-N'-(2-(3,4-dichlorophenyl)acetyl)propanehydrazide.



Compound **10** (0.300 g, 1.02 mmol) was dissolved in DCM (10.0 mL). To this solution, 3,4-dichlorophenylacetic acid (0.209 g, 1.02 mmol, 1.0 equiv) and DCC (1.0 M in DCM, 1.02 mL, 1.0 equiv) were added. The mixture was stirred at room temperature for 12 h. The resultant white precipitate was removed by filtration and the filtrate was concentrated *in vacuo* to give a colorless oil. The crude material was purified using silica gel chromatography (1 EtOAc/1 Hexanes) to give a white solid (0.218 g, 44%). The material was carried on without characterization.

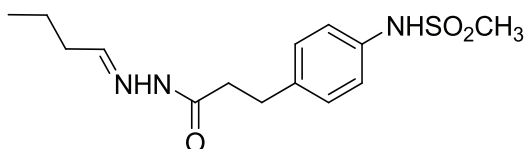
N'-(2-(3,4-dichlorophenyl)acetyl)-3-(4-hydroxyphenyl)propanehydrazide (96-3).



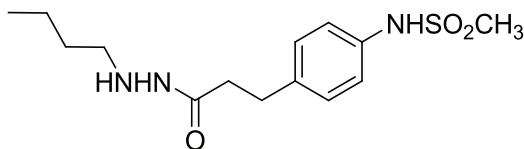
The above compound (0.218 g, 0.45 mmol) was dissolved in THF (5.0 mL). To this solution, TBAF (1.0 M in THF, 1.0 mL, 1.0 mmol, 2.2 equiv) was added dropwise. The mixture was stirred at room temperature for 12 h, after which the solution was

concentrated *in vacuo*. The crude material was purified by silica gel chromatography (7% MeOH/DCM) to give an off-white solid. This material was further purified by recrystallization with ethyl acetate to give a white solid (0.020 g, 7.2%). Multiple purifications required to obtain material which passed elemental analysis. ^1H NMR (400 MHz, d_6 -DMSO) δ 10.16 (s, 1H), 9.90 (s, 1H), 9.21 (s, 1H), 7.65 (d, $J = 8.4$ Hz, 1H), 7.63 (d, $J = 1.9$ Hz, 1H), 7.34 (dd, $J_1 = 8.4$ Hz, $J_2 = 1.9$ Hz, 1H), 7.05 (d, $J = 8.6$ Hz, 2H), 6.71 (d, $J = 8.6$ Hz, 2H), 3.56 (s, 2H), 2.76 (t, $J = 7.3$ Hz, 2H), 2.41 (t, $J = 8.6$ Hz, 2H). HRMS calc'd for $\text{C}_{17}\text{H}_{16}\text{Cl}_2\text{N}_2\text{O}_3$, 367.06174 $[\text{M}+\text{H}]^+$; found, 367.06101 $[\text{M}+\text{H}]^+$. Anal ($\text{C}_{17}\text{H}_{16}\text{Cl}_2\text{N}_2\text{O}_3$) C, H, N.

N-(4-(3-(2-butylidenehydrazinyl)-3-oxopropyl)phenyl)methanesulfonamide (11).

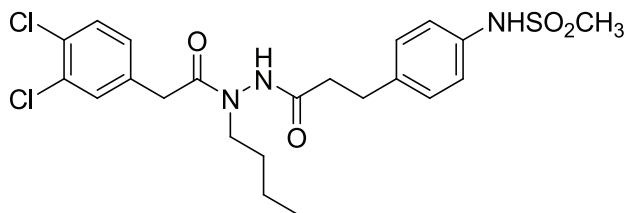


Compound **2** (2.8 g, 11 mmol) was dissolved in THF (30.0 mL). To this solution, butyraldehyde (0.97 mL, 11 mmol, 1.0 equiv) was added dropwise. The solution was stirred at room temperature for 12 h. TLC indicated no starting material remained. The mixture was concentrated *in vacuo* to give a white solid. The crude material was purified by passing sample (dissolved in DCM) through a silica plug (2% MeOH/DCM) to give a white solid (3.4 g, quant). HRMS calc'd for $\text{C}_{14}\text{H}_{21}\text{N}_3\text{O}_3\text{S}$, 312.13830 $[\text{M}+\text{H}]^+$; found, 312.22642 $[\text{M}+\text{H}]^+$. The material was carried on without further characterization.

N-(4-(3-(2-butyldrazinyl)-3-oxopropyl)phenyl)methanesulfonamide (12).

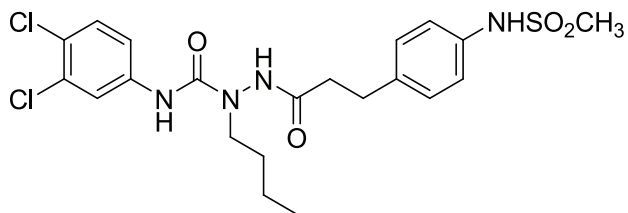
Compound **11** (3.4 g, 11 mmol) was suspended in ethanol (50.0 mL). After cooling to 0°C, sodium borohydride (2.1 g, 55 mmol, 5.0 equiv) was added. The suspension was stirred for 5 min further at 0°C before warming to room temperature and stirring for 12 h. The resulting colorless solution was quenched with water and partitioned with DCM. The mixture was extracted with DCM (3x). The combined organics were washed with brine, dried over MgSO₄, and concentrated *in vacuo* to give a white solid. The crude material was purified using silica gel chromatography (10% MeOH/DCM) to give a white solid (0.105 g, 11%). ¹H NMR (400 MHz, CDCl₃) δ 7.25 (d, *J* = 8.0 Hz, 2H), 7.13 (d, *J* = 8.0 Hz, 2H), 3.02-2.95 (mult, 5H), 2.77 (t, *J* = 6.0 Hz, 2H), 2.43 (t, *J* = 7.5 Hz, 2H), 1.41-1.32 (mult, 4H), 0.89 (t, *J* = 7.1 Hz, 3H). ¹³C NMR (100 MHz, CDCl₃) δ 137.9, 135.5, 129.8, 121.4, 52.1, 39.5, 36.4, 31.0, 30.0, 20.4, 14.2. HRMS calc'd for C₁₄H₂₃N₃O₃S, 313.14601 [M]⁺; found, 314.15322 [M]⁺.

N-(4-(3-(2-butyl-2-(2-(3,4-dichlorophenyl)acetyl)hydrazinyl)-3-oxopropyl)phenyl)methanesulfonamide (96-6).



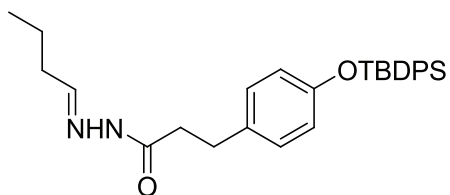
Compound **12** (0.305 g, 0.97 mmol) was dissolved in DCM (5.0 mL). TO this solution, 3,4-dichlorophenylacetic acid (0.210 g, 0.97 mmol, 1.0 equiv) and DCC (1.0 M in DCM, 1.1 mL, 1.1 mmol, 1.1 equiv) was added. The mixture was stirred at room temperature for 12 h. The white precipitate was removed by filtration and the filtrate was concentrated *in vacuo* to give a colorless oil. The crude material was purified using silica gel chromatography (5% MeOH/DCM) to give a colorless oil (0.322 g, 66%). ^1H NMR (400 MHz, CDCl_3) δ 7.93 (s, 1H), 7.29 (d, J = 8.2 Hz, 1H), 7.21 (d, J = 1.9 Hz, 1H), 7.15 (d, J = 8.6 Hz, 2H), 7.06 (d, J = 8.6 Hz, 2H), 6.88 (dd, J_1 = 8.2 Hz, J_2 = 1.9 Hz, 1H), 3.70 (bs, 1H), 3.31 (s, 2H), 2.98-2.89 (mult, 4H), 2.86 (s, 3H), 2.50 (t, J = 7.1 Hz, 2H), 1.34-1.29 (mult, 2H), 1.22-1.16 (mult, 2H), 0.83 (t, J = 7.1 Hz, 3H). ^{13}C NMR (100 MHz, CDCl_3) δ 172.4, 171.0, 137.4, 135.6, 135.2, 132.4, 131.5, 131.1, 130.6, 129.9, 129.8, 129.1, 121.4, 121.3, 48.0, 39.4, 38.6, 35.7, 30.5, 29.0, 20.1, 14.0. HRMS calc'd for $\text{C}_{22}\text{H}_{27}\text{Cl}_2\text{N}_3\text{O}_4\text{S}$, 500.11787 $[\text{M}+\text{H}]^+$; found, 500.56221 $[\text{M}+\text{H}]^+$. Anal ($\text{C}_{22}\text{H}_{27}\text{Cl}_2\text{N}_3\text{O}_4\text{S}$) C, H, N.

1-Butyl-N-(3,4-dichlorophenyl)-2-(3-(4-(methylsulfonamido)phenyl)propanoyl)hydrazinecarboxamide (96-7).



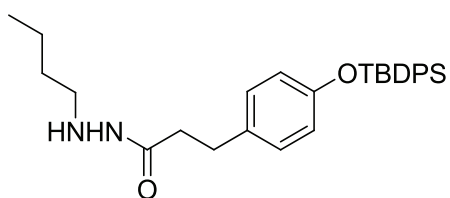
Compound **12** (0.212 g, 0.68 mmol) was dissolved in DCM (15.0 mL). To this solution, 3,4-dichlorophenylisocyanate (0.201 g, 0.74 mmol, 1.1 equiv) was added. The mixture was stirred at room temperature for 12 h. The solution was concentrated *in vacuo* to give a colorless oil. The crude material was purified using silica gel chromatography (5% - 10% MeOH/DCM gradient) to give a colorless oil (0.221 g, 65%). ^1H NMR (400 MHz, CDCl_3) δ 8.02 (s, 1H), 7.39 (d, $J = 8.2$ Hz, 1H), 7.30 (d, $J = 1.6$ Hz, 1H), 7.22 (d, $J = 8.6$ Hz, 2H), 7.06 (dd, $J_1 = 8.2$ Hz, $J_2 = 1.6$ Hz, 1H), 6.88 (d, $J = 8.6$ Hz, 2H), 3.55 (mult, 2H), 3.06 (t, $J = 6.9$ Hz, 2H), 2.99 (s, 3H), 2.62 (t, $J = 6.9$ Hz, 2H), 1.39-1.20 (mult, 4H), 0.90 (t, $J = 6.9$ Hz, 3H). HRMS calc'd for $\text{C}_{21}\text{H}_{26}\text{Cl}_2\text{N}_4\text{O}_4\text{S}$, 501.11312 $[\text{M}+\text{H}]^+$; found, 501.11241 $[\text{M}+\text{H}]^+$.
 Anal ($\text{C}_{21}\text{H}_{26}\text{Cl}_2\text{N}_4\text{O}_4\text{S}$) C, H, N.

3-(4-(Tert-butyldiphenylsilyloxy)phenyl)-N'-butylidenepropanehydrazide (14).



Compound **10** (1.31 g, 5.09 mmol) was dissolved in DCM (10.0 mL). To this solution butyraldehyde (0.46 mL, 5.09 mmol 1.0 equiv) was added dropwise. The solution was stirred at room temperature for 12 h. TLC indicated no starting material remained. The mixture was concentrated *in vacuo* to give a white solid. The crude material was purified using silica gel chromatography (5% MeOH/DCM) to give a white solid (1.00 g, 63%). HRMS calc'd for $C_{29}H_{36}N_2O_2Si$, 473.26254 $[M+H]^+$; found 473.23682 $[M+H]^+$. The material was carried on without further characterization.

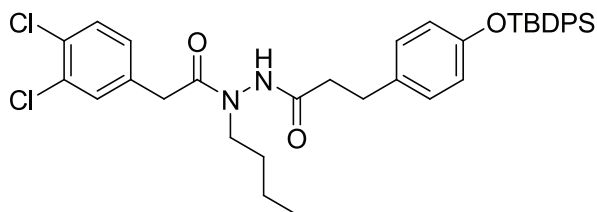
N'-butyl-3-(4-(tert-butyldiphenylsilyloxy)phenyl)propanehydrazide (15).



Compound **14** (1.00 g, 2.12 mmol) was dissolved in methanol (20.0 mL) and the suspension was cooled to 0°C. Sodium borohydride (0.208 g, 5.50 mmol, 2.6 equiv) was added. The suspension was stirred for 5 min further at 0°C before warming to room temperature and stirring for 12 h. The resulting colorless solution was quenched with water and partitioned with DCM. The mixture was extracted with DCM (3x). The combined organics were washed with brine, dried over $MgSO_4$, and concentrated *in*

vacuo to give a yellow residue. The crude material was purified using silica gel chromatography (5% MeOH/DCM) to give a colorless oil (0.105 g, 11%). ^1H NMR (400 MHz, CDCl_3) δ 7.71-7.68 (mult, 4H), 7.42-7.32 (mult, 6H), 6.94 (d, $J = 8.2$ Hz, 1H), 6.88 (d, $J = 8.2$ Hz, 1H), 6.66 (dd, $J_1 = 8.2$ Hz, $J_2 = 1.9$ Hz, 2H), 3.02-2.98 (mult, 2H), 2.71 (t, $J = 7.3$ Hz, 2H), 2.31 (t, $J = 7.3$ Hz, 2H), 1.54-1.24 (mult, 4H), 1.07 (s, 9H), 0.90 (t, $J = 7.0$ Hz, 3H). HRMS calc'd for $\text{C}_{29}\text{H}_{38}\text{N}_2\text{O}_2\text{Si}$, 474.27026 $[\text{M}]^+$, found 474.28033 $[\text{M}]^+$.

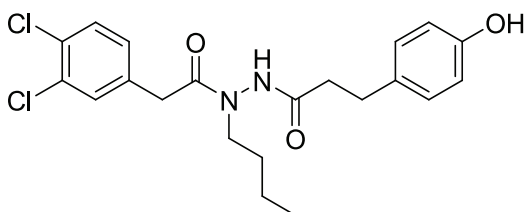
N'-butyl-3-(4-(tert-butyldiphenylsilyloxy)phenyl)-N'-(2-(3,4-dichlorophenyl)acetyl)propanehydrazide (16).



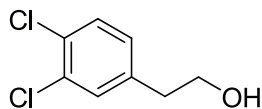
Compound **15** (0.243 g, 0.51 mmol) was dissolved in DCM (5.0 mL). To this solution, 3,4-dichlorophenylacetic acid (0.105 g, 0.51 mmol, 1.0 equiv) and DCC (1.0 M sol'n in DCM, 0.56 mL, 0.56 mmol, 1.1 equiv) was added. The mixture was stirred at room temperature for 5 h. The white precipitate was removed by filtration and the filtrate was concentrated *in vacuo* to give a colorless oil. The crude material was purified using silica gel chromatography (1 EtOAc/ 9 DCM) to give a white foam upon trituration with ether (0.256 g, 76%). ^1H NMR (600 MHz, CDCl_3) δ 8.05 (s, 1H), 7.65 (d, $J = 8.1$ Hz, 4H), 7.38 (t, $J = 7.1$ Hz, 2H), 7.30 (t, $J = 7.1$ Hz, 4H), 7.22 (d, $J = 8.1$ Hz, 1H), 7.08 (s, 1H), 6.91 (d, $J = 8.6$ Hz, 2H), 6.79 (d, $J = 8.1$ Hz, 1H), 6.67 (d, $J = 8.6$ Hz, 2H), 3.54 (mult, 2H), 3.22 (s, 2H), 2.83 (bs, 2H), 2.37 (bs, 2H), 1.31-1.29 (mult, 2H) 1.19-1.15 (mult, 2H), 1.06 (s,

9H), 0.83 (t, $J = 7.1$ Hz, 3H). ^{13}C NMR (150 MHz, CDCl_3) δ 166.0, 164.8, 148.0, 129.2, 128.8, 126.5, 125.99, 125.98, 125.0, 124.6, 124.0, 123.6, 123.0, 122.6, 121.5, 113.5, 41.5, 32.1, 29.4, 23.8, 22.5, 20.2, 13.7, 13.1, 7.5. HRMS calc'd for $\text{C}_{37}\text{H}_{42}\text{Cl}_2\text{N}_2\text{O}_3\text{Si}$, 661.24212 $[\text{M}+\text{H}]^+$; found, 661.22967 $[\text{M}+\text{H}]^+$.

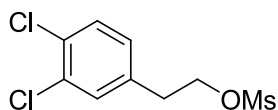
N'-butyl-N'-(2-(3,4-dichlorophenyl)acetyl)-3-(4-hydroxyphenyl)propanehydrazide (96-8).



Compound **16** (0.256 g, 0.39 mmol) was dissolved in THF (4.0 mL). To this solution, TBAF (1.0 M in THF, 1.2 mL, 1.2 mmol, 3.0 equiv) was added dropwise. The solution was stirred for 12 h then concentrated *in vacuo* to give a yellow residue. The crude material was purified by silica gel chromatography (10% - 30% EtOAc/DCM gradient) to give a white solid (0.103 g, 63%). ^1H NMR (600 MHz, d_6 -acetone) δ 9.46 (s, 1H), 8.12 (1H, s), 7.43 (d, $J = 8.1$ Hz, 1H), 7.29 (d, $J = 1.9$ Hz, 1H), 7.08 (d, $J = 8.6$ Hz, 2H), 7.05 (dd, $J_1 = 8.1$ Hz, $J_2 = 1.9$ Hz, 1H), 6.73 (d, $J = 8.6$ Hz, 2H), 3.79 (s, 2H), 3.52-3.37 (mult, 2H), 2.88 (bs, 2H), 2.58 (t, $J = 7.1$ Hz, 2H), 1.38-1.34 (t, $J = 7.1$ Hz, 2H), 1.22-1.18 (mult, 2H), 0.83 (t, $J = 7.1$ Hz, 3H). HRMS calc'd for $\text{C}_{21}\text{H}_{24}\text{Cl}_2\text{N}_2\text{O}_3$, 423.12434 $[\text{M}+\text{H}]^+$; found, 423.2320 $[\text{M}+\text{H}]^+$.
 Anal. ($\text{C}_{21}\text{H}_{24}\text{Cl}_2\text{N}_2\text{O}_3$) C, H, N.

2-(3,4-Dichlorophenyl)ethanol (18).

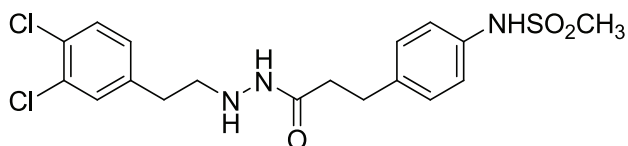
Lithium aluminum hydride (0.90 g, 24 mmol, 1.0 equiv) was dissolved in THF (50.0 mL) at 0°C, and then warmed to room temperature for 30 minutes. To this suspension, a solution of 3,4-dichlorophenyl acetic acid (**17**, 5.0 g, 24 mmol) and triethyl amine (3.0 mL, 24 mmol, 1.0 equiv) in THF (37.5mL) was added dropwise. The reaction mixture was refluxed for 1 hour. The reaction was cooled to room temperature and poured into water (125 mL) to give a bright yellow solution. The mixture was extracted with EtOAc (2x). The organics were dried over Na₂SO₄ and concentrated *in vacuo* to give a yellow oil (3.76 g, 81%). The crude material was carried on without further purification. ¹H NMR (300 MHz, CDCl₃) δ 7.38 (d, *J* = 8.3 Hz, 1H), 7.35 (d, *J* = 1.9 Hz, 1H), 7.08 (dd, *J*₁ = 8.3 Hz, *J*₂ = 1.9 Hz), 3.87 (quart, *J* = 6.6 Hz, 2H), 2.83 (t, *J* = 6.6 Hz, 2H), 1.45 (bs, 1H).

3,4-Dichlorophenethyl methanesulfonate (19).

Crude alcohol **18** (3.76 g, 2.79 mmol) was dissolved in pyridine (30.0 mL). Methanesulfonyl chloride (1.7 mL, 3.0 mmol, 1.1 equiv) was added dropwise at room temperature and the reaction was stirred for 1 hour. The mixture was poured into ice water and warmed to room temperature. The organics were extracted with EtOAc (3x), dried over Na₂SO₄, and concentrated *in vacuo* to give a yellow liquid. The crude material

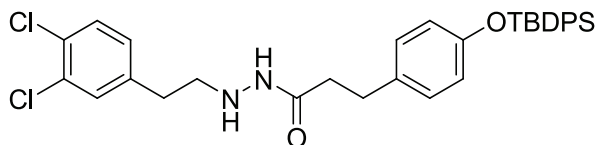
was purified using silica gel chromatography (1 EtOAc/1 Hexanes) to give a yellow oil (4.25 g, 80%). ^1H NMR (300 MHz, CDCl_3) δ 7.41 (d, J = 8.1 Hz, 1H), 7.35 (d, J = 1.9 Hz, 1H), 7.10 (dd, J_1 = 8.1 Hz, J_2 = 1.9 Hz, 1H), 4.41 (t, J = 6.6 Hz, 2H), 3.03 (t, J = 6.6 Hz, 2H), 2.95 (s, 3H).

N'-(3,4-Dichlorophenethyl)-3-(4-(methylsulfonamido)phenyl)propanehydrazide (96-9).



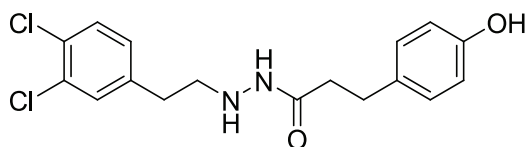
Hydrazide **12** (1.00 g, 3.9 mmol) was dissolved in methanol (15.0 mL). To this solution, mesylate **20** was added dropwise (1.0 g, 3.9 mmol, 1.0 equiv). The solution was refluxed for 48 h, cooled to room temperature, and concentrated *in vacuo* to give a white solid. The crude material was purified using silica gel chromatography (10% MeOH/DCM) to give a white foam (0.690 g, 41%). ^1H NMR (400 MHz, CDCl_3) δ 7.37 (d, J = 8.2 Hz, 1H), 7.29 (d, J = 1.90 Hz, 1H), 7.20 (d, J = 8.7 Hz, 2H), 7.14 (d, J = 8.7 Hz, 2H), 7.04 (dd, J_1 = 8.2 Hz, J_2 = 2.2 Hz, 2H), 6.73 (bs, 1H), 6.25 (bs, 1H), 4.60 (bs, 1H), 3.04 (mult, 2H), 2.99 (s, 3H), 2.96 (t, J = 7.3 Hz, 2H), 2.69 (t, J = 7.3 Hz, 2H), 2.41 (t, J = 7.6 Hz, 2H). ^{13}C NMR (150 MHz, CDCl_3) δ 172.0, 139.8, 137.7, 135.4, 132.4, 130.8, 130.6, 130.4, 129.7, 128.3, 121.4, 52.6, 39.4, 36.2, 33.6, 30.9. HRMS calc'd for $\text{C}_{18}\text{H}_{21}\text{Cl}_2\text{N}_3\text{O}_3\text{S}$, 430.07604 [M+H]; found, 430.07001 [M+H] $^+$ Anal. ($\text{C}_{18}\text{H}_{21}\text{Cl}_2\text{N}_3\text{O}_3\text{S}$) C, H, N.

3-(4-(Tert-butyldiphenylsilyloxy)phenyl)-N'-(3,4-dichlorophenethyl)propanehydrazide.



Compound **10** (0.699 g, 1.67 mmol) was dissolved in methanol (11.0 mL). To this solution, mesylate **20** (0.494 g, 1.84 mmol, 1.1 equiv) was added dropwise. The mixture was refluxed for 48 h. Although TLC indicated the reaction had not reached completion, the solution was cooled to room temperature and concentrated *in vacuo* to give a green oil. The crude material was purified using silica gel chromatography (5%-10% MeOH/DCM gradient) to give an off-white foam (0.272 g, 28%). ^1H NMR (600 MHz, CDCl_3) δ 8.30 (1H, bs), 7.74-7.70 (mult, 4H), 7.43-7.32 (mult, 8H), 7.01-6.95 (mult, 1H), 6.89 (dd, $J_1 = 8.2$ Hz, $J_2 = 1.9$ Hz, 1H), 6.68 (d, $J = 8.6$ Hz, 2H), 2.99 (t, $J = 7.1$ Hz, 2H), 2.64 (t, $J = 7.1$ Hz, 2H), 2.43 (t, $J = 7.6$ Hz, 2H), 2.33 (t, $J = 7.6$ Hz, 2H), 1.02 (s, 9H). ^{13}C NMR (150 MHz, CDCl_3) δ 169.1, 154.3, 139.9, 135.7, 133.1, 132.7, 130.8, 130.4, 130.1, 130.0, 129.2, 129.1, 128.0, 119.9, 52.8, 36.5, 33.7, 30.6, 26.7, 19.6. HRMS calc'd for $\text{C}_{33}\text{H}_{36}\text{Cl}_2\text{N}_2\text{O}_2\text{Si}$, 591.20025 $[\text{M}+\text{H}]^+$; found, 591.20031 $[\text{M}+\text{H}]^+$.

N'-(3,4-dichlorophenethyl)-3-(4-hydroxyphenyl)propanehydrazide (96-11).

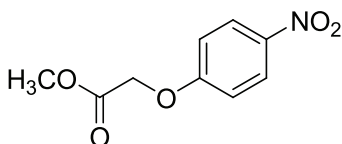


The above compound (0.229 g, 0.39 mmol) was dissolved in THF (5.0 mL). To this solution TBAF (1.0 M in THF, 1.2 mL, 1.2 mmol, 3.0 equiv) was added dropwise. The

mixture was stirred at room temperature for 3 h, then concentrated *in vacuo* to give an orange residue. The crude material was purified using silica gel chromatography (10% MeOH/DCM) to give a white powder (0.076 g, 56%). ^1H NMR (600 MHz, CD_3OD) δ 7.40 (d, J = 8.5 Hz, 1H), 7.36 (d, J = 2.1 Hz, 1H), 7.09 (dd, J_1 = 8.5 Hz, J_2 = 2.1 Hz, 1H), 7.03 (d, J = 8.6 Hz, 2H), 6.68 (d, J = 8.6 Hz, 2H), 2.89 (bt, J = 6.7 Hz, 2H), 2.82 (t, J = 7.6 Hz, 2H), 2.59 (t, J = 7.6 Hz, 2H), 2.39 (t, J = 7.6 Hz, 2H). ^{13}C NMR (150 MHz, CD_3OD) δ 176.6, 159.7, 144.7, 135.8, 135.3, 134.7, 134.2, 133.8, 133.3, 132.6, 119.0, 56.3, 40.1, 37.0, 34.7. HRMS calc'd for $\text{C}_{17}\text{H}_{18}\text{Cl}_2\text{N}_2\text{O}_2$, 353.08247 $[\text{M}+\text{H}]^+$; found 353.08182 $[\text{M}+\text{H}]^+$. Anal ($\text{C}_{17}\text{H}_{18}\text{Cl}_2\text{N}_2\text{O}_2$) C, H, N.

Synthesis of methyl esters **29** and **30**, exemplified by **29**.

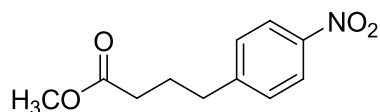
Methyl 2-(4-nitrophenoxy)acetate (29).



Thionyl chloride (17 mL, 234 mmol, 3.3 equiv) was added dropwise to a solution of dry methanol (70 mL, 1704 mmol, 24 equiv) at -10°C . After stirring for 10 minutes, 4-nitrophenoxyacetic acid (14.0 g, 71 mmol) was added. The solution stirred for 1 hour and slowly warmed to room temperature. The resulting solution was concentrated *in vacuo* to give an off-white solid. The solid was dissolved in EtOAc, and NaHCO_3 (sat'd) was added. The layers were separated and the organics were washed with brine, dried over MgSO_4 , and concentrated *in vacuo* to give a white solid (14.3 g, 95%). ^1H NMR (300

MHz, CDCl₃) δ 8.23 (d, J = 9.2 Hz, 2H), 6.98 (d, J = 9.2 Hz), 4.75 (s, 2H), 3.84 (s, 3H). ¹³C NMR (100 MHz, CDCl₃) δ 168.4, 162.7, 142.5, 126.2, 114.9, 65.5, 52.8.

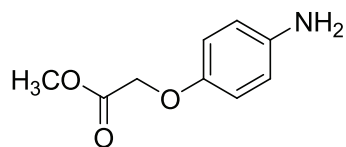
Methyl 4-(4-nitrophenyl)butanoate (30).



Compound **30** was obtained from 4-(4-nitrophenyl)butanoic acid (off-white solid, 5.01 g, 94%). ¹H NMR (600 MHz, CDCl₃) δ 7.98 (d, J = 9.1 Hz, 2H), 7.22 (d, J = 9.1 Hz, 2H), 3.53 (s, 3H), 2.63 (t, J = 7.6 Hz, 2H), 2.22 (t, J = 7.1 Hz, 2H), 1.85 (quint, J = 7.6 Hz, 2H). ¹³C NMR (150 MHz, CDCl₃) δ 173.3, 149.4, 146.3, 129.2, 123.5, 51.4, 34.7, 32.9, 25.4.

Synthesis of anilines **31** and **32**, exemplified by **32**.

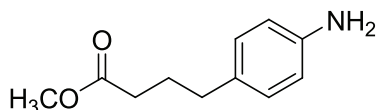
Methyl 2-(4-aminophenoxy)acetate (31).



Ester **29** (14.3 g, 68 mmol) was dissolved in dry methanol (100 mL) and 5% palladium on carbon catalyst (1.43 g, 10 wt%) was added. The suspension was hydrogenolyzed using a balloon for 12 hours. The mixture was filtered over a pad of celite, and the resulting solution was concentrated *in vacuo* to give a pink oil which turned to a solid upon trituration with chloroform. The crude material was purified using silica gel chromatography (1 EtOAc/2 Hexanes) to give a pink solid (11.7 g, 95%). ¹H NMR (400

MHz, CDCl₃) δ 6.74 (d, J = 8.6 Hz, 2H), 6.60 (d, J = 8.6 Hz), 4.54 (s, 2H), 3.77 (s, 3H), 3.50 (bs, 2H). ¹³C NMR (100 MHz, CDCl₃) δ 169.9, 150.9, 141.2, 116.3, 116.0, 66.4, 51.2. m/z calc'd for C₉H₁₁NO₃, 182.18 [M]⁺; found, 182.081 [M]⁺.

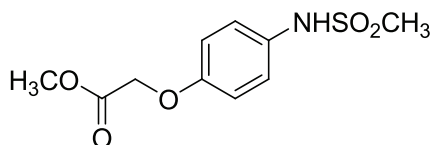
Methyl 4-(4-aminophenyl)butanoate (32).



Compound **32** was obtained from compound **30** (pink solid, 4.34 g, 100%). ¹H NMR (400 MHz, CDCl₃) δ 6.93 (d, J = 6.9 Hz, 2H), 6.57 (d, J = 6.9 Hz, 2H), 3.68 (bs, 2H), 3.63 (s, 3H), 2.51 (t, J = 7.3 Hz, 2H), 2.30 (t, J = 7.3 Hz, 2H), 1.88 (quint, J = 7.3 Hz, 2H). ¹³C NMR (100 MHz, CDCl₃) δ 173.9, 114.5, 130.8, 129.0, 115.0, 51.2, 34.0, 33.1, 26.6. HRMS calc'd for C₁₁H₁₅NO₂, 194.11824 [M+H]⁺; found, 194.11743 [M+H]⁺.

Synthesis of methanesulfonamides **33**, **6**, and **34**, were carried out the same as exemplified for **6**.

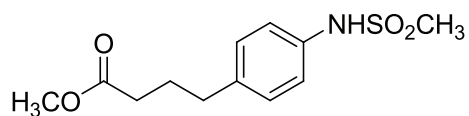
Methyl 2-(4-(methylsulfonamido)phenoxy)acetate (33).



Compound **33** was obtained from compound **31** (orange solid, 15.0 g, 90%). ¹H NMR (300 MHz, CDCl₃) δ 7.22 (d, J = 9.0 Hz, 2H), 6.88 (d, J = 9.0 Hz, 2H), 4.65 (s, 2H), 3.83 (s,

3H), 2.96 (s, 3H). ^{13}C NMR (75 MHz, CDCl_3) δ 169.5, 155.8, 130.6, 124.2, 115.6, 65.5, 52.5, 38.7.

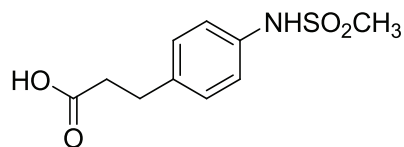
Methyl 4-(4-(methylsulfonamido)phenyl)butanoate (34).



Compound **34** was obtained from compound **32** (pink solid, 6.5 g, 107%). The crude material was used without further purification. ^1H NMR (300 MHz, CDCl_3) δ 7.43 (bs, 1H), 7.16 (d, $J = 8.5$ Hz, 2H), 7.10 (d, $J = 8.5$ Hz, 2H), 3.62 (s, 3H), 2.94 (s, 3H), 2.57 (t, $J = 7.3$ Hz, 2H), 2.29 (t, $J = 7.3$ Hz, 2H), 1.88 (quint, $J = 7.6$ Hz, 2H). ^{13}C NMR (75 MHz, CDCl_3) δ 174.1, 138.7, 134.9, 129.6, 121.5, 51.6, 39.3, 38.5, 33.3, 26.4.

Synthesis of carboxylic acids **35-37**, exemplified by **36**.

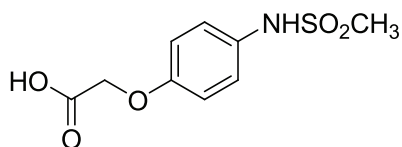
3-(4-(Methylsulfonamido)phenyl)propanoic acid (36).



The sulfonamide ester **6** (1.16 g, 4.5 mmol) was dissolved in methanol (50 mL). To this solution, 1.0 N NaOH (17.0 mL, 17.0 mmol, 3.8 equiv) was added. The mixture was stirred at room temperature for 12 hours. The pH of the solution was adjusted to ~ 3 with a solution of aqueous HCl. The volume of methanol was reduced by rotary evaporation (40 mbar), upon which the product crashed out of solution. The yellow

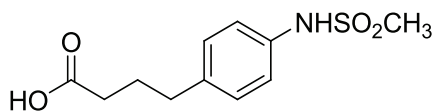
crystals were collected by filtration and dried *in vacuo* (0.900 g, 82%). ^1H NMR (400 MHz, CD_3OD) δ 7.21 (d, $J = 8.6$ Hz, 2H), 7.17 (d, $J = 8.6$ Hz, 2H), 2.91 (s, 3H), 2.89 (t, $J = 7.6$ Hz, 2H), 2.59 (t, $J = 7.6$ Hz, 2H). ^{13}C NMR (100 MHz, CD_3OD) δ 176.7, 139.0, 137.7, 130.5, 122.3, 39.1, 36.8, 31.4. m/z (APCI) calc'd for $\text{C}_{10}\text{H}_{13}\text{NO}_4\text{S}$, 242.06 $[\text{M}-\text{H}]^+$; found, 242.05 $[\text{M}-\text{H}]^+$.

2-(4-(Methylsulfonamido)phenoxy)acetic acid (35).

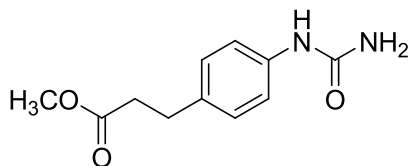


Compound **35** was obtained from compound **33** (pink crystals, 5.6 g, 97%). ^1H NMR (300 MHz, CD_3OD) δ 7.20 (d, $J = 9.0$ Hz, 2H), 6.92 (d, $J = 9.0$ Hz, 2H), 4.65 (s, 2H), 2.88 (s, 3H). ^{13}C NMR (75 MHz, CD_3OD) δ 172.7, 157.3, 132.8, 125.0, 116.5, 66.2, 38.8.

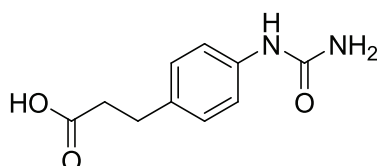
4-(4-(Methylsulfonamido)phenyl)butanoic acid (37).



Compound **37** was obtained from compound **34** (off-white solid, 3.24 g, 53%). ^1H NMR (300 MHz, d_6 -DMSO) δ 12.04 (bs, 1H), 9.58 (bs, 1H), 7.12 (mult, 4H), 2.91 (s, 3H), 2.51 (t, $J = 7.3$ Hz, 2H), 2.18 (t, $J = 7.3$ Hz, 2H), 1.74 (quint, $J = 7.3$ Hz, 2H). ^{13}C NMR (75 MHz, d_6 -DMSO) δ 175.0, 138.0, 136.8, 129.8, 121.0, 34.4, 33.7, 28.3, 27.0. HRMS calc'd for $\text{C}_{11}\text{H}_{15}\text{NO}_4\text{S}$, 256.06426 $[\text{M}-\text{H}]^+$; found, 256.06500 $[\text{M}-\text{H}]^+$.

Methyl 3-(4-ureidophenyl)propanoate (38).

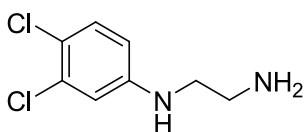
Compound **5** (0.500 g, 2.79 mmol) was dissolved in DMF (10.0 ml). To this solution trimethylisocyanate (0.408 ml, 3.07 mmol, 1.1 equiv) was added dropwise. The solution was stirred at room temperature for 24 hours. TLC indicated starting material remained. Another equivalent of isocyanate was added and the mixture was again stirred at room temperature for 12 hours. Starting material still remained. Triethylamine (0.384 ml, 2.79 mmol, 1.0 equiv) was added and the mixture was refluxed for 3 hours, upon which the reaction went to completion. The reaction was cooled to room temperature and quenched with water. The mixture was extracted with ethyl acetate (2x). The combined organics were washed with brine, dried over MgSO_4 , and concentrated *in vacuo* to give an orange solid. The crude material was purified using silica gel chromatography (100% EtOAc) to give a white solid (0.366 g, 59%). ^1H NMR (600 MHz, CD_3OD) δ 7.27 (d, $J = 8.6$ Hz, 2H), 7.10 (d, $J = 8.6$ Hz, 2H), 2.85 (t, $J = 7.6$ Hz, 2H), 2.59 (t, $J = 7.6$ Hz, 2H). ^{13}C NMR (150 MHz, CD_3OD) δ 175.3, 159.7, 139.0, 136.4, 129.8, 120.9, 52.1, 36.9, 31.4. HRMS calc'd for $\text{C}_{11}\text{H}_{14}\text{N}_2\text{O}_3$, 223.10838 $[\text{M}+\text{H}]^+$; found, 223.10717 $[\text{M}+\text{H}]^+$.

3-(4-Ureidophenyl)propanoic acid (39).

Ester **38** (0.336 g, 1.5 mmol) was dissolved in methanol (10.0 mL). To this solution 1.0 N NaOH (5.7 mL, 5.7 mmol, 3.8 equiv) was added dropwise. The mixture was stirred at room temperature for 12 hours. The pH of the solution was adjusted to 3 with an unknown molarity solution of aqueous HCl. The volume of methanol was reduced by rotary evaporation (40 mbar), upon which the product crashed out of solution. The white solid was obtained by filtration and washed with hexanes (0.300 g, 95%). ^1H NMR (400 MHz, CD_3OD) δ 7.26 (d, $J = 8.6$ Hz, 2H), 7.13 (d, $J = 8.6$ Hz, 2H), 2.85 (t, $J = 7.7$ Hz, 2H), 2.56 (t, $J = 7.7$ Hz, 2H). ^{13}C NMR (100 MHz, CD_3OD) δ 175.6, 158.4, 137.6, 135.4, 128.5, 119.6, 35.7, 30.2.

General synthesis of amines **45-47**, exemplified by **45**.

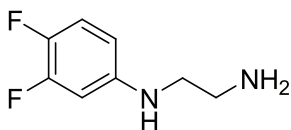
N^1 -(3,4-dichlorophenyl)ethane-1,2-diamine (45).



Bromoethylamine hydrobromide salt (5.0 g, 25 mmol) was suspended in toluene (100 mL) and 3,4-dichloroaniline (**44**, 12 g, 74 mmol, 3.0 equiv) was added. The brown solution was refluxed for 1 hour. The resulting mixture was cooled to room temperature to give a brown precipitate that was filtered off and washed with toluene. The solid was then treated with 20% w/v NaOH (100 mL) and extracted with DCM (2x). The organics were extracted with an acetic acid/sodium acetate buffer (300 mL of 0.1 M pH 5.5). The resulting aqueous layer was then basified with 20% w/v NaOH (100 mL) and extracted

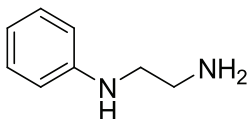
with DCM (2x). The combined organics were collected and washed with water, dried over MgSO_4 , and concentrated *in vacuo* to give a brown oil. The crude material was purified using silica gel chromatography (100% DCM to 10% MeOH/DCM + 1% Et_3N gradient) to give a brown residue (3.60 g, 72 %). ^1H NMR (400 MHz, CDCl_3) δ 7.17 (d, $J = 8.6$ Hz, 1H), 6.69 (s, 1H), 6.46 (d, $J = 8.6$ Hz, 1H), 4.25 (bs, 1H), 3.13 (t, $J = 5.1$ Hz, 2H), 2.96 (t, $J = 5.1$ Hz, 2H), 1.41 (bs, 2H). ^{13}C NMR (150 MHz, CDCl_3) δ 148.1, 133.0, 131.8, 114.0, 113.0, 46.2, 40.9. HRMS calc'd for $\text{C}_8\text{H}_{10}\text{Cl}_2\text{N}_2$, 205.03004 $[\text{M}+\text{H}]^+$; found, 205.02914 $[\text{M}+\text{H}]^+$.

N^1 -(3,4-difluorophenyl)ethane-1,2-diamine (46).



Compound **46** was prepared from 3,4-difluoroaniline (**41**) to give a brown oil (3.5 g, 86%). ^1H NMR (400 MHz, CDCl_3) δ 6.88 (1H, d, $J = 8.4$ Hz), 6.38 (1H, s), 6.24 (1H, d, $J = 8.4$ Hz), 4.21 (1H, bs), 3.34 (2H, t, $J = 6.0$ Hz), 2.04 (2H, t, $J = 6.0$ Hz), 1.16 (2H, bs). ^{13}C NMR (150 MHz, CDCl_3) δ 147.9, 138.6, 134.5, 115.2, 113.6, 46.5, 41.2

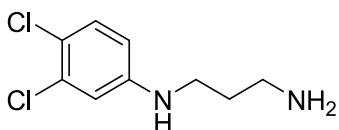
N^1 -phenylethane-1,2-diamine (47).



Compound **47** was prepared from aniline (**42**) to give a purple oil (2.36 g, 44%). ^1H NMR (400 MHz, CDCl_3) δ 7.18 (t, $J = 7.3$ Hz, 2H), 6.71 (t, $J = 7.3$ Hz, 1H), 6.61 (d, $J = 7.9$ Hz, 2H),

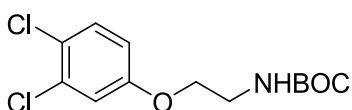
3.08-3.01 (mult, 2H), 2.90-2.73 (mult, 2H). ^{13}C NMR (100 MHz, CDCl_3) δ 148.0, 128.7, 116.5, 112.2, 45.5, 40.3.

N^1 -(3,4-dichlorophenyl)propane-1,3-diamine (50).



Compound **50** was obtained from compound **40** and bromopropylamine hydrobromide (brown residue, 45%). ^1H NMR (400 MHz, CDCl_3) δ 7.06 (d, $J = 8.0$ Hz, 1H), 6.54 (d, $J = 2.9$ Hz, 1H), 6.32 (dd, $J_1 = 8.0$ Hz, $J_2 = 2.9$ Hz, 1H), 4.76-4.27 (bs, 1H), 3.01 (t, $J = 6.7$ Hz, 2H), 2.73 (t, $J = 6.7$ Hz, 2H), 2.25-1.84 (bs, 2H), 1.64 (quint, $J = 6.7$ Hz, 2H). ^{13}C NMR (100 MHz, CDCl_3) δ 148.0, 132.3, 130.3, 118.6, 113.2, 112.3, 41.9, 39.9, 31.7. HRMS calc'd for $\text{C}_9\text{H}_{12}\text{Cl}_2\text{N}_2$, 219.04574 $[\text{M}+\text{H}]^+$; found, 219.04479 $[\text{M}+\text{H}]^+$.

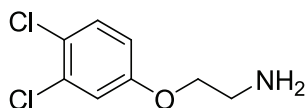
Tert-butyl 2-(3,4-dichlorophenoxy)ethylcarbamate (52).



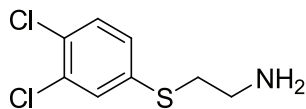
To a solution of dry THF (40.0 mL), 3,4-dichlorophenol (**51**, 1.11 g, 6.82 mmol, 1.1 equiv), *N*-Boc-aminoethanol (0.962 mL, 6.20 mmol) and triphenyl phosphine (2.28 g, 8.68 mmol, 1.40 equiv) were added. Diisopropylazodicarboxylate (1.71 mL, 8.68 mmol, 1.4 equiv) was added dropwise over 5 minutes at 0°C . The mixture was warmed to room temperature and stirred for 12 hours. The resulting solution was washed with 1.0N NaOH (20 mL), water (20 mL), and brine (20 mL). The organics were dried over MgSO_4

and concentrated *in vacuo* to give a yellow oil. The crude material was purified using silica gel chromatography (1 EtOAc/1 Hexanes) to give a colorless oil (1.30 g, 68%). ^1H NMR (400 MHz, CDCl_3) δ 7.33 (d, $J = 8.9$ Hz, 1H), 7.00 (d, $J = 2.9$ Hz, 1H), 6.76 (dd, $J_1 = 8.9$ Hz, $J_2 = 2.9$ Hz, 1H), 4.96 (bs, 1H), 3.99 (t, $J = 5.1$ Hz, 2H), 3.55-3.50 (mult, 2H), 1.46 (s, 9H).

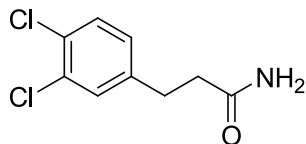
2-(3,4-Dichlorophenoxy)ethanamine (53).



Carbamate **52** (1.30 g, 4.25 mmol) was dissolved in THF (30.0 mL) and cooled to 0°C . To this solution trifluoroacetic acid (10.0 mL, 130 mol, 31 equiv) was added dropwise to give a brown solution, which was warmed to room temperature and stirred for 2 days. The mixture was basified with solid sodium bicarbonate and partitioned between water and ethyl acetate. The layers were separated and the organics were washed with brine, dried over MgSO_4 , and concentrated *in vacuo* to give a yellow residue. The crude material was purified using silica gel chromatography (10% MeOH/DCM) to give a yellow oil (0.826 g, 94%). ^1H NMR (300 MHz, CDCl_3) δ 7.28 (d, $J = 9.0$ Hz, 1H), 6.92 (d, $J = 2.8$ Hz, 1H), 6.67 (dd, $J_1 = 9.0$ Hz, $J_2 = 2.8$ Hz), 4.05 (t, $J = 4.5$ Hz, 2H), 3.52 (t, $J = 4.5$ Hz, 2H). ^{13}C NMR (75 MHz, CDCl_3) δ 156.6, 133.2, 125.5, 116.7, 114.4, 64.3, 39.5.

2-(3,4-Dichlorophenylthio)ethanamine (55).

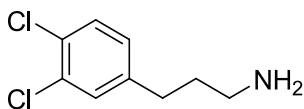
Thiophenol (**54**, 1.00 g, 5.58 mmol) and oxazolidinone (0.486 g, 5.58 mmol, 1.0 equiv) were heated to 130°C, and stirred for 2 hours. After cooling to room temperature, the resulting green solid was taken up in 10% HCl and heated for several minutes. The mixture was filtered and the filtrate was made basic (pH 10) with solid NaOH and extracted with DCM. The combined extracts were washed with water and brine, dried over MgSO₄, and concentrated *in vacuo* to give a colorless residue. The crude material was purified using silica gel chromatography (10% MeOH/DCM) to give a colorless residue (0.338 g, 27%). ¹H NMR (600 MHz, CDCl₃) δ 7.43 (d, *J*=1.9 Hz, 1H), 7.35 (d, *J*=8.6 Hz, 1H), 7.18 (dd, *J*₁=8.6 Hz, *J*₂=1.9 Hz, 1H), 3.02 (t, *J*=6.7 Hz, 2H), 2.94 (t, *J*=6.2 Hz, 2H), 1.59 (bs, 2H). HRMS calc'd for C₈H₉Cl₂NS, 221.99094 [M+H]⁺; found, 221.99072 [M+H]⁺.

3-(3,4-Dichlorophenyl)propanamide (57).

3-(3,4-dichlorophenyl)propionic acid (**56**, 3.00 g, 14 mmol) was dissolved in benzene (30.0 mL) and treated with oxalyl chloride (5.8 mL, 68 mmol, 5.0 equiv) and DMF (catalytic). The mixture was stirred for 12 hours at room temperature. The resulting solution was concentrated *in vacuo* to give an opaque liquid and dried *in vacuo* overnight. ¹H, ¹³C NMR confirms the presence of the acid chloride. The acid chloride

was dissolved in ether (24.0 mL), and ammonia (0.5 M solution in 1,4-dioxane, 82 mL, 41 mmol, 3.0 equiv) was added dropwise to give a white precipitate. The mixture was stirred at room temperature for 2 hours. The reaction was quenched with water and diluted with ether, and the layers were separated. The organics were washed with 2.0 N HCl, 10% NaHCO₃ solution, and brine. They were then dried over MgSO₄ and concentrated *in vacuo* to give a colorless oil which solidified upon trituration with DCM and hexanes (1.40 g, 47%). ¹H NMR (400 MHz, CDCl₃) δ 7.33 (d, *J* = 8.3 Hz, 1H), 7.29 (d, *J* = 1.9 Hz, 1H), 7.04 (dd, *J*₁ = 8.3 Hz, *J*₂ = 1.9 Hz, 1H), 6.04 (bs, 1H), 5.61 (bs, 1H), 2.90 (t, *J* = 7.6 Hz, 2H), 2.49 (t, *J* = 7.6 Hz, 2H). ¹³C NMR (100 MHz, CDCl₃) δ 174.3, 141.1, 132.5, 130.1, 128.1, 37.0, 30.4.

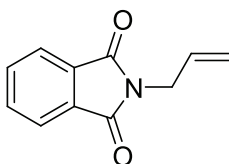
3-(3,4-Dichlorophenyl)propan-1-amine (58).



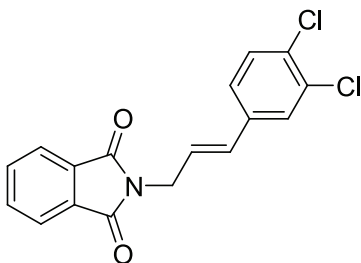
Amide **57** (0.446 g, 2.0 mmol) was dissolved in THF (15.0 mL). After cooling to 0°C, lithium aluminum hydride (2.0 M sol'n in THF, 3.1 mL, 6.1 mmol, 3.0 equiv) was added dropwise. The mixture was stirred at room temperature for 12 hours. The mixture was diluted with EtOAc and water, filtered over a pad of celite, and the resulting layers were separated. The organics were washed with brine, dried over MgSO₄, and concentrated *in vacuo* to give a yellow residue (0.400 g, 96%). ¹H NMR (400 MHz, CD₃OD) δ 7.40-7.36 (mult, 2H), 7.13 (dd, *J*₁ = 8.9 Hz, *J*₂ = 2.0 Hz, 1H), 2.68-2.61 (mult, 4H), 1.80-1.73 (mult,

2H). ^{13}C NMR (100 MHz, CD_3OD) δ 143.0, 131.9, 130.3, 130.2, 129.4, 128.2, 40.5, 33.5, 32.0. HRMS calc'd for $\text{C}_9\text{H}_{11}\text{Cl}_2\text{N}$, 204.03484 $[\text{M}+\text{H}]^+$; found, 204.03458 $[\text{M}+\text{H}]^+$.

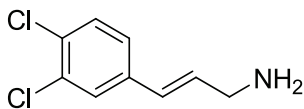
2-Allylisindoline-1,3-dione (60).



Potassium phthalimide (**59**, 2.59 g, 14 mmol, 1.4 equiv) was added to anhydrous DMF (100 mL). To this solution allyl bromide (0.86 mL, 10.0 mmol) was added dropwise. The reaction was heated to 50°C and stirred for 12 hours. The DMF was removed *in vacuo* and the remaining yellow liquid was dissolved in DCM. The solution was washed with water (2x) and brine (2x). The organics were dried over MgSO_4 and concentrated *in vacuo* to give an off-white solid. The crude material was purified using silica gel chromatography (50% DCM/50% hexanes) to give a white solid (1.80 g, 96%). ^1H NMR (400 MHz, CDCl_3) δ 7.87 (dd, $J_1 = 5.7$ Hz, $J_2 = 2.9$ Hz, 2H), 7.73 (dd, $J_1 = 5.7$ Hz, $J_2 = 2.9$ Hz, 2H), 5.90 (mult, 1H), 5.26 (dd $J_1 = 16.1$ Hz, $J_2 = 1.4$ Hz, 2H), 5.20 (dd, $J_1 = 10.1$ Hz, $J_2 = 1.4$ Hz, 1H) 4.31 (dt, $J_1 = 5.4$ Hz, $J_2 = 1.4$ Hz, 2H). ^{13}C NMR (100 MHz, CDCl_3) δ 168.2, 134.2, 132.3, 131.7, 123.5, 118.0, 40.2.

2-(3,4-Dichlorocinnamyl)isoindoline-1,3-dione (61).

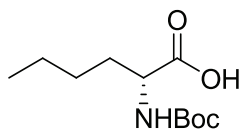
N-allylphthalimide **60** (0.660 g, 3.53 mmol, 1.25 equiv) and 3,4-dichloroiodobenzene (0.770 g, 2.82 mmol) were dissolved in triethylamine (10.0 mL) and acetonitrile (10 mL). Palladium acetate (6 mg, 0.028 mmol, 0.01 equiv) was added. The yellow solution was heated at 100°C in a thick-walled glass container for 20 hours. The reaction was cooled to room temperature, upon which precipitation occurred to give a brown solid. The solid was filtered and washed with water. The solid was then dissolved in hot DMF to give an orange liquid which was filtered through Celite to remove Pd(0). The resulting hot DMF filtrate was diluted with an equal volume of water, upon which precipitation occurred. The yellow solid was filtered off and dried *in vacuo* (6.9 g, 85%). ¹H NMR (400 MHz, *d*₆-DMSO) δ 7.92-7.84 (mult, 4H), 7.73 (d, *J* = 1.9 Hz, 1H), 7.56 (d, *J* = 8.3 Hz, 1H), 7.44 (dd, *J*₁ = 8.3 Hz, *J*₂ = 1.9 Hz, 1H), 6.55 (d, *J* = 15.9 Hz, 1H), 6.50-6.43 (dt, *J*₁ = 10.8 Hz, *J*₂ = 5.1 Hz, 1H), 4.35 (d, *J* = 4.1 Hz, 2H). ¹³C NMR (100 MHz, *d*₆-DMSO) δ 167.6, 137.1, 134.4, 131.7, 131.4, 130.6, 129.7, 128.7, 128.5, 128.2, 126.9, 126.3. HRMS calc'd for C₁₇H₁₁Cl₂NO₂, 332.02464 [M+H]⁺; found, 332.01368 [M+H]⁺.

(E)-3-(3,4-dichlorophenyl)prop-2-en-1-amine (62).

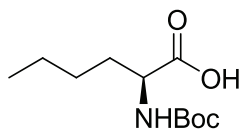
Compound **61** (0.660 g, 1.99 mmol) was suspended in ethanol (7.5 mL) and hydrazine hydrate (0.1 mL, 2.0 mmol, 1.1 equiv) was added. The solution was refluxed (heating dissolved to give an orange solution) overnight to give a yellow precipitate. The suspension was cooled to room temperature, and the precipitate was filtered off and washed with ethanol. The yellow solid was then suspended in water, and 1.0 N NaOH was added until the solid mostly dissolved. DCM was added and the layers were separated. The organics were washed with water, dried over MgSO₄, and concentrated *in vacuo* to give a yellow residue (0.221 g, 55%). ¹H NMR (400 MHz, CDCl₃) δ 7.42 (d, *J* = 2.2 Hz, 1H), 7.35 (d, *J* = 8.6 Hz, 1H), 7.17 (dd, *J*₁ = 8.6 Hz, *J*₂ = 2.2 Hz, 1H), 6.41 (d, *J* = 15.9 Hz, 1H), 6.31 (dt, *J*₁ = 15.9 Hz, *J*₂ = 5.1 Hz, 1H), 3.47 (d, *J* = 5.1 Hz, 2H), 1.23 (bs, 2H). ¹³C NMR (150 MHz, CDCl₃) δ 137.6, 133.7, 130.6, 128.2, 127.2, 125.6, 44.3. *m/z* (APCI) calc'd for C₉H₉Cl₂N, 202.0 [M]⁺; found, 202.1 [M]⁺.

General method for synthesis of N-Boc-norleucine **65** and **66**, exemplified by **65**.

(R)-2-(tert-butoxycarbonylamino)hexanoic acid (65).

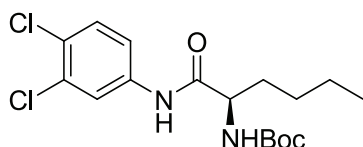


D-Norleucine (**63**, 0.500 g, 3.8 mmol) was dissolved in *tert*-butanol (5.0 ml) and 2.0 N NaOH (5.0 ml, 2.6 equiv) To this solution Boc₂O (0.920 g, 4.2 mmol, 1.1 equiv) was added. The clear mixture was stirred at room temperature for 12 hours. The solvent was removed *in vacuo* and the resulting white solid was partitioned between water and ether. The water layer was extracted 2x with ethyl ether, and the ether layers were discarded. The water layer was acidified with 1.0 N HCl and partitioned with ethyl acetate. The water layer was extracted 3x with ethyl acetate, and the combined organics were dried over MgSO₄ and concentrated *in vacuo* to give a colorless oil. The crude material was purified using silica gel chromatography (1 EtOAc/2 Hexanes) to give a colorless oil (0.572, 65%). ¹H NMR (300 MHz, CDCl₃) δ 9.96 (bs, 1H), 5.03 (d, *J* = 8.0 Hz, 1H), 4.33-4.22 (mult, 1H), 1.82-1.64 (mult, 2H), 1.41 (s, 9H), 1.40-1.30 (mult, 4H), 0.91 (t, *J* = 6.8 Hz, 3H). ¹³C NMR (75 MHz, CDCl₃) δ 178.5, 155.9, 80.6, 54.0, 33.4, 28.8, 27.7, 22.9, 14.6. HRMS calc'd for C₁₁H₂₁NO₄, 232.1500 [M+H]⁺; found, 232.15423 [M+H]⁺.

(S)-2-(tert-butoxycarbonylamino)hexanoic acid (66).

Compound **66** was obtained from L-norleucine (1.61 g, 91%). ^1H NMR (300 MHz, CDCl_3) δ 9.96 (bs, 1H), 5.05 (d, $J = 8.0$ Hz, 1H), 4.34-4.25 (mult, 1H), 1.84-1.67 (mult, 2H), 1.45 (s, 9H), 1.41-1.32 (mult, 4H), 0.91 (t, $J = 6.8$ Hz, 3H). ^{13}C NMR (75 MHz, CDCl_3) δ 178.1, 155.8, 80.4, 53.6, 32.4, 28.5, 27.6, 22.5, 14.1. HRMS calc'd for $\text{C}_{11}\text{H}_{21}\text{NO}_4$, 232.15500 $[\text{M}+\text{H}]^+$; found, 232.15423 $[\text{M}+\text{H}]^+$.

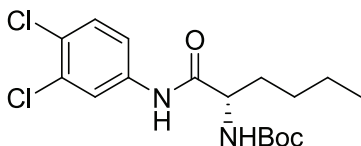
General method for synthesis of α -alkyl benzylamines **67** and **68**, exemplified by **67**.

(R)-tert-butyl 1-(3,4-dichlorophenylamino)-1-oxohexan-2-ylcarbamate (67).

A solution of N-Boc-D-Norleucine (0.572 g, 2.5 mmol) in THF (20.0 ml) was cooled to -5°C and N-methyl morpholine (0.30 ml, 2.7 mmol, 1.1 equiv) was added. After stirring for 5 min, isopropyl chloroformate (1.0 M sol'n in toluene, 2.7 ml, 2.7 mmol, 1.1 equiv) was added dropwise, forming a white precipitate. After stirring for 5 additional min, a solution of 3,4-dichloroaniline (0.400 g, 2.5 mmol, 1.0 equiv) in THF (7.0 ml) was added dropwise over 10 minutes to give a brown solution. The mixture was stirred at room temperature for 5 hours. The NMM-HCl salt was removed by filtration, and the resulting solution was concentrated *in vacuo* to give a brown oil. The crude material was purified

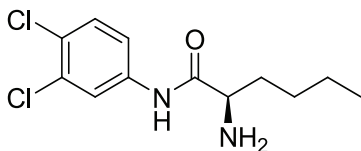
using silica gel chromatography (RediSep 40 g column; 1 EtOAc/4 Hexanes) to give a white foam (0.769, 83%). ^1H NMR (300 MHz, CDCl_3) δ 9.26 (bs, NH), 7.69 (s, 1H), 7.17 (mult, 2H), 5.41 (d, $J = 7.8$ Hz, 1H, N-H), 4.30-4.27 (mult, 1H), 1.83-1.80 (mult, 1H), 1.71-1.67 (mult, 1H), 1.45 (s, 9H), 1.39-1.30 (mult, 4H), 0.89 (t, $J = 6.6$ Hz, 3H). ^{13}C NMR (75 MHz, CDCl_3) δ 171.7, 156.8, 137.6, 132.6, 130.3, 127.2, 121.3, 118.7, 81.0, 55.8, 32.3, 28.6, 28.2, 22.6, 14.1. HRMS calc'd for $\text{C}_{17}\text{H}_{24}\text{Cl}_2\text{N}_2\text{O}_3$, 375.12434 $[\text{M}+\text{H}]^+$; found: 375.12466 $[\text{M}+\text{H}]^+$.

(S)-tert-butyl 1-(3,4-dichlorophenylamino)-1-oxohexan-2-ylcarbamate (68).

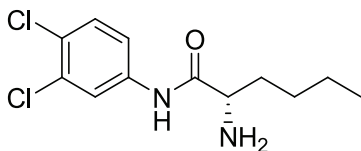


Compound **68** was prepared from N-Boc-L-Norleucine (**66**, 1.60 g, 6.9 mmol) to give a white foam (2.24 g, 86%). ^1H NMR (600 MHz, CDCl_3) δ 9.32 (s, 1H), 7.69 (s, 1H), 7.16 (mult, 2H), 5.47 (d, $J = 8.1$ Hz, 1H), 4.31 (mult, 1H), 1.84-1.79 (mult, 1H), 1.70-1.67 (mult, 1H), 1.45 (s, 9H), 1.34-1.30 (mult, 4H), 0.88 (t, $J = 6.6$ Hz, 3H). ^{13}C NMR (150 MHz, CDCl_3) δ 171.9, 156.9, 137.6, 132.6, 130.3, 127.2, 121.3, 118.7, 80.9, 55.9, 32.3, 28.5, 28.2, 22.6, 14.1. HRMS calc'd for $\text{C}_{17}\text{H}_{24}\text{Cl}_2\text{N}_2\text{O}_3$, 375.12434 $[\text{M}+\text{H}]^+$; found: 375.12367 $[\text{M}+\text{H}]^+$.

General method for amines **69** and **70**, exemplified by **69**.

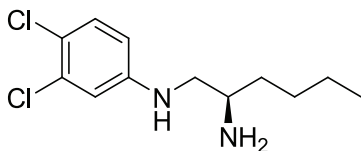
(R)-2-amino-N-(3,4-dichlorophenyl)hexanamide (69).

Ethanol (3.0 mL, excess) was cooled to -5°C . Acetyl chloride (1.46 mL, 20.5 mmol, 10 equiv) was added dropwise. The mixture was warmed to room temperature and stirred for 20 minutes. In a separate flask, a solution of amide **67** (0.769 g, 2.05 mmol) in THF (10.0 mL) was cooled to 0°C , and the ethanolic HCl was added dropwise. The solution was warmed to room temperature and stirred for 12 hours. The mixture was concentrated *in vacuo* to give a yellow solid. The solid was dissolved in EtOAc and solid sodium bicarbonate was added, followed by water. The layers were separated and the organics were washed with water and brine, dried over MgSO_4 , and concentrated *in vacuo* to give an orange oil, which was used without purification (0.491 g, 87%). ^1H NMR (400 MHz, CDCl_3) δ 9.67 (s, 1H), 7.83 (s, 1H), 7.37-7.33 (mult, 2H), 5.27 (s, 1H), 4.09 (mult, 1H), 3.43 (mult, 2H), 1.90 (mult, 1H), 1.55-1.28 (mult, 5H), 0.88 (t, $J = 6.6$ Hz, 3H). ^{13}C NMR (75 MHz, CDCl_3) δ 173.7, 137.5, 132.8, 130.6, 127.1, 121.1, 118.7, 55.6, 34.6, 28.1, 22.7, 22.2, 14.3. HRMS calc'd for $\text{C}_{12}\text{H}_{16}\text{Cl}_2\text{N}_2\text{O}$, 275.07194 $[\text{M}+\text{H}]^+$; found, 275.07111 $[\text{M}+\text{H}]^+$.

(S)-2-amino-N-(3,4-dichlorophenyl)hexanamide (70).

Compound **70** was prepared from compound **68** to give an orange oil (1.84 g, quant). ^1H NMR (400 MHz, CDCl_3) δ 9.63 (s, 1H), 7.81 (s, 1H), 7.36-7.33 (mult, 2H), 5.28 (s, 1H), 4.03 (mult, 1H), 3.43 (mult, 2H), 1.91 (mult, 1H), 1.55-1.26 (mult, 5H), 0.88 (t, $J = 6.6$ Hz, 3H). ^{13}C NMR (75 MHz, CDCl_3) δ 173.8, 137.4, 132.4, 130.3, 126.8, 121.0, 118.7, 55.4, 34.4, 27.9, 22.4, 22.0, 13.9. HRMS calc'd for $\text{C}_{12}\text{H}_{16}\text{Cl}_2\text{N}_2\text{O}$, 275.07194 $[\text{M}+\text{H}]^+$; found, 275.07111 $[\text{M}+\text{H}]^+$.

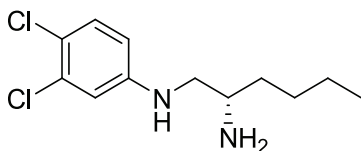
General method for reduction to give ethanediamine compounds **71** and **72**, exemplified by **71**.

(R)-N¹-(3,4-dichlorophenyl)hexane-1,2-diamine (71).

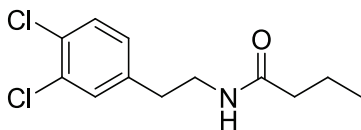
Amide **69** (0.460 g, 1.67 mmol) was dissolved in THF (15.0 mL). To this solution, borane dimethyl sulfide (0.47 mL, 5.02 mmol, 3.0 equiv) was added dropwise at room temperature. The brown solution was refluxed for 6 hours before cooling to room temperature. The reaction was quenched with water and partitioned with EtOAc. The layers were separated, and the organics were washed with 1.0 N HCl, water, and brine.

The organics were dried over MgSO_4 and concentrated *in vacuo* to give a colorless oil. The crude material was purified using silica gel chromatography (5% MeOH/DCM + 1% Et_3N) to give a yellow oil (0.295 g, 68%). ^1H NMR (300 MHz, CDCl_3) δ 7.15 (d, $J = 8.8$ Hz, 1H), 6.67 (d, $J = 2.8$ Hz, 1H), 6.44 (dd, $J_1 = 8.8$ Hz, $J_2 = 2.8$ Hz, 1H), 4.40 (bs, 1H), 3.18-3.06 (mult, 1H), 2.93 (mult, 1H), 2.81-2.74 (mult, 1H), 1.49-1.30 (mult, 8H), 0.92 (t, $J = 6.6$ Hz, 3H). ^{13}C NMR (75 MHz, CDCl_3) δ 148.2, 132.8, 130.6, 119.5, 113.8, 112.8, 50.7, 50.1, 36.4, 28.4, 22.9, 14.2. HRMS calc'd for $\text{C}_{12}\text{H}_{18}\text{Cl}_2\text{N}_2$, 261.09264 $[\text{M}+\text{H}]^+$; found, 261.09161 $[\text{M}+\text{H}]^+$.

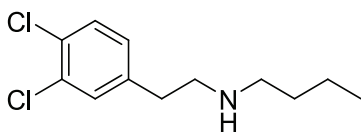
(S)-N¹-(3,4-dichlorophenyl)hexane-1,2-diamine (72).



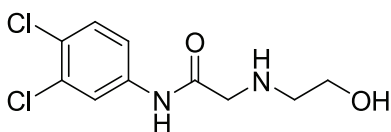
Compound **72** was prepared from **70** to give a white foam (0.700 g, 63%). ^1H NMR (400 MHz, CDCl_3) δ 7.16 (d, $J = 8.8$ Hz, 1H), 6.68 (d, $J = 2.8$ Hz, 1H), 6.44 (dd, $J_1 = 8.8$ Hz, $J_2 = 2.8$ Hz, 1H), 4.45 (bs, 1H), 3.20-3.06 (mult, 1H), 2.91 (mult, 1H), 2.81-2.77 (mult, 1H), 1.49-1.27 (mult, 8H), 0.91 (t, $J = 6.6$ Hz, 3H). ^{13}C NMR (75 MHz, CDCl_3) δ 146.6, 133.1, 131.0, 120.9, 114.2, 112.7, 52.3, 45.7, 30.8, 27.8, 22.5, 14.0. HRMS calc'd for $\text{C}_{12}\text{H}_{18}\text{Cl}_2\text{N}_2$, 261.09264 $[\text{M}+\text{H}]^+$; found, 261.09185 $[\text{M}+\text{H}]^+$.

N-(3,4-dichlorophenethyl)butyramide (74).

Butyric acid (2.00 g, 22.7 mmol) was dissolved in DCM (50.0 mL). After cooling to 0°C, DMAP (3.05 g, 25.0 mmol, 1.1 equiv) and EDCI (4.79 g, 25.0 mmol, 1.1 equiv) were added. The mixture was stirred for 45 minutes at 0°C, then 3,4-dichlorophenylethylamine (**73**, 3.74 mL, 225.0 mmol, 1.1 equiv) was added dropwise to give a colorless solution. The mixture was warmed to room temperature and stirred for 12 hours. The DCM was removed *in vacuo*, and the resulting residue was partitioned between ethyl acetate and 1.0 N HCl. The organics were extracted with EtOAc (3x). The combined organics were washed with brine, dried over MgSO₄, and concentrated *in vacuo* to give a yellow residue. The crude material was purified using silica gel chromatography (ISCO 80 g column, 50% EtOAc/50% Hexanes to 100% EtOAc gradient) to give a light yellow oil, which solidified to a white solid under vacuum (5.45 g, 92%). ¹H NMR (400 MHz, CDCl₃) δ 7.51 (bt, *J* = 5.1 Hz, 1H), 7.39-7.35 (mult, 2H), 7.11 (d, *J* = 8.3 Hz, 1H), 3.53 (quart, *J* = 6.8 Hz, 2H), 2.89 (t, *J* = 6.8 Hz, 2H), 2.24 (t, *J* = 7.3 Hz, 2H), 1.71 (sextet, *J* = 7.3 Hz, 2H), 1.00 (t, *J* = 7.3 Hz, 3H). ¹³C NMR (100 MHz, CDCl₃) δ 173.0, 139.2, 131.5, 130.1, 129.7, 129.5, 127.7, 39.7, 37.7, 34.2, 18.7, 13.2. HRMS calc'd for C₁₂H₁₅Cl₂NO, 260.10104 [M+H]⁺; found, 260.06042 [M+H]⁺.

N-(3,4-dichlorophenethyl)butan-1-amine (75).

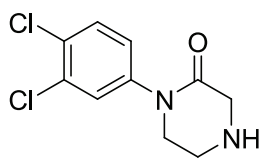
Amide **74** (5.45 g, 0.93 mmol) was dissolved in THF (150.0 mL). To this solution, borane dimethyl sulfide (6.0 mL, 63 mmol, 3.0 equiv) was added dropwise at room temperature. The solution was then refluxed for 3 hours. The reaction was quenched with 1.0 N HCl and partitioned with EtOAc. The mixture was extracted with EtOAc (3x). The combined organics were washed with water and brine, dried over MgSO_4 , and concentrated *in vacuo* to give a white solid. The crude material was recrystallized using DCM and hexanes to give a white solid (1.48 g, 29%). ^1H NMR (400 MHz, d_6 -DMSO) δ 7.60-7.58 (mult, 2H), 7.29 (dd, $J_1=8.3$ Hz, $J_2=1.9$ Hz, 1H), 3.15-3.10 (mult, 2H), 2.99 (t, $J = 8.6$ Hz, 2H), 2.91-2.83 (mult, 2H), 1.64-1.56 (mult, 2H), 1.34-1.29 (mult, 2H), 0.88 (t, $J = 7.3$ Hz, 3H). ^{13}C NMR (100 MHz, d_6 -DMSO) δ 139.2, 131.7, 131.5, 131.2, 130.1, 130.0, 129.8, 47.7, 47.1, 31.1, 28.1, 20.0, 14.2. HRMS calc'd for $\text{C}_{12}\text{H}_{17}\text{Cl}_2\text{N}$, 246.08174 $[\text{M}+\text{H}]^+$; found, 246.08063 $[\text{M}+\text{H}]^+$.

N-(3,4-dichlorophenyl)-2-(2-hydroxyethylamino)acetamide (77).

3,4-dichloroaniline (**40**, 10.0 g, 61.7 mmol) was combined with EtOAc (60.0 mL) and 20% aq. KHCO_3 (52.5 mL, 524 mmol, 8.5 equiv). The biphasic mixture was cooled to -5°C and treated with chloroacetyl chloride (5.90 mL, 74.1 mmol, 1.2 equiv) dropwise over 30

minutes. The ice bath was removed, and the reaction mixture was warmed to room temperature to give a brown biphasic mixture. The aqueous layer was removed, and the organic layer was combined with ethanolamine (13.0 mL, 216 mmol, 3.5 equiv), heated to 60°C and stirred for 1 hour to give brown crystals. Water and EtOAc were added to the reaction mixture, and the mixture was reheated to 60°C and the aqueous layer was removed. The organic layer was cooled to 0°C over 1 hour, yielding an orange solution with white crystals. The solids were collected by filtration and washed with chilled EtOAc. The product was dried *in vacuo* to give a white solid (13.46 g, 83%). ¹H NMR (400 MHz, *d*₆-DMSO) δ 8.00 (s, 1H), 7.55 (d, *J* = 8.2 Hz, 1H), 7.50 (d, *J* = 8.2 Hz, 1H), 3.42 (s, 2H), 3.27 (bs, 2H), 2.57 (t, *J* = 4.7 Hz, 2H). ¹³C NMR (100 MHz, *d*₆-DMSO) δ 171.2, 138.7, 131.0, 130.6, 124.7, 120.4, 119.3, 60.4, 52.8, 51.6. HRMS calc'd for C₁₀H₁₂Cl₂N₂O₂, 263.03552 [M+H]⁺; found, 263.03458 [M+H]⁺.

1-(3,4-Dichlorophenyl)piperazin-2-one (**78**).



The amidoalcohol **77** (5.00 g, 19.0 mmol) and tributylphosphine (6.64 mL, 26.6 mmol, 1.4 equiv) were suspended in dry EtOAc (100.0 mL) and cooled to 0°C. To this solution, di-*tert*-butyl azodicarboxylate (6.13 g, 26.6 mmol, 1.4 equiv) in EtOAc (50.0 mL) was added dropwise over 45 min, resulting in a yellow solution. The reaction mixture was stirred at 0°C for 30 minutes, warmed to room temperature and stirred for an additional 12 h. The reaction was quenched with 1.0 M NaOH, and the mixture was extracted

with EtOAc (2x). The combined organics were washed with brine, dried over MgSO_4 , and concentrated *in vacuo* to give a brown oil. The crude material was purified using silica gel chromatography (5%-10%MeOH/DCM gradient) to give a light brown oil (3.50 g, 75%). ^1H NMR (600 MHz, CDCl_3) δ 7.47 (d, J = 8.5 Hz, 1H), 7.45 (d, J = 2.4 Hz, 1H), 7.19 (dd, J_1 = 8.5 Hz, J_2 = 2.4 Hz), 3.70 (s, 2H), 3.67 (t, J = 4.9 Hz, 2H), 3.23 (t, J = 4.9 Hz, 2H). ^{13}C NMR (150 MHz, CDCl_3) δ 168.0, 141.6, 133.1, 131.0, 130.9, 128.0, 125.5, 51.5, 51.0, 43.6. HRMS calc'd for $\text{C}_{10}\text{H}_{10}\text{Cl}_2\text{N}_2\text{O}$, 245.02496 $[\text{M}+\text{H}]^+$; found, 245.12276 $[\text{M}+\text{H}]^+$.

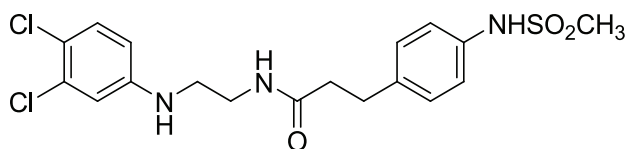
Compound **78** can also be prepared by a Buchwald coupling:

A pyrex thick-walled flask was charged with CuI (0.035 g, 0.18 mmol, 0.10 equiv), K_3PO_4 (0.62 g, 2.9 mmol, 1.6 equiv), 3,4-dichloriodobenzene (0.500 g, 1.8 mmol), and 2-oxopiperidone (0.152 g, 1.52 mmol, 0.83 equiv). DMF (10.0 mL) and trans-N,N-dimethylcyclohexane-1,3-diamine (0.049 mL, 0.31 mmol, 0.17 equiv) were added and the flask was heated to 110°C for 18 hours. Addition of the diamine turned the suspension green to bright blue. The reaction mixture was cooled to room temperature, and a solution of ammonium hydroxide (3 mL) in water (40 mL) was added. The resulting aqueous layer was extracted with ethyl acetate (3x). The organic layers were dried over MgSO_4 and concentrated *in vacuo* to give a brown residue. The crude material was purified using silica gel chromatography (10% MeOH/DCM) to give a light brown oil (0.126 g, 28%).

General method for preparation of amides in Table 2.3 exemplified by **96-13**.

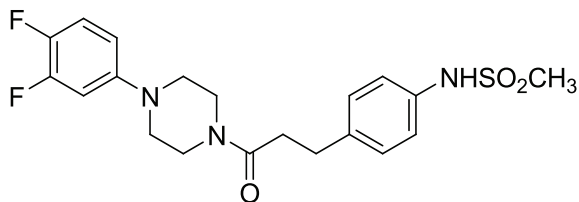
N-(2-(3,4-dichlorophenylamino)ethyl)-3-(4-(methylsulfonamido)phenyl)propanamide

(96-13).



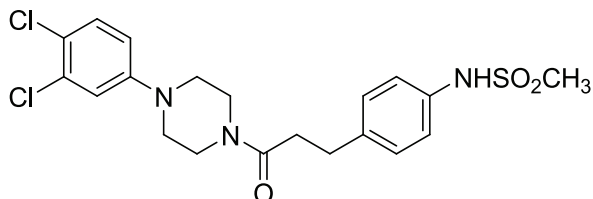
Carboxylic acid **36** (0.700 g, 2.88 mmol) was dissolved in DMF (30.0 mL) and cooled to 0°C. To this solution, DMAP (0.352 g, 2.28 mmol, 1.1 equiv), and EDCI (0.552 g, 2.88 mmol, 1.0 equiv) were added to give a clear suspension. After stirring for 45 minutes, amine **45** (0.590 g, 2.88 mmol, 1.0 equiv) in THF (5.0 mL) was added dropwise. The mixture was warmed to room temperature and stirred for 12 hours. The mixture was concentrated *in vacuo*, and the resulting residue was partitioned between 1.0 N HCl, and EtOAc. After extracting with EtOAc (2x), the combined organic layers were dried over MgSO₄ and concentrated *in vacuo*. The crude material was purified by taking the residue up in DCM and stirring. Immediately a white powder precipitated, which was collected by filtration (0.920 g, 74%). ¹H NMR (400 MHz, CD₃OD) δ 7.14-7.10 (mult, 5H), 6.72 (d, *J* = 2.9 Hz, 1H), 6.51 (dd, *J*₁ = 8.9 Hz, *J*₂ = 2.6 Hz, 1H), 3.27 (t, 2H), 3.10 (t, *J* = 6.4 Hz, 2H), 2.88 (s, 3H), 2.87 (t, *J* = 6.5 Hz, 2H), 2.46 (t, *J* = 6.4 Hz, 2H). ¹³C NMR (75 MHz, CDCl₃) δ 175.8, 150.0, 138.7, 138.3, 131.7, 130.5, 122.3, 114.4, 113.6, 44.0, 39.8, 39.2, 39.0, 32.3. HRMS calc'd for C₁₈H₂₁Cl₂N₃O₃S, 431.07604 [M+H]⁺; found, 431.08143 [M+H]⁺. Anal. (C₁₈H₂₁Cl₂N₃O₃S) C, H, N.

N-(4-(3-(4-(3,4-difluorophenyl)piperazin-1-yl)-3-oxopropyl)phenyl)methanesulfonamide (96-14).

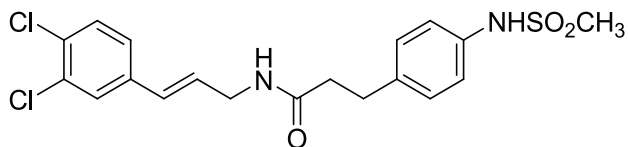


Compound **96-14** was obtained from carboxylic acid **36** (0.349 g, 1.4 mmol) and 3,4-difluorophenylpiperazine (**81**, 0.310 g, 1.6 mmol, 1.1 equiv). The crude material was purified using silica gel chromatography to give a white foam (0.240 g, 40%). ^1H NMR (600 MHz, CDCl_3) δ 7.7(bs, 1H), 7.27-7.22 (4H, mult), 7.11 (quart, $J = 9.1$ Hz, 1H), 6.78-6.72 (qd $J_1 = 7.0$, $J_2 = 2.9$ Hz, 1H, mult), 6.65 (d, $J = 9.0$ Hz, 1H), 3.84 (t, $J = 4.8$ Hz, 2H), 3.63 (t, $J = 4.8$ Hz, 2H), 3.12 (t, $J = 5.1$ Hz), 3.10-3.02 (mult, 6H), 2.74 (t, $J = 7.9$ Hz). ^{13}C NMR (100 MHz, CDCl_3) δ 170.9, 150.5 (dd, $J_1 = 246$ Hz, $J_2 = 13.7$ Hz), 148.7 (d, $J = 5.3$ Hz), 144.8 (dd, $J_1 = 246$ Hz, $J_2 = 13.7$ Hz), 138.3, 135.4, 129.7, 121.5, 117.4 (d, $J = 17.6$ Hz), 112.2 (d, $J = 5.2$ Hz), 106.0 (d, $J = 19.8$ Hz), 50.0, 49.7, 45.4, 41.6, 39.1, 34.9, 30.7. HRMS calc'd for $\text{C}_{20}\text{H}_{23}\text{F}_2\text{N}_3\text{O}_3\text{S}$, 424.15076 $[\text{M}+\text{H}]^+$; found, 424.14934 $[\text{M}+\text{H}]^+$. Anal. ($\text{C}_{20}\text{H}_{23}\text{F}_2\text{N}_3\text{O}_3\text{S}$) C: 56.15, H: 5.61, N: 9.54.

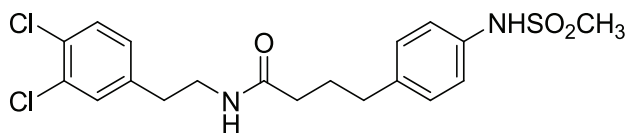
N-(4-(3-(4-(3,4-dichlorophenyl)piperazin-1-yl)-3-oxopropyl)phenyl)methanesulfonamide (96-15).



Compound **96-15** was obtained using carboxylic acid **36** and 1-(3,4-dichlorophenyl)piperazine (**82**). The crude material was purified using silica gel chromatography (100% EtOAc) to give an off-white foam (0.320 g, 28%). ^1H NMR (600 MHz, CDCl_3) δ 7.37 (s, 1H), 7.34 (d, $J=8.6$ Hz, 1H), 7.15 (s, 4H), 6.88 (d, $J=2.4$ Hz, 1H), 6.67 (dd, $J_1=8.8$ Hz, $J_2=2.8$ Hz, 1H), 3.71 (t, $J=4.8$ Hz, 2H), 3.51 (t, $J=4.8$ Hz, 2H), 3.06 (t, $J=5.2$ Hz, 2H), 3.01 (t, $J=5.2$ Hz, 2H), 2.92 (t, $J=7.6$ Hz, 2H), 2.91 (s, 3H), 2.62 (t, $J=7.6$ Hz, 2H). ^{13}C NMR (150 MHz, CDCl_3) δ 170.9, 150.4, 138.5, 135.4, 133.1, 130.8, 129.9, 123.2, 121.6, 118.0, 116.0, 49.1, 49.0, 45.3, 41.5, 39.3, 34.9, 30.9. HRMS calc'd for $\text{C}_{20}\text{H}_{23}\text{Cl}_2\text{N}_3\text{O}_3\text{S}$, 456.09164 $[\text{M}+\text{H}]^+$; found, 456.09066 $[\text{M}+\text{H}]^+$. (a) 99.5% (c) 99.6%.

N-(3,4-dichlorocinnamyl)-3-(4-(methylsulfonamido)phenyl)propanamide (96-17).

Compound **96-17** was obtained using carboxylic acid **36** and amine **62**. The crude material was purified using silica gel chromatography (100% EtOAc) to give yellow crystals (1.05 g, 80%). ^1H NMR (400 MHz, d_6 -DMSO) δ 9.61 (s, 1H), 8.11 (bt, $J = 5.7$ Hz, 1H), 7.69 (d, $J = 1.9$ Hz, 1H), 7.57 (d, $J = 8.6$ Hz, 2H), 7.38 (dd, $J_1 = 8.6$ Hz, $J_2 = 1.9$ Hz, 1H), 7.18 (d, $J = 8.3$ Hz, 2H), 7.11 (d, $J = 8.6$ Hz, 2H), 6.41 (d, $J = 15.9$ Hz, 1H), 6.31 (dt, $J_1 = 15.9$ Hz, $J_2 = 5.1$ Hz, 1H), 3.83 (t, $J = 5.1$ Hz, 2H), 2.80 (t, $J = 7.6$ Hz, 2H), 2.92 (s, 3H), 2.41 (t, $J = 8.2$ Hz, 2H). ^{13}C NMR (100 MHz, d_6 -DMSO) δ 171.2, 137.5, 137.0, 136.2, 131.4, 130.7, 130.1, 129.4, 129.1, 127.9, 127.3, 126.2, 120.2, 39.0, 36.9, 30.4. HRMS calc'd for $\text{C}_{19}\text{H}_{20}\text{Cl}_2\text{N}_2\text{O}_3\text{S}$, 427.07514 $[\text{M}+\text{H}]^+$; found, 427.06418 $[\text{M}+\text{H}]^+$. Anal. ($\text{C}_{19}\text{H}_{20}\text{Cl}_2\text{N}_2\text{O}_3\text{S}$) C, H, N.

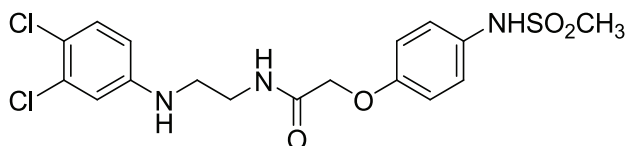
N-(3,4-dichlorophenethyl)-4-(4-(methylsulfonamido)phenyl)butanamide (96-19).

Compound **96-19** was obtained using carboxylic acid **37** and 3,4-dichlorophenylethylamine (**73**). The crude material was purified using silica gel chromatography (50% EtOAc/50% Hexanes to 100% EtOAc gradient) to give a white foam which solidified *in vacuo* (0.571 g, 68%). ^1H NMR (600 MHz, CDCl_3) δ 7.57 (s, 1H), 7.29 (d, $J = 8.1$ Hz, 1H), 7.23 (d, $J = 1.9$ Hz, 1H), 7.12 (d, $J = 8.6$ Hz, 2H), 7.03 (d, $J = 8.1$ Hz,

2H), 6.99 (dd, $J_1 = 8.1$ Hz, $J_2 = 1.9$ Hz, 1H), 5.82 (bt, $J = 6.2$ Hz, 1H), 3.44 (quart, $J = 6.2$ Hz, 2H), 2.92 (s, 3H), 2.73 (t, $J = 7.1$ Hz, 2H), 2.52 (t, $J = 7.1$ Hz, 2H), 2.11 (t, $J = 7.1$ Hz, 2H), 1.84 (quint, $J = 8.1$ Hz, 2H). ^{13}C NMR (150 MHz, CDCl_3) δ 173.3, 139.4, 138.9, 135.2, 132.5, 130.9, 130.7, 130.6, 129.7, 128.5, 121.6, 40.4, 39.3, 35.9, 35.0, 34.6, 27.3. HRMS calc'd for $\text{C}_{19}\text{H}_{22}\text{Cl}_2\text{N}_2\text{O}_3\text{S}$, 429.08074 $[\text{M}+\text{H}]^+$; found, 429.08027 $[\text{M}+\text{H}]^+$. Anal. ($\text{C}_{19}\text{H}_{22}\text{Cl}_2\text{N}_2\text{O}_3\text{S}$) C, H, N.

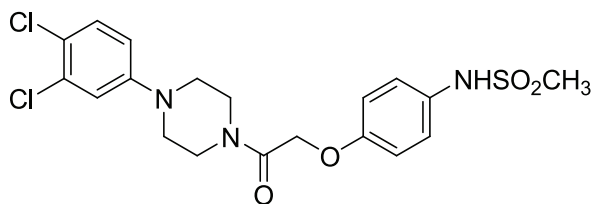
N-(2-(3,4-dichlorophenylamino)ethyl)-2-(4-(methylsulfonamido)phenoxy)acetamide

(96-22)



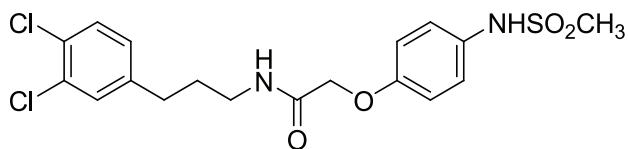
Compound **96-22** was obtained using carboxylic acid **35** and amine **45**. The crude material was purified using silica gel chromatography (100% EtOAc) to give a white powder (0.970 g, 55%). ^1H NMR (400 MHz, d_6 -acetone) δ 7.28 (d, $J = 8.8$ Hz, 2H), 7.20 (d, $J = 8.8$ Hz, 1H), 6.96 (d, $J = 8.9$ Hz, 2H), 6.79 (d, $J = 2.9$ Hz, 1H), 6.61 (dd, $J_1 = 8.8$ Hz, $J_2 = 2.9$ Hz, 1H), 4.47 (s, 2H), 3.78 (s, 1H), 3.49 (quint, $J = 6.3$ Hz, 2H), 3.28 (quint, $J = 6.3$ Hz, 2H), 2.89 (s, 3H). ^{13}C NMR (100 MHz, d_6 -acetone) δ 169.3, 156.3, 149.7, 132.9, 131.5, 129.0, 124.4, 118.5, 116.4, 113.9, 113.5, 68.4, 43.8, 38.9, 38.7. HRMS calc'd for $\text{C}_{17}\text{H}_{19}\text{Cl}_2\text{N}_3\text{O}_4\text{S}$, 432.05524 $[\text{M}+\text{H}]^+$; found: 432.05383 $[\text{M}+\text{H}]^+$. Anal. ($\text{C}_{17}\text{H}_{19}\text{Cl}_2\text{N}_3\text{O}_4\text{S}$) C, H, N.

N-(4-(2-(4-(3,4-dichlorophenyl)piperazin-1-yl)-2-oxoethoxy)phenyl)methanesulfonamide (96-30).



Compound **96-30** was obtained using carboxylic acid **35** and 1-(3,4-dichlorophenyl)piperazine (**82**). Upon addition of 1.0 N HCl precipitation occurred. The white solid was obtained by filtration and washing with hexanes (0.775 g, 85%). ¹H NMR (600 MHz, *d*₆-DMSO) δ 9.39 (s, 1H), 7.42 (d, *J* = 9.1 Hz, 1H), 7.17 (d, *J* = 2.3 Hz, 1H), 7.13 (d, *J* = 9.1 Hz, 2H), 6.96 (dd, *J*₁ = 9.1 Hz, *J*₂ = 2.3 Hz, 1H), 6.92 (d, *J* = 9.1 Hz, 2H), 4.84 (s, 2H), 3.27-3.18 (mult, 4H), 2.88 (s, 3H). ¹³C NMR (150 MHz, *d*₆-DMSO) δ 165.9, 155.3, 150.4, 131.5, 131.2, 130.5, 123.2, 120.0, 116.6, 115.6, 115.3, 59.8, 47.7, 47.4, 43.7, 40.7, 38.7. HRMS calc'd for C₁₉H₂₁Cl₂N₃O₄S, 458.07094 [M+H]⁺; found, 458.07034 [M+H]⁺. Anal. (C₁₉H₂₁Cl₂N₃O₄S · 0.8 H₂O) C: 48.38, H:4.86, N: 8.39.

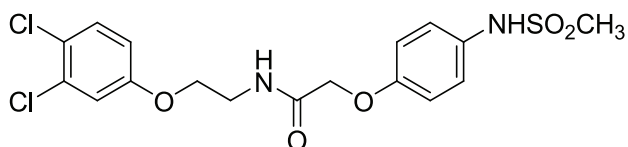
N-(3-(3,4-dichlorophenyl)propyl)-2-(4-(methanesulfonamido)phenoxy)acetamide (96-32).



Compound **96-32** was obtained using carboxylic acid **35** and amine **58**. The crude material was purified using silica gel chromatography (3 EtOAc/1 Hexanes) to give a

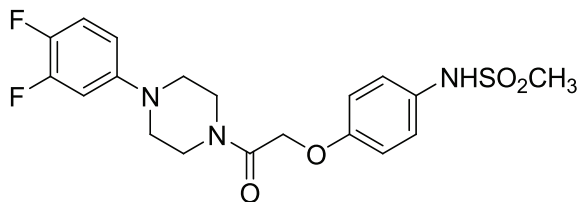
yellow oil (0.380 g, 43%). ^1H NMR (400 MHz, CDCl_3) δ 7.37 (bs, 1H), 7.31 (d, $J = 8.3$ Hz, 1H), 7.26-7.23 (mult, 3H), 7.00 (dd, $J_1 = 8.1$ Hz, $J_2 = 2.2$ Hz, 1H), 6.89 (d, $J = 8.8$ Hz, 2H), 6.67 (bt, $J = 5.7$ Hz, 1H), 4.46 (s, 2H), 3.38 (q, $J = 6.7$ Hz, 2H), 2.95 (s, 3H), 2.60 (t, $J = 7.3$ Hz, 2H), 1.87 (quint, $J = 7.3$ Hz, 2H). ^{13}C NMR (100 MHz, CDCl_3) δ 168.4, 155.3, 141.6, 132.4, 131.2, 130.5, 130.4, 130.1, 128.0, 124.3, 115.8, 67.7, 39.1, 38.7, 34.4, 30.9. HRMS calc'd for $\text{C}_{18}\text{H}_{20}\text{Cl}_2\text{N}_2\text{O}_4\text{S}$, 431.06004 $[\text{M}+\text{H}]^+$; found, 431.05898 $[\text{M}+\text{H}]^+$. HPLC (a) 99.7% (b) 98.6%

N-(2-(3,4-dichlorophenoxy)ethyl)-2-(4-(methylsulfonamido)phenoxy)acetamide (96-34).



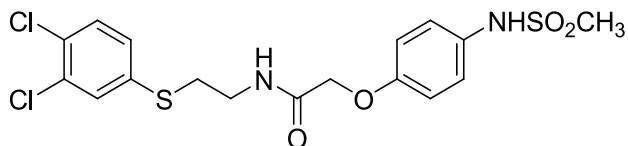
Compound **96-32** was obtained using carboxylic acid **35** and amine **53**. The crude material was purified using silica gel chromatography (2 EtOAc/1 Hexanes) to give a white foam (0.366 g, 41%). ^1H NMR (300 MHz, CDCl_3) δ 7.32 (s, 1H), 7.23 (d, $J = 9.0$ Hz, 2H), 7.05 (bt, $J = 5.7$ Hz, 1H), 6.96 (d, $J = 2.8$ Hz, 1H), 6.89 (d, $J = 9.0$ Hz, 2H), 6.73 (dd, $J_1 = 9.0$ Hz, $J_2 = 2.8$ Hz, 1H), 4.50 (s, 2H), 4.04 (t, $J = 5.3$ Hz, 2H), 3.76 (q, $J = 5.3$ Hz, 2H), 2.94 (s, 3H). ^{13}C NMR (75 MHz, CDCl_3) δ 168.6, 157.5, 155.2, 133.0, 131.1, 130.9, 124.6, 124.2, 116.6, 115.8, 114.5, 67.7, 67.2, 39.1, 38.6. HRMS calc'd for $\text{C}_{17}\text{H}_{18}\text{Cl}_2\text{N}_2\text{O}_5\text{S}$, 433.03924 $[\text{M}+\text{H}]^+$; found, 433.03824 $[\text{M}+\text{H}]^+$. Anal. ($\text{C}_{18}\text{H}_{18}\text{Cl}_2\text{N}_2\text{O}_4\text{S}$) C, H, N.

N-(4-(2-(4-(3,4-difluorophenyl)piperazin-1-yl)-2-oxoethoxy)phenyl)methanesulfonamide (96-35).



Compound **96-35** was obtained using carboxylic acid **35** and amine **81**. The crude material was purified using silica gel chromatography (2 EtOAc/1 Hexanes) to give a white foam (0.366 g, 41%). ^1H NMR (400 MHz, CDCl_3) δ 7.21 (d, J = 8.9 Hz, 2H), 7.07 (quart, J = 9.1 Hz, 1H) 6.96 (d, J = 8.9 Hz, 2H), 6.79-6.68 (qd J_1 = 7.0, J_2 = 2.9 Hz, 1H), 6.76-6.72 (mult, 1H), 6.38 (bs, 1H), 4.74 (s, 2H), 3.78 (bs, 2H), 3.31 (t, J = 1.3 Hz, 2H), 3.17 (t, J = 5.1 Hz, 2H), 3.13 (t, J = 5.1 Hz, 2H) 2.88 (s, 3H). ^{13}C NMR (100 MHz, CDCl_3) d 171.6, 152.3 (dd, J_1 = 248 Hz, J_2 = 14.1 Hz), 148.9 (d, J = 5.4 Hz), 145.2 (dd, J_1 = 248 Hz, J_2 = 14.1 Hz), 138.6, 137.5, 129.9, 121.8, 116.6 (d, J = 18.8 Hz), 113.1 (d, J = 5.4 Hz), 107.7 (d, J = 21.0 Hz), 64.8, 50.1, 49.6, 46.7, 41.9, 31.0. HRMS calc'd for $\text{C}_{19}\text{H}_{21}\text{F}_2\text{N}_3\text{O}_4\text{S}$, 425.12208 $[\text{M}]^+$; found, 425.13174 $[\text{M}]^+$.

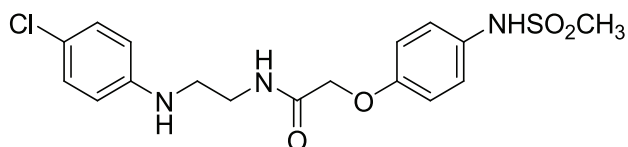
N-(2-(3,4-dichlorophenylthio)ethyl)-2-(4-(methanesulfonamido)phenoxy)acetamide (96-37).



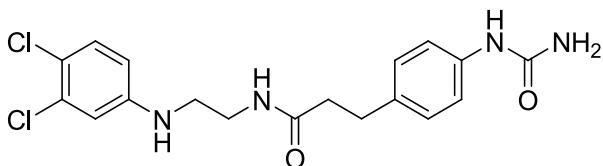
Compound **96-37** was obtained using carboxylic acid **34** and amine **79**. The crude material was purified using silica gel chromatography (3 EtOAc/1 Hexanes) to give a

white foam (0.389 g, 69%). ^1H NMR (600 MHz, CDCl_3) δ 7.44 (d, $J = 2.4$ Hz, 1H), 7.32 (d, $J = 8.6$ Hz, 1H), 7.29 (bs, 1H), 7.24 (d, $J = 8.6$ Hz, 2H), 7.19 (dd, $J_1 = 8.3$ Hz, $J_2 = 2.4$ Hz, 1H), 6.98 (bt, $J = 5.7$ Hz, 1H), 6.88 (d, $J = 9.0$ Hz), 4.45 (s, 2H), 3.58 (quart, $J = 6.4$ Hz, 2H), 3.10 (t, $J = 6.4$ Hz, 2H), 2.96 (s, 3H). ^{13}C NMR (150 MHz, CDCl_3) δ 168.6, 155.3, 135.6, 133.2, 131.2, 131.0, 130.9, 130.8, 128.8, 124.4, 115.9, 67.7, 39.2, 39.1, 38.5, 33.3. HRMS calc'd for $\text{C}_{17}\text{H}_{18}\text{Cl}_2\text{N}_2\text{O}_4\text{S}_2$, 449.01644 $[\text{M}+\text{H}]^+$; found, 449.01536 $[\text{M}+\text{H}]^+$. Anal. ($\text{C}_{17}\text{H}_{18}\text{Cl}_2\text{N}_2\text{O}_4\text{S}_2$) C, H, N.

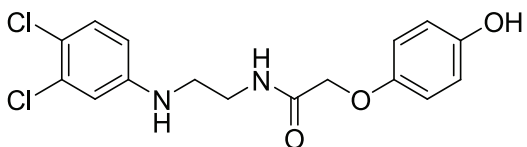
N-(2-(4-chlorophenylamino)ethyl)-2-(4-(methylsulfonamido)phenoxy)acetamide (96-38).



Compound **96-38** was obtained using carboxylic acid **35** and amine **48**. The crude material was purified using silica gel chromatography (ISCO, RediSep 12 g column, 100% EtOAc) to give an off-white solid (0.484 g, 59.7%) ^1H NMR (400 MHz, d_6 -acetone) δ 7.69 (bs, 1H), 7.29 (d, $J = 9.2$ Hz, 2H), 7.08 (d, $J = 8.9$ Hz, 2H), 6.97 (d, $J = 9.2$ Hz, 2H), 6.64 (d, $J = 8.9$ Hz, 2H), 4.52 (s, 2H), 3.78 (s, 2H, N-H), 3.50 (q, $J = 6.0$ Hz, 2H), 3.26 (t, $J = 6.4$ Hz, 2H), 2.9 (s, 3H). ^{13}C NMR (400 MHz, d_6 -acetone) 169.2, 156.3, 148.5, 147.0, 132.9, 129.6, 124.4, 116.4, 114.4, 68.5, 44.0, 38.9. HRMS calc'd for $\text{C}_{17}\text{H}_{20}\text{ClN}_3\text{O}_4\text{S}$, 398.09424 $[\text{M}+\text{H}]^+$; found, 398.09285 $[\text{M}+\text{H}]^+$.

N-(2-(3,4-dichlorophenylamino)ethyl)-3-(4-ureidophenyl)propanamide (96-39).

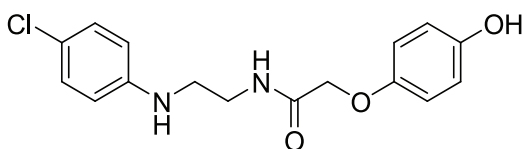
Compound **96-39** was obtained from carboxylic acid **39** and amine **45**. The crude material was recrystallized with methanol to give an off-white solid which was collected by filtration (0.106 g, 25%). ^1H NMR (400 MHz, d_6 -acetone) 7.37 (d, $J = 8.6$ Hz, 2H), 7.26 (bs, 1H), 7.20 (d, $J = 8.6$ Hz, 1H), 7.06 (d, $J = 8.6$ Hz, 2H), 6.76 (d, $J = 2.5$ Hz, 1H), 6.58 (dd, $J_1 = 8.6$ Hz, $J_2 = 2.5$ Hz, 1H), 5.38 (bs, 1H), 3.35 (t, $J = 6.2$ Hz, 2H), 3.27 (t, $J = 6.2$ Hz, 2H), 2.82 (t, $J = 7.3$ Hz, 2H), 2.41 (t, $J = 7.3$ Hz, 2H). HRMS calc'd for $\text{C}_{18}\text{H}_{20}\text{Cl}_2\text{N}_4\text{O}_2$, 395.10427 $[\text{M}+\text{H}]^+$; found 395.10345 $[\text{M}+\text{H}]^+$.

N-(2-(3,4-dichlorophenylamino)ethyl)-2-(4-hydroxyphenoxy)acetamide (96-40).

Compound **96-40** was obtained from carboxylic acid **82** and amine **45**. The crude material was purified using silica gel chromatography (ISCO, 40 g RediSep column, 3 EtOAc/1 Hexanes) to give a white foam. Trituration with DCM and collected via filtration yielded a white powder (0.561 g, 53%). ^1H NMR (400 MHz, CDCl_3) δ 7.13 (d, $J = 8.6$ Hz, 1H), 7.03 (bt, $J = 5.7$ Hz, 1H), 6.78 (d, $J = 8.9$ Hz, 2H), 6.72 (d, $J = 8.9$ Hz, 2H), 6.61 (d, $J = 2.9$ Hz, 1H), 6.39 (dd, $J_1 = 8.6$ Hz, $J_2 = 2.9$ Hz, 1H), 4.42 (s, 2H), 3.59-3.55 (mult, 2H), 3.24 (t, $J = 5.7$ Hz, 2H). ^{13}C NMR (100 MHz, CDCl_3) δ 170.5, 151.6, 150.9, 147.5, 132.9, 130.8,

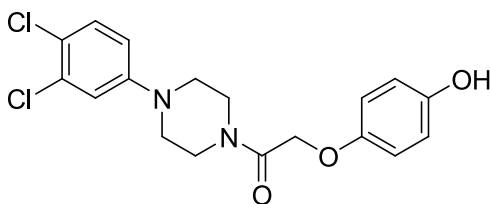
120.1, 116.5, 116.0, 113.8, 112.6, 68.2, 44.0, 38.7. HRMS calc'd for $C_{16}H_{16}Cl_2N_2O_3$, 355.06174 $[M+H]^+$; found, 355.06094 $[M+H]^+$. Anal ($C_{16}H_{16}Cl_2N_2O_3$) C, H, N.

N-(2-(4-chlorophenylamino)ethyl)-2-(4-hydroxyphenoxy)acetamide (96-42).



Compound **96-42** was obtained from carboxylic acid **82** and amine **48**. The crude material was purified using recrystallization with DCM, MeOH, and hexanes to give an off-white powder which was obtained by filtration (0.469 g, 49%). 1H NMR (600 MHz, d_6 -DMSO) δ 9.00 (s, 1H), 8.14 (bt, $J = 5.2$ Hz, 1H), 7.08 (d, $J = 8.6$ Hz, 2H), 6.80 (d, $J = 9.1$ Hz, 2H), 6.68 (d, $J = 8.6$ Hz, 2H), 6.58 (d, $J = 8.6$ Hz, 2H), 5.88 (bt, $J = 5.2$ Hz, 1H), 4.35 (s, 2H), 3.31-3.27 (mult, 2H), 3.10-3.01 (mult, 2H). ^{13}C NMR (150 MHz, d_6 -DMSO) δ 168.3, 151.8, 150.5, 147.6, 128.6, 118.9, 115.9, 115.7, 113.2, 68.0, 42.3, 37.6. HRMS calc'd for $C_{16}H_{17}ClN_2O_3$, 321.10071 $[M+H]^+$; found, 321.10001 $[M+H]^+$. Anal. ($C_{16}H_{17}ClN_2O_3$) C, H, N.

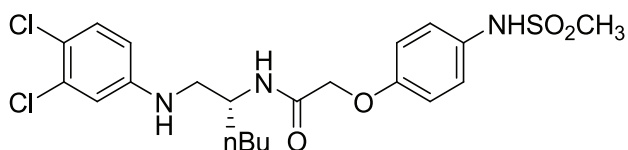
1-(4-(3,4-Dichlorophenyl)piperazin-1-yl)-2-(4-hydroxyphenoxy)ethanone (96-43).



Compound **96-43** was obtained from carboxylic acid **83** and amine **82**. The crude material was purified using recrystallization with DCM, MeOH, and hexanes to give an off-white powder which was obtained by filtration (0.696 g, 62%). 1H NMR (400 MHz, d_6 -

DMSO) δ 8.99 (bs, 1H), 7.34 (d, J = 8.9 Hz, 2H), 7.15 (d, J = 2.9 Hz, 1H), 6.93 (dd, J_1 =8.9 Hz, J_2 = 2.9 Hz, 1H), 6.78 (d, J = 8.9 Hz, 2H), 6.68 (d, J = 8.9 Hz, 2H), 4.72 (s, 2H), 3.58 (mult, 4H), 3.24-3.17 (mult, 4H). ^{13}C NMR (100 MHz, d_6 -DMSO) δ 166.4, 151.6, 150.8, 150.4, 131.6, 130.5, 120.0, 116.6, 115.6, 115.6, 66.9, 47.8, 47.4, 43.8, 40.8. HRMS calc'd for $\text{C}_{18}\text{H}_{18}\text{Cl}_2\text{N}_2\text{O}_3$, 381.07739 $[\text{M}+\text{H}]^+$; found, 381.07663 $[\text{M}+\text{H}]^+$. Anal. ($\text{C}_{18}\text{H}_{18}\text{Cl}_2\text{N}_2\text{O}_3$) C, H, N.

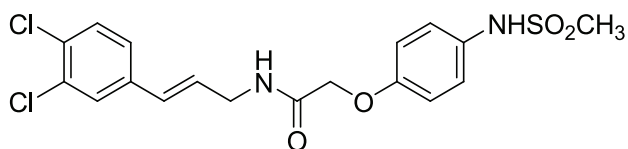
(R)-N-(1-(3,4-dichlorophenylamino)hexan-2-yl)-2-(4-(methylsulfonamido)phenoxy)acetamide (96-47).



Compound **96-47** was obtained from carboxylic acid **35** and amine **71**. The crude material was purified using silica gel chromatography (ISCO, RediSep 40 g column, 2 EtOAc/1 Hexanes) to give a white foam (0.402 g, 72%). ^1H NMR (300 MHz, CDCl_3) δ 7.20 (d, J = 9.0 Hz, 2H), 7.12 (d, J = 9.0 Hz, 2H), 6.86 (d, J = 9.0 Hz, 2H), 6.64 (d, J = 2.6 Hz, 1H), 6.46 (bs, 1H), 6.42 (dd, J_1 = 9.0 Hz, J_2 = 2.6 Hz, 1H), 4.47 (d, J = 5.5 Hz, 2H), 4.39-4.32 (mult, 1H), 4.21-4.12 (mult, 1H), 3.28-3.21 (mult, 1H), 3.11-3.09 (mult, 1H), 2.94 (s, 3H), 1.68-1.31 (mult, 6H), 0.89 (t, J = 6.9 Hz, 3H). ^{13}C NMR (75 MHz, CDCl_3) δ 169.2, 155.2, 147.8, 132.9, 131.1, 130.7, 124.3, 119.7, 115.9, 113.6, 112.6, 67.8, 49.5, 49.2, 39.2, 32.6, 28.3, 22.6, 14.1. HRMS calc'd for $\text{C}_{21}\text{H}_{27}\text{Cl}_2\text{N}_3\text{O}_4\text{S}$, 488.11787 $[\text{M}+\text{H}]^+$; found, 488.11700 $[\text{M}+\text{H}]^+$. Anal ($\text{C}_{21}\text{H}_{27}\text{Cl}_2\text{N}_3\text{O}_4\text{S}$) C, H, N. 98.2% ee based on chiral HPLC with Chiralcel AD-

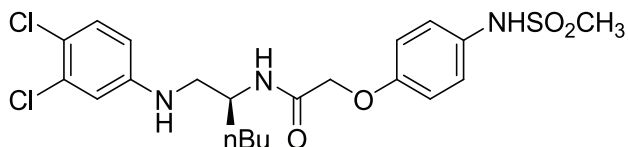
H column (46 mm i.d. x 250 mm), eluent 10%-90% iPrOH/hexane gradient, flow rate, 1.0 mL/min; UV monitoring at 254 nm, retention time 13.8 minutes.

N-(3,4-dichlorocinnamyl)-2-(4-(methylsulfonamido)phenoxy)acetamide (96-50).



Compound **96-50** was obtained using carboxylic acid **35** and amine **62**. The crude material was purified using silica gel chromatography (2 EtOAc/1 Hexanes) to give a white solid (0.247, 71%). ^1H NMR (300 MHz, d_6 -DMSO) δ 9.43 (s, 1H), 8.40 (bt, $J = 5.7$ Hz, 1H), 7.68 (d, $J = 1.9$ Hz, 1H), 7.56 (d, $J = 8.2$ Hz, 1H), 7.39 (dd, $J_1 = 8.2$ Hz, $J_2 = 1.9$ Hz, 1H), 7.17 (d, $J = 9.0$ Hz, 2H), 8.96 (d, $J = 9.0$ Hz, 2H), 6.41-6.39 (mult, 2H), 4.52 (s, 2H), 3.94-3.92 (mult, 2H), 2.89 (s, 3H). ^{13}C NMR (75 MHz, d_6 -DMSO) δ 167.6, 154.9, 137.5, 131.5, 131.4, 130.4, 129.7, 129.5, 127.9, 127.4, 126.2, 123.0, 115.4, 67.2, 39.0. HRMS calc'd for $\text{C}_{18}\text{H}_{18}\text{Cl}_2\text{N}_2\text{O}_4\text{S}$, 427.02846 $[\text{M}-\text{H}]^+$; found, 427.02960 $[\text{M}-\text{H}]^+$. Anal. ($\text{C}_{18}\text{H}_{18}\text{Cl}_2\text{N}_2\text{O}_4\text{S}$) C, H, N.

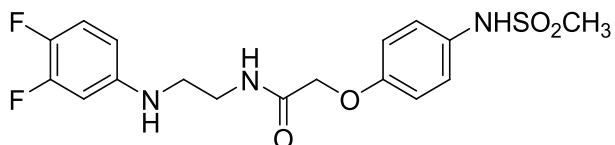
(S)-N-(1-(3,4-dichlorophenylamino)hexan-2-yl)-2-(4-(methylsulfonamido)phenoxy)acetamide (96-51).



Compound **96-51** was obtained from carboxylic acid **35** and amine **72**. The crude material was purified using silica gel chromatography (ISCO, RediSep 40 g column, 2 EtOAc/1 Hexanes) to give a white foam (0.470 g, 79%). 97.5% ee based on chiral HPLC with Chiralcel AD-H column (46 mm i.d. x 250 mm), eluent 10%-90% iPrOH/hexane gradient, flow rate, 1.0 mL/min; UV monitoring at 254 nm, retention time 12.0 minutes. ^1H NMR (400 MHz, CDCl_3) δ 7.28 (s, 1H), 7.20 (d, $J = 9.0$ Hz, 2H), 7.12 (d, $J = 8.9$ Hz, 1H), 6.85 (d, $J = 9.0$ Hz, 2H), 6.64 (d, $J = 2.6$ Hz, 1H), 6.49 (bd, $J = 8.9$ Hz, 1H), 6.42 (dd, $J_1 = 9.0$ Hz, $J_2 = 2.6$ Hz), 4.46 (d, $J = 8.6$ Hz, 2H), 4.35 (bt, $J = 5.1$ Hz, 1H), 4.24-.20 (mult, 1H), 3.25-3.19 (mult, 1H), 3.11-3.05 (mult, 1H), 2.94 (s, 3H), 1.68-1.29 (mult, 6H), 0.89 (t, $J = 6.9$ Hz, 3H). ^{13}C NMR (100 MHz, CDCl_3) δ 169.3, 155.2, 147.8, 132.8, 131.2, 30.7, 124.3, 119.7, 115.9, 113.6, 112.6, 67.7, 49.5, 49.1, 39.1, 32.5, 28.3, 22.6, 14.1. HRMS calc'd for $\text{C}_{21}\text{H}_{27}\text{Cl}_2\text{N}_3\text{O}_4\text{S}$, 488.11787 $[\text{M}+\text{H}]^+$; found, 488.11694 $[\text{M}+\text{H}]^+$. Anal. ($\text{C}_{21}\text{H}_{27}\text{Cl}_2\text{N}_3\text{O}_4\text{S}$) C, H, N.

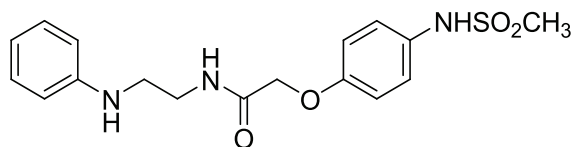
N-(2-(3,4-difluorophenylamino)ethyl)-2-(4-(methylsulfonamido)phenoxy)acetamide

(96-53).



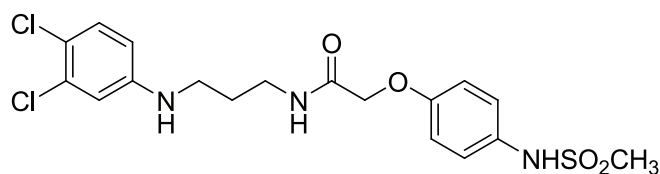
Compound **96-53** was obtained from carboxylic acid **35** and amine **46**. The crude material was purified using silica gel chromatography (ISCO, RediSep 12 g column, 4 EtOAc/1 Hexanes) to give a yellow solid. The title compound was further purified by trituration with DCM. The off-white solid was obtained by filtration and washed with hexanes (0.150, 46%). ^1H NMR (400 MHz, CDCl_3) δ 7.21 (d, J = 8.9 Hz, 2H), 6.95 (quart, J = 8.9 Hz, 1H), 6.90 (d, J = 8.9 Hz, 2H), 6.90-6.86 (bs 1H), 6.59 (bs, 1H), 6.38 (qd, J_1 = 6.7 Hz, J_2 = 2.9 Hz, 1H), 6.29-6.25 (mult, 1H), 4.50 (s, 2H), 4.14-4.07 (bs, 1H), 3.61 (quart, J = 5.7 Hz, 2H), 3.27 (t, J = 5.7 Hz, 2H), 2.97 (s, 3H). ^{13}C NMR (100 MHz, CDCl_3) δ 169.2, 155.5 (dd, J_1 = 246 Hz, J_2 = 13.5 Hz), 149.6 (d, J = 5.4 Hz), 130.9 (dd, J_1 = 246 Hz, J_2 = 13.5 Hz), 124.6, 117.9 (d, J = 19.1 Hz), 115.9, 108.0 (d, J = 5.4 Hz), 101.4 (d, J = 19.2 Hz), 67.8, 44.7, 39.4, 38.8. HRMS calc'd for $\text{C}_{17}\text{H}_{19}\text{F}_2\text{N}_3\text{O}_4\text{S}$, 400.11437 $[\text{M}+\text{H}]^+$; found 400.25332 $[\text{M}+\text{H}]^+$.
 Anal. ($\text{C}_{17}\text{H}_{19}\text{F}_2\text{N}_3\text{O}_4\text{S}$) C: 50.83, H: 4.75, N: 10.39.

2-(4-(methylsulfonamido)phenoxy)-N-(2-(phenylamino)ethyl)acetamide (96-56).



Compound **96-56** was obtained from carboxylic acid **35** and amine **47**. The crude material was purified using silica gel chromatography (ISCO, RediSep 12 g column, 1 EtOAc/1 Hexanes to 100% EtOAc gradient) to give a white foam (0.097 g, 33%). ^1H NMR (600 MHz, CDCl_3) δ 7.18-7.14 (mult, 4H), 6.85 (d, $J = 9.1$ Hz, 2H) 6.82 (bs, 1H), 6.70 (t, $J = 7.6$ Hz, 1H), 6.61 (bs, 1H), 6.59 (d, $J = 7.6$ Hz, 2H), 4.46 (s, 2H), 3.59 (quart, $J = 5.7$ Hz, 2H), 3.31 (t, $J = 5.7$ Hz, 2H), 2.91 (s, 3H). ^{13}C NMR (100 MHz, CD_3OD) δ 171.6, 157.0, 150.0, 133.2, 130.3, 125.0, 118.3, 116.8, 114.0, 68.6, 44.3, 39.8, 38.9. HRMS calc'd for $\text{C}_{17}\text{H}_{21}\text{N}_3\text{O}_4\text{S}$, 364.13324 $[\text{M}+\text{H}]^+$; found, 364.13219 $[\text{M}+\text{H}]^+$. Anal. ($\text{C}_{17}\text{H}_{21}\text{N}_3\text{O}_4\text{S}$) C, H, N.

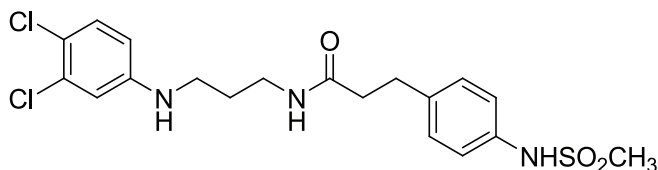
N-(3-(3,4-dichlorophenylamino)propyl)-2-(4-(methylsulfonamido)phenoxy)acetamide (96-58).



Compound **96-58** was obtained using carboxylic acid **35** and amine **50**. The crude material was purified using silica gel chromatography (2 EtOAc/1 Hexanes to 100% EtOAc gradient) to give a white foam. Trituration with MeOH give a white solid which was obtained by filtration (0.177 g, 64%). ^1H NMR (600 MHz, CD_3OD) δ 7.22 (d, $J = 9.1$ Hz, 2H), 7.14 (d, $J = 9.1$ Hz, 1H), 6.97 (d, $J = 9.1$ Hz, 2H), 6.68 (d, $J = 2.9$ Hz, 1H), 6.48 (dd,

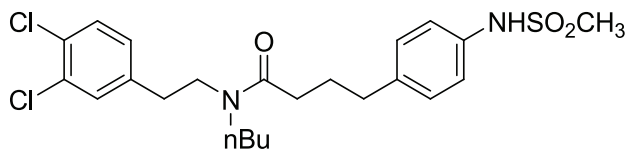
$J_1 = 9.1$ Hz, $J_2 = 2.9$ Hz, 1H), 4.50 (s, 2H), 3.38 (mult, 2H), 3.05 (t, $J = 6.7$ Hz, 2H), 2.87 (s, 3H), 1.81 (quint, $J = 6.7$ Hz, 2H). ^{13}C NMR (150 MHz, CD_3OD) δ 171.3, 156.9, 150.3, 133.6, 133.3C, 125.0, 119.4, 116.8, 114.5, 113.7, 68.6, 42.0, 38.9, 38.0, 29.8. HRMS calc'd for $\text{C}_{18}\text{H}_{21}\text{Cl}_2\text{N}_3\text{O}_4\text{S}$, 446.07094 $[\text{M}+\text{H}]^+$; found, 446.07031 $[\text{M}+\text{H}]^+$. Anal ($\text{C}_{18}\text{H}_{21}\text{Cl}_2\text{N}_3\text{O}_4\text{S}$) C: 47.79, H: 4.89, N: 9.19.

N-(3-(3,4-dichlorophenylamino)propyl)-3-(4-(methylsulfonamido)phenyl)propanamide (96-59).



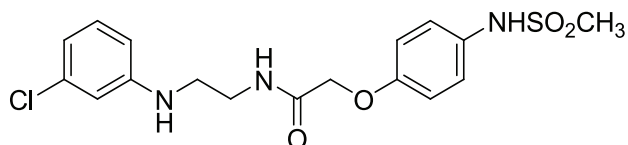
Compound **96-59** was obtained using carboxylic acid **36** and amine **50**. The crude material was purified using silica gel chromatography (2 EtOAc/1 Hexanes to 100% EtOAc gradient) to give a white foam which solidified *in vacuo* (0.182 g, 40%). ^1H NMR (300 MHz, CD_3OD) δ 7.99 (bs, 1H), 7.21-7.14 (mult, 5H), 6.68 (d, $J = 2.6$ Hz, 1H), 6.48 (dd, $J_1 = 8.8$ Hz, $J_2 = 2.6$ Hz, 1H), 3.23-3.19 (mult, 2H), 2.95 (t, $J = 6.7$ Hz, 2H), 2.89 (s, 3H), 2.93-2.86 (mult, 2H), 2.47 (t, $J = 7.6$ Hz, 2H), 1.68 (quint, $J = 6.7$ Hz, 2H). ^{13}C NMR (150 MHz, CD_3OD) δ 174.0, 148.9, 137.5, 136.4, 132.3, 130.4, 129.2, 120.9, 118.0, 113.1, 112.3, 40.5, 37.8, 37.6, 36.7, 31.0, 28.5. HRMS calc'd for $\text{C}_{19}\text{H}_{23}\text{Cl}_2\text{N}_3\text{O}_3\text{S}$, 444.09164 $[\text{M}+\text{H}]^+$; found, 444.09059 $[\text{M}+\text{H}]^+$. Anal ($\text{C}_{19}\text{H}_{23}\text{Cl}_2\text{N}_3\text{O}_3\text{S}$) C: 50.89, H: 5.20, N: 9.19.

N-butyl-N-(3,4-dichlorophenethyl)-4-(4-(methylsulfonamido)phenyl)butanamide (96-62).



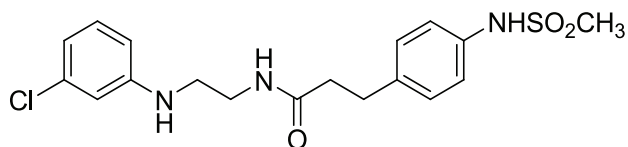
Compound **96-62** was obtained using carboxylic acid **37** and amine **75**. The crude material was purified using silica gel chromatography (ISCO, RediSep 80 g column, 50% EtOAc/50% Hexanes to 100% EtOAc gradient) to give a colorless oil, which foamed slightly upon trituration with DCM and hexanes (0.596, 63%). ^1H NMR (400 MHz, CDCl_3) δ 7.74 (bs, 1H), 7.29 (d, $J = 8.3$ Hz, 1H), 7.27 (d, $J = 1.9$ Hz, 1H), 7.18 (d, $J = 8.3$ Hz, 2H), 7.09 (d, $J = 8.3$ Hz, 2H), 7.04 (dd, $J_1 = 8.3$ Hz, $J_2 = 1.9$ Hz, 1H), 3.50 (t, $J = 7.3$ Hz, 2H), 3.07 (t, $J = 7.3$ Hz, 2H), 2.94 (s, 3H), 2.78 (t, $J = 7.3$ Hz, 2H), 2.60 (t, $J = 7.3$ Hz, 2H), 2.31 (t, $J = 7.3$ Hz, 2H), 1.92 (t, $J = 7.3$ Hz, 2H) 1.51-1.40 (mult, 2H), 1.31-1.21 (mult, 2H), 0.91- 0.86 (mult, 3H). ^{13}C NMR (100 MHz, CDCl_3) δ 172.7, 139.8, 139.0, 135.2, 132.3, 130.9, 130.7, 130.5, 129.6, 128.5, 121.5, 48.5, 47.4, 39.1, 34.8, 33.3, 32.4, 31.3, 27.0, 20.2, 13.9. HRMS calc'd for $\text{C}_{23}\text{H}_{30}\text{Cl}_2\text{N}_2\text{O}_3\text{S}$, 485.14336 $[\text{M}+\text{H}]^+$; found, 485.14240 $[\text{M}+\text{H}]^+$.

N-(2-(3-chlorophenylamino)ethyl)-2-(4-(methylsulfonamido)phenoxy)acetamide (96-63).



Compound **96-63** was obtained using carboxylic acid **35** and amine **49**. The crude material was purified using silica gel chromatography (ISCO, RediSep 40 g column, 2 EtOAc/1 Hexanes to 100% EtOAc gradient) to give a white foam which solidified under high vacuum (0.778 g 69%). ^1H NMR (400 MHz, d_6 -DMSO) δ 9.45 (s, 1H), 8.22 (bt, $J = 5.7$ Hz, 1H), 7.18 (d, $J = 8.9$ Hz, 2H), 7.07 (t, $J = 8.3$ Hz, 1H), 6.97 (d, $J = 8.9$ Hz, 2H), 6.62 (s, 1H), 6.56-6.52 (mult, 2H), 6.06 (bt, $J = 5.4$ Hz, 1H), 4.47 (s, 2H), 3.33-3.28 (mult, 2H), 3.15-3.10 (mult, 2H), 2.90 (s, 3H). ^{13}C NMR (100 MHz, d_6 -DMSO) δ 168.0, 154.9, 150.1, 133.8, 131.6, 130.4, 123.1, 115.5, 115.1, 110.9, 110.7, 67.3, 42.0, 38.7, 37.6. HRMS calc'd for $\text{C}_{17}\text{H}_{20}\text{ClN}_3\text{O}_4\text{S}$, 398.09424 $[\text{M}+\text{H}]^+$; found, 398.09342 $[\text{M}+\text{H}]^+$. Anal. ($\text{C}_{17}\text{H}_{20}\text{ClN}_3\text{O}_4\text{S}$) C, H, N.

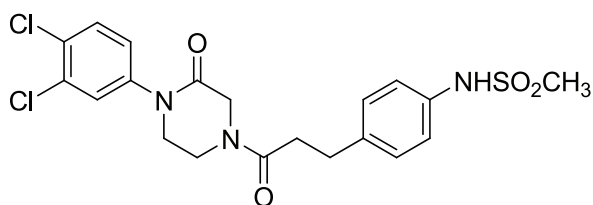
N-(2-(3-chlorophenylamino)ethyl)-3-(4-(methylsulfonamido)phenyl)propanamide (96-64).



Compound **96-64** was obtained using carboxylic acid **36** and amine **49**. The crude material was purified using silica gel chromatography (ISCO, RediSep 40 g column, 2

EtOAc/1 Hexanes to 100% EtOAc gradient) to give a white foam (0.778 g 68%). ^1H NMR (400 MHz, CDCl_3) δ 7.15 (d, J = 8.6 Hz, 2H), 7.09 (d, J = 8.6 Hz, 2H), 7.06 (t, J = 8.3 Hz, 1H), 6.96 (bs, 1H), 6.65 (dd, J_1 = 7.9 Hz, J_2 = 1.6 Hz, 1H), 6.52 (t, J = 2.2 Hz, 1H), 6.44 (dd, J_1 = 7.9 Hz, J_2 = 2.22 Hz, 1H), 5.88 (bt, J = 6.0 Hz, 1H), 4.23 (bs, 1H), 3.47-3.42 (mult, 2H), 3.15 (t, J = 6.0 Hz, 2H), 2.95 (s, 3H), 2.93 (t, J = 7.4 Hz, 2H), 2.46 (t, J = 7.4 Hz, 2H). ^{13}C NMR (100 MHz, CDCl_3) δ 173.3, 149.4, 138.3, 135.2, 135.1, 130.5, 129.8, 121.7, 117.5, 112.3, 111.3, 44.3, 39.5, 39.1, 38.4, 31.1. HRMS calc'd for $\text{C}_{18}\text{H}_{22}\text{ClN}_3\text{O}_3\text{S}$, 396.11494 $[\text{M}+\text{H}]^+$; found, 396.11418 $[\text{M}+\text{H}]^+$. Anal. ($\text{C}_{18}\text{H}_{22}\text{ClN}_3\text{O}_3\text{S}$) C, H, N.

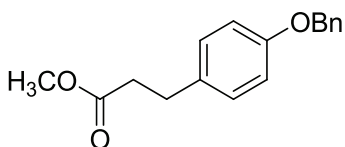
N-(4-(3-(4-(3,4-dichlorophenyl)-3-oxopiperazin-1-yl)-3-oxopropyl)phenyl)methanesulfonamide (96-68).



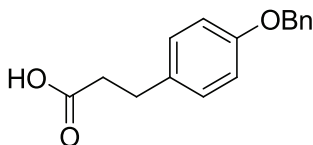
Compound **96-68** was obtained using carboxylic acid **36** and amine **78**. The crude material was purified using silica gel chromatography (ISCO, RediSep 12 g column, 1 EtOAc/1 Hexanes to 100% EtOAc gradient) to give a white foam (0.152 g, 69%). ^1H NMR (300 MHz, CDCl_3) δ 7.48 (d, J = 8.8 Hz, 1H), 7.42 (d, J = 2.3 Hz, 1H), 7.21 (d, J = 8.2 Hz, 2H), 7.16-7.13 (mult, 3H), 6.45 (bs, 1H), 4.18 (s, 2H), 3.96 (t, J = 5.3 Hz, 2H), 3.69 (t, J = 5.3 Hz, 2H), 2.97 (t, J = 5.3 Hz, 2H), 2.93 (s, 3H), 2.66 (t, J = 5.3 Hz, 2H). ^{13}C NMR (150 MHz, CDCl_3) δ 170.9, 164.9, 140.6, 137.9, 135.5, 133.2, 131.5, 131.1, 129.8, 127.7, 125.0,

121.4, 49.6, 46.8, 43.0, 39.3, 35.0, 30.6. HRMS calc'd for $C_{20}H_{21}Cl_2N_3O_4S$, 468.05504 [M-H]⁺; found, 468.05560 [M-H]⁺. Anal. ($C_{20}H_{21}Cl_2N_3O_4S$) C, H, N.

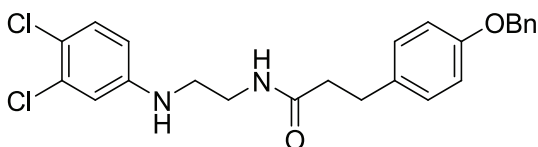
Methyl 3-(4-(benzyloxy)phenyl)propanoate (85).



Ester **84** (5.0 g, 28 mmol) was dissolved in DMF (40.0 mL). To this solution, potassium carbonate (23.0 g, 166 mmol, 6.0 equiv) was added, followed by benzyl bromide (3.6 mL, 31 mmol, 1.1 equiv). The mixture was heated to 120°C and stirred for 12 hours. The mixture was cooled to room temperature and poured into icewater (225 mL). Concentrated HCl (ca. 20 mL) was added to give a pH of 1. The resulting white precipitate was collected by filtration and dried *in vacuo* (7.26 g, 97%). ¹H NMR (400 MHz, CD₃OD) δ 7.41 (d, *J* = 7.0 Hz, 2H), 7.35 (t, *J* = 7.0 Hz, 2H), 7.23 (mult, 1H), 7.12 (d, *J* = 9.0 Hz, 1H), 7.10 (d, *J* = 9.0 Hz, 1H), 6.91-6.86 (mult, 2H), 5.03 (s, 2H), 3.62 (s, 3H), 2.84 (t, *J* = 6.0 Hz, 2H), 2.58 (t, *J* = 7.6 Hz, 1H), 2.40 (t, *J* = 7.6 Hz, 1H). ¹³C NMR (100 MHz, CD₃OD) δ 175.4, 158.9, 139.1, 135.5, 134.4, 130.4, 129.7, 128.9, 128.7, 116.1, 71.1, 52.2, 37.0, 32.3, 31.3.

3-(4-(Benzyloxy)phenyl)propanoic acid (86).

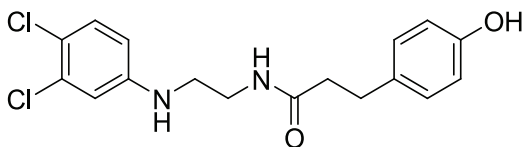
Ester **85** (6.27 g, 23 mmol) was suspended in methanol (60.0 mL). To this suspension, 0.4 N KOH (116 mL, 46 mmol, 2.0 equiv) was added. The mixture was heated to 60°C and stirred for 12 hours. The mixture was cooled to room temperature, and the methanol was removed *in vacuo*. The pH was adjusted to 1 with concentrated HCl. The resultant white precipitate was collected by filtration and washed with hexanes (5.86 g, 99%). ¹H NMR (600 MHz, CD₃OD) δ 7.43 (d, *J* = 7.6 Hz, 2H), 7.35 (t, *J* = 7.6 Hz, 2H), 7.29 (t, *J* = 7.2 Hz, 1H), 7.13 (d, *J* = 8.6 Hz, 2H), 6.88 (d, *J* = 8.6 Hz, 2H), 5.03 (s, 2H), 2.84 (t, *J* = 8.1 Hz, 2H), 2.46 (t, *J* = 8.1 Hz, 2H).

3-(4-(benzyloxy)phenyl)-N-(2-(3,4-dichlorophenylamino)ethyl)propanamide (96-26).

Compound **96-26** was prepared in the manner described for **96-13**. Compound **96-26** was obtained from carboxylic acid **85** and amine **45**. The crude material was suspended in DCM and filtered. The solid was washed with hexanes, ether, and DCM to give a brown solid (0.972 g, 56%). ¹H NMR (600 MHz, CD₃OD) δ 7.40 (d, *J* = 7.1 Hz, 2H), 7.34 (t, *J* = 7.1 Hz, 2H), 7.28 (t, *J* = 7.6 Hz, 1H), 7.15 (d, *J* = 8.6 Hz, 1H), 7.10 (d, *J* = 8.6 Hz, 2H), 6.86 (d, *J* = 8.6 Hz, 2H), 6.69 (d, *J* = 2.4 Hz, 1H), 6.49 (dd, *J*₁ = 8.6 Hz, *J*₂ = 2.4 Hz, 1H), 5.00

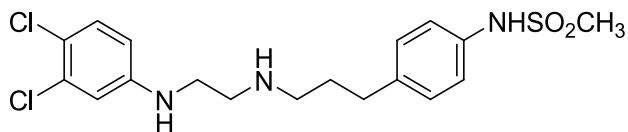
(s, 2H), 3.29 (t, $J = 6.2$ Hz, 2H), 3.06 (t, $J = 6.4$ Hz, 2H), 2.84 (t, $J = 7.6$ Hz, 2H), 2.43 (t, $J = 7.6$ Hz, 2H). ^{13}C NMR (300 MHz, CD_3OD) δ 174.7, 157.5, 149.7, 148.7, 137.6, 133.1, 132.3, 130.4, 129.2, 128.3, 127.6, 127.3, 114.7, 113.1, 112.3, 69.7, 42.8, 38.6, 38.1, 30.9. HRMS calc'd for $\text{C}_{24}\text{H}_{24}\text{Cl}_2\text{N}_2\text{O}_2$, 443.12942 $[\text{M}+\text{H}]^+$; found, 443.12869 $[\text{M}+\text{H}]^+$.

N-(2-(3,4-dichlorophenylamino)ethyl)-3-(4-hydroxyphenyl)propanamide (96-27).



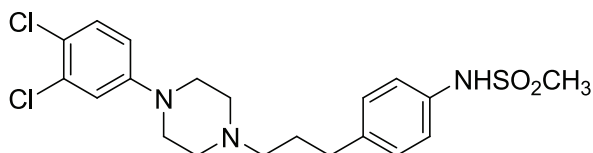
Compound **96-26** (0.150 g, 0.34 mmol) was dissolved in methanol (10.0 mL) in a hydrogenation flask. To this solution, 10% palladium on carbon catalyst (0.034 g, 10 mol%) was added and the mixture was hydrogenolyzed at 40 psi for 12 hours. The mixture was filtered over a pad of celite and the resulting solution was concentrated *in vacuo* to give a brown residue. The crude material was purified using silica gel chromatography (100% EtOAc) to give a brown residue. The material was further purified using silica gel chromatography (2 EtOAc/1 Hexanes) to give a white foam (0.083 g, 69%). ^1H NMR (600 MHz, CDCl_3) δ 7.15 (d, $J = 8.6$ Hz, 1H), 7.02 (d, $J = 8.1$ Hz, 2H), 6.75 (d, $J = 8.6$ Hz, 2H), 6.58 (d, $J = 2.9$ Hz, 1H), 6.36 (dd, $J_1 = 8.8$ Hz, $J_2 = 2.9$ Hz, 1H), 5.7 (t, $J = 6.2$ Hz, 1H), 3.39 (q, $J = 5.7$ Hz, 2H), 3.08 (t, $J = 5.7$ Hz, 2H), 2.88 (t, $J = 7.1$ Hz, 2H), 2.46 (t, $J = 7.1$ Hz, 2H). ^{13}C NMR (600 MHz, CDCl_3) δ 174.0, 154.8, 147.5, 133.0, 132.8, 130.8, 129.7, 119.9, 115.7, 113.7, 112.6, 44.2, 39.0, 38.9, 31.1. HRMS calc'd for $\text{C}_{17}\text{H}_{18}\text{Cl}_2\text{N}_2\text{O}_2$, 353.08247 $[\text{M}+\text{H}]^+$; found, 353.08141 $[\text{M}+\text{H}]^+$. Anal. ($\text{C}_{17}\text{H}_{18}\text{Cl}_2\text{N}_2\text{O}_2$) C, H, N.

N-(4-(3-(2-(3,4-dichlorophenylamino)ethylamino)propyl)phenyl)methanesulfonamide·HCl (96-20).

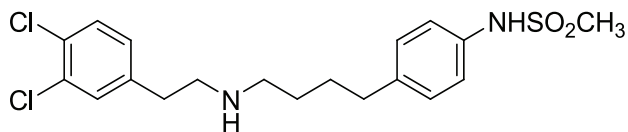


Amide **96-22** (0.500 g, 1.2 mmol) was dissolved in THF (30.0 mL). After cooling to 0°C, a solution of lithium aluminum hydride (2.0 M solution in THF, 2.3 mL, 4.6 mmol, 4.0 equiv) was added dropwise. After stirring for 10 minutes at 0°C, the ice bath was removed and the reaction mixture was warmed to room temperature and stirred for 12 hours. The mixture was diluted with DCM and water to give an emulsion. Rochelle's salt (sat'd) was added and the mixture stirred for 20 minutes before filtering over a pad of celite. The resulting liquid was separated, and the organics were washed with brine, dried over MgSO₄, and concentrated *in vacuo* to give a white foam. The free base was converted to the HCl salt by bubbling HCl (g) through a solution of substrate dissolved in ethanol. The resultant white powder which precipitated was collected by filtration (0.358 g, 74%). ¹H NMR (300 MHz, CDCl₃) δ 7.20-7.11 (mult, 5H), 6.69 (d, *J* = 2.8 Hz, 1H), 6.46 (dd, *J*₁ = 8.8 Hz, *J*₂ = 2.8 Hz, 1H), 4.36 (bs, 1H), 3.16 (mult, 2H), 3.00 (s, 3H), 2.88 (t, *J* = 6.2 Hz, 2H), 2.66 (t, *J* = 7.1 Hz, 4H), 1.86-1.79 (mult, 3H). ¹³C NMR (75 MHz, CDCl₃) δ 148.1, 139.4, 134.8, 132.8, 130.7, 129.7, 121.6, 119.7, 113.9, 112.9, 49.0, 48.2, 43.2, 39.3, 32.9, 31.5. HRMS calc'd for C₁₈H₂₂Cl₂N₃O₂S, 430.07604 [M+H]⁺; found, 430.08143 [M+H]⁺. Anal. (C₁₈H₂₃Cl₂N₃O₂S·0.45 HCl) C, H, N.

N-(4-(3-(4-(3,4-dichlorophenyl)piperazin-1-yl)propyl)phenyl)methanesulfonamide-HCl
(96-21).

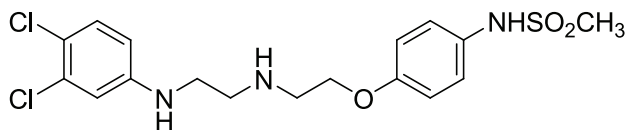


Amide **96-15** (0.250 g, 0.33 mmol) was dissolved in THF (7.0 mL) and cooled to 0°C. To this solution, lithium aluminum hydride (2.0 M solution in diethyl ether, 1.1 ml, 2.2 mmol, 4.0 equiv) was added dropwise. The ice was allowed to melt as the reaction warmed to room temperature and stirred for 3 hours. The reaction mixture was diluted with water and ethyl acetate and filtered over a pad of celite. The layers were separated and the organics were washed with brine, dried over MgSO₄, and concentrated *in vacuo* to give an off-white residue. The crude material was purified using silica gel chromatography (ISCO, RediSep 12 g column 5-10% MeOH/DCM gradient) to give a white oil. The free amine was converted to the HCl salt by bubbling HCl gas (NaCl/Sulfuric Acid method) with sample dissolved in ethanol. The solvent was removed *in vacuo* to give an off-white foam, which was triturated with hexanes to give a white powder (0.33 g, 21%). ¹H NMR (300 MHz, d₆-acetone) 7.34 (d, *J* = 4.7 Hz, 1H), 7.28-7.21 (mult, 4H), 7.06 (d, *J* = 3.1 Hz, 1H), 6.95-6.89 (mult, 1H), 3.23-3.15 (mult, 4H), 2.94 (s, 3H), 2.66 (t, *J* = 7.3 Hz, 2H), 2.53 (t, *J* = 5.2 Hz, 4H), 2.37 (t, *J* = 6.8 Hz, 2H), 1.80 (pentet, *J* = 7.3 Hz, 2H). ¹³C NMR (300 MHz, d₆-acetone) 151.5, 139.0, 136.3, 132.3, 130.6, 129.5, 128.9, 121.0, 116.6, 115.5, 57.5, 53.0, 48.4, 38.6, 32.7, 28.7 (under acetone peak). HRMS calc'd for C₂₀H₂₅Cl₂N₃O₂S, 442.11239 [M+H]⁺; found, 442.11200 [M+H]⁺. Anal. (C₂₀H₂₅Cl₂N₃O₂S·HCl) C: 50.89, H: 5.24, N: 8.38.

N-(4-(4-(3,4-dichlorophenethylamino)butyl)phenyl)methanesulfonamide (96-24).

Amide **96-19** (0.400 g, 0.93 mmol) was dissolved in THF (25.0 mL). To this solution, borane dimethyl sulfide (0.27 mL, 2.8 mmol, 3.0 equiv) was added dropwise at room temperature. The solution was refluxed for 3 hours before cooling to room temperature. The reaction was quenched with 1.0 N HCl. The mixture was extracted with EtOAc (3x). The combined organics were washed with water and brine, dried over MgSO₄, and concentrated *in vacuo* to give a white solid. The crude material was purified using silica gel chromatography (ISCO, RediSep 12 g column, 10% MeOH/DCM) to give a white solid (0.090 g, 23%). ¹H NMR (400 MHz, CD₃OD) δ 7.51-7.48 (mult, 2H), 7.23 (dd, *J*₁=8.3 Hz, *J*₂=1.9 Hz, 1H), 7.21-7.16 (mult, 4H), 3.23-3.19 (mult, 2H), 3.04-2.96 (mult, 4H), 2.92 (s, 3H), 2.65 (mult, 2H), 1.93 (bs, 1H), 1.72-1.70 (mult, 2H). ¹³C NMR (100 MHz, CD₃OD) δ 139.7, 139.0, 137.5, 133.7, 132.2, 132.1, 130.6, 130.0, 122.4, 49.6, 39.1, 35.6, 32.6, 29.5, 27.0. HRMS calc'd for C₁₉H₂₄Cl₂N₂O₂S, 415.10154 [M+H]⁺; found: 415.10148 [M+H]⁺.

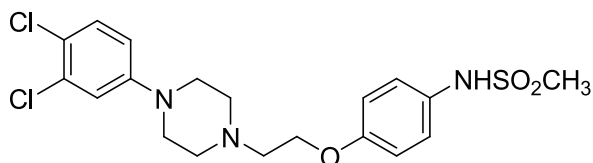
N-(4-(2-(2-(3,4-dichlorophenylamino)ethylamino)ethoxy)phenyl)methanesulfonamide·HCl (96-25).



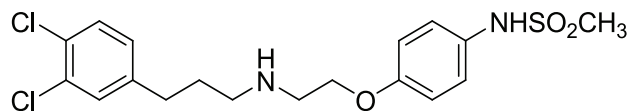
Amide **96-22** (1.01 g, 2.3 mmol) was dissolved in THF (25.0 mL) and cooled to 0°C. To this solution, lithium aluminum hydride (2.0 M solution in diethyl ether, 4.7 mL, 9.3 mmol, 4.0 equiv) was added dropwise. The mixture was warmed to room temperature and stirred for 12 hours. The reaction mixture was diluted with water and ethyl acetate and then filtered over a pad of celite. The layers were separated and the organics were washed with brine, dried over MgSO₄, and concentrated *in vacuo* to give a yellow oil. The crude material was purified using silica gel chromatography (2%-10% MeOH/DCM gradient) to give a white oil. The free amine was converted to the HCl salt by bubbling HCl gas (NaCl/sulfuric acid method) with sample dissolved in ethanol. The resultant white powder was obtained by filtration and washed with cold ethanol (0.350 g, 34%).

¹H NMR (300 MHz, CDCl₃) δ 7.16 (dd, *J*₁ = 8.9 Hz, *J*₂ = 2.4 Hz, 3H), 6.81 (d, *J* = 8.8 Hz, 2H), 6.68 (d, *J* = 2.8 Hz, 1H), 6.46 (dd, *J*₁ = 8.6 Hz, *J*₂ = 2.6 Hz, 1H), 4.06 (t, *J* = 5.0 Hz, 2H), 3.23 (t, *J* = 5.2 Hz, 2H), 3.05 (t, *J* = 5.0 Hz, 2H), 2.98 (t, *J* = 5.2 Hz, 2H), 2.93 (s, 3H). ¹³C NMR (300 MHz, CDCl₃) δ 157.1, 147.9, 132.9, 130.7, 129.7, 124.8, 119.8, 115.5, 113.9, 112.9, 67.2, 48.3, 48.0, 43.1, 39.1. HRMS calc'd for C₁₇H₂₁Cl₂N₃O₃S, 418.07601 [M+H]⁺; found, 418.07543 [M+H]⁺. Anal. (C₁₇H₂₁Cl₂N₃O₃S·1.0 HCl) C, H, N.

N-(4-(2-(4-(3,4-dichlorophenyl)piperazin-1-yl)ethoxy)phenyl)methanesulfonamide (96-31).



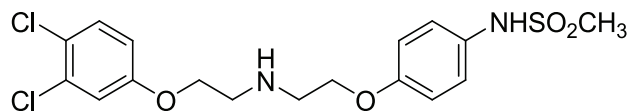
Amide **96-30** (0.250 g, 0.51 mmol) was dissolved in THF (10.0 mL) and cooled to 0°C. To this solution, lithium aluminum hydride (2.0 M solution in diethyl ether, 1.0 mL, 2.0 mmol, 4.0 equiv) was added dropwise. The mixture was warmed to room temperature and stirred for 12 hours. The reaction mixture was diluted with water and ethyl acetate and then filtered over a pad of celite. The layers were separated and the organics were washed with brine, dried over MgSO₄, and concentrated *in vacuo* to give a white foam. The crude material was purified using silica gel chromatography (5-10% MeOH/DCM gradient) to give a white foam (0.180 g, 79%). ¹H NMR (400 MHz, CDCl₃) δ 7.28 (d, *J* = 9.0 Hz, 1H), 7.22 (d, *J* = 9.0 Hz, 2H), 6.96 (d, *J* = 2.9 Hz, 1H), 6.91 (d, *J* = 9.0 Hz, 2H), 6.75 (dd, *J*₁ = 9.0 Hz, *J*₂ = 2.9 Hz, 1H), 4.14 (t, *J* = 5.7 Hz, 2H), 3.21 (t, *J* = 5.1 Hz, 4H), 2.96 (s, 3H), 2.89 (t, *J* = 5.7 Hz, 2H), 2.71 (t, *J* = 5.1 Hz, 4H). ¹³C NMR (100 MHz, CDCl₃) δ 157.2, 150.7, 132.9, 130.6, 129.6, 129.1, 124.8, 122.2, 117.4, 115.6, 66.3, 57.2, 53.4, 48.7, 39.0. HRMS calc'd for C₁₉H₂₃Cl₂N₃O₃S, 444.09166 [M+H]⁺; found, 444.07237 [M+H]⁺. Anal. (C₁₉H₂₃Cl₂N₃O₃S) C, H, N.

N-(4-(2-(3-(3,4-dichlorophenyl)propylamino)ethoxy)phenyl)methanesulfonamide·HCl**(96-33).**

Amide **96-32** (0.111 g, 0.26 mmol) was dissolved in THF (5.0 mL) and cooled to 0°C. To this solution, lithium aluminum hydride (2.0 M solution in diethyl ether, 0.39 mL, 0.77 mmol, 3.0 equiv) was added dropwise. The mixture was warmed to room temperature and stirred for 12 hours. The reaction mixture was diluted with water and ethyl acetate and then filtered over a pad of celite. The layers were separated and the organics were washed with brine, dried over MgSO₄, and concentrated *in vacuo* to give a white foam. The free amine was converted to the HCl salt by bubbling HCl gas (NaCl/sulfuric acid method) with sample dissolved in ethanol. The addition of hexane and ether with cooling gave an off-white precipitate which was obtained by filtration (0.050 g, 42%). ¹H NMR (600 MHz, CD₃OD) δ 7.46-7.45 (mult, 1H), 7.39 (t, *J* = 8.6 Hz, 1H), 7.25 (d, *J* = 9.1 Hz, 3H), 7.20 (dd, *J*₁ = 8.6 Hz, *J*₂ = 2.6 Hz, 1H), 6.99 (d, *J* = 9.1 Hz, 2H), 4.26 (t, *J* = 5.2 Hz, 2H), 3.46 (t, *J* = 7.8 Hz, 2H), 3.11 (t, *J* = 8.1, 2H), 2.89 (s, 3H), 2.74 (t, *J* = 8.0 Hz, 2H), 2.06-2.03 (mult, 2H). ¹³C NMR (600 MHz, CD₃OD) δ 157.1, 133.3, 131.9, 131.7, 131.2, 129.9, 129.6, 125.1, 116.6, 64.9, 48.6, 48.2, 39.0, 32.7, 28.6. HRMS calc'd for C₁₈H₂₂Cl₂N₂O₃S, 417.08076 [M+H]⁺; found, 417.07971 [M+H]⁺.

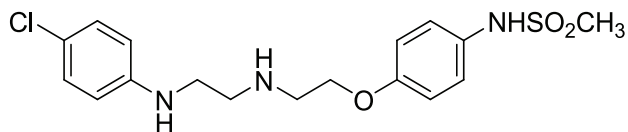
N-(4-(2-(2-(3,4-dichlorophenoxy)ethylamino)ethoxy)phenyl)methanesulfonamide·HCl

(96-36).



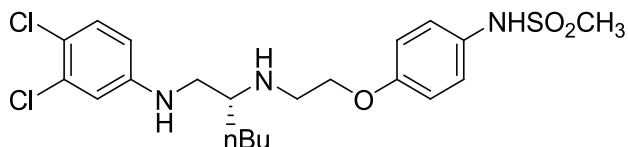
Amide **96-34** (1.01 g, 2.3 mmol) was dissolved in THF (25.0 mL) and cooled to 0°C. To this solution, lithium aluminum hydride (2.0 M solution in diethyl ether, 4.7 mL, 9.3 mmol, 4.0 equiv) was added dropwise. The mixture was warmed to room temperature and stirred for 12 hours. The reaction mixture was diluted with water and ethyl acetate and then filtered over a pad of celite. The layers were separated and the organics were washed with brine, dried over MgSO₄, and concentrated *in vacuo* to give a yellow oil. The crude material was purified using silica gel chromatography (2%-10% MeOH/DCM gradient) to give a white oil. The free amine was converted to the HCl salt by bubbling HCl gas (NaCl/sulfuric acid method) with sample dissolved in ethanol. The resultant white powder was obtained by filtration (0.352 g, 34%). ¹H NMR (300 MHz, CDCl₃) δ 7.16 (dd, *J*₁ = 8.9 Hz, *J*₂ = 2.4 Hz, 3H), 6.81 (d, *J* = 8.9 Hz, 2H), 6.68 (d, *J* = 2.7 Hz, 1H), 6.46 (dd, *J*₁ = 8.6 Hz, *J*₂ = 2.7 Hz, 1H), 4.06 (t, *J* = 5.0 Hz, 2H), 3.23 (t, *J* = 5.2 Hz, 2H), 3.05 (t, *J* = 5.0 Hz, 2H), 2.98 (t, *J* = 5.2 Hz, 2H), 2.93 (s, 3H). ¹³C NMR (300 MHz, CDCl₃) δ 157.1, 147.9, 132.9, 130.7, 129.7, 124.8, 119.8, 115.5, 113.9, 112.9, 67.2, 48.3, 48.0, 43.1, 39.1. HRMS calc'd for C₁₇H₂₀Cl₂N₂O₄S, 419.06002 [M+H]⁺; found, 419.05875 [M+H]⁺. Anal. (C₁₇H₂₀Cl₂N₂O₄S·1.0 HCl) C, H, N.

**N-(4-(2-(2-(4-chlorophenylamino)ethylamino)ethoxy)phenyl)methanesulfonamide·HCl
(96-41).**



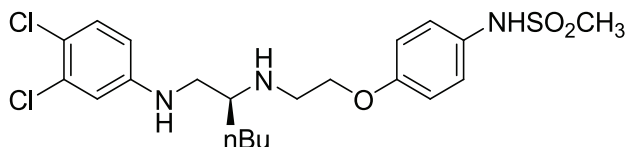
Amide **96-38** (0.100 g, 0.25 mmol) was dissolved in THF (15.0 mL) and cooled to 0°C. To this solution lithium aluminum hydride (2.0 M sol'n in THF, 0.50 mL, 1.0 mmol, 4.0 equiv) was added dropwise. The mixture was warmed to room temperature and stirred for 12 hours. The reaction mixture was diluted with water and ethyl acetate and then filtered over a pad of celite. The layers were separated and the organics were washed with brine, dried over MgSO₄, and concentrated *in vacuo* to give a yellow oil. The crude material was purified using silica gel chromatography (2%-10% MeOH/DCM gradient) to give a white oil. The free amine was converted to the HCl salt by bubbling HCl gas (NaCl/sulfuric acid method) with sample dissolved in ethanol. The resultant white powder was obtained by filtration (0.082 g, 78%). ¹H (600 MHz, *d*₆-DMSO) δ 9.49 (s, 1H), 9.42 (s, 1H), 7.19 (d, *J* = 9.1 Hz, 2H), 7.12 (d, *J* = 8.6 Hz, 2H), 6.98 (d, *J* = 9.1 Hz, 2H), 6.65 (d, *J* = 8.6 Hz, 2H), 4.27 (t, *J* = 5.8 Hz, 2H), 3.41 (t, *J* = 5.8 Hz, 2H), 3.37 (mult, 2H), 3.15 (mult, 2H), 2.89 (s, 3H). ¹³C NMR (150 MHz, *d*₆-DMSO) δ 154.9, 146.9, 131.7, 128.7, 123.2, 119.7, 115.4, 113.8, 63.6, 45.9, 38.7, 38.6. HRMS calc'd for C₁₇H₂₂ClN₃O₃S, 384.11498 [M+H]⁺; found, 384.11418 [M+H]⁺.

(R)-N-(4-(2-(1-(3,4-dichlorophenylamino)hexan-2-ylamino)ethoxy)phenyl)methanesulfonamide·HCl (96-48).



Amide **96-47** (0.100 g, 0.205 mmol) was dissolved in THF (5.0 mL). To this solution borane dimethyl sulfide (0.78 mL, 82 mmol, 4.0 equiv) was added dropwise at room temperature. The solution was refluxed for 6 hours. After cooling to room temperature, the reaction was quenched with water. The mixture was extracted with EtOAc (2x). The combined organics were washed with 1.0 N HCl, water, and brine, dried over MgSO₄, and concentrated *in vacuo* to give a colorless oil. The crude material was purified using silica gel chromatography (2-5% MeOH/DCM gradient) to give a colorless oil (0.070, 72%). The free amine was converted to the HCl salt by bubbling HCl gas (NaCl/sulfuric acid method) with sample dissolved in ethanol. Evaporation of the solvent gave an off-white foam (0.067 g, 63%). 98.5% ee based on chiral HPLC with Chiralcel AD-H column (46 mm i.d. x 250 mm), eluent 10%-90% iPrOH/hexane gradient, flow rate, 1.0 mL/min; UV monitoring at 254 nm, retention time 18.31 minutes ¹H NMR (600 MHz, CD₃OD) δ 7.32-7.20 (mult, 3H), 6.94 (d, *J* = 9.1 Hz, 2H), 6.87 (d, *J* = 2.4 Hz, 1H), 6.67 (dd, *J*₁ = 8.0 Hz, *J*₂ = 2.4 Hz, 1H), 4.29-4.28 (mult, 2H), 3.54-3.49 (mult, 4H), 3.45-3.40 (mult, 1H), 2.89 (s, 3H), 1.86-1.79 (mult, 2H), 1.51-1.42 (mult, 4H), 0.97 (t, *J* = 7.2 Hz, 3H). ¹³C NMR (150 MHz, CD₃OD) δ 157.0, 149.1, 133.9, 133.2, 132.0, 125.0, 121.5, 116.6, 115.7, 114.6, 64.7, 58.9, 45.5, 44.8, 39.0, 29.8, 28.8, 23.8, 14.3. HRMS calc'd for C₂₁H₂₉Cl₂N₃O₃S, 474.13864 [M+H]⁺; found: 474.13754 [M+H]⁺. Anal. (C₂₁H₂₉Cl₂N₃O₃S·1.0 HCl) C, H, N.

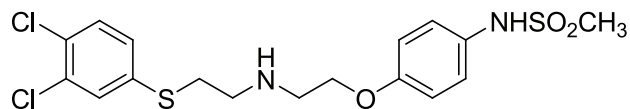
(S)-N-(4-(2-(1-(3,4-dichlorophenylamino)hexan-2-ylamino)ethoxy)phenyl)methanesulfonamide·HCl (96-52).



Amide **96-51** (0.150 g, 0.21 mmol) was dissolved in THF (10.0 mL). To this solution, borane dimethyl sulfide (0.12 mL, 1.2 mmol, 4.0 equiv) was added dropwise at room temperature. The solution was refluxed for 3 hours. After cooling to room temperature, the reaction was quenched with water. The mixture was extracted with EtOAc (2x). The combined organics were washed with 1.0 N HCl, water, and brine, dried over MgSO_4 , and concentrated *in vacuo* to give a colorless oil. The crude material was purified using silica gel chromatography (2-5% MeOH/DCM gradient) to give a colorless oil. The free amine was converted to the HCl salt by bubbling HCl gas (NaCl/sulfuric acid method) with sample dissolved in ethanol. Evaporation of the solvent gave an off-white foam (0.087 g, 82%). 97.2% ee based on chiral HPLC with Chiralcel AD-H column (46 mm i.d. x 250 mm), eluent 10%-90% iPrOH/hexane gradient, flow rate, 1.0 mL/min; UV monitoring at 254 nm, retention time 18.31 minutes. ^1H NMR (400 MHz, CD_3OD) δ 7.23 (d, $J = 8.0$ Hz, 1H), 7.20 (d, $J = 9.1$ Hz, 2H), 6.93 (d, $J = 9.1$ Hz, 2H), 6.91 (d, $J = 2.4$ Hz, 1H), 6.70 (dd, $J_1 = 8.0$ Hz, $J_2 = 2.4$ Hz, 1H), 4.29 (t, $J = 4.8$ Hz, 1H), 3.55-3.40 (mult, 5H), 2.89 (s, 3H), 1.87-1.79 (mult, 2H), 1.52-1.40 (mult, 4H), 0.97 (t, $J = 7.2$ Hz, 3H). ^{13}C NMR (100 MHz, CD_3OD) δ 157.0, 148.7, 133.8, 133.1, 132.0, 125.0, 121.7, 116.6, 116.0, 114.8, 64.7, 58.8, 45.5, 45.0, 38.9, 29.7, 28.8, 23.8, 14.3. HRMS calc'd for $\text{C}_{21}\text{H}_{29}\text{Cl}_2\text{N}_3\text{O}_3\text{S}$ 474.13861 $[\text{M}+\text{H}]^+$; found, 474.12886 $[\text{M}+\text{H}]^+$. Anal. ($\text{C}_{21}\text{H}_{27}\text{Cl}_2\text{N}_3\text{O}_4\text{S}\cdot 1.0$ HCl) C, H, N.

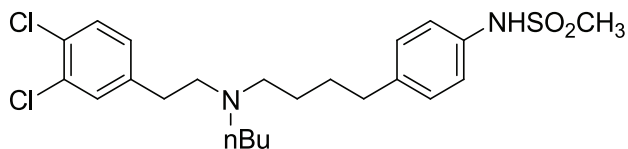
N-(4-(2-(2-(3,4-dichlorophenylthio)ethylamino)ethoxy)phenyl)methanesulfonamide

(96-55).



Amide **96-37** (0.100 g, 0.22 mmol) was dissolved in THF (10.0 mL). To this solution borane dimethyl sulfide (0.08 mL, 0.89 mmol, 4.0 equiv) was added dropwise at room temperature. The solution was refluxed for 3 hours. After cooling to room temperature, the reaction was quenched with water. The mixture was extracted with EtOAc (2x). The combined organics were washed with 1.0 N HCl, water, and brine, dried over MgSO₄, and concentrated *in vacuo* to give a white residue. The crude material was purified using silica gel chromatography (ISCO, 12 g RediSep column, 40% EtOAc/60% Hexanes to 100% EtOAc gradient) to give a white foam. The free amine was converted to the HCl salt by bubbling HCl gas (NaCl/sulfuric acid method) with sample dissolved in ethanol. Evaporation of the solvent gave a white solid (0.042 g, 41%). ¹H NMR (400 MHz, CD₃OD) δ 7.52 (d, *J* = 2.2 Hz, 1H), 7.35 (d, *J* = 8.6 Hz, 1H), 7.25 (dd, *J*₁ = 8.6 Hz, *J*₂ = 2.2 Hz, 1H), 7.20 (d, *J* = 8.9 Hz, 2H), 6.88 (d, *J* = 8.9 Hz, 2H), 5.43 (bs, 1H), 4.26-4.20 (mult, 1H), 4.14-4.09 (mult, 1H), 3.39-3.34 (mult, 2H), 3.17-2.98 (mult, 3H), 2.90-2.85 (mult, 4H). ¹³C NMR (100 MHz, CD₃OD) δ 157.5, 137.0, 134.1, 132.7, 132.2, 131.7, 131.5, 130.1, 125.1, 116.5, 65.1, 55.4, 54.2, 38.9, 30.4. HRMS calc'd for C₁₇H₂₀Cl₂N₂O₃S₂, 435.03718 [M+H]⁺; found, 435.03662 [M+H]⁺.

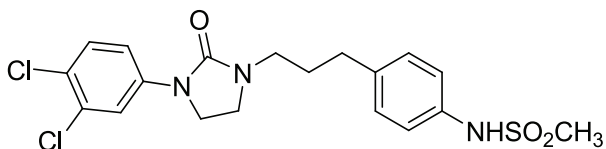
N-(4-(4-(butyl(3,4-dichlorophenethyl)amino)butyl)phenyl)methanesulfonamide (96-60).



Amide **96-60** (0.180 g, 0.37 mmol) was dissolved in THF (10.0 mL). To this solution, borane dimethyl sulfide (0.11 mL, 1.1 mmol, 3.0 equiv) was added dropwise at room temperature. The solution was refluxed for 3 hours. After cooling to room temperature, the reaction was quenched with water. The mixture was extracted with EtOAc (2x). The combined organics were washed with 1.0 N HCl, water, and brine, dried over MgSO₄, and concentrated *in vacuo* to give a colorless residue. The crude material was purified by silica gel chromatography (1 EtOAc/2 Hexanes to 1 EtOAc/1 Hexanes gradient) to give a colorless residue (0.146 g, 78%). ¹H NMR (400 MHz, CDCl₃) δ 7.30 (d, *J* = 8.3 Hz, 1H), 7.26-7.26 (mult, 1H), 7.15-7.13 (mult, 4H), 6.99 (dd, *J*₁ = 8.3 Hz, *J*₂ = 1.6 Hz, 1H), 2.97 (s, 3H), 2.64-2.61 (mult, 4H), 2.56 (t, *J* = 7.6 Hz, 2H), 2.44 (quart, *J* = 7.9 Hz, 4H), 1.57-1.53 (mult, 2H), 1.45-1.37 (mult, 4H), 1.29-1.24 (mult, 2H), 0.89 (t, *J* = 7.3 Hz, 3H). ¹³C NMR (100 MHz, CDCl₃) δ 141.4, 140.4, 134.4, 132.2, 130.9, 130.4, 129.9, 129.8, 128.5, 121.7, 55.7, 53.9, 39.4, 35.4, 32.9, 29.4, 27.0, 20.9, 14.3. HRMS calc'd for C₂₃H₃₂Cl₂N₂O₂S, 471.16414 [M+H]⁺, found: 471.16327 [M+H]⁺.

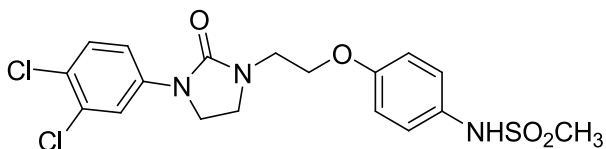
General method for preparation of imidazolinones **96-23** and **96-45**, exemplified by **96-23**.

N-(4-(3-(3-(3,4-dichlorophenyl)-2-oxoimidazolidin-1-yl)propyl)phenyl)methanesulfonamide (96-23).



Amine **70** (0.113 g, 0.27 mmol) was dissolved in THF (10.0 mL). To this solution 1,1-carbonyldimidazole (0.048 g, 0.30 mmol, 1.1 equiv) was added, and the mixture was stirred at room temperature for 12 hours. The solution was concentrated *in vacuo* and the residue was taken up in ethyl acetate, washed with brine, dried over Na₂SO₄, and concentrated *in vacuo* to give a colorless oil. The crude material was purified using silica gel chromatography (100% EtOAc) to give a white foam (0.070 g, 58%). ¹H NMR (400 MHz, CDCl₃) δ 7.72 (s, 1H), 7.16 (d, *J*=8.6 Hz, 2H), 7.07 (d, *J*=8.6 Hz, 2H), 7.02 (s, 1H), 6.64 (d, *J*=2.9 Hz, 1H), 6.41 (dd, *J*₁=8.5 Hz, *J*₂=2.9 Hz, 1H), 3.64 (t, *J*=6.0 Hz, 2H), 3.40-3.36 (mult, 4H), 2.97 (s, 3H), 2.57 (t, *J*=7.3 Hz, 2H), 1.26 (t, *J*=7.3 Hz, 2H). ¹³C (75 MHz, CDCl₃) δ 152.6, 147.1, 137.3, 136.8, 135.6, 130.9, 129.5, 121.6, 118.0, 113.6, 112.5. HRMS calc'd for C₁₉H₂₁Cl₂N₃O₃S, 442.07604 [M+H]⁺; found, 442.07527 [M+H]⁺. HPLC (a) 99.1% (b) 99.6%.

N-(4-(2-(3-(3,4-dichlorophenyl)-2-oxoimidazolidin-1-yl)ethoxy)phenyl)methanesulfonamide (96-45).



Compound **96-45** was obtained using amine **96-29**. The crude material was purified using silica gel chromatography (100% EtOAc) to give a white foam (white foam, 0.100 g, 56%). ^1H NMR (400 MHz, CDCl_3) δ 7.62 (d, $J=2.5$ Hz, 1H), 7.30 (dd, $J_1=8.9$ Hz, $J_2=2.5$ Hz, 1H), 7.25 (d, $J=8.9$ Hz, 1H), 7.12 (d, $J=8.9$ Hz, 2H), 6.77 (d, $J=8.9$ Hz, 2H), 4.05-4.02 (mult, 2H), 3.70-3.59 (mult, 6H), 2.84 (s, 3H). ^{13}C NMR (100 MHz, CDCl_3) δ 157.4, 156.8, 140.0, 132.6, 130.4, 130.0, 125.5, 124.6, 118.9, 116.6, 115.4, 67.4, 38.9. HRMS calc'd for $\text{C}_{18}\text{H}_{19}\text{Cl}_2\text{N}_3\text{O}_4\text{S}$, 444.0473 $[\text{M}]^+$; found, 444.05451 $[\text{M}]^+$. HPLC (a) 98.3% (b) 97.6%.

2.10.2 Combustion analysis (Atlantic Microlab, Inc)

ID	Molecular Formula	Theoretical	Experimental
96-1	$\text{C}_{17}\text{H}_{18}\text{Cl}_2\text{N}_4\text{O}_3\text{S}_2$	C: 44.25, H: 3.93, N: 12.14	C: 44.21, H:4.03, N: 12.34
96-2	$\text{C}_{16}\text{H}_{15}\text{Cl}_2\text{N}_3\text{O}_3$	C: 52.19, H: 4.11; N: 11.41	C: 52.08, H: 4.10, N: 11.21
96-3	$\text{C}_{17}\text{H}_{16}\text{Cl}_2\text{N}_2\text{O}_3$	C: 55.60, H: 4.39, N: 7.63	C: 55.20, H: 4.40, N: 7.47
96-4	$\text{C}_{18}\text{H}_{19}\text{Cl}_2\text{N}_3\text{O}_4\text{S}$	C: 48.66, H: 4.31, N: 9.46	C: 48.62, H: 4.29, H: 9.41
96-5	$\text{C}_{17}\text{H}_{18}\text{Cl}_2\text{N}_4\text{O}_4\text{S}$	C: 45.85, H: 4.07, N: 12.58	C: 45.77, H:3.98, N:12.37
96-6	$\text{C}_{22}\text{H}_{27}\text{Cl}_2\text{N}_3\text{O}_4\text{S}$	C: 52.80, H: 5.44, N: 8.40	C: 51.98, H: 5.11, N: 8.13
96-7	$\text{C}_{21}\text{H}_{26}\text{Cl}_2\text{N}_4\text{O}_4\text{S}$	C: 50.30, H: 5.23, N: 11.17	C: 50.11, H: 5.13, N: 10.98
96-8	$\text{C}_{21}\text{H}_{24}\text{Cl}_2\text{N}_2\text{O}_3$	C: 59.58, H: 5.71, N: 6.62	C: 59.69, H: 5.73, N: 6.60
96-9	$\text{C}_{18}\text{H}_{21}\text{Cl}_2\text{N}_3\text{O}_3\text{S}$	C: 50.24, H: 4.92; N: 9.76	C: 50.38, H:4.97, N: 9.60
96-10	$\text{C}_{17}\text{H}_{17}\text{Cl}_2\text{N}_3\text{O}_4\text{S}$	C: 47.45, H: 3.98, N: 9.77	C: 47.45, H:4.10, N:9.94
96-11	$\text{C}_{17}\text{H}_{18}\text{Cl}_2\text{N}_2\text{O}_2$	C: 57.80, H: 5.14, N: 7.93	C: 57.74, H:5.18, N: 7.91
96-12	$\text{C}_{18}\text{H}_{15}\text{Cl}_2\text{N}_3\text{O}_5\text{S} \cdot 0.25 \text{CH}_3\text{OH}$	C: 47.21, H: 3.47 N: 9.05	C: 47.38, H: 3.31, N: 9.21
96-13	$\text{C}_{18}\text{H}_{21}\text{Cl}_2\text{N}_3\text{O}_3\text{S}$	C: 50.24, H: 4.92, N: 9.76	C: 49.94, H: 4.92, N:9.57
96-14	$\text{C}_{20}\text{H}_{23}\text{F}_2\text{N}_3\text{O}_3\text{S}$	C: 56.72, H:5.47, N:9.92	C: 56.15, H: 5.61, N: 9.54*

96-19	C ₁₉ H ₂₂ Cl ₂ N ₂ O ₃ S	C: 53.15, H: 5.16, N: 6.52	C: 52.99, H: 5.15, N: 6.52
96-17	C ₁₉ H ₂₀ Cl ₂ N ₂ O ₃ S	C: 53.40, H: 4.72, N: 6.56	C: 53.24, H: 4.75, N: 6.52
96-20	C ₁₈ H ₂₃ Cl ₂ N ₃ O ₂ S·0.45 HCl	C: 47.07, H: 5.25, N: 8.96	C: 47.21, H: 5.34, N: 8.92
96-21	C ₂₀ H ₂₅ Cl ₂ N ₃ O ₂ S·HCl	C: 50.16, H: 5.47, N: 8.76	C: 50.89, H: 5.24, N: 8.38*
96-22	C ₁₇ H ₁₉ Cl ₂ N ₃ O ₄ S	C: 47.23, H: 4.43, N: 9.72	C: 47.39, H: 4.47, N: 9.62
96-27	C ₁₇ H ₁₈ Cl ₂ N ₂ O ₂	C: 57.80, H: 5.14, N: 7.93	C: 58.00, H: 5.34, N: 7.75
96-25	C ₁₇ H ₂₁ Cl ₂ N ₃ O ₃ S·HCl	C: 44.90, H: 4.88, N: 9.23	C: 45.03, H: 4.87, N: 9.24
96-30	C ₁₉ H ₂₁ Cl ₂ N ₃ O ₄ S·0.8 H ₂ O	C: 48.27, H: 4.82, N: 8.89	C: 48.38, H: 4.86, N: 8.39*
96-31	C ₁₉ H ₂₃ Cl ₂ N ₃ O ₃ S	C: 47.36, H: 5.23, N: 8.72	C: 47.17, H: 5.35, N: 8.57
96-34	C ₁₇ H ₁₈ Cl ₂ N ₂ O ₅ S·0.25 H ₂ O	C: 46.64, H: 4.26, N: 6.40	C: 46.67, H: 4.17, N: 6.28
96-36	C ₁₇ H ₂₀ Cl ₂ N ₂ O ₄ S·1.0HCl	C: 47.64, H: 5.11, N: 6.17	C: 47.49, H: 5.04, N: 6.08
96-37	C ₁₇ H ₁₈ Cl ₂ N ₂ O ₄ S ₂	C: 45.44, H: 4.04, N: 6.23	C: 45.25, H: 4.02, N: 6.15
96-40	C ₁₆ H ₁₆ Cl ₂ N ₂ O ₃	C: 54.10, H: 4.54, N: 7.89	C: 53.98, H: 4.56, N: 7.73
96-42	C ₁₆ H ₁₇ ClN ₂ O ₃	C: 59.91, H: 5.34, N: 8.73	C: 59.88, H: 5.29, N: 8.64
96-43	C ₁₈ H ₁₈ Cl ₂ N ₂ O ₃	C: 56.71, H: 4.76, N: 7.35	C: 56.68, H: 4.56, N: 7.26
96-47	C ₂₁ H ₂₇ Cl ₂ N ₃ O ₄ S	C: 51.64, H: 5.57, N: 8.60	C: 51.63, H: 5.67, N: 8.44
96-48	C ₂₁ H ₂₉ Cl ₂ N ₃ O ₃ S·1.0 HCl	C: 49.37; H: 5.92, N: 8.22	C: 49.32, H: 5.87, N: 8.13
96-50	C ₁₈ H ₁₈ Cl ₂ N ₂ O ₄ S	C: 50.36; H: 4.23, N: 6.53	C: 50.41, H: 4.28, N: 6.53
96-51	C ₂₁ H ₂₇ Cl ₂ N ₃ O ₄ S·1.0 HCl	C: 49.37; H: 5.92, N: 8.22	C: 49.49, H: 5.68, N: 8.31
96-53	C ₁₇ H ₁₉ F ₂ N ₃ O ₄ S	C: 51.12, H: 4.79, N: 10.52	C: 50.83, H: 4.75, N: 10.39
96-56	C ₁₇ H ₂₁ N ₃ O ₄ S	C: 56.18, H: 5.82, N: 11.56	C: 56.17, H: 5.85, N: 11.32
96-58	C ₁₈ H ₂₁ Cl ₂ N ₃ O ₄ S	C: 48.44, H: 4.74, N: 9.41	C: 47.79, H: 4.89, N: 9.19*
96-59	C ₁₉ H ₂₃ Cl ₂ N ₃ O ₃ S	C: 51.35, H: 5.22, N: 9.46	C: 50.89, H: 5.20, N: 9.19*
96-63	C ₁₇ H ₂₀ ClN ₃ O ₄ S	C: 51.32, H: 5.07, N: 10.56	C: 51.21, H: 5.20, N: 10.36
96-64	C ₁₈ H ₂₂ ClN ₃ O ₃ S	C: 54.61, H: 5.60; N: 10.61	C: 54.45, H: 5.64, N: 10.58
96-68	C ₂₀ H ₂₁ Cl ₂ N ₃ O ₄ S	C: 51.07, H: 4.50, N: 8.93;	C: 51.01, H: 4.33, N: 8.91

* Did not pass within ± 0.4%

2.11. Biology Experimental Detail

2.11.1. *In vitro* NMDA antagonism assay (Dr. Stephen Traynelis Laboratory, Emory University School of Medicine)

Expression of glutamate receptors in *Xenopus laevis* oocytes.

All protocols involving the use of animals were approved by the Emory University IACUC. cRNA was synthesized from linearized template cDNA for rat glutamate receptor subunits according to manufacturer specifications (Ambion). Quality of synthesized cRNA was assessed by gel electrophoresis, and quantity was estimated by spectroscopy and gel electrophoresis. Stage V and VI oocytes were surgically removed from the ovaries of large, well-fed and healthy *Xenopus laevis* anesthetized with 3-amino-benzoic acid ethyl ester (1-3 gm/l) as previously described.⁵⁹ Clusters of isolated oocytes were incubated with 292 U/ml Worthington (Freehold, NJ) type IV collagenase or 1.3 mg/ml collagenase (Life Technologies, Gaithersburg, MD; 17018-029) for 2 hr in Ca²⁺-free solution comprised of (in mM) 89 NaCl, 1 KCl, 2.4 NaHCO₃, 0.82 MgSO₄, 10 HEPES, with slow agitation to remove the follicular cell layer. Oocytes were then washed extensively in the same solution and maintained in Barth's solution comprised of (in mM) 88 NaCl, 1 KCl, 2.4 NaHCO₃, 10 HEPES, 0.82 MgSO₄, 0.33 Ca(NO₃)₂, and 0.91 CaCl₂ and supplemented with 100 µg/ml gentamycin, 10 µg/ml streptomycin, and 10 µg/ml penicillin. Oocytes were manually defolliculated and injected within 24 hrs of isolation with 3-5 ng of NR1-1a (hereafter NR1) subunit and 7-10 ng of NR2 subunit in a 50 nl volume, or 5-10 ng in 50 nl of AMPA or kainate receptor cRNAs, and incubated in Barth's

solution at 15°C for 1–7 d. Glass injection pipettes had tip sizes ranging from 10-20 microns, and were backfilled with mineral oil.

Two electrode voltage clamp recording from *Xenopus laevis* oocytes

Two electrode voltage-clamp recordings were made 2–7 days post-injection as previously described.⁵⁹ Oocytes were placed in a dual-track plexiglass recording chamber with a single perfusion line that splits in a Y-configuration to perfuse two oocytes. Dual recordings were made at room temperature (23°C) using two Warner OC725B or OC725C two-electrode voltage clamp amplifiers, arranged as recommended by the manufacturer. Glass microelectrodes (1-10 Megaohms) were filled with 300 mM KCl (voltage electrode) or 3 M KCl (current electrode). The bath clamps communicated across silver chloride wires placed into each side of the recording chamber, both of which were assumed to be at a reference potential of 0 mV. Oocytes were perfused with a solution comprised of (in mM) 90 NaCl, 1 KCl, 10 HEPES, and 0.5 BaCl₂; pH was adjusted to 7.4 or 7.6 by addition of 1 M NaOH. Oocytes expressing NR1/NR2A were pre-incubated before recording in recording solution supplemented with 50 μM BAPTA-AM at room temperature. Oocytes were recorded under voltage clamp at -40 mV. Final concentrations for control application of glutamate (50-100 μM) plus glycine (30 μM) to oocytes expressing NMDA receptors were achieved by dilution from 100 and 30-100 mM stock solutions, respectively. In addition, 10 μM final EDTA was obtained by adding a 1:1000 dilution of 10 mM EDTA, in order to chelate contaminant divalent ions such as extracellular Zn²⁺. Homomeric GluR1 AMPA receptors were activated by 100 μM

glutamate. Homomeric GluR6 kainate receptors were incubated in concanavalin A (10 μ M) for 5 minutes, and activated by 100 μ M glutamate. Concentration-response curves for experimental compounds acting on NMDA receptors were obtained by applying in successive fashion a maximally effective concentration of glutamate/glycine, followed by glutamate/glycine plus variable concentrations of experimental compounds. Concentration-response curves consisting of 5 to 8 concentrations were obtained in this manner. The baseline leak current at -40 mV was measured before and after recording, and the full recording linearly corrected for any change in leak current. Oocytes with glutamate-evoked responses smaller than 50 nA were not included in the analysis. The level of inhibition produced by experimental compounds was expressed as a percent of the initial glutamate response, and averaged together across oocytes from a single frog. Each experiment consisted of recordings from 3 to 10 oocytes obtained from a single frog. Results from ≥ 3 experiments using oocytes from 3 different frogs were pooled, and the percent responses at antagonist concentrations for each oocyte were fitted by the equation,

$$\text{Percent Response} = (100 - \text{minimum}) / (1 + ([\text{conc}] / IC_{50})^{nH}) + \text{minimum}$$

where *minimum* is the residual percent response in saturating concentration of the experimental compounds, IC_{50} is the concentration of antagonist that causes half of the achievable inhibition, and nH is a slope factor describing steepness of the inhibition curve. *Minimum* was constrained to be greater than or equal to 0.

2.11.2. *In vitro* binding studies for secondary effects (MDS Pharma, Inc.)

Compounds were evaluated for binding to the human ether-a-go-go potassium channel (hERG) expressed in HEK293 cells by displacement of $^3\text{[H]}$ -astemizole according to the methods by Finlayson et al.⁶⁰ Compounds were incubated at 10 μM , in duplicate, and the amount of $^3\text{[H]}$ -astemizole determined by liquid scintillation spectroscopy. In some cases, a seven concentration (each concentration in duplicate) displacement curve was generated to determine IC_{50} .

K_i values for human hERG channels determined by displacement of 1.5 nM $^3\text{[H]}$ astemizole from HEK-293 cell membranes transfected with human recombinant hERG channels (MDS Pharma).⁶⁰ Data from multipoint displacement curves were fit by a non-linear, least squares regression analysis and the K_i calculated using the Cheng and Prusoff equation.

Binding to the rat α_1 -adrenergic receptor in rat brain membranes was determined by displacement of $^3\text{[H]}$ -prazosin.⁶¹ Compounds were incubated at 3 μM , in duplicate, and the amount of displaced $^3\text{[H]}$ -prazosin determined by liquid scintillation spectroscopy.

2.11.3. Homology Modeling (Computational lab of Dr. Dennis Liotta, Department of Chemistry, Emory University)

The homology model of NR2B was built using a published alignment between NR2B and mGluR1⁶² and the closed structure of mGluR1⁶³ using Prime (Schrodinger, LLC, New York 2006). Ifenprodil and Ro25,6981 were docked into this model using the Induced Fit

Docking algorithm, and constrained to interact with D101, and residue known to be critical for these two compounds. Seven different poses of the ligands were used as templates for further docking of novel compounds **96-22**, **96-5**, and **96-20** using GlideXP (Schrodinger, LLC, New York 2006). MM-GBSA rescoring was performed the results, and consensus poses were identified and their scores compared.

2.11.4 Rotarod assay (Dr. Stephen Traynelis Laboratory, Emory University School of Medicine)

Male C57BL/6 mice (3 months old, The Jackson Laboratory) were tested in the rotarod assay using a four-chamber Rotamex 4/8 rotarod (Columbus Instruments, Columbus, OH). The test was initiated by placing mice on a 3.8 cm diameter rotating rod (5 rpm) suspended 30 cm from the floor of an isolated chamber. After 10 sec the rod rotation was accelerated from 5 to 35 rpm over a 5 minute period and the length of time the mice stayed on the rod was automatically recorded (latency time) by light-activated sensors in the bottom of the chamber. Animals were trained four times each day for two consecutive days, with a within-day inter-trial interval of 20-25 min. On day 3, mice were randomly assigned to groups and injected i.p. with vehicle, drug, or positive control (3 ml/kg volume) and tested as before. All drugs were dissolved in 10% DMA: 10% EtOH: 40% PEG: 40% aqueous. Mean latency values for each trial were calculated on day three. The technician conducting the rotarod assay was blinded throughout the study.

2.11.5. Lactate dehydrogenase (LDH) assay (Dr. Stephen Traynelis Laboratory, Emory University School of Medicine)

Primary Cortical Neurons prepared from Sprague Dawley rat embryos (E16-19), preferably E18. DIV 4-5 refed with neurobasal media (with all additives except FBS) containing uridine and 5-fluoro-2-deoxuridine (10uM Final). Primary neuronal cultures (DIV 17) treated with 10uM Drug, Vehicle, or NMDA (100uM) and Glycine (10uM) overnight in culture media (with no additives). After 20-24 hours cytotoxicity was assessed by measuring lactase dehydrogenase released in media. The data was normalized to the % of the total LDH in the culture.

After 20-24 hours excitotoxicity was assessed by measuring lactase dehydrogenase release into media. Removed media/supernatant from wells and placed into a new 24 well-plate. Put 1mL 2% Triton into each well of original plate. Scrape bottom w/ 1ml pipette tip, then sonicate for 5 secs @ 2.5 setting. Spin plate for 5mins @ 250,000RPM. Created 1-96 well plate for both the released (media) and unreleased (in triton). Measured on plate reader @ 490 wavelength by adding 100ul of dye solution to each well; incubate dye for 25 mins, then read. Used dye kits from Sigma Tox-7 and Roche Cytotoxicity Detection Kit.

Primary dissociated cortical cultures were prepared from Sprague-Dawley rat embryos (E16-E19) as previously described. After 9-12 days in culture, pretreatment and treatment of cells with experimental compounds were performed using buffered artificial cerebrospinal fluid (ACSF) solution (pH 7.6). ACSF was comprised of (in mM) 130 NaCl, 3.5KCl, 2 MgSO₄, 1.25 NaH₂PO₄, 2 CaCl₂, 15 NaHCO₃, 10 glucose, and 10 HEPES

and saturated with 95%O₂/5% CO₂. Cells were pretreated with ACSF alone, variable concentrations of test compound, or D-APV (100 μM) for 15 min. Excitotoxicity was induced by treating cultures with NMDA (100 μM) plus glycine(10 μM) at room temperature for 10 min in the presence of test compound or D-APV (100 μM). Cells were subsequently washed twice with fresh medium containing D-APV (100 μM) and CNQX (1-10 μM) to limit the period of excitotoxicity to the 10 min exposure. Rinsed plates were returned to the incubator in fresh medium without D-APV or CNQX. After 16-24 h, excitotoxic damage was assessed spectrophotometrically measuring the amount of lactate dehydrogenase (LDH) released into the culture medium(Tox-7 kit; Sigma Chemical Co, St. Louis, MO). Released LDH was expressed as the fraction of total LDH present in each well, determined by lysing the cells. Neuroprotection produced by experimental compounds was quantified by scaling LDH release in wells between minimum and maximum degree of LDH release. We defined percent inhibition as:

$$\% \text{ Inhibition} = 100 - 100(\text{LDH}_{\text{treated}} - \text{LDH}_{\text{min}}) / (\text{LDH}_{\text{max}} - \text{LDH}_{\text{min}})$$

where LDH_{treated} is the amount of LDH released from wells treated with variable concentrations of experimental compound, LDH_{min} was the LDH release from wells treated with ACSF+D-APV, and LDH_{max} was the maximum LDH released from wells treated with glutamate and glycine. Cultures in which the NMDA-evoked excitotoxic cell death was less than 10% were discarded.

2.11.6 Transient focal ischemia (Dr. Manuel Yepes Laboratory, Emory University School of Medicine)

Transient focal cerebral ischemia was induced in mice by intraluminal middle cerebral artery occlusion (MCAO) with a monofilament suture as previously described.⁶⁴ Male C57BL/6 mice (3-5 months old, The Jackson Laboratory) were anesthetized with 2% isoflurane in 98% O₂. The rectal temperature was controlled at 37 °C (range 36.5-37.5) with a homeothermic blanket. Relative changes in regional cerebral blood flow were monitored with a laser Doppler flowmeter (Perimed). To do this, the probe was glued directly to the skull 2 mm posterior and 4-6 mm lateral of the bregma. An 11 mm 5-0 Dermalon or Look (SP185) black nylon nonabsorbable suture with the tip flame rounded was introduced into the left internal carotid artery through the external carotid artery stump until monitored blood flow was reduced below 20% or stopped (at 10.5-11 mm of suture insertion). After 30 min MCA occlusion, blood flow was restored by withdrawing the suture. After 24 h survival, the brain was removed and cut into 2 mm sections. The lesion was identified with 2% 2,3,5-triphenyltetrazolium chloride (TTC) in PBS at 37 °C for 20 min. The infarct area of each section was measured using NIHIMAGE (Scion Corporation, Beta 4.0.2 release) and multiplied by the section thickness to give the infarct volume of that section. The density slice option in NIH IMAGE was used to segment the images based on the intensity determined as 70% of that in the contralateral undamaged cortex. This standard was maintained throughout the analysis in all animals, and only objects at this intensity were highlighted for area measurement. The area of the lesion, as identified by digital threshold reductions in TTC staining, was

manually outlined. A ratio of the contralateral to ipsilateral hemisphere section volume was multiplied by the corresponding infarct section volume to correct for edema. Infarct volume was determined by summing the infarct area times section thickness for all sections. C57Bl/6 mice received an intraperitoneal (ip) injection of compound **96-22** 10 min before MCA occlusion surgery, resulting in receipt of compound **96-22** 30 min before occlusion. A second dose of 30 mg/kg was delivered 30 minutes post reperfusion. A 30 mg/mL stock solution in 50% DMSO was prepared by adding 30 mg of compound into 0.5 mL of DMSO followed by addition of 0.5 mL of 0.9% saline with vortexing. The working solution for the ip injection solution was 3 mg/mL in 0.9% saline (50% v/v DMSO) and was prepared by transferring 0.2 mL of the stock solution into a new tube and adding 0.9 mL of DMSO and 0.9 mL of 0.9% saline with vortexing. A dose of 30 mg/kg compound **96-22** was administered to mice with a 10 mL/kg injection volume. The technician performing both the surgical procedure and analysis of stained sections by NIH IMAGE was blinded from the compound injected.

2.11.7. Chung model of neuropathic pain (Algos Therapeutics, Inc.)

Male Sprague Dawley rats (Harlan, Indianapolis, Indiana, USA) weighing 262 ± 2 g were housed three per cage with soft bedding material. Animals had free access to food and water and were maintained on a 12:12h light/dark schedule for the entire duration of the study. The animal colony was maintained at 21°C and 60% humidity. All experiments were conducted in accordance with the International Association for the Study of Pain guidelines. The spinal nerve ligation (SNL) model was used to induce chronic

neuropathic pain. The animals were anesthetized with isoflurane, the left L6 transverse process was removed, and the L5 and L6 spinal nerves were tightly ligated with 6-0 silk suture. The wound was then closed with internal sutures and external staples. Baseline, post-injury and post-treatment values for non-noxious mechanical sensitivity were evaluated using 8 Semmes-Weinstein filaments with varying stiffness (0.4, 0.7, 1.2, 2.0, 3.6, 5.5, 8.5, and 15 g) according to the up-and-down method. Animals were placed on a perforated metallic platform and allowed to acclimate to their surrounding for a minimum of 30 minutes before testing. The mean and standard error of the mean (SEM) were determined for each paw and each treatment group. Compounds were administered by a separate experimenter who was not involved with conducting the behavioral testing. **96-22** was formulated in 5% DMA, 5% DMSO, 50% PEG, and 40% water. Vehicle was 5% DMA, 5% DMSO, 50% PEG, and 40% water.

2.11.8. Estimation of brain penetration (Absorption Systems)

Transwell wells containing MDR1-MDCK cell monolayers were used for measuring the percent recovery of compound after dosing both sides of a cell monolayer with the test article (performed by Absorption Systems, Exton, PA, USA). Briefly, monolayers were grown for 7-11 days at which time 5 μ M of the test article was made by dilution from DMSO stocks into a Hank's balanced salt solution (pH 7.4), final DMSO not greater than 1% and added to: (a) the apical side for A-B permeability assessment, or separately (b) the basal side for B-A permeability assessment, all at pH 7.4. After 2 h incubation (37°C) both the apical and the basal compartments were sampled and the amount of test

article present determined by generic LC-MS/MS methods against a > 4 point calibration curve. Apparent permeability (P_{app}) units are reported in $\times 10^{-6}$ cm/s. Experiments were done in duplicate.

References

- (1) Tahirovic, Y. A.; Geballe, M.; Gruszecka-Kowalik, E.; Myers, S. J.; Lyuboslavsky, P.; Le, P.; French, A.; Irier, H.; Choi, W. B.; Easterling, K.; Yuan, H.; Wilson, L. J.; Kotloski, R.; McNamara, J. O.; Dingledine, R.; Liotta, D. C.; Traynelis, S. F.; Snyder, J. P. *J. Med. Chem.* **2008**, *51*, 5506.
- (2) Zhong, H. Y.; Minneman, K. P. *Eur. J. Pharmacol.* **1999**, *375*, 261.
- (3) Kojima, Y.; Sasaki, S.; Hayashi, Y.; Tsujimoto, G.; Kohri, K. *Nat. Clin. Pract. Urol.* **2009**, *6*, 44.
- (4) Bishop, M. J. *Curr. Top. Med. Chem.* **2007**, *7*, 135.
- (5) Mosley, C. A.; Myers, S. J.; Murray, E. E.; Santangelo, R.; Tahirovic, Y. A.; Kurtkaya, N.; Mullasseril, P.; Yuan, H. J.; Lyuboslavsky, P.; Le, P.; Wilson, L. J.; Yepes, M.; Dingledine, R.; Traynelis, S. F.; Liotta, D. C. *Biorg. Med. Chem.* **2009**, *17*, 6463.
- (6) Prata, J. V.; Clemente, D. T. S.; Prabhakar, S.; Lobo, A. M.; Mourato, I.; Branco, P. S. *J. Chem Soc Perk T 1* **2002**, 513.
- (7) Khan, K. M.; Rasheed, M.; Zia-Ullah; Hayat, S.; Kaukab, F.; Choudhary, M. I.; Atta-ur-Rahman; Perveen, S. *Biorg. Med. Chem.* **2003**, *11*, 1381.
- (8) Liotta, D. C.; Snyder, J. P.; Traynelis, S. F.; Wilson, L. J.; Mosley, C. A.; Dingledine, R. J.; Myers, S.; Tahirovic, Y. A. (Emory University, USA and NeurOp, Inc., USA). NMDA Receptor Antagonists for Neuroprotection. WO 2009006437, January 8, 2009
- (9) Borza, I.; Domany, G. *Curr Top Med Chem* **2006**, *6*, 687.
- (10) Jamieson, C.; Moir, E. M.; Rankovic, Z.; Wishart, G. *J. Med. Chem.* **2006**, *49*, 5029.
- (11) Jakobsen, C. M.; Denmeade, S. R.; Isaacs, J. T.; Gady, A.; Olsen, C. E.; Christensen, S. B. *Journal of Medicinal Chemistry* **2001**, *44*, 4696.
- (12) Jiang, G. C.; Stalewski, J.; Galyean, R.; Dykert, J.; Schteingart, C.; Broqua, P.; Aebi, A.; Aubert, M. L.; Semple, G.; Robson, P.; Akinsanya, K.; Haigh, R.; Riviere, P.; Trojnar, J.; Junien, J. L.; Rivier, J. E. *Journal of Medicinal Chemistry* **2001**, *44*, 453.

- (13) Perillo, I.; Caterina, M. C.; Lopez, J.; Salerno, A. *Synthesis-Stuttgart* **2004**, 851.
- (14) Miller, J. F.; Brieger, M.; Furfine, E. S.; Hazen, R. J.; Kaldor, I.; Reynolds, D.; Sherrill, R. G.; Spaltenstein, A. *Bioorganic & Medicinal Chemistry Letters* **2005**, *15*, 3496.
- (15) Poindexter, G. S.; Owens, D. A.; Dolan, P. L.; Woo, E. J. *Org. Chem.* **1992**, *57*, 6257.
- (16) Fuller, R. W.; Molloy, B. B.; Day, W. A.; Roush, B. W.; Marsh, M. M. *Journal of Medicinal Chemistry* **1973**, *16*, 101.
- (17) Kao, L. C.; Stakem, F. G.; Patel, B. A.; Heck, R. F. *J. Org. Chem.* **1982**, *47*, 1267.
- (18) Heyes, J. A.; Niculescu-Duvaz, D.; Cooper, R. G.; Springer, C. J. *Journal of Medicinal Chemistry* **2002**, *45*, 99.
- (19) Malek, N. J.; Moormann, A. E. *J. Org. Chem.* **1982**, *47*, 5395.
- (20) Cabri, W.; Candiani, I.; Bedeschi, A.; Santi, R. *J. Org. Chem.* **1992**, *57*, 3558.
- (21) Ho, B.; Crider, A. M.; Stables, J. P. *Eur. J. Med. Chem.* **2001**, *36*, 265.
- (22) Weissman, S. A.; Lewis, S.; Askin, D.; Volante, R. P.; Reider, P. J. *Tetrahedron Lett* **1998**, *39*, 7459.
- (23) Klapars, A.; Antilla, J. C.; Huang, X. H.; Buchwald, S. L. *J Am Chem Soc* **2001**, *123*, 7727.
- (24) Lewin, A. H.; Szewczyk, J.; Wilson, J. W.; Carroll, F. I. *Tetrahedron* **2005**, *61*, 7144.
- (25) Abdelmagid, A. F.; Maryanoff, C. A. *Synlett* **1990**, 537.
- (26) Naito, H.; Ohsuki, S.; Sugimori, M.; Atsumi, R.; Minami, M.; Nakamura, Y.; Ishii, M.; Hirotsu, K.; Kumazawa, E.; Ejima, A. *Chem. Pharm. Bull. (Tokyo)* **2002**, *50*, 453.
- (27) Fischer, G.; Mutel, V.; Trube, G.; Malherbe, P.; Kew, J. N.; Mohacsi, E.; Heitz, M. P.; Kemp, J. A. *J. Pharmacol. Exp. Ther.* **1997**, *283*, 1285.
- (28) Williams, K. *Mol. Pharmacol.* **1993**, *44*, 851.
- (29) Ilyin, V. I.; Whittemore, E. R.; Guastella, J.; Weber, E.; Woodward, R. M. *Mol. Pharmacol.* **1996**, *50*, 1541.
- (30) Kew, J. N.; Trube, G.; Kemp, J. A. *J Physiol* **1996**, *497 (Pt 3)*, 761.
- (31) Kew, J. N.; Trube, G.; Kemp, J. A. *Br. J. Pharmacol.* **1998**, *123*, 463.
- (32) Perin-Dureau, F.; Rachline, J.; Neyton, J.; Paoletti, P. *J. Neurosci.* **2002**, *22*, 5955.
- (33) Gallagher, M. J.; Huang, H.; Lynch, D. R. *J. Neurochem.* **1998**, *70*, 2120.

- (34) Wong, E.; Ng, F. M.; Yu, C. Y.; Lim, P.; Lim, L. H.; Traynelis, S. F.; Low, C. M. *Protein Sci.* **2005**, *14*, 2275.
- (35) Marinelli, L.; Cosconati, S.; Steinbrecher, T.; Limongelli, V.; Bertamino, A.; Novellino, E.; Case, D. A. *Chemmedchem* **2007**, *2*, 1498.
- (36) Mony, L.; Krzaczkowski, L.; Leonetti, M.; Le Goff, A.; Alarcon, K.; Neyton, J.; Bertrand, H. O.; Acher, F.; Paoletti, P. *Molecular Pharmacology* **2009**, *75*, 60.
- (37) Ellison, G. *Brain Res Rev* **1995**, *20*, 250.
- (38) Thornberg, S. A.; Saklad, S. R. *Pharmacotherapy* **1996**, *16*, 82.
- (39) Andine, P.; Widermark, N.; Axelsson, R.; Nyberg, G.; Olofsson, U.; Martensson, E.; Sandberg, M. *J. Pharmacol. Exp. Ther.* **1999**, *290*, 1393.
- (40) Koh, J. Y.; Choi, D. W. *J. Neurosci. Methods* **1987**, *20*, 83.
- (41) Wang, C. X.; Shuaib, A. *Curr Drug Targets CNS Neurol Disord* **2005**, *4*, 143.
- (42) Miyabe, M.; Kirsch, J. R.; Nishikawa, T.; Koehler, R. C.; Traystman, R. J. *Crit. Care Med.* **1997**, *25*, 1037.
- (43) Dogan, A.; Rao, A. M.; Baskaya, M. K.; Rao, V. L. R.; Rastl, J.; Donaldson, D.; Dempsey, R. *J. J. Neurosurg.* **1997**, *87*, 921.
- (44) Sah, D. W. Y.; Ossipov, M. H.; Porreca, F. *Nat Rev Drug Discov* **2003**, *2*, 460.
- (45) Kirk, E. J. *J. Comp. Neurol.* **1974**, *155*, 165.
- (46) Wall, P. D.; Gutnick, M. *Exp. Neurol.* **1974**, *43*, 580.
- (47) Ma, Q. P.; Woolf, C. J. *Pain* **1995**, *61*, 383.
- (48) Woolf, C. J.; Thompson, S. W. N. *Pain* **1991**, *44*, 293.
- (49) Merskey, H. *Pain* **2002**, *96*, 408.
- (50) Taniguchi, K.; Shinjo, K.; Mizutani, M.; Shimada, K.; Ishikawa, T.; Menniti, F. S.; Nagahisa, A. *Br. J. Pharmacol.* **1997**, *122*, 809.
- (51) Davidson, E. M.; Carlton, S. M. *Brain Res.* **1998**, *785*, 136.
- (52) Gaunitz, C.; Schuttler, A.; Gillen, C.; Allgaier, C. *Amino Acids* **2002**, *23*, 177.
- (53) McCormack, K. *Pain Rev.* **1999**, *6*, 99.
- (54) Ma, Q. P.; Hargreaves, R. J. *Neuroscience* **2000**, *101*, 699.
- (55) Kim, K. J.; Yoon, Y. W.; Chung, J. M. *Exp. Brain Res.* **1997**, *113*, 200.

- (56) Li, J. C.; McRoberts, J. A.; Nie, J. J.; Ennes, H. S.; Mayer, E. A. *Pain* **2004**, *109*, 443.
- (57) Marvizon, J. C. G.; McRoberts, J. A.; Ennes, H. S.; Song, B. B.; Wang, X. R.; Jinton, L.; Corneliussen, B.; Mayer, E. A. *J. Comp. Neurol.* **2002**, *446*, 325.
- (58) Gingrich, M. B.; Traynelis, S. F. *Trends Neurosci.* **2000**, *23*, 399.
- (59) Traynelis, S. F.; Burgess, M. F.; Zheng, F.; Lyuboslavsky, P.; Powers, J. L. *J Neurosci* **1998**, *18*, 6163.
- (60) Finlayson, K.; Turnbull, L.; January, C. T.; Sharkey, J.; Kelly, J. S. *Eur. J. Pharmacol.* **2001**, *430*, 147.
- (61) Greengrass, P.; Bremner, R. *Eur. J. Pharmacol.* **1979**, *55*, 323.
- (62) Malherbe, P.; Kratochwil, N.; Knoflach, F.; Zenner, M. T.; Kew, J. N. C.; Kratzeisen, C.; Maerki, H. P.; Adam, G.; Mutel, V. *J. Biol. Chem.* **2003**, *278*, 8340.
- (63) Kunishima, N.; Shimada, Y.; Tsuji, Y.; Sato, T.; Yamamoto, M.; Kumasaka, T.; Nakanishi, S.; Jingami, H.; Morikawa, K. *Nature* **2000**, *407*, 971.
- (64) Junge, C. E.; Sugawara, T.; Mannaioni, G.; Alagarsamy, S.; Conn, P. J.; Brat, D. J.; Chan, P. H.; Traynelis, S. F. *Proc. Natl. Acad. Sci. U. S. A.* **2003**, *100*, 13019.

Part 2:

Design, Synthesis, and Biological
Evaluation of First-in-Class
NR2C/2D-Selective NMDA
Receptor Antagonists

Chapter 3.

Design, Synthesis, and Biological Evaluation of NR2C/2D- selective NMDA Receptor Antagonists

3.1 Statement of Purpose

Ifenprodil was the first described potent and subunit-selective NMDA inhibitor,¹ specifically targeting the NR1/NR2B-subtype of NMDA receptor. This initial finding inspired the development of a plethora of ifenprodil-type analogues (including the Liotta group contributions), which were utilized as both drugs and pharmacological tools. Since ifenprodil's discovery in 1993, greater than 1000 biological studies have been conducted which probe the role of the NR2B subunit in multiple facets of brain function including cognition, synaptic plasticity, neuronal development, and neuropathology (see Chapter 1 and Chapter 2). However, in the past 16 years, no significantly subunit-selective antagonists have been described for NR2A-, NR2C-, or NR2D-containing NMDA receptors. As a result, very little is known about the role of these subunits in both normal brain function and neurological diseases. The Traynelis group sought to identify non-competitive allosteric modulators of NR2C- and NR2D-containing receptors in order to develop pharmacological tools and gain an understanding of the contribution of the NR2C and NR2D subunits to brain function. The goal was to lay the foundation for further expansion, by both chemists and biologists in the research community, in developing a vast knowledge base of the role of NR2C and NR2D antagonists with the first-in-class compounds described herein.

Similar to their effort toward discovering novel NR2B NMDA receptor antagonists, the Traynelis laboratory undertook a massive screening effort of nearly 100,000 compounds to identify NR2C- and NR2D-selective NMDA receptor antagonists. Three classes were identified to study in depth: quinazolin-4-ones (987 series, i.e. **987**, Figure 3.1), phenyl alkylcarbamothioates (1063 series, **1063**, Figure 3.1), and dihydropyrazolquinolines (1105 series, **1105**, Figure 3.1).

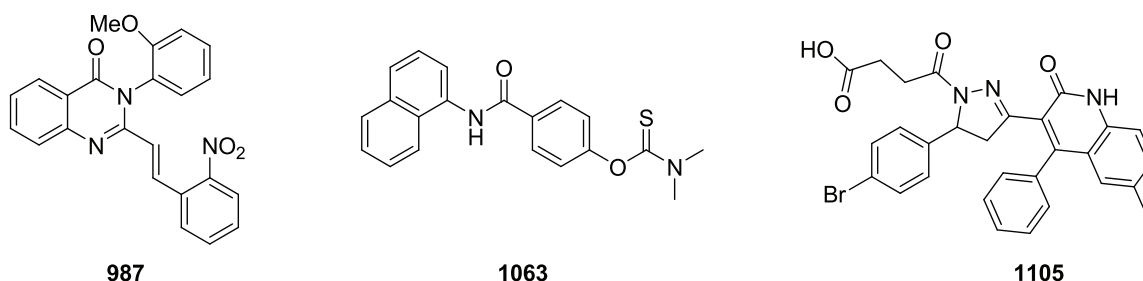


Figure 3.1 Screening hits identified in Traynelis laboratory NR2C/NR2D inhibitor screening effort

The three classes represented distinct chemical scaffolds with differing selectivity towards NR2C/NR2D-containing receptors. The 987 class generally exhibited 5 to 20-fold selectivity for NR2D receptors, the 1105 class exhibited 100-fold, and the 1063 class had greater than 500-fold selectivity. We envisaged exploring the structure activity relationships surrounding each class of inhibitors in collaboration with the Traynelis laboratory. We sought to increase the NR1/NR2D on-target potency of each family of compounds. In addition, exemplary compounds would possess selectivity versus other glutamate family members (AMPA and kainate) and other NR2 subunit-containing receptors. These project goals were achieved using the following strategy:

1. Design and synthesis of novel 987 analogues, with emphasis on improving selectivity and potency.
2. Design and synthesis of novel 1063 analogues, with emphasis on improving stability, and selectivity, and potency.
3. Determination of the important binding interactions of 987 and 1063 compounds on the NR1/NR2D-containing NMDA receptors *in vitro*.
4. Determination of preliminary *in vivo* pharmacokinetic properties of 987 and 1063 compounds.

3.2. Introduction and Background

3.2.1. Previously Developed NR2-subunit selective Antagonists

Despite significant effort, no significantly selective (> 10-fold) inhibitors of NR2A, NR2C-, or NR2D-containing NMDA receptors have been described (Figure 3.2). The highly conserved ligand binding sites for NMDA receptor agonists glutamate and glycine has stymied progress in the development of subunit-selective antagonists among NR2 subunits. Initially **NVP-AAM07** was thought to be a selective glutamate antagonist for NR2A, but subsequent calculations proved the compound to be only weakly selective for NR2A (5-fold).²⁻³ Feng, et al. reported a series of piperazine-based compounds which were 50-fold selective NR2D antagonists.⁴ However, K_i values were estimated for IC_{50} values determined at a single glutamate concentration, this was not agreed to be an accurate measure of selectivity.⁵ A series of novel piperazine-containing glutamate analogues showed weak selectivity for NR2D over NR2A.⁶ Finally, the subunit selective

organic cations discussed in Chapter 1 also show only modest (< 10-fold) selectivity. Thus, while ifenprodil was a first-in-class NR2B-selective antagonist with greater than 400-fold selectivity, there is an obvious lack of sufficiently selective antagonists for NR2A-, NR2C-, or NR2D-containing receptors.

Drug name	Site	Type	2A (μM)	2B (μM)	2C (μM)	2D (μM)	Value	2A/2B	2A/2D	Ref
GV150,526A	glycine	Competitive	0.08	0.08	0.11	0.05	Ki *	1.0 *	1.6 *	Chopra et al 2000
ACEA-1021	glycine	Competitive	0.004	0.004	0.003	0.011	Kb	1.0	0.4	Woodward et al 1995
NVP-AAM07	glutamate	Competitive	15.2	78	--	--	Kb	0.2	--	Frizelle et al 2008
UBP141	glutamate	Competitive	14.2	19.3	4.2	2.8	Ki **	0.7 **	5.1 **	Morley et al 2005
(R)CPP	glutamate	Competitive	0.04	0.27	0.63	2.0	Ki **	0.2 **	0.02 **	Morley et al 2005
(-)-MK-801	pore	Uncompetitive	0.35	0.03	0.04	0.17	IC50	12	2.1	Dravid et al 2007
Dextromethorphan	pore	Uncompetitive	11.3	3.7	1.1	1.5	IC50	3.1	7.5	Dravid et al 2007
Pentamidine	pore	Uncompetitive	0.72	1.5	10.3	9.1	IC50	0.5	0.1	Dravid et al 2007
Ifenprodil	NR2B ATD	Allosteric	40	0.11	29	76	IC50	429	--	Hess 1998

Figure 3.2 Summary of weakly-subunit selective antagonists

* K_i values determined from equilibrium binding displacement curves using the IC_{50} values at a single concentration to estimate affinity. Only the low affinity site is shown.

** K_i values for competitive antagonists estimated from functionally determined IC_{50} values at a single agonist concentration can be complex to interpret, and needs to be confirmed.

3.2.2. Potential use of NR2D-selective NMDA antagonists: Parkinson's disease (PD)

Movement is coordinated by transient excitatory (glutamate-mediated) signals from the thalamus to the pre-frontal cortex (Figure 3.3, Left Panel). The thalamus, in turn, is regulated by a direct and indirect pathway, both originating in the substantia nigra pars compacta (SNc). Under normal physiologic conditions, inhibitory signals (GABA-mediated) regulate the output signaling of the internal global pallidus (Gpi) and external global pallidus (GPe) through the striatum (caudate and putamen structures). The subthalamic nucleus (STN), which receives inhibitory signals from the GPe, sends excitatory signals to the Gpi. The accumulated Gpe and STN signaling result in tonic inhibition of thalamus, which prevents movement from occurring via the pre-

frontal cortex. During movement, the inhibitory control of the SNc on the GPi and GPe is attenuated by simultaneously decreasing inhibitory GABA signaling and increasing excitatory glutamate signaling. Ultimately, decreased inhibition (and thus increased glutamate-mediated excitation) of the thalamus by the GPi results. Lessened thalamic inhibition gives rise to increased thalamo-cortical stimulation which allows voluntary movement.

Parkinson's disease is a neurodegenerative disorder characterized by loss of both dopaminergic neurons in the substantia nigra pars compacta (SNc) and dopaminergic projection terminals which input the striatum (Right Panel, Figure 3.3).⁷ The result is increased inhibitory (i.e. disinhibitory) signaling upon the GPi, resulting in disinhibition of the thalamus. As a result, fewer excitatory signals reach the pre-frontal cortex (decreased thalamo-cortical stimulation) to affect movement. The effects of the malfunctioning pathway can be observed in patients with bradykinesia (slow movement), akinesia (inability to initiate movement), resting tremor, rigidity, and postural disturbances.

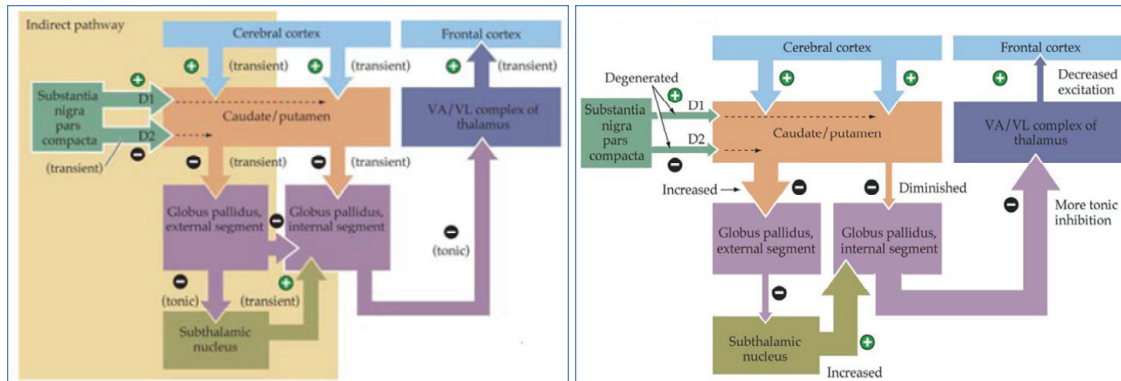


Figure 3.3 Basal ganglionic circuitry of Parkinson's Disease. Left Panel: Normal functioning signalling pathway. Right panel: Parkinson's disease circuitry imbalances. Arrow width is indicative of signal strength

The Traynelis group hypothesized that because PD is characterized by decreased inhibitory signals, the motor deficit could be returned to the proper balance by a concomitant decrease in excitatory signaling. Excitatory signals in the brain are mediated by glutamate receptors, most notably NMDA receptors. In addition, the NR2D subunit is abundantly expressed in basal ganglionic nuclei associated with PD signaling defects including the STN, SNc, GPi and cholinergic striatal interneurons.⁸⁻¹¹ Inhibition of NR2D-containing NMDA receptors in these areas would reduce the overactive output pathways, thus rectifying the circuitry imbalance. NR2D subunits are also found in the SNc, the epicenter of all PD dysfunction.¹²⁻¹³ The hypothesis follows that blockade of glutamate signaling in the SNc could be neuroprotective for dopaminergic neurons and prevent further loss of dopaminergic projections.

3.2.3. Rationale for proposed styryl quinazolone analogues (987 series)

Analysis of the results from the Traynelis NR2C/D screen revealed multiple compounds which contained the styryl quinazolone core. After purchasing a number of commercially available analogues, simple structure activity relationships emerged. One such SAR relationship is illustrated in Figure 3.4.

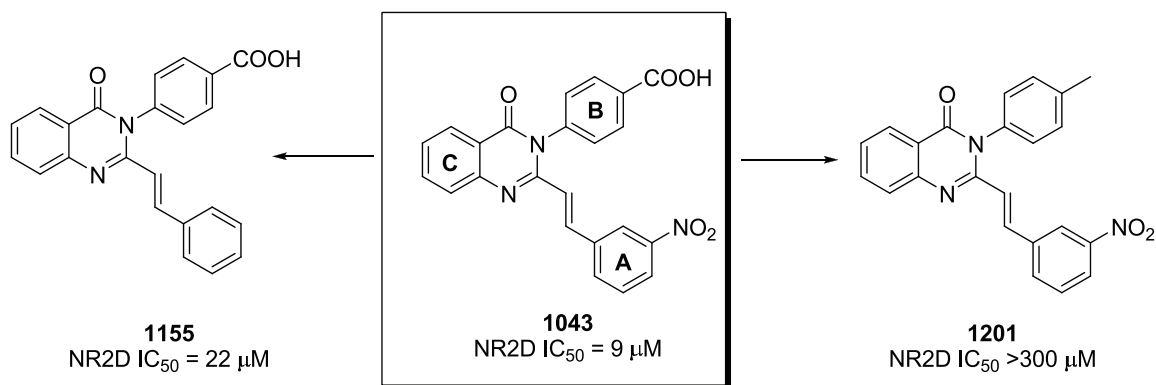


Figure 3.4 Comparison of purchased 987 analogues at NR1/NR2D-containing NMDA receptors

The deletion of the A ring *meta*-nitro group of **1043** resulted in a ca. 2-fold reduction of potency (**1155** $IC_{50} = 22 \mu M$). However, replacement of the B ring *para*-carboxylic acid of **1043** with a methyl group of **1201** gave a complete loss of activity ($IC_{50} > 300 \mu M$). We hypothesized the charge of the carboxylate might be important for binding. Therefore, we proposed to probe the position and substitution of the B ring by first identifying the optimal (*ortho*-, *meta*-, or *para*-) substituent placement (Figure 3.5). Then a number of substituents would be introduced at the above-identified position to determine the effect of neutralizing the charge associated with the carboxylate group found in **1043**.

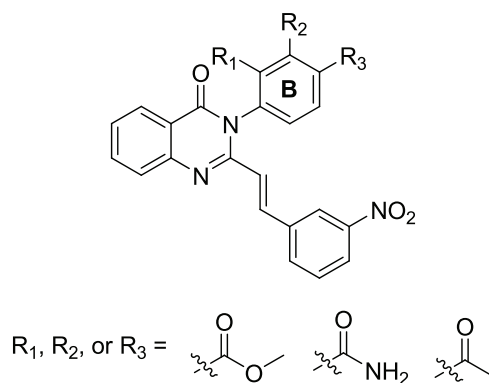


Figure 3.5 Proposed B ring 987 analogues

We were also interested in exploring the structure activity relationships of both the A and C rings. The C ring in particular showed sensitivity to substituents in the course of the biological screen (Figure 3.6). Compound **1116**, with a iodo-containing C ring for instance, exhibited a potency of 600 nM. The parent hydrogen-containing analogue **1043** had an IC₅₀ of 9 μM.

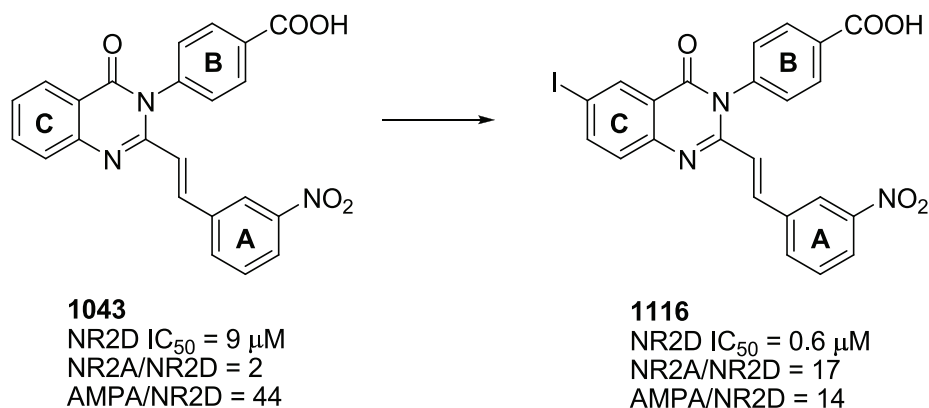
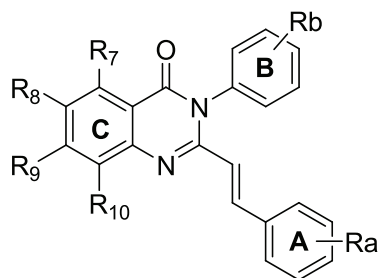


Figure 3.6 Effect of C ring substitution on potency and selectivity

The C ring appeared to dramatically affect potency; hence a number of C ring positional isomers were proposed as well as incorporation of alternative steric and electronic moieties (Figure 3.7).



Proposed R₇ - R₁₀ substituents = F, Cl, Br, Me, -OMe, Ph

Figure 3.7 Proposed C ring 987 analogues

Compounds with a number of other substitutions were also proposed to glean information about tolerated alterations to the A, B, and C rings (see synthesis and results and discussion). The impetus for further compound development was driven by biological results obtained. In summary, we sought to generate a number of 987 analogues to develop the structure activity relationships, with regards to both potency and selectivity, surrounding this scaffold.

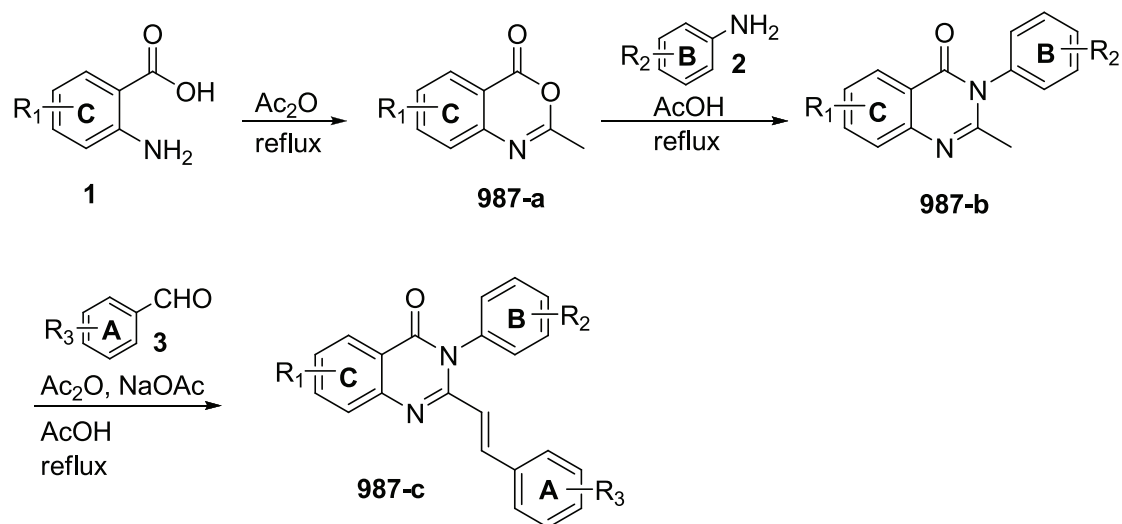
3.3 Synthesis of 987 Analogues

A family of styryl quinazolinones were readily generated via a three-step sequence which combines three simple starting materials: anthranilic acids, anilines, and aryl aldehydes (Scheme 3.1).¹⁴⁻¹⁵

Briefly, a substituted anthranilic acid (**1**) was converted to the benzoxazine-4-one **987-a** by refluxing in acetic anhydride. The quinazolinone core was generated by a ring opening-ring closure reaction under acid-catalyzed conditions. The use of an

appropriately substituted aniline (**2**) yielded compounds of type **987-b**. Finally, an acid-catalyzed aldol-type condensation with the terminal methyl group of the quinazolinone and a substituted aryl aldehyde (**3**) afforded the target (*E*)-3-phenyl-2-styryl-quinazolin-4(3H)-one (**987-c**).

Scheme 3.1 Synthesis of (*E*)-3-phenyl-2-styryl-quinazolin-4(3H)-ones

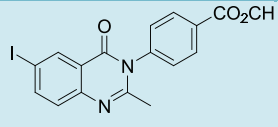
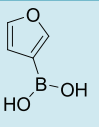
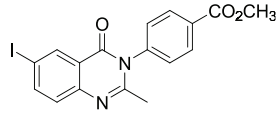
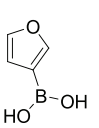


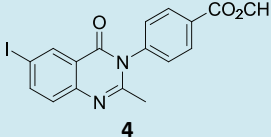
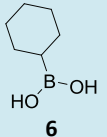
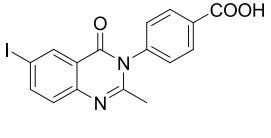
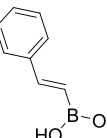
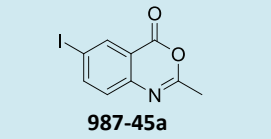
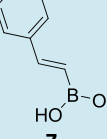
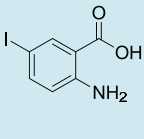
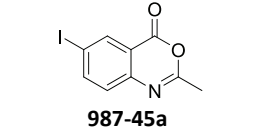
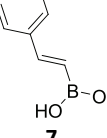
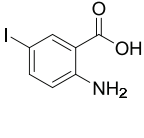
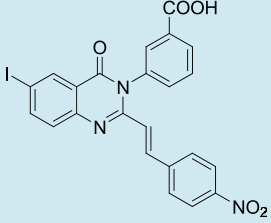
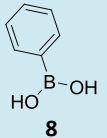
While a number of anilines and aryl aldehydes are readily available, anthranilic acids are more limited in their commercial availability. Suzuki couplings were attempted with the aryl halide styryl quinazolinone final products (**987-c**), as well as intermediate benzoxazinones (**987-a**) and quinazolinones (**987-b**), in an effort to rapidly generate chemical diversity. Both intermediate quinazolinones (**987-b**) and styryl quinazolinone products (**987-c**) are poorly soluble in both organic and aqueous solvents unless heated. Suzuki reactions with a variety of solvents, temperatures, catalysts, organic solvents, and bases were attempted, however isolation of the product proved difficult. Reaction

depended on catalyst, base, microwave conditions, and the presence of a protecting group on the benzoic acid moiety. A sample of attempted reaction conditions is illustrated in Table 3.1.

Protected benzoic acid aryl halide **4** did not react with 3-furan boronic acid (**5**) with either Pd(II) or Pd(0) sources. When **4** was heated in the microwave and reacted with cyclohexylboronic acid **6**, decomposition of **4** occurred. Product was detected in the reaction of unprotected aryl halide **987-45b** with **7** in the microwave with a Pd(II) source. However, pure material was never isolated. Similarly, benzoic acid **987-43** and phenylboronic acid (**8**) underwent Suzuki coupling with sodium carbonate. However, pure product could not be obtained. In both of the above cases isolation involved silica gel chromatography with silica cakes formed from DMF, unfavorable for rapid isolation. Finally, Suzuki reactions with benzoxazinone intermediates (i.e. **987-45a**) resulted in water-catalyzed ring opening resulting from the basic aqueous conditions, ultimately regenerating the starting material anthranilic acids.

Table 3.1 Sample of attempted Suzuki conditions

Aryl Halide	Boronic Acid	Catalyst	Solvent	Base	Temperature	Result
 4	 5	Pd(PPh ₃) ₄	1:1 toluene: DMF	KF	80°C	NR
 4	 5	Pd(PPh ₃) ₂ Cl ₂	1:1 toluene: DMF	KF	80°C	NR

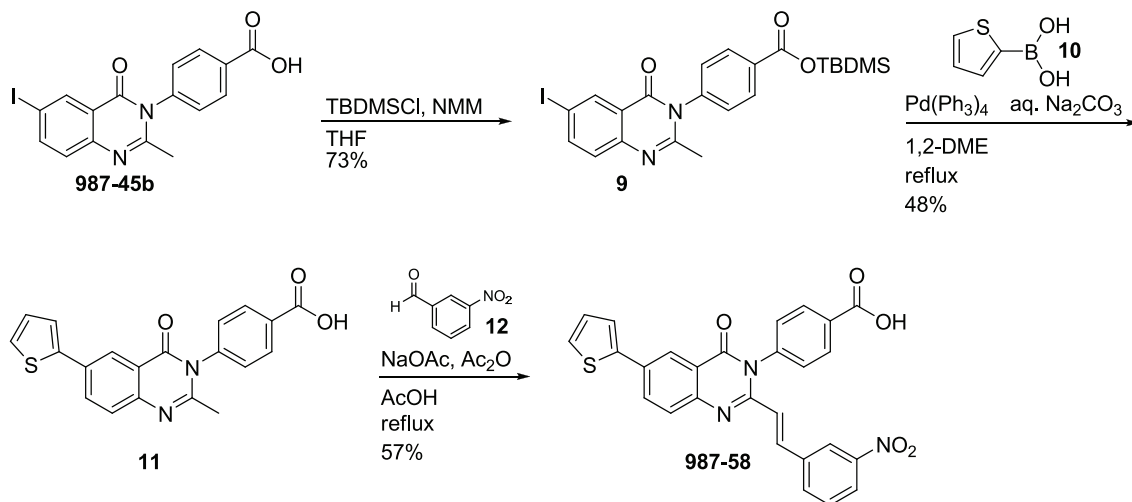
 <p>4</p>	 <p>6</p>	Pd(PPh ₃) ₂ Cl ₂	1:1 acetone: toluene	KF	MW, 180°C, 15 min	Decomposition
 <p>987-45b</p>	 <p>7</p>	Pd(PPh ₃) ₂ Cl ₂	DMF	KF	MW, 180°C, 15 min	41%, impure
 <p>987-45a</p>	 <p>7</p>	Pd(PPh ₃) ₄	1:1 Acetone: toluene	KF	MW, 180°C, 15 min	
 <p>987-45a</p>	 <p>7</p>	Pd(PPh ₃) ₄	1:1 Acetone: toluene	NaHCO ₃	MW, 180°C, 15 min	
 <p>987-43</p>	 <p>8</p>	Pd(PPh ₃) ₄	1:1 Acetone: toluene	NaHCO ₃	80°C	30%, impure

MW = Microwave

The most efficient Suzuki methodology on 987 series intermediates utilized **9**, the TBDMS-protected benzoic acid intermediate (Scheme 3.2). Protection of the carboxylic acid of **987-45b** with TBDMSCl and N-methylmorpholine gave **9**.¹⁶ A Suzuki coupling between **9** and 2-thiopheneboronic acid (**10**) gave the C ring R₈-substituted thiophene quinazolinone **11** in decent yield. The TBDMS protecting group was removed with the addition of 1.0 N HCl during work-up. The condensation reaction with *meta*-nitrobenzaldehyde proceeded in the usual fashion to give **987-58**. Unfortunately, isolation of both **11** and **987-58** require column chromatography by forming silica cakes

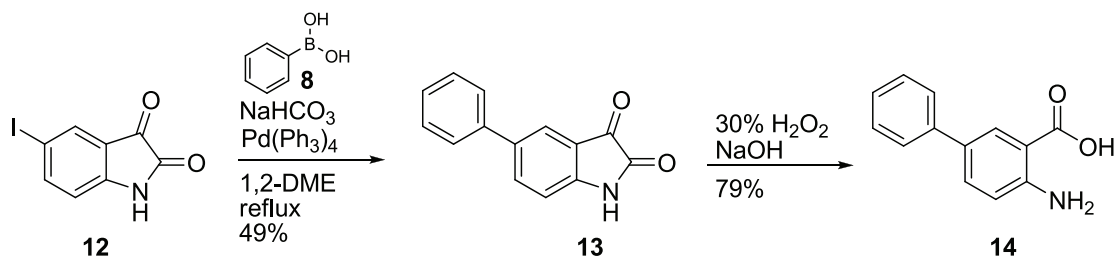
with DMF, which is a time-consuming procedure. Thus, alternative routes of generating chemical diversity were explored.

Scheme 3.2 Synthesis of C ring R₈-thiophene analogue 987-58



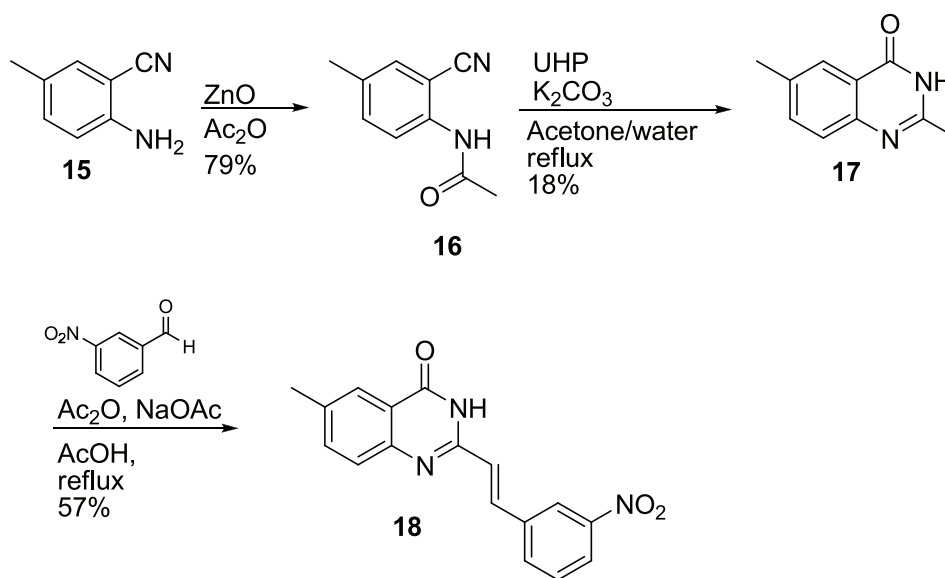
Non-commercially available anthranilic acids were ultimately optimally generated by Suzuki coupling of 5-iodoisatin (**12**) and the appropriate boronic acid (Scheme 3.3). For example, coupling of **12** and **8** afforded functionalized isatin **13**.¹⁷⁻¹⁸ The isatin was then converted to the anthranilic acid (**14**) by oxidation with alkaline hydrogen peroxide.¹⁹

Scheme 3.3 Synthesis anthranilic acids from 5-iodoisatin



Synthesis of 987 analogues lacking the B ring was carried out as illustrated in Scheme 3.4. Solvent-free acylation of aniline **15** with catalytic zinc oxide gave *ortho*-amidobenzonitrile **16** in 79% yield.²⁰ Treatment of **16** with urea hydrogen peroxide (UHP) under basic conditions yielded cyclization to quinazolinone **17**.²¹ Finally, condensation of **17** with *meta*-nitrobenzaldehyde afforded **18**. Unfortunately, this compound was completely insoluble in DMSO and buffer solution, and it was not evaluated for biological activity.

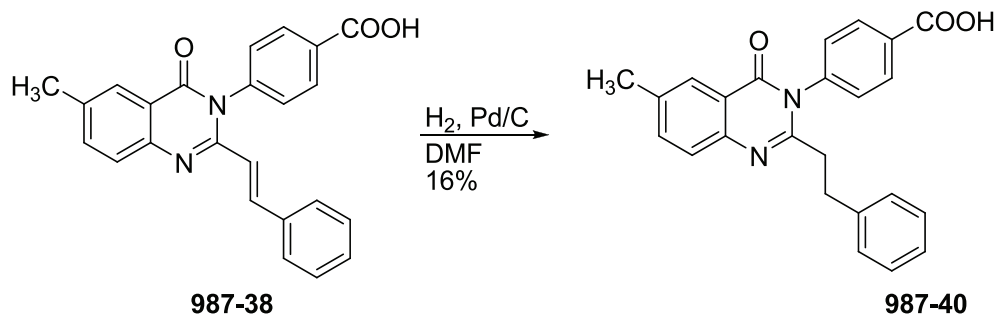
Scheme 3.4 Synthesis of quinazolinone **18**



Synthesis of a 987 compound with saturated linker was prepared as illustrated in Scheme 3.5. Hydrogenolysis of the styryl quinazolinone **987-38** with palladium on carbon catalyst yielded the alkyl linker analogue **987-40**.¹⁴ The non-nitro containing

analogue **987-38** was used to prevent reduction of the (normally present) nitro group during hydrogenolysis. We assumed the relative effect of removing the double bond would remain similar between all 987 compounds.

Scheme 3.5 Synthesis of saturated linker analogue **987-40**



3.4 Results and Discussion

3.4.1. Structure activity relationships of 987 series

Styryl quinazolinones similar to the ones described herein have previously been shown to be potent and relatively selective AMPA receptor antagonists.^{14-15,22-23} In particular, Pfizer disclosed non-competitive antagonist **CP-465,022**, which was developed for the treatment of neurodegenerative diseases (Figure 3.8).

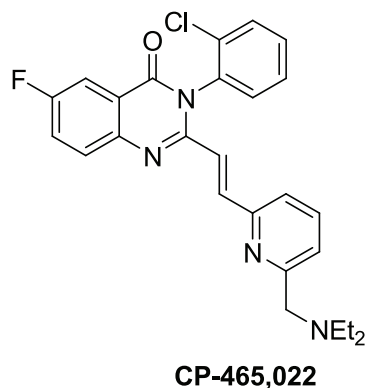
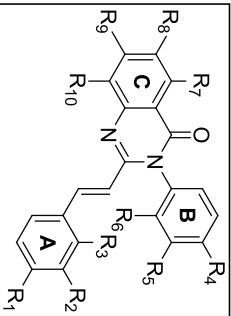


Figure 3.8 Pfizer's styryl quinazolinone AMPA antagonist CP-465,022

The AMPA receptor, like the NMDA receptor, is an ionotropic glutamate receptor.²⁴ We envisaged our quinazolinone compounds could potentially inhibit the AMPA receptor as well as other glutamate receptor family members. Consequently, we tested commercially purchased and synthetic compounds for activity at AMPA, kainate, and all NR1/NR2A-D subtypes of NMDA receptors. We envisaged developing compounds which were selective for both NMDA receptors over AMPA and kainate receptors. In addition, we sought compounds selective for NR2D-containing receptors.

Two-electrode voltage-clamp (TEVC) recordings were performed on *Xenopus* oocytes expressing recombinant rat NR1/NR2A, NR1/NR2B, NR1/NR2C, NR1/NR2D, GluR1, or GluR6 receptors. The biological results of both commercially purchased and synthesized quinazolinones are summarized in Table 3.2 through Table 3.7.

Table 3.2 Optimization of subunit selectivity through evaluation of A and B ring substituents



Number	R ₁	R ₂	R ₃	R ₄	R ₅	R ₆	NR2A IC ₅₀ μM	NR2B IC ₅₀ μM	NR2C IC ₅₀ μM	NR2D IC ₅₀ μM	Glur1 IC ₅₀ μM	Glur6 IC ₅₀ μM	IC ₅₀ NR2A NR2D	IC ₅₀ Glur1 NR2D
1206	NO ₂			COOH			64	93	15	15	>300	NE	4	>20
1208	NO ₂				COOH		135	177	33	27	>300	NE	5	>10
987-26	NO ₂					COOH	>300	197	>300	278	>300	NE	1	1
1043	NO ₂			COOH			21	30	12	9	32	NE	2	4
1160	NO ₂				COOH		100	69	19	15	32	NE	7	2
987-27	NO ₂					COOH	>300	235	258	148	>300	NE	2	2
1422			NO ₂	COOH			11	17	8	6	6	NE	2	1
987-25 [†]			NO ₂		COOH		17	20	8	7	5	NE	2	1
1492	NO ₂			OCH3			>300	98	181	221	>300	NE	1	1
1505	NO ₂				OCH3		>300	>300	>300	>300	120	NE	1	1
1493	NO ₂					OCH3	>300	>300	>300	290	>300	NE	1	1
1503	NO ₂			OCH3			>300	>300	152	168	>300	NE	1	1
1494	NO ₂				OCH3		>300	262	205	186	>300	NE	1	1
1504	NO ₂					CH3	>300	>300	>300	>300	>300	NE	1	1
1127	NO ₂			OCH3			>300	>300	143	125	223	NE	2	2
1126	NO ₂				OCH3		>300	>300	>300	>300	>300	NE	1	1
987	NO ₂					OCH3	4	7	4	5	14	NE	1	3

IC₅₀ values were determined by fitting the Hill equation to average composite concentration-effect curves from 4-20 oocytes injected with NR1/NR2A, NR1/NR2B, NR1/NR2C, NR1/NR2D, Glur1, or Glur6 cRNA. Oocytes were obtained from 1-3 frogs; NE indicates no effect. IC₅₀ values greater than 300 nM are not reported. [†] Prepared by Timothy Acker

Table 3.3 Optimization of subunit selectivity through evaluation of A ring substituents

Number	R ₁	R ₂	R ₃	R ₄	NR2A IC ₅₀ μM	NR2B IC ₅₀ μM	NR2C IC ₅₀ μM	NR2D IC ₅₀ μM	Glur1 IC ₅₀ μM	IC ₅₀ NR2A IC ₅₀ NR2D	IC ₅₀ Glur1 IC ₅₀ NZD
1155				COOH	84	85	39	33	25	3	1
1455	OCH3			COOH	100	98	42	31	250	3	8
1461		OCH3		COOH	24	36	17	9	27	3	3
1467			OCH3	COOH	88	51	32	16	38	6	2
1456	CF3			COOH	61	55	23	15	233	4	16
1506		CF3		COOH	13	26	8	12	22	1	2
1457			CF3	COOH	>300	>300	88	28	>300	>10	>11
1436	OH			COOH	38	35	50	36	110	1	3
1466		OH		COOH	52	30	24	17	24	3	1
1045			OH	COOH	20	18	20	18	36	1	2
1206	NO2			COOH	64	93	15	15	>300	4	>20
1043/987-4		NO2		COOH	21	30	12	9	32	2	4
1422			NO2	COOH	11	17	8	6	6	2	1
987-58*	CH3			COOH	41	300	65	39	>300	1	>7
1469		CH3		COOH	21	34	28	18	>300	1	>17
1462			CH3	COOH	86	93	80	81	62	1	1

IC₅₀ values were determined by fitting the Hill equation to average composite concentration-effect curves from 4-20 oocytes injected with NR1/NR2A, NR1/NR2B, NR1/NR2C, NR1/NR2D, Glur1, or Glur6 cRNA. Oocytes were obtained from 1-3 frogs; NE indicates no effect; IC₅₀ values greater than 300 μM are not reported. * Prepared by Timothy Acker

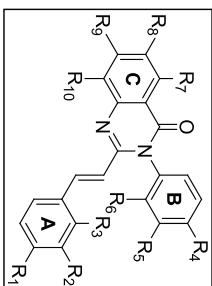
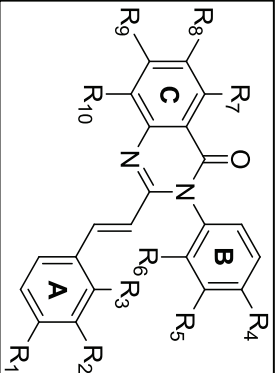


Table 3.4 Optimization of subunit selectivity through evaluation of C ring substituents

Number	R ₁	R ₂	R ₄	R ₇	R ₈	R ₉	R ₁₀	NR2A IC ₅₀ μM	NR2B IC ₅₀ μM	NR2C IC ₅₀ μM	NR2D IC ₅₀ μM	Glur1 IC ₅₀ μM	IC ₅₀ /NR2A IC ₅₀ /NR2D	IC ₅₀ /Glur1 IC ₅₀ /NR2D
987-28	NO ₂	COOH	Cl					>300	110	22	14	>300	>20	>20
987-5	NO ₂	COOH		Cl				16	13	2	1	7	16	7
987-31	NO ₂	COOH			Cl		Cl	32	52	16	15	41	2	3
987-32	NO ₂	COOH					Cl	56	243	12	9	87	6	10
987-30 [†]	NO ₂	COOH			Cl		Cl	224	109	16	10	>300	22	30
987-34 [†]	NO ₂	COOH			Cl		Cl	>300	>300	9	5.8	>300	>50	>50
987	NO ₂	COOH			H			21	30	12	9	32	2	4
987-7	NO ₂	COOH			F			36	33	14	7	7	5	1
987-5	NO ₂	COOH			Cl			16	13	2	7	7	16	7
987-6	NO ₂	COOH			Br			17	13	2	1	8	17	8
1116	NO ₂	COOH			I			18	6	1	0.6	31	30	52
987-11	NO ₂	COOH			CH ₃			12	15	5	2	27	6	14
987-8	NO ₂	COOH			OCH ₃			178	234	5	3	>300	59	>100
987-29 [†]	NO ₂	COOH			NO ₂			NE	NE	204	90	>300	-	-
987-24	NO ₂	COOH			OH			237	>300	43	10	96	24	10
987-35 *	NO ₂	COOH			C ₆ H ₅			11	3	1.8	1.8	5	6	2
987-23 *	NO ₂	COOH			R ₈ -C ₆ H ₄ -R ₉			11	5	2	2	4	6	2
987-54	NO ₂	COOH			R ₈ -OC ₂ H ₄ -O-R ₉			>300	>300	281	213	>300	1	1
987-55	NO ₂	COOH			R ₈ -O-CH ₂ -O-R ₉			112	162	40	36	>300	3	9
987-36	NO ₂	COOH			CH(CH ₃) ₂			101	98	6	7	200	14	29
987-37	NO ₂	COOH			CH ₂ CH ₂ CH ₃			28	18	3	4	50	7	13

IC₅₀ values were determined by fitting the Hill equation to average composite concentration-effect curves from 6-26 oocytes injected with NR1/NR2A, NR1/NR2B, NR1/NR2C, NR1/NR2D, Glur1 cRNA. Oocytes were obtained from 2-5 frogs. IC₅₀ values greater than 300 μM are not reported. NE indicates no effect. * data were fitted with a variable minimum. [†] Prepared by Timothy Acker.

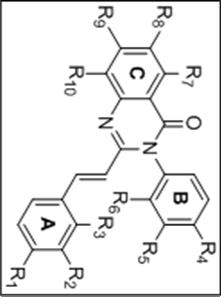
Table 3.5 Substitutions for Ring B carboxylic acid and Ring A nitro groups



Number	R ₁	R ₂	R ₄	R ₈	NR2A IC ₅₀ μM	NR2B μM	IC ₅₀	NR2C μM	IC ₅₀	NR2D μM	IC ₅₀	GIUR1 IC ₅₀ μM	IC ₅₀ NR2A IC ₅₀ NR2D	IC ₅₀ GIUR1 IC ₅₀ NR2D
987-8		NO ₂	COOH	OCH ₃	178	234	>300	5	>300	3	>300	>300	59	>100
987-19		NO ₂	-CN	OCH ₃	>300	>300	>300	>300	>300	>300	>300	>300	1	1
987-20		NO ₂	-COCH ₃	OCH ₃	>300	>300	>300	>300	>300	>300	>300	>300	1	1
987-21		NO ₂	-CONH ₂	OCH ₃	>300	82	>300	58	>300	>300	>300	>300	1	1
987-22		NO ₂	-COOCH ₃	OCH ₃	218	46	>300	39	>300	38	>300	138	6	4
987-13		OCH ₃	COOH	OCH ₃	73	109	>300	18	>300	9	>300	220	8	24
987-16		COOH	COOH	OCH ₃	>300	>300	>300	>300	>300	131	>300	>300	>9	>9
987-18		COOCH ₃	COOH	OCH ₃	113	>300	>300	>300	>300	145	>300	>300	1	2
987-15		COOCH ₃	COOH	OCH ₃	>300	>300	>300	124	>300	52	>300	>300	>6	>6
1206	NO ₂	COOH	COOH	OCH ₃	64	93	>300	15	>300	15	>300	>300	4	>20
1468	-SCH ₃	COOH	COOH		211	79	>300	42	>300	22	>300	244	10	11
1463	-CN	COOH	COOH		94	106	>300	28	>300	34	>300	>300	3	>10
1159	-N(CH ₃) ₂	COOH	COOH		>300	>300	>300	63	>300	53	>300	>300	6	6
1459	-OCHF ₂	COOH	COOH		73	89	>300	33	>300	22	>300	208	3	9
1471	-OCH ₂ CH ₂	COOH	COOH		194	144	>300	111	>300	30	>300	>300	6	>10
1472	-OCH ₂ COOH	COOH	COOH		>300	>300	>300	>300	>300	>300	>300	>300	1	1
1460	COOH	COOH	COOH		>300	>300	>300	>300	>300	>300	>300	>300	1	1

IC₅₀ values were determined by fitting the Hill equation to average composite concentration-effect curves from 6-20 oocytes injected with NR1/NR2A, NR1/NR2B, NR1/NR2C, NR1/NR2D, GIUR1 cRNA. Oocytes were obtained from 1-4 frogs. IC₅₀ values greater than 300 μM are not reported. * data were fitted with a variable minimum.

Table 3.6. Optimization of A and B ring substituents with best C ring substituents

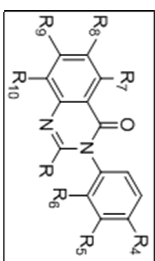


Number	R ₁	R ₂	R ₄	R ₅	R ₆	NR2A IC ₅₀ μM	NR2B μM	NR2C IC ₅₀ μM	NR2D IC ₅₀ μM	GIUR1 IC ₅₀ μM	IC ₅₀ NR2A NR2D	IC ₅₀ GIUR1 NR2D
987-45 *	NO ₂	NO ₂	COOH		I	>300	>300	1.7 *	1.3 *	>300	>150	>150
1116	NO ₂	NO ₂	COOH		I	18	6	1	0.6	31	30	52
987-43	NO ₂	NO ₂	COOH		I	>300	279	9	8	>300	>37	>37
987-44	NO ₂	NO ₂	COOH		I	8	11	1.5	1	21	8	21
987-48	NO ₂	NO ₂	COOH		OCH ₃	197	206	13	7	>300	28	>42
987-8	NO ₂	NO ₂	COOH		OCH ₃	178	234	5	3	>300	59	>100
987-47	NO ₂	NO ₂	COOH		OCH ₃	238	238	21	16	>300	15	>19
987-46	NO ₂	NO ₂	COOH		OCH ₃	208	>300	24	13	289	16	22
987-41	NO ₂	NO ₂	COOH		C ₆ H ₅	>300	42	53	42	>300	>7	>7
987-41	NO ₂	NO ₂	COOH		C ₆ H ₅	>300	40	4	3	287	>100	96
987-35	NO ₂	NO ₂	COOH		C ₆ H ₅	78	324	11	14	146	6	10
987-50	NO ₂	NO ₂	COOH		C ₆ H ₅	28	46	8	5	218	6	44

IC₅₀ values were determined by fitting the Hill equation to average composite concentration-effect curves from 6-20 oocytes injected with NR1/NR2A, NR1/NR2B, NR1/NR2C, NR1/NR2D, GIUR1 cRNA. Oocytes were obtained from 2-5 frogs. IC₅₀ values greater than 300 μM are not reported. * data were fitted with a variable minimum.

Table 3.7 Optimization of linker and A ring substituents

Number	R	R ₄	R ₃	NR2A	NR2B	NR2C	NR2D	GIUR1	IG ₅₀ NR2A	IG ₅₀ GIUR1
				IC ₅₀ μM	μM	IC ₅₀ μM	μM	IC ₅₀ μM	IC ₅₀ NR2D	IC ₅₀ NR2D
987-9	CH ₃	COOH	I	>300	>300	>300	>300	>300	1	1
987-10		COOH	I	53	66	13	4	23	13	6
987-38		COOH	CH ₃	39	25	22	26	21	2	1
987-40		COOH	CH ₃	>300	78	184	282	>300	1	1
1507		COOH		21	31	14	6	>300	4	>50
1157		COOH		3	7	1	1	10	3	10
1508		COOH		63	36	20	11	103	6	9
1437		COOH		25	68	22	6	82	4	14
1427		COOH		>300	122	284	171	>300	1	1
1443		COOH		>300	262	26	16	>300	>18	30



IC₅₀ values were determined by fitting the Hill equation to average composite concentration-effect curves from 6-12 oocytes injected with NR1/NR2A, NR1/NR2B, NR1/NR2C, NR1/NR2D, GIUR1 cRNA. Oocytes were obtained from 1-2 frogs. IC₅₀ values greater than 300 μM are not reported.

Table 3.8 Optimization of B ring substituents of pyridinyl A ring analogues



Number	R ₄	R ₅	R ₆	R ₈	NR2A IC ₅₀ μM	NR2B IC ₅₀ μM	NR2C IC ₅₀ μM	NR2D IC ₅₀ μM	GIUR1 IC ₅₀ μM	IC ₅₀ NR2A IC ₅₀ NR2D	IC ₅₀ GIUR1 IC ₅₀ N2D
1445					40	51	140	35	74	1	2
1447					132	>300	>300	108	>300	1	1
1476	OCH ₃				>300	>300	>300	>300	>300	1	1
1448		OCH ₃			>300	>300	>300	200	>300	1	1
1451			OCH ₃		31	30	3.4	2.5	199	12	80
1474	CH ₃				>300	>300	>300	>300	>300	1	1
1475		CH ₃			>300	>300	241	>300	>300	1	1
1449			CH ₃		>300	156	70	25	83	12	2
1477	NO ₂				>300	>300	204	218	>300	1	1
1478		NO ₂			>300	>300	>300	>300	>300	1	1
1450			NO ₂		206	105	19	4.7	>300	44	64
987.56 [†]	COOH				26	31	5.7	3.9	61	7	16
987.57 [†]		COOH			45	49	7.4	4.3	64	10	15

IC₅₀ values were determined by fitting the Hill equation to average composite concentration-effect curves from 6-12 oocytes injected with NR1/NR2A, NR1/NR2B, NR1/NR2C, NR1/NR2D, GIUR1 cRNA. Oocytes were obtained from 1-2 frogs. IC₅₀ values greater than 300 nM are not reported. [†] Prepared by Timothy Acker.

Positional Isomer Manipulation of Screening Hits **1043** and **987**.

The two most active NR2C/2D inhibitors found in the course of the library screen (**1043** and **987**) were inactive at kainate receptors, and 4-5-fold more potent (i.e. lower IC₅₀) at NMDA receptors than AMPA receptors (Table 3.2). To evaluate whether we could improve the selectivity for NMDA receptors over AMPA receptors, positional isomer combinations of both **987** (A ring R₃ = NO₂, B ring R₆ = OMe) and **1043** (A ring R₂ = NO₂, B ring R₄ = COOH) were evaluated (Table 3.2). All isomers of A and B ring substitution led to significantly decreased potency (increased IC₅₀ values) compared to the screening hit **987**, and thus no further work was conducted within this series. Two positional isomeric analogues of compound **1043** appeared to inhibit responses fully with IC₅₀ values of 15 μM (**1206**) and 6 μM (**1422**), both notably contained a *para*-carboxylic acid B ring substituent despite differential *ortho*-, *meta*-, or *para*-substitution of the A ring nitro group. This suggested optimal placement of the *para*-carboxylic acid B ring substituent would likely yield the most active analogues within this scaffold. Moreover, a number of these compounds showed improved selectivity for NMDA receptors over the AMPA receptor GluR1, as well as improved selectivity for NR2D-containing receptors over receptors containing the NR2A subunit, although the substitution patterns controlling these effects are unclear. The IC₅₀ values for inhibition of NR2C- and NR2D-containing receptors were more similar than those for NR2A- and NR2B-containing receptors. These initial experiments suggested that it might be possible to identify derivatives within this class that selectively inhibit NR2C/D-

containing receptors compared to AMPA, kainate, or NR2A/B-containing NMDA receptors.

The effect of substituent position and identity on rings A, B, and C

To further evaluate the effects of different aryl ring substituents, we measured the IC_{50} values for inhibition at NR1/NR2A, NR1/NR2B, NR1/NR2C, NR1/NR2D, and GluR1 receptors expressed in *Xenopus* oocytes. The position of a variety of A ring substituents was tested while holding the B ring substituent constant ($R_4 = \text{COOH}$), as this proved to be the optimal positioning with respect to potency (Table 3.3). Given the lack of any detectable activity at recombinant kainate receptors (Table 3.2), responses at GluR6 were not studied further. Substitution at the *meta* position (R_2) modestly improved potency at NR2D-containing receptors among analogues containing methoxy (**1461**), trifluoromethyl (**1506**), methyl (**1469**), and hydroxyl (**1466**) A ring substituents, while *ortho*- (R_3) and *meta*- positions are nearly equivalent for nitro-containing analogues (**1043**, **1422**).

The positional preference for C ring substitutions was explored utilizing chlorinated derivatives while retaining optimal A ring ($R_2 = \text{NO}_2$) and B ring ($R_4 = \text{COOH}$) substitutions (Table 3.4). Substitution at position R_8 , specifically compound **987-5**, gave both improved potency ($IC_{50} = 1 \mu\text{M}$) and selectivity ($IC_{50} \text{ 2A/2D} = 16$) for mono-substituted compounds. Interestingly, the R_8, R_{10} -dichloro compound **987-30** showed enhanced NR2D selectivity ($IC_{50} \text{ 2A/2D} = 22$) with decreased on-target potency ($IC_{50} = 10 \mu\text{M}$).

Evaluation of a series of R₈ C ring substituents revealed a correlation between van der Waals radii of the series H, F, Cl, Br, I and both the IC₅₀ value at NR1/NR2D ($r = -0.96$; $p < 0.01$; Fig. 9) and the selectivity for NR2D over NR2A ($r = 0.91$; $p < 0.03$). In particular, the iodinated derivative **1116** inhibited NR1/NR2D receptor responses with an IC₅₀ value of 600 nM and is 18- and 52-fold selective over NR2A and AMPA GluR1 receptors, respectively (Table 3.4).

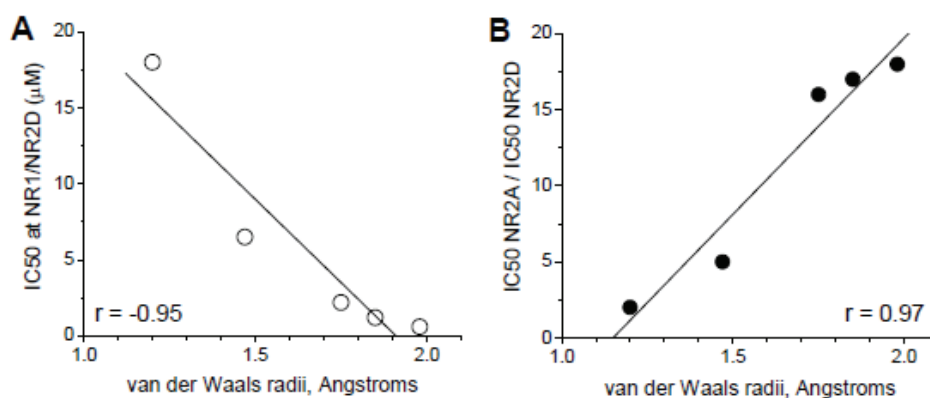


Figure 3.9 Correlation between van der Waals radii and both potency and selectivity of 987 series. Panel A: A plot of IC₅₀ value determined in two electrode voltage clamp recordings from *Xenopus* oocytes versus the C ring R₈ side chain van der Waals radii, which were 1 Å for hydrogen, 1.47 Å for fluorine, 1.75 Å for chlorine, 1.85 Å for bromine, and 1.98 Å for iodine ($r = -0.96$, $p < 0.01$). Panel B: Plot of selectivity, defined here as IC₅₀ at NR1/NR2A divided by the IC₅₀ at NR1/NR2D, versus the side chain van der Waals radii ($r = 0.91$, $p < 0.03$).

It is unclear whether the increased potency and selectivity of **1116** can be attributed to an electropositive effect or a steric effect. Consistent with a steric effect, we observed that other analogues containing large R₈ substituents also improve NR2D apparent selectivity such as R₈ = Ph (**987-35**) and R₇,R₈-naphthyl (**987-23**) when it is assumed that inhibition is complete at saturating concentrations. However, the inhibition curves with these larger hydrophobic substituents were shallow, and often

revealed incomplete inhibition. Fitting the concentration-effect data for these compounds with a variable minimum (see Experimental detail) resulted in little difference in potency between the various NR2 subunits (see IC₅₀ values in Table 3.4). However, the fitted curves do reveal striking differences in degree of inhibition. For example, **987-23** is predicted to reduce responses at saturating concentrations for receptors containing NR2A, NR2B, NR2C, or NR2D to 68, 50, 26, or 20% of control respectively. Similarly, **987-35** is predicted to reduce responses at saturating concentrations for receptors containing NR2A, NR2B, NR2C, or NR2D to 68, 51, 22, or 14% of control, respectively. These classes of compounds were not studied further.

Robust combined selectivity for NR2D over NR2A, NR2B and GluR1 was achieved with the R₈ = OMe derivative **987-8** (IC₅₀ = 3 μM), which was greater than 100-fold selective for NR1/NR2D over GluR1. This compound series is characterized by poor solubility above 100 μM, thus we were unable to attain an accurate measure of IC₅₀ value at AMPA receptors. Therefore it is possible that **987-8** is even more selective for NR2D over AMPA than our conservative estimate. IC₅₀ values for **987-8** at NR2C were similar to those at NR2D. Likewise, IC₅₀ values at NR2A were typically similar to NR2B, and were greater than 50 fold higher than at NR2C/D containing receptors (Table 3.4).

We subsequently tested the effect of altering the nitro and carboxylic acid substituents on the A and B rings respectively, for compounds with C ring OMe at R₈ (Table 3.5). Replacement of the *p*-carboxylic acid functionality on the B ring with a methyl ester (**987-22**), amide (**987-21**), nitrile (**987-19**), or ketone (**987-20**) moiety led to compounds that were either substantially less potent or inactive (Table 3.5). These

results suggest an anionic component, such as in the carboxylate of **987-8**, which would be anionic at physiologic pH, is crucial for binding. Similar results were found for substitutions of the A ring nitro group. With the exception of $R_2 = \text{OMe}$ (**987-13**, $\text{IC}_{50} = 9 \mu\text{M}$), no other functional groups exhibited similar potency compared to **987-8**. Only modest activity was maintained a *para*-nitro substituents on the A ring (Table 3.5). These data suggest the binding pocket prefers the electron rich nitro and carboxylic acid groups on rings A and B, respectively.

Although compounds with $R_2 = \text{NO}_2$ (**1043**) and $R_3 = \text{NO}_2$ (**1422**) A ring substitution gave the best potency, improved selectivity for NMDA over AMPA receptors was noted for $R_1 = \text{NO}_2$ analogues **1206** and **1208** in (Table 3.2), as well as modestly improved selectivity for NR2D over NR2A with $R_5 = \text{COOH}$ B ring substitution (**1160** in Table 3.2). This led us to perform a systematic comparison of ring substituents among these two positions (A ring: $R_1, R_2 = \text{NO}_2$; B ring: $R_4, R_5 = \text{COOH}$) for our most potent and selective ring C substitutions where R_8 was iodo, methoxy, and phenyl. Table 3.6 summarizes data describing these compounds, fitted as described in the methods. The best potency was obtained for compounds with *para*-carboxylic acid substitution on the B ring ($R_4 = \text{COOH}$), in particular compounds **1116**, **987-8**, and **987-41**. Among iodo-substituted compounds, **987-45**, which contains a *para*-nitro A ring ($R_1 = \text{NO}_2$), inhibited NR2C/D containing receptors with the best apparent selectivity over NR2A, NR2B or AMPA receptors. However, the low solubility of this compound prevented an accurate determination of its ability to inhibit NR2A, NR2B, and GluR1 AMPA receptors. **987-45** required addition of $1 \mu\text{M}$ 2-hydroxypropyl- β -cyclodextrin at

concentrations above 10 μM to prevent precipitation, and it is possible concentrations in free solution were below nominal levels. Inhibition by **987-45** at NR1/NR2C and NR1/NR2D was incomplete, leading us to fit the data with a variable minimum (see Methods), which was on average 31% and 26% of control, respectively.

Effect of changes to the backbone on subunit selectivity and potency at NR2C/D receptors

Modifications to the styryl A ring linker were also explored to determine the nature of the backbone structure in terms of both potency and subunit selectivity (Table 3.7). Complete removal of ring, as in compound **987-9**, which contains merely the quinazolin-4-one core structure, resulted in a total loss of activity with an IC_{50} value of greater than 300 μM . We further investigated the saturation level of the styryl linker between the A ring and the quinazolin-4-one core structure. Reduction the styryl linker of **987-38** (No A ring substitutions, B ring: *p*-carboxylic acid, C ring: R₈ methyl; IC_{50} 26 μM) to the fully saturated linker analogue **987-40** (IC_{50} 282 μM ; Table 3.6) resulted in 10-fold potency reduction. These data suggest the geometry of the *trans*-unsaturated linker is preferred for binding. Incorporation of larger ring systems pendant to the C ring led to compounds with modest activity, as shown by the various naphthyl derivatives **1508**, **1157**, **1507**, and **1437**, as well as phenyl-1,4-dioxane compound **1443** (Table 3.7), suggesting the presence of an extended space in the binding pocket for hydrophobic interactions with larger hydrophobic groups.

Replacement of the phenyl A ring with a 3-pyridyl system also induced increased potency. Further evaluation of 3-pyridyl A ring analogues was conducted for the most potent R₈ C ring iodine substitution (Table 3.8). Compound **1451** with an (R₆ = OMe) exhibited reasonable potency (IC₅₀ 2.5 mM) with modest selectivity (12-fold) over NR2A and good selectivity over GluR1 (80-fold). Introduction of a carboxylic acid at position R₅ (**987-56**) or R₆ (**987-57**) gave reasonable potency; however selectivity over NR2A and GluR1 was only modest.

3.4.2. In vitro analysis of 987 series mechanism of action and binding interactions

Inhibition by 30 μM of compound **1043** at NR1/NR2D receptors (33±0.6% control) could not be surmounted by increasing the concentration of glutamate and glycine from 100/30 μM to 1000/300 μM (31±0.7% control; n=4; Fig. 3.10A). The fitted inhibition curve for **1043** predicted complete inhibition at saturating concentrations (fitted minimum was <0.1%; Figure 3.10B). Inhibition of NR1/NR2D responses by 10 μM of compound **1043** appeared voltage-independent over the range of -60 to +50 mV, with no significant difference in inhibition at -40 mV compared to +40 mV (p>0.05; n=5; Fig 3.10C). Inhibition of NR1/NR2C receptors by compound **1043** was similarly complete at saturating concentrations (n=8), non-competitive (n=6), and voltage-independent (n=6). These data suggest that quinazolin-4-ones are noncompetitive antagonists of NMDA receptors that likely act at a site independent of the channel pore.

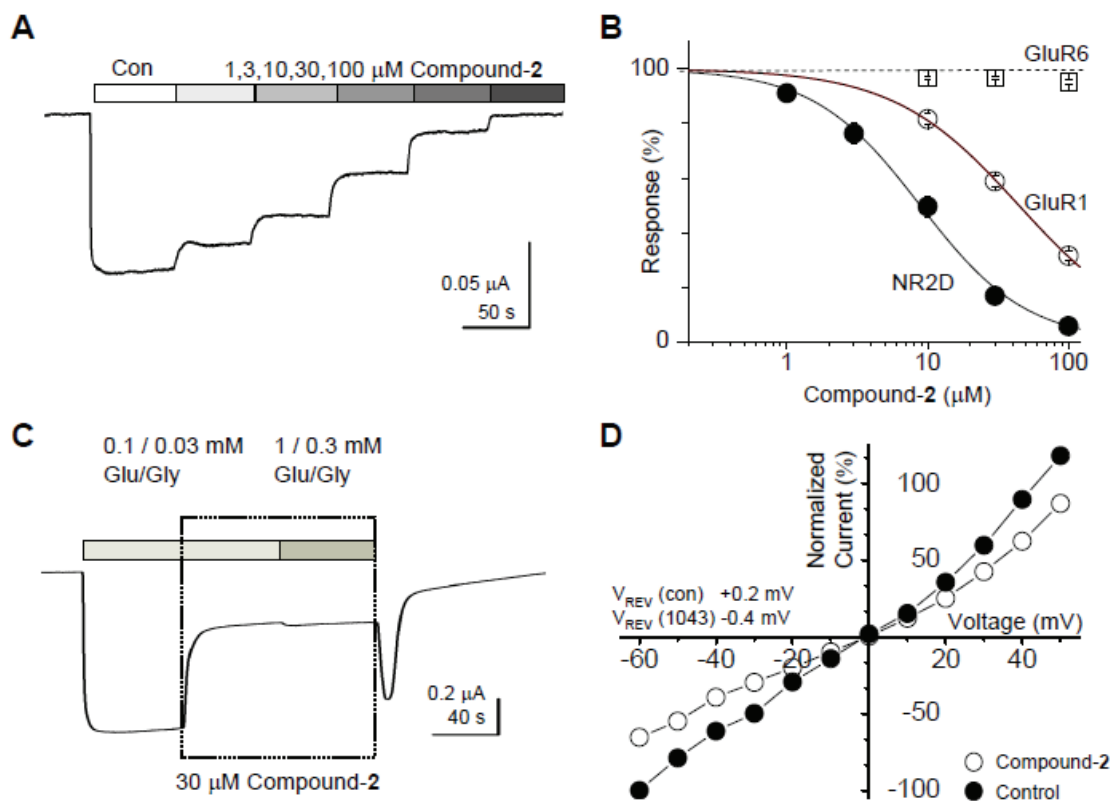


Figure 3.10 *In vitro* analysis of 987 class: Panel A: Representative current recording from a *Xenopus* oocyte expressing NR1/NR2D in response to 100 μM glutamate / 30 μM glycine plus increasing concentrations of 1043 (compound 2). Panel B: Composite concentration-effect curves for 1043. Panel C: Representative current recording showing that inhibition by 1043 cannot be surmounted by increasing concentrations of agonist, suggesting inhibition is non-competitive (n=4). Panel D: Current-voltage relationship for responses to glutamate plus glycine (100 μM and 30 μM , respectively) in the absence and presence of 10 μM 1043 suggesting that inhibition is voltage-independent.

To gain insight into where 987 series compounds bind on the NR2D subunit of the NMDA receptor, the Traynelis lab performed a number of chimera experiments (Figure 3.11). Transfer of the S2 region of the ligand binding domain from NR2D to NR2A receptors conferred enhanced response to **1116**. By contrast, transfer of the S1 region from NR2D to NR2A did not alter receptor sensitivity to **1116**. These results indicate 987 series interactions with the S2 domain is responsible for receptor inhibition.

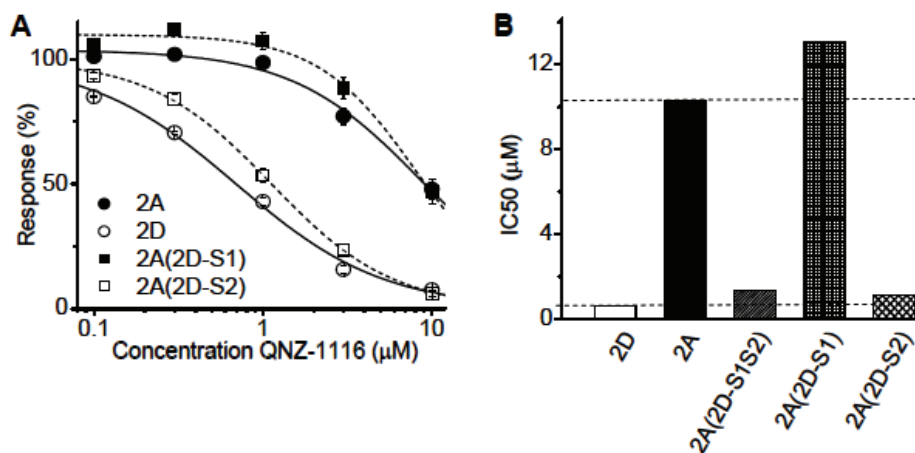


Figure 3.11 Mutagenesis studies of 987 class compounds. Panel A: replacement of the S2 region in NR2A with that of NR2D confers sensitivity to 1116. Panel B: IC₅₀ values represented in panel A.

The NR2D S2 domain encompasses both part of the lower lobe of the ligand binding domain, the linker region between the ligand binding domain and the transmembrane helices, and the M3 transmembrane helix (Figure 3.12, A and B). Interestingly, binding of AMPA-selective compound **CP-465,022** has been localized to the linker region between the S2 region and the M3 helix. The similar locations between our NMDA-selective quinazolinones and Pfizer's AMPA-selective quinazolinones suggest that the glutamate receptor family may have a conserved pharmacophore for quinazolinone-type compounds which can be tuned towards NMDA or AMPA activity based on A, B, and C ring substituents.

In addition, molecular dynamics simulations suggest the S2 region exhibited the greatest structural differences between NR2A and NR2D receptor subtypes (Figure 3.12, C).²⁵ In light of this information, it is not unexpected that we achieved selectivity for NR2D over NR2A most readily.

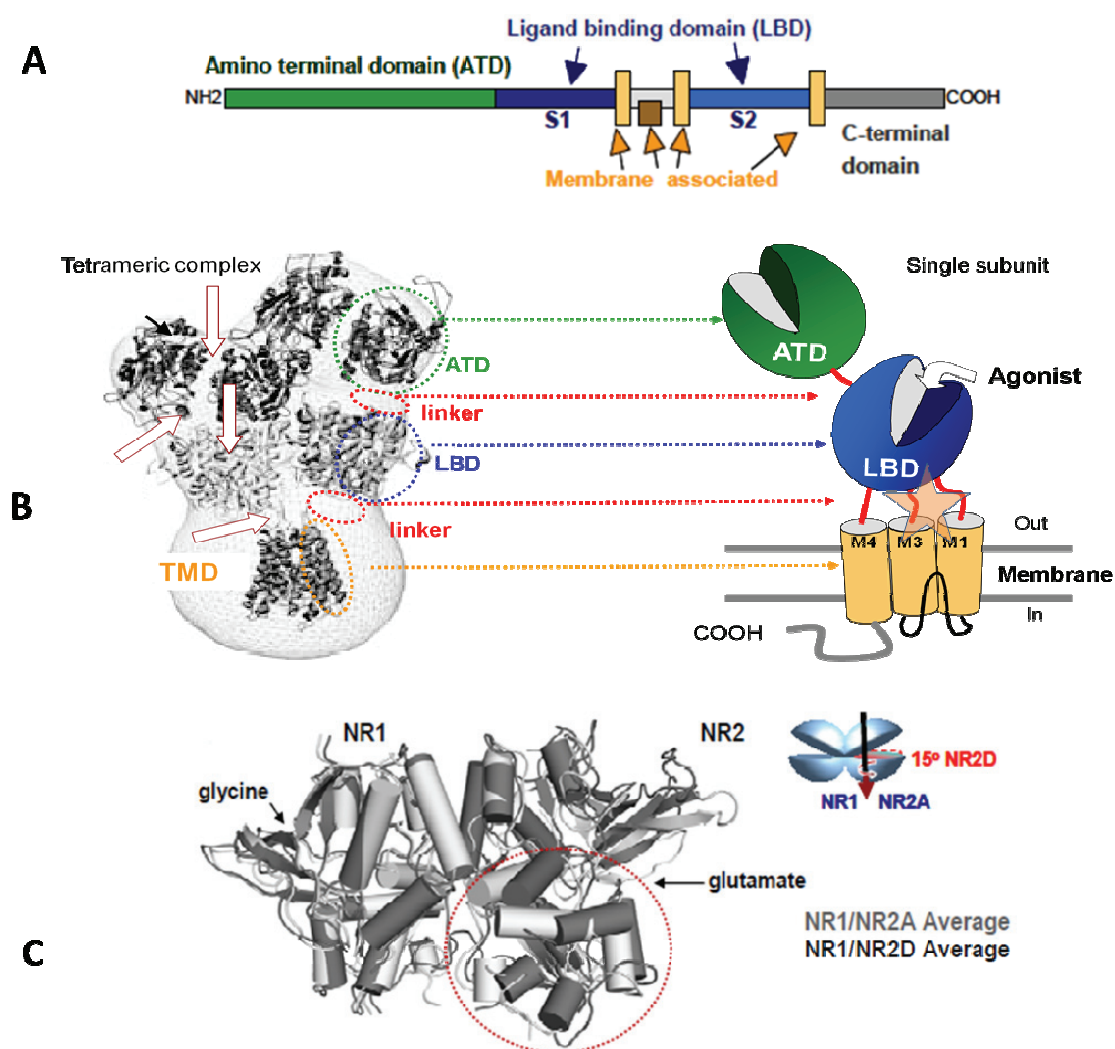


Figure 3.12. Proposed binding site of 987 series compounds. Panel A: NMDA receptor architecture of linearized protein. Panel B: tetrameric architecture of NMDA receptor, adapted from AMPA receptor crystal structure.²⁶ Each domain is mapped onto one NMDA subunit, illustrated in the right panel. Colors coordinate with panel A. The orange star represents the proposed binding site of 987 class compounds. Panel C: Average structure for NR1/NR2D after 15 ns molecular dynamics simulation at 300K built from NR1/NR2A crystal. Superposition of NR1/NR2A and NR1/NR2D show divergence in S2 region, which is actually a 15° counterclockwise rotation (modified).²⁵

3.5 Conclusions

These data show that a previously unknown and novel pharmacophore exists in the S2 domain on the NMDA receptor, at which modulators can act with strong

selectivity for NR2C/D subunits. The two most potent and selective compounds in terms of inhibition of NR2C/D-containing receptors to emerge from these experiments are compounds **987-8** and **987-45** (Figure 3.13). Both **987-8** and **987-45** are highly selective over AMPA and kainate receptors. Compound **987-8** is over 50-fold selective for NR2D over NR2A/B, and 100-fold selective over GluR1. Compound **987-45** also appears to be highly selective over NR1A/B-containing receptors; however we cannot tell the full selectivity profile given the low solubility above 10 μM as well as the apparent incomplete inhibition (Figure 3.13). Although we did not identify compounds more potent **1116** (600 nM), we did significantly improve selectivity of the 987 series through medicinal chemistry efforts. The selectivity exhibited by **987-8** and **987-45** represents a significant improvement over the 20-fold selectivity observed with initial screening hits.

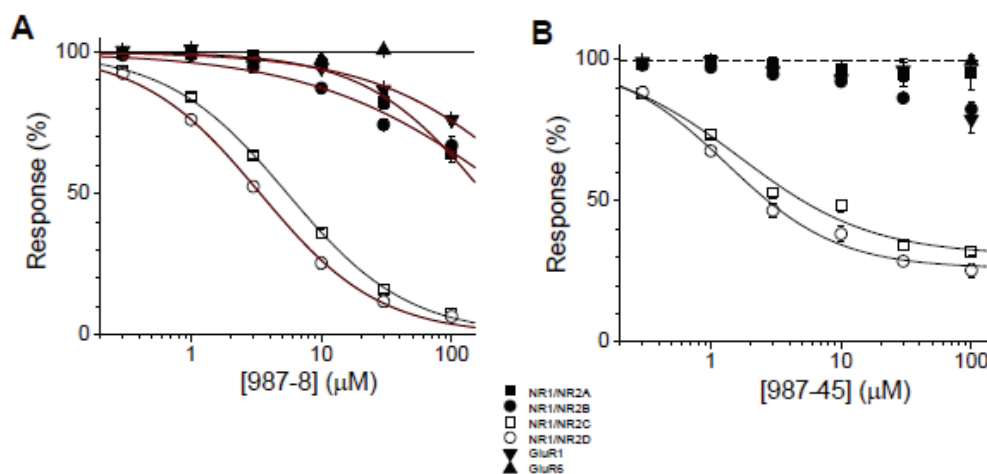


Figure 3.13 Concentration-effect curves for more selective 987 series compounds. Panel A: IC₅₀ curves for 987-8. Panel B: IC₅₀ curve for 987-45.

Overall, this class of compounds is characterized by poor aqueous solubility. As a result, undetectable precipitation during the biological evaluation may have occurred, reducing the actual concentration of compound in solution. Consequently, the compounds discussed here may be more selective than we have conservatively reported.

These compounds represent the first set of non-competitive antagonists at NR2C- and NR2D-containing receptors with selectivity for NMDA receptors containing NR2C/D subunits over receptors containing NR2A/B subunits. Further work on this pharmacophore is ongoing to yield compounds with improved potency and heightened selectivity over other members of the glutamate receptor family.

3.6 Introduction and rationale for naphthylphenyl carbamothioate analogues (1063 series)

A second class of inhibitors to emerge from the Traynelis NR2C/2D screening effort was the 1063 series (Figure 3.14), characterized by a centrally located *para*-substituted phenyl ring. The left (A side) of the compound contained a naphthyl amide, and the right (B side) contained a carbamothioate.

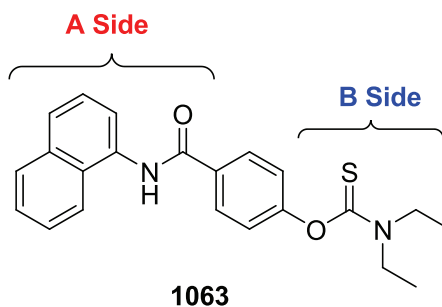


Figure 3.14 Hit compound 1063 found during NR2C/2D screening effort

Compound **1063** showed significantly enhanced selectivity compared to the quinazolinones previously described (Figure 3.15). While medicinal chemistry efforts increased selectivity from 20 to 50-100 fold in the 987 series, screening hit **1063** exhibited NR2D selectivity of greater than 500-fold.

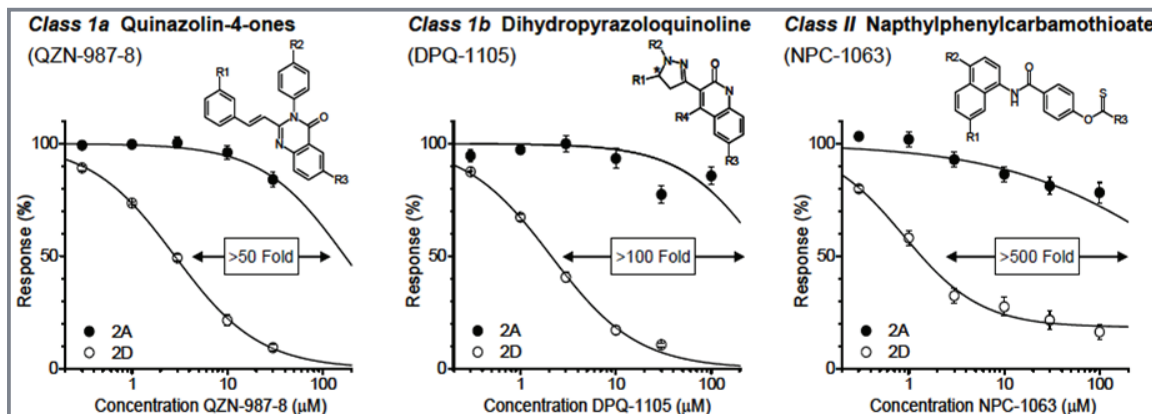


Figure 3.15 Selectivity comparison of 987, 1105, and 1063 class NR2C/2D inhibitors

The 1063 class offered a number of advantages over the aforementioned 987 class as a starting to explore structure activity relationships. In addition to the increased selectivity observed by the screening hit, the compounds were hypothesized to have enhanced solubility compared to the ionic 987 class. As a result, we envisaged obtaining

more accurate measurements of selectivity among glutamate receptors, which would aid in guiding future medicinal chemistry efforts more efficiently than in the 987 series. As well as increased solubility, the heightened hydrophobicity of the compound suggested blood brain barrier permeation was more likely than with the quinazolinones. Finally, initial mutagenesis studies indicated the 1063 class bound to the NR2D subunit in a location distinct from the 987 class. Thus, analysis of 1063 and related antagonists would lead to the elucidation of two novel NR2D allosteric binding sites.

Initial biological analysis suggested **1063** was unstable in buffer solution over time. While freshly dissolved samples of **1063** gave excellent potency and selectivity in NR2D antagonism assays, after 30 minutes in solution the inhibition became aberrant and diminished. We hypothesized the carbamothioate was degrading *in vitro*, and proposed replacing this moiety with the corresponding N,N-diethylcarbamate **1063-2** (Figure 3.16). Pharmacology dogma suggests sulfur is rapidly oxidized to oxygen in biological systems,²⁷⁻³⁰ and thus carbamate **1063-2** would most likely represent the a high percentage of species present, were 1063 to be dosed in animal models.

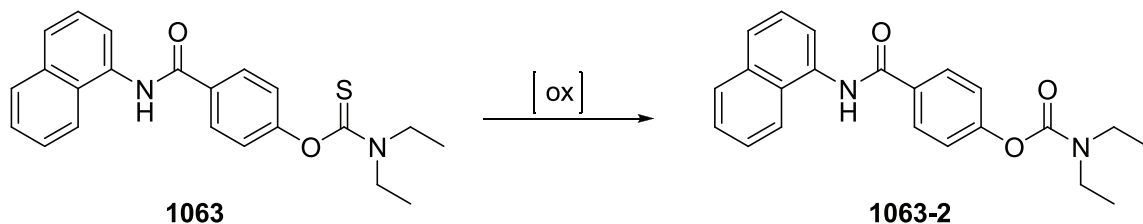


Figure 3.16 Proposed sulfur to oxygen oxidation of 1063

We also envisaged analysis of a number of B side modifications. In particular, we were interested in exploring multiple X,Y,Z configurations of the parent carbamothiate. This included the introducing ureas, esters, and carbamates as the B side carbamothioate replacement to affect stability, hydrogen bonding, and conformational flexibility. We hypothesized varying the N-alkyl substituents pendant to the XYZ moiety would allow us to probe a number of conformations as well. Contraction, extension, and rigidification would be analyzed through a number of alkyl analogues (R_1 in Figure 3.17).

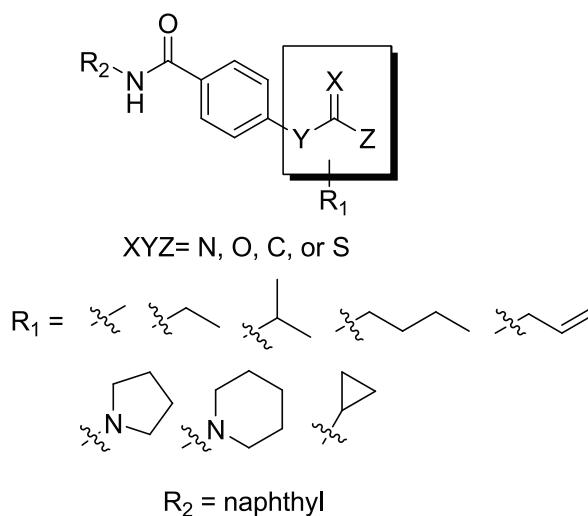


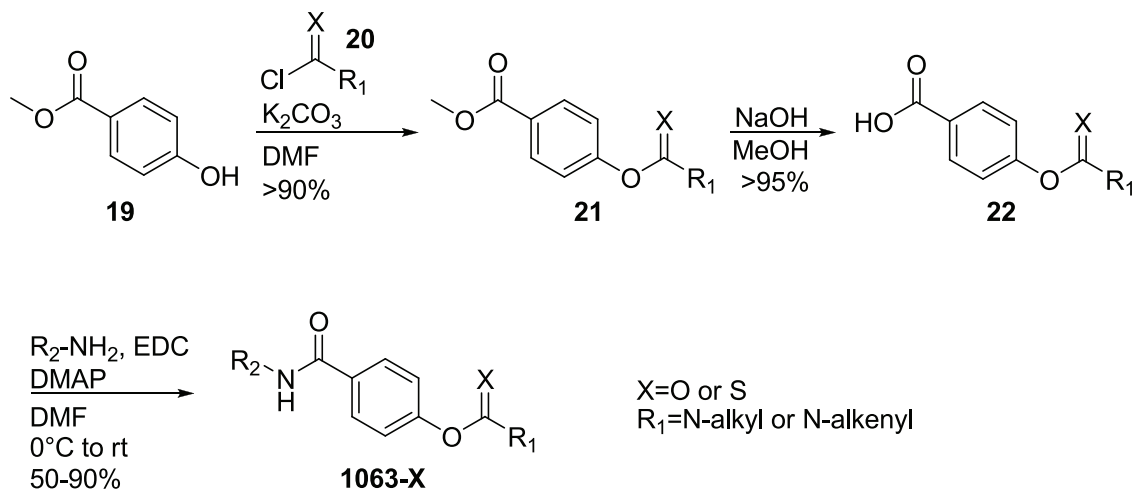
Figure 3.17 Proposed analogues of 1063 series

3.7 Synthesis of 1063 Analogues

The proposed compounds were prepared by one of two general routes, depending on the B side moiety.

For compounds containing carbamates and thiocarbamates, analogue synthesis was accomplished as illustrated in scheme 3.6.

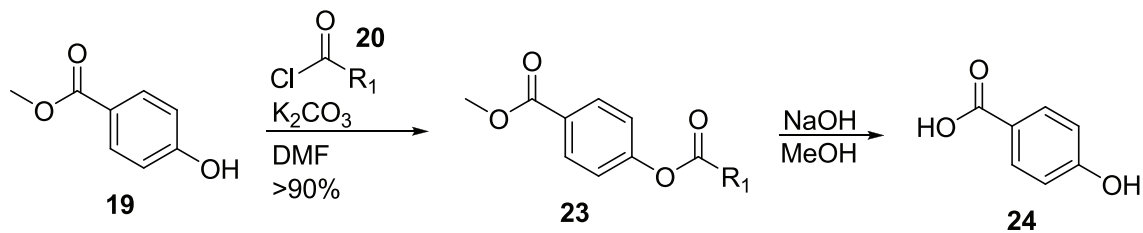
Scheme 3.6 Synthesis of thiocarbamate and carbamate 1063 analogues



Methyl paraben (**19**) was allowed to react with the appropriate electrophilic chloride species, either a carbamoyl chloride or thiocarbamoyl chloride, to give the corresponding carbamate or carbamothioate (**21**). Saponification of the methyl ester yielded benzoic acid **22**. Finally, **22** was coupled to an arylamine using EDC to give the 1063 analogue.

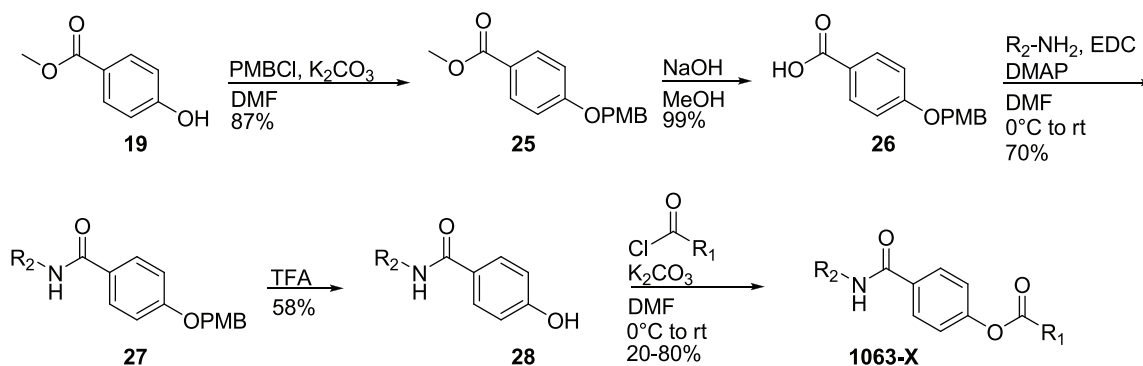
Attempts to synthesize esters via the above route led to saponification of both A and B side esters during hydrolysis of **23** to give the undesired phenol **24** (Scheme 3.7).

Scheme 3.7 Failed syntheses of ester 1063 analogues via saponification



To prevent saponification of the desired B side ester functionality, the phenol was protected, and the order of the reaction sequence was reversed compared with Scheme 3.6 (Scheme 3.8). Protection of **19** as the *para*-methoxybenzyl (PMB) ester afforded **25**, which was saponified to give benzoic acid **26**. Carbodiimide-mediated coupling with naphthylamine yielded **27**. Deprotection of the PMB group was achieved readily with trifluoroacetic acid, however preparative HPLC was required to obtain pure phenol **28**. Final 1063 compounds were then afforded from acylation of **28** with acyl chlorides. Compound **28** was also allowed to react with carbamoyl chlorides, which generated additional carbamate 1063 analogues.

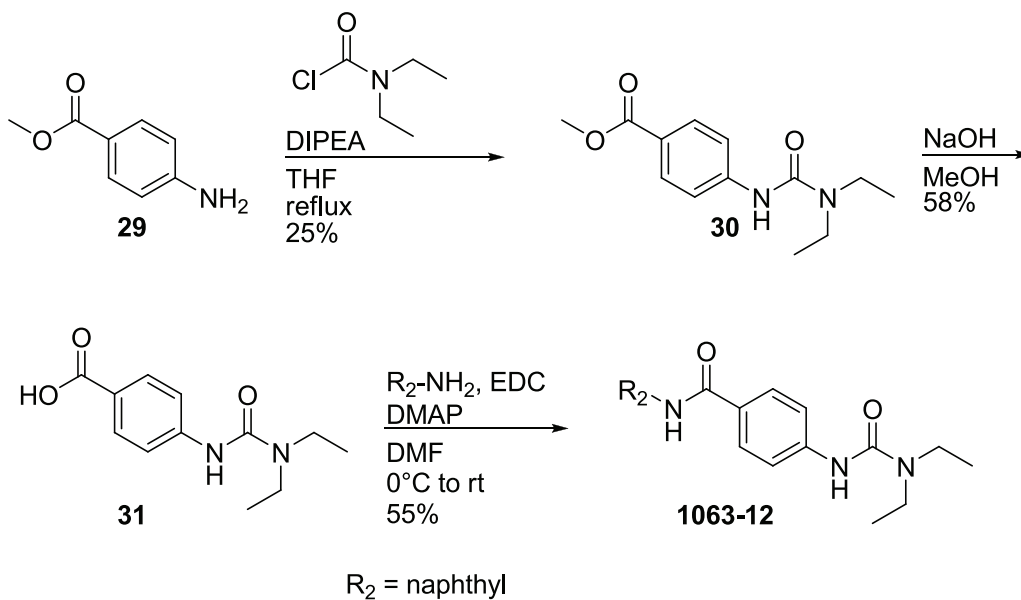
Scheme 3.8 Synthesis of ester 1063 analogues



The corresponding urea analogue of **1036**, **1063-12**, was synthesized in a similar manner as the carbamothioates and carbamates (Scheme 3.9). Methyl 4-aminobenzoate (**29**) was allowed to react with *N,N*-diethylcarbamoyl chloride under

basic conditions to give urea **30**.³¹ Saponification of **30** yielded benzoic acid **31**, which was coupled with naphthylamine to afford **1063-12**.

Scheme 3.9 Synthesis of urea analogue **1063-12**

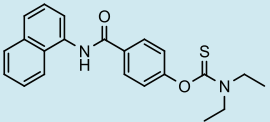
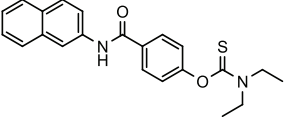
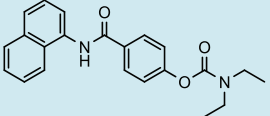
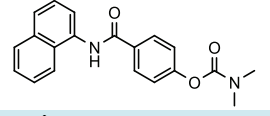
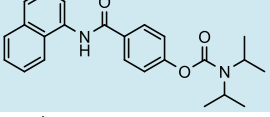
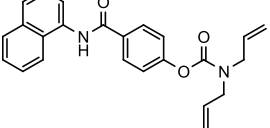
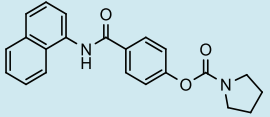
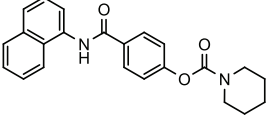
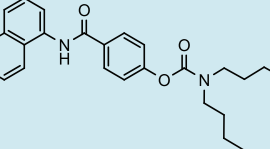
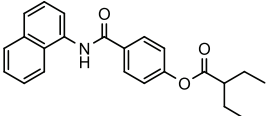
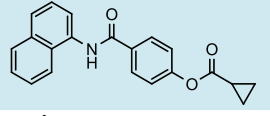
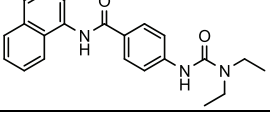


3.8 Results and Discussion

3.8.1. Structure activity relationships of 1063 series

The activity of all synthesized 1063 compounds was evaluated in *Xenopus* oocytes over-expressing each NR2 subunit of the NMDA receptor. The results are given in Table 3.9

Table 3.9 Summary of 1063 series *in vitro* activity[†] at NMDA receptors

ID	Structure	IC ₅₀ (μM) NR2A [‡]	IC ₅₀ (μM) NR2B [‡]	IC ₅₀ (μM) NR2C [‡]	IC ₅₀ (μM) NR2D [‡]	$\frac{IC_{50} \text{ NR2A}^{\ddagger}}{IC_{50} \text{ NR2D}^{\ddagger}}$
1063		1365	1228	2.2	1.2	1138
1063-1		NA	NA	243	91.2	--
1063-2		874	164	5.8	3.9	224
1063-3		NA	1454	619	194	>5
1063-4		702	150	4.9	4.1	171
1063-5		NA	719	42	28	>50
1063-6		NA	502	135	257	--
1063-7		NA	NA	NA	84% ^a	--
1063-8		NA	NA	NA	87% ^a	--
1063-9		NA	NA	NA	86% ^a	--
1063-10		NA	NA	86%	81% ^a	--
1063-11		NA	88%	687	527 ^a	--

[†] In vitro activity measured with two electrode voltage clamp recordings with *Xenopus* oocytes

[‡] NR1 subunit is assumed: NR1A/NR2A, NR1A/NR2B, NR1A/NR2C, NR1A/NR2D.

NA = not active up to 100 μ M

^aActivity give as percentages correspond to percent inhibition at 100 μ M.

The parent screening hit **1063** exhibited an in vitro potency of 1.2 μ M, and was 1138-fold selective for NR2D-containing NMDA receptors.

Replacement of the sulfur present in the carbamothioate of **1063** with an oxygen, as in carbamate **1063-2**, gave slightly decreased potency (IC_{50} = 3.9 μ M), but a significant reduction in selectivity (224-fold). Although the potency and selectivity of **1063-2** was diminished compared to **1063**, the stability was improved in buffer solution and *in vitro* analysis of **1063-2** was consistently reproducible. This supports our initial hypothesis that the instability of **1063** was caused by degradation of the sulfur-containing moiety.

Further modifications of alkyl substituents flanking the carbamate did not result in further improvements in either potency or selectivity. The N,N-diethyl substituent was optimal. Shortening to a N,N-dimethyl group significantly reduced potency (**1063-5**, IC_{50} = 194 μ M). Extension of the carbamate, as in N,N-diisopropyl analogue **1063-4**, only modestly decreased potency and selectivity compared to **1063-2** (IC_{50} = 4.1 μ M, 171-fold selective). Thus the binding pocket may prefer bulky and branched hydrophobic carbamates. Extended linear substituents such as N,N-diallyl analogue **1063-5** and N,N-dibutyl analogue **1063-8** led to near-abolished NR2D activity.

Incorporation of the carbamate N,N-dialkyl chains into ring systems yielded compounds with increased conformational rigidity. Notably, pyrrolidine analogue **1063-**

6 exhibited an IC_{50} of 257 μ M. The significant potency reduction observed with pyrrolidine **1063-6** from N,N-diethyl analogue **1063-2** suggest the optimal binding mode of the compounds with the receptor requires a conformation the pyrrolidine moiety cannot adopt as readily as the more flexible N,N-dialkyl substituents.

The nature of the XYZ moiety also proved crucial to potency. While analogues containing a carbamate exhibited decreased activity compared to carbamothioates, both esters (**1063-9** and **1063-10**) and ureas (**1063-11**) were inactive.

3.8.2. *In vitro* analysis of 1063 series mechanism of action and binding interactions

Eight splice variants of NR1 exist in NMDA receptors. The concentration-effect curves for **1063-2** at various NR1/NR2D-containing receptors indicated there was no significant alteration in inhibition between NR1-1a, 1b-, 3a-, or 3b-containing receptors (Figure 3.18).

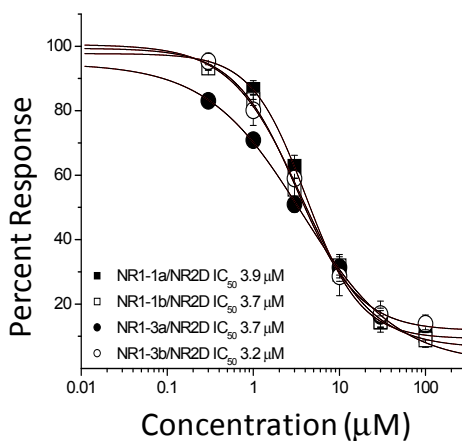


Figure 3.18 Activity of 1063-2 at various NR1-splice variant-containing NR1/NR2D receptors

While binding of 987 series compounds was localized to the S2 domain, compound **1063-2** showed sensitization in chimera studies involving the transmembrane domain (Left Panel, Figure 3.19). Replacement of the NR2A transmembrane domain with that of 2D [2A – (2D M1M2M3)] gave inhibition in NR2A receptors similar to observed results with NR2D receptors when treated with **1063-2**. Binding was further localized to only one transmembrane helix, M1 [2A – (2D S1M1)] (Left Panel, Figure 3.19). Finally, point mutagenesis within the M1 helix of NR2D receptors showed replacement of cysteine with lysine at position 590 resulted in near-complete loss of inhibition (Right Panel, Figure 3.19), suggesting this residue is crucial for 1063 series binding.

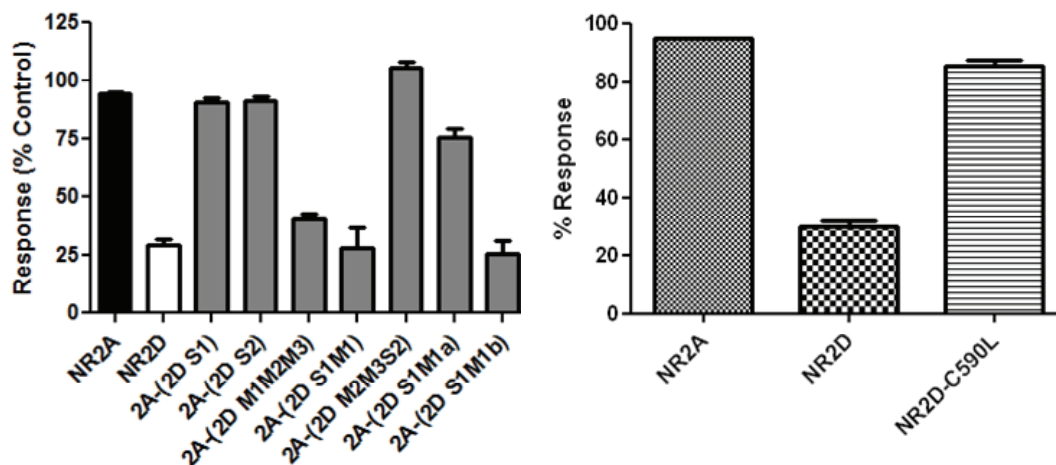


Figure 19 Mutagenesis studies of binding interactions of 1063-2 with NR2D

Figure 3.20 highlights the two distinct binding regions on the NR2 subunit, specific for either the 987 series or 1063 series. The 987 class was found to bind in the

ligand binding domain at an allosteric site within S2. In contrast, the 1063 class binds within the M1 helix, embedded within the transmembrane domain of the receptor.

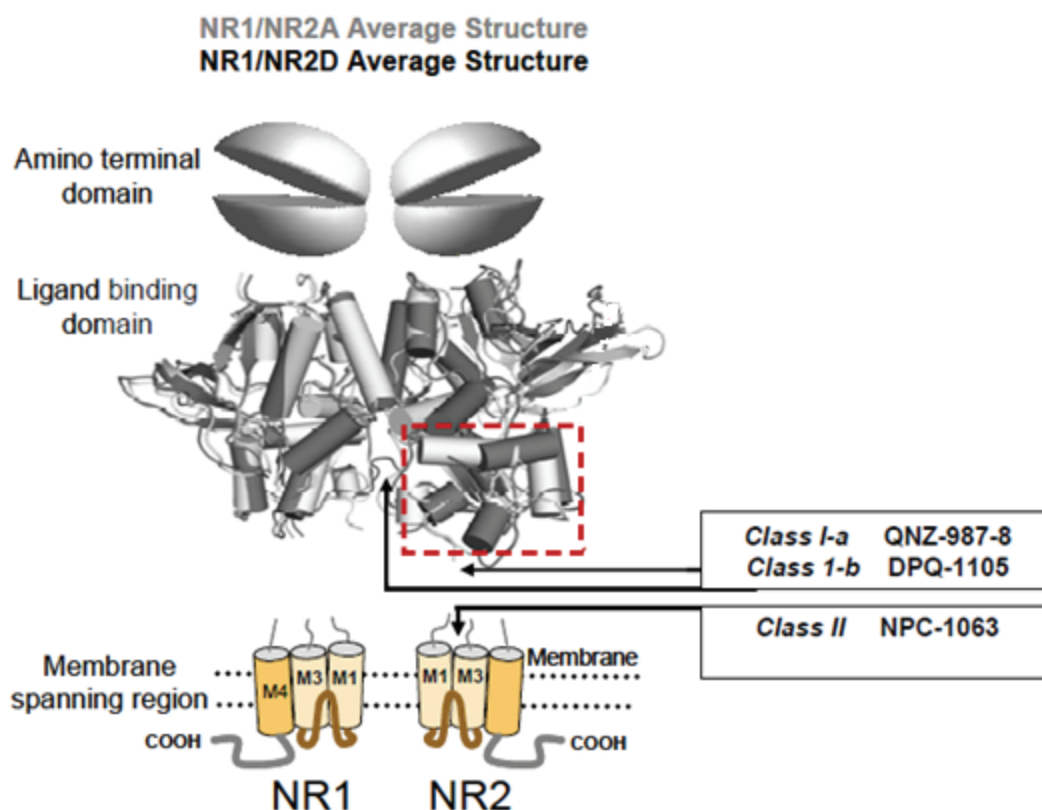


Figure 3.20 Binding regions of 987 series, 1063 series, and 1105 series of NR2D inhibitors

3.8.3. *In vivo* analysis of NR1/NR2D—containing NMDA receptors.

The best 987 series and 1063 series compounds were analyzed for pharmacokinetic parameters *in vivo*, particularly half-life ($T_{1/2}$) and blood brain barrier penetration (Table 3.10). As expected, the quinazolinones **987-8** and **987-23** did not appreciably cross the blood brain barrier due to the charged nature of the compounds. In addition, both quinazolinones were poorly absorbed into the plasma after oral

dosing. By contrast, compound **1063-2** did enter the plasma, and was found to partition well into the brain.

Table 3.10 *In vivo* pharmacokinetics parameters of NR2D inhibitors (mice)

ID	Dose (mg/kg)	Peak Plasma (ng/mL)	T _{1/2} (h)	Brain: Plasma
1063-2	20	146	< 30 min	3.2
987-8	20	28	ND	0.00
987-23	20	3.69	ND	0.00

* Performed by Lundbeck (Copenhagen, Denmark)

Analogous PK studies in rats determined the concentration of **1063-2** in the brain increased over time (Figure 3.21), further supporting the heightened drug-like nature of the 1063 series compared to the 987 series.

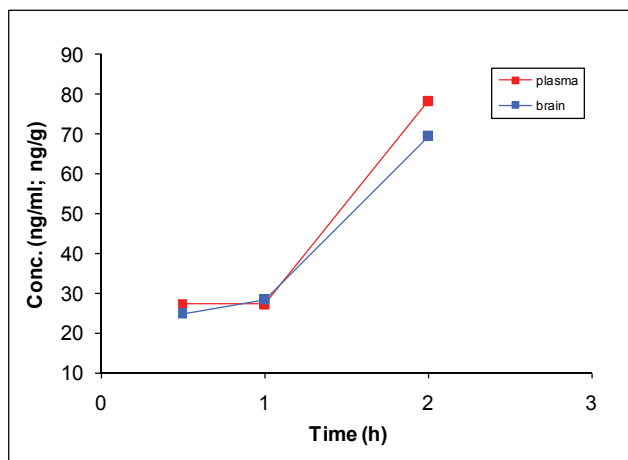


Figure 3.21 The concentration of 1063-2 increases in the brain and plasma of rats over time

3.9 Conclusions regarding both 987 and 1063 series inhibitors

Two classes of compounds were developed, each specific for novel and distinct binding sites within the NR2D subunit. Medicinal chemistry efforts within the 987 series led to significant (100-fold) increases in selectivity. However, this class is plagued by poor solubility. As a result, the compounds do not absorb well into the bloodstream or partition into the brain. Thus, at present, these compounds represent excellent pharmacological tools. Further efforts are underway to increase solubility and drug-like characteristics.

The 1063 series offers increased selectivity (100-1000 fold), but similar potency to the 987 series. Although initial carbamothioates were found to degrade in buffer solutions which gave erratic results, the introduction of a carbamate yielded analogues with increased *in vitro* stability. This class exhibited more drug-like properties such as absorption into plasma after oral dosing and passage through the blood brain barrier. Further efforts are underway to increase the potency of the 1063 analogues.

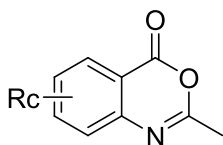
Taken together, the 987 and 1063 class both represent first-in-class NR2D-specific NMDA receptor antagonists. Each class of compound binds to a distinct location on the receptor, and may confer differential properties. Development of more potent and selective analogues, beyond this initial work, could lead to elucidation of the role of the NR2D subunit in normal brain function and disease states.

3.10 Chemistry Experimental Detail

All reagents were obtained from commercial suppliers and used without further purification. Reaction progress was monitored by thin layer chromatography (TLC) on precoated glass plates (silica gel 60 F254, 0.25 mm). Proton and carbon NMR spectra were recorded on an INOVA-400 (400 MHz), VNMRS 400 (400 MHz), INOVA-600 (600 MHz), or Mercury 300 Vx (300 MHz). The spectra obtained were referenced to the residual solvent peak. Mass spectra were performed by the Emory University Mass Spectroscopy Center on either a VG 70-S Nier Johnson or JEOL instrument. Elemental analyses were performed by Atlantic Microlab Inc. C, H, N agreed with proposed structures within $\pm 4\%$ of theoretical values unless indicated. When noted, flash chromatography was performed on a Teledyne ISCO Combiflash Companion with prepackaged Teledyne RediSep disposable normal phase silica columns. HPLC (Varian) was used to determine the purity of some compounds. HPLC was performed to determine purity of selected compounds. The conditions used are noted per example.

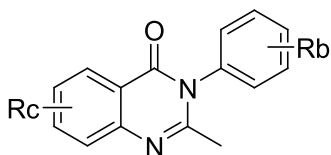
3.10.1 Experimental detail of compounds synthesized in Chapter 3

General procedure for synthesis of 2-methyl-4H-benzo[d][1,3]oxazin-4-one (**987-a**) intermediates (Procedure A).



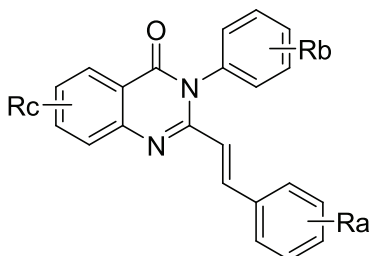
The anthranilic acid (**1**, 1.0 mmol) was suspended in acetic anhydride (8.7 equiv). Upon refluxing all material went into solution, and the mixture was refluxed until TLC indicated the reaction was finished (generally 1 hr). The solvent was removed *in vacuo* to give a solid. The crude material was recrystallized using either hexanes or hexanes and ethyl acetate. The product was collected by filtration and washed with hexanes.

General procedure for synthesis of 2-methyl-3-phenylquinazolin-4(3H)-one (**987-b**) intermediates (Procedure B).



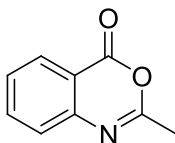
The benzoxazinone (**987-a**, 1.0 mmol) and aniline (**2**, 1.2 equiv) were dissolved in glacial acetic acid (56 equiv). The solution was refluxed until TLC indicated the reaction was finished (generally 6-12 hours). After cooling to room temperature, the mixture was concentrated *in vacuo* to give a solid. The crude material was recrystallized and the product was collected by filtration and washed with ethyl acetate.

General procedure for synthesis of (*E*)-3-phenyl-2-styrylquinazolin-4(3*H*)-one (**987-c**) products (Procedure C).



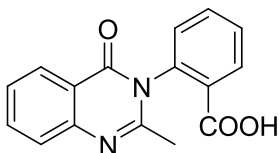
The quinazolinone (**987-b**, 1.0 mmol), benzaldehyde (**3**, 1.33 equiv), and sodium acetate (1.63 equiv) were suspended in a mixture of glacial acetic acid (58 equiv) and acetic anhydride (7.0 equiv). The mixture was refluxed until TLC indicated the reaction was finished (generally 12-18 hours). After cooling to room temperature, the mixture was filtered and washed with methanol. Further purification was performed (chromatography or recrystallization) as necessary.

2-Methyl-4H-benzo[d][1,3]oxazin-4-one (**987-26a**).



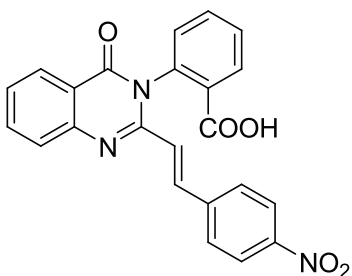
Compound **987-26a** was prepared via procedure A with anthranilic acid (1.00 g). Recrystallization was performed with hexanes to give a white solid (0.772 g, 66%). ¹H NMR (600 MHz, *d*₆-DMSO) δ 8.02 (d, *J* = 7.6 Hz, 1H), 7.85 (t, *J* = 7.6 Hz, 1H), 7.53 (t, *J* = 7.6 Hz, 1H), 7.49 (d, *J* = 7.6 Hz, 1H), 2.37 (s, 3H). ¹³C NMR (150 MHz, *d*₆-DMSO) δ 160.0, 159.1, 146.0, 136.6, 128.2, 127.7, 126.0, 116.3, 20.9.

2-(2-Methyl-4-oxoquinazolin-3(4H)-yl)benzoic acid (987-26b).



Compound **987-26b** was prepared via procedure B with compound **987-26a** (1.00 g, 3.48 mmol) and anthranilic acid (0.570 g, 4.18 mmol, 1.2 equiv). Recrystallization was performed with methanol to give a white solid (0.580 g, 41%). ^1H NMR (400 MHz, d_6 -DMSO) δ 13.13 (bs, 1H), 8.13 (dd, $J_1 = 7.8$ Hz, $J_2 = 1.6$ Hz, 1H), 8.09 (dd, $J_1 = 7.8$ Hz, $J_2 = 1.6$ Hz, 1H), 7.87-7.80 (mult, 2H), 7.70-7.67 (mult, 2H), 7.58 (d, $J = 7.4$ Hz, 1H), 7.52 (t, $J = 7.4$ Hz, 1H), 2.11 (s, 3H). ^{13}C NMR (100 MHz, DMSO- d_6) δ 165.8, 161.5, 154.4, 147.5, 137.6, 134.7, 133.8, 131.7, 130.3, 129.7, 128.9, 126.7, 126.4, 126.3, 120.4, 23.8 HRMS calcd for $\text{C}_{16}\text{H}_{12}\text{N}_2\text{O}_3$, 281.09273 $[\text{M}+\text{H}]^+$; found, 281.09246 $[\text{M}+\text{H}]^+$.

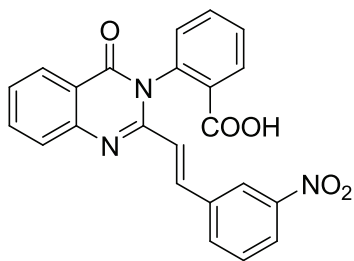
(E)-2-(2-(4-nitrostyryl)-4-oxoquinazolin-3(4H)-yl)benzoic acid (987-26).



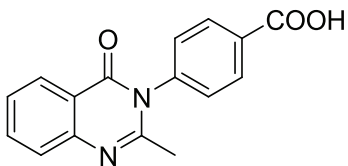
Compound **987-26** was prepared via procedure C with compound **987-26b** (1.00 g, 3.57 mmol) and *para*-nitrobenzaldehyde (0.717 g, 4.75 mmol, 1.33 equiv) to give the title compound as a yellow solid (1.18 g, 80%). ^1H NMR (400 MHz, d_6 -DMSO) δ 8.20-8.14 (mult, 4 H), 7.96 (d, $J = 15.9$ Hz, 1H), 7.92-7.81 (mult, 3H), 7.74 (t, $J = 7.6$ Hz, 1H), 7.68 (d,

$J = 7.9$ Hz, 2H), 7.61-7.56 (mult, 2H), 6.50 (d, $J = 15.6$ Hz, 1H). ^{13}C NMR (100 MHz, d_6 -DMSO) δ 165.7, 161.3, 151.0, 147.5, 147.3, 141.2, 136.6, 136.5, 134.9, 133.8, 131.8, 130.7, 130.0, 128.6, 127.4, 127.0, 126.5, 124.1, 124.0, 120.7, HRMS calcd for $\text{C}_{23}\text{H}_{15}\text{N}_3\text{O}_5$, 414.10911 $[\text{M}+\text{H}]^+$; found, 414.10903 $[\text{M}+\text{H}]^+$. Anal. ($\text{C}_{23}\text{H}_{15}\text{N}_3\text{O}_5$) C, H, N. MP $> 260^\circ\text{C}$.

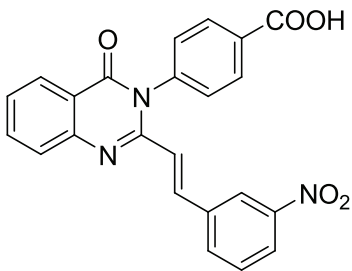
(E)-2-(2-(3-nitrostyryl)-4-oxoquinazolin-3(4H)-yl)benzoic acid (987-27).



Compound **987-27** was prepared via procedure C with compound **987-26b** (0.250 g, 0.89 mmol) and *meta*-nitrobenzaldehyde (0.179 g, 1.19 mmol, 1.33 equiv) to give the title compound as a yellow solid (0.202 g, 55%). ^1H (400 MHz, d_6 -DMSO) δ 8.22-8.13 (mult, 4H), 7.99 (d, $J = 15.4$ Hz, 1H), 7.93-7.80 (mult, 4H), 7.75 (t, $J = 7.2$ Hz, 1H), 7.65-7.60 (mult, 2H), 7.57 (t, $J = 7.2$ Hz, 1H), 6.47 (d, $J = 15.4$ Hz, 1H). ^{13}C NMR (150 MHz, d_6 -DMSO) δ 165.7, 161.3, 151.1, 148.3, 147.4, 136.6, 136.6, 136.6, 134.9, 133.8, 133.3, 131.8, 130.7, 130.5, 129.9, 129.4, 127.3, 126.8, 126.5, 124.0, 122.6, 122.1, 120.7. HRMS calcd for $\text{C}_{23}\text{H}_{15}\text{N}_3\text{O}_5$, 414.10911 $[\text{M}+\text{H}]^+$; found, 414.10822 $[\text{M}+\text{H}]^+$. Anal. ($\text{C}_{23}\text{H}_{15}\text{N}_3\text{O}_5$) C, H, N. MP $> 260^\circ\text{C}$.

4-(2-Methyl-4-oxoquinazolin-3(4H)-yl)benzoic acid (987-4b).

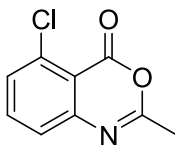
Compound **987-4b** was prepared via procedure B with compound **987-26a** (0.300 g, 1.86 mmol) and *para*-aminobenzoic acid (0.306 g, 69.9 mmol, 1.20 equiv). Recrystallization was performed with ethyl acetate and methanol to give a white solid (0.200 g, 28%). ^1H NMR (400 MHz, d_6 -DMSO) δ 8.12 (t, $J = 7.9$ Hz, 3H), 7.85 (t, $J = 7.6$ Hz, 1H), 7.68 (d, $J = 7.9$ Hz, 1H), 7.61 (d, $J = 7.9$ Hz, 2H), 7.53 (t, $J = 7.6$ Hz, 1H), 2.14 (s, 3H). ^{13}C NMR (100 MHz, d_6 -DMSO) δ 166.7, 161.3, 153.9, 147.4, 141.8, 134.7, 131.4, 130.6, 129.0, 126.8, 126.6, 126.3, 120.4, 24.0. HRMS calcd for $\text{C}_{16}\text{H}_{12}\text{N}_2\text{O}_3$, 281.09723 $[\text{M}+\text{H}]^+$; found, 281.09195 $[\text{M}+\text{H}]^+$.

(E)-4-(2-(3-nitrostyryl)-4-oxoquinazolin-3(4H)-yl)benzoic acid (1043/987-4).

Compound **1043** was prepared via procedure C with compound **987-4b** (0.100 g, 0.36 mmol) and *meta*-nitrobenzaldehyde (0.072 g, 0.48 mmol, 1.3 equiv). The crude material was purified via silica gel chromatography (ISCO RediSep 12 g column, silica cake, 5-10% MeOH/DCM gradient) to give an off-white solid (0.030 g, 20%). ^1H NMR (600 MHz, d_6 -

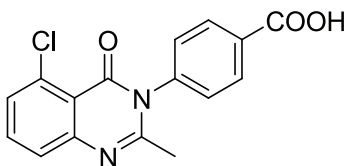
DMSO) δ 8.26 (s, 1H), 8.17 (d, $J = 7.6$ Hz, 4H), 8.01 (d, $J = 15.5$ Hz, 1H), 7.92 (t, $J = 7.1$ Hz, 1H), 7.86 (d, $J = 7.6$ Hz, 1H), 7.81 (d, $J = 8.1$ Hz, 1H), 7.65-7.62 (mult, 3H), 7.58 (t, $J = 7.6$ Hz, 1H), 6.51 (d, $J = 15.5$ Hz, 1H). ^{13}C NMR (150 MHz, d_6 -DMSO) δ 166.7, 161.1, 150.6, 148.3, 147.2, 140.7, 136.7, 136.6, 135.0, 133.3, 131.6, 130.6, 130.5, 129.5, 127.4, 127.1, 126.5, 124.0, 122.8, 122.4, 120.7, 103.3. HRMS calcd for $\text{C}_{23}\text{H}_{15}\text{N}_3\text{O}_5$, 414.10911 $[\text{M}+\text{H}]^+$; found, 414.10791 $[\text{M}+\text{H}]^+$. Anal. ($\text{C}_{23}\text{H}_{15}\text{N}_3\text{O}_5$) C, H, N. MP > 260°C.

5-Chloro-2-methyl-4H-benzo[d][1,3]oxazin-4-one (987-28a).



Compound **987-28a** was prepared via procedure A using 2-amino-6-chlorobenzoic acid (1.00 g, 5.83 mmol). The crude material was purified using recrystallization with hexanes to give yellow needles (0.862 g, 76%). ^1H NMR (400 MHz, CDCl_3) δ 7.59 (t, $J = 7.9$ Hz, 1H), 7.43 (d, $J = 7.9$ Hz, 1H), 7.35 (d, $J = 7.9$ Hz, 1H), 2.39 (s, 3H). ^{13}C NMR (100 MHz, CDCl_3) δ 161.1, 156.2, 148.8, 136.0, 135.8, 130.7, 125.5, 114.4, 21.3.

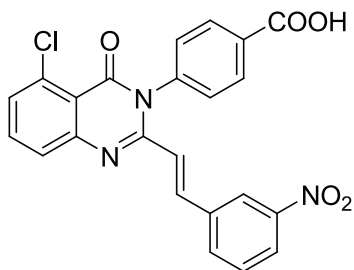
4-(5-Chloro-2-methyl-4-oxoquinazolin-3(4H)-yl)benzoic acid (987-27b).



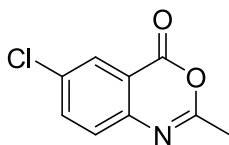
Compound **987-28b** was prepared via procedure B using compound **987-28a** (0.862 g, 4.09 mmol) and *para*-aminobenzoic acid (0.673 g, 4.91 mmol, 1.20 equiv). The crude

material was recrystallized with ethyl acetate to give an off-white solid (0.343 g, 27%). ^1H NMR (400 MHz, d_6 -DMSO) δ 13.27 (bs, 1H), 8.12 (d, J = 8.2 Hz, 2H), 7.76 (t, J = 8.2 Hz, 1H), 7.61 (d, J = 8.2 Hz, 3H), 7.53 (d, J = 7.8 Hz, 1H), 2.09 (s, 3H). ^{13}C NMR (100 MHz, d_6 -DMSO) δ 166.7, 159.3, 154.9, 149.9, 141.7, 134.5, 132.7, 131.4, 130.6, 129.0, 129.0, 126.4, 117.4, 24.0. HRMS calcd for $\text{C}_{16}\text{H}_{11}\text{ClN}_2\text{O}_3$, 315.05376 $[\text{M}+\text{H}]^+$; found, 315.05325 $[\text{M}+\text{H}]^+$.

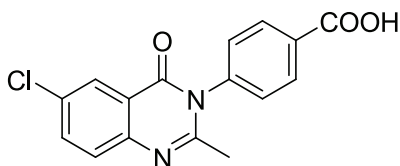
(*E*)-4-(5-chloro-2-(3-nitrostyryl)-4-oxoquinazolin-3(4H)-yl)benzoic acid (987-28).



Compound **987-28** was prepared via procedure C using compound **987-28b** (0.300 g, 0.95 mmol) and *meta*-nitrobenzaldehyde (0.192 g, 1.27 mmol, 1.33 equiv) to give the title compound as a bright yellow solid (0.251 g, 59%). ^1H NMR (400 MHz, d_6 -DMSO) δ 13.31 (bs, 1H), 8.22 (s, 1H), 8.19-8.15 (mult, 2H), 7.99 (d, J = 15.7 Hz, 1H), 7.83-7.78 (mult, 1H), 7.65 (d, J = 8.6 Hz, 2H), 7.61 (t, J = 7.7 Hz, 1H), 7.55 (d, J = 7.7 Hz, 1H), 6.42 (d, J = 15.7 Hz, 1H). ^{13}C NMR (100 MHz, d_6 -DMSO) δ 166.7, 159.1, 151.2, 149.7, 148.2, 140.6, 137.3, 136.3, 134.7, 133.3, 132.9, 131.6, 130.7, 130.5, 129.5, 129.3, 126.9, 124.1, 122.4, 122.3, 117.6. HRMS calcd for $\text{C}_{23}\text{H}_{14}\text{ClN}_3\text{O}_5$, 448.07014 $[\text{M}+\text{H}]^+$; found, 448.06970 $[\text{M}+\text{H}]^+$. Anal. ($\text{C}_{23}\text{H}_{14}\text{ClN}_3\text{O}_5$) C, H, N. MP > 260 °C.

6-Chloro-2-methyl-4H-benzo[d][1,3]oxazin-4-one (987-5a).

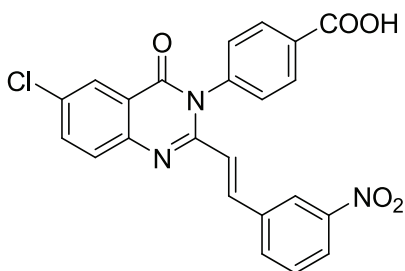
Compound **987-5a** was prepared via procedure A using 2-amino-5-chlorobenzoic acid (1.00 g, 5.80 mmol). The crude material was purified by recrystallization with hexanes to give an orange solid (0.927 g, 81%). ^1H NMR (400 MHz, CDCl_3) δ 8.07 (d, $J = 2.2$ Hz, 1H), 7.69 (dd, $J_1 = 8.6$ Hz, $J_2 = 2.2$ Hz, 1H), 7.45 (d, $J = 8.6$ Hz, 1H), 2.44 (s, 3H). ^{13}C NMR (100 MHz, CDCl_3) δ 160.6, 158.6, 145.0, 136.9, 133.8, 128.1, 127.8, 117.9, 21.5.

4-(6-Chloro-2-methyl-4-oxoquinazolin-3(4H)-yl)benzoic acid (987-5b).

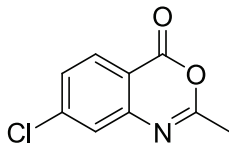
Compound **987-5b** was prepared via procedure B using compound **987-5a** (0.500 g, 2.56 mmol) and *para*-aminobenzoic acid (0.421 g, 3.10 mmol, 1.20 equiv). The crude material was purified by trituration with ethyl acetate to give a white solid (0.507 g, 63%). ^1H NMR (400 MHz, d_6 -DMSO) δ 8.14 (d, $J = 8.6$ Hz, 2H), 8.04 (d, $J = 2.5$ Hz, 1H), 7.90 (dd, $J_1 = 8.9$ Hz, $J_2 = 2.5$ Hz, 1H), 7.72 (d, $J = 8.9$ Hz, 1H), 7.64 (d, $J = 8.6$ Hz, 2H), 2.15 (s, 3H). ^{13}C NMR (100 MHz, d_6 -DMSO) δ 166.7, 160.3, 154.6, 146.1, 141.5, 134.8, 131.5, 130.7,

130.6, 130.4, 129.0, 128.9, 125.2, 121.7, 118.2, 24.1. HRMS calcd for $C_{16}H_{11}ClN_2O_3$, 315.05376 $[M+H]^+$; found, 315.05256 $[M+H]^+$.

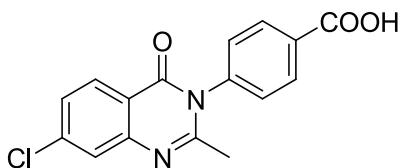
(E)-4-(6-chloro-2-(3-nitrostyryl)-4-oxoquinazolin-3(4H)-yl)benzoic acid (987-5).



Compound **987-5** was prepared via procedure C using **987-5b** (0.300 g, 0.950 mmol) and *meta*-nitrobenzaldehyde (0.192 g, 1.30 mmol, 1.33 equiv). The crude material was purified using recrystallization with methanol and dioxane. Further trituration with water yielded the title compound as a yellow solid after filtration and washing with hexanes (0.060 g, 14%). 1H NMR (400 MHz, d_6 -DMSO) δ 8.24 (s, 1H), 8.19-1.66 (mult, 3H), 8.05 (d, J = 2.2 Hz, 1H), 8.01 (d, J = 15.6 Hz, 1H), 7.94 (dd, J_1 = 8.7 Hz, J_2 = 2.2 Hz, 1H), 7.85-7.81 (mult, 2H), 7.66-7.61 (mult, 3H), 6.48 (d, J = 15.6 Hz, 1H). ^{13}C NMR (100 MHz, d_6 -DMSO) δ 167.4, 160.9, 151.8, 148.9, 146.6, 141.0, 137.9, 137.1, 135.7, 134.0, 133.0, 132.4, 131.9, 131.4, 131.8, 130.2, 130.0, 126.1, 124.8, 123.1, 122.6. HRMS calcd for $C_{23}H_{14}ClN_3O_5$, 446.05426 $[M-H]^+$; found, 446.05511 $[M-H]^+$. Anal. ($C_{23}H_{14}ClN_3O_5$) C, H, N. MP > 260 °C.

7-Chloro-2-methyl-4H-benzo[d][1,3]oxazin-4-one (987-31a).

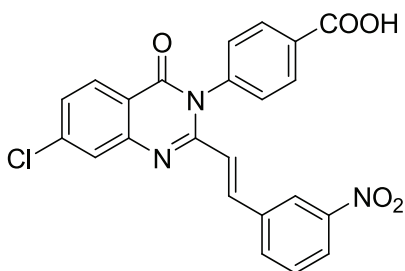
Compound **987-31a** was prepared via procedure A using 2-amino-4-chlorobenzoic acid (1.00 g, 5.83 mmol). The crude material was purified by recrystallization with hexanes to give yellow needles (0.928 g, 81%). ^1H NMR (400 MHz, CDCl_3) δ 8.10 (d, $J = 8.6$ Hz, 1H), 7.53 (d, $J = 2.0$ Hz, 1H), 7.45 (dd, $J_1 = 8.6$ Hz, $J_2 = 2.0$ Hz, 1H), 2.47 (s, 3H). ^{13}C NMR (100 MHz, CDCl_3) δ 161.8, 159.1, 147.7, 143.1, 129.9, 129.9, 126.5, 115.2, 21.6.

4-(7-Chloro-2-methyl-4-oxoquinazolin-3(4H)-yl)benzoic acid (987-31b).

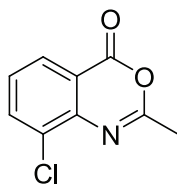
Compound **987-31b** was prepared via procedure B using compound **987-31a** (0.500 g, 2.56 mmol) and *para*-aminobenzoic acid (0.421 g, 3.07 mmol, 1.20 equiv). The crude material was purified by recrystallization with ethyl acetate to give partially pure product which was further purified by recrystallization with methanol to give a white solid (0.235 g, 29%). ^1H NMR (400 MHz, d_6 -DMSO) δ 13.23 (bs, 1H), 8.11 (mult, 3H), 7.47 (d, $J = 2.0$ Hz, 1H), 7.62 (d, $J = 8.2$ Hz, 2H), 7.56 (dd, $J_1 = 8.6$ Hz, $J_2 = 2.0$ Hz, 1H), 2.14 (s, 3H). ^{13}C NMR (100 MHz, d_6 -DMSO) δ 166.7, 160.7, 155.7, 148.4, 141.5, 139.3, 131.6,

130.6, 128.9, 128.4, 126.8, 125.9, 119.3, 24.1. HRMS calcd for $C_{16}H_{11}ClN_2O_3$, 315.05376 $[M+H]^+$; found 315.05319 $[M+H]^+$.

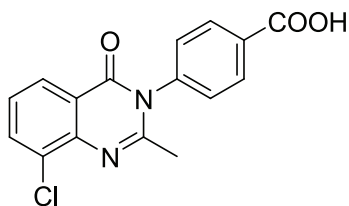
(E)-4-(7-chloro-2-(3-nitrostyryl)-4-oxoquinazolin-3(4H)-yl)benzoic acid (987-31).



Compound **987-31** was prepared via procedure C using compound **987-31b** (0.200 g, 0.640 mmol) and *meta*-nitrobenzaldehyde (0.128 g, 0.850 mmol, 1.33 equiv) to give the title compound as a yellow solid (0.135 g, 47%). 1H NMR (400 MHz, d_6 -DMSO) δ 8.24 (s, 1H), 8.18-8.13 (mult, 4H), 8.00 (d, J = 15.6 Hz, 1H), 7.85 (d, J = 8.3 Hz, 1H), 7.83 (d, J = 1.9 Hz, 1H), 7.65 (d, J = 8.6 Hz, 3H), 7.60 (dd, J_1 = 8.3 Hz, J_2 = 1.9 Hz, 1H). ^{13}C NMR (100 MHz, d_6 -DMSO) δ 166.7, 160.6, 152.0, 148.3, 148.2, 140.4, 139.5, 137.6, 136.3, 133.4, 131.7, 130.7, 130.6, 130.5, 129.4, 128.6, 127.2, 126.3, 124.2, 122.4, 119.5. HRMS calcd for $C_{23}H_{14}ClN_3O_5$, 448.07014 $[M+H]^+$; found, 448.06890 $[M+H]^+$. Anal. ($C_{23}H_{14}ClN_3O_5$) C, H, N. MP > 260 °C.

8-Chloro-2-methyl-4H-benzo[d][1,3]oxazin-4-one (987-32a).

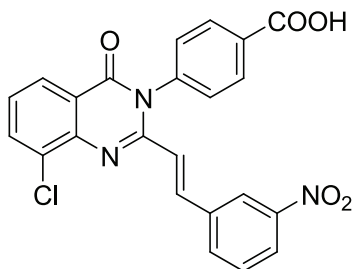
Compound **987-32a** was prepared via procedure A using 2-amino-3-chlorobenzoic acid (1.00 g, 5.83 mmol). The crude material was purified by recrystallization with hexanes to give yellow needles (0.868 g, 76%). ^1H NMR (400 MHz, CDCl_3) δ 8.04 (d, $J = 7.9$ Hz, 1H), 7.80 (d, $J = 7.5$ Hz, 1H), 7.39 (t, $J = 7.9$ Hz, 1H), 2.50 (s, 3H). ^{13}C NMR (100 MHz, CDCl_3) δ 161.3, 158.9, 143.3, 136., 131.1, 128.4, 127.2, 118.3, 21.8.

4-(8-Chloro-2-methyl-4-oxoquinazolin-3(4H)-yl)benzoic acid (987-32b).

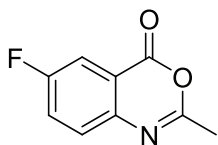
Compound **987-32b** was prepared via procedure B using compound **987-32a** (0.899 g, 4.50 mmol) and *para*-aminobenzoic acid (0.756 g, 5.52 mmol, 1.20 equiv). The crude material was recrystallized with ethyl acetate and methanol to give a white solid (0.833 g, 58%). ^1H NMR (400 MHz, d_6 -DMSO) δ 13.24 (bs, 1H), 8.08 (d, $J = 7.8$ Hz, 2H), 8.02 (d, $J = 7.8$ Hz, 1H), 7.96 (d, $J = 7.8$ Hz, 1H), 7.59 (d, $J = 7.8$ Hz, 2H), 7.45 (d, $J = 7.9$ Hz, 1H), 2.13 (s, 3H). ^{13}C NMR (400 MHz, d_6 -DMSO) δ 166.7, 160.8 155.1, 143.7, 141.5, 134.7, 131.6,

130.7, 130.3, 128.9, 126.8, 125.5, 122.2, 24.4. HRMS calcd for $C_{16}H_{11}ClN_2O_3$, 314.04582; found 315.05355 $[M+H]^+$.

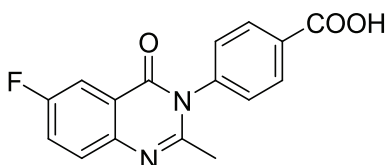
(E)-4-(8-chloro-2-(3-nitrostyryl)-4-oxoquinazolin-3(4H)-yl)benzoic acid (987-32).



Compound **987-32** was prepared via procedure C using compound **987-32b** (0.400 g, 1.27 mmol) and *meta*-nitrobenzaldehyde (0.255 g, 1.69 mmol, 1.33 equiv) to yield the title compound as a yellow solid (0.071 g, 12%). 1H NMR (400 MHz, d_6 -DMSO) δ 13.24 (bs, 1H), 8.26 (s, 1H), 8.17 (d, J = 8.2 Hz, 3H), 8.10-8.02 (mult, 3H), 7.86 (d, J = 7.8 Hz, 1H), 7.67-7.62 (mult, 3H), 7.53 (t, J = 7.8 Hz, 1H), 6.51 (d, J = 15.6 Hz, 1H). ^{13}C NMR (100 MHz, d_6 -DMSO) δ 167.3, 161.4, 151.9, 148.9, 144.3, 141.0, 138.4, 137.0, 135.5, 134.0, 132.3, 131.5, 131.4, 131.1, 130.0, 127.9, 126.2, 124.8, 123.2, 123.0. HRMS calcd for $C_{23}H_{14}ClN_3O_5$, 448.07014 $[M+H]^+$; found 448.07015 $[M+H]^+$. Anal. ($C_{23}H_{14}ClN_3O_5$) C, H, N. MP > 260 °C.

6-Fluoro-2-methyl-4H-benzo[d][1,3]oxazin-4-one (987-7a).

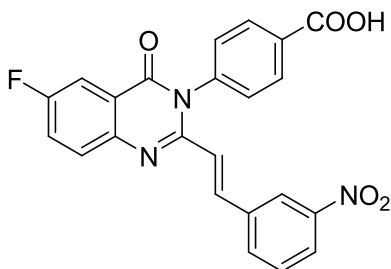
Compound **987-7a** was prepared via procedure A using 2-amino-5-fluorobenzoic acid (1.00 g, 6.50 mmol). The crude material was purified by recrystallization with hexanes to give off-white needles (0.571 g, 49%). ^1H NMR (400 MHz, CDCl_3) δ 7.79 (dd, $J_1 = 8.0$ Hz, $J_2 = 2.9$ Hz, 1H), 7.53 (dd, $J_1 = 8.1$ Hz, $J_2 = 4.8$ Hz, 1H), 7.49 (td, $J_1 = 8.5$ Hz, $J_2 = 2.9$ Hz, 1H), 2.45 (s, 3H). ^{13}C NMR (100 MHz, CDCl_3) δ 161.4 (d, $J = 250.2$ Hz), 159.6, 159.1, 143.1, 128.9 (d, $J = 7.6$ Hz) 124.7 (d, $J = 23.7$ Hz), 118.1 (d, $J = 9.2$ Hz) 113.8 (d, $J = 24.4$ Hz). ^{19}F NMR (282.4 Hz, CDCl_3) δ -110.7.

4-(6-Fluoro-2-methyl-4-oxoquinazolin-3(4H)-yl)benzoic acid (987-7b).

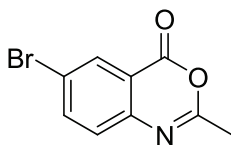
Compound **987-7b** was prepared via procedure B using compound **987-7a** (0.500 g, 2.79 mmol) and *para*-aminobenzoic acid (0.459 g, 3.40 mmol, 1.20 equiv). The crude material was purified by recrystallization with ethyl acetate to give a white solid (0.531 g, 64%). ^1H NMR (400 MHz, CDCl_3) δ 8.08 (d, $J = 8.7$ Hz, 2H), 7.73-7.69 (mult, 3H), 7.58 (d, $J = 8.7$ Hz, 2H), 2.09 (s, 3H). ^{13}C NMR (100 MHz, CDCl_3) δ 166.7, 159.9 (d, $J = 244.9$ Hz), 160.6,

153.4, 144.2, 141.6, 131.5, 130.6, 129.6 (d, $J = 8.4$ Hz), 128.9, 123.1 (d, $J = 23.7$ Hz), 121.6 (d, $J = 8.4$ Hz), 110.9 (d, $J = 22.9$ Hz), 23.9. HRMS calcd for $C_{16}H_{11}FN_2O_3$, 299.08331 $[M+H]^+$; found, 299.08221 $[M+H]^+$.

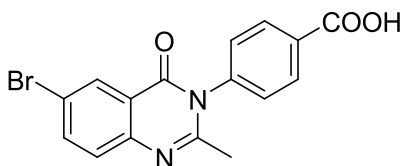
(E)-4-(6-fluoro-2-(3-nitrostyryl)-4-oxoquinazolin-3(4H)-yl)benzoic acid (987-7).



Compound **987-7** was prepared via procedure C using **987-7b** (0.400 g, 1.34 mmol) and *meta*-nitrobenzaldehyde (0.270 g, 1.78 mmol, 1.33 equiv). The crude material was purified by recrystallization with methanol and dioxane and further purification by trituration with methanol and ethyl acetate to remove residual dioxane to yield the title compound as a pale yellow solid (0.268 g, 43%). 1H NMR (600 MHz, d_6 -DMSO) δ 8.24 (s, 1H), 8.18-8.16 (mult, 3H), 7.99 (d, $J = 15.6$ Hz, 1H), 7.89-7.80 (mult, 4H), 7.66-7.62 (mult, 3H), 6.49 (d, $J = 15.6$, 1H). ^{13}C NMR (100 MHz, d_6 -DMSO) δ 166.7, 160.5, 159.8 (d, $J = 245$ Hz), 150.2, 148.3, 144.1, 140.5, 136.8, 136.5, 133.3, 131.6, 130.7, 130.5, 130.3, 130.0, 129.4, 124.0, 123.3 (d, $J = 24$ Hz), 122.4 (d, $J = 15$ Hz), 121.9 (d, $J = 8.4$ Hz), 111.2 (d, $J = 24$ Hz). HRMS calcd for $C_{23}H_{14}FN_3O_5$, 432.09969 $[M+H]^+$; found, 432.09850 $[M+H]^+$. Anal. ($C_{23}H_{14}FN_3O_5$) C, H, N. MP > 260 °C.

6-Bromo-2-methyl-4H-benzo[d][1,3]oxazin-4-one (987-6a).

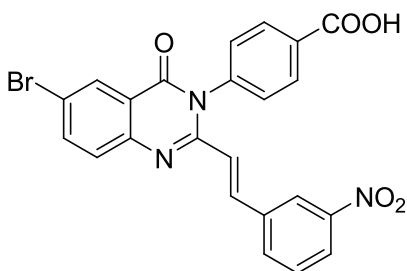
Compound **987-6a** was prepared via procedure A using 2-amino-5-bromobenzoic acid (1.00 g, 4.60 mmol). The solid was recrystallized with hexanes to give a white solid (0.796 g, 72%). ^1H NMR (600 MHz, CDCl_3) δ 8.25 (s, 1H), 7.84 (d, $J = 8.6$ Hz, 1H), 7.39 (d, $J = 8.1$ Hz, 1H), 2.44 (s, 3H). ^{13}C NMR (150 MHz, CDCl_3) δ 160.8, 158.5, 145.4, 139.8, 131.0, 128.3, 121.5, 119.5, 118.2, 21.6.

4-(6-Bromo-2-methyl-4-oxoquinazolin-3(4H)-yl)benzoic acid (987-6b).

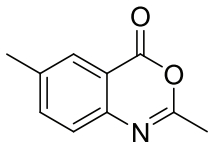
Compound **987-6b** was prepared via procedure B using **987-6a** (0.500 g, 2.08 mmol) and *para*-aminobenzoic acid (0.343 g, 2.50 mmol, 1.20 equiv). The crude material was purified by recrystallization with ethyl acetate to give an off-white solid (0.511 g, 68%). ^1H NMR (600 MHz, d_6 -DMSO) δ 8.16 (d, $J = 2.4$ Hz, 1H), 8.22 (d, $J = 8.4$ Hz, 2H), 7.98 (dd, $J_1 = 8.4$ Hz, $J_2 = 2.4$ Hz, 1H), 7.63-7.61 (mult, 3H), 2.12 (s, 3H). ^{13}C NMR (150 MHz, d_6 -DMSO) δ 166.8, 160.2, 154.7, 146.4, 141.5, 137.5, 131.5, 130.6, 130.4, 129.2, 128.9,

128.3, 122.1, 118.8, 118.2, 24.1. HRMS calcd for $C_{16}H_{11}BrN_2O_3$, 359.00324 $[M+H]^+$; found, 359.00006 $[M+H]^+$.

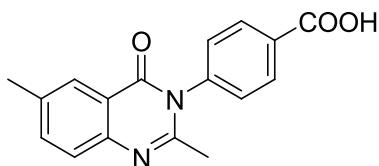
(E)-4-(6-bromo-2-(3-nitrostyryl)-4-oxoquinazolin-3(4H)-yl)benzoic acid (987-6).



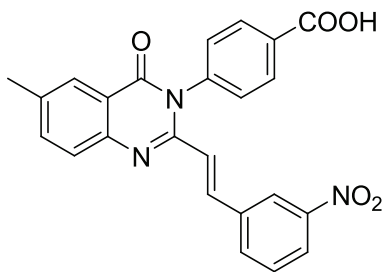
Compound **987-6** was prepared via procedure C using compound **987-6b** (0.300 g, 0.840 mmol) and *meta*-nitrobenzaldehyde (0.168 g, 1.10 mmol, 1.33 equiv). The crude material was recrystallized using methanol and dioxane and further purified by hot trituration with methanol and ethyl acetate to remove residual dioxane to yield the title compound as a yellow solid (0.120 g, 30%). 1H NMR (300 MHz, d_6 -DMSO) δ 8.22 (s, 1H), 8.19-8.14 (mult, 4H), 8.04 (dd, $J_1 = 8.5$ Hz, $J_2 = 2.3$ Hz, 1H), 8.00 (d, $J = 2.3$ Hz, 1H), 7.82 (d, $J = 7.6$ Hz, 1H), 7.73 (d, $J = 8.5$ Hz, 1H), 7.64-7.59 (mult, 3H), 6.46 (d, $J = 15.5$ Hz, 1H). ^{13}C NMR (100 MHz, d_6 -DMSO) δ 166.8, 160.0, 151.1, 148.2, 146.1, 140.0, 137.7, 137.2, 136.4, 133.2, 132.5, 130.7, 130.5, 129.6, 129.2, 128.5, 124.1, 122.4, 122.2, 119.3. HRMS calcd for $C_{23}H_{14}BrN_3O_5$, 492.01962 $[M+H]^+$; found, 492.00228 $[M+H]^+$. Anal. ($C_{23}H_{14}BrN_3O_5$) C, H, N. MP > 260 °C.

2,6-Dimethyl-4H-benzo[d][1,3]oxazin-4-one (96-11a).

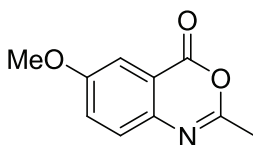
Compound **987-11a** was prepared via procedure A using 2-amino-5-methylbenzoic acid (3.00 g, 19.8 mmol). The crude material was purified by recrystallization with hexanes to give an off-white solid (3.21 g, 92%). ^1H NMR (400 MHz, d_6 -DMSO) δ 7.82 (s, 1H), 7.66 (dd, $J_1 = 8.3$ Hz, $J_2 = 1.6$ Hz, 1H), 7.40 (d, $J = 8.3$ Hz, 1H), 2.38 (s, 3H), 2.34 (s, 3H). ^{13}C NMR (100 MHz, d_6 -DMSO) δ 159.3, 143.9, 138.1, 137.7, 127.2, 125.9, 116.0, 20.8, 20.6.

4-(2,6-Dimethyl-4-oxoquinazolin-3(4H)-yl)benzoic acid (987-11b).

Compound **987-11b** was prepared via procedure B using compound **987-11a** (1.00 g, 5.71 mmol) and *para*-aminobenzoic acid (0.939 g, 6.85 mmol, 1.20 equiv). The crude material was purified by recrystallization with ethyl acetate to give an off-white solid (0.898 g, 54%). ^1H NMR (600 MHz, d_6 -DMSO) δ 8.11 (d, $J = 8.6$ Hz, 2H), 7.90 (s, 1H), 7.67 (dd, $J_1 = 8.6$ Hz, $J_2 = 1.4$ Hz, 1H), 7.60-7.57 (mult, 3H), 2.45 (s, 3H), 2.11 (s, 3H). ^{13}C NMR (150 MHz, d_6 -DMSO) δ 166.7, 161.2, 152.9, 145.4, 141.8, 136.2, 131.4, 130.5, 129.0, 126.5, 125.6, 120.1, 23.9, 20.8.

(E)-4-(6-methyl-2-(3-nitrostyryl)-4-oxoquinazolin-3(4H)-yl)benzoic acid (987-11).

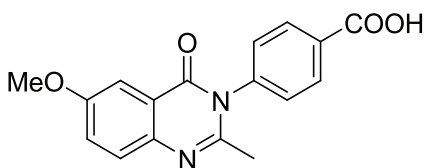
Compound **987-11** was prepared via procedure C using compound **987-11b** (0.507 g, 1.72 mmol) and *meta*-nitrobenzaldehyde (0.346 g, 2.29 mmol, 1.33 equiv) to yield the title compound as a yellow solid (0.498 g, 68%). ^1H NMR (400 MHz, d_6 -DMSO) δ 13.34 (bs, 1H), 8.22 (s, 1H), 8.18-8.14 (mult, 3H), 7.96 (d, $J = 15.6$ Hz), 7.93 (s, 1H), 7.83 (d, $J = 7.8$ Hz, 1H), 7.73-7.77 (mult, 2H), 7.64-7.60 (mult, 3H), 6.47 (d, $J = 15.6$ Hz, 1H), 2.48 (s, 3H). ^{13}C (100 MHz, d_6 -DMSO) δ 166.7, 161.0, 149.8, 148.2, 145.2, 140.8, 136.9, 136.6, 136.3, 133.3, 131.6, 130.7, 130.5, 129.5, 127.2, 125.8, 123.9, 122.8, 122.3, 120.4, 20.9. HRMS calcd for $\text{C}_{24}\text{H}_{17}\text{N}_3\text{O}_5$, 428.12476 $[\text{M}+\text{H}]^+$; found 428.12422 $[\text{M}+\text{H}]^+$. Anal. ($\text{C}_{24}\text{H}_{17}\text{N}_3\text{O}_5$) C, H, N. MP > 260 °C.

6-Methoxy-2-methyl-4H-benzo[d][1,3]oxazin-4-one (987-8a).

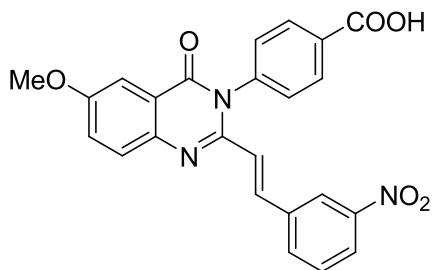
Compound **987-8a** was prepared via procedure A using 2-amino-5-methoxybenzoic acid (1.00 g, 6.00 mmol). The crude material was purified by recrystallization with hexanes to

give yellow needles (0.623 g, 55%). ^1H NMR (400 MHz, CDCl_3) δ 7.54 (d, $J = 2.9$ Hz, 1H), 7.45 (d, $J = 8.9$ Hz, 1H), 7.34 (dd, $J_1 = 8.9$ Hz, $J_2 = 2.9$ Hz, 1H), 3.89 (s, 3H), 2.44 (s, 3H). ^{13}C NMR (100 MHz, CDCl_3) δ 160.2, 159.3, 158.2, 140.8, 128.1, 126.0, 117.5, 108.6, 56.1, 21.3. HRMS calcd for $\text{C}_{10}\text{H}_9\text{NO}_3$, 192.06618 $[\text{M}+\text{H}]^+$; found, 192.06535 $[\text{M}+\text{H}]^+$.

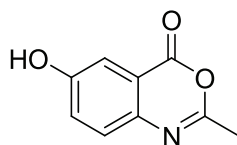
4-(6-Methoxy-2-methyl-4-oxoquinazolin-3(4H)-yl)benzoic acid (987-8b).



Compound **987-8b** was prepared via procedure B using compound **987-8a** (0.500 g, 2.62 mmol) and *para*-aminobenzoic acid (0.430 g, 3.10 mmol, 1.20 equiv). The crude material was purified by trituration with ethyl acetate to give a white solid (0.548 g, 68%). ^1H NMR (400 MHz, d_6 -DMSO) δ 8.08 (d, $J = 8.3$ Hz, 2H), 7.60-7.55 (mult, 3H), 7.44-7.40 (mult, 2H), 3.83 (s, 3H), 2.07 (s, 3H). ^{13}C NMR (100 MHz, d_6 -DMSO) δ 166.7, 161.0, 157.6, 151.4, 141.8, 131.4, 130.6, 128.9, 128.4, 124.1, 121.1, 118.2, 106.3, 55.6, 23.7. HRMS calcd for $\text{C}_{17}\text{H}_{14}\text{N}_2\text{O}_4$, 311.1033 $[\text{M}+\text{H}]^+$; found, 311.10211 $[\text{M}+\text{H}]^+$.

(E)-4-(6-methoxy-2-(3-nitrostyryl)-4-oxoquinazolin-3(4H)-yl)benzoic acid (987-8).

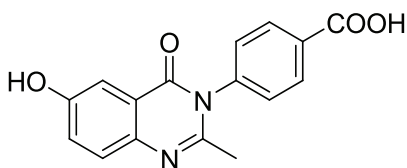
Compound **987-8** was prepared via procedure C using compound **987-8b** (0.120 g, 0.390 mmol) and *meta*-nitrobenzaldehyde (0.078 g, 0.51 mmol, 1.3 equiv) to yield the title compound as a yellow solid (0.094 g, 55%). ^1H NMR (400 MHz, d_6 -DMSO) δ 8.24 (s, 1H), 8.16 (d, J = 8.3 Hz, 3H), 7.94 (d, J = 15.6 Hz, 1H), 7.84 (d, J = 7.9 Hz, 2H), 7.62 (d, J = 9.8 Hz, 1H), 7.65-7.61 (mult, 3H), 7.54-7.53 (mult, 2H), 6.49 (d, J = 15.6 Hz, 1H). ^{13}C NMR (100 MHz, d_6 -DMSO) δ 167.7, 161.5, 158.8, 149.2, 148.9, 142.5, 140.9, 137.4, 136.4, 133.8, 133.7, 131.2, 129.9, 129.8, 129.7, 125.2, 124.5, 123.4, 122.9, 122.2, 56.4. HRMS calcd for $\text{C}_{24}\text{H}_{17}\text{N}_3\text{O}_6$, 444.11968 $[\text{M}+\text{H}]^+$; found, 444.11849 $[\text{M}+\text{H}]^+$. Anal. ($\text{C}_{24}\text{H}_{17}\text{N}_3\text{O}_6$) C, H, N. MP > 260°C.

2-methyl-4-oxo-4H-benzo[d][1,3]oxazin-6-yl acetate (987-24a).

Compound **987-24a** was prepared via procedure A using 2-amino-5-(tert-butyl)diphenylsilyloxy)benzoic acid (1.00 g, 2.55 mmol). The crude material was purified

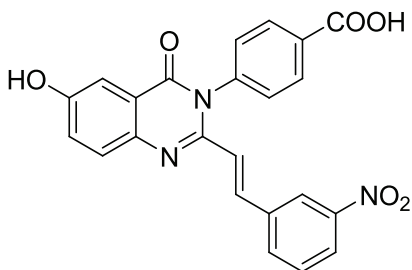
by recrystallization with hexanes to give yellow needles. ^1H NMR (400 MHz, CDCl_3) δ 7.86 (d, $J = 2.3$ Hz, 1H), 7.54-7.45 (mult, 2H), 2.43 (s, 3H), 2.31 (s, 3H). ^{13}C NMR (100 MHz, CDCl_3) δ 169.1, 160.1, 159.2, 149.9, 144.3, 130.7, 128.0, 120.8, 117.6, 21.5, 21.2.

4-(6-hydroxy-2-methyl-4-oxoquinazolin-3(4H)-yl)benzoic acid (987-24b).



Compound **987-24b** was prepared via procedure B using compound **987-24a** (0.400 g, 2.05 mmol) and *para*-aminobenzoic acid (0.338 g, 2.50 mmol, 1.20 equiv). The crude material was carried on without purification.

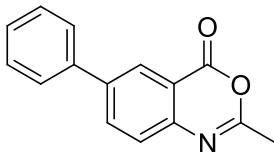
(E)-4-(6-acetoxy-2-(3-nitrostyryl)-4-oxoquinazolin-3(4H)-yl)benzoic acid (987-24).



Compound **987-24** was prepared via procedure C using compound **987-24b** (0.262 g, 0.770 mmol) and *meta*-nitrobenzaldehyde (0.156 g, 1.0 mmol, 1.33 equiv). The crude material was purified by recrystallization with methanol and dioxane and further

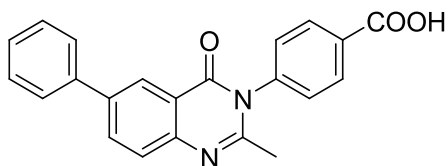
purified by hot gravity filtration after trituration with ethyl acetate and methanol (0.095 g, 29%). ^1H NMR (400 MHz, d_6 -DMSO) δ 8.23 (s, 1H), 8.15 (d, J = 8.6 Hz, 3H), 7.90 (d, J = 15.6 Hz, 1H), 7.83 (d, J = 7.8 Hz, 1H), 7.69 (d, J = 9.0 Hz, 1H), 7.62-7.59 (mult, 3H), 7.45 (d, J = 2.9 Hz, 1H), 7.36 (dd, J_1 = 8.6 Hz, J_2 = 2.9 Hz, 1H), 6.47 (d, J = 15.7 Hz, 1H). ^{13}C NMR (100 MHz, d_6 -DMSO) δ 166.7, 160.8, 156.7, 148.3, 147.6, 140.9, 140.4, 136.8, 135.3, 133.2, 131.4, 130.6, 130.5, 129.5, 129.2, 124.5, 123.7, 122.8, 122.2, 121.7, 109.4. HRMS calcd for $\text{C}_{23}\text{H}_{15}\text{N}_3\text{O}_6$, 430.10403 $[\text{M}+\text{H}]^+$; found, 430.10455 $[\text{M}+\text{H}]^+$. Anal. ($\text{C}_{23}\text{H}_{15}\text{N}_3\text{O}_6$) C, H, N. MP > 260°C.

2-Methyl-6-phenyl-4H-benzo[d][1,3]oxazin-4-one (987-35a).



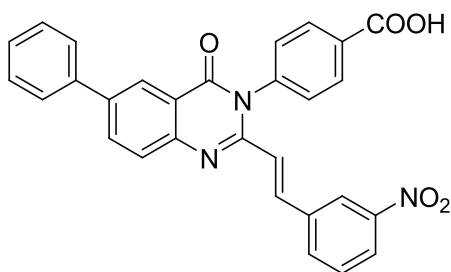
Compound **987-35a** was prepared via procedure A using 4-aminobiphenyl-3-carboxylic acid (0.500 g, 2.3 mmol). The crude material was purified by recrystallization with hexanes to give orange needles (0.363 g, 65%). ^1H NMR (400 MHz, CDCl_3) δ 8.32 (s, 1H), 7.96 (d, J = 7.9 Hz, 1H), 7.59-7.54 (mult, 3H), 7.44 (t, J = 7.0 Hz, 2H), 7.38 (d, J = 7.0 Hz, 1H), 2.44 (s, 3H). ^{13}C NMR (100 MHz, CDCl_3) δ 160.1, 159.8, 145.5, 141.2, 138.8, 135.2, 129.2, 128.3, 127.1, 126.9, 126.3, 116.9, 21.4.

4-(2-Methyl-4-oxo-6-phenylquinazolin-3(4H)-yl)benzoic acid (987-35b).



Compound **987-35b** was prepared via procedure B using **987-35a** (0.363 g, 1.53 mmol) and *para*-aminobenzoic acid (0.252 g, 1.84 mmol, 1.20 equiv). The crude material was purified by recrystallization with ethyl acetate (0.218 g, 40%). ^1H NMR (400 MHz, d_6 -DMSO) δ 13.27 (bs, 1H), 8.31 (d, $J = 2.0$ Hz, 1H), 8.18-8.13 (mult, 3H), 7.76 (d, $J = 8.2$ Hz, 3H), 7.63 (d, $J = 8.6$ Hz, 2H), 7.51 (t, $J = 7.0$ Hz, 2H), 7.41 (t, $J = 7.4$ Hz, 1H), 2.16 (s, 3H). ^{13}C NMR (100 MHz, DMSO- d_6) δ 166.7, 161.3, 154.0, 146.7, 141.8, 138.8, 138.2, 133.2, 131.4, 130.6, 129.2, 129.0, 128.0, 127.5, 126.8, 123.6, 120.8, 24.1. HRMS calcd for $\text{C}_{22}\text{H}_{16}\text{N}_2\text{O}_3$, 357.12403 $[\text{M}+\text{H}]^+$; found, 357.12312 $[\text{M}+\text{H}]^+$.

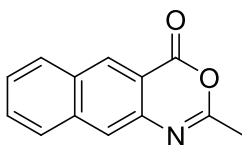
(E)-4-(2-(3-nitrostyryl)-4-oxo-6-phenylquinazolin-3(4H)-yl)benzoic acid (987-35).



Compound **987-35** was prepared via procedure C using **987-35b** (0.200 g, 0.560 mmol) and *meta*-nitrobenzaldehyde (0.113 g, 0.750 g, 1.33 equiv) to yield the title compound

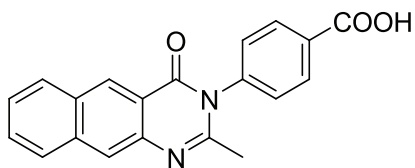
as a yellow solid (0.210 g, 76%). ^1H NMR (400 MHz, d_6 -DMSO) δ 8.35 (d, $J = 2.0$ Hz, 1H), 8.26-8.25 (mult, 1H), 8.23 (d, $J = 2.3$ Hz, 1H), 8.19-8.15 (mult, 3H), 8.03 (d, $J = 15.7$ Hz, 1H), 7.89 (d, $J = 8.2$ Hz, 1H), 7.86 (d, $J = 7.8$ Hz, 1H), 7.67-7.65 (mult, 3H), 7.53 (t, $J = 7.4$ Hz, 2H), 7.43 (t, $J = 7.0$ Hz, 1H), 6.51 (d, $J = 15.7$ Hz, 1H). ^{13}C NMR (100 MHz, d_6 -DMSO) δ 166.8, 161.1, 150.6, 148.2, 146.5, 140.4, 138.7, 138.6, 136.8, 136.5, 133.4, 133.3, 132.2, 130.7, 130.5, 129.4, 129.2, 128.1, 126.8, 124.0, 123.7, 122.7, 122.4, 121.0. HRMS calcd for $\text{C}_{29}\text{H}_{19}\text{N}_3\text{O}_5$, 490.14041 $[\text{M}+\text{H}]^+$; found, 490.13965 $[\text{M}+\text{H}]^+$. Anal. ($\text{C}_{29}\text{H}_{19}\text{N}_3\text{O}_5$) C, H, N. MP > 260°C.

2-Methyl-4H-naphtho[2,3-d][1,3]oxazin-4-one (987-23a).



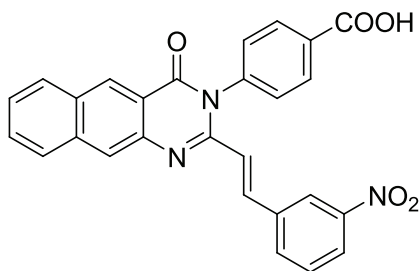
Compound **987-23a** was prepared via procedure A using 3-amino-2-naphthoic acid (1.00 g, 4.30 mmol). The crude material was purified by recrystallization with hexanes and ethyl acetate gave yellow flakes (0.638 g, 71%). ^1H NMR (400 MHz, CDCl_3) δ 8.77 (s, 1H), 7.99 (d, $J = 8.4$ Hz, 1H), 7.92 (d, $J = 8.4$ Hz, 2H), 7.65 (t, $J = 7.6$ Hz, 1H), 7.56 (t, $J = 7.6$ Hz, 1H), 2.48 (s, 3H). ^{13}C NMR (100 MHz, CDCl_3) δ 160.2, 158.4, 141.0, 137.6, 132.2, 131.1, 129.8, 129.7, 128.4, 127.2, 124.4, 115.4, 21.5. HRMS calcd for $\text{C}_{13}\text{H}_9\text{NO}_2$, 212.07127 $[\text{M}+\text{H}]^+$; found, 212.07040 $[\text{M}+\text{H}]^+$.

4-(2-Methyl-4-oxobenzo[g]quinazolin-3(4H)-yl)benzoic acid (987-23b).



Compound **987-23b** was prepared via procedure B using **987-23a** (0.200 g, 0.950 mmol) and *para*-aminobenzoic acid (0.156 g, 1.14 mmol, 1.20 equiv). The crude material was purified by recrystallization with ethyl acetate to give an off-white solid (0.152 g, 49%). ¹H NMR (400 MHz, *d*₆-DMSO) δ 8.85 (s, 1H), 8.24 (d, *J* = 6.7 Hz, 2H), 8.13 (d, *J* = 8.3 Hz, 3H), 7.71-7.65 (mult, 3H), 7.59 (t, *J* = 7.9 Hz, 1H), 2.17 (s, 3H). ¹³C NMR (100 MHz, *d*₆-DMSO) δ 166.7, 161.7, 152.8, 142.7, 141.9, 136.3, 131.4, 130.9, 130.6, 129.3, 129.2, 128.6, 127.8, 126.2, 124.0, 24.2. HRMS calcd for C₂₀H₁₄N₂O₃, 331.10838 [M+H]⁺; found, 331.10773 [M+H]⁺.

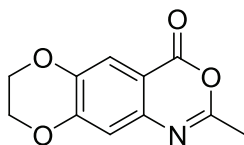
(E)-4-(2-(3-nitrostyryl)-4-oxobenzo[g]quinazolin-3(4H)-yl)benzoic acid (987-23).



Compound **987-23** was prepared via procedure C using compound **987-23b** (0.250 g, 0.760 mmol) and *meta*-nitrobenzaldehyde (0.152 g, 1.01 mmol, 1.33 equiv). The crude material was purified by hot gravity filtration with methanol (0.194 g, 55%). ¹H NMR (400 MHz, *d*₆-DMSO) δ 13.31 (bs, 1H), 8.87 (s, 1H), 8.28 (s, 1H), 8.25 (mult, 2H), 8.20-

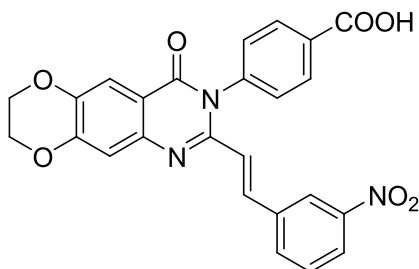
8.16 (mult, 4H), 8.02 (d, $J = 15.7$ Hz, 1H), 7.86 (d, $J = 7.8$ Hz, 1H), 7.33-7.59 (mult, 5H), 6.52 (d, $J = 15.7$ Hz, 1H). ^{13}C NMR (100 MHz, d_6 -DMSO) δ 166.8, 161.6, 149.6, 148.3, 142.6, 140.9, 136.7, 136.5, 133.3, 131.5, 131.2, 130.7, 130.5, 129.7, 129.4, 128.8, 128.0, 126.6, 124.9, 124.0, 123.0, 122.3, 119.8. HRMS calcd for $\text{C}_{27}\text{H}_{17}\text{N}_3\text{O}_5$, 464.12476 $[\text{M}+\text{H}]^+$; found, 464.125661 $[\text{M}+\text{H}]^+$. Anal. ($\text{C}_{27}\text{H}_{17}\text{N}_3\text{O}_5$) C, H, N. MP $> 260^\circ\text{C}$.

6,7-Dioxane-2-methyl-4H-benzo[d][1,3]oxazin-4-one (987-54a).



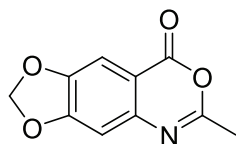
Compound **987-54a** was prepared via procedure A using 7-amino-2,3-dihydrobenzo[b][1,4]dioxine-6-carboxylic acid (0.500 g, 2.6 mmol). The crude material was purified by recrystallization with hexanes to give an orange solid. (0.399 g, 71%). ^1H NMR (400 MHz, CDCl_3) δ 7.60 (s, 1H), 6.97 (s, 1H), 4.37-4.31 (mult, 4H), 2.41 (s, 3H). ^{13}C NMR (100 MHz, CDCl_3) δ 159.5, 159.1, 151.3, 144.2, 142.1, 115.9, 115.8, 113.92, 113.86, 110.5, 64.9, 64.2, 21.4. HRMS calcd for $\text{C}_{11}\text{H}_9\text{NO}_4$, 220.06110 $[\text{M}+\text{H}]^+$; found, 220.06039 $[\text{M}+\text{H}]^+$. MP $169\text{-}171^\circ\text{C}$.

(E)-4-(2-(3-nitrostyryl)-4-oxo-7,8-dihydro-[1,4]dioxino[2,3-g]quinazolin-3(4H)-yl)benzoic acid (987-54).



Compound **987-54** was prepared via procedure C using compound **987-54b** (0.150 g, 0.44 mmol) and *meta*-nitrobenzaldehyde (0.089 g, 0.59 mmol, 1.33 equiv). The crude material was purified by hot gravity filtration with methanol to give a yellow solid (0.056 g, 27%). ¹H NMR (400 MHz, *d*₆-DMSO) δ 8.19 (s, 1H), 8.14 (d, *J* = 8.2 Hz, 1H), 8.03 (d, *J* = 8.2 Hz, 2H), 7.89 (d, *J* = 15.7 Hz, 1H), 7.75 (d, *J* = 7.8 Hz, 1H), 7.64 (t, *J* = 7.8 Hz, 1H), 7.51 (s, 1H), 7.26 (d, *J* = 8.2 Hz, 2H), 7.21 (s, 1H), 6.49 (d, *J* = 15.7 Hz, 1H), 4.44-4.38 (mult, 4H). ¹³C NMR (100 MHz, *d*₆-DMSO) δ 168.1, 160.3, 149.8, 149.7, 148.3, 143.7, 142.7, 142.0, 136.8, 136.7, 135.5, 132.9, 130.6, 130.1, 127.6, 123.8, 123.0, 122.1, 115.0, 114.2, 113.4, 112.6, 64.4, 64.3. HRMS calcd for C₂₅H₁₇N₃O₇, 472.11459 [M+H]⁺; found, 472.11429 [M+H]⁺. Anal. (C₂₅H₁₇N₃O₇) C, H, N. MP > 260 °C.

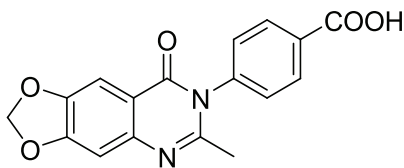
6,7-Dioxolane-2-methyl-4H-benzo[d][1,3]oxazin-4-one (987-55a).



Compound **987-55a** was prepared via procedure A using 7-aminobenzo[d][1,3]dioxole-5-carboxylic acid (0.500 g, 2.80 mmol). The crude material was purified by

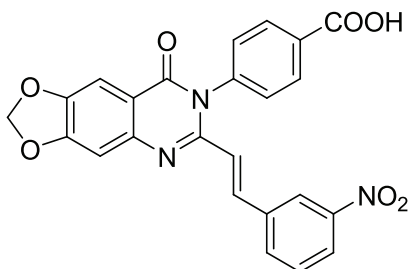
recrystallization with hexanes to give an orange solid (0.245 g, 43%). ^1H NMR (600 MHz, CDCl_3) δ 7.37 (s, 1H), 6.92 (s, 1H), 6.13 (s, 2H), 2.43 (s, 3H). ^{13}C NMR (150 MHz, CDCl_3) δ 159.6, 155.1, 148.2, 144.7, 110.9, 105.7, 105.6, 102.8, 21.4. MP 148-150°C

4-(6-Methyl-8-oxo-[1,3]dioxolo[4,5-g]quinazolin-7(8H)-yl)benzoic acid (987-55b).



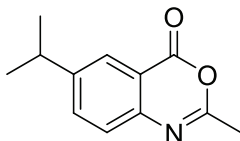
Compound **987-55b** was prepared via procedure B using **987-55a** (0.220 g, 1.07 mmol) and *para*-aminobenzoic acid (0.176 g, 1.29 mmol, 1.2 equiv). The crude material was purified by recrystallization with ethyl acetate to give an off-white solid (0.115 g, 33%). ^1H NMR (400 MHz, CDCl_3) δ 13.27 (bs, 1H), 8.10 (d, $J = 8.2$ Hz, 2H), 7.58 (d, $J = 8.2$ Hz, 2H), 7.39 (s, 1H), 7.15 (s, 1H), 6.23 (s, 2H), 2.09 (s, 3H). ^{13}C NMR (400 MHz, d_6 -DMSO) δ 166.7, 160.5, 153.3, 152.4, 146.9, 145.2, 141.8, 131.3, 130.5, 129.0, 114.9, 105.1, 102.8, 102.5. HRMS calcd for $\text{C}_{17}\text{H}_{12}\text{N}_2\text{O}_5$, 325.08256 $[\text{M}+\text{H}]^+$; found 325.08196 $[\text{M}+\text{H}]^+$. MP > 260°C.

(E)-4-(6-(3-nitrostyryl)-8-oxo-[1,3]dioxolo[4,5-g]quinazolin-7(8H)-yl)benzoic acid (987-55).



Compound **987-55** was prepared via procedure C using compound **987-55b** (0.100 g, 0.31 mmol) and *meta*-nitrobenzaldehyde (0.062 g, 0.41 mmol, 1.33 equiv). The crude material was purified by hot gravity filtration with methanol to give a yellow solid (0.048 g, 34%). ^1H NMR (400 MHz, d_6 -DMSO) δ 8.21 (s, 1H), 8.15 (d, J = 8.6 Hz, 1H), 8.00 (d, J = 8.3 Hz, 2H), 7.91 (d, J = 15.6 Hz, 1H), 7.76 (d, J = 7.0 Hz, 1H), 7.65 (t, J = 7.9 Hz, 1H), 7.46 (s, 1H), 7.28 (d, J = 8.3 Hz, 2H), 7.24 (s, 1H), 6.49 (d, J = 15.6 Hz, 1H), 6.27 (s, 2H). HRMS calcd for $\text{C}_{24}\text{H}_{15}\text{N}_3\text{O}_7$, 458.09894 $[\text{M}+\text{H}]^+$; found, 458.09772 $[\text{M}+\text{H}]^+$. Anal. ($\text{C}_{24}\text{H}_{15}\text{N}_3\text{O}_7$) C, H, N. MP > 260°C.

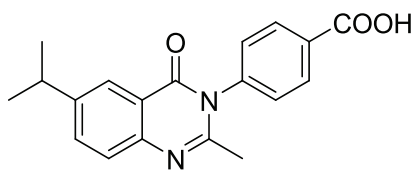
6-Isopropyl-2-methyl-4H-benzo[d][1,3]oxazin-4-one (987-36a).



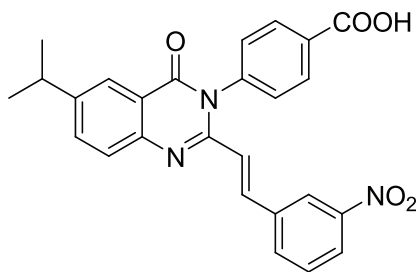
Compound **987-36a** was prepared via procedure A using 2-amino-5-isopropylbenzoic acid (0.400 g, 2.20 mmol). The crude material was purified by silica gel chromatography (ISCO RediSep 24 g column, 0-50% EtOAc/hexanes gradient) to give a yellow residue (0.439 g, 97%). ^1H NMR (400 MHz, CDCl_3) δ 7.92 (d, J = 2.0 Hz, 1H), 7.57 (dd, J_1 = 8.4 Hz,

$J_2 = 2.0$ Hz, 1H), 7.36 (d, $J = 8.2$ Hz, 1H), 2.04 (sept, $J = 7.0$ Hz, 1H), 2.36 (s, 3H), 1.22 (d, $J = 7.0$ Hz, 6H). ^{13}C NMR (100 MHz, CDCl_3) δ 159.9, 159.4, 149.4, 144.5, 135.4, 126.3, 125.4, 116.4, 33.9, 23.8, 21.2.

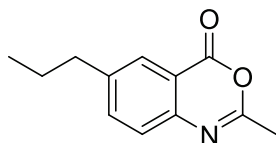
4-(6-Isopropyl-2-methyl-4-oxoquinazolin-3(4H)-yl)benzoic acid (987-36b).



Compound **987-36b** was prepared via procedure B using compound **987-23a** (0.439 g, 2.20 mmol) and *para*-aminobenzoic acid (0.355 g, 2.60 mmol, 1.20 equiv). The crude material was purified by recrystallization with methanol to give an off-white solid (0.190 g, 27%). ^1H NMR (400 MHz, d_6 -DMSO) δ 8.12 (d, $J = 8.3$ Hz, 2H), 7.93 (s, 1H), 7.75 (d, $J = 8.6$ Hz, 1H), 7.62-7.58 (mult, 3H), 3.01 (sept, $J = 7.0$ Hz, 1H), 2.11 (s, 3H), 1.25 (d, $J = 7.0$ Hz, 6H). ^{13}C NMR (100 MHz, d_6 -DMSO) δ 166.7, 161.3, 153.0, 147.0, 145.7, 141.9, 133.6, 131.3, 130.6, 129.0, 126.8, 122.9, 120.2, 33.2, 23.9, 23.8. HRMS calcd for $\text{C}_{19}\text{H}_{18}\text{N}_2\text{O}_3$, 323.13968 $[\text{M}+\text{H}]^+$; found 323.13879 $[\text{M}+\text{H}]^+$.

(E)-4-(6-isopropyl-2-(3-nitrostyryl)-4-oxoquinazolin-3(4H)-yl)benzoic acid (987-36).

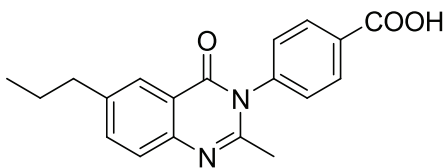
Compound **987-36** was prepared via procedure C using **987-36b** (0.150 g, 0.47 mmol) and *meta*-nitrobenzaldehyde (0.094 g, 0.62 mmol, 1.3 equiv) to yield the title compound as a yellow solid (0.137 g, 65%). ^1H NMR (400 MHz, d_6 -DMSO) δ 13.34 (bs, 1H), 8.26 (s, 1H), 8.16 (d, $J = 8.6$ Hz, 3H), 8.00 (d, $J = 15.7$ Hz, 1H), 7.99 (d, $J = 2.0$ Hz, 1H), 7.87-7.83 (mult, 3H), 7.75 (d, $J = 8.2$ Hz, 1H), 7.66-7.61 (mult, 3H), 6.49 (d, $J = 15.7$ Hz, 1H), 3.11 (sept, $J = 7.0$ Hz, 1H), 1.29 (d, $J = 7.0$ Hz, 6H). ^{13}C NMR (100 MHz, d_6 -DMSO) δ 166.8, 161.1, 149.9, 148.3, 147.6, 145.6, 140.7, 136.6, 136.3, 133.8, 133.3, 131.8, 130.7, 130.5, 129.4, 127.5, 123.9, 123.1, 122.7, 122.3, 120.4, 33.3, 23.7. HRMS calcd for $\text{C}_{26}\text{H}_{21}\text{N}_3\text{O}_5$, 456.15606 $[\text{M}+\text{H}]^+$; found, 456.15557 $[\text{M}+\text{H}]^+$. Anal. ($\text{C}_{26}\text{H}_{21}\text{N}_3\text{O}_5$) C, H, N. MP > 260°C.

2-Methyl-6-propyl-4H-benzo[d][1,3]oxazin-4-one (987-37a).

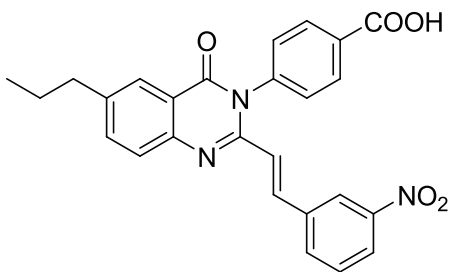
Compound **987-37a** was prepared via procedure A using 2-amino-5-propylbenzoic acid (0.500 g, 2.80 mmol). The crude material was purified by silica gel chromatography (ISCO RediSep 24 g column, 0-50% EtOAc/Hexanes gradient) to give a yellow residue (0.534 g, 94%). ^1H NMR (400 MHz, CDCl_3) δ 7.75 (d, $J = 1.2$ Hz, 1H), 7.41 (dd, $J_1 = 8.2$ Hz,

$J_2 = 1.2$ Hz, 1H), 7.24 (d, $J = 8.2$ Hz, 1H), 2.51 (t, $J = 7.4$ Hz, 2H), 2.60 (s, 3H), 1.50 (sext, $J = 7.4$ Hz, 2H), 0.78 (t, $J = 7.4$ Hz, 3H). ^{13}C NMR (100 MHz, CDCl_3) δ 159.6, 159.2, 144.3, 143.0, 136.9, 127.2, 126.0, 116.2, 37.4, 24.1, 21.1, 13.5.

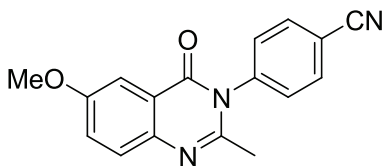
4-(2-Methyl-4-oxo-6-propylquinazolin-3(4H)-yl)benzoic acid (987-37b).



Compound **987-37b** was prepared via procedure B using **987-37a** (0.534 g, 2.60 mmol) and *para*-aminobenzoic acid (0.432 g, 3.20 mmol, 1.20 equiv). The crude material was purified by trituration with methanol and concentration of the filtrate (0.578 g, 68%). ^1H NMR (400 MHz, d_6 -DMSO) δ 8.30 (d, $J = 8.6$ Hz, 2H), 8.07 (d, $J = 2.0$ Hz, 1H), 7.75 (d, $J = 8.2$ Hz, 1H), 7.64 (dd, $J_1 = 8.2$ Hz, $J_2 = 2.0$ Hz, 1H), 7.41 (d, $J = 8.6$ Hz, 2H), 2.73 (t, $J = 7.4$ Hz, 1H), 2.58 (t, $J = 7.4$ Hz, 1H), 2.12 (s, 3H), 1.74-1.61 (mult, 2H), 0.97-0.91 (mult, 3H). HRMS calcd for $\text{C}_{19}\text{H}_{18}\text{N}_2\text{O}_3$, 323.13968 $[\text{M}+\text{H}]^+$; found, 323.12896 $[\text{M}+\text{H}]^+$.

(E)-4-(2-(3-nitrostyryl)-4-oxo-6-propylquinazolin-3(4H)-yl)benzoic acid (987-37).

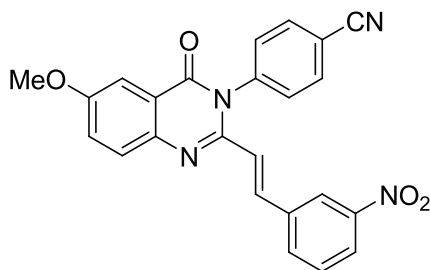
Compound **987-37** was prepared via procedure C using compound **987-37b** (0.578 g, 1.79 mmol) and *meta*-nitrobenzaldehyde (0.360 g, 2.38 mmol). The crude material was purified by silica gel chromatography (ISCO, RediSep 24 g column, silica cake, 0-10% MeOH/DCM gradient) to give a yellow solid (0.086 g, 11%). ^1H NMR (400 MHz, d_6 -DMSO) δ 8.26 (s, 1H), 8.16 (d, J = 8.6 Hz, 3H), 7.96 (d, J = 15.6 Hz, 2H), 7.85 (d, J = 7.6 Hz, 1H), 7.79-7.73 (mult, 3H), 7.64 (t, J = 7.9 Hz, 3H), 6.50 (d, J = 15.6 Hz, 1H), 2.75 (t, J = 7.3 Hz, 2H), 1.67 (sext, J = 7.3 Hz, 2H), 0.93 (t, J = 7.3 Hz, 3H). ^{13}C NMR (100 MHz, d_6 -DMSO) δ 166.8, 161.1, 149.9, 148.3, 145.5, 141.5, 140.8, 136.6, 136.3, 135.7, 133.3, 131.6, 130.7, 130.5, 129.5, 127.3, 125.4, 123.9, 122.8, 122.3, 120.4, 36.8, 24.1, 13.5. HRMS calcd for $\text{C}_{26}\text{H}_{21}\text{N}_3\text{O}_5$, 456.15606 $[\text{M}+\text{H}]^+$; found, 456.15568 $[\text{M}+\text{H}]^+$. Anal. ($\text{C}_{26}\text{H}_{21}\text{N}_3\text{O}_5$) C, H, N. MP > 260°C.

4-(6-Methoxy-2-methyl-4-oxoquinazolin-3(4H)-yl)benzonitrile (987-19b).

Compound **987-19b** was prepared via procedure B using compound **987-8a** (0.300 g, 1.57 mmol) and *para*-aminobenzonitrile (0.222 g, 1.90 mmol, 1.20 equiv). After cooling

to room temperature the resulting white solid was collected by filtration and washed with hexanes (0.205 g, 45%). ^1H NMR (400 MHz, CDCl_3) δ 7.87 (d, $J = 7.8$ Hz, 2H), 7.62 (d, $J = 9.0$ Hz, 1H), 7.59 (s, 1H), 7.43 (d, $J = 7.8$ Hz, 2H), 7.38 (d, $J = 9.0$ Hz, 1H), 3.90 (s, 3H), 2.21 (s, 3H). ^{13}C NMR (100 MHz CDCl_3) δ 162.0, 158.7, 150.5, 142.1, 142.0, 134.1, 129.7, 128.7, 125.3, 121.3, 117.9, 113.8, 106.6, 56.0, 24.2. HRMS calcd for $\text{C}_{17}\text{H}_{13}\text{N}_3\text{O}_2$, 292.10872 $[\text{M}+\text{H}]^+$; found, 292.10787 $[\text{M}+\text{H}]^+$.

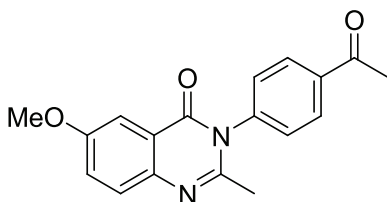
(E)-4-(6-methoxy-2-(3-nitrostyryl)-4-oxoquinazolin-3(4H)-yl)benzonitrile (987-19).



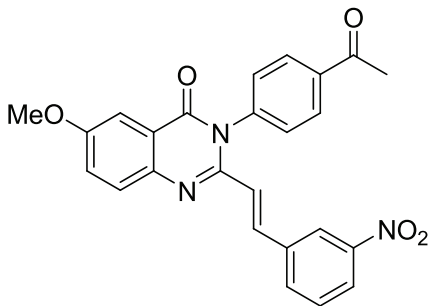
Compound **987-19** was prepared via procedure C using compound **987-19b** (0.150 g, 0.520 mmol) and *meta*-nitrobenzaldehyde (0.103 g, 0.690 mmol, 1.33 equiv). The crude material was purified by recrystallization with hexanes and chloroform to yield the title compound as a bright yellow solid (0.112 g, 51%). ^1H NMR (400 MHz, CDCl_3) δ 8.19-8.17 (mult, 2H), 8.00 (d, $J = 15.7$ Hz, 1H), 7.93 (d, $J = 8.6$ Hz, 2H), 7.76 (d, $J = 9.0$ Hz, 1H), 7.66 (d, $J = 2.7$ Hz, 1H), 7.63-7.61 (mult, 1H), 7.54 (d, $J = 8.6$ Hz, 1H), 7.51 (d, $J = 8.6$ Hz, 2H), 7.45 (dd, $J_1 = 9.0$ Hz, $J_2 = 2.7$ Hz, 1H), 3.95 (s, 3H), 1.57 (s, 3H). ^{13}C NMR (100 MHz, CDCl_3) δ 161.8, 159.3, 148.9, 147.2, 142.1, 141.2, 137.3, 137.0, 134.1, 132.9, 130.3, 130.1, 129.6, 125.7, 124.3, 122.8, 122.1, 121.8, 118.0, 114.0, 106.9, 56.1. HRMS calcd for

$C_{24}H_{16}N_4O_4$, 425.12510 $[M+H]^+$; found, 425.12473 $[M+H]^+$. Anal. ($C_{24}H_{16}N_4O_4$) C, H, N. MP > 260°C.

3-(4-Acetylphenyl)-6-methoxy-2-methylquinazolin-4(3H)-one (987-20b).

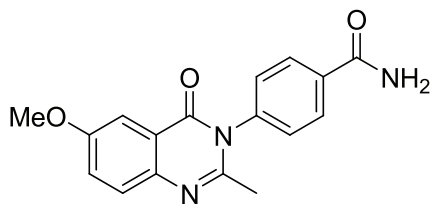


Compound **987-20b** was prepared via procedure B using compound **987-8a** (0.300 g, 1.57 mmol) and *para*-aminoacetophenone (0.255 g, 1.90 mmol, 1.20 equiv). The crude material was purified by silica gel chromatography (ISCO, RediSep 12 g column, 50-70% EtOAc/hexanes gradient) to give an off-white solid (0.400 g, 83%). 1H NMR (400 MHz, $CDCl_3$) δ 8.10 (d, J = 8.3 Hz, 2H), 7.58 (d, J = 9.0 Hz, 1H), 7.55 (d, J = 2.7 Hz, 1H), 7.36 (d, J = 8.3 Hz, 2H), 7.34 (dd, J_1 = 9.0 Hz, J_2 = 2.7 Hz, 1H), 3.85 (s, 3H), 2.63 (s, 3H), 2.18 (s, 3H). ^{13}C NMR (100 MHz, $CDCl_3$) δ 197.1, 162.1, 158.5, 150.9, 142.1, 137.7, 130.1, 129.7, 128.7, 125.1, 121.3, 118.8, 106.4, 55.9, 26.9, 24.2 HRMS calcd for $C_{18}H_{16}N_2O_3$, 309.12403 $[M+H]^+$; found, 309.10630 $[M+H]^+$.

(E)-3-(4-acetylphenyl)-6-methoxy-2-(3-nitrostyryl)quinazolin-4(3H)-one (987-20).

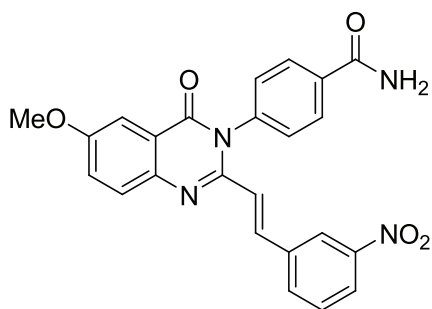
Compound **987-20** was prepared via procedure C using compound **987-20b** (0.200 g, 0.650 mmol) and *meta*-nitrobenzaldehyde (0.130 g, 0.860 mmol, 1.33 equiv). The crude material was purified using silica gel chromatography (ISCO, RediSep 12 g column, 0-50% EtOAc/hexanes gradient) to yield the title compound as a yellow solid (0.057 g, 20%). ^1H NMR (400 MHz, d_6 -DMSO) δ 8.20 (d, J = 8.2 Hz, 2H), 8.15 (s, 1H), 7.97 (d, J = 15.3 Hz, 1H), 7.75 (d, J = 9.0 Hz, 1H), 7.67 (d, J = 2.7 Hz, 1H), 7.59 (d, J = 7.8 Hz, 1H), 7.52-7.42 (mult, 4H), 6.41 (d, J = 15.3 Hz, 1H), 3.92 (s, 3H), 2.72 (s, 3H). ^{13}C NMR (100 MHz, d_6 -DMSO) δ 197.5, 160.8, 158.2, 148.5, 148.3, 141.7, 141.1, 137.1, 136.7, 135.8, 133.2, 130.5, 129.6, 129.5, 129.2, 124.6, 123.9, 122.8, 122.3, 122.2, 121.5, 55.8, 27.0. HRMS calcd for $\text{C}_{25}\text{H}_{19}\text{N}_3\text{O}_5$, 442.14041 $[\text{M}+\text{H}]^+$; found, 442.14017 $[\text{M}+\text{H}]^+$. Anal. ($\text{C}_{25}\text{H}_{19}\text{N}_3\text{O}_5$) C, H, N. MP > 260°C.

4-(6-Methoxy-2-methyl-4-oxoquinazolin-3(4H)-yl)benzamide (987-21b).



Compound **987-21b** was prepared via procedure B using compound **987-8a** (0.300 g, 1.57 mmol) and *para*-aminobenzamide (0.256 g, 1.88 mmol, 1.20 equiv). The crude material was purified by trituration with ethyl acetate and collection of the white solid by filtration (0.416 g, 86%). ^1H NMR (400 MHz, d_6 -DMSO) δ 8.16 (s, 1H), 8.05 (d, J = 8.2 Hz, 1H), 7.64-7.62 (mult, 2H), 7.76-7.54 (mult, 3H), 7.48-7.44 (mult, 2H), 3.87 (s, 3H), 2.11 (s, 3H). ^{13}C NMR (100 MHz, d_6 -DMSO) δ 167.2, 161.1, 157.6, 151.6, 141.8, 140.5, 134.8, 128.8, 128.5, 128.4, 128.4, 124.1, 121.1, 118.0, 106.2, 55.8, 55.7, 23.8. HRMS calcd for $\text{C}_{17}\text{H}_{15}\text{N}_3\text{O}_3$, 310.11928 $[\text{M}+\text{H}]^+$; found, 310.11819 $[\text{M}+\text{H}]^+$.

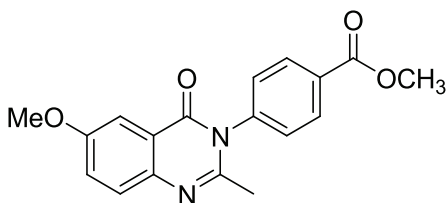
(E)-4-(6-Methoxy-2-(3-nitrostyryl)-4-oxoquinazolin-3(4H)-yl)benzamide (987-21).



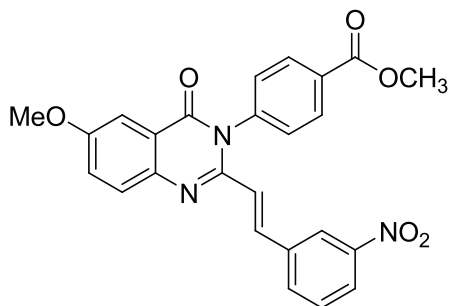
Compound **987-21** was prepared via procedure C using compound **987-21b** (0.200 g, 0.650 mmol) and *meta*-nitrobenzaldehyde (0.130 g, 0.860 mmol, 1.33 equiv). The crude material was purified by hot gravity filtration after boiling with methanol and collection of the title compound as the resulting yellow solid (0.162 g, 57%). ^1H NMR (400 MHz, d_6 -

DMSO) δ 8.24 (s, 1H), 8.16 (d, J = 8.6 Hz, 2H), 8.09 (d, J = 8.6 Hz, 2H), 7.94 (d, J = 15.7 Hz, 1H), 7.83 (d, J = 7.8 Hz, 1H), 7.77 (d, J = 8.6 Hz, 1H), 7.64 (t, J = 7.8 Hz, 1H), 7.58 (d, J = 8.6 Hz, 2H), 7.54-7.51 (mult, 3H), 6.49 (d, J = 15.7 Hz, 1H), 3.91 (s, 3H). ^{13}C NMR (100 MHz, d_6 -DMSO) δ 167.1, 160.9, 158.1, 148.6, 148.3, 141.7, 139.4, 136.7, 135.7, 134.9, 133.1, 130.5, 129.2, 129.0, 128.9, 124.5, 123.8, 122.8, 122.2, 121.6, 55.8. HRMS calcd for $\text{C}_{24}\text{H}_{18}\text{N}_4\text{O}_5$, 443.13566 $[\text{M}+\text{H}]^+$; found, 443.13529 $[\text{M}+\text{H}]^+$. Anal. ($\text{C}_{24}\text{H}_{18}\text{N}_4\text{O}_5$) C, H, N. MP > 260°C.

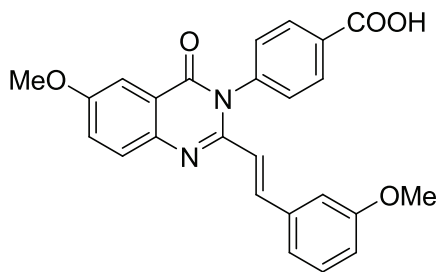
Methyl 4-(6-methoxy-2-methyl-4-oxoquinazolin-3(4H)-yl)benzoate (987-22b).



Compound **987-22b** was prepared via procedure B using compound **987-8a** (0.300 g, 1.57 mmol) and *para*-aminomethylbenzoate (0.285 g, 1.88 mmol, 1.20 equiv). After the crude mixture was concentrated *in vacuo*, the resulting yellow residue was partitioned between ethyl acetate and saturated sodium bicarbonate. The organics were extracted 2x with EtOAc, washed with brine, dried over MgSO_4 , and concentrated *in vacuo* to give an off-white solid (0.368 g, 72%). ^1H NMR (400 MHz, CDCl_3) δ 8.22 (d, J = 8.2 Hz, 2H), 7.95 (d, J = 9.0 Hz, 1H), 7.63-7.55 (mult, 2H), 7.38-7.35 (mult, 2H), 3.96 (s, 3H), 3.88 (s, 3H), 2.23 (s, 3H). ^{13}C NMR (100 MHz, CDCl_3) δ 166.2, 158.6, 151.1, 142.2, 142.1, 131.5, 131.3, 130.9, 128.7, 128.6, 125.2, 121.5, 118.9, 56.0, 52.7, 24.3. HRMS calcd for $\text{C}_{18}\text{H}_{16}\text{N}_2\text{O}_4$, 325.11895 $[\text{M}+\text{H}]^+$; found, 325.11787 $[\text{M}+\text{H}]^+$.

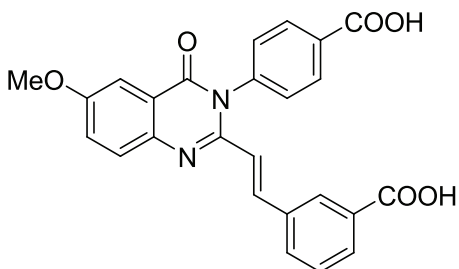
(E)-methyl 4-(6-methoxy-2-(3-nitrostyryl)-4-oxoquinazolin-3(4H)-yl)benzoate (987-22).

Compound **987-22** was prepared via procedure C using compound **987-22b** (0.200 g, 0.650 mmol) and *meta*-nitrobenzaldehyde (0.124 g, 0.860 mmol, 1.33 equiv) to yield the title compound as a yellow solid (0.143 g, 51%). ¹H NMR (400 MHz, *d*₆-DMSO) δ 8.29 (d, *J* = 8.2 Hz, 1H), 8.15 (d, *J* = 6.7 Hz, 2H), 7.96 (d, *J* = 15.7 Hz, 1H), 7.76 (d, *J* = 9.0 Hz, 1H), 7.67 (d, *J* = 2.7 Hz, 1H), 7.59 (d, *J* = 7.8 Hz, 1H), 7.50 (t, *J* = 7.8 Hz, 1H), 7.45-7.43 (mult, 3H), 6.42 (d, *J* = 15.7 Hz, 1H), 4.01 (s, 3H), 3.95 (s, 3H). ¹³C NMR (100 MHz, *d*₆-DMSO) δ 166.3, 161.9, 159.1, 148.8, 148.3, 142.2, 141.1, 137.2, 136.8, 132.9, 131.6, 131.5, 130.0, 129.5, 129.2, 125.5, 124.1, 122.7, 122.6, 121.9, 106.8, 56.4, 53.1. HRMS calcd for C₂₅H₁₉N₃O₆, 458.13533 [M+H]⁺; found, 458.13473 [M+H]⁺. Anal. (C₂₅H₁₉N₃O₆) C, H, N. MP > 260°C.

(E)-4-(6-methoxy-2-(3-nitrostyryl)-4-oxoquinazolin-3(4H)-yl)benzoic acid (987-13).

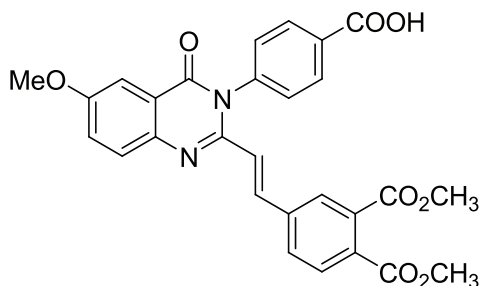
Compound **987-13** was prepared via procedure C using compound **987-8b** (0.200 g, 0.650 mmol) and *ortho*-anisaldehyde (0.104 mL, 0.860 mmol, 1.33 equiv) to yield the title compound as a yellow solid (0.150 g, 54%). ^1H NMR (300 MHz, d_6 -DMSO) δ 13.32 (bs, 1H), 8.16 (d, $J = 8.5$ Hz, 2H), 7.78 (d, $J = 15.3$ Hz, 1H), 7.75 (d, $J = 9.4$ Hz, 1H), 7.52-7.49 (mult, 2H), 7.26 (t, $J = 7.9$ Hz, 1H), 6.92 (d, $J = 8.5$ Hz, 3H), 6.28 (d, $J = 15.3$ Hz, 1H), 3.90 (s, 3H), 3.72 (s, 3H). ^{13}C NMR (100 MHz, d_6 -DMSO) δ 166.7, 160.9, 159.5, 157., 148.8, 141.9, 141.0, 138.0, 136.3, 131.6, 130.6, 130.1, 129.5, 129.0, 124.5, 121.3, 120.2, 119.1, 115.1, 113.5, 106.5, 55.7, 55.1. HRMS calcd for $\text{C}_{25}\text{H}_{20}\text{N}_2\text{O}_5$, 429.14516 $[\text{M}+\text{H}]^+$; found, 429.14404 $[\text{M}+\text{H}]^+$. Anal. ($\text{C}_{25}\text{H}_{20}\text{N}_2\text{O}_5$) C, H, N. MP > 260°C.

(E)-3-(2-(3-(4-carboxyphenyl)-6-methoxy-4-oxo-3,4-dihydroquinazolin-2-yl)vinyl)benzoic acid (987-16).

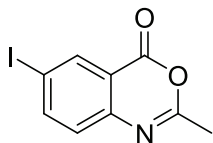


Compound **987-16** was prepared via procedure C using compound **987-8b** (0.200 g, 0.650 mmol) and *meta*-formylbenzoic acid (0.129 g, 0.860 mmol, 1.33 equiv) to yield the title compound as a yellow solid (0.259 g, 45%). ^1H NMR (400 MHz, d_6 -DMSO) δ 8.16 (d, $J = 8.6$ Hz, 2H), 7.89 (mult, 3H), 7.76 (d, $J = 9.5$ Hz, 1H), 7.63 (d, $J = 8.6$ Hz, 2H), 7.53-7.50 (mult, 2H), 7.58 (t, $J = 7.9$ Hz, 1H), 6.37 (d, $J = 15.6$ Hz, 1H), 3.90 (s, 3H). ^{13}C NMR (100 MHz, d_6 -DMSO) δ 166.8, 166.7, 160.9, 158.1, 148.7, 141.8, 141.0, 137.2, 135.3, 131.52, 131.49, 130.7, 130.2, 129.5, 129.1, 128.1, 124.5, 121.4, 120.9, 106.5, 55.8. HRMS calcd for $\text{C}_{25}\text{H}_{18}\text{N}_2\text{O}_6$, 443.12443 $[\text{M}+\text{H}]^+$; found, 443.12393 $[\text{M}+\text{H}]^+$. Anal. ($\text{C}_{25}\text{H}_{18}\text{N}_2\text{O}_6$) C, H, N. MP > 260°C.

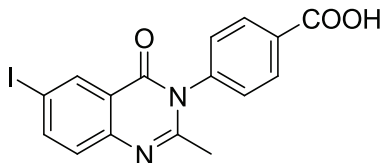
(E)-4-(2-(3,4-diacetoxystyryl)-6,7-dimethoxy-4-oxoquinazolin-3(4H)-yl)benzoic acid (987-15).



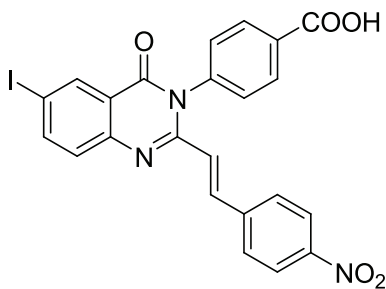
Compound **987-15** was prepared via procedure C using **987-8b** (0.400 g, 1.29 mmol) and 3,4-dihydroxybenzaldehyde (0.237 g, 1.71 g, 1.33 equiv). The crude material was purified by silica gel chromatography (ISCO, RediSep 40 g column, silica cake, 0-10% MeOH/DCM gradient) to yield the title compound as a yellow solid (0.221 g, 33%). ^1H NMR (400 MHz, d_6 -DMSO) δ 8.15 (d, $J = 8.3$ Hz, 2H), 7.91 (d, $J = 15.6$ Hz, 1H), 7.76 (d, $J = 7.6$ Hz, 1H), 7.60 (d, $J = 8.3$ Hz, 2H), 7.52 (d, $J = 7.3$ Hz, 2H), 7.25 (d, $J = 8.3$ Hz, 1H), 6.32 (d, $J = 15.6$ Hz, 1H), 3.90 (s, 3H), 2.27 (s, 6H). ^{13}C NMR (100 MHz, d_6 -DMSO) δ 168.81, 168.76, 161.5, 158.6, 149.4, 143.3, 143.0, 142.5, 141.5, 137.2, 134.4, 132.3, 131.3, 130.0, 129.8, 126.3, 125.1, 124.9, 123.4, 123.3, 122.0, 121.6, 107.2, 56.4, 21.02, 20.98. HRMS calcd for $\text{C}_{28}\text{H}_{22}\text{N}_2\text{O}_8$, 515.14556 $[\text{M}+\text{H}]^+$; found, 515.14526 $[\text{M}+\text{H}]^+$. Anal. ($\text{C}_{28}\text{H}_{22}\text{N}_2\text{O}_8$) C, H, N. MP 247-252°C.

6-Iodo-2-methyl-4H-benzo[d][1,3]oxazin-4-one (987-45a).

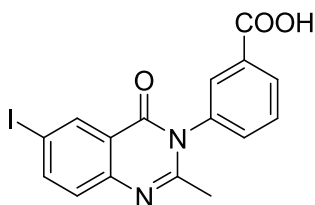
Compound **987-45a** was prepared via procedure A using 2-amino-5-iodobenzoic acid (1.00 g, 3.80 mmol). The crude material was purified by recrystallization with hexanes and ethyl acetate to give off-white needles (0.884 g, 81%). ^1H NMR (300 MHz, d_6 -DMSO) δ 8.32 (d, J = 1.9 Hz, 1H), 8.19 (dd, J_1 = 8.1 Hz, J_2 = 1.9 Hz, 1H), 7.34 (d, J = 8.1 Hz, 1H), 2.39 (s, 3H). ^{13}C NMR (150 MHz, d_6 -DMSO) δ 161.0, 158.3, 146.0, 145.5, 137.2, 128.4, 118.4, 92.3, 21.7.

4-(6-Iodo-2-methyl-4-oxoquinazolin-3(4H)-yl)benzoic acid (987-45b).

Compound **987-45b** was prepared via procedure B using compound **987-45a** (2.00 g, 7.00 mmol) and *para*-aminobenzoic acid (1.15 g, 8.40 mmol, 1.20 equiv). The crude material was recrystallized with ethyl acetate and methanol to give an off-white solid (1.27 g, 45%). ^1H NMR (400 MHz, d_6 -DMSO) δ 13.27 (bs, 1H), 8.36 (d, J = 2.0 Hz, 1H), 8.15-8.11 (mult, 3H), 7.61 (d, J = 8.5 Hz, 2H), 7.47 (d, J = 8.5 Hz, 1H), 2.11 (s, 3H). ^{13}C NMR (100 MHz, d_6 -DMSO) δ 166.7, 160.0, 154.7, 146.6, 143.0, 141.5, 134.5, 131.5, 130.7, 128.9, 122.3, 91.3, 24.2. HRMS calcd for $\text{C}_{16}\text{H}_{11}\text{IN}_2\text{O}_3$, 406.98938 $[\text{M}+\text{H}]^+$; found, 406.98893 $[\text{M}+\text{H}]^+$.

(E)-4-(6-iodo-2-(4-nitrostyryl)-4-oxoquinazolin-3(4H)-yl)benzoic acid (987-45).

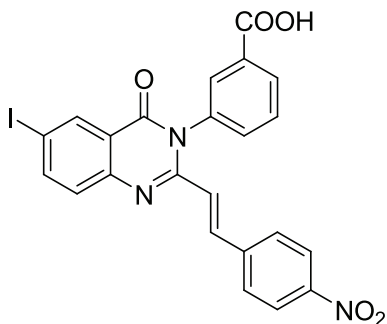
Compound **987-45** was prepared via procedure C using compound **987-45b** (0.200 g, 0.490 mmol) and *para*-nitrobenzaldehyde (0.099 g, 0.65 mmol, 1.3 equiv) to yield the title compound as a yellow solid (0.174 g, 66%). ^1H NMR (400 MHz, d_6 -DMSO) δ 8.32 (s, 1H), 8.16-8.12 (mult, 4H), 8.05 (s, 1H), 7.98 (d, $J = 15.6$ Hz, 1H), 7.77-7.68 (mult, 3H), 7.61-7.54 (mult, 2H), 6.41 (d, $J = 15.6$ Hz, 1H). ^{13}C NMR (150 MHz, d_6 -DMSO) δ 166.6, 159.9, 151.4, 148.2, 146.4, 143.1, 137.0, 136.5, 136.4, 134.6, 133.3, 130.5, 130.1, 129.8, 129.3, 124.0, 122.5, 122.4, 122.1, 91.9. HRMS calcd for $\text{C}_{23}\text{H}_{14}\text{IN}_3\text{O}_5$, 540.00575 $[\text{M}+\text{H}]^+$; found, 540.00559 $[\text{M}+\text{H}]^+$. Anal. ($\text{C}_{23}\text{H}_{14}\text{IN}_3\text{O}_5$) C, H, N. MP > 260°C.

3-(6-iodo-2-methyl-4-oxoquinazolin-3(4H)-yl)benzoic acid (987-43b).

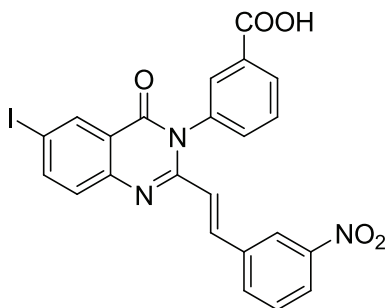
Compound **987-43b** was prepared via procedure B using compound **987-45a** (3.00 g, 10.5 mmol) and *meta*-aminobenzoic acid (1.72 g, 12.5 mmol, 1.20 equiv). The crude material was purified by trituration with methanol and collection of the resulting white solid by filtration (3.32 g, 78%). ^1H NMR (400 MHz, d_6 -DMSO) δ 8.31 (d, $J = 1.9$ Hz, 1H),

8.10-8.05 (mult, 3H), 7.47-7.69 (mult, 2H), 7.42 (d, $J = 8.6$ Hz, 1H), 2.11 (s, 3H). ^{13}C NMR (100 MHz, d_6 -DMSO) δ 166.6, 160.1, 154.9, 146.6, 142.9, 137.9, 134.5, 132.9, 132.5, 130.1, 130.0, 129.4, 128.9, 122.3, 91.2, 24.3. HRMS calcd for $\text{C}_{16}\text{H}_{11}\text{IN}_2\text{O}_3$, 406.98938 $[\text{M}+\text{H}]^+$; found, 406.98882 $[\text{M}+\text{H}]^+$.

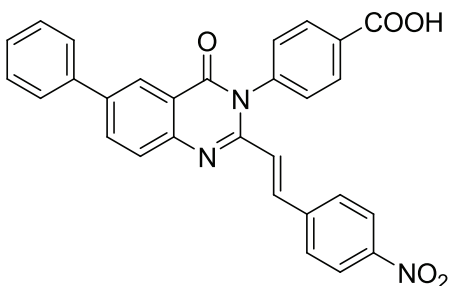
(*E*)-3-(6-iodo-2-(4-nitrostyryl)-4-oxoquinazolin-3(4H)-yl)benzoic acid (987-43).



Compound **987-43** was prepared via procedure C using compound **987-43b** (0.800 g, 1.97 mmol) and *para*-nitrobenzaldehyde (0.396 g, 2.62 mmol, 1.33 equiv) to yield the title compound as a yellow solid (0.572 g, 54%). ^1H NMR (400 MHz, d_6 -DMSO) δ 13.29 (bs, 1H), 8.32 (mult, 1H), 8.16-8.09 (mult, 5H), 7.94 (d, $J = 15.3$ Hz, 1H), 7.77 (s, 2H), 7.65-7.54 (mult, 3H), 6.47 (d, $J = 15.3$ Hz, 1H). ^{13}C NMR (150 MHz, d_6 -DMSO) δ 166.8, 158.7, 151.6, 148.7, 147.2, 142.8, 136.7, 136.6, 135.9, 134.3, 133.2, 130.8, 130.6, 129.4, 128.9, 128.8, 123.9, 123.5, 123.4, 122.1, 92.2 HRMS calcd for $\text{C}_{23}\text{H}_{14}\text{IN}_3\text{O}_5$, 540.00575 $[\text{M}+\text{H}]^+$; found, 540.00548 $[\text{M}+\text{H}]^+$. Anal. ($\text{C}_{23}\text{H}_{14}\text{IN}_3\text{O}_5$) C, H, N. MP > 260°C.

(E)-3-(6-iodo-2-(3-nitrostyryl)-4-oxoquinazolin-3(4H)-yl)benzoic acid (987-44).

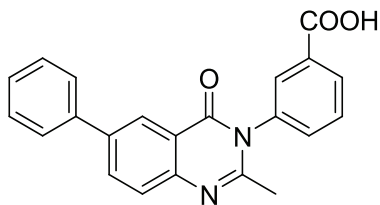
Compound **987-44** was prepared via procedure C using compound **987-43b** (0.800 g, 1.97 mmol) and *meta*-nitrobenzaldehyde (0.396 g, 2.62 mmol, 1.33 equiv) to yield the title compound as a yellow solid (0.626 g, 59%). ^1H NMR (400 MHz, d_6 -DMSO) δ 8.32 (s, 1H), 8.16-8.12 (mult, 4H), 8.05 (s, 1H), 7.98 (d, J = 15.6 Hz, 1H), 7.77-7.68 (mult, 3H), 7.61-7.54 (mult, 2H), 6.41 (d, J = 15.6 Hz, 1H). ^{13}C NMR (150 MHz, d_6 -DMSO) δ 166.6, 159.9, 151.4, 148.2, 146.4, 143.1, 137.0, 136.5, 136.4, 134.6, 133.3, 130.5, 130.1, 129.8, 129.3, 124.0, 122.5, 122.4, 122.1, 91.9. HRMS calcd for $\text{C}_{23}\text{H}_{14}\text{IN}_3\text{O}_5$, 540.00575 $[\text{M}+\text{H}]^+$; found, 540.00546 $[\text{M}+\text{H}]^+$. Anal. ($\text{C}_{23}\text{H}_{14}\text{IN}_3\text{O}_5$), C, H, N. MP > 260°C.

(E)-4-(2-(4-nitrostyryl)-4-oxo-6-phenylquinazolin-3(4H)-yl)benzoic acid (987-41).

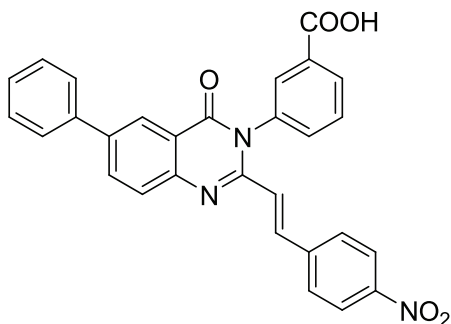
Compound **987-41** was prepared via procedure C using compound **987-35b** (0.150 g, 0.42 mmol) and *para*-nitrobenzaldehyde (0.085 g, 0.056 mmol, 1.3 equiv) to yield the

title compound as a yellow solid (0.138 g, 67%). ^1H NMR (400 MHz, d_6 -DMSO) δ 13.39 (bs, 1H), 8.37 (s, 1H), 8.25 (dd, $J_1 = 8.7$ Hz, $J_2 = 2.0$ Hz, 1H), 8.21-8.17 (mult, 4H), 8.01 (d, $J = 15.7$ Hz, 1H), 7.91 (d, $J = 8.2$ Hz, 1H), 7.81 (d, $J = 7.4$ Hz, 2H), 7.18-7.66 (mult, 4H), 7.56 (t, $J = 7.4$ Hz, 2H), 7.44 (t, $J = 7.4$ Hz, 1H), 6.55 (d, $J = 15.7$ Hz, 1H). ^{13}C NMR (150 MHz, d_6 -DMSO) δ 166.8, 161.1, 150.4, 147.5, 146.4, 141.1, 140.5, 138.7, 136.6, 133.4, 131.9, 130.7, 129.4, 129.2, 128.7, 128.2, 128.1, 126.8, 124.1, 123.7, 121.0. HRMS calcd for $\text{C}_{29}\text{H}_{19}\text{N}_3\text{O}_5$, 490.14041 $[\text{M}+\text{H}]^+$; found, 490.14033 $[\text{M}+\text{H}]^+$. Anal. ($\text{C}_{29}\text{H}_{19}\text{N}_3\text{O}_5$) C, H, N. MP $> 260^\circ\text{C}$.

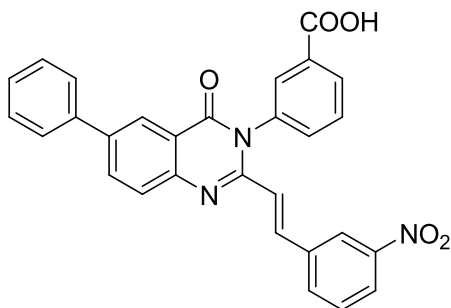
3-(2-Methyl-4-oxo-6-phenylquinazolin-3(4H)-yl)benzoic acid (987-50b).



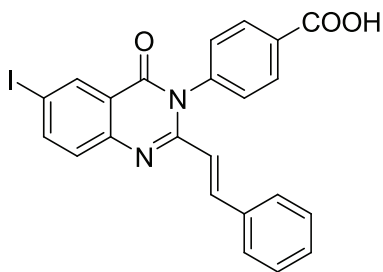
Compound **987-50b** was prepared via procedure B using compound **987-35a** (0.319 g, 1.98 mmol) and *meta*-aminobenzoic acid (0.326 g, 2.38 mmol, 1.20 equiv). The crude material was purified using recrystallization with methanol (0.303 g, 43%). ^1H (400 MHz, d_6 -DMSO) δ 13.29 (bs, 1H), 8.30 (d, $J = 1.2$ Hz, 1H), 8.16 (d, $J = 8.6$ Hz, 1H), 8.10 (d, $J = 7.0$ Hz, 1H), 8.05 (s, 1H), 7.77-7.72 (mult, 5H), 7.52 (t, $J = 7.4$ Hz, 2H), 7.42 (t, $J = 7.4$ Hz, 1H), 2.15 (s, 3H). ^{13}C NMR (100 MHz, d_6 -DMSO) δ 166.6, 161.5, 154.3, 146.7, 138.8, 138.2, 138.1, 133.14, 133.06, 132.5, 130.1, 129.9, 129.5, 129.2, 128.0, 127.5, 126.8, 123.6, 120.8, 24.2. HRMS calcd for $\text{C}_{22}\text{H}_{16}\text{N}_2\text{O}_3$, 357.12403 $[\text{M}+\text{H}]^+$; found, 357.12363 $[\text{M}+\text{H}]^+$.

(E)-3-(2-(4-nitrostyryl)-4-oxo-6-phenylquinazolin-3(4H)-yl)benzoic acid (987-50).

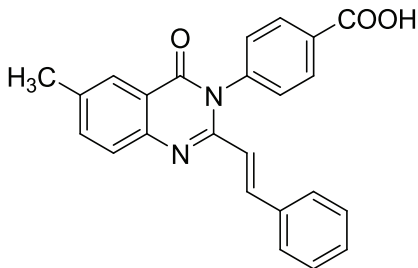
Compound **987-50** was prepared via procedure C using compound **987-50b** (0.125 g, 0.350 mmol) and *para*-nitrobenzaldehyde (0.071 g, 0.47 mmol, 1.3 equiv) to yield the title compound as a yellow solid (0.077 g, 45%). ^1H NMR (400 MHz, d_6 -DMSO) δ 13.40 (s, 1H), 8.36 (d, $J = 2.0$ Hz, 1H), 8.25 (dd, $J_1 = 8.6$ Hz, $J_2 = 2.0$ Hz, 1H), 8.20-8.14 (mult, 3H), 8.08 (s, 1H), 8.01 (d, $J = 15.7$ Hz, 1H), 7.91 (d, $J = 8.6$ Hz, 1H), 7.80 (d, $J = 7.8$ Hz, 2H), 7.77-7.74 (mult, 2H), 7.69 (d, $J = 8.6$ Hz, 2H), 7.54 (t, $J = 7.8$ Hz, 2H), 7.44 (t, $J = 7.0$ Hz, 1H), 6.55 (d, $J = 15.7$ Hz, 1H). ^{13}C NMR (100 MHz, d_6 -DMSO) δ 167.4, 161.9, 151.4, 148.2, 147.2, 141.8, 139.35, 139.31, 137.6, 137.2, 134.0, 133.8, 130.9, 130.7, 130.6, 129.9, 129.4, 128.85, 128.76, 127.5, 124.8, 124.4. HRMS calcd for $\text{C}_{29}\text{H}_{19}\text{N}_3\text{O}_5$, 490.14041[M+H] $^+$; found, 490.13988 [M+H] $^+$. Anal. ($\text{C}_{29}\text{H}_{19}\text{N}_3\text{O}_5$) C, H, N. MP > 260°C.

(E)-3-(2-(3-nitrostyryl)-4-oxo-6-phenylquinazolin-3(4H)-yl)benzoic acid (987-49).

Compound **987-49** was prepared via procedure C using compound **987-50b** (0.125 g, 0.350 mmol) and *meta*-nitrobenzaldehyde (0.071 g, 0.47 mmol, 1.3 equiv) to yield the title compound as a yellow solid (0.101 g, 59%). ^1H NMR (400 MHz, d_6 -DMSO) δ 13.53 (bs, 1H), 8.36 (s, 1H), 8.27-8.24 (mult, 2H), 8.18-8.16 (mult, 2H), 8.07 (s, 1H), 8.04 (d, $J = 15.7$ Hz, 1H), 7.90 (d, $J = 8.6$ Hz, 1H), 7.87 (d, $J = 8.2$ Hz, 1H), 7.82-7.75 (mult, 4H), 7.65 (t, $J = 8.2$ Hz, 1H), 7.54 (t, $J = 7.8$ Hz, 2H), 7.44 (t, $J = 7.4$ Hz, 1H), 6.52 (d, $J = 15.7$ Hz, 1H). ^{13}C NMR (100 MHz, d_6 -DMSO) δ 166.6, 161.3, 150.8, 148.3, 146.6, 138.7, 138.5, 137.1, 136.7, 136.6, 133.5, 133.4, 132.4, 130.5, 130.1, 130.0, 129.3, 128.1, 126.8, 124.0, 123.8, 122.8, 122.3, 121.1. HRMS calcd for $\text{C}_{29}\text{H}_{19}\text{N}_3\text{O}_5$, 490.14041 $[\text{M}+\text{H}]^+$; found, 490.13985 $[\text{M}+\text{H}]^+$. Anal. ($\text{C}_{29}\text{H}_{19}\text{N}_3\text{O}_5$) C, H, N. MP > 260°C.

(E)-4-(6-iodo-4-oxo-2-styrylquinazolin-3(4H)-yl)benzoic acid (987-10).

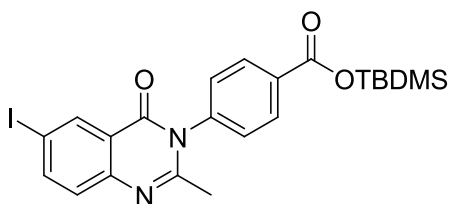
Compound **987-10** was prepared via procedure C using compound **987-45b** (0.300 g, 0.740 mol) and benzaldehyde (0.100 mL, 0.980 mmol, 1.33 equiv). The crude material was purified by hot gravity filtration of the title compound as a yellow solid after boiling in methanol (0.070 g, 19%). ^1H NMR (400 MHz, d_6 -DMSO) δ 8.40 (d, $J=1.9$ Hz, 1H), 8.19-8.15 (mult, 3H), 7.92 (d, $J=15.5$ Hz, 1H), 7.62-7.57 (mult, 3H), 7.39-7.35 (mult, 5H), 6.30 (d, $J=15.5$ Hz, 1H). ^{13}C NMR (150 MHz, d_6 -DMSO) δ 166.8, 160.0, 151.6, 146.7, 143.2, 140.4, 139.7, 134.6, 132.3, 130.7, 130.0, 129.3, 129.2, 129.0, 127.7, 122.4, 119.5, 114.0, 91.5. HRMS calcd for $\text{C}_{23}\text{H}_{15}\text{IN}_2\text{O}_3$, 495.02068 $[\text{M}+\text{H}]^+$; found, 495.01987 $[\text{M}+\text{H}]^+$. Anal. ($\text{C}_{23}\text{H}_{15}\text{IN}_2\text{O}_3$) C, H, N. MP > 260°C.

(E)-4-(6-methyl-4-oxo-2-styrylquinazolin-3(4H)-yl)benzoic acid (987-38).

Compound **987-38** was prepared via procedure C using compound **987-11b** (0.400 g, 1.36 mmol) and benzaldehyde (0.183 mL, 1.81 mmol, 1.33 equiv to yield the title

compound as a yellow solid (0.216 g, 42%). ^1H NMR (400 MHz, d_6 -DMSO) δ 13.3 (bs, 1H), 8.16 (d, J = 8.2 Hz, 2H), 7.91 (s, 1H), 7.86 (d, J = 15.6 Hz, 1H), 7.69 (s, 2H), 7.61 (d, J = 7.8 Hz, 2H), 7.34 (bs, 5H), 6.28 (d, J = 15.6 Hz, 1H), 2.46 (s, 3H). ^{13}C NMR (100 MHz, d_6 -DMSO) δ 166.8, 161.1, 150.1, 145.4, 141.0, 138.7, 136.5, 136.2, 134.8, 131.5, 130.7, 129.8, 129.5, 129.0, 127.6, 127.1, 125.8, 120.2, 119.8, 20.9. HRMS calcd for $\text{C}_{24}\text{H}_{18}\text{N}_2\text{O}_3$, 383.13968 $[\text{M}+\text{H}]^+$; found, 383.13887 $[\text{M}+\text{H}]^+$. Anal. ($\text{C}_{24}\text{H}_{18}\text{N}_2\text{O}_3$) C, H, N. MP > 260°C.

tert-Butyldimethylsilyl 4-(6-iodo-2-methyl-4-oxoquinazolin-3(4H)-yl)benzoate (9).

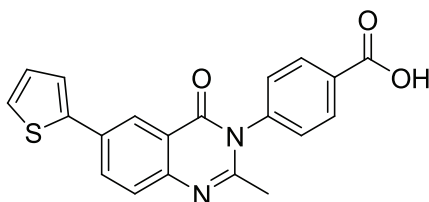


Carboxylic acid **987-45b** (0.300 g, 0.74 mmol) was dissolved in THF (10.0 mL). To this solution was added N-methylmorpholine (0.081 mL, 0.74 mmol, 1.0 equiv) and TBDMS-Cl (0.111 g, 0.74 mmol, 1.0 equiv). The mixture was stirred at room temperature for 1 hour. The yellow suspension was concentrated *in vacuo*, and the resulting residue was partitioned between ethyl acetate and water. The mixture was extracted 3x with ethyl acetate. The combined organics were washed with brine, dried over MgSO_4 , and concentrated *in vacuo* to give a white solid. The crude material was purified using silica gel chromatography (ISCO, RediSep 12 g column, 100% EtOAc) to give a white foam (0.280 g, 73%). ^1H NMR (400 MHz, CDCl_3) δ 8.57 (d, J = 2.1 Hz, 1H), 8.23 (d, J = 8.8 Hz, 2H), 8.02 (dd, J_1 = 8.7 Hz, J_2 = 2.1 Hz, 1H), 7.41 (d, J = 8.6 Hz), 7.34 (d, J = 8.8 Hz, 2H), 2.22 (s, 3H), 1.05 (s, 9H), 0.41 (s, 6H). ^{13}C NMR (100 MHz, CDCl_3) δ 165.5, 160.8, 154.3, 146.9,

143.7, 141.5, 135.9, 132.9, 132.1, 129.0, 128.4, 122.5, 91.3, 25.8, 24.6, 18.0, -4.6.

HRMS calcd for $C_{22}H_{25}IN_2O_3Si$, 521.07585 $[M+H]^+$; found, 521.07527 $[M+H]^+$.

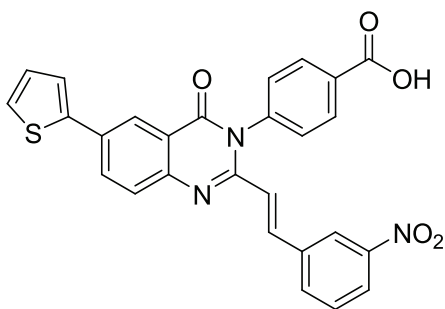
4-(2-Methyl-4-oxo-6-(thiophen-2-yl)quinazolin-3(4H)-yl)benzoic acid (11).



To a 100 mL 3-neck round-bottom flask fitted with a reflux condenser was added **9** (0.250 g, 0.48 mmol) and $Pd(PPh_3)_4$ (0.028 g, 0.024 mmol, 0.05 equiv). The vessel was made inert by opening to vacuum and then administering positive pressure with Ar (g) three times. 1,2-dimethoxyethane (5.0 mL), 2-thiopheneboronic acid (**10**, 0.068 g, 0.53 mmol, 1.1 equiv), and solution of sodium carbonate (0.081 g, 0.96 mmol, 2.0 equiv) in water (5.0 mL) was added. The evacuation/argon procedure was performed one more time. The reaction mixture was refluxed for 12 hours. After cooling to room temperature, the 1,2-DME was removed *in vacuo*. The resulting orange residue was diluted with 0.5 N HCl and extracted with EtOAc (3x). The combined organics were washed with brine, dried over $MgSO_4$, and concentrated *in vacuo* to give an orange residue. The crude material was purified using silica gel chromatography (ISCO, RediSep 12 g column, 0-100% EtOAc/Hexanes gradient) to give an off-white solid (0.083 g, 48%). 1H NMR (400 MHz, $CDCl_3$) δ 13.21 (bs, 1H), 8.26 (d, $J = 2.0$, 1H), 8.20 (dd, $J_1 = 8.6$ Hz, $J_2 = 2.0$ Hz, 1H), 8.13 (d, $J = 8.2$ Hz, 2H), 7.72 (d, $J = 8.6$ Hz, 1H), 7.69 (d, $J = 3.9$ Hz, 1H), 7.64-7.63 (mult, 2H-but extra integrations), 7.57-7.55 (mult, 1H), 7.20 (dd, $J_1 = 5.1$ Hz, $J_2 = 3.9$

Hz, 1H), 2.15 (s, 3H). HRMS calcd for $C_{20}H_{14}N_2O_3S$, 363.08045 $[M+H]^+$; found, 363.07995 $[M+H]^+$.

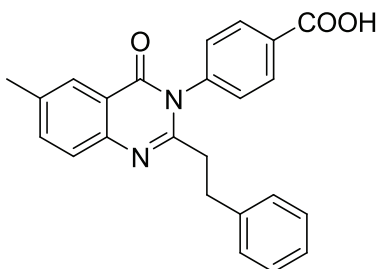
(E)-4-(2-(3-nitrostyryl)-4-oxo-6-(thiophen-2-yl)quinazolin-3(4H)-yl)benzoic acid (987-58).



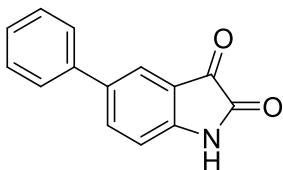
Compound **11** (0.077 g, 0.212 mmol) was dissolved in a mixture of acetic acid (0.71 mL, 12.3 mmol, 58 equiv) and acetic anhydride (0.14 mL, 1.4 mmol, 7.0 equiv). To this solution was added *meta*-nitrobenzaldehyde (**12**, 0.043 g, 0.283 mmol, 1.33 equiv) and sodium acetate (0.028 g, 0.35 mmol, 1.63 equiv). The mixture was refluxed for 6 hours. After cooling to room temperature, the resultant yellow solid was collected by filtration and washed with methanol. The crude material was purified using silica gel chromatography (silica cake, ISCO, RediSep 24 g column, 0-10% MeOH/DCM gradient) to give a yellow solid (0.049 g, 48%). 1H NMR (400 MHz, d_6 -DMSO) δ 13.35 (bs, 1H), 8.31-8.25 (mult, 3H), 8.17 (d, J = 8.2 Hz, 3H), 8.03 (d, J = 15.7 Hz, 1H), 7.87 (t, J = 7.4 Hz, 2H), 7.74 (dd, J_1 = 3.5 Hz, J_2 = 1.2 Hz, 1H), 7.68-7.63 (mult, 4H), 7.21 (dd, J_1 = 5.1 Hz, J_2 = 3.51 Hz, 1H), 6.51 (d, J = 15.7 Hz, 1H). ^{13}C NMR (150 MHz, d_6 -DMSO) δ 166.7, 160.9, 150.5, 148.3, 146.4, 141.9, 140.6, 136.8, 136.5, 131.3, 132.3, 131.9, 131.7, 130.7, 130.5, 129.4, 129.0, 128.3, 126.8, 124.9, 124.0, 122.6, 122.4, 121.9, 121.2. HRMS calcd for $C_{27}H_{17}N_3O_5S$,

496.09683 [M+H]⁺; found, 496.10655 [M+H]⁺. Anal. (C₂₇H₁₇N₃O₅S) C, H, N. MP > 260°C.

4-(6-Methyl-4-oxo-2-phenethylquinazolin-3(4H)-yl)benzoic acid (987-40).



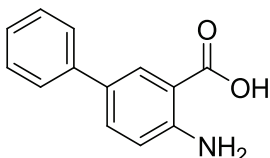
Compound (**987-38**, 0.100 g, 0.26 mmol) was dissolved in DMF (5.0 mL). Palladium on carbon (10%, 0.10 g, 10 wt %) was added. A balloon filled with hydrogen was added and the mixture was stirred at room temperature for 1 hour. The mixture was filtered over a pad of celite, and the resulting solution was concentrated *in vacuo* to give a white solid. The solid was triturated with DCM and obtained by filtration (0.016 g, 16%). ¹H NMR (400 MHz, *d*₆-DMSO) δ 13.27 (bs, 1H), 8.09 (d, *J* = 8.2 Hz, 2H), 7.93 (s, 1H), 7.71 (d, *J* = 8.6 Hz, 1H), 7.65 (d, *J* = 8.2 Hz, 1H), 7.54 (d, *J* = 8.1 Hz, 2H), 7.22 (t, *J* = 7.4 Hz, 2H), 7.14 (t, *J* = 7.0 Hz, 1H), 7.06 (d, *J* = 7.0 Hz, 2H), 2.98 (t, *J* = 7.4 Hz, 2H), 2.58 (t, *J* = 7.4 Hz, 2H), 2.47 (s, 3H). ¹³C NMR (100 MHz, *d*₆-DMSO) δ 166.7, 161.2, 154.6, 145.1, 141.3, 140.8, 136.4, 136.1, 131.5, 130.5, 129.2, 128.4, 128.2, 126.9, 126.1, 125.7, 120.2, 37.1, 32.0, 20.8. HRMS calc'd for C₂₄H₂₀N₂O₃, 385.15533 [M+H]⁺; found, 385.15459 [M+H]⁺. Anal. (C₂₄H₂₀N₂O₃) C: 72.02, H: 5.03, N: 7.19. MP > 260°C.

5-Phenylindoline-2,3-dione (13).

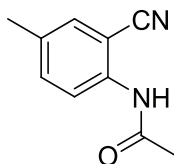
To a 500 mL 3-neck round bottom flask fitted with a reflux condenser 5-iodoisatin (1.50 g, 5.5 mmol) and Pd(PPh₃)₄ (0.320 g, 0.27 mmol, 0.05 equiv) were added. The vessel was made inert by opening to vacuum and then to positive pressure with Ar (g) three times, followed by addition of 1,2-dimethoxyethane (50.0 mL) to give an orange solution. Phenylboronic acid (0.740 g, 6.0 mmol, 1.1 equiv) and a solution of sodium bicarbonate (0.93 g, 8.8 mmol, 2.0 equiv) in water (50.0 mL) was added, upon which the color changed to deep purple. The evacuation/nitrogen procedure was performed one more time. The reaction mixture was refluxed for 1 hr. After cooling to room temperature, the 1,2-DME was removed *in vacuo*. The residue was diluted with 1N HCl and extracted with EtOAc (3x). The combined organics were washed with brine, dried over MgSO₄, and concentrated *in vacuo* to give an orange solid. The crude material was purified using silica gel chromatography (ISCO, RediSep 12 g column, silica cake, 0-50% EtOAc/Hexanes gradient) to give a bright red solid, but was impure by NMR. The material was further recrystallized using hexanes and EtOAc to yield a red solid which was collected by filtration (0.597 g, 49%). ¹H NMR (400 MHz, CDCl₃) δ 8.18 (bs, 1H), 7.87 (s, 1H), 7.82 (dd, J₁ = 8.2 Hz, J₂ = 2.0 Hz, 1H), 7.54 (d, J = 7.0 Hz, 2H), 7.47 (t, J = 7.4 Hz, 2H), 7.40 (t, J = 7.0 Hz, 1H), 7.02 (d, J = 8.2 Hz, 1H). ¹³C NMR (100 MHz, CDCl₃) δ 184.4, 159.6, 150.0, 138.7,

136.5, 134.9, 129.0, 127.5, 126.2, 122.4, 118.5, 112.7. HRMS calcd for $C_{14}H_9NO_2$, 224.07127 $[M+H]^+$; found, 224.07070 $[M+H]^+$.

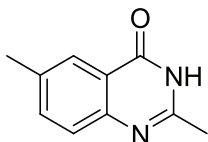
4-Aminobiphenyl-3-carboxylic acid (14).



A stirred solution of isatin **13** (0.247 g, 1.1 mmol) in 1.5 N NaOH (2.6 mL, 3.9 mmol, 3.5 equiv) was heated to 50°C. To this solution, 30% hydrogen peroxide solution (0.27 mL, 2.7 mmol, 2.4 equiv) was added. The mixture was cooled to room temperature and left without stirring for 12 hours. The mixture was carefully neutralized, then acidified with 12 N HCl solution to pH 4, upon which an off-white solid precipitated out. The off-white solid was collected by filtration and washed with hexanes (0.187 g, 79%). 1H NMR (400 MHz, d_6 -DMSO) δ 9.57-8.02 (bs, 2H), 7.99 (d, $J = 2.0$ Hz, 1H), 7.59 (dd, $J_1 = 8.6$ Hz, $J_2 = 2.0$ Hz, 1H), 7.55 (d, $J = 7.4$ Hz, 2H), 7.40 (t, $J = 7.8$ Hz, 2H), 7.25 (t, $J = 7.4$ Hz, 1H), 6.86 (d, $J = 8.6$ Hz, 1H). ^{13}C NMR (100 MHz, d_6 -DMSO) δ 169.6, 150.9, 139.8, 132.2, 128.9, 126.6, 126.2, 125.5, 117.2, 110.0. HRMS calcd for $C_{13}H_{11}NO_2$, 214.08692 $[M+H]^+$; found, 214.08636 $[M+H]^+$. MP 202-206°C.

N-(2-cyano-4-methylphenyl)acetamide (16).

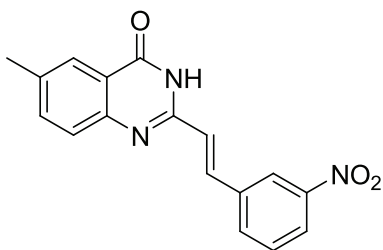
To a mixture of zinc oxide powder (0.172 g, 2.12 mmol, 0.5 equiv) and acetic anhydride, (0.40 mL, 4.23 mmol, 1.0 equiv) 2-aminobenzonitrile (**15**, 0.500 g, 4.23 mmol) was added. The mixture was stirred at room temperature for 1 hour, and the reaction mixture solidified. The solid was taken up in DCM and the remaining solids were removed by filtration. The filtrate was partitioned with aqueous NaHCO₃, and the organics were dried over MgSO₄ and concentrated *in vacuo* to give a yellow solid (0.522 g, 79%). ¹H NMR (400 MHz, CDCl₃) δ 8.15 (d, *J* = 8.6 Hz, 1H), 7.83 (bs, 1H), 7.36 (d, *J* = 7.4 Hz, 2H), 2.32 (s, 3H), 2.24 (s, 3H). ¹³C NMR (100 MHz, CDCl₃) δ 169.0, 138.2, 135.1, 134.4, 132.4, 122.1, 116.8, 102.4, 24.8, 20.6. HRMS calcd for C₁₀H₁₀N₂O, 175.08725 [M+H]⁺; found, 175.08652 [M+H]⁺.

2,6-Dimethylquinazolin-4(3H)-one (17).

Nitrile **16** (0.522 g, 3.0 mmol) was dissolved in an acetone/water mixture (10 mL of each). To this solution was added anhydrous potassium carbonate (0.050 g, 0.36 mmol, 0.12 equiv) and urea hydrogen peroxide (0.056 g, 6.0 mmol, 2.0 equiv). The mixture was refluxed for 12 hours, although the reaction did not go to completion. The mixture was

cooled to room temperature and the acetone was removed *in vacuo*. The resulting yellow residue was chilled in the freezer for a 10 minutes, upon which a yellow solid precipitated. The solid was collected by filtration and washed with water and ether. The crude material was purified using silica gel chromatography (ISCO, 24 g column, 0-100% EtOAc gradient) to give a white solid (0.092 g, 18%). ^1H NMR (400 MHz, d_6 -DMSO) δ 12.1 (bs, 1H), 7.87 (s, 1H), 7.59 (dd, $J_1 = 8.2$ Hz, $J_2 = 2.0$ Hz, 1H), 7.47 (d, $J = 8.2$ Hz, 1H), 2.43 (s, 3H), 2.33 (s, 3H).

(E)-6-methyl-2-(3-nitrostyryl)quinazolin-4(3H)-one (18).

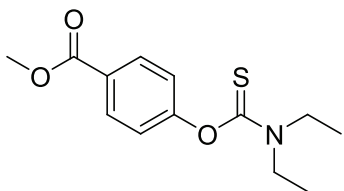


Quinazolinone **17** (0.092 g, 0.53 mmol), 3-nitrobenzaldehyde (0.110 g, 0.70 mmol, 1.33 equiv), and sodium acetate (0.071 g, 0.86 mmol, 1.63 equiv) were dissolved in a mixture of glacial acetic acid (1.8 mL, 31 mmol, 58 equiv) and acetic anhydride (0.35 mL, 3.7 mmol, 7.0 equiv). The mixture was refluxed for 6 hours. The yellow suspension was cooled to room temperature and the solid was obtained by filtration (0.093 g, 57%). ^1H NMR (400 MHz, d_6 -DMSO) δ 8.47 (s, 1H), 8.25 (d, $J = 6.7$ Hz, 1H), 8.13 (d, $J = 7.6$ Hz, 1H), 8.03 (d, $J = 16.1$ Hz, 1H), 7.94 (s, 1H), 7.77 (t, $J = 7.9$ Hz, 1H), 7.68-7.60 (mult, 1H), 7.20 (d, $J = 16.1$ Hz, 1H), 3.33 (s, 3H). The sample did not significantly dissolve in DMSO, so neither further characterization nor biological evaluation was performed.

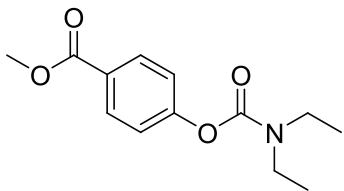
General preparation of carbamothioates esters and carbamate esters, exemplified by

32.

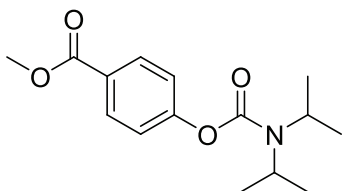
Methyl 4-(diethylcarbamothioxy)benzoate (32).



Methyl-4-hydroxybenzoate (1.00 g, 6.57 mmol) and finely ground potassium carbonate (1.82 g, 13.1 mmol, 2.0 equiv) were dissolved in DMF (25.0 mL). The mixture was stirred at room temperature for 1 hour to give an opaque suspension. Diethylthiocarbamoyl chloride (1.10 g, 7.23 mmol, 1.1 equiv) was then added and the mixture was stirred at room temperature for 12 hours. The mixture was diluted with water (75 mL) and extracted with diethyl ether (2 x 100 mL). The combined organics were washed with water and brine, dried over MgSO_4 , and concentrated *in vacuo* to give a yellow solid. The crude material was purified using silica gel chromatography (ISCO, RediSep 12 g column, 1 EtOAc/6 Hexanes) to give an off-white solid (1.24 g, 71%). ^1H NMR (400 MHz, CDCl_3) δ 8.07 (d, $J = 8.6$ Hz, 2H), 7.13 (d, $J = 8.6$ Hz, 2H), 3.90 (s, 3H), 3.87 (mult, 2H), 3.68 (quart, $J = 7.0$ Hz, 2H), 1.31 (t, $J = 7.3$ Hz, 3H). ^{13}C NMR (100 MHz, CDCl_3) δ 186.1, 166.5, 157.6, 131.0, 127.7, 123.0, 52.3, 48.5, 44.5, 13.7, 11.9. HRMS calcd for $\text{C}_{13}\text{H}_{17}\text{NO}_3\text{S}$, 268.10084 $[\text{M}+\text{H}]^+$; found, 268.10017 $[\text{M}+\text{H}]^+$.

Methyl 4-(diethylcarbamoyloxy)benzoate (33).

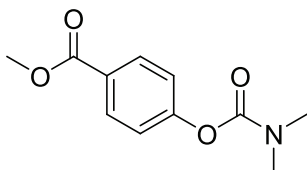
Compound **33** was prepared in the same manner as **32** utilizing methyl-4-hydroxybenzoate (1.00 g, 6.57 mmol) and N,N-diethylthiocarbamoyl chloride (0.96 mL, 7.23 mmol, 1.1 equiv). The crude material was purified using silica gel chromatography (ISCO, RediSep 12 g column, 1 EtOAc/6 Hexanes) to give a colorless oil (1.50 g, 91%). ^1H NMR (400 MHz, CDCl_3) δ 7.95 (d, J = 8.6 Hz, 2H), 7.12 (d, J = 8.9 Hz, 2H), 3.78 (s, 3H), 3.30-3.27 (mult, 4H), 1.16-1.08 (mult, 6H). ^{13}C NMR (100 MHz, CDCl_3) δ 166.1, 155.1, 153.1, 130.7, 126.6, 121.4, 51.8, 42.1, 41.8, 14.0, 13.1.

Methyl 4-(diisopropylcarbamoyloxy)benzoate (34).

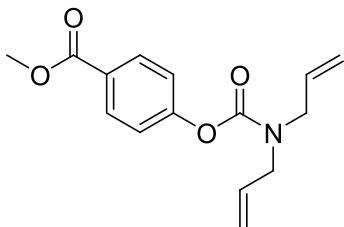
Compound **34** was prepared in the same manner as **32** utilizing methyl-4-hydroxybenzoate (1.00 g, 6.57 mmol) and N,N-diisopropylcarbamoyl chloride (0.77 mL, 7.23 mmol, 1.1 equiv). The reaction was incomplete after 36 hours, however. The crude material was purified using silica gel chromatography (ISCO, RediSep 24 g column, 0-10% EtOAc/Hexanes gradient) to give a white solid (0.975 g, 53%). ^1H NMR (400 MHz, CDCl_3) δ 8.03 (d, J = 9.0 Hz, 2H), 7.20 (d, J = 9.0 Hz, 2H), 4.20-3.91 (mult, 2H), 3.89 (s, 3H),

1.41-1.28 (mult, 12 H). ^{13}C NMR (100 MHz, CDCl_3) δ 166.6, 155.3, 153.1, 131.1, 126.8, 121.7, 52.2, 47.1, 46.4, 21.6, 20.5. HRMS calcd for $\text{C}_{15}\text{H}_{21}\text{NO}_4$, 280.15500 $[\text{M}+\text{H}]^+$; found, 280.15421 $[\text{M}+\text{H}]^+$.

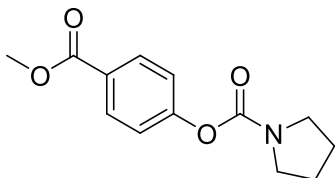
Methyl 4-(dimethylcarbamoyloxy)benzoate (35).



Compound **35** was prepared in the same manner as **32** utilizing methyl-4-hydroxybenzoate (1.00 g, 6.57 mmol) and N,N-dimethylcarbamoyl chloride (0.66 mL, 7.23 mmol, 1.1 equiv). The crude white solid was pure by NMR and used without further purification (1.36 g, 93%). ^1H NMR (400 MHz, CDCl_3) δ 8.00 (d, $J = 8.6$ Hz, 2H), 7.15 (d, $J = 8.6$ Hz, 2H), 3.84 (s, 3H), 3.03 (s, 3H), 2.96 (s, 3H). ^{13}C NMR (100 MHz, CDCl_3) δ 166.4, 155.2, 154.0, 130.9, 126.8, 121.6, 52.1, 36.6, 36.4. HRMS calcd for $\text{C}_{11}\text{H}_{13}\text{NO}_4$, 224.09240 $[\text{M}+\text{H}]^+$; found, 224.09163 $[\text{M}+\text{H}]^+$.

Methyl 4-(diallylcarbamoyloxy)benzoate (36).

Compound **36** was prepared in the same manner as **32** utilizing methyl-4-hydroxybenzoate (1.00 g, 6.57 mmol) and N,N-diallylcarbamoyl chloride (1.1 mL, 7.23 mmol, 1.1 equiv). The crude material was purified by silica gel chromatography (ISCO, RediSep 24 g column, 0-15% EtOAc/Hexanes gradient) to give a colorless oil (1.68 g, 92%). ^1H NMR (400 MHz, CDCl_3) δ 8.00 (d, J = 8.9 Hz, 2H), 7.16 (d, J = 8.9 Hz, 2H), 5.82-5.77 (mult, 2H), 5.20-5.14 (mult, 4H), 4.01-3.92 (mult, 4H), 3.84 (s, 3H). ^{13}C NMR (100 MHz, CDCl_3) δ 166.3, 155.1, 153.6, 133.0, 132.8, 130.9, 126.9, 121.5, 117.8, 117.0, 52.0, 49.5, 49.0. HRMS calcd for $\text{C}_{15}\text{H}_{17}\text{NO}_4$, 276.12370 $[\text{M}+\text{H}]^+$; found, 276.12292 $[\text{M}+\text{H}]^+$.

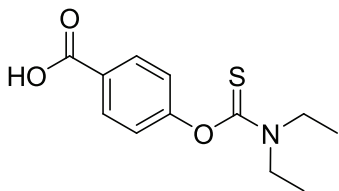
4-(Methoxycarbonyl)phenyl pyrrolidine-1-carboxylate (37).

Compound **37** was prepared in the same manner as **32** utilizing methyl-4-hydroxybenzoate (1.00 g, 6.57 mmol) and pyrrolidine-1-carbonyl chloride (0.80 mL, 7.23 mmol, 1.1 equiv). The crude white solid was pure by NMR and used without further purification (1.36 g, 93%). ^1H NMR (400 MHz, CDCl_3) δ 8.03 (d, J = 8.6 Hz, 2H), 7.21 (d, J =

8.6 Hz, 2H), 3.89 (s, 3H), 3.55 (t, $J = 6.7$ Hz, 2H), 3.47 (t, $J = 6.7$ Hz, 2H), 1.96-1.86 (mult, 4H). ^{13}C NMR (100 MHz, CDCl_3) δ 166.7, 155.3, 152.4, 131.1, 126.9, 121.7, 52.2, 46.7, 46.6, 25.9, 25.1. HRMS calcd for $\text{C}_{13}\text{H}_{15}\text{NO}_4$, 295.10805 $[\text{M}+\text{H}]^+$; found, 250.10729 $[\text{M}+\text{H}]^+$.

General preparation of carbamothioate benzoic acids and carbamate benzoic acids, exemplified by **38**

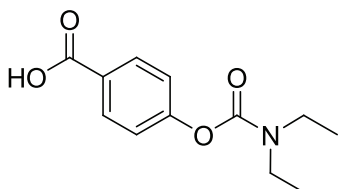
4-(Diethylcarbamothioxy)benzoic acid (**38**).



Compound **32** (0.933 g, 3.49 mmol) was dissolved in methanol (40.0 mL). To this solution, 1.0 N sodium hydroxide (13.3 mL, 13.3 mmol, 3.8 equiv) was added. Immediately a solid precipitated. The mixture was stirred at room temperature for 12 hours, upon which all material went into solution. The pH was adjusted to ca. 3 with concentrated HCl. The mixture was then concentrated *in vacuo* to remove the methanol, upon which a white solid precipitated. The mixture was chilled at 4°C for 3 hours, and the product was collected by filtration and washed with hexanes to give a white solid (0.798 g, 90%). ^1H NMR (600 MHz, d_6 -DMSO) δ 7.98 (d, $J = 9.1$ Hz, 2H), 7.19 (d, $J = 8.6$ Hz, 2H), 3.81 (quart, $J = 6.7$ Hz, 2H), 3.67 (quart, $J = 6.7$ Hz, 2H), 1.25 (t, $J = 7.1$ Hz, 3H), 1.23 (t, $J = 7.1$ Hz, 3H). ^{13}C NMR (150 MHz, d_6 -DMSO) δ 184.9, 166.7, 157.0,

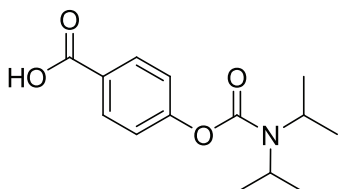
130.6, 128.1, 123.1, 123.0, 47.9, 44.2, 13.5, 13.4, 11.6, 11.5. HRMS calcd for $C_{12}H_{15}NO_3S$, 254.08524 $[M+H]^+$; found 254.08452 $[M+H]^+$.

4-(Diethylcarbamoyloxy)benzoic acid (39).



Compound **39** was prepared in the same manner as **38**, utilizing ester **33** (1.50 g, 5.97 mmol). The title compound was obtained as a white solid (1.23 g, 87%). 1H NMR (400 MHz, d_6 -DMSO) δ 12.98 (bs, 1H), 7.97 (d, J = 9.0 Hz, 2H), 7.24 (d, J = 8.6 Hz, 2H), 3.41-3.30 (mult, 4H), 1.19 (t, J = 6.7 Hz, 3H), 1.12 (t, J = 6.7 Hz, 3H). ^{13}C NMR (100 MHz, d_6 -DMSO) δ 166.8, 154.9, 152.7, 130.7, 127.5, 121.9. HRMS calcd for $C_{12}H_{15}NO_4$, 238.10804 $[M+H]^+$; found 238.21147 $[M+H]^+$.

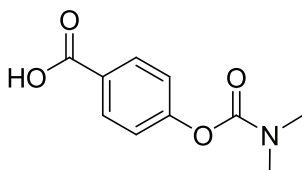
4-(Diisopropylcarbamoyloxy)benzoic acid (40).



Compound **40** was prepared in the same manner as **38**, utilizing ester **34** (0.975 g, 3.49 mmol). The title compound was obtained as a white solid (0.652 g, 70%). 1H NMR (400 MHz, d_6 -DMSO) δ 7.96 (d, J = 8.2 Hz, 2H), 7.21 (d, J = 8.2 Hz, 2H), 3.98-3.65 (mult, 2H), 1.46-1.25 (mult, 12H). ^{13}C NMR (100 MHz, d_6 -DMSO) δ 166.9, 154.9, 152.3, 130.9, 127.5,

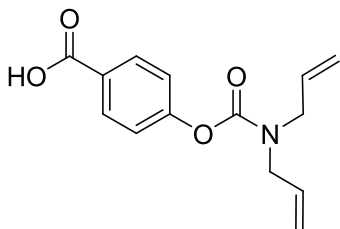
122.9, 45.6, 43.9, 21.4, 20.2. HRMS calcd for $C_{14}H_{19}NO_4$, 266.13935 $[M+H]^+$; found, 266.13856 $[M+H]^+$.

4-(Dimethylcarbamoyloxy)benzoic acid (41).



Compound **41** was prepared in the same manner as **38**, utilizing ester **35** (1.36 g, 6.09 mmol). The title compound was obtained as a white solid (0.562 g, 44%). 1H NMR (400 MHz, d_6 -DMSO) δ 7.97 (d, J = 8.2 Hz, 2H), 7.24 (d, J = 8.2 Hz, 2H), 3.04 (s, 3H), 2.92 (s, 3H). ^{13}C NMR (100 MHz, d_6 -DMSO) δ 166.8, 155.0, 153.5, 130.8, 127.6, 122.0, 36.4, 36.2 $[M+H]^+$. HRMS calcd for $C_{10}H_{11}NO_4$, 210.07675 $[M+H]^+$; found, 210.07594 $[M+H]^+$.

4-(Diallylcarbamoyloxy)benzoic acid (42).

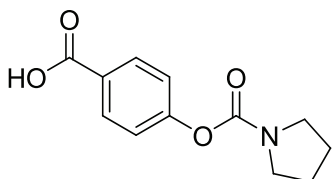


Compound **42** was prepared in the same manner as **38**, utilizing ester **36** (1.68 g, 6.10 mmol). The title compound was obtained as a white solid (1.22 g, 77%). 1H NMR (400 MHz, d_6 -DMSO) δ 12.99 (bs, 1H), 8.00 (d, J = 7.4 Hz, 2H), 7.23 (d, J = 7.4 Hz, 2H), 5.99-5.76 (mult, 2H), 5.24-5.16 (mult, 4H), 3.90-3.72 (mult, 4H). ^{13}C NMR (100 MHz, d_6 -

DMSO) δ 166.8, 154.7, 153.2, 133.7, 133.2, 130.8, 127.8, 121.9, 117.4, 116.7, 49.4, 49.1.

HRMS calcd for $C_{14}H_{15}NO_4$, 262.10805 $[M+H]^+$; found, 262.10727 $[M+H]^+$.

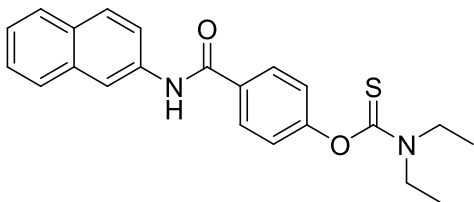
4-(Pyrrolidine-1-carboxyloxy)benzoic acid (**43**).



Compound **43** was prepared in the same manner as **38**, utilizing ester **37** (1.57 g, 6.30 mmol). The title compound was obtained as a white solid (0.856 g, 58%). 1H NMR (400 MHz, d_6 -DMSO) δ 12.97 (bs, 1H), 7.97 (d, J = 8.8 Hz, 2H), 7.25 (d, J = 8.8 Hz, 2H), 3.51-3.48 (mult, 2H), 3.35-3.32 (mult, 2H), 1.88-1.84 (mult, 4H). ^{13}C NMR (100 MHz, d_6 -DMSO) δ 166.8, 154.8, 151.6, 130.8, 127.5, 121.9, 46.4, 46.2, 25.3, 24.5. HRMS calcd for $C_{12}H_{13}NO_4$, 236.09240 $[M+H]^+$; found, 236.09163 $[M+H]^+$.

General preparation of 1063 analogues **1063-1** through **1063-6**, exemplified by **1063-1**.

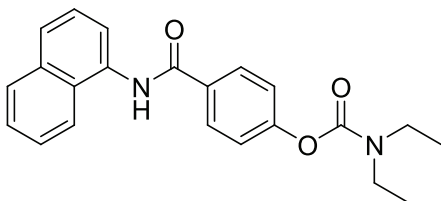
O-4-(naphthalen-2-ylcarbamoyl)phenyl diethylcarbamothioate (**1063-1**)



Acid **38** (0.500 g, 1.97 mmol) was dissolved in DMF (15.0 mL) and cooled to 0°C. To this solution, DMAP (0.265 g, 2.17 mmol, 1.1 equiv), and EDC (0.378 g, 1.97 mmol, 1.0

equiv) were added to give a colorless suspension. After stirring for 45 minutes, all material was in solution. Finally, β -naphthylamine (0.311 g, 2.17 mmol, 1.1 equiv) was added. The mixture was warmed to room temperature and stirred for 12 hours. The solvent was removed *in vacuo* and the residue was partitioned between 1.0 N HCl and EtOAc. The mixture was extracted with ethyl acetate (2x). The combined organics were washed with brine, dried with MgSO_4 , and concentrated *in vacuo* to give a white solid. The crude material was purified by silica gel chromatography (ISCO, RediSep 12 g column, 0-30% EtOAc/Hexanes gradient) to give a white solid. ^1H NMR (400 MHz, CDCl_3) δ 8.34 (d, $J = 2.3$ Hz, 1H), 8.00 (bs, 1H), 7.95 (d, $J = 9.0$ Hz, 2H), 7.86-7.80 (mult, 3H), 7.59 (dd, $J_1 = 8.9$ Hz, $J_2 = 2.3$ Hz, 1H), 7.51-7.42 (mult, 2H), 7.22 (d, $J = 8.6$ Hz, 8.6 Hz, 2H), 3.92 (quart, $J = 7.0$ Hz, 2H), 3.72 (quart, $J = 7.0$ Hz, 2H), 1.38-1.34 (mult, 6H). ^{13}C NMR (100 MHz, CDCl_3) δ 186.2, 165.5, 156.7, 135.5, 134.0, 132.7, 131.0, 129.0, 128.5, 127.9, 127.7, 126.7, 125.3, 123.5, 120.3, 117.2, 48.7, 44.7, 13.8, 12.0. HRMS calcd for $\text{C}_{22}\text{H}_{22}\text{N}_2\text{O}_2\text{S}$, 379.14814 $[\text{M}+\text{H}]^+$; found, 379.14712 $[\text{M}+\text{H}]^+$. Anal. ($\text{C}_{22}\text{H}_{22}\text{N}_2\text{O}_2\text{S}$) C, H, N.

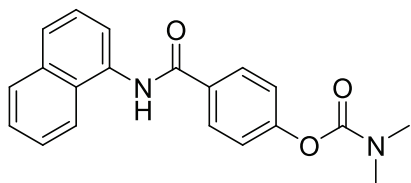
4-(naphthalen-1-ylcarbamoyl)phenyl diethylcarbamate (1063-2).



Compound **1063-2** was prepared in the same manner as **1063-1** utilizing carboxylic acid **39** (0.500 g, 2.11 mmol) and α -naphthylamine (0.332 g, 2.32 mmol, 1.1 equiv). The crude material was purified by silica gel chromatography (ISCO, RediSep 12 g column,

step gradient 0-15% EtOAc/Hexanes over 15 mins, upped to 30% for 15 mins gradient) to give a pink foam. The foam was triturated with hexanes and ether, and the resultant white solid was collected by filtration and washed with hexanes (428 mg, 56%). ^1H NMR (400 MHz, CDCl_3) δ 8.82 (s, 1H), 7.89 (d, $J = 8.6$ Hz, 2H), 7.85-7.82 (mult, 2H), 7.70 (d, $J = 8.2$ Hz, 1H), 7.69 (d, $J = 7.4$ Hz, 1H), 7.48-7.39 (mult, 3H), 7.11 (d, $J = 8.6$ Hz, 2H), 3.38 (quart, $J = 7.0$ Hz, 2H), 3.25 (quart, $J = 7.4$ Hz, 2H), 1.20 (t, $J = 7.0$ Hz, 3H), 1.07 (t, $J = 7.0$ Hz, 3H). ^{13}C NMR (100 MHz, CDCl_3) δ 166.0, 154.1, 153.7, 134.2, 132.9, 131.3, 128.8, 128.5, 128.4, 126.4, 126.1, 126.0, 125.6, 122.6, 122.0, 121.7, 42.6, 42.0, 14.2, 13.2. HRMS calcd for $\text{C}_{22}\text{H}_{22}\text{N}_2\text{O}_3$, 363.17094 $[\text{M}+\text{H}]^+$; found, 363.17081 $[\text{M}+\text{H}]^+$. Anal. ($\text{C}_{22}\text{H}_{22}\text{N}_2\text{O}_3$) C, H, N.

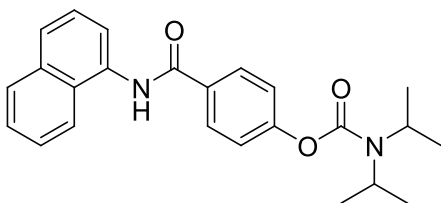
4-(Naphthalen-1-ylcarbamoyl)phenyl diethylcarbamate (1063-3).



Compound **1063-3** was prepared in the same manner as **1063-1** utilizing carboxylic acid **41** (0.400 g, 1.91 mmol) and α -naphthylamine (0.301 g, 2.10 mmol, 1.1 equiv). The crude material was purified by silica gel chromatography (ISCO, RediSep 24 g column, 0% Hexanes to 2 EtOAc/1 Hexanes gradient) to give a pinkish foam. The foam was triturated with hexanes and ether to yield an off-white solid which was obtained by filtration and washed with hexanes (0.431 g, 67%). ^1H NMR (400 MHz, CDCl_3) δ 8.49 (bs, 1H), 7.94 (d, $J = 8.2$ Hz, 2H), 7.89-7.86 (mult, 3H), 7.74 (d, $J = 8.2$ Hz, 1H), 7.51-7.46

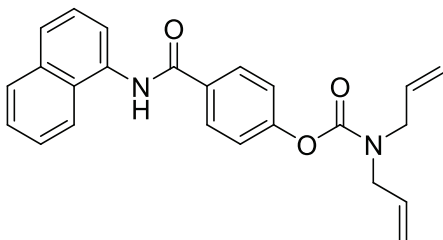
(mult, 3H), 7.20 (d, $J = 8.2$ Hz, 2H), 3.08 (s, 3H), 2.92 (s, 3H). ^{13}C NMR (100 MHz, CDCl_3) δ 165.9, 155.44, 154.35, 134.3, 132.8, 131.7, 128.8, 128.7, 128.1, 126.4, 126.2, 125.8, 122.1, 122.0, 121.5, 36.8, 36.6. HRMS calcd for $\text{C}_{20}\text{H}_{18}\text{N}_2\text{O}_3$, 335.13968 $[\text{M}+\text{H}]^+$; found, 335.13885 $[\text{M}+\text{H}]^+$. Anal. ($\text{C}_{20}\text{H}_{18}\text{N}_2\text{O}_3$) C, H, N.

4-(Naphthalen-1-ylcarbamoyl)phenyl diisopropylcarbamate (1063-4).



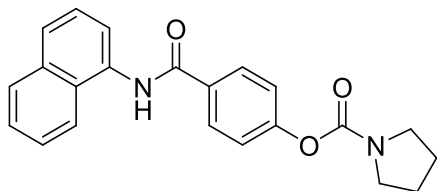
Compound **1063-4** was prepared in the same manner as **1063-1** utilizing carboxylic acid **40** (0.400 g, 1.51 mmol) and α -naphthylamine (0.237 g, 1.66 mmol, 1.1 equiv). The crude material was purified by silica gel chromatography (ISCO, RediSep 12 g column, step gradient 0-15% EtOAc/Hexanes over 15 mins, 20% for 15 mins gradient) to give an off-white foam (0.373 g, 63%). ^1H NMR (400 MHz, CDCl_3) δ 8.35 (bs, 1H), 7.98 (d, $J = 8.5$ Hz, 2H), 7.95 (d, $J = 7.4$ Hz, 1H), 7.91-7.88 (mult, 2H), 7.75 (d, $J = 8.2$ Hz, 1H), 7.54-7.49 (mult, 3H), 7.26 (d, $J = 8.5$ Hz, 2H), 4.18-4.95 (mult, 2H), 1.39-1.24 (mult, 12 H). ^{13}C NMR (100 MHz, CDCl_3) δ 165.9, 154.4, 153.4, 134.4, 132.7, 131.6, 129.0, 128.8, 127.9, 126.6, 126.4, 126.2, 126.0, 122.3, 121.8, 121.2, 47.3, 46.4, 21.8, 21.5. HRMS calcd for $\text{C}_{24}\text{H}_{26}\text{N}_2\text{O}_3$, 391.20228 $[\text{M}+\text{H}]^+$; found, 391.20157 $[\text{M}+\text{H}]^+$. Anal. ($\text{C}_{24}\text{H}_{26}\text{N}_2\text{O}_3$) C, H, N.

4-(Naphthalen-1-ylcarbamoyl)phenyl diallylcarbamate (1063-5).



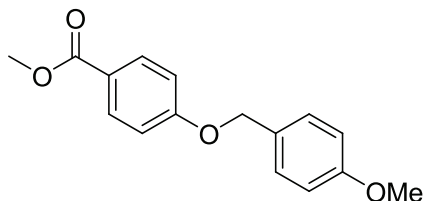
Compound **1063-5** was prepared in the same manner as **1063-1** utilizing carboxylic acid **42** (0.500 g, 1.91 mmol) and α -naphthylamine (0.301 g, 2.11 mmol, 1.1 equiv). The crude material was purified by silica gel chromatography (ISCO, RediSep 24 g, 0-15% EtOAc/Hexanes gradient column) to give a pink oil. The oil was triturated with ether and hexanes to yield an off-white solid which was collected by filtration (0.346 g, 47%). ^1H NMR (400 MHz, CDCl_3) δ 8.48 (bs, 1H), 7.94 (d, $J = 8.6$ Hz, 2H) 7.89-7.83 (mult, 3H), 7.73 (d, $J = 8.2$ Hz, 1H), 7.51-7.45 (mult, 3H), 7.02 (d, $J = 8.6$ Hz, 2H), 5.87-5.76 (mult, 2H), 5.25-5.19 (mult, 4H), 4.02-3.92 (mult, 4H). ^{13}C NMR (100 MHz, CDCl_3) δ 165.9, 154.2, 154.1, 134.3, 133.1, 132.9, 132.7, 131.8, 128.8, 128.7, 128.3, 126.4, 126.2, 125.8, 122.1, 122.0, 121.5, 118.1, 117.3, 49.6, 49.2. HRMS calcd for $\text{C}_{24}\text{H}_{22}\text{N}_2\text{O}_3$, 387.17098 $[\text{M}+\text{H}]^+$; found, 387.16989 $[\text{M}+\text{H}]^+$. Anal. ($\text{C}_{24}\text{H}_{22}\text{N}_2\text{O}_3$) C, H, N.

4-(Naphthalen-1-ylcarbamoyl)phenyl pyrrolidine-1-carboxylate (1063-6).



Compound **1063-6** was prepared in the same manner as **1063-1** utilizing carboxylic acid **43** (0.500 g, 2.13 mmol) and α -naphthylamine (0.335 g, 2.34 mmol, 1.1 equiv). The crude material was purified by silica gel chromatography (ISCO, RediSep 24 g column, 0-25% EtOAc/Hexanes gradient) to give a pink solid. The solid was triturated with hexanes and ether to give a white solid which was obtained by filtration (0.642 g, 84%). ^1H NMR (400 MHz, CDCl_3) δ 8.55 (bs, 1H), 7.96 (d, $J = 8.2$ Hz, 2H), 7.89-7.84 (mult, 3H), 7.75 (d, $J = 8.2$ Hz, 1H), 7.51-7.46 (mult, 3H), 7.23 (d, $J = 8.2$ Hz, 2H), 3.52 (t, $J = 6.7$ Hz, 2H), 3.31 (t, $J = 6.7$ Hz, 2H), 1.91 (quint, $J = 6.7$ Hz, 2H), 1.83 (quint, $J = 6.7$ Hz, 2H). ^{13}C NMR (100 MHz, CDCl_3) δ 165.9, 154.3, 152.7, 134.3, 132.9, 131.5, 128.9, 126.2, 125.9, 122.2, 122.0, 121.6, 25.9, 25.1. HRMS calcd for $\text{C}_{22}\text{H}_{20}\text{N}_2\text{O}_3$, 361.15533 $[\text{M}+\text{H}]^+$; found, 361.15430 $[\text{M}+\text{H}]^+$. Anal. ($\text{C}_{22}\text{H}_{20}\text{N}_2\text{O}_3$) C: 71.42, H: 5.47, N: 7.56.

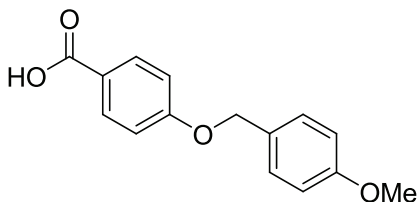
Methyl 4-(4-methoxybenzyloxy)benzoate (25).



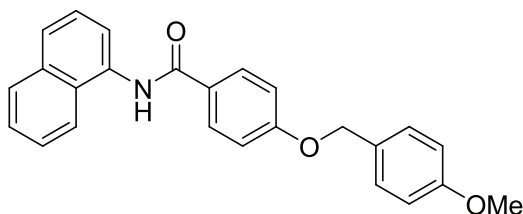
Compound **19** (12.00 g, 78.9 mmol) was dissolved in DMF (85.0 mL). 4-methoxybenzyl chloride (13.9 mL, 103 mmol, 2.00 equiv) was added, followed by potassium carbonate

(21.8 g, 158 mmol, 2.0 equiv). The mixture was stirred at room temperature for 12 hours. The mixture was poured into an ice bath and warmed to room temperature. The white precipitate was collected by filtration and washing with hexanes (1.56 g, 87%). ^1H NMR (400 MHz, CDCl_3) δ 8.01 (d, $J = 8.6$ Hz, 2H), 7.36 (d, $J = 8.2$ Hz, 2H), 6.99 (d, $J = 9.0$ Hz, 2H), 6.93 (d, $J = 8.6$ Hz, 2H), 5.03 (s, 2H), 3.89 (s, 3H), 3.82 (s, 3H). ^{13}C NMR (100 MHz, CDCl_3) δ 167.0, 162.7, 159.7, 131.7, 129.5, 128.4, 122.8, 114.6, 114.2, 70.0, 55.4, 52.0.

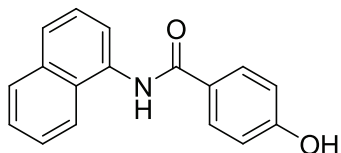
4-(4-Methoxybenzyloxy)benzoic acid (26).



Ester **25** (1.00 g, 3.67 mmol) was dissolved in methanol (50.0 mL). To this solution, 1.0 N sodium hydroxide (14.0 mL, 14.0 mmol, 3.8 equiv) was added. The solution was refluxed for 12 hours. The pH was adjusted to 3 with concentrated HCl. The resultant white precipitate was obtained by filtration and washed with hexanes (0.936 g, 99%). ^1H NMR (400 MHz, CDCl_3) δ 7.88 (d, $J = 9.0$ Hz, 2H), 7.39 (d, $J = 8.6$ Hz, 2H), 7.05 (d, $J = 9.0$ Hz, 2H), 6.96 (d, $J = 9.0$ Hz, 2H), 5.08 (s, 2H), 3.76 (s, 3H). ^{13}C NMR (100 MHz, CDCl_3) δ 167.2, 136.2, 159.3, 131.5, 129.9, 128.5, 123.2, 114.7, 114.0, 69.4, 55.2, 48.8.

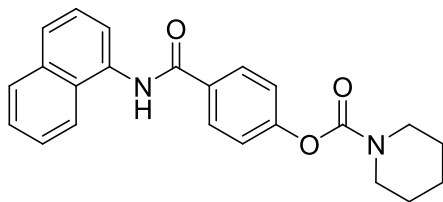
4-(4-Methoxybenzyloxy)-N-(naphthalen-1-yl)benzamide (27).

Carboxylic acid **26** (5.00 g, 19.4 mmol) was dissolved in DMF (100.0 mL). To this solution, DMAP (2.60 g, 21.3 mmol, 1.1 equiv), and EDC (4.08 g, 21.3 mmol, 1.1 equiv) were added to give a colorless suspension. After stirring for 45 minutes, α -naphthylamine (3.05 g, 21.3 mmol, 1.1 equiv) was added. The mixture was warmed to room temperature and stirred for 12 hours. The solvent was removed *in vacuo* and the residue was partitioned between 1.0 N HCl and EtOAc. A purple solid precipitated, which was obtained by filtration and washed with ether. The crude material was further recrystallized with EtOAc to give a white solid (5.22 g, 70%). ^1H NMR (400 MHz, d_6 -DMSO) δ 10.37 (bs, 1H), 8.15 (d, J = 8.2 Hz, 2H), 8.03-7.98 (mult, 2H), 7.87 (d, J = 7.8 Hz, 1H), 7.64 (d, J = 7.0 Hz, 1H), 7.59-7.55 (mult, 3H), 7.45 (d, J = 8.6 Hz, 2H), 7.19 (d, J = 8.2 Hz, 2H), 6.99 (d, J = 8.2 Hz, 2H), 5.16 (s, 2H), 3.78 (s, 3H). ^{13}C NMR (100 MHz, d_6 -DMSO) δ 165.6, 161.1, 159.1, 134.1, 133.8, 129.8, 129.7, 129.4, 128.5, 128.1, 126.7, 126.2, 126.1, 125.9, 125.6, 123.9, 123.5, 114.6, 113.9, 69.3, 55.1.

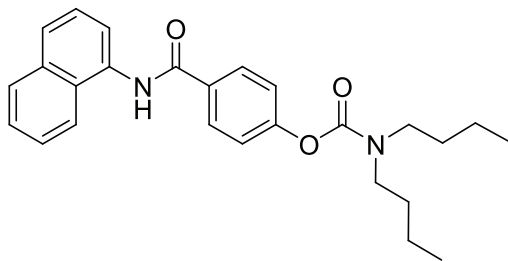
4-Hydroxy-N-(naphthalen-1-yl)benzamide (28).

Ester **27** (0.500 g, 1.00 mmol) was dissolved in TFA (3.0 mL, 39 mmol, 30 equiv). The mixture immediately turned purple, and was stirred at room temperature for 30 minutes. The solution was concentrated *in vacuo* to give a yellow residue. The residue was partitioned between ethyl acetate and water. The organics were separated and washed with sat'd NaHCO₃ and brine, dried over MgSO₄, and concentrated *in vacuo* to give a white foam. The foam was taken up in DCM, upon which a white solid precipitated, which was collected by filtration. The crude material was purified using silica gel chromatography (ISCO, RediSep 24 g column, 1 EtOAc/3 DCM gradient) to give a white foam. The crude material was further purified using reverse phase preparative HPLC. The sample was dissolved in THF. Method: 40% MeOH/H₂O to 90% MeOH/H₂O over 40 mins at 10 mL/min, 1 min ramp to 100% MeOH, 100% MeOH for 40 mins. Product comes out near 80% MeOH (first peak). The title compound was obtained as a white solid (0.200 g, 58%). ¹H NMR (300 MHz, *d*₆-DMSO) δ 10.20 (s, 1H), 10.14 (bs, 1H), 8.10-7.96 (mult, 4H), 7.85 (d, *J* = 7.6 Hz, 1H), 7.60-7.53 (mult, 4H), 6.92 (d, *J* = 8.5 Hz, 2H).

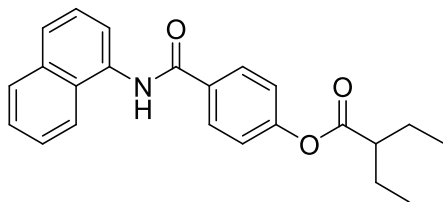
4-(Naphthalen-1-ylcarbamoyl)phenyl piperidine-1-carboxylate (1063-7).



Phenol **28** (0.092 g, 0.35 mmol), finely ground potassium carbonate (0.097 g, 0.70 mmol, 2.0 equiv) and DMF (5.0 mL) was stirred at 23°C for 1 hr to give an opaque suspension. Piperidine carbonyl chloride (0.048 mL, 0.38 mmol, 1.1 equiv) was then added. The mixture was stirred at room temperature for 3 hours. The DMF was removed *in vacuo* and the resulting residue was poured into water yielding a white solid. The white solid was collected by filtration and washed with ether (0.086 g, 66%). ¹H NMR (400 MHz, *d*₆-DMSO) δ 10.46 (s, 1H), 8.12 (d, *J* = 7.9 Hz, 2H), 8.01 (bm, 2H), 7.88 (d, *J* = 7.9 Hz, 1H), 7.62-7.55 (mult, 4H), 7.32 (d, *J* = 8.3 Hz, 2H), 3.60 (bs, 2H), 3.45 (bs, 2H), 1.62 (bmult, 6H). ¹³C NMR (100 MHz, *d*₆-DMSO) δ 166.0, 154.5, 153.3, 134.3, 132.7, 131.6, 128.8, 128.8, 128.1, 126.4, 126.2, 125.8, 122.1, 121.5, 45.8, 45.3, 26.0, 25.5, 24.3. HRMS calcd for C₂₃H₂₂N₂O₃, 375.17094 [M+H]⁺; found 375.16991 [M+H]⁺. Anal. (C₂₃H₂₂N₂O₃) C: 71.58, H: 5.74, N: 7.36.

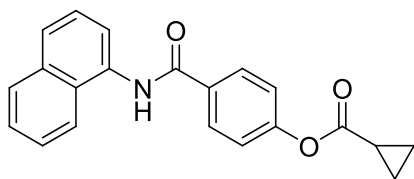
4-(Naphthalen-1-ylcarbamoyl)phenyl dibutylcarbamate (1063-8).

Compound **1063-8** was prepared in the same manner as **1063-7** utilizing phenol **28** (0.085 g, 0.32 mmol) and dibutyl carbamoyl chloride (0.069 mL, 0.36 mmol, 1.1 equiv). No solid precipitated, and the solution was extracted with ether (2x). The organics were washed with brine, dried over MgSO_4 , and concentrated *in vacuo* to give a yellow oil. The crude material was purified using silica gel chromatography (ISCO, RediSep 24 g column, 0-20% EtOAc/Hexanes gradient) to give a colorless oil (0.114 g, 84%). ^1H NMR (400 MHz, CDCl_3) δ 8.57 (s, 1H), 7.92 (d, $J = 8.6$ Hz, 2H), 7.85-7.83 (mult, 2H), 7.78 (d, $J = 7.0$ Hz, 1H), 7.70 (d, $J = 8.2$ Hz, 1H), 7.40-7.42 (mult, 3H), 7.15 (d, $J = 8.6$ Hz, 2H), 3.33 (t, $J = 7.4$ Hz, 2H), 3.21 (t, $J = 7.4$ Hz, 2H), 1.60-1.47 (mult, 4H), 1.35-1.23 (mult, 4H), 0.97-0.88 (mult, 6H). ^{13}C NMR (100 MHz, CDCl_3) δ 165.9, 154.4, 154.2, 134.3, 132.8, 131.5, 128.9, 128.7, 128.3, 126.4, 126.4, 126.1, 125.8, 122.2, 121.9, 121.7, 47.6, 47.3, 31.0, 30.1, 20.1, 14.0. HRMS calcd for $\text{C}_{26}\text{H}_{30}\text{N}_2\text{O}_3$, 419.23358 $[\text{M}+\text{H}]^+$; found, 419.23261 $[\text{M}+\text{H}]^+$. Anal. ($\text{C}_{26}\text{H}_{30}\text{N}_2\text{O}_3$) C, H, N.

4-(Naphthalen-1-ylcarbamoyl)phenyl 2-ethylbutanoate (1063-9).

Phenol **28** (0.100 g, 0.38 mmol), finely ground potassium carbonate (0.105 g, 0.76 mmol, 2.0 equiv) and DMF (5.0 mL) was stirred at 23°C for 30 min to give an opaque suspension. 2-ethylbutyryl chloride (0.057 mL, 0.42 mmol, 1.1 equiv) was then added. The mixture was stirred at room temperature for 12 hours, then heated to 90°C for an additional 12 hours. The DMF was removed *in vacuo* and the resulting residue was poured into water. No solid precipitated, so the solution was extracted with ether (2x). The organics were washed with brine, dried over MgSO₄, and concentrated *in vacuo* to give a yellow oil. The crude material was purified using silica gel chromatography (ISCO, RediSep 24 g column, 0-20% EtOAc/Hexanes gradient) to give a colorless oil (0.028, 20%). ¹H NMR (400 MHz, CDCl₃) δ 8.22 (bs, 1H), 7.97 (d, *J* = 7.9 Hz, 3H), 7.88 (d, *J* = 9.0 Hz, 2H), 7.74 (d, *J* = 8.3 Hz, 1H), 7.55-7.49 (mult, 3H), 7.26 (d, *J* = 9.0 Hz, 2H), 3.63-3.59 (mult, 2H), 3.49-3.44 (mult, 2H), 1.79-1.69 (mult, 4H). HRMS calcd for C₂₃H₂₃NO₃, 362.17573 [M+H]⁺; found, 362.17475 [M+H]⁺. HPLC 1: Reverse Phase C₁₈ column. Method: 100% MeOH/0% water over 15 mins at 1 mL/min. 99.8% purity (retention time = 3.31 minutes). HPLC 2: Normal Phase Si column. Method: 20% iPrOH/80% Hexanes to 80% iPrOH/20% Hexanes over 15 mins at 1 mL/min. 100% purity (retention time 5.85 minutes).

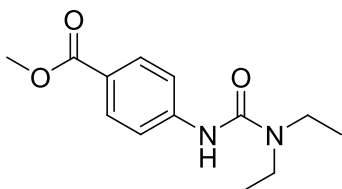
4-(Naphthalen-1-ylcarbamoyl)phenyl cyclopropanecarboxylate (1063-10).



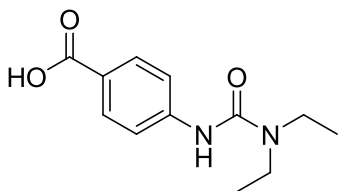
Phenol **28** (0.100 g, 0.38 mmol), finely ground potassium carbonate (0.105 g, 0.76 mmol, 2.0 equiv) and DMF (5.0 mL) was stirred at 23°C for 30 min to give an opaque suspension. Cyclopropanecarbonyl chloride (0.035 mL, 0.38 mmol, 1.0 equiv) was then added. The mixture was stirred at room temperature for 12 hours, then heated to 90°C for an additional 12 hours. The DMF was removed *in vacuo* and the resulting residue was poured into water. No solid precipitated, so the solution was extracted with ether (2x). The organics were washed with brine, dried over MgSO₄, and concentrated *in vacuo* to give a yellow oil. The crude material was purified using silica gel chromatography (ISCO, RediSep 24 g column, 0-30% EtOAc/Hexanes gradient) to give a white solid (0.028, 22%). ¹H NMR (400 MHz, CDCl₃) δ 8.25 (bs, 1H), 7.98 (d, *J* = 8.6 Hz, 2H), 7.94 (d, *J* = 7.6 Hz, 1H), 7.91-1.87 (mult, 2H), 7.75 (d, *J* = 8.3 Hz, 1H), 7.55-7.48 (mult, 3H), 7.24 (d, *J* = 8.6 Hz, 2H), 1.91-1.84 (mult, 1H), 1.22-1.19 (mult, 2H), 1.10-1.05 (mult, 2H). ¹³C NMR (400 MHz, CDCl₃) δ 173.4, 153.8, 134.4, 132.5, 132.4, 129.1, 128.9, 127.7, 126.7, 126.5, 126.3, 126.0, 122.3, 121.6, 121.0, 29.9, 13.3, 9.79. HRMS calcd for C₂₁H₁₇NO₃, 332.12878 [M+H]⁺; found, 332.12802 [M+H]⁺. HPLC 1: Reverse Phase C₁₈ column. Method: 100% MeOH/0% water over 15 mins at 1 mL/min. 98.9% purity (retention time = 3.92 minutes). HPLC 2: Normal Phase Si column. Method: 20%

iPrOH/80% Hexanes to 80% iPrOH/20% Hexanes over 15 mins at 1 mL/min. 99.6% purity (retention time 6.01 minutes).

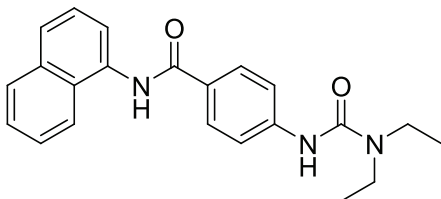
Methyl 4-(3,3-diethylureido)benzoate (30).



To a solution of amine **29** (0.300 g, 1.98 mmol) and DIPEA (3.46 mL, 19.8 mmol, 10 equiv) in THF (20 mL) was added diethylcarbonyl chloride (2.51 mL, 19.8 mmol, 10 equiv). The mixture was refluxed for 16 hours. The reaction was poured into water and extracted with DCM. The organics were washed with brine, dried over MgSO_4 , and concentrated in vacuo to give an orange residue. The crude material was purified using silica gel chromatography (ISCO, RediSep 12 g column, 0-30% EtOAc/Hexanes) to give a white solid (0.124 g, 25%). ^1H NMR (400 MHz, CDCl_3) δ 7.92 (d, $J = 9.0$ Hz, 2H), 7.48 (d, $J = 9.0$ Hz, 2H), 6.75 (bs, 1H), 3.86 (s, 3H), 3.36 (quart, $J = 7.4$ Hz, 4H), 1.20 (t, $J = 7.4$ Hz, 6H). ^{13}C NMR (100 MHz, CDCl_3) δ 167.1, 154.2, 144.1, 130.8, 123.9, 118.6, 52.0, 41.8, 14.1. HRMS calcd for $\text{C}_{13}\text{H}_{18}\text{N}_2\text{O}_3$, 251.13968 $[\text{M}+\text{H}]^+$; found, 251.13899 $[\text{M}+\text{H}]^+$.

4-(3,3-diethylureido)benzoic acid (31).

Ester **30** (0.124 g, 0.495 mmol) was dissolved in methanol (5.0 mL). To this solution 1.0 N sodium hydroxide (1.88 mL, 1.88 mmol, 3.8 equiv) was added. The mixture was stirred at room temperature for 12 hours. The pH was adjusted to 3 with concentrated HCl. The mixture was concentrated *in vacuo* to remove the methanol, upon which a white solid precipitated. The mixture was chilled at 4°C for 3 hours, and the resultant product was obtained by filtration and washed with hexanes to give a white solid (0.065 g, 56%). ¹H NMR (400 MHz, *d*₆-DMSO) δ 8.49 (s, 1H), 7.81 (d, *J* = 9.0 Hz, 2H), 7.63 (d, *J* = 9.0 Hz, 2H), 3.36 (quart, *J* = 7.0 Hz, 4H), 1.10 (t, *J* = 7.0 Hz, 6H). HRMS calcd for C₁₂H₁₆N₂O₃, 237.12403 [M+H]⁺; found, 237.12554 [M+H]⁺.

4-(3,3-Diethylureido)-N-(naphthalen-1-yl)benzamide (1063-11).

Carboxylic acid **31** (0.062 g, 0.26 mmol) was dissolved in DMF (5.0 mL) and cooled to 0°C. To this solution, DMAP (0.035 g, 0.29 mmol, 1.1 equiv), and EDC (0.055 g, 0.29 mmol, 1.0 equiv) were added. After stirring for 45 minutes, α-naphthylamine (0.041 g,

0.29 mmol, 1.1 equiv) was added to give a brown solution. The mixture was warmed to room temperature and stirred for 12 hours. The solvent was removed *in vacuo*, and the resultant residue treated with 1.0 N HCl, upon which a solid precipitated out. The precipitate was obtained by filtration and washed with ether. ^1H NMR (400 MHz, CDCl_3) δ 8.24 (bs, 1H), 8.02 (d, $J = 7.4$ Hz, 1H), 7.95-7.89 (mult, 3H), 7.75 (d, $J = 8.2$ Hz, 2H), 7.59-7.50 (mult, 6H), 6.59 (bs, 1H), 3.39 (quart, $J = 7.0$ Hz, 4H), 1.25 (d, $J = 7.0$ Hz, 6H). HRMS calcd for $\text{C}_{22}\text{H}_{23}\text{N}_3\text{O}_2$, 362.18697 $[\text{M}+\text{H}]^+$; found, 362.18614 $[\text{M}+\text{H}]^+$. Anal. ($\text{C}_{22}\text{H}_{23}\text{N}_3\text{O}_2$) C, H, N.

3.10.2. Combustion Analysis (Atlantic Microlab, Inc)

987 Series Compounds

Compound ID	Molecular Formula	Theoretical	Experimental
987-5	$\text{C}_{23}\text{H}_{14}\text{ClN}_3\text{O}_5$	C: 61.69, H: 3.15, N: 9.38	C: 61.84, H: 3.17, N: 9.56
987-6	$\text{C}_{23}\text{H}_{14}\text{BrN}_3\text{O}_5$	C: 56.12, H: 2.87, N: 8.54	C: 56.10, H: 3.83, N: 8.42
987-7	$\text{C}_{23}\text{H}_{14}\text{FN}_3\text{O}_5$	C: 64.04, H: 3.27, N: 9.74	C: 63.86, H: 3.31, N: 9.59
987-8	$\text{C}_{24}\text{H}_{17}\text{N}_3\text{O}_6$	C: 65.10, H: 3.86, N: 9.48	C: 64.97, H: 3.79, N: 9.42
987-10	$\text{C}_{23}\text{H}_{15}\text{IN}_2\text{O}_3$	C: 55.89, H: 3.06, N: 5.67	C: 55.78, H: 3.03, N: 5.64
987-11	$\text{C}_{24}\text{H}_{17}\text{N}_3\text{O}_5$	C: 67.44, H: 4.01, N: 9.83	C: 67.50, H: 3.85, N: 9.82
987-13	$\text{C}_{25}\text{H}_{20}\text{N}_2\text{O}_5$	C: 70.08, H: 4.71, N: 6.54	C: 69.88, H: 4.64, N: 6.55
987-15	$\text{C}_{28}\text{H}_{22}\text{N}_2\text{O}_8$	C: 65.37, H: 4.31, N: 5.44	C: 65.30, H: 4.40, N: 5.34
987-16	$\text{C}_{25}\text{H}_{18}\text{N}_2\text{O}_6$	C: 67.87, H: 4.10, N: 6.33	C: 67.82, H: 4.09, N: 6.33
987-19	$\text{C}_{24}\text{H}_{16}\text{N}_4\text{O}_4$	C: 67.92, H: 3.80, N: 13.20	C: 67.96, H: 3.88, N: 13.18
987-20	$\text{C}_{25}\text{H}_{19}\text{N}_3\text{O}_5$	C: 68.02, H: 4.34, N: 9.52	C: 67.93, H: 4.21, N: 9.50
987-21	$\text{C}_{24}\text{H}_{18}\text{N}_4\text{O}_5$	C: 65.15, H: 4.10, N: 12.66	C: 64.66, H: 3.88, N: 12.36*
987-22	$\text{C}_{25}\text{H}_{19}\text{N}_3\text{O}_6$	C: 65.64, H: 4.19, N: 9.19	C: 65.31, H: 4.01, N: 9.09*
987-23	$\text{C}_{27}\text{H}_{17}\text{N}_3\text{O}_5$	C: 69.97, H: 3.70, N: 9.07	C: 69.80, H: 3.53, N: 8.92
987-24	$\text{C}_{23}\text{H}_{15}\text{N}_3\text{O}_6$	C: 64.34, H: 3.52, N: 9.79	C: 63.44, H: 3.35, N: 9.60
987-26	$\text{C}_{23}\text{H}_{15}\text{N}_3\text{O}_5$	C: 66.83, H: 3.66, N: 10.16	C: 66.86, H: 3.62, N: 10.06
987-27	$\text{C}_{23}\text{H}_{15}\text{N}_3\text{O}_5$	C: 66.83, H: 3.66, N: 10.16	C: 66.75, H: 3.61, N: 10.03
1043	$\text{C}_{23}\text{H}_{15}\text{N}_3\text{O}_5$	C: 66.83, H: 3.66, N: 10.16	C: 66.79, H: 3.61, N: 10.05
987-28	$\text{C}_{23}\text{H}_{14}\text{ClN}_3\text{O}_5$	C: 61.69, H: 3.15, N: 9.38	C: 61.73, H: 3.00, N: 9.27
987-31	$\text{C}_{23}\text{H}_{14}\text{ClN}_3\text{O}_5$	C: 61.69, H: 3.15, N: 9.38	C: 61.72, H: 3.01, N: 9.22
987-32	$\text{C}_{23}\text{H}_{14}\text{ClN}_3\text{O}_5$	C: 61.69, H: 3.15, N: 9.38	C: 61.77, H: 3.13, N: 9.21
987-35	$\text{C}_{29}\text{H}_{19}\text{N}_3\text{O}_5$	C: 71.16, H: 3.91, N: 8.58	C: 71.07, H: 3.89, N: 8.48
987-36	$\text{C}_{26}\text{H}_{21}\text{N}_3\text{O}_5$	C: 68.56, H: 4.65, N: 9.23	C: 68.48, H: 4.52, N: 9.11
987-37	$\text{C}_{26}\text{H}_{21}\text{N}_3\text{O}_5$	C: 68.56, H: 4.65, N: 9.23	C: 68.49, H: 4.61, N: 9.18

Compound ID	Molecular Formula	Theoretical	Experimental
987-38	C ₂₄ H ₁₈ N ₂ O ₃	C: 75.38, H: 4.74, N: 7.33	C: 75.25, H: 4.68, N: 7.32
987-40	C ₂₄ H ₂₀ N ₂ O ₃	C: 74.98, H: 5.24, N: 7.29	C: 72.02, H: 5.03, N: 7.19*
987-41	C ₂₉ H ₁₉ N ₃ O ₅	C: 71.16, H: 3.91, N: 8.58	C: 70.96, H: 3.83, N: 8.48
987-43	C ₂₃ H ₁₄ IN ₃ O ₅	C: 51.23, H: 2.62, N: 7.79	C: 51.34, H: 2.55, N: 7.76
987-44	C ₂₃ H ₁₄ IN ₃ O ₅	C: 51.23, H: 2.62, N: 7.79	C: 51.28, H: 2.56, N: 7.78
987-45	C ₂₃ H ₁₄ IN ₃ O ₅	C: 51.23, H: 2.62, N: 7.79	C: 51.29, H: 2.64, N: 7.80
987-49	C ₂₉ H ₁₉ N ₃ O ₅	C: 71.16, H: 3.91, N: 8.58	C: 71.01, H: 3.77, N: 8.57
987-50	C ₂₉ H ₁₉ N ₃ O ₅	C: 71.16, H: 3.91, N: 8.58	C: 71.29, H: 3.88, N: 8.55
987-54	C ₂₅ H ₁₇ N ₃ O ₇	C: 63.69, H: 3.63, N: 8.91	C: 63.62, H: 3.56, N: 8.78
987-55	C ₂₄ H ₁₅ N ₃ O ₇	C: 63.02, H: 3.31, N: 9.19	C: 62.92, H: 3.30, N: 9.06
987-58	C ₂₇ H ₁₇ N ₃ O ₅ S	C: 65.45, H: 3.46, N: 8.48	C: 65.49, H: 3.42, N: 8.44

*did not pass within $\pm 0.4\%$

1063 Series Compounds

Compound ID	Molecular Formula	Theoretical	Experimental
1063-1	C ₂₂ H ₂₂ N ₂ O ₂ S	C: 69.81, H: 5.86, N: 7.40	C: 69.79, H: 5.82, N: 7.27
1063-2	C ₂₂ H ₂₂ N ₂ O ₃	C: 72.91, H: 6.12, N: 7.73	C: 72.79, H: 6.05, N: 7.63
1063-3	C ₂₀ H ₁₈ N ₂ O ₃	C: 71.84, H: 5.43, N: 8.38	C: 71.91, H: 5.44, N: 8.31
1063-4	C ₂₄ H ₂₆ N ₂ O ₃	C: 73.82, H: 6.71, N: 7.17	C: 73.64, H: 6.72, N: 7.13
1063-5	C ₂₄ H ₂₂ N ₂ O ₃	C: 74.59, H: 5.74, N: 7.25	C: 74.46, H: 5.77, N: 7.26
1063-6	C ₂₂ H ₂₀ N ₂ O ₃	C: 73.32, H: 5.59, N: 7.77	C: 71.42, H: 5.47, N: 7.56*
1063-7	C ₂₃ H ₂₂ N ₂ O ₃	C: 73.78, H: 5.92, N: 7.48	C: 71.58, H: 5.74, N: 7.36*
1063-8	C ₂₆ H ₃₀ N ₂ O ₃	C: 74.61, H: 7.22, N: 6.69	C: 74.71, H: 7.23, N: 6.76
1063-11	C ₂₂ H ₂₃ N ₃ O ₂	C: 73.11, H: 6.41, N: 11.63	C: 73.03, H: 6.36, N: 11.61

*did not pass within $\pm 0.4\%$

3.11 Biology Experimental Detail

3.11.1 *In vitro* NMDA antagonism assay (Dr. Stephen Traynelis, Emory University School of Medicine).

Two-electrode voltage-clamp electrophysiology

Two-electrode voltage-clamp (TEVC) recordings were performed on *Xenopus* oocytes expressing recombinant rat NR1/NR2A, NR1/NR2B, NR1/NR2C, NR1/NR2D, GluR1, or GluR6 receptors. cDNAs for rat NR1-1a (GenBank accession numbers U11418 and U08261; hereafter NR1), NR2A (D13211), NR2B (U11419), NR2C (M91563), NR2D

(L31611), GluR1 (X17184), GluR6 (Z11548) were provided by Drs. S. Heinemann (Salk Institute), S. Nakanishi (Kyoto University), and P. Seeburg (University of Heidelberg). Oocyte isolation and RNA injection were completed as described in detail elsewhere³²; all protocols involving *Xenopus laevis* were approved by the Emory University Institutional Animal Care and Use Committee. During TEVC recordings, oocytes were placed into a perfusion chamber and continually washed with recording solution containing (in mM) 90 NaCl, 1.0 KCl, 0.5 BaCl₂, 0.005 EDTA, and 10 HEPES at pH 7.4 (23°C). Glass electrodes with a tip resistance of 0.5-2.5 MΩ were pulled from thin-walled glass capillary tubes using a PP-83 puller (Narashige). Voltage electrodes were filled with 0.3 M KCl and current electrodes were filled with 3.0 M KCl. The current and voltage electrodes were connected to an OC-725C amplifier (Warner Instrument Co), which held the membrane potential of the oocytes at -40 mV during recording. All compounds were made as 20 mM stocks in DMSO, and dissolved to reach the desired final concentration in recording solution containing 100 μM glutamate and 30 μM glycine for use on oocytes expressing NMDA receptors. Final DMSO content was 0.05-0.5% (vol/vol). Oocytes expressing GluR6 receptors were pre-treated with 10 μM concanavalin-A for 10 minutes. Recombinant GluR1 and GluR6 receptors were activated by 100 μM glutamate. In order to prevent a gradual increase in current response over the course of the experiment, which appears to be a common feature of NR1/NR2A receptor responses, some oocytes expressing NR1/NR2A were either pretreated with 50 μM BAPTA-AM for 10 minutes or injected with 50 nl of 2 mM K-BAPTA.

For a select group of compounds, the maximum solubility was determined using a BMG Labtech Nephelostar nephelometer (Offenburg, Germany), according to manufacturer's instructions. Maximum solubility of each test compound was determined in oocyte recording solution (components given below) and 1% DMSO. Values for the IC₅₀ (half maximally effective concentration of inhibitor) were determined by fitting the equation

$$Response = (100 - minimum) / (1 + ([I] / IC_{50})^N) + minimum$$

to the mean composite concentration-response data normalized to the response in the absence of inhibitor (100%). N is the Hill slope, [I] is the inhibitor concentration, and *minimum* is the residual inhibition at saturating concentrations of ligand. Because inhibition was complete for most compounds tested, the *minimum* was fixed to 0 for all fitted curves, unless otherwise indicated. For a few compounds with bulky hydrophobic C ring substituents (e.g. **987-23**, **987-35**), minimum was allowed to vary. Only responses for concentrations below the experimentally determined limit of solubility were determined. For some compounds, we included 1-10 mM 2-hydroxypropyl- β -cyclodextrin in the recording solution to ensure the compounds remained in solution; 2-hydroxypropyl- β -cyclodextrin had no detectable effect on NMDA response amplitude (data not shown).

References

- (1) Williams, K. *Mol. Pharmacol.* **1993**, *44*, 851.
- (2) Frizelle, P. A.; Chen, P. E.; Wyllie, D. J. A. *Mol. Pharmacol.* **2006**, *70*, 1022.

- (3) Neyton, J.; Paoletti, P. *J. Neurosci.* **2006**, *26*, 1331.
- (4) Feng, B. H.; Morley, R. M.; Jane, D. E.; Monaghan, D. T. *Neuropharmacology* **2005**, *48*, 354.
- (5) Wyllie, D. J. A.; Chen, P. E. *Br. J. Pharmacol.* **2007**, *150*, 541.
- (6) Morley, R. M.; Tse, H. W.; Feng, B. H.; Miller, J. C.; Monaghan, D. T.; Jane, D. E. *J. Med. Chem.* **2005**, *48*, 2627.
- (7) Olanow, C. W.; Tatton, W. G. *Annu. Rev. Neurosci.* **1999**, *22*, 123.
- (8) Standaert, D. G.; Testa, C. M.; Young, A. B.; Penney, J. B. *J. Comp. Neurol.* **1994**, *343*, 1.
- (9) Wenzel, A.; Villa, M.; Mohler, H.; Benke, D. *J. Neurochem.* **1996**, *66*, 1240.
- (10) Standaert, D. G.; Landwehrmeyer, G. B.; Kerner, J. A.; Penney, J. B.; Young, A. B. *Mol. Brain Res.* **1996**, *42*, 89.
- (11) Counihan, T. J.; Landwehrmeyer, G. B.; Standaert, D. G.; Kosinski, C. M.; Scherzer, C. R.; Daggett, L. P.; Velicelebi, G.; Young, A. B.; Penney, J. B. *J. Comp. Neurol.* **1998**, *390*, 91.
- (12) Jones, S.; Gibb, A. J. *J. Physiol-London* **2005**, *569*, 209.
- (13) Brothwell, S. L. C.; Barber, J. L.; Monaghan, D. T.; Jane, D. E.; Gibb, A. J.; Jones, S. *J. Physiol-London* **2008**, *586*, 739.
- (14) Chenard, B. L.; Welch, W. M.; Blake, J. F.; Butler, T. W.; Reinhold, A.; Ewing, F. E.; Menniti, F. S.; Pagnozzi, M. J. *J. Med. Chem.* **2001**, *44*, 1710.
- (15) Welch, W. M.; Ewing, F. E.; Huang, J.; Menniti, F. S.; Pagnozzi, M. J.; Kelly, K.; Seymour, P. A.; Guanowsky, V.; Guhan, S.; Guinn, M. R.; Critchett, D.; Lazzaro, J.; Ganong, A. H.; DeVries, K. M.; Staigers, T. L.; Chenard, B. L. *Bioorg. Med. Chem. Lett.* **2001**, *11*, 177.
- (16) Perich, J. W.; Johns, R. B. *Synthesis-Stuttgart* **1989**, 701.
- (17) Gerard, A. L.; Lisowski, V.; Rault, S. *Tetrahedron* **2005**, *61*, 6082.
- (18) Kaila, N.; Janz, K.; Huang, A.; Moretto, A.; DeBernardo, S.; Bedard, P. W.; Tam, S.; Clerin, V.; Keith, J. C.; Tsao, D. H. H.; Sushkova, N.; Shaw, G. D.; Camphausen, R. T.; Schaub, R. G.; Wang, Q. *J. Med. Chem.* **2007**, *50*, 40.
- (19) Snow, R. A.; Cottrell, D. M.; Paquette, L. A. *J. Am. Chem. Soc.* **1977**, *99*, 3734.
- (20) Sarvari, M. H.; Sharghi, H. *Tetrahedron* **2005**, *61*, 10903.
- (21) Bandgar, B. P. *Synth. Commun.* **1997**, *27*, 2065.
- (22) Menniti, F. S.; Buchan, A. M.; Chenard, B. L.; Critchett, D. J.; Ganong, A. H.; Guanowsky, V.; Seymour, P. A.; Welch, W. M. *Stroke* **2003**, *34*, 171.

- (23) Lazzaro, J. T.; Paternain, A. V.; Lerma, J.; Chenard, B. L.; Ewing, F. E.; Huang, J.; Welch, W. M.; Ganong, A. H.; Menniti, F. S. *Neuropharmacology* **2002**, *42*, 143.
- (24) Dingledine, R.; Borges, K.; Bowie, D.; Traynelis, S. F. *Pharmacol. Rev.* **1999**, *51*, 7.
- (25) Erreger, K.; Geballe, M. T.; Kristensen, A.; Chen, P. E.; Hansen, K. B.; Lee, C. J.; Yuan, H.; Le, P.; Lyuboslavsky, P. N.; Micale, N.; Jorgensen, L.; Clausen, R. P.; Wyllie, D. J.; Snyder, J. P.; Traynelis, S. F. *Mol. Pharmacol.* **2007**, *72*, 907.
- (26) Nakagawa, T.; Cheng, Y. F.; Ramm, E.; Sheng, M.; Walz, T. *Nature* **2005**, *433*, 545.
- (27) Schulman, J. *J. Biol. Chem.* **1950**, *186*, 717.
- (28) Schulman, J.; Keating, R. P. *J Clin Endocrinol* **1949**, *9*, 664.
- (29) Schulman, J.; Keating, R. P. *J. Biol. Chem.* **1950**, *183*, 215.
- (30) Winters, W. D.; Spector, E.; Wallach, D. P.; Shideman, F. E. *J. Pharmacol. Exp. Ther.* **1955**, *114*, 343.
- (31) Ogita, H.; Isobe, Y.; Takaku, H.; Sekine, R.; Goto, Y.; Misawa, S.; Hayashi, H. *Biorg. Med. Chem.* **2002**, *10*, 1865.
- (32) Traynelis, S. F.; Burgess, M. F.; Zheng, F.; Lyuboslavsky, P.; Powers, J. L. *J Neurosci* **1998**, *18*, 6163.